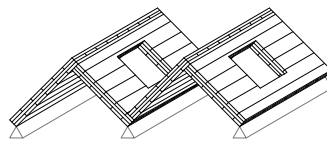
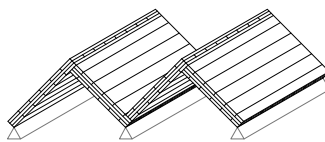
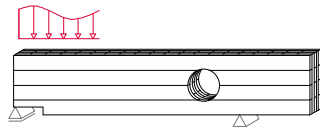
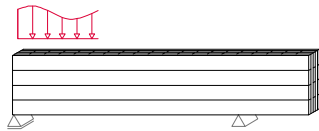
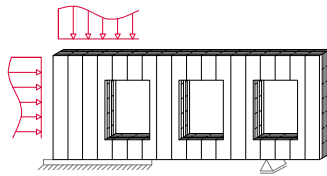
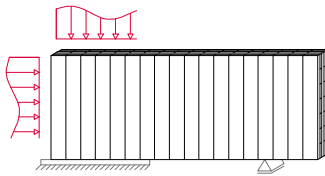
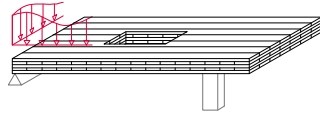
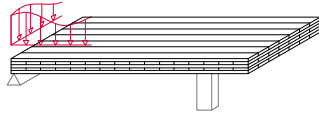


Properties, Testing and Design of Cross Laminated Timber



Editors:
Reinhard Brandner, Roberto Tomasi, Thomas
Moosbrugger, Erik Serrano and Philipp Dietsch

Properties, Testing and Design of Cross Laminated Timber

A state-of-the-art report by
COST Action FP1402 / WG 2

With contributions by:

Ishan K. Abeysekera, Stefano Bezzi, Andrii Bidakov, Anders Björnfot, Thomas Bogensperger, Reinhard Brandner, Daniele Casagrande, Thomas Ehrhart, Mariano Fiorencis, Maurizio Follesa, Andrew C. Lawrence, Ildiko Lukacs, Thomas Moosbrugger, Peter Niebuhr, Dag Pasca, Claudio Pradel, Gerhard Schickhofer, Erik Serrano, Elizabeth Shotton, Mike Sieder, Christophe Sigrist, Gregor Silly, Andrew J. R. Smith, Marta Stojmanovska, Roberto Tomasi, Vasileios Tsipiras, Tobias Wiegand

Editors:

Reinhard Brandner, Roberto Tomasi, Thomas Moosbrugger, Erik Serrano and Philipp Dietsch

Bibliographic information published by the Deutsche Nationalbibliothek

The Deutsche Nationalbibliothek lists this publication in the Deutsche Nationalbibliografie; detailed bibliographic data are available in the Internet at <http://dnb.d-nb.de>.

This publication is based upon work from COST Action FP1402, supported by COST (European Cooperation in Science and Technology).

COST (European Cooperation in Science and Technology) is a funding agency for research and innovation networks. Our Actions help connect research initiatives across Europe and enable scientists to grow their ideas by sharing them with their peers. This boosts their research, career and innovation.

www.cost.eu



Funded by the Horizon 2020 Framework Programme of the European Union

No permission to reproduce or utilise the contents of this book by any means is necessary, other than in the case of images, diagrams or other material from other copyright holders. In such cases, permission of the copyright holders is required.

This book may be cited as: Brandner, R., Tomasi, R., Moosbrugger, T., Serrano, E., Dietsch, P. (eds.), Properties, Testing and Design of Cross Laminated Timber: A state-of-the-art report by COST Action FP1402 / WG 2, Shaker Verlag Aachen, 2018.

Neither the COST Office nor any person acting on its behalf is responsible for the use which might be made of the information contained in this publication. The COST Office is not responsible for the external websites referred to in this publication.

Copyright Shaker Verlag 2018

All rights reserved. No part of this publication may be reproduced, stored in a retrieval system, or transmitted, in any form or by any means, electronic, mechanical, photocopying, recording or otherwise, without the prior permission of the publishers.

Printed in Germany.

ISBN 978-3-8440-6143-7

ISSN 0945-067X

Shaker Verlag GmbH • P.O. BOX 101818 • D-52018 Aachen

Phone: 0049/2407/9596-0 • Telefax: 0049/2407/9596-9

Internet: www.shaker.de • e-mail: info@shaker.de

Preface WG 2

Cross laminated timber (CLT), as structural, plate-like timber product, was developed in Central Europe about 30 years ago. Meanwhile, it gained global recognition due to its high resistance and stiffness in- and out-of-plane and its versatile applicability. It provoked some revolution in the international building sector as it allows rather easily to substitute mineral-based building products, like concrete and brick, in for example family and multi-storey residential, office and school buildings. Building with CLT even has led to a renaissance of timber in our cities. Reasons therefore are the fast erection times and dry building sites allowing concurrent works of other crafts. Furthermore, CLT allows relatively thin wall and floor elements increasing the utilizable living and working space, relatively low masses of total wall and floor elements reducing demands on lifting and mounting equipment, and easy fixing of installations and other finishing works without anchors.

Now and after the construction market / industry crisis, which started in US in 2007, again and worldwide a dynamic development of CLT production capacities is observed, which exceeded one million cubic meter per year already in 2017. Although these capacities have been erected globally, the vast majority of CLT still comes from Central Europe, with a share of two-thirds of the worldwide production from Austria. Despite its important position and relevance in the timber construction sector, in Europe standardization of CLT is still in a very early phase. In a first step the European product standard for CLT, EN 16351, was established but it is still not in force. In addition, it misses regulations and information on a number of important issues, e.g. establishment of a CLT strength class system, regulations on mechanical properties and harmonization of layer thicknesses and layups. Apart from missing regulations for the product itself, there are many other issues which mandate for European standardization. These comprise: testing and evaluation, design and execution. Also missing are details and regulations on building services also in conjunction with building physics detailing, in particular guidelines for execution and monitoring, taking care of the vulnerability of timber at high moisture content. Meanwhile, some national regulations as supplements to Eurocode 5, the European design standard for timber structures, contain rules for the design and execution of CTL structures, e.g. the Austrian National Annex K in ÖNORM B 1995-1-1 (2015).

The European design standard for timber structures, Eurocode 5, is currently in revision. Apart from revising existing chapters it is also aimed at implementing new products and design approaches which have become engineering practice but so far miss European standardization. This comprises also the design of CLT. The preparation work for implementing CLT in Eurocode 5 and related background documentation was the task of the project team PT SC5.T1. Their proposal is now ready for implementation as long as a European consensus can be achieved.

Parallel to this revision process of Eurocode 5, the COST Action FP1402 “Basis of Structural Timber Design – from research to standards” started its work in Autumn 2014 in frame of the European Cooperation in Science and Technology (COST). The aim of this Action was to overcome the gap between established scientific outcomes and demands from engineers, industry and authorities. The work within this COST Action was accompanied by semi-annual meetings organized mainly as workshops and theme specific conferences and training schools as well as short-term scientific missions (STSMs) which outcomes substantially contributed to the overall success of our Action.

Working group 2 (WG 2) “Solid/Massive Timber”, one of four working groups in COST Action FP1402, aimed on collecting, discussing, assessing, harmonizing and condensing of fragmented state-of-the-art concerning CLT with focus on testing and design. Initial intensive WG 2 discussions identified and outlined open issues, missing approaches and regulations. Further focus was on these issues which were categorized as median or high priority. These intensive discussions were followed and supported by an online questionnaire sent to engineers worldwide with overwhelming response and unison with WG 2 internal discussions in most issues. Parallel to this, literature related to CLT and engineering questions was collected and categorized according to four main topics addressed in WG 2 which were later dealt with in the four Task Groups (TGs):

- TG 1: Design of CLT elements (chaired by Thomas Moosbrugger),
- TG 2: Testing and evaluation (chaired by Erik Serrano),
- TG 3: Properties of CLT (chaired by Tobias Wiegand; later merged with TG 1),
- TG 4: Design of CLT systems (chaired by Roberto Tomasi).

Each TG aimed on presenting the state-of-the-art in TG STAR (state-of-the-art report) documents, outlining a condensed knowledge, relevant for scientists and lecturers; base documents of agreed content, as basis for code writers and standardization committees; proposals and suggestions, dedicated to practice; and identified open points and gaps, as source for potential initiators of future research

projects and investigations. Beside these internal activities, collaboration was sought and kept alive with other WGs in COST Action FP1402 as well as with other COST Actions, standardisation committees and the project team PT SC5.T1. A number of joint activities and publications underline these liaisons.

The WG 2 / TG STAR documents represent one of the main written outputs of each TG and constitute the main chapters of the WG 2 STAR, as presented in the following. This STAR aims on discussing many points related to CLT from an objective point-of-view, providing possible solutions, and outlining necessary further steps to go. It demonstrates a compilation of important written outcomes from WG 2 and represents and involves contributions from academia and practice across Europe, representing some European point-of view on CLT as building product, related to properties, testing and design. It is the result of a number of extraordinarily motivated WG 2 members, scientists, engineers and architects, to contribute, on a voluntary basis, to the success of our WG 2 and our COST Action FP1402. The efforts of all these WG 2 members and their TG chairs are thankfully acknowledged! As chair of WG 2 we express our sincere thanks to all participants at meetings and conferences, all members which had been in some liaison with our group and especially to all members of WG 2 and their colleague who had been active in the background. It has been impressive, enriching and motivating working with all of you in frame of this group! We also take the liberty to say thanks to the chair of COST Action FP1402, for initiating and leading this COST Action, implementing our WG 2 and for all support provided throughout these last four years.

Now it is time to let the readers and users of this STAR speak! Any response to our work is appreciated. Enjoy studying and working with our STAR.

Reinhard Brandner and Roberto Tomasi, Chair of COST Action FP1402 / WG 2

Table of Content

TG 1 – Design of CLT Elements & TG 3 – CLT Properties

Foreword	3
<i>A Discussions on Eurocode 5 Chapters for CLT on the Basis of PT SC5.T1 Document & Background Document (Status Oct. 2017)</i> <i>(please note: the following chapter numbers correspond to them in EC 5)</i>	
1 General	9
1.5 Terms and Definitions	11
2 Basis of Design	15
2.4 Verification by the Partial Factor Method	15
2.4.1 Design values of material properties	15
3 Material Properties	18
3.1 General	18
3.1.3 Strength modification factors for service classes and load-duration classes	18
3.1.4 Deformation modification factors for service classes	20
3.8 Cross Laminated Timber (CLT)	25
4 Durability	42
5 Basis of Structural Analysis	43
5.4 Assemblies	43
5.4.5 Cross laminated timber members	43
6 Ultimate and Serviceability Limit States	46
6.1 Design of Cross-Sections	46
6.1.1 General	46
6.1.2 Tension parallel to the grain	48
6.1.3 Tension perpendicular to the grain	49
6.1.4 Compression parallel to the grain	51
6.1.5 Compression perpendicular to the plane	52
6.1.6 Bending	54

6.1.7	Shear	56
6.2	Design of Cross-Sections Subjected to Combined Stresses	61
6.3	Stability of Members	62
6.3.2	Members subjected to either compression or combined compression and bending ...	62
6.3.3	Beams subjected to either bending or combined bending and compression	64
6.4	Design of Cross-Sections in Members with Varying Cross-Section or Curved Shape	67
6.5	Notched Members	68
6.5.2	Beams and plates with a notch at the support	68
6.6	System Strength	69
6.7	Vibrations	70
7	Connections with Metal Fasteners	73
8	Components and Assemblies	73
9	Execution and Control	73

B Thematic Contributions

Fatigue behaviour of CLT under in-plane shear loading		
	<i>Mike Sieder and Peter Niebuhr</i>	107

TG 2 – Testing and Evaluation

A General Motivation, Comments and Overview

Summary		125
1	Introduction	127
1.1	Testing for product properties	127
1.2	Aims and limitations	127
1.3	Outline	127
2	CLT – considerations regarding denomination and testing	128
2.1	Introduction	128
2.2	Standards and guidelines	131
2.3	Denominations	132

2.4	Test configurations	136
2.4.1	Requirements for bending and shear	136
2.4.2	Sample dimensions and testing configurations	138
2.4.3	Sampling	139
2.5	Conclusion and summary	141
3	Conclusions and recommendations	142
3.1	Main findings	142
3.2	Recommendations for future work	142
4	References	143

B *Test Methods – State-of-Art and Future Developments*

Some Comments on and Proposals for Determining the Compression Perpendicular to Grain Properties of CLT: Brief Summary of a Recent Publication <i>Reinhard Brandner</i>	147
Test Configurations for Determining Rolling Shear Properties with Focus on Cross Laminated Timber: A Critical Review <i>Thomas Ehrhart and Reinhard Brandner</i>	151
Test Methods for In-plane Shear Tests of Cross Laminated Timber <i>Erik Serrano</i>	171
CLT Strength by Tension Perpendicular to Grain <i>Andrii Bidakov</i>	183

TG 4 – Design of CLT Systems

Foreword	199
----------------	-----

A *Mechanical Characterization of Floor and Wall Diaphragms*

State-of-the-art: Cross Laminated Timber shear wall capacity and stiffness assessment methods <i>Ildiko Lukacs, Anders Björnfot and Roberto Tomasi</i>	203
State-of-the-art: Timber floor diaphragms <i>Ildiko Lukacs, Claudio Pradel, Anders Björnfot and Roberto Tomasi</i>	217
Safe design of indeterminate systems in a brittle material <i>Ishan K. Abeysekera, Andrew J. R. Smith and Andrew C. Lawrence</i>	231

B *Seismic Design*

General rules
Maurizio Follesa 245

The capacity design approach of Cross Laminated Timber structures:
a state-of-the-art review
Daniele Casagrande 259

Assessment of the q-factor for timber building with CLT panels:
state-of-the-art
Stefano Bezzi 269

Definition of the most suitable value of the q-factor for CLT structural systems
Marta Stojmanovska 287

Assessment of the over-strength factor for CLT structures:
a state-of-the-art review
Roberto Tomasi, Dag Pasca and Mariano Fiorencis 291

C *General Design Issues*

An Architectural Perspective on Cross Laminated Timber
Elizabeth Shotton 307

Supplemental Material

Comparison of Methods of Approximate Verification Procedures
for Cross Laminated Timber (reprint)
Thomas Bogensperger, Gregor Silly and Gerhard Schickhofer 323

COST Action FP1402
Basis of Structural Timber Design:
From Research to Standards

WG 2 – Solid Timber Constructions:
Cross Laminated Timber (CLT)

TG 1 – Design of CLT Elements
TG 3 – CLT Properties

Foreword

This State-of-the-Art Report (STAR) was written by the core group of Working Group 2 / Task Group 1 and 3 (WG 2 / TG 1 & TG 3) of COST Action FP1402 “Basis of Structural Timber Design – from Research to Standards” and it addresses all those who are interested in the properties and design of cross laminated timber (CLT) elements used as plates, diaphragms or as beams.

The present output is based on the work of the Project Team SC5.T1 responsible for development of a draft for implementation of cross laminated timber (CLT) in a revised version of Eurocode 5 (EN 1995-1-1), the European design code for timber structures, as well as the discussions, presentations and agreements made in past meetings of COST Action FP1402 in Karlsruhe / Germany (03 / 2015), Pamplona / Spain (10 / 2015), Stockholm / Sweden (03 / 2016), Mons / Belgium (09 / 2016), Zagreb / Croatia (03 / 2017) and Graz / Austria (09 / 2017).

In addition to the draft for implementation of CLT in EN 1995-1-1, SC5.T1 prepared also a “background document”, consisting of detailed information explaining the paragraphs of the CLT draft. Furthermore, a reference list is provided. As some members of COST Action FP1402 / WG 2 / TG 1 & TG 3 contributed also to the work of the Project Team SC5.T1 and vice versa, a close cooperation and support of the work on both sides was achieved reflecting also a broad consensus within all involved European delegates. Consequently, both documents written by the SC5.T1 project team serve also as basis for the STAR of WG 2 / TG 1 & TG 3. Due to different durations of SC5.T1 project team and COST Action FP1402, finally, the following two draft documents were applied:

- PT1 document, version 2017_10_13 [42], and
- PT1 background document, version 2017_10_13 [43].

The intention of this STAR is a more detailed summary of the relevant work, done during the last 20 years on the topic of CLT. Additional references not included in the documents of SC5.T1 were added highlighting also CLT relevant publications not directly addressing content of the CLT draft version for EC 5. Apart from providing additional references for all topics and chapters of SC5.T1 draft documents edited by WG2 / TG 1 & TG 3 within this STAR, further necessary scientific work was identified and listed. In doing so, the formal structure of EN 1995-1-1 [63] was kept. All chapters of EN 1995-1-1 [63] have been evaluated in respect to missing parts and regulations which seem to be necessary for designing CLT. In the following, for getting a holistic overview of relevant and missing topics as well as to summarize the output of all work

within COST Action FP1402 / WG 2 / TG 1 & TG 3, tables were used which are organised as follows:

Chapter	Numbering of edited chapters corresponds to the chapter number in EN 1995-1-1 [63]
Focus of work	Description of necessary focus of work for COST WG 2 / TG 1 & TG 3 meetings
Collaboration inclusive short motivation – WGs – TGs	Definition of possible or necessary collaborations with other WG's and / or WG 2 / TG's within COST Action FP1402
Currently available Literature	List of relevant references extended by well known publications on CLT which are not directly relevant but of interest
Suggestions for possible papers, scientific theses and further work	Collection of topics which are still open after COST Action FP1402 and / or outside the existing network of scientists

It should be noted that due to the progressively raising interest on CLT within the last five to ten years, a large number of scientific publications has been published internationally. Thus, the references cited may not be exhaustive nor does it represent only the most important references. The aim was that the cited references provide sufficient knowledge to describe the relevant subject areas in depth.

Based on these tabulated basis, the background information from the SC5.T1 background document was reviewed and edited as well for all chapters. In the grey boxes a summary of the SC5.T1 background information with small modifications made by COST Action FP1402 / WG 2 / TG 1 & TG 3 is given.

The background information given in the grey boxes is placed directly after the base tables for each relevant chapter.

Background

Consolidated background information, created by combining the evaluation results of the SC5.T1 background document in version 2017_10_13 [43] and the information generated during the meetings of COST Action FP1402 / WG 2 / TG 1 & TG 3.

In addition to the above-mentioned periodic working meetings of COST Action FP1402 / WG 2 / TG 1 & TG 3, a short term scientific mission (STSM) on the subject of “Investigation on the creep factor k_{def} for CLT elements loaded out-of-plane, taking into account CLT layup and lamination properties” was held within the scope of WG 2 / TG 1. Thereby, generated information and knowledge also represents essential input of the work of the COST Action FP1402 / WG 2 / TG 1.

Thomas Moosbrugger, leader of TG 1

*A Discussions on Eurocode 5 Chapters for CLT on the Basis of the
PT SC5.T1 Document & Background Document (Status Oct. 2017)*

1 General

1.5 Terms and Definitions

1.5.2 Additional terms and definitions used in this present standard

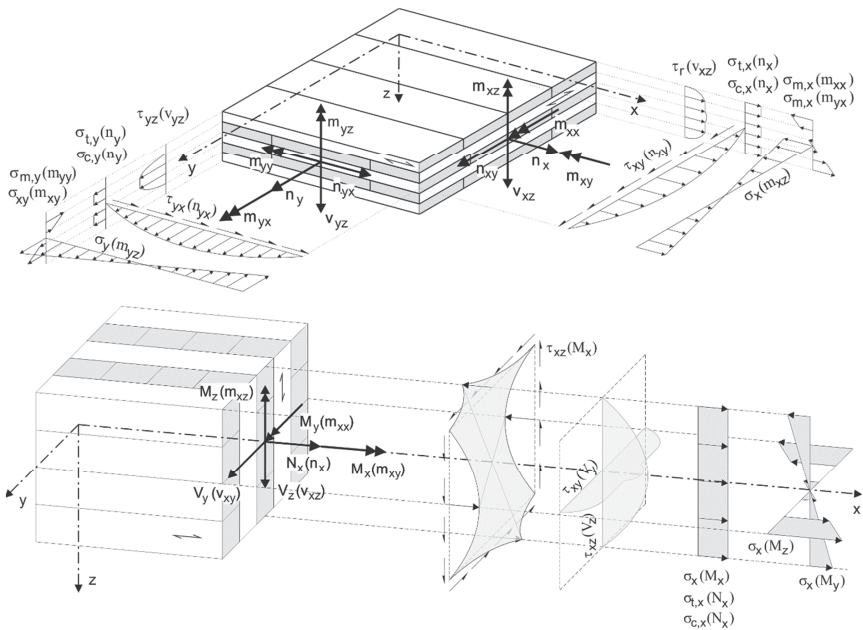
Chapter	General Information
Focus of work	<ul style="list-style-type: none">– Definition of generally valid terms and definitions– Consequent definition of CLT
Further steps To Do's	<ul style="list-style-type: none">– summary of state-of-knowledge (update) + proposal for possible regulation in design standards
Currently available Literature	<ul style="list-style-type: none">– TC250/SC5/PT1: Working draft; Version 2017_10_13 [42]– TC250/SC5/PT1: Background document; Version 2017_10_13 [43]– EN 13353– EN 16351– EN 1995-1-1– Z9.1-501
Suggestions for possible papers, scientific theses and further work	<ul style="list-style-type: none">– Definition of generally valid terms and definitions with a harmonisation between plate- and beam-like members– Definition of a general valid convention of axes between EC 5 and calculation software

Background: PT.1-3.1.2.11 cross laminated timber

[EN 16351] allows for the production of cross laminated timber comprising wood-based panel layers. Within EN 16351 it is stated that any joints between wood-based panels within a layer shall be taken as butt joints as no specific rules for the production of structural joints between wood-based panels are given in the standard.

The national technical approval of one company [Z 9.1-501] provides rules for the design of cross laminated timber comprising outer layers made from single- or multi-layered solid wood panels according to [EN 13353] or made from slabs cut from glulam made from laminated veneer lumber.

Though cross laminated timber comprising plywood or laminated veneer lumber is seldom used up to now, PT SC5.T1 recommends, not to exclude cross laminated timber from the scope of the future EN 1995-1-1 as the calculation models allow the design of such products.



Terms and Definitions

$A_{ef,x}$	effective cross section of the layers with grain direction parallel to the x-direction
$A_{ef,y}$	effective cross section of the layers with grain direction parallel to the y-direction
$(E \cdot I)_x$	bending stiffness in direction parallel to the grain of the outermost layers (x-direction)
$(E \cdot I)_y$	bending stiffness in direction perpendicular to the grain of the outermost layers (y-direction) per one meter width
E_{05}	5 %-quantile of modulus of elasticity
E_{mean}	mean modulus of elasticity
$E_{x,mean}$	mean modulus of elasticity parallel to the grain of the outermost layers (x-direction)
$E_{y,mean}$	mean modulus of elasticity perpendicular to the grain of the outermost layers (y-direction)
$E_{z,mean}$	mean modulus of elasticity perpendicular to the plane (z-direction)
$E_{0,l,mean}$	mean modulus of elasticity parallel to the grain of a lamination
$E_{90,lay,mean}$	mean modulus of elasticity perpendicular to the grain of a layer
F	force
$F_{ax, Rd}$	design axial load-bearing capacity of a screw
F_0	vertical load of a walking person
G_{05}	5 %-quantile of shear modulus
$G_{l,mean}$	mean shear modulus of a lamination
G_{mean}	mean shear modulus
$G_{r,mean}$	mean rolling shear modulus
$G_{tor,mean}$	mean torsional shear modulus
$G_{xy,mean}$	mean shear modulus in plane
$G_{xz,mean}$	mean shear modulus out of plane
$G_{yx,mean}$	mean shear modulus in plane
$G_{yz,mean}$	mean shear modulus out of plane
I_{tor}	torsional moment of inertia
M^*	modal mass
$V_{xy,d}$	design shear force in the direction of the y-axis acting at a cross section perpendicular to the x-axis

Latin lower case letters

a	acceleration
a_{req}	required root mean square acceleration
a_1	spacing parallel to the grain
a_2	spacing perpendicular to the grain
$a_{z,ef}$	effective spacing perpendicular to the grain
$f_{c,x,k}$	characteristic compression strength parallel to the grain of the outermost layers (x-direction)
$f_{c,y,k}$	characteristic compression strength perpendicular to the grain of the outermost layers (y-direction)

$f_{c,z,d}$	design compression strength perpendicular to the plane (z-direction)
$f_{m,edge,x,k}$	characteristic edgewise bending strength parallel to the grain of the outermost layers (x-direction)
$f_{m,edge,y,k}$	characteristic edgewise bending strength perpendicular to the grain of the outermost layers (y-direction)
$f_{m,l,k}$	characteristic edgewise bending strength parallel to the grain of laminations
$f_{m,x,k}$	characteristic bending strength parallel to the grain of the outermost layers (x-direction)
$f_{m,y,k}$	characteristic bending strength perpendicular to the grain of the outermost layers (y-direction)
f_{req}	required fundamental bending frequency
$f_{r,d}$	design rolling shear strength
$f_{r,k}$	characteristic rolling shear strength
$\overline{f_{r,ref,d}}$	design load-bearing capacity of the reinforced cross laminated timber member under shear stress
$\overline{f_{rd}}$	design value of rolling shear strength for local load introductions
$f_{t,x,k}$	characteristic tension strength parallel to the grain of the outermost layers (x-direction)
$f_{t,y,k}$	characteristic tension strength perpendicular to the grain of the outermost layers (y-direction)
$f_{t,z,k}$	characteristic tension strength perpendicular to the plane (z-direction)
$f_{tor,node,d}$	design torsional shear strength of the glued area of crosswise bonded laminations
$f_{tor,node,k}$	characteristic torsional shear strength of the glued area of crosswise bonded laminations
$f_{t,0,l,k}$	characteristic tension strength parallel to the grain of a lamination
$f_{v,k}$	characteristic shear strength out of plane
$f_{v,xy,gross,k}$	characteristic shear strength in plane related to the gross cross section
$f_{v,xy,k}; f_{v,yx,k}$	characteristic shear strength in plane
$f_{v,yx,gross,k}$	characteristic shear strength in plane related to the gross cross section
f_i	fundamental bending frequency
h	height
h_{ef}	effective height
h_{slam}	overall height of a cross laminated timber member
h_1	height of a notch
$k_{c,90,xlam}$	factor taking into account the load configuration and the layup of the cross laminated timber element
k_{cr}	factor taking into account the effects of cracks
k_{def}	deformation modification factor for service classes
$k_{e,1}$	factor for the fundamental bending frequency of a two-span floor
k_l	factor taking into account the possibility of stress dispersion in the direction of the length
k_{ls}	factor taking into account the load application
k_{mod}	strength modification factor for service classes and load-duration classes
$k_{m,loc}$	factor considering the effects of local stress concentration
k_n	factor for the determination of the reduction factor k_v for notches
$k_{r,90}$	factor to account for stress interaction with compression perpendicular to the grain

$k_{r,pu}$	factor to account for the non-linear behaviour
k_{sys}	system factor
$k_{sys,x}$	system factor for edgewise bending taking into account the number of layers with grain parallel to the x-axis
$k_{sys,y}$	system factor for edgewise bending taking into account the height of the cross laminated timber
k_w	factor taking into account the possibility of stress dispersion in the direction of the width
l	length or span
l_{dis}	dispersion length
l_{ef}	effective length
l_1	distance between the centre of a support and the corner of a notch
m	mass per unit area
n_{bond}	number of bondlines between orthogonally bonded adjacent layers
n_l	number of laminations in a layer having their grain parallel to the x-direction
n_x	number of layers in a cross laminated timber member with grain parallel to x-direction
n_y	number of fastener lines perpendicular to the grain of the outermost layers (y-direction)
t	thickness
t_{xlam}	overall thickness of the cross laminated timber
t_l	thickness of a lamination
$t_{l,max}$	maximum thickness of a lamination within a cross laminated timber layup
w	width
$w_{A,x}$	width of contact area parallel to the grain of the outermost layers (x-direction)
$w_{A,y}$	width of contact area perpendicular to the grain of the outermost layers (x-direction)
w_{dis}	dispersion width
w_{ef}	effective width
$w_{ef,B}$	effective width for the determination of the modal mass
$w_{ef,x}$	effective width parallel to the grain of the outermost layers (x-direction)
$w_{ef,y}$	effective width perpendicular to the grain of the outermost layers (x-direction)
w_l	width of a lamination
$w_{l,mean}$	mean width of laminations
$w_{l,x}$	lamination width in x-direction
$w_{l,y}$	lamination width in y-direction
w_{req}	maximum deflection for the stiffness criteria
w_{xlam}	overall width of the cross laminated timber
w_{1kN}	maximum deflection due to a vertical single load of 1 kN
x	x-axis
y	y-axis
z	z-axis

Greek lower case letters

α	Fourier coefficient depending on the fundamental frequency
β_c	factor for members within the straightness limits defined in Section 10
γ_M	partial safety factor for materials
ζ	maximum modal damping ratio for cross laminated timber
ρ_k	characteristic density
$\rho_{k,l}$	characteristic density of a lamination
$\rho_{l,mean}$	mean density of a lamination
ρ_{mean}	mean density
$\sigma_{c,z,d}$	design compression stress perpendicular to the plane
$\tau_{r,d}$	design rolling shear stress
$\tau_{tor,node,d}$	design shear stress of a glued area of crosswise bonded laminations
$\tau_{v,xy,d}; \tau_{v,yx,d}$	design shear stress in plane related to the effective cross section

2 Basis of Design

2.4 Verification by the Partial Factor Method

2.4.1 Design values of material properties

Chapter	Design values of material properties
Focus of work	– Investigation of safety factor for CLT: suggestion 1.25
Further steps To Do's	– summary of state-of-knowledge (update) + proposal for possible regulation in design standards
Currently available Literature	<ul style="list-style-type: none"> – TC250/SC5/PT1: Working draft; Version 2017_10_13 [42] – TC250/SC5/PT1: Background document; Version 2017_10_13 [43] – National approvals from Germany: Z9.1-482, Z9.1-501, Z9.1-534, Z9.1-555, Z9.1-559, Z9.1-576, Z9.1-680, Z9.1-721, Z9.1-793 – Brandner (2016) [28] – DIN EN 1995-1-1/NA – EN 14080, EN 14081-1 and EN 1995-1-1 – ETAs: 06/0009, 09/0138, 09/0036, 09/0211, 11/0189, 11/0210, 12/0327, 14/0349, 16/0055 – ON B 1995-1-1 Annex K – Schickhofer (2015) [155] – Unterwieser (2013b) [175]
Suggestions for possible papers, scientific theses and further work	<ul style="list-style-type: none"> – summary of available test data and statistics, with focus on variabilities (within and between batches as well as between CLT producers / productions), at least of all design relevant product properties is recommended; this to be able to quantify the partial safety factor for CLT in a broader context – partial safety factor has to cover also model uncertainties; however, current design practice in EC 5 does not consider adjustment of structural elements to climatic conditions in service class (SC) 1 & 2; for ease of use for the designers also no differentiation is made in respect to the properties individual sensitivity to moisture; it is required that dimensions, load configurations other than tested or considered as basis for the product properties are treated in

	<p>a consistent and complete way; in context to CLT, in particular size and volume effects as well as system effects are still missing or only regulated on a conservative and / or weak theoretical and / or experimental basis; there is need for action.</p> <ul style="list-style-type: none"> - For CLT layups comprising wood-based panels featuring γ_M-factors other than proposed for CLT, regulations on how the γ_M shall be derived are missing.
--	---

Background: Table 2.3 – Recommended partial factors γ_M for material properties and resistances

There are several reasons for identical γ_M -factors for cross laminated timber according to [EN 16351] and glued laminated timber according to [EN 14080]:

- Both, glued laminated timber and cross laminated timber made from timber layers, are made of boards / laminations from coniferous species or poplar, strength graded according to [EN 14081-1], having the same range of dimensions and moisture content and being classified to the same strength classes.
- Provisions for preservative treatment, if any, are identical.
- For the production of glulam and cross laminated timber the same adhesive families, verified by the same set of test standards and fulfilling the same requirements, are used.
- The provisions for the minimum production requirements are almost identical for comparable components of both products.
- The system of assessment and verification of constancy of performance is the same for both products and the number of specimens to be tested within Type Testing (TT) and Factory Production Control (FPC) is almost identical for comparable components.
- For tests in bending out of plane and tension or compression in plane the number of laminations and the overall reference cross sectional sizes are the same for glulam and cross laminated timber: In Schickhofer, G., Bauer, H. and Thiel, A. [Schickhofer et al., 2015] and Brandner, R. et al. [Brandner et al., 2016] a reference cross section for cross laminated timber to be used for tests in bending out of plane and tension or compression in plane is given, see Figure BI.1. This reference cross section has the same overall sizes as the reference cross section for glued laminated timber according to [EN 14080:2013] and approximately the same number of laminations with

grain parallel to the span of the specimens.

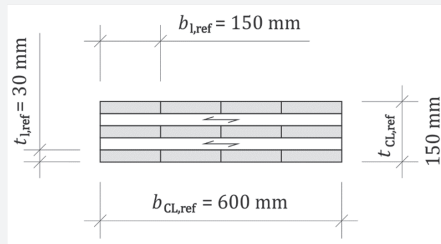


Figure BI.1: Reference cross section for cross laminated timber according to [Schickhofer et al., 2015]

The degree of equivalence allows concluding that the same partial safety factor for glued laminated timber and cross laminated timber made of timber layers could be used. Different National Annexes, see e.g. [ÖNORM B1995-1-1] and [DIN EN 1995-1-1/NA] already provide such γ_M -factors for cross laminated timber.

Wood-based panels allowed for the production of cross laminated timber (structural plywood, LVL, single- and multi-layered solid wood panels) are assigned to γ_M -factors which are less than or equal to the γ_M -factor of structural glued timber products such as cross laminated timber. Therefore γ_M -factors for cross laminated timber solely produced from timber layers should be identical with γ_M -factors for cross laminated timber comprising wood-based panel layers.

PT SC5.T1 proposes to apply the γ_M -factors for glued laminated timber for both, cross laminated timber solely build up from timber layers and cross laminated timber comprising wood-based panel layers according to [EN 16351].

3 Material Properties

3.1 General

3.1.3 Strength modification factors for service classes and load-duration classes

Chapter	k_{mod} -factors
Focus of work	– literature research for a binding statement on k_{mod}
Further steps To Do's	– summary of state-of-knowledge (update) – proposal for possible regulation in design standards
Currently available Literature	<ul style="list-style-type: none"> – TC250/SC5/PT1: Working draft; Version 2017_10_13 [42] – TC250/SC5/PT1: Background document; Version 2017_10_13 [43] – National approvals from Germany: Z9.1-482, Z9.1-501, Z9.1-534, Z9.1-555, Z9.1-559, Z9.1-576, Z9.1-680, Z9.1-721, Z9.1-793 – DIN EN 1995-1-1/NA – EN 1995-1-1 – ETA documents: 06/0009, 09/0138, 09/0036, 09/0211, 11/0189, 11/0210, 12/0327, 14/0349, 16/0055 – ON B 1995-1-1 Annex K – Unterwieser (2013b) [175]
Suggestions for possible papers, scientific theses and further work	<ul style="list-style-type: none"> – currently proposed k_{mod}-factors are argued by the circumstance that CLT is made of sawn timber, equally to solid timber and glulam; therefore, the same k_{mod}-factors, as harmonized for these products, are proposed for CLT; in respect to heterogeneous CLT layups, e.g. by using wood-based panels as substitute for some layers within CLT, like OSB, a note addressing the necessity to adjust the k_{mod} of such CLT if layers of material with k_{mod}-factors other than regulated currently for solid timber, glulam, solid wood-based panels and LVL should be added; an approach for calculating a k_{mod}-factor for CLT composed of layers featuring different k_{mod}-factors should be added. – As stated above, the same k_{mod}-factors, as harmonized for sawn timber and glulam products, are proposed for CLT. However, in several loading situations such as out-of-plane actions, CLT layers are subjected to rolling shear stresses. Such stresses rarely appear in sawn timber and glulam

products; thus they are not regarded in the regulation of k_{mod} . Due to the fact that timber is sensitive under rolling shear, one could argue that duration of load effects, beside influences from moisture covered via k_{mod} , are more pronounced in this loading situation as compared to others. Thus, experimental investigations should address this topic in the future, noting also that in an older report of 1987 (“Eurocode No. 5 – Common unified rules for timber structures”), k_{mod} -factors in dependency of the type of stress are prescribed. In respect to ease of use, instead of regulating k_{mod} -values in dependency of the type of stress there is also the possibility to adjust the characteristic properties as input parameters for the design, i.e. by regulating characteristic properties differently to outcomes from performance based tests. In doing so a clear and traceable regulation and quantification of made adjustments is highly suggested to have a transparent link between test and design properties.

- Investigations generally addressing the behaviour of CLT exposed to different and varying climatic conditions over a longer period of time would be of interest, not only for k_{mod} but also for adjustment of cross sections, i. e. calculation of net cross section or effective cross section accountable in the design of narrow face bonded CLT diaphragms in respect to gross in-plane shear, but also for quantification of limits in tests conducted within the quality control in CLT productions, e.g. delamination limits.
- currently, use of CLT for structural purposes is restricted to SC 1 & SC 2; however, in respect to possible future developments of new CLT products and in particular of new adhesive systems with the potential to enable the use of CLT also in SC 3, it is recommended not to exclude a potential use of CLT in SC 3 as far as all general requirements on building products used for structural purposes can be fulfilled → a note could be probably added in EC 5 which addresses this aspect, e.g. *“Restriction of CLT to be used only in SC 1 and SC 2 are valid as long as the safe use of CLT as structural building product in SC 3 has not been approved.”*

Background: Table 3.1 – k_{mod} -factors for timber and wood-based materials

Cross laminated timber is typically used in service classes (SC) 1 and 2 according to EN 1995-1-1. This is also reflected in the scope of [EN 16351], which excludes the application in SC 3.

For moisture contents covered by SC 1 and 2 the influence of moisture content and load duration on the properties of cross laminated timber made from timber layers will be similar to the influence of moisture content and load duration on the properties of the layers.

Eurocode 5-1-1:2010 recommends identical k_{mod} -factors for solid timber, glued laminated timber, plywood and laminated veneer lumber. In existing National Annexes (e.g. [ÖNORM B 1995-1-1], [DIN EN 1995-1-1/NA]) identical values are also given for multi-layered solid wood panels and cross laminated timber.

PT SC5.T1 recommends, applying the k_{mod} -factors for solid timber, glued laminated timber, plywood and laminated veneer lumber also for cross laminated timber.

3.1.4 Deformation modification factors for service classes

Chapter	k_{def} -factors
Focus of work	– Reliability of the use of a single “global” k_{def} -factor at the CLT element level (investigations part of a short term scientific mission (STSM)).
Further steps To Do’s	– summary of state-of-knowledge (update) – proposal for possible regulation in design standards
Currently available Literature	<ul style="list-style-type: none"> – TC250/SC5/PT1: Working draft; Version 2017_10_13 [42] – TC250/SC5/PT1: Background document; Version 2017_10_13 [43] – Brandner et al. (2016) [28] – DIN EN 1995-1-1/NA and EN 1995-1-1 – ETAs: 06/0009, 08/0238, 09/0138, 09/0036, 09/0211, 11/0189, 11/0210, 11/0464, 12/0327, 14/0349, 16/0055 – Jöbstl, Schickhofer (2007) [108] – Nakajima et al. (2014) [133] – Niemz. (1993) [134] – ON B 1995-1-1 Annex K – Park et al. (2002) [141], Park et al. (2006) [142] – Pirvu, Karacabeyli (2014) [144]

- Thiel, Schickhofer (2010) [168]
- Unterwieser, Schickhofer (2013b) [175]

Short literature review

Wood is essentially orthotropic in nature. It has been observed that its creep effects are also dependent on the material axes of orthotropy [Niemz (1993)]. As expected, creep effects are much more pronounced in the radial-tangential plane (rolling shear) where wood is weaker (both in stiffness and strength) compared to the longitudinal-tangential and longitudinal-radial planes [Niemz (1993)]. Due to the characteristic laminar structure of CLT consisting of timber layers arranged crosswise at an angle of 90°, it becomes evident that all types of out-of-plane loading resulting in flexural deformations (i.e. simultaneous bending and shear deformations), cause (i) out-of-plane longitudinal shear stresses at longitudinal layers and (ii) rolling shear stresses at cross layers of a CLT section. Thus, they are affected by the aforementioned differential creep effects.

Also, it has been already shown [Thiel, Schickhofer (2010), Brandner et al. (2016)] that in most span to depth ratios employed in engineering practice, shear deformations (and especially rolling shear deformations) should not be neglected in the deflection evaluation of CLT elements loaded out-of-plane.

The modelling of creep deformations has received relatively small attention in the research community; as compared to other subjects such as rolling shear strength and in-plane shear behaviour. In [Park et al. (2002), (2006)] small beam-like cross laminated timber specimens made of Sugi have been experimentally and analytically investigated. The authors employed several creep deformation factors in the calculation of deflections, while all the specimens had the same length-to-thickness ratios. Much more recently, [Nakajima et al. (2014)] have reported some results of creep tests of cross laminated timber elements made of Japanese Cedar. Also [Pirvu, Karacabeyli (2014)] performed creep tests of cross laminated timber elements made of Canadian lumber and discussed the corresponding results. Before this contribution, [Jöbstl, Schickhofer (2007)] performed a comparative experimental examination of creep effects in simply supported CLT and glued laminated slabs made of spruce (strength class C24) under 4-point bending. By

	<p>comparing the experimentally obtained instantaneous and long-term deformations, they evaluated a "global" ("smeared") k_{def}-factor which can be applied as a single reduction factor for all stiffness properties of the CLT element. By exploiting the experimental results and employing the prescribed k_{def}-factor to reduce the bending and longitudinal shear stiffness properties, they also managed to calculate the k_{def}-factor of rolling shear deformations. By using the obtained value in parametric numerical analyses of CLT elements with 3 to 19 layers, they calculated "global" k_{def}-factors for such layups. In all of the aforementioned numerical and experimental results, single values of length-to-thickness ratios have been employed at each contribution.</p>
<p>Suggestions for possible papers, scientific theses and further work</p>	<p>Suggestions for further work:</p> <ul style="list-style-type: none"> – The knowledge base of the current background document to the new section on CLT in EC 5 is restricted to CLT elements loaded out-of-plane. However, the k_{def}-factor proposed for the chapter on CLT in the revised version of EC 5 is essentially applicable to all types of loading. Different k_{def}-factors based on the type of loading (in-plane and out-of-plane) are suggested in two ETAs, (ETA 08/0238, ETA 11/0464) the in-plane ones being smaller than the out-of-plane ones. This discrepancy has a sound physical basis: a significant portion of long term deformations are due to rolling shear which appears mostly on CLT panels loaded-out-of-plane. A note in the chapter on CLT in the revised version of EC 5 could be added addressing this issue. – The knowledge base of the current background document to the new chapter on CLT in the revised version of EC 5 is restricted to homogeneous CLT elements made of solid wood. It proposes the use of a single k_{def}-factor at the CLT element level. The determination and use of single k_{def}-factors even for heterogeneous CLT layups (which are within the scope of the new chapter on CLT in the revised version of EC 5), could be problematic. A note in the new chapter on CLT in the revised version of EC 5 could be added addressing this issue. <p>Suggestions for future research projects:</p> <ul style="list-style-type: none"> – STSM of Vasileios Tsipiras at Graz University of Technology approved by the core group of COST Action

	<p>FP1402 (topic: Investigation on the creep factor k_{def} for CLT elements loaded out-of-plane, taking into account CLT layup and lamination properties, date: 2018_03_18 to 2018_04_06):</p> <p>It is envisaged to check if a single k_{def}-factor to be applied for the whole CLT element is adequate to be employed or several k_{def}-factors for each deformation mode (longitudinal shear, rolling shear, etc.) should be used instead. The investigation will cover a broad range of CLT products currently used in engineering practice under both ULS and SLS design scenarios.</p> <ul style="list-style-type: none"> – Paper or other form of scientific publication to be published containing the findings of the aforementioned STSM. – In respect to possible future developments of new CLT products with the potential to enable the use of CLT also in SC 3 (see the previous section), meaningful would be an experimental campaign investigating the k_{def}-factor of CLT products in SC 3.
--	---

Background: Table 3.2 – k_{def} -factors for timber and wood-based materials

Related to the effects of changes of moisture content on the creep deformations of timber members subjected to stresses parallel to the grain the effects on timber members subjected to rolling shear stresses are reasonable higher. Jöbstl, R. et al. [Jöbstl et al., 2007] have determined k_{def} -factors depending on the number of layers. They state, that especially the assumed shear moduli have a major influence on the determined values. Jöbstl, R. et al. [Jöbstl et al., 2007] propose to apply k_{def} -factors for plywood taken from EN 1995-1-1:2010 for cross laminated timber having more than seven layers and to multiply those values by 1.1 if the number of layers is less than or equal to seven.

Some National Annexes already provide k_{def} -factors for cross laminated timber. According to the Austrian National Annex [ÖNORM B 1995-1-1] the same values as for plywood (0,8 for SC 1 and 1,0 for SC 2) shall apply whereas the German National Annex [DIN EN 1995-1-1/NA] states that the same values as for solid timber and glued laminated timber (0,6 for SC 1 and 0,8 for SC 2) can be applied.

The proposed k_{def} -factors from [Jöbstl et al., 2007] are up to 10 % higher than the values given in the Austrian National Annex [ÖNORM B 1995-1-1] but as already stated above values estimated according to [Jöbstl et al., 2007] will be different for different assumed shear moduli applied in the analysis of the test

results.

Designers would like to apply only a limited number of sets of k_{def} -factors in order to avoid a faulty choice of values.

Deformations can only be estimated due to e. g. the scatter of MOE values or varying moisture contents in use within one service class. A difference in the k_{def} -factors of 10 % will not significantly influence the correctness of the estimated deformations.

PT SC5.T1 therefore recommends applying the k_{def} -factors for plywood given in EN 1995-1-1:2010 also for cross laminated timber.

3.8 Cross Laminated Timber (CLT)

Chapter	Cross laminated timber – product properties & strength class system
Focus of work	<ul style="list-style-type: none"> – Basically, not the task of EN 1995-1-1 – Set of characteristic values – Size, volume and system effect factors (e.g. k_h, k_{size} and k_{sys}) for adjustment of CLT properties to the dimensions used for structural purposes, load configurations, stress distributions, layups and system actions in respect to the reference geometries and conditions used in testing and as basis for outlined characteristic CLT properties.
Further steps To Do's	<ul style="list-style-type: none"> – summary of state-of-knowledge (update) + proposal for possible regulations in design standards
Currently available Literature	<ul style="list-style-type: none"> – TC250/SC5/PT1: Working draft; Version 2017_10_13 [42] – TC250/SC5/PT1: Background document; Version 2017_10_13 [43] – Andreolli, Rigamonti, Tomasi (2014) [4] – National approvals from Germany: Z9.1-482, Z9.1-501, Z9.1-534, Z9.1-555, Z9.1-559, Z9.1-576, Z9.1-680, Z9.1-721, Z9.1-793 – Bejtka (2010) [10] – Blaß, Flaig (2014) [14] – Blaß, Görlacher (2002) [12] – Bogensperger, Augustin, Schickhofer (2011) [18] – Bogensperger, Moosbrugger, Schickhofer (2007) [19] – Bogensperger, Moosbrugger, Silly (2010) [20] – Bosl (2002) [24] – Brandner, Bogensperger, Schickhofer (2013) [25] – Brandner, Dietsch, Dröscher, Schulte-Wrede, Kreuzinger, Schickhofer, Winter (2015) [27] – Brandner, Schickhofer (2014) [29] – Brandner, Schickhofer (2008) [32] – Brandner, Schickhofer (2006) [31] – Brandner, Schickhofer (2014) [33]

- Bratulic (2013) [34]
- Ciampitti (2013) [45]
- Dröscher (2014) [53]
- EAD 13005-000304
- Ehrhart, Brandner, Schickhofer, Frangi (2015) [56]
- EN 14080
- EN 16351
- EN 1995-1-1
- EN 408
- ETAs: 06/0009, 09/0138, 09/0036, 09/0211, 11/0189, 11/0210, 12/0327, 14/0349, 16/0055
- Flaig (2013) [82]
- Flaig (2015) [84]
- Flaig, Blaß (2014)
- Görlacher (2002)
- Halili (2008) [94]
- Hasuni, Al-douri, Hamodi (2009) [99]
- Hirschmann (2011) [102]
- Jacobs (2005) [105]
- Jeitler (2004) [106]
- Jeitler, Brandner (2008) [107]
- Jöbstl, Bogensperger, Schickhofer (2006) [109]
- Jöbstl, Bogensperger, Schickhofer (2008) [110]
- Jöbstl, Bogensperger, Schickhofer, Jeitler (2004) [111]
- Kreuzinger, Sieder (2013) [122]
- Mestek (2011) [124]
- ON B 1995-1-1 Annex K
- Salzmann (2010) [151]
- Schickhofer, Bauer, Thiel (2015) [155]
- Serrano, Enquist (2010) [158]
- Silly (2014) [161]
- Silly, Thiel (2013) [162]
- Unterwieser, Schickhofer (2013a) [174]
- van der Put (2008) [177]
- Wallner (2004) [180]
- Watson, van Beerschoten, Smith, Pampanin, Buchanan,

	(2013) [183]
<p>Suggestions for possible papers, scientific theses and further work</p>	<p>Suggestions for further work:</p> <ul style="list-style-type: none"> – In PT.1-5.4, it is stated that: "For cross laminated timber having layups different to those described in PT.1(4) and PT.1(5) the properties of the cross laminated timber shall be derived from the layer properties by composite theory. For timber layers, system effects may be considered". This provision holds for both stiffness and strength properties. In PT.1-7.3.2, it is stated that: "The calculation model shall consider the influence of the layup e.g. thickness, material and orientation of layers, influence of gaps, grooves and lamination sizes, on the cross laminated timber properties". It is suggested to harmonize the section "Analysis of test results" of EN 16351 with the above provisions, especially in the case of CLT elements comprising wood-based panel layers (in PT.1-3.1.2.11, it is stated that cross laminated timber may be comprised from wood-based panel layers). <p>Suggestions for future research projects:</p> <ul style="list-style-type: none"> – Investigation of the model uncertainty of the bearing model for the bending strength of homogeneous CLT elements developed in Jöbstl, Bogensperger, Schickhofer [Jöbstl et al., 2006] and Brandner, Schickhofer [Brandner et al., 2006]. – Investigations on size, system and volume effects, considering also stress dispersion effects are suggested for all properties in order to adapt characteristic properties according to the relevant design cases / load configurations.

Table PT.1-5.3: Characteristic values of strength and elastic properties in N/mm² and density in kg/m³ for cross laminated timber comprising timber layers derived from the properties of the timber laminations¹⁾

Property		Symbol	Value	Example for cross laminated timber nominated class CL24 ²⁾
Bending strength	for bending moments m_{xx} or m_{yy} out of plane, see Figure PT.1-6.13	$f_{m,x,k}$ $f_{m,y,k}$	3 $f_{t,0,1,k}^{0.8}$	24.0
	for bending moments m_{yz} or m_{xz} in plane, see Figure PT.1-6.13	$f_{m,edge,x,k}$ $f_{m,edge,y,k}$	$f_{m,1,k}^{3)}$	20.5
Tension strength	in plane	$f_{t,x,k}^{4)}$ $f_{t,y,k}^{4)}$	1.2 $f_{t,0,1,k}$	16.0
	perpendicular to the plane	$f_{t,z,k}$	0.50	0.50
Compression strength	in plane	$f_{c,x,k}$ $f_{c,y,k}$	3 $f_{t,0,1,k}^{0.8}$	24.0
	perpendicular to the plane	$f_{c,z,k}$	3.00	3.00
Shear strength out of plane	longitudinal	$f_{v,k}$	3.50	3.50
	rolling shear	$f_{r,k}$	$\min \left\{ 0.2 + 0.3 \frac{w_1^{5)} }{t_1} \right\}$	0.80 ⁶⁾
Shear and torsional shear strength in plane	shear strength of the effective cross section	$f_{v,xy,k}$ $f_{v,yx,k}$	5.50	5.50
	torsional shear strength of the glued area of crosswise bonded laminations	$f_{tor,node,k}$	2.50	2.50
	rolling shear	$f_{r,k}$	as for shear strength out of plane	
Modulus of Elasticity	loaded in plane	$E_{x,mean}$ $E_{y,mean}$	1.05 $E_{0,1,mean}^{7)}$	11,600 ⁷⁾
	loaded perpendicular to the plane	$E_{z,mean}$	450 ⁷⁾	450 ⁷⁾
Shear Modulus	loaded out of plane	$G_{xz,mean}$ $G_{yz,mean}$	$G_{1,mean}^{7)}$	650 ⁷⁾

	loaded in plane	$G_{xy,mean}$ $G_{yx,mean}$ $G_{tor,mean}$	$\min \begin{cases} \frac{650^{5)7)}}{1 + 2.6 \left(\frac{t_1}{w_1} \right)^{1.2}} \\ 450 \end{cases}$	$450^{6)7)}$
	rolling shear	$G_{r,mean}$	$\min \begin{cases} 30 + 17.5 \left(\frac{w_1}{t_1} \right)^{5)7)} \\ 100 \end{cases}$	$65,0^{6)7)}$
Density		ρ_k	1.1 $\rho_{l,k}^{8)}$	$385^{8)}$
		ρ_{mean}	$\rho_{l,mean}$	420

- 1) The reference cross section is five layered and has a width to thickness ratio of $w_{xlam} / t_{xlam} = 600 \text{ mm} / 150 \text{ mm}$ with the exception of edgewise bending strength, for which reference is made to a three layered cross laminated timber beam with a height of $t_{xlam} = 150 \text{ mm}$ and only one lamination with grain direction parallel to the respective stress.
- 2) Cross laminated timber made of timber layers made of laminations assigned to strength class T14 according to EN 338, having a characteristic bending strength parallel to grain $f_{m,l,k} \geq 20.5 \text{ N/mm}^2$.
- 3) For cross laminated timber made from laminations having a characteristic tension strength parallel to grain $f_{t,0,l,k} \geq 14 \text{ N/mm}^2$. $f_{m,l,k}$ is the characteristic edgewise bending strength according to EN 338.
- 4) This value takes into account a system factor for at least 15 laminations loaded in x-direction or y-direction, respectively.
- 5) Where w_1 is either the width of the lamination or the distance between the edge and a groove or spacing between grooves within the lamination and t_1 is the thickness of the lamination. The minimum nominal ratio of w_1 / t_1 can be taken from the Declaration of Performance.
- 6) For a ratio $w_1 / t_1 \geq 2$.
- 7) The 5 %-quantile of the modulus of elasticity and the shear modulus are equal to 5 / 6 of the mean values: $E_{05} = E_{mean} \cdot 5/6$ and $G_{05} = G_{mean} \cdot 5 / 6$.
- 8) For connections in only one lamination of a layer the characteristic density of the lamination $\rho_{l,k}$ shall be applied.

Background: PT.1(4)

Determination of properties of homogeneous cross laminated timber from layer properties

According to [EN 16351] cross laminated timber properties shall be declared as geometrical data and layer properties which may be taken from the product standards of the layer materials or may be determined by full scale testing of cross laminated timber. European technical assessments on the basis of the European Assessment document [EAD 13005-000304] are based on full scale

testing. Table PT.1-5.3 is the link between the declaration of layer properties according to EN 16351 or an ETA and cross laminated timber properties applicable for designs according to EN 1995-1-1.

Background: PT.1(5)

Determination of properties of combined cross laminated timber from layer properties

Comparative calculations on the basis of the composite theory have been done with symmetrically build up inhomogeneous cross laminated timber plates having up to seven layers. It can be shown, that manufacturing only the outermost layer from laminations of a higher strength class allows to determine the bending strength, the tension strength parallel to the grain and the compression strength parallel to the grain in x-direction of the cross laminated timber on the basis of the lamination properties of the outermost layers. This is also true for the y-direction, if also the outermost timber layers with grain parallel to that direction are assigned to a higher strength class.

The same applies for cross laminated timber diaphragms and beams without a limitation of the number of layers.

Background: Table PT.1-5.3

Reference cross section

As already stated in the background information on the amendment to EN 1995-1-1, Table 2.3, the reference cross section for cross laminated timber shown in Figure BI.1 has the same overall size and a slightly lower number of interacting laminations ($n = 12$ for cross laminated timber compared to $n = 15$ for glulam) with almost identical lamination properties as the reference cross section for glulam according to EN 14080:2013.

For edgewise bending strength the reference cross section is smaller. A conservative value referring to a three-layered cross laminated timber with only one layer having grain parallel to the x-axis and related to a beam height of 150 mm is given in Table PT.1-5.3. This value can be multiplied by a $k_{sys,x}$ -factor for a higher number of layers with grain parallel to the grain and by a $k_{sys,y}$ -factor for the positive height effect for cross laminated timber subjected to edgewise bending, see PT.1-5.4, PT.1(7).

The cross laminated timber properties are also affected by the layup, i. e. the ratio of layer-thicknesses in x- and y-direction.

Provisions for tests

Full scale tests for the determination of strength, stiffness and density values are typically done based on modified test configurations according to [EN 408]. Such modifications are e.g. laid down in the European Assessment document [EAD 13005-000304], being the basis for a number of European Technical Approvals & Assessments, e.g. [ETA-06/0009], [ETA-09/0036], [ETA-16/0055], [ETA-06/0138], [ETA-11/0189], [ETA-11/0210], [ETA-09/0211] [ETA-14/0349], [ETA-12/0327], in national technical approvals, e.g. [Z 9.1-482], [Z 9.1-501], [Z 9.1-534], [Z 9.1-555], [Z 9.1-559], [Z 9.1-576], [Z 9.1-680], [Z 9.1-721], [Z 9.1-793], or in the future harmonised product standard [EN 16351].

Further test configurations have been investigated in research works. An overview of test configurations for some properties is given in Unterwieser, H. and Schickhofer, G. [Unterwieser et al., 2013]. Further test provisions can be taken from literature cited in the background information of the respective property.

Strength class and coefficient of variation (COV) of laminations

Almost all cross laminated timber produced in Europe is made of laminations assigned to lamination strength class T14 (the class name indicates a characteristic tension strength parallel to the grain of $f_{t,0,1,k} = 14 \text{ N/mm}^2$, see EN 338). Brandner, R. and Schickhofer, G. [Brandner et al., 2006], [Brandner et al., 2008], Jöbstl, R., Bogensperger, T. and Schickhofer, G. [Jöbstl et al., 2006] and Jeitler, G. and Brandner, R. [Brandner et al., 2008] showed, that because of different grading procedures (visual or machine grading; grading into one or more strength classes) the coefficient of variation (COV) of the characteristic tension strength parallel to the grain of the laminations can vary significantly. A higher $\text{COV}(f_{t,0,1,k})$ results in a higher capability of stress (re)distribution in parallel systems, also called “homogenization”. Unterwieser, H. and Schickhofer, G. [Unterwieser et al., 2013] therefore propose to distinguish between two strength classes for cross laminated timber both made from laminations of class T14 but having different $\text{COV}(f_{t,0,1,k})$.

EN 16351:2015 does not require the declaration of $\text{COV}(f_{t,0,1,k})$. A continuous verification of the $\text{COV}(f_{t,0,1,k})$ is extensive. It might be subject to significant changes during production caused by changes of the timber source, the number of strength classes to which the graded material is assigned and, in the case of laminations graded at the sawmill, the grading procedure (visual or machine grading). PT SC5.T1 proposes to give only equations for the determination of cross laminated timber properties from lamination properties based on a conservative $\text{COV}(f_{t,0,1,k}) = 25 \pm 5 \%$. Appropriate equations for a

$\text{COV}(f_{t,0,1,k}) = 35 \pm 5 \%$ may be taken from [Unterswieser et al., 2013].

Bending strength for bending moments m_x or m_y out of plane

Failures in bending out of plane starts with failures of laminations in tension. Due to the large difference between the characteristic tension strengths parallel and perpendicular to the grain and due to the presence of gaps, grooves and/or cracks the cross layers do not contribute to the bending strengths out of plane. This is also true for the bending and tension strengths in plane.

The bending strength of cross laminated timber subjected to bending moments m_x or m_y out of plane depends on the characteristic tension strength of the laminations, its coefficient of variation and the number of laminations acting as a parallel system. On the basis of tests with cross laminated timber and glulam and simulations Jöbstl, R., Bogensperger, T.; Schickhofer, G. [Jöbstl et al., 2006] and Brandner, R.; Schickhofer, G. [Brandner et al., 2006] developed equation (BI.1):

$$f_{m,x,k} = k_{\text{sys},m} k_{\text{xlam/GL}} k_{h_{\text{CLT}}} k_{\text{CV}} f_{t,0,1,k}^{0.8} \quad (\text{BI.1})$$

where:

- $f_{m,x,k}$ is the characteristic bending strength of the cross laminated timber;
- $f_{t,0,1,k}$ is the characteristic tension parallel to grain strength of the laminations;
- k_{CV} is a factor considering the coefficient of variation of the tension strength of the laminations ($\text{COV}(f_{t,0,1,k})$);
- $k_{h_{\text{CLT}}}$ is a factor considering the height effect;
- $k_{\text{sys},m}$ is a factor considering the number of laminations acting parallel in the outer layer with grain in x-direction of a cross laminated timber member subjected to bending;
- $k_{\text{xlam/GL}}$ is a factor considering the ability of transverse load distribution by cross layers;

Equation (BI.1) applies for the effective cross sections stressed parallel to the grain.

The factor $k_{\text{sys},m}$ taking into account the number of laminations acting parallel has been derived for floors made of glulam slabs. The factor $k_{\text{xlam/GL}}$ gives the relation between the homogenization (the lamination effect) in cross laminated timber compared to glulam. Jöbstl et al. [Jöbstl et al., 2006] report on a reduced homogenisation for cross laminated timber. Therefore, a $k_{\text{xlam/GL}} = 0.94$ is given. For a given reference cross section as shown up in Figure BI.1, a

$\text{COV}(f_{t,0,1,k}) = 25 \pm 5 \%$ and a lamination strength class T14 equation (BI.1) changes to (BI.2):

$$f_{m,x,k} = 3 \cdot f_{t,0,1,k}^{0.8} = 3 \cdot 14^{0.8} = 24.8 \approx 24 \text{ N/mm}^2 \quad (\text{BI. 2})$$

For a $\text{COV}(f_{t,0,1,k}) = 35 \pm 5 \%$ equation (BI. 3) would apply:

$$f_{m,x,k} = 3.5 \cdot f_{t,0,1,k}^{0.8} = 3.5 \cdot 14^{0.8} = 28.9 \text{ N/mm}^2 \quad (\text{BI. 3})$$

In the case of two- or multi-span systems, the increase of stresses at the supports is compensated by an increase of strength due to the interaction with compression perpendicular to the grain stresses.

The modulus of elasticity parallel to the grain of cross laminated timber is directly linked to the modulus of elasticity of its layer materials. The provisions for glulam according to EN 14080:2013 can also be applied for cross laminated timber.

Height factor for cross laminated timber subjected to bending out of plane

PT SC5.T1 is not aware of publications on height factors for cross laminated timber or of national technical rules for such height factors.

Due to the relatively small number of layers (compared to e.g. the high number of laminations in glulam) in almost all cases bending failure of cross laminated timber plates is caused by brittle failure in tension of the outermost layer. Therefore, PT SC5.T1 omits to introduce a k_h -factor for cross laminated timber plates.

Bending strength for bending moments m_z in plane

Beitka reports on cross laminated timber used as beam elements [Bjetka., 2010]. According to Flaig, M. [Bejtka, 2010], [Blaß et al., 2014] and Blaß, H.J.; Flaig, M., [Flaig, 2013], [Flaig et al., 2014] the bending strength in plane of cross laminated timber having a height of $h_{CL} = 600 \text{ mm}$ made from laminations graded in edgewise bending can approximately be taken as the bending strength of a homogeneous glued laminated timber made from such laminations according to [EN 14080].

In order to prevent the compulsory application of reduction factors, a conservative edgewise bending strength related to a cross laminated timber beam with only one layer with grain parallel to the span direction and a beam height of 150 mm is proposed by PT SC5.T1. Increasing factors are given in PT.1-5.4 PT.1(7).

Tension strength in plane

As the bending strength out of plane, the tension strength in plane depends on the characteristic tension parallel to grain strength of the laminations, its coefficient of variation and the number of laminations acting as a parallel system.

Up to now no sufficient theoretical or experimental results exist. Therefore, no factor taking into account a possible load distribution as for the bending strengths out of plane can be given. On the basis of factors $k_{\text{sys,t,0/CV}}$, describing the system effect taking into account the coefficient of variation of the tension parallel to grain strength of the laminations, $\text{COV}(f_{t,0,1,k})$, which have been determined by Brandner, R. and Schickhofer, G. [Brandner et al., 2006], [Brandner et al., 2008], Jöbstl, R., Bogensperger, T. and Schickhofer, G. [Jöbstl et al., 2006] and Jeitler, G. and Brandner, R. [Brandner et al., 2008], Schickhofer, G. Bauer, H. and Thiel, A. [Schickhofer et al., 2015] propose Eq. (BI.4):

$$f_{t,x,k} = k_{\text{sys,t,0/CV}} \cdot f_{t,0,1,k} \quad (\text{BI.4})$$

where:

$f_{t,x,k}$ is the characteristic tension strength of the cross laminated timber in x-direction;

$f_{t,0,1,k}$ is the characteristic tension parallel to grain strength of the laminations;

$k_{\text{sys,t,0/CV}}$ is a factor considering the number of laminations acting parallel in a glulam or glued solid timber member subjected to tension parallel to the grain and the coefficient of variation of the tension parallel to grain strength of the laminations ($\text{COV}(f_{t,0,1,k})$).

Eq. (BI.4) applies for the effective cross sections stressed parallel to the grain.

For $\text{COV}(f_{t,0,1,k}) = 25 \pm 5 \%$ Eq. (BI.5) and for $\text{COV}(f_{t,0,1,k}) = 35 \pm 5 \%$ Eq. (BI.6) applies.

$$k_{\text{sys,t,0/CV}} = \min \begin{cases} 0.075 \cdot \ln(n_{1,x}) + 1 \\ 1.2 \end{cases} \quad \text{for } \text{COV}(f_{t,0,1,k}) = 25 \pm 5 \% \text{ and } n_{1,x} \leq 15 \quad (\text{BI. 5})$$

$$k_{\text{sys,t,0/CV}} = \min \begin{cases} 0.130 \cdot \ln(n_{1,x}) + 1 \\ 1.35 \end{cases} \quad \text{for } \text{COV}(f_{t,0,1,k}) = 35 \pm 5 \% \text{ and } n_{1,x} \leq 15 \quad (\text{BI. 6})$$

where:

$n_{l,x}$ is the number of laminations acting as a parallel system.

Within the reference cross section according to Figure BI.1 $n_x = 12$. For a lamination strength class T14 and a $\text{COV}(f_{t,0,l,k}) = 25 \pm 5 \%$ Eq. (BI.4) gives:

$$f_{t,x,k} = 1.186 \cdot f_{t,0,l,k} = 1.186 \cdot 14 = 16.6 \approx 16 \text{ N/mm}^2 \quad (\text{BI.7})$$

For a $\text{COV}(f_{t,0,l,k}) = 35 \pm 5 \%$ Eq. (BI.4) results in:

$$f_{t,x,k} = 1.323 \cdot f_{t,0,l,k} = 1.323 \cdot 14 = 18.5 \text{ N/mm}^2 \quad (\text{BI.8})$$

Tension strength perpendicular to the plane

One European Technical approval [ETA-16/0055] deals with curved cross laminated timber members. PT SC5.T1 is not aware of scientific reports on tension strength perpendicular to the plane for cross laminated timber.

EN 16351:2013 does not give specific test provisions but tests should be done with specimens similar to those for glulam according to [EN 408]. PT SC5.T1 proposes to choose the same characteristic tension strength perpendicular to the plane (grain) as for glulam according to EN 14080:2013. Attention should be given to the fact, that PT SC5.T1 will neither propose to apply EN 1995-1-1, 6.1.3 on curved cross laminated timber members subjected to bending nor propose any distribution factors and equations for volume effects needed for such a design.

Compression strength in plane

As for the bending strength out of plane, the compression strength in plane will depend on the characteristic compression strength of the laminations, the coefficient of variation and the number of laminations acting as a parallel system. The cross layers will act as a load distributing system but beside this will not significantly contribute to the load transfer.

As for glulam it can be assumed that full scale tests according to EN 408 with cross laminated timber subjected to compression parallel to the grain will lead to higher strength values than for cross laminated timber subjected to bending out of plane. But as for glulam it should be taken into account that test conditions according to EN 408 only reflect Service Class 1 conditions according to EN 1995-1-1. A higher moisture content will have a much higher effect on the compression strength compared to the bending strength out of plane. As long as EN 1995-1-1 gives only one k_{mod} -factor for both, Service class 1 and 2, characteristic compression strengths in plane determined for SC 1

conditions need to be reduced.

As PT SC5.T1 is not aware of specific research it proposes to fix the compression parallel to the plane values for cross laminated timber as for glulam, being equivalent to the bending strengths out of plane.

Compression strength and modulus of elasticity perpendicular to the plane

Halili, Y. [Halili, 2008], Bratulic, K. [Bratulic 2013], Hasuni, H.; Al-douri, K.; Hamodi, M. [Hasuni et al., 2009], Salzmann, C. [Salzmann, 2010], Serrano, E.; Enquist, B. [Serrano et al., 2010], Bogensperger, T.; Augustin, M., Schickhofer, G. [Bogensperger et al., 2011], Ciampitti, A. [Ciampitti, 2013] and Brandner, R.; Schickhofer, G. [Brandner et al., 2014] performed compression perpendicular to the plane tests mostly with cross laminated timber made from T14 laminations.

Brandner, R. and Schickhofer, G. [Brandner et al., 2014] showed that $f_{c,z,k} = 3 \text{ N/mm}^2$ derived from prism specimens according to EN 408 can be adjusted to any kind of load configuration using a modified stress dispersion model according to van der Put, TACM [van der Put, 2008], see also the background information on EN 1995-1-1, PT.1-11.2.5.4.

Characteristic values for compression strength perpendicular to the grain for cross laminated timber made from laminations other than T14 lamination will not significantly differ from those determined for cross laminated timber made of T14 laminations. PT SC5.T1 therefore proposes to fix a value of $f_{c,z,k} = 3 \text{ N/mm}^2$ for any lamination strength class.

For cross laminated timber comprising wood-based panel layers, a detailed analysis of the compression stresses in any layer taking into account the characteristic strength values perpendicular to the grain of the layers is needed, if higher loads are to be transferred.

Halili, Y. [Halili, 2008] reports that modulus of elasticity perpendicular to grain of cross laminated timber is higher compared to glulam due to a restraining effect caused by the cross layers. This is reflected by the proposed value given in Table PT.1-5.3, which is 50 % higher than the corresponding value given in EN 14080:2013.

Longitudinal shear strength and shear modulus (shear out of plane)

For shear stresses parallel to the grain shear strength values according to EN 14080:2013 can be applied.

Rolling shear strength and rolling shear modulus (shear out of plane)

In cross layers a rolling shear failure can occur. As shown e.g. by Görlacher, R. [Görlacher, 2002], Blaß, H. and Görlacher, R. [Blaß et al., 2002], Wallner, G.

[Wallner, 2004], Jacobs, A. [Jacobs, 2005], Mestek, P. [Mestek, 2011], Silly, G. and Thiel, A. [Silly et al., 2013] and Ehrhart, T.; Brandner, R.; Schickhofer, G.; Frangi, A. [Ehrhart et al., 2015a] rolling shear strength values are much lower than longitudinal shear strength values and significantly depending on the ratio of lamination width to lamination thickness w_1 / t_1 . Grooves in laminations need to be taken as lamination edges.

The proposed equation given in Table PT.1-5.3 is taken from Ehrhart, T.; Brandner, R.; Schickhofer, G.; Frangi, A. [Ehrhart et al., 2015a] and is valid for ratios $w_1 / t_1 \leq 4$. For ratios $w_1 / t_1 > 4$ the rolling shear value is limited to 1.4 N/mm^2 .

Görlacher, R. [Görlacher, 2002], Jacobs, A. [Jacobs, 2005] and Ehrhart, T.; Brandner, R.; Schickhofer, G.; Frangi, A. [Ehrhart et al., 2015a] report, that the rolling shear modulus heavily depends on the annual ring orientation and the geometry of the cross section. If the board center is closer to the pith, higher rolling shear moduli can be observed. Ehrhart, T.; Brandner, R.; Schickhofer, G.; Frangi, A. [Ehrhart et al., 2015a] determined higher rolling shear moduli compared to earlier studies, which can be explained by the fact, that in earlier cross laminated timber production almost only sidecuts had been used. The equation given in Table PT.1-5.3 is again taken from [Ehrhart et al., 2015a] and is valid for ratios $w_1 / t_1 \leq 4$. For ratios $w_1 / t_1 > 4$ the rolling shear modulus is limited to 100 N/mm^2 .

Shear strength and shear modulus in plane

Bogensperger, T.; Moosbrugger, T.; Schickhofer, G. [Bogensperger et al., 2007], Bogensperger, T.; Moosbrugger, T.; Silly, G. [Bogensperger et al., 2010] and Flaig, M. and Blaß, H. [Flaig et al., 2013] describe three different failure modes for cross laminated timber subjected to shear in plane:

- a) Longitudinal shear can cause a shear failure throughout the gross cross section of cross laminated timber comprising edge glued timber layers. This failure mode can be relevant for cross laminated timber with edge glued layers and almost no cracks during the entire service life, if a high characteristic shear strength value is taken into account. As cross laminated timber is typically not produced with structural edge bonds, cracking cannot be avoided in most of the cases and a conservative characteristic strength value of shear strength for verifications with gross cross sections covering all possible layups is relatively low. PT SC5.T1 will not propose equations for procedure for such shear verifications.
- b) Layers with grain parallel to the “weak” direction of cross laminated timber comprising gaps or cracks might fail due to shear in plane.

c) Gluing interfaces between orthogonally bonded adjacent layers can fail due to torsional shear and rolling shear.

Outcomes for shear strength of gluing interfaces between orthogonally bonded adjacent layers can be taken from Wallner, G. [Wallner 2004], Jöbstl, R.; Bogensperger, T.; Schickhofer, G. [Jöbstl et al., 2008] and Hirschmann, B. [Hirschmann, 2011].

Bosl, R. [Bosl, 2002], Bogensperger, T.; Moosbrugger, T.; Silly, G. [Bogensperger et al., 2010], Watson, C.; van Beerschoten, W.; Smith, T.; Pampanin, S.; Buchanan, Andrew H. [Watson et al., 2013], Dröscher, J. [Dröscher, 2014] and Andreolli, M.; Rigamonti, M; Tomasi, R. [Andreolli et al., 2014] report on tests with cross laminated timber elements.

Blaß, H. and Görlacher, R. [Blaß et al., 2002], Jeitler, G. [Jeitler, 2004] and Jöbstl, R.; Bogensperger, T.; Schickhofer, G., Jeitler, G. [Jöbstl et al., 2004] report on outcomes regarding the gluing interfaces.

Existing test methods have been analyzed e.g. by Brandner, R.; Bogensperger, T.; Schickhofer, G. [Brandner et al., 2013] and Silly, G. [Silly, 2014]. Brandner, R. et al. [Brandner et al., 2015] report on a comprehensive test campaign on the basis of a new test method developed by Kreuzinger, H. and Sieder, M. [Kreuzinger et al., 2013] which allows to reliably assess gross- and net-shear properties.

Density

Regarding the density cross laminated timber with homogeneous and combined layup exhibits the same properties as glulam having the same layering. Thus, the provisions for density are taken from [EN 14080].

Background: PT.1(6)P

Reduction factors for members with reduced width

Within cross laminated timber plates with reduced widths and thereby the strengths of the laminations with grain parallel to the span might be significantly reduced.

If a structural cross laminated timber plate is intended to be structural, the minimum width $w_{x,lam}$ shall be at least its thickness $t_{x,lam}$. For cross laminated timber plates of typical thickness, it can be assumed to either have one untrimmed lamination or two or three laminations, two of them trimmed, in the layers having fibres parallel to the span. In the latter case a system factor could be applied.

Cross laminated timber subjected to bending out of plane having a width w_{xlam} of less than the thickness t_{xlam} shall not be taken as structural.

For member widths w_{xlam} between t_{xlam} and 600 mm PT SC5.T1 proposes linear interpolation.

Background: PT.1(7)

Increasing factors for edgewise bending

In order to prevent the compulsory application of reduction factors, a conservative edgewise bending strength related to a cross laminated timber beam with only one layer with grain parallel to the grain and a beam height of 150 mm is proposed by PT SC5.T1.

In case of a diaphragm in bending verification is done for the outermost laminations in tension parallel to grain disregarding the homogenisation. According to Blaß and Flaig [Flaig et al., 2014] a reversed height effect was observed, i. e. an increase of the bending strength with increased beam height h_{xlam} . The given increasing factor $k_{\text{sys},y}$ has been determined from test data given in Flaig [Flaig, 2013] and Blaß and Flaig [Flaig et al., 2014].

According to [Flaig et al., 2014] a $k_{\text{sys},x}$ -factor can be applied for a higher number of layers $n_{\text{lay},x}$ with grain parallel to the x-direction, if – typically in a late design step – this number is known.

Chapter	Material Properties: Shrinkage and Swelling
Focus of work	<ul style="list-style-type: none"> – Literature research – Comparing the products CLT and Solid wood panel
Collaboration inclusive short motivation <ul style="list-style-type: none"> – WGs – TGs 	<ul style="list-style-type: none"> – meaningful would be a concerted regulation with other TG's of WG 2, at least with TG 2
Further steps To Do's	<ul style="list-style-type: none"> – summary of state-of-knowledge (update) + proposal for possible regulation in design standards
Currently available	<ul style="list-style-type: none"> – TC250/SC5/PT1: Working draft; Version 2017_10_13 [42] – TC250/SC5/PT1: Background document; Version

Literature	<p>2017_10_13 [43]</p> <ul style="list-style-type: none"> – Bader, Niemz, Sonderegger (2007) [9] – Bonigut, Stephani, Dube (2010) [23] – Clauß, Kröppelin, Niemz (2010a) [46] – Clauß, Kröppelin, Niemz, (2010b) [47] – DIN 52184 (1979) – EN 1995-1-1 – Gereke (2009) [90] – Gereke, Hass, Niemz (2010) [91] – Keylwerth (1962) [113] – Keylwerth (1968) [114] – Moosbrugger et al. (2017) [128] – Moosbrugger et al. (2018) [129] – Niemz, Bärtsch, Howald (2005) [135] – Niemz, Petzold, Häupl (2003) [136] – ON B 1995-1-1 Annex K – ÖNORM B 3012 – ÖNORM EN 16351 – ÖNORM EN 318 – Popper, Niemz, Eberle (2004) [148] – Schwab, Steffen, Korte (1997) [157] – Tobisch (2006) [171]
Suggestions for possible papers, scientific theses and further work	<ul style="list-style-type: none"> – investigation of automatic photo evaluation to determine local behaviour envisaged – swelling and shrinkage under consideration of the layup of CLT

Background: PT.1(8)

Swelling and shrinking values

As for glulam the swelling and shrinkage values of cross laminated timber perpendicular to its plane can be taken as the mean value of the radial and tangential swelling and shrinkage value.

Due to the crosswise orientation of the layers swelling and shrinking in plane is

restrained. Measurements show differences in x- and y-direction as especially the outermost layers (x-direction) are affected by moisture changes.

PT SC5.T1 is not aware of studies on swelling and shrinkage values and therefore recommends applying the values given in the Austrian National Annex [ÖNORM B 1995-1-1].

Moosbrugger et al. (2017) confirm current values in ÖNORM B 1995-1-1.

4 Durability

Chapter	Durability
Focus of work	<ul style="list-style-type: none">– Literature research– Comparing the products CLT and glulam (GLT)
Further steps To Do's	<ul style="list-style-type: none">– summary of state-of-knowledge (update) + proposal for possible regulation in design standards
Currently available Literature	<ul style="list-style-type: none">– TC250/SC5/PT1: Working draft; Version 2017_10_13 [42]– TC250/SC5/PT1: Background document; Version 2017_10_13 [43]– EN 16351– EN 1995-1-1
Suggestions for possible papers, scientific theses and further work	<ul style="list-style-type: none">– Comparing the products CLT and glulam (GLT)

Background

As for other structural glued laminated products, the durability against biological attack of cross laminated timber can be taken as the durability of the wood from which the layers are made of.

Unless no specific provisions for wood protection by design and preservative treatment are given in the new EN 1995-1-1, Clause 6, nothing has to be added with regard to cross laminated timber.

5 Basis of Structural Analysis

5.4 Assemblies

5.4.5 Cross laminated timber members

Chapter	Appropriate analysis methods for out-of-plane loading of plate and beam elements
Focus of work	<ul style="list-style-type: none"> – Literature research – Comparing the calculation methods for CLT and glulam (GLT). The principal requirements for modelling CLT or GLT beams should be harmonised, since the basic behaviour of the two products is the same.
Further steps To Do's	<ul style="list-style-type: none"> – summary of state-of-knowledge.
Currently available Literature	<ul style="list-style-type: none"> – Bogensperger, Silly, Schickhofer (2012) (A printed version of this publication is part of this report in a separate section) – TC250/SC5/PT1: Working draft; Version 2017_10_13 [42] – TC250/SC5/PT1: Background document; Version 2017_10_13 [43] – National approvals from Germany: Z9.1-482, Z9.1-501, Z9.1-534, Z9.1-555, Z9.1-559, Z9.1-576, Z9.1-680, Z9.1-721, Z9.1-793 – Brandner, Dietsch et al. (2015) [27] – CEN/TC 250/SC 5: EN 1995-1-1 working draft – Christovasilis et al. (2016) [44] – EN 16351 and EN 1995-1-1 – ETAs: 06/0009, 09/0138, 09/0036, 09/0211, 11/0189, 11/0210, 12/0327, 14/0349, 16/0055 – Guggenberger, Moosbrugger (2006) [93] – Karabeyli, Douglas (2013) – Mestek, Kreuzinger and Winter (2008) [125] – Resch (2016) [150] – Thiel, Brandner (2016) [167]
Suggestions for possible papers,	<p>Suggestions for further work:</p> <ul style="list-style-type: none"> – The knowledge base of the background document could be enhanced with the reference of Christovasilis et al. [44]

scientific theses and further work	<p>which contains also experimental data.</p> <p>Suggestions for future research projects:</p> <ul style="list-style-type: none"> – The relevant future research ideas mentioned in Bogensperger, Silly, Schickhofer [Bogensperger et al., 2012], could be pursued: It could be analytically investigated which is the most suitable effective length to be used in continuous beam systems analysed with the modified γ-method.
---	--

<p>Background: PT.1-7.3.2 Cross laminated timber members</p> <p>PT.1(2)P and PT.1(3)</p> <p>Design models for cross laminated timber</p> <p>Different models for the design of cross laminated timber plates, diaphragms and beams can be taken from reports, publications and handbooks (see e.g. [Kreuzinger/Scholz, 2004], [Brandner et al., 2015] to [Karabeyli et al., 2013]), National Annexes to Eurocode 5-1-1 ([ÖNORM B 1995-1-1/NA], [DIN EN 1995-1-1/NA]) and national and European technical approvals (e.g. [ETA-06/0009], [ETA-12/0327], [ETA-06/0138], [ETA-09/0211], [ETA-09/0036], [ETA-11/02103], [ETA-14/0349], [ETA-11/0189], [ETA-16/0055] [Z 9.1-501], [Z 9.1-534], [Z 9.1-721], [Z 9.1-680], [Z 9.1-482], [Z 9.1-555], [Z 9.1-793], [Z 9.1-559], [Z 9.1-576]).</p> <p>A comprehensive comparison of methods of approximate verification procedures for cross laminated timber can be taken from Bogensperger, T.; Silly, G.; Schickhofer, G. [Bogensperger et al., 2012]. Note: This report, in its original text and format, constitutes the second main chapter of WG 2 / TG 1 STAR of COST Action FP1402.</p> <p>As all of the methods for the determination of stresses and strains are simply based on mechanics and can be taken from existing literature PT SC5.T1 proposes neither to include them in the main part of the Eurocode 5-1-1 nor in an Annex.</p>

<p>Background: PT.1(4)</p> <p>Gaps in timber layers</p> <p>The maximum width measured at any point of a timber layer is allowed to be up to 6 mm according to [EN 16351]. This rule reflects the usual quality of cross laminated timber. The mean value of gap widths is significantly lower.</p>
--

As the Equations given in Table PT.1-5.3 are based on tests with cross laminated timber having typical gap widths, gaps may be disregarded for the design of cross laminated timber members. They need, of course, be taken into account for the design of joints and fasteners.

Background: PT.1(5)

Influence of shear deformations

In Augustin, M.; Blaß, HJ.; Bogensperger, T.; Ebner; Ferik, H.; Fontana, M.; Frangi, A.; Hamm, P.; Jöbstl, R.; Moosbrugger, T.; Richter, K.; Schickhofer, G.; Thiel, A.; Traetta, G.; Uibel, T. [Augustin et al., 2009] it is shown that for slender cross laminated timber the influence of the shear stiffness on the distribution of internal forces and moments can be disregarded.

6 Ultimate and Serviceability Limit States

6.1 Design of Cross-Sections

6.1.1 General

Chapter	General provisions for the ULS design of CLT cross-sections
Focus of work	<ul style="list-style-type: none"> – Literature research – Comparing the products CLT and glulam (GLT)
Further steps To Do's	<ul style="list-style-type: none"> – None.
Currently available Literature	<ul style="list-style-type: none"> – TC250/SC5/PT1: Working draft; Version 2017_10_13 [42] – TC250/SC5/PT1: Background doc.; Ver. 2017_10_13 [43] – Bogensperger, Silly, Schickhofer (2012) [21] – EN 1995-1-1 – EN 16351
Suggestions for possible papers, scientific theses and further work	<p>Suggestions for further work:</p> <ul style="list-style-type: none"> – In PT.1-5.4, it is stated that: "For cross laminated timber having layups different to those described in PT.1(4) and PT.1(5) the properties of the cross laminated timber shall be derived from the layer properties by composite theory. For timber layers, system effects may be considered". This provision holds for strength properties as well. In PT.1-7.3.2, it is stated that: "The calculation model shall consider the influence of the layup e.g. thickness, material and orientation of layers, influence of gaps, grooves and lamination sizes, on the cross laminated timber properties". It is suggested to harmonize PT.1-8.1.1(2)P with the above provisions, in order to cover also the cases of layers with non-negligible strength properties perpendicular to the grain (in PT.1-3.1.2.11, it is stated that cross laminated timber may be comprised from wood-based panel layers). E.g. "PT.1(2)P Unless the verifications are explicitly related to the cross section of the cross laminated timber, verifications shall be done for each decisive layer with the effective cross sections of those layers with non-negligible strength parallel to the respective stresses, see Figure PT.1-8.13."

Background: PT.1(3)P**System effects**

System effects are already covered in the strength model according to PT.1-5.4 PT.1(3) and PT.1(4). If the strength properties are determined according to those paragraphs, no additional system factor shall be taken into account.

Background: PT.1(4)**Tension and compression strength in plane of large finger joints in cross laminated timber**

The characteristic bending strength in edge or flatwise bending of large finger joints in cross laminated timber shall be determined according to the procedures given in EN 16351 or ETAs, if relevant.

EN 16351:2014 does not give information on test procedures for the tension or compression strength in plane of large finger joints. PT SC5.T1 is not aware of reports on tension or compression strength in plane, but it can be assumed that the ratios of those values by the bending strength are similar to the ratios of the unjointed cross laminated timber. Alternatively, values may be taken from ETAs on the basis of full scale test, if any.

6.1.2 Tension parallel to the grain

Chapter	Tension parallel to the grain
Focus of work	<ul style="list-style-type: none"> – Summary of state of knowledge – Literature research
Further steps To Do's	<ul style="list-style-type: none"> – None.
Currently available Literature	<ul style="list-style-type: none"> – TC250/SC5/PT1: Working draft; Version 2017_10_13 [42] – TC250/SC5/PT1: Background document; Version 2017_10_13 [43]
Suggestions for possible papers, scientific theses and further work	<ul style="list-style-type: none"> – E_{90} not equal to zero for SWP (Solid Wood Panels, according to EN 13353), harmonisation between CLT and SWP should be conducted

Background: PT.1(2)P

In cross layers made of timber laminations the stresses perpendicular to the grain will be low because of a low modulus of elasticity in that direction. Strength and stiffness properties perpendicular to the grain of the timber layers are low compared to parallel to grain. Due to gaps, grooves and cracks no load transfer perpendicular to the grain of the timber layers can be ensured over the expected service time of the members and therefore should not be taken into account.

If in a design the load bearing capacity perpendicular to the grain of the cross layers is taken into account for verification of bending, tension or compression stresses in plane, this will lead to unrealistically low load bearing capacities of the cross laminated timber member.

It is recommended to disregard any contribution of cross layers to the load bearing capacity by taking the modulus of elasticity of those layers as zero. This background information also applies to compression in plane according to 8.1.4 and bending out of plane according to 8.1.6.

6.1.3 Tension perpendicular to the grain

Chapter	Tension perpendicular to the grain
Focus of work	<ul style="list-style-type: none"> – Literature research – Comparing the products CLT and glulam (GLT)
Further steps To Do's	<ul style="list-style-type: none"> – summary of state-of-knowledge (update) + proposal for possible regulation in design standards
Currently available Literature	<ul style="list-style-type: none"> – TC250/SC5/PT1: Working draft; Version 2017_10_13 [42] – TC250/SC5/PT1: Background document; Version 2017_10_13 [43] – EN 16351 and EN 1995-1-1 – ETA-16/0055 – Z9.1-509 – STSM Bidakov [163] <p>Short literature review</p> <p>As it is well known from curved glulam elements, tension perpendicular to the grain occurs when curved elements are subjected to bending. This effect could be the decisive design criterion. In the national technical approval [Z9.1-509], curved CLT elements are covered. In [STSM Bidakov], several aspects of tension perpendicular to the grain in CLT elements have been outlined. Test data for tension perpendicular to the grain strength properties of CLT elements have been gained within 2017 [STSM Bidakov].</p>
Suggestions for possible papers, scientific theses and further work	<ul style="list-style-type: none"> – A note could be added in the background document stating this effect could arise in the transportation and assembling of non-curved CLT elements at the building site. Some other scenarios have also been presented in [STSM Bidakov]. – testing, production, transportation and assembling at building site

Background

[EN 16351], a national technical approval [Z 9.1-509] and one European Technical Assessment [ETA-16/0055]) allow the production of curved cross laminated timber. PT SC5.T1 is not aware of sufficient publications on experience or test data for the verification of tension perpendicular stresses due to bending of curved cross laminated timber. Particularly publications on distribution factors and volume effects are missing.

6.1.4 Compression parallel to the grain

Chapter	Compression parallel to the grain
Focus of work	<ul style="list-style-type: none"> – Literature research – Comparing the products CLT and glulam (GLT)
Further steps To Do's	<ul style="list-style-type: none"> – summary of state-of-knowledge (update) + proposal for possible regulation in design standards
Currently available Literature	<ul style="list-style-type: none"> – TC250/SC5/PT1: Working draft; Version 2017_10_13 [42] – TC250/SC5/PT1: Background document; Version 2017_10_13 [43] – EN 16351 – EN 1995-1-1 – Wang et al. (2016) [182] – Horvat (2013) [101]
Suggestions for possible papers, scientific theses and further work	<ul style="list-style-type: none"> – E_{90} not equal to zero for SWP (Solid Wood Panels, according to EN 13353), harmonisation between CLT and SWP should be conducted. – Meaningful would be an experimental investigation of CLT elements produced from European timber species under compression along the grain, similar to the one performed in Horvat (2013) (see also Wang et al. 2016).

Background

In cross layers made of timber laminations the stresses perpendicular to the grain will be low because of a low modulus of elasticity in that direction. Due to gaps, grooves and cracks no load transfer perpendicular to the grain of the timber layers can be ensured over the expected service time of the members and therefore should not be taken into account. It is recommended to disregard any contribution of cross layers to the load bearing capacity by taking the modulus of elasticity of those layers as zero.

6.1.5 Compression perpendicular to the plane

Chapter	Compression perpendicular to the plane
Focus of work	<ul style="list-style-type: none"> – Literature research – Comparing the products CLT and glulam (GLT)
Further steps To Do's	<ul style="list-style-type: none"> – summary of state-of-knowledge (update) + proposal for possible regulation in design standards
Currently available Literature	<ul style="list-style-type: none"> – TC250/SC5/PT1: Working draft; Version 2017_10_13 [42] – TC250/SC5/PT1: Background document; Version 2017_10_13 [43] – Bogensperger, Augustin, Schickhofer (2011) [18] – Brandner and Schickhofer (2014) [33] – Ciampitti (2013) [45] – EN 16351 and EN 1995-1-1 – Halili (2008) [94] – Hasuni (2009) [99] – Salzmann (2010) [151] – Serrano (2010) [158]
Suggestions for possible papers, scientific theses and further work	<ul style="list-style-type: none"> – Peer-reviewed paper on CLT compression perp. to grain is envisaged, summarizing also the state-of-knowledge in general and with focus on CLT as well as the outcomes of a comprehensive test campaign, with the aim to present proposals for testing, evaluation and design. – The orthogonal layup of CLT leads to higher base compression perpendicular to plane (grain) strength and modulus in CLT in comparison to glulam; reason is the reinforcement caused by the transverse layers which limit transverse deformations; an increase of 30 % on strength and elastic modulus is reported in Brandner and Schickhofer (2014) [33]. – Apart from reference test setup on uniformly and over their entire surface loaded and supported prism-like specimen $k_{c,90}$-factors different to glulam have been observed, in case of partial loading and / or support. Reason is the limited stress transfer perpendicular to grain. Consequently, whereas basic values of strength and elastic modulus in CLT are higher than in glulam, in case of partial loading / support the gain by stress transfer to adjacent unloaded

	<p>timber volume is lower.</p> <ul style="list-style-type: none"> – Brandner and Schickhofer (2014) [33] adapted the stress dispersion model proposed by van der Put (1991 [176], 2008 [177], 2012 [178]), originally developed for linear structural members, for CLT plates; this was made by implementation of a stress dispersion angle perpendicular to grain of 15° additional to the 45° in grain direction. Comparison of model calculations with test data of various load configurations demonstrated the applicability of van der Put’s stress dispersion model and reflected the apparent increase in strength and modulus of elasticity with increasing surrounding area and CLT thickness in comparison to the basic tests.
--	--

Background

Characteristic values for strengths perpendicular to the grain are derived from compression tests with cubical specimens referring to [EN 408]. Such values need to be adjusted taking into account the load situation (e.g. continuous support or load transfer), the shape of the contact areas (point- vs. line loads), the layup of the cross laminated timber and the possibility of stress dispersion at one, two or more sides of the contact area.

In Brandner, R. and Schickhofer, G. [Brandner et al., 2014] it is shown, that an adopted stress dispersion model based on the model for linear members according to van der Put, T. [van der Put, 2008], [van der Put, 2012] properly reflects test results for very different load situations, if a stress dispersion of 45° parallel to the grain and of 15° perpendicular to the grain is assumed. The accordance with test results can be improved assuming, that the dispersion of compression stresses within layers having gaps, grooves or cracks is reduced to the half.

For typical layups a load dispersion of 35° throughout all layers may be used, covering also the effects of cracks, grooves and gaps.

6.1.6 Bending

Chapter	Bending – Appropriate design methods for out-of-plane loading of plate and beam elements
Focus of work	<ul style="list-style-type: none"> – Literature research – Comparing the products CLT and glulam (GLT)
Further steps To Do's	<ul style="list-style-type: none"> – summary of state-of-knowledge (update) + proposal for possible regulation in design standards
Currently available Literature	<ul style="list-style-type: none"> – TC250/SC5/PT1: Working draft; Version 2017_10_13 [42] – TC250/SC5/PT1: Background document; Version 2017_10_13 [43] – Aicher (1987) – EN 16351 and EN 1995-1-1 – Heimeshoff (1997) [100] – Kreuzinger (1999) [117], [118] – Kreuzinger (2000) [119] – Kreuzinger (2002) [120] – Pischl (1968) [145] – Pischl (1969) [146] – Schelling (1968) [152] – Schelling (1998) [153] <p>References with focus on CLT:</p> <ul style="list-style-type: none"> – Bogensperger, Silly, Schickhofer (2012) [21] – Schickhofer (2010) [154] – Scholz (2003) [156]
Suggestions for possible papers, scientific theses and further work	<p>Suggestions for further work</p> <ul style="list-style-type: none"> – Formulation of a link to the current design procedure of EN 1995-1-1 for light weight composite elements (especially for cases such as inhomogeneous CLT where additional verifications of tension stresses at the centre of the boards of CLT layers are required). – Investigation and inclusion of additional verifications for tension stresses parallel to grain in the centre of the board at the layer level, if necessary (e.g. German NA, DIN EN 1995-1-1/NA - 2013).

Suggestions for future research projects:

The relevant future research ideas mentioned in Bogensperger, Silly, Schickhofer [Bogensperger et al., 2012] could be pursued: it could be experimentally investigated if the significant stress peaks occurring locally for example at the internal supports of continuous CLT beams lead indeed to the necessity to include strength reduction factors in the verification process of the out-of-plane bending. First tests, conducted at the Competence Centre holz.bau forschungs gmbh, indicated a rather higher than lower resistance; unfortunately, an official report on the analysed small sample is not available. Consequently, a strength reduction factor to consider local increased stresses (single load) is currently not proposed for the CLT chapter in the revised version of EC 5.

Background: PT.1(5)**Necessity of additional tension strength verifications**

The characteristic bending strength values for bending out of plane according to Table PT.1-5.3 take into account the effects of combined bending and tension stresses in the layers. Therefore, no additional verification is needed.

It can be shown on the basis of Equations 5 to 7 from Flaig, M.; Blaß, H. [Flaig et al., 2015] that also for cross laminated timber subjected to edgewise bending having a slenderness larger than $l / t_{\text{lam}} > 5$ verifications on tension stresses in laminations will not govern the design.

6.1.7 Shear

Chapter	Shear
Focus of work	– Literature research
Further steps To Do's	– summary of state-of-knowledge (update) + proposal for possible regulation in design standards
Currently available Literature	<ul style="list-style-type: none"> – TC250/SC5/PT1: Working draft; Version 2017_10_13 [42] – TC250/SC5/PT1: Background document; Version 2017_10_13 [43] – Andreolli (2014) [4] – Blaß, Görlacher (2002) [12] – Blaß, Flaig (2012) – Blaß, Flaig (2014) – Bogensperger, Moosbrugger, Schickhofer (2007) [19] – Bogensperger, Moosbrugger, Silly (2010) [20] – Bosl (2002) [24] – Brandner, Bogensperger, Schickhofer (2013) [25] – Brandner, Dietsch et al. (2017) [27] – Dröscher, Brandner (2013) [54] – Dröscher (2014) [53] – EN 16351 – EN 1995-1-1 – Flaig, Blaß (2013) [82] – Hirschmann (2011) [102] – Jeitler (2004) [106] – Jöbstl, Bogensperger, Schickhofer (2004) [111] – Jöbstl et al. (2008) [110] – Kreuzinger, Sieder (2013) [122] – Silly (2014) [161] – Wallner (2004) [180]
Suggestions for possible papers, scientific theses and	– Peer-reviewed paper on that subject was published recently, by Brandner, Dietsch et al. (2017) [27]. This paper addresses all three possible failure modes, net-shear, gross-shear and torsion, and gives recommendations for testing, evaluation and design.

<p>further work</p>	<p>– Concerning the question if there is still the necessity regulating the design of shear stresses in CLT diaphragms different to CLT beams loaded in-plane, Brandner, Dietsch et al. (2017) give the following statement: <i>“The presented characteristic in-plane shear properties derived for CLT diaphragms can also be applied in the design of CLT beams exposed to in-plane shear stresses. It is recognized that the shear stress distribution over the cross section in CLT beams differs from that in CLT diaphragms, and that the peak shear stresses in CLT beams apply more to single nodes. However and following the conclusions in Brandner et al. [10] [note: Brandner et al. 2013 [25]], the characteristic shear properties for single nodes shear compare well with the shear properties of CLT diaphragms. It is rather a question of what base material properties should be considered in particular in CLT beams randomly cut from larger CLT elements. In such cases there is a high probability that the lengthwise cuts parallel to CLT layers, mainly responsible for load bearing, are not in the gap between but rather within lamellas. The position of this cut significantly affects the residual resistance of these lamellas and hence of the whole CLT beam. In any case, a quadratic parabolic shear stress distribution over the depth of such beams should be considered.”.</i></p>
----------------------------	---

Background: PT.1(4)P

Shear verifications for cross laminated timber plates

In a cross laminated timber plate subjected to a shear force, part of the shear stresses act parallel to the fibres (parallel layers) and another part perpendicular to the fibres (cross layers). Because of the big differences between shear moduli and strengths parallel and perpendicular to the fibre, shear verifications need to be done in each decisive layer.

If specimens fail in shear perpendicular to the grain the fibres along the plane of fracture or the laminations in a cross layer seem to be twisted along their axes. Therefore, shear stresses acting perpendicular to the grain of a layer are denominated as rolling shear stresses.

See also background information on shear strengths given for Table PT.1-5.3.

Background: PT.1(5)P

Shear verifications for cross laminated timber diaphragms and walls

For cross laminated timber diaphragms or walls subjected to shear in plane different failure mechanisms are described, see e.g. Wallner-Novak et al. [Wallner-Novak et al., 2013].

Mechanism 1: In an edge glued cross laminated timber without cracks shear failure may occur through the entire plate. This mechanism is typically not relevant, see also background information on Table PT.1-5.3, shear strength and shear modulus in plane, and has therefore not been taken into account by PT SC5.T1.

Mechanism 2: If the gaps between the laminations are small, the laminations of the cross layers will act as reinforcements of the parallel layers. This lead to shear strength values which are significantly higher than the shear strengths of the laminations. In Jöbstl et al. [Jöbstl et al., 2008] shear strength values $f_{v,xy,k}$ of up to $f_{v,xy,k} = 10 \text{ N/mm}^2$ have been reported. For unfavourable layups, lower values will be achieved. Within Table PT.1-5.3 a conservative value of $f_{v,xy,k} = 5.5 \text{ N/mm}^2$ is given, covering all possible layups. Failure occurs perpendicular to the grain of the boards in either x- or y-direction, see Figure BI.2. This mechanism is reflected in PT.1(5)P a).

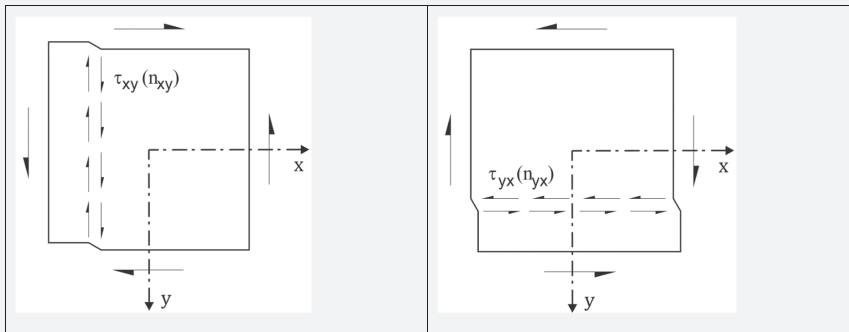


Figure BI.2: Shear failure mechanism 2 [taken from Wallner-Novak et al., 2013].

Mechanism 3: For larger gaps between the laminations the nodal areas between adjacent orthogonally glued layers will be subjected to torsional stresses, see Figure BI.3. This mechanism is reflected in PT.1(5)P b).

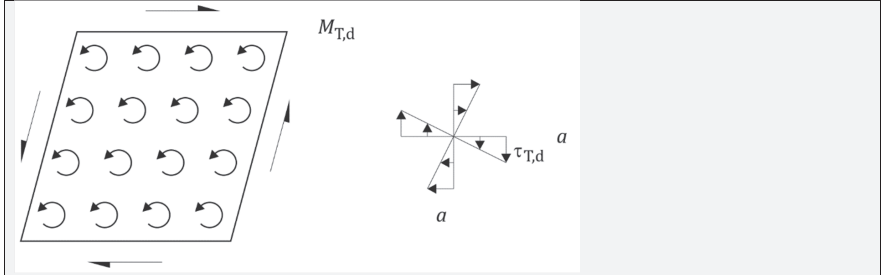


Figure BI.3: Shear failure mechanism 3 [taken from Wallner-Novak et al., 2013].

Background: PT.1(6)P

Shear verifications for cross laminated timber beams

According to Flaig, M. [Flaig, 2013] and Blaß, H. and Flaig, M. [Blaß et al., 2014] shear verifications with cross laminated timber beams need to be done with effective and gross cross sections. In the case of cross laminated timber which is not made from edge glued timber layers also the torsional and rolling shear stresses in the glue lines between laminations of adjacent orthogonal layers need to be verified.

For the latter case the torsional shear stress in the node area is according to Flaig:

$$\tau_{\text{tor,node,d}} = \frac{3 V_{xy,d}}{w_{l,x}^2 \cdot n_{CA}} \left(\frac{1}{n_{l,x}} - \frac{1}{n_{l,x}^3} \right) k_b \quad \text{with } k_b = \frac{2 \cdot w_{l,\max} w_{l,x}}{w_{l,x}^2 + w_{l,y}^2}. \quad (\text{BI.9})$$

The symbols can be taken from 8.1.7, PT.1(6)P b).

The factor k_b , taking into account different lamination widths in x- and y-direction, may be skipped, if within [BI.9] $b_{l,x}$ is equal to $b_{l,y}$.

For example, a three-layered cross laminated timber element ($n = 3$) leads to $n_{CA} = n_{\text{bond}} - 1 = 2$, where n_{bond} is the number of bond lines between orthogonally bonded adjacent layers. If the number of laminations within a layer is taken as $n_{l,x} = 2$ and the lamination width as $w_{l,x} = w_{l,y} = 80 \text{ mm}$ (BI.9) becomes:

$$\tau_{\text{tor,node,d}} = \frac{3 V_{xy,d}}{w_{l,\min}^2 \cdot 2} \left(\frac{1}{2} - \frac{1}{2^3} \right) \cdot 1 \approx 0.56 \cdot \frac{V_{xy,d}}{w_{l,\min}^2} = 8.75 \cdot 10^{-5} \frac{1}{\text{mm}^2} \cdot V_{xy,d} \quad (\text{BI.10})$$

According to Flaig the rolling shear in the node area is determined as follows:

$$\tau_{xy,d} = \frac{6 V_{xy,d}}{w_{l,x}^2 \cdot n_{CA}} \left(\frac{1}{n_{l,x}^2} - \frac{1}{n_{l,x}^3} \right). \quad (\text{BI.11})$$

The symbols can again be taken from 8.1.7, PT.1(6)P b).

For example, a three-layered cross laminated timber element ($n = 3$) leads to $n_{CA} = n_{\text{bond}} - 1 = 2$, where n_{bond} is the number of bond lines between orthogonally bonded adjacent layers. If the number of laminations within a layer is taken as $n_{l,x} = 2$ and the lamination width as $w_{l,x} = w_{l,y} = 80 \text{ mm}$ (BI.11) becomes:

$$\tau_{xy,d} = \frac{6 V_{xy,d}}{w_{l,\min}^2 \cdot 2} \left(\frac{1}{2^2} - \frac{1}{2^3} \right) \approx 0.375 \frac{V_{xy,d}}{w_{l,\min}^2} \approx 0.6 \cdot 10^{-5} \frac{1}{\text{mm}^2} V_{xy,d} \quad (\text{BI.12})$$

For the same reasons as for shear verifications of diaphragms and walls no verification related to the gross cross section is proposed.

Background: PT.1(7)P

k_{cr}

Swelling and shrinking and stresses caused by restraining effects are limited compared to solid timber and glued laminated timber. Changes in moisture content will especially affect the outermost layers. The depth of cracks within the outermost parallel layers is limited by the outermost cross layers.

The effects of cracking are already considered in the shear strength values according to Table PT.1 - 5.3. Therefore no additional k_{cr} -factor is needed.

6.2 Design of Cross-Sections Subjected to Combined Stresses

Chapter	Design of cross-sections subjected to combined stresses
Further steps To Do's	– summary of state-of-knowledge (update) + proposal for possible regulation in design standards
Currently available Literature	<ul style="list-style-type: none"> – TC250/SC5/PT1: Working draft; Version 2017_10_13 [42] – TC250/SC5/PT1: Background doc.; Vers. 2017_10_13 [43] – EN 16351 and EN 1995-1-1
Suggestions for possible papers, scientific theses and further work	<ul style="list-style-type: none"> – The interaction between shear and rolling shear stresses is considered to be linear; for validation further investigations are needed. – The exact format of all the design equations for the combined shear verification should be clearly expressed. – Currently, stresses due to twisting (drilling) moments in plate elements are disregarded from the ULS design. Additional research should be performed in loading situations (e.g. point-supported CLT plates) where stresses due to twisting (drilling) moments could notably affect the ULS design of CLT plates. – Dealing with CLT under pure bending only bending stresses are verified at the edges, although the outer layers must resist an interaction between normal forces and bending moments. Considering combined cross sections, e.g. timber concrete composite beams, the CLT members are not only under pure bending, the whole cross section is loaded by a combination of normal forces and bending moments. Currently, the interaction equations employed for solid timber are employed for CLT as well due to lack of relevant investigations. Further investigations are necessary to enable the application.

Background: PT.1(1)P

Combined shear

Beside the combined influence of shear and rolling shear stresses in nodal areas of cross laminated timber subjected to edgewise bending, see 8.1.7 PT.1(6)P b), PT SC5.T1 is not aware of sufficient reports on such combinations of shear stresses. Linear interpolation is proposed.

6.3 Stability of Members

6.3.2 Members subjected to either compression or combined compression and bending

Chapter	Stability of members: Buckling
Focus of work	<ul style="list-style-type: none"> – Literature research – Comparing the products CLT and glulam (GLT)
Further steps To Do's	<ul style="list-style-type: none"> – summary of state-of-knowledge (update) + proposal for possible regulation in design standards
Currently available Literature	<ul style="list-style-type: none"> – TC250/SC5/PT1: Working draft; Version 2017_10_13 [42] – TC250/SC5/PT1: Background document; Version 2017_10_13 [43] – EN 16351 – EN 1995-1-1 – Wang et al. (2016) [182]
Suggestions for possible papers, scientific theses and further work	<ul style="list-style-type: none"> – Meaningful would be an attempt to transfer the design proposal of Wang et al. (2016) for the Canadian standard CSA-O86 to the new EC5. Also a similar experimental investigation of CLT produced from European timber species should be pursued. – Influence of windows and doors on the overall load bearing capacity of CLT – Investigation of imperfections

Background (2)

Straightness of members

Augustin, M.; Flatscher, G.; Tripolt, M. and Schickhofer, G. [Augustin et al. 2017] report on measurements of straightness of cross laminated timber diaphragms. The calculated 95 %-quantiles of the mean depth gauges are reasonable smaller compared to values for glulam taken from literature. It can be assumed that cross laminated members have at least similar straightness and flatness as glued laminated timber and that equal β_c -values can be taken for design.

Background: PT.1(4)P

Verification for compression or combined compression and bending

Shear deformations in slender cross laminated timber members for which verifications for compression or combined compression and bending might govern the cross-sectional sizes are small and may therefore be disregarded.

6.3.3 Beams subjected to either bending or combined bending and compression

Chapter	Stability of members: Torsional Buckling
Focus of work	<ul style="list-style-type: none"> – Literature research – Comparing the products CLT and glulam (GLT)
Further steps To Do's	<ul style="list-style-type: none"> – summary of state-of-knowledge (update) + proposal for possible regulation in design standards
Currently available Literature	<ul style="list-style-type: none"> – TC250/SC5/PT1: Working draft; Version 2017_10_13 [42] – TC250/SC5/PT1: Background document; Version 2017_10_13 [43] – Blaß (2015) [13] – EN 16351 – EN 1995-1-1 – Krenn (2016) [115] – Moosbrugger, Bogensperger, Krenn (2015) [130]
Suggestions for possible papers, scientific theses and further work	<ul style="list-style-type: none"> – The increase factor 1.4 (defined for glulam) to calculate the term $(E G)_{05} = 1.4 E_{05} G_{05}$ must be examined – Investigations on imperfections

Background: (2)

Torsional moment of inertia of a cross laminated timber diaphragm, wall or beam

According to Moosbrugger, T., Bogensperger, T. and Krenn, H. [Moosbrugger et al., 2015] the torsional stiffness of a slender cross laminated timber beam can be derived by equating the torsional drill moment of a plate with the torsional moment of a slender beam according to St. Venant's theory. It is assumed, that the torsional moments acting along the borders of the plate being parallel to the span, can be substituted by a pair of forces acting in the z-direction at both ends of the beam, see Figure BI.4.

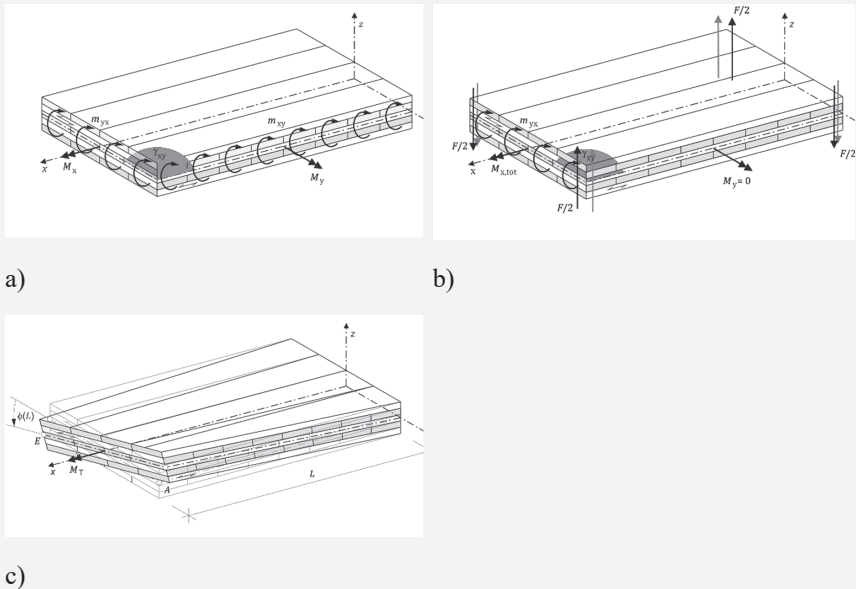


Figure BI.4: Replacement of torsional moments acting at the borders of a plate by pairs of forces

By doing so, the torsional stiffness D_{xy}^* of a strip with a width of 1 m can be determined according to Silly, G. [Silly, G., 2010] as:

$$D_{xy}^* = \frac{G_{xz,mean} \frac{t_{xlam}^3}{12}}{1 + 6 p_D \left(\frac{t_{l,max}}{w_{l,mean}} \right)^{q_D}} \cdot "1" \quad (BI.13)$$

where

- $G_{xz,mean}$ is the mean the shear modulus in plane in N/mm²;
 t_{xlam} is the thickness of the cross laminated timber member, in mm;
 $t_{l,max}$ is the maximum thickness of the layer, in mm;
 $w_{l,mean}$ is the mean width of the laminations within the thickest timber layer, in mm;
 p_D, q_D are parameters according to Silly, G. [Silly, G., 2010], Table 1.

For a three layered cross laminated timber with parameters $p_D = 0.89$ and $q_D = 1.33$ and a ratio of $t_{l,max} / w_{l,mean} = 0.5$ (BI.13) becomes approximately (BI.14):

$$D_{xy}^* \approx \frac{G_{xz,mean}}{3.124} \cdot \frac{t_{xlam}^3}{12} \cdot "1" \quad (\text{BI.14})$$

In Silly, G. [Silly, G., 2010] the torsional moment of inertia is given as:

$$I_{tor} = \frac{4D_{xy}^*}{G_{xz,mean}} \left(1 - 0.63 \frac{t_{xlam}}{h_{xlam}} \right) \cdot "1" \quad (\text{BI.15})$$

Where h_{xlam} is the overall height of the cross laminated timber member. Replacing D_{xy}^* in (BI.15) by (BI.14) results in (BI.16):

$$I_{tor} = \frac{4}{3.124} \cdot \frac{t_{xlam}^3}{12} \left(1 - 0.63 \frac{t_{xlam}}{h_{xlam}} \right) \cdot h_{xlam} \approx \frac{t_{xlam}^3 \cdot h_{xlam}}{9} \left(1 - 0.6 \frac{t_{xlam}}{h_{xlam}} \right) \quad (\text{BI.16})$$

Background: PT.1(3)

M_{crit} and product $(E G)_{05}$

(6.30) should read:

$$M_{crit} = \frac{\pi}{l_{ef}} \sqrt{(E G)_{05} I_z I_{tor}} \quad (\text{BI.17})$$

Blaß, H. [Blaß, 2015] showed, that modulus of elasticity and shear modulus for laminations in glued laminated timber are almost statistically independent and that $(E G)_{05}$ can approximately be taken as $(E G)_{05} = 1.4 E_{05} G_{05} \approx E_{mean} G_{mean}$. This is also applicable for cross laminated timber.

6.4 Design of Cross-Sections in Members with Varying Cross-Section or Curved Shape

Chapter	Design of cross-sections in members with varying cross-section or curved shape
Focus of work	<ul style="list-style-type: none"> – Literature research – Comparing the products CLT and glulam (GLT)
Further steps To Do's	– summary of state-of-knowledge (update) + proposal for possible regulation in design standards
Currently available Literature	<ul style="list-style-type: none"> – TC250/SC5/PT1: Working draft; Version 2017_10_13 [42] – TC250/SC5/PT1: Background document; Version 2017_10_13 [43] – EN 16351 – EN 1995-1-1 – ETA-16/0055
Suggestions for possible papers, scientific theses and further work	– Evaluation and transfer of the design models from glulam to cross laminated timber

Background

None

6.5 Notched Members

6.5.2 Beams and plates with a notch at the support

Chapter	Notched members
Focus of work	<ul style="list-style-type: none">– Literature research– Comparing the products CLT and glulam (GLT)
Further steps To Do's	<ul style="list-style-type: none">– summary of state-of-knowledge (update)– proposal for possible regulation in design standards
Currently available Literature	<ul style="list-style-type: none">– TC250/SC5/PT1: Working draft; Version 2017_10_13 [42]– TC250/SC5/PT1: Background document; Version 2017_10_13 [43]– EN 16351 and EN 1995-1-1
Suggestions for possible papers, scientific theses and further work	<ul style="list-style-type: none">– Evaluation and transfer of the design models for notches in glulam to cross laminated timber with notches.

Background: PT 1.(3)

Effective height in a notched cross laminated timber plate

PT SC5.T1 still intends to find a verification method for notches in cross laminated timber plates. Such verifications are part of one national technical approval [Z 9.1-482] and proposals for a verification deducted from verifications for LVL can be found in [Wallner-Novak et. al., 2013].

6.6 System Strength

Chapter	System strength
Focus of work	<ul style="list-style-type: none"> – k_{sys} – definition of quantile values for cross section width smaller than one board width (remaining cross sections due to cut-outs, windows ...)
Further steps To Do's	– summary of state-of-knowledge (update) + proposal for possible regulation in design standards
Currently available Literature	<ul style="list-style-type: none"> – TC250/SC5/PT1: Working draft; Version 2017_10_13 [42] – TC250/SC5/PT1: Background doc.; Vers. 2017_10_13 [43] – EN 16351 – EN 1995-1-1
Suggestions for possible papers, scientific theses and further work	– Investigation of the influence on the strength properties of CLT due to the reduction of the board widths according to subsequently produced cut-outs (windows)

Background: PT.1-5.4 Cross laminated timber

Reduction factors for members with reduced width

Within cross laminated timber plates with reduced widths, laminations might be reduced in width and strengths too.

If a cross laminated timber plate is intended to be structural, the minimum width b_{CL} shall be at least its thickness t_{CL} . For cross laminated timber plates having such a width, it can be assumed to either have one untrimmed lamination or two or three laminations, two of them trimmed, in the layers having fibres parallel to the span. In the latter case a system factor could be applied.

Cross laminated timber subjected to bending out of plane having a width b_{CL} of less than the thickness t_{CL} shall not be taken as structural.

For member widths b_{CL} between t_{CL} and 600 mm PT SC5.T1 proposes linear interpolation.

6.7 Vibrations

Chapter	Vibrations
Focus of work	<ul style="list-style-type: none"> – Literature research – Comparing CLT and other types of floor systems
Further steps To Do's	<ul style="list-style-type: none"> – summary of state-of-knowledge (update) + proposal for possible regulation in design standards
Currently available Literature	<ul style="list-style-type: none"> – TC250/SC5/PT1: Working draft; Version 2017_10_13 [42] – TC250/SC5/PT1: Background document; Version 2017_10_13 [43] – Bachmann (1997) [8] – Blaß (2004) [16] – DIN 1052:2004-08. – DIN 1055-100:2001-03 – Eibl (1997) – EN 16351 – EN 1995-1-1:2004 – Fitz (2012) – Hamm (2006) – Hamm (2008) – Hamm (2009) – ISO 2631-2 – Kreuzinger (1995) [116] – Kreuzinger (1999) [117], [118] – Kreuzinger (2003) [121] – Mohr (2001) [127] – Murray (2003) [132] – ON B 1995-1-1 – Petersen (1996) [143] – SIA 265 – Tredgold (1828) [173] – Winter (2009) [184]
Suggestions for possible papers,	<ul style="list-style-type: none"> – Harmonisation of the verification procedures of CLT and GLT taking into account light and heavy floor structures – Considering the effects resulting from boundary conditions

scientific theses and further work	along the edges (semi rigid moment connection between wall and ceiling, etc.) – Application of the advanced method (ISO 10137)
---	---

Background PT.1-9.3.4 Heavyweight floors

The vibrational behaviour of floors is typically checked by three verifications, see e.g. EN 1995-1-1:2010:

- a check of the natural frequency (frequency criteria);
- a check of the deflection or stiffness due to a single load (stiffness criteria); and
- a check of the velocity or acceleration due to an impulse (velocity criteria).

Hamm, P.; Richter, A. and Winter S. [Hamm et al., 2010] report on measurements of floors in residential buildings classified as floors with higher, lower or no demands. For timber beam floors in residential buildings a deflection limit of 0.5 mm under a point load of 2 kN for floors with higher demands and of 1 mm for floors with lower demands are given. A frequency limit of 8 Hz is given for floors with higher demands and of 6 Hz for floors with lower demands. An additional verification of the acceleration criteria is needed, if the natural frequency is above 4.5 Hz but below the frequency limits given above.

Thiel, A. and Schickhofer, G. [Thiel et al., 2012] and Thiel, A.; Zimmer, S.; Augustin, M. [Thiel, A. et al., 2013] compare different verification methods for vibrational behaviour with a large number of results from testing CLT floors. They report, that the calculated results in almost all cases were very conservative and advise to take into account the shear flexibility of cross laminated timber, the transverse bending stiffness and the influence of the flexibility of supports. In Thiel, A. and Schickhofer, G. [Thiel et al., 2012] a modified procedure for the verification similar to the verification according to Hamm / Richter is proposed.

Zimmer, S.; Augustin, A. [Zimmer, S. et al., 2016] report on measurements on cross laminated timber floors in residential buildings. They propose to distinguish between floor classes representing different levels of demands, similar to those given in [Hamm et al., 2010]. The proposed equations for verification and the criteria they applied are almost identical to those given in [Hamm et al., 2010]. Only the stiffness criteria is given for a point load of 1 kN instead of 2 kN with limit values which are half the values given in [Hamm et al., 2010]. Additional information on the consideration of the transverse bending strength is given.

PT SC5.T1 proposes to apply the floor classes, verification process and limit values according to [Zimmer et al., 2016] not only for cross laminated timber floorings but also for other floors with an overall permanent weight per unit area of at least 50 kg/m².

It should be checked, if the proposed equations are also applicable for lightweight floorings.

7 Connections with Metal Fasteners

Not part of work in WG 2 / TG 1 & TG 3.

8 Components and Assemblies

Not part of work in WG 2 / TG 1 & TG 3.

- T-Beam
- Ribbed Beams

9 Execution and Control

Not part of work in WG 2 / TG 1 & TG 3.

Literature for COST FP1402 WG2-TG1 document

- [1] Aicher, S. (1987): *Bemessung biegebeanspruchter Sandwichbalken mit dem modifizierten γ -Verfahren*, In: Bautechnik; Nr.: 03/1987, S. 79-86.
- [2] Aicher, S.; Roth, W. (1987): *Ein modifiziertes γ -Verfahren für das mechanische Analogon: dreischichtiger Sandwichverbund-zweiteiliger verschieblicher Verbund*, In: Bautechnik; Nr.: 01/1987, S. 21-29.
- [3] Allgemeine bauaufsichtliche Zulassung des Deutschen Instituts für Bautechnik Z 9.1-501, *Leno Brettsperrholz*, Holder: Merk Timber GmbH, valid until 03.06.2019
- [4] Andreolli M, Rigamonti, MA Tomasi R (2014): *Diagonal compression test on cross laminated timber panels*. WCTE, Quebec, Canada.
- [5] Augustin, M.; Bogensperger, T.; Schickhofer, G. and Thiel, A. (2017): *Lasteinleitung in Wandscheiben aus BSP – Bestimmung der wirksamen Lastverteilmittigkeit – Kurzfassung und Anwendungsbeispiel*, Report holz.bau forschungsgmbh and TU Graz Graz, 2017.
- [6] Augustin, M.; Flatscher, G.; Tripolt, M. and Schickhofer, G. (2017): *Messung der Vorkrümmungsamplituden von planmäßig mittig gedrückten BSP-Elementen zur Festlegung des Imperfektionsbeiwertes für den Knicknachweis*, holz.bau forschung GmbH Graz und TU Graz, 2017
- [7] Augustin, M.; Thiel, A. (2017): *Proposal for the determination of the effective width and the verification of ribbed plates*, Report holz.bau forschungsgmbh and TU Graz Graz, 2017.
- [8] Bachmann, H. et al. (1997), *Vibration Problems in Structures – Practical Guidelines*, 2nd Edition, Birkhäuser Verlag Basel, Berlin, Boston.
- [9] Bader, H., Niemz, P., Sonderegger, W., (2007): *Untersuchungen zum Einfluss des Plattenaufbaus auf ausgewählte Eigenschaften von Massivholzplatten*, Holz Roh Werkst. 65: 173-181
- [10] Bejtka, I. (2010): *Cross (CLT) and diagonal (DLT) laminated timber as innovative material for beam elements*, Karlsruher Institut für Technologie (KIT), Lehrstuhl für Ingenieurholzbau und Baukonstruktionen. KIT Scientific Publishing: Karlsruher Berichte zum Ingenieurholzbau 17, ISBN 978-3-86644-604-5, 2010

- [11] Blaß H.J., Flaig M. (2012): *Stabförmige Bauteile aus Brettsperrholz*, Karlsruher Berichte zum Ingenieurholzbau, No. 24, Karlsruhe Institute of Technology (KIT), ISBN 978-3-86644-922-0 (in German).
- [12] Blaß H.J., Görlacher R. (2002): *Zum Trag- und Verformungsverhalten von Brettsperrholz-Elementen bei Beanspruchung in Plattenebene: Teil 2. Bauen mit Holz*, 12:30–34 (in German).
- [13] Blaß, H. (2015): *Ermittlung des 5%-Quantils des Produkts aus Elastizitätsmodul und Torsionsschubmodul für Brettschichtholz*. Report Lehrstuhl für Ingenieurholzbau und Baukonstruktionen, KIT, 2015.
- [14] Blaß, H., Flaig, M. (2014): *Keilgezinkte Rahmenecken und Satteldachträger aus Brettsperrholz*. Karlsruher Berichte zum Ingenieurholzbau, Bd. 29, KIT Scientific Publishing, Karlsruhe, Germany, 2014.
- [15] Blaß, H.J., Fellmoser, P. (2003): *Bemessung von Mehrschichtplatten*, Forschungsbericht, Universität Karlsruhe.
- [16] Blaß, H.J.; Ehlbeck, J.; Kreuzinger, H. (2004); Steck, G., *Erläuterungen zu DIN 1052:2004-08; Entwurf, Berechnung und Bemessung von Holzbauwerken*, 1. Auflage, Hrsg.: DGfH Innovations- und Service GmbH, München, 2004.
- [17] Bogensperger, T. (2014): *Lasteinleitung in Wandscheiben aus Brettsperrholz*. Forschungsbericht, holz.bau forschungs gmbh, 2014
- [18] Bogensperger, T., Augustin, M., Schickhofer, G. (2011): *Properties of CLT-panels exposed to compression perpendicular to their plane. International Council for Research and Innovation in Building and Construction, Working Commission W18 – Timber Structures, Meeting 44, CIB-W18/44-12-1, Alghero, Italy, pp15*
- [19] Bogensperger, T., Moosbrugger, T., Schickhofer, G. (2007): *New test configuration for CLT-wall-elements under shear load*. CIBW18/40-21-2, Bled, Slovenia.
- [20] Bogensperger, T., Moosbrugger, T., Silly, G. (2010): *Verification of CLT-plates under loads in plane*. WCTE, Riva del Garda, Italy.
- [21] Bogensperger, T., Silly, G., Schickhofer, G. (2012): *Comparison of methods of approximate verification procedures for cross laminated timber*, TU Graz, 2012.

- [22] Bogensperger, T.; Jöbstl, R. (2015): *Concentrated load introductions*, In: CLT Proceedings of INTER, Paper 48-12-1 ,INTER, Šibenik /SL
- [23] Bonigut, J.; Stephani, B.; Dube, H. (2010): *Eigenschaften thermisch vergüteter Massivholzplatten und OSB*. Teil 2: Langzeiteigenschaften. In: Holztechnologie 51 (5), S. 16-20.
- [24] Bosl R. (2002): *Zum Nachweis des Trag- und Verformungsverhaltens von Wandscheiben aus Brettsperrholz* (in German). Military University Munich, Munich (in German).
- [25] Brandner R, Bogensperger T, Schickhofer G (2013): *In plane Shear Strength of Cross Laminated Timber (CLT)*, Test Configuration, Quantification and influencing Parameters. CIB-W18/46-12-2, Vancouver, Canada.
- [26] Brandner, R., Flatscher, G., Ringhofer, A, Schickhofer, G. and Thiel, A (2013): *Cross laminated timber (CLT) – Overview and development*, In: European Journal of Wood and Wood products, Vol. 74, No. 3, 03.2013
- [27] Brandner, R., Dietsch, P., Dröscher, J., Schulte-Wrede, M., Kreuzinger, H. and Sieder, M. (2017), *Cross laminated timber (CLT) diaphragms under shear: Test configuration, properties and design*, Construction and Building Materials, 2017, Vol. 147, pp. 312–327.
- [28] Brandner, R., Flatscher, G., Ringhofer, A., Schickhofer, G., Thiel, A. (2016): *Cross laminated timber (CLT): overview and development*, 2016, European Journal of Wood and Wood Products, 74, 331–351.
- [29] Brandner, R., Schickhofer, G. (2014): *Properties of cross laminated timber (CLT) in compression perpendicular to the grain*, Proceedings of INTER, Paper INTER/47-12-5, Bath / UK
- [30] Brandner, R.; Dietsch, P.; Dröscher, J.; Schulte-Wrede, M.; Kreuzinger, H.; Sieder, M.; Schickhofer, G.; Winter, S. (2015): *Shear properties of cross laminated timber (CLT) under in-plane load. Test configuration and experimental study*, 2nd INTER Meeting, Sibenik, Croatia, 2015
- [31] Brandner, R.; Schickhofer, G. (2006): *System effects of structural elements – determined for bending and tension*, 9th World Conference on Timber Engineering (WCTE 2006), Portland, Oregon, United States, 2006

- [32] Brandner, R.; Schickhofer, G. (2008): *Glued laminated timber in bending: new aspects concerning modelling*, Wood science and Technology. 42(5): 401-425, 2008
- [33] Brandner, R.; Schickhofer, G. (2014): *Properties of cross laminated timber (CLT) in compression perpendicular to the grain*, Proceedings of INTER, Paper INTER/47-12-5, Bath / UK, 2014
- [34] Bratulic, K. (2013): *Untersuchung ausgewählter Einflussparameter auf die Querdruckkenngrößen von Brettsper Holz*, Masterarbeit am Institut für Holzbau und Holztechnologie der TU Graz 2013
- [35] Casagrande D., Rossi S., Sartori T., Tomasi R. (2016): *Proposal of an analytical procedure and a simplified numerical model for elastic response of single-storey timber shear-walls*, Construction and Building Materials, ISSN 0950-0618, pp. 1101-1112, 2016
- [36] CEN/TC 250/SC 5: *Structural Eurocodes – Timber Structures – SC5.PT1 ‘CLT’ (2016)*, Working draft of design of CLT in a revised Eurocode 5-1-1: Version 2017_03_25.
- [37] CEN/TC 250/SC 5: *Structural Eurocodes – Timber Structures – SC5.PT1 ‘CLT’ (2016)*, Background document for design of cross laminated timber in a revised Eurocode 5-1-1: Version 2017_03_06.
- [38] CEN/TC 250/SC 5: *Structural Eurocodes – Timber Structures – SC5.PT1 ‘CLT’ (2016)*, Working draft of design of CLT in a revised Eurocode 5-1-1: Version 2017_07_11.
- [39] CEN/TC 250/SC 5: *Structural Eurocodes – Timber Structures – SC5.PT1 ‘CLT’ (2016)*, Background document for design of cross laminated timber in a revised Eurocode 5-1-1: Version 2017_04_13.
- [40] CEN/TC 250/SC 5: *Structural Eurocodes – Timber Structures – SC5.PT1 ‘CLT’ (2016)*, Working draft of design of CLT in a revised Eurocode 5-1-1: Version 2017_08_09.
- [41] CEN/TC 250/SC 5: *Structural Eurocodes – Timber Structures – SC5.PT1 ‘CLT’ (2016)*, Background document for design of cross laminated timber in a revised Eurocode 5-1-1: Version 2017_08_09.
- [42] CEN/TC 250/SC 5: *Structural Eurocodes – Timber Structures – SC5.PT1 ‘CLT’ (2016)*, Working draft of design of CLT in a revised Eurocode 5-1-1: Version 2017_10_13.

- [43] CEN/TC 250/SC 5: *Structural Eurocodes – Timber Structures – SC5.PT1 ‘CLT’ (2016)*, Background document for design of cross laminated timber in a revised Eurocode 5-1-1: Version 2017_10_13.
- [44] Christovasilis I.P., Brunetti M., Follesa M., Nocetti M., Vassalo D. (2016): *Evaluation of the mechanical properties of cross laminated timber with elementary beam theories*, IN: Construction and building materials, 122, 202-213.
- [45] Ciampitti, A. (2013): *Untersuchung ausgewählter Einflussparameter auf die Querdruckkenngrößen von Brettsperrholz*, Master Thesis, Institute of Timber Engineering and Wood Technology, Graz University of Technology, pp133 (in German)
- [46] Clauß, S.; Kröppelin, U.; Niemz, P. (2010a): *Quellverhalten dreischichtiger Massivholzplatten. Teil 1: Freie Quellung*, In: Holztechnologie 51 (1), S. 5-10.
- [47] Clauß, S.; Kröppelin, U.; Niemz, P. (2010b): *Quellverhalten dreischichtiger Massivholzplatten. Teil 2: Partiiell behinderte Quellung*, In: Holztechnologie 51 (2), S. 5-10.
- [48] CSA O86-14: *Engineering design in wood*, Toronto, Canada: CSA, Canadian Standard Association, 2014
- [49] DIN 1052:2004-08, *Entwurf, Berechnung und Bemessung von Holzbauwerken – Allgemeine Bemessungsregeln und Bemessungsregeln für den Hochbau*, Berlin, August 2004.
- [50] DIN 1055-100:2001-03, *Einwirkungen auf Tragwerke, Teil 100: Grundlagen der Tragwerksplanung, Sicherheitskonzept und Bemessungsregeln*, Berlin, März 2001.
- [51] DIN 52184 (1979): *Bestimmung der Quellung und Schwindung*, Ausgabe Mai 1979
- [52] DIN EN 1995-1-1/NA, *Nationaler Anhang - National festgelegte Parameter – Eurocode 5: Bemessung und Konstruktion von Holzbauten – Teil 1-1: Allgemeines - Allgemeine Regeln und Regeln für den Hochbau*
- [53] Dröscher, J. (2014): *Prüftechnische Ermittlung der Schubkenngrößen von BSP-Scheibenelementen und Studie ausgewählter Parameter (in German)*, Master Thesis, Graz University of Technology, Graz (in German).

- [54] Dröscher, J., Brandner, R. (2013): *Abschätzung der Scheibenschubfestigkeit mit dem Prüfverfahren nach Kreuzinger und Sieder (2013)*, Research Report, Institute of Timber Engineering and Wood Technology, Graz University of Technology (in German).
- [55] Dujic, B., Klobcar, S., Zarnic, R. (2008): *Shear capacity of cross-laminated wooden walls*, 10th World Conference on Timber Engineering 2008, 3, pp. 1641-1648, 2008
- [56] Ehrhart, T., Brandner, R., Schickhofer, G., Frangi, A. (2015): *Rolling shear properties of some European timber species with focus on cross laminated timber (CLT): test configuration and parameter study*, 2nd Inter-meeting, Sibenik, Croatia, 2015
- [57] Bogensperger, T, Jöbstl, R. (2015); *Concentrated load introduction*, In: CLT Proceedings of INTER, Paper 48-12-1 INTER, Šibenik, Croatia, 2015
- [58] Eibl, J.; Häussler-Combe, U. (1997): *Baudynamik*, In: Beton-Kalender 1997, Teil II; Verlag Ernst & Sohn, Berlin, 1997; S. 755-861
- [59] EN 13353, Solid wood panels (SWP) – Requirements
- [60] EN 14080:2013, *Timber structures – Glued laminated timber and glued solid timber – Requirements*
- [61] EN 14081-1, *Timber structures – Strength graded structural timber with rectangular cross section – Part 1: General requirements*
- [62] EN 16351:2015, *Timber structures – Cross laminated timber – Requirements*
- [63] EN 1995-1-1:2004, *Eurocode 5: Bemessung und Konstruktion von Holzbauten – Teil 1-1: Allgemeines – Allgemeine Regeln und Regeln für den Hochbau*, Deutsche Fassung, November 2004.
- [64] EN 338:2016 *Structural timber – Strength classes*, Release April 2016
- [65] EN 408, *Timber structures – Structural timber and glued laminated timber – Determination of some physical and mechanical properties*
- [66] ETA 06/0138: KLH ETA including commentary.
- [67] ETA-08/0238: Schilliger Holz-Industrie AG: *Solid wood slab element to be used as a structural element in buildings*, ETA-08/0238, valid until June 10, 2018.

- [68] ETA-11/0464: EGOIN SA: *Solid wood slab element to be used as a structural element in buildings*, ETA-11/0464, issued at 20 April 2017.
- [69] ETA-06/0009: Binderholz Bausysteme GmbH: Binderholz Brettspertholz BBS – Multilayered timber elements for walls, ceilings, roofs and special construction purposes, ETA-06/0009, valid until 20.12.2016
- [70] ETA-06/0138: KLH Massivholz GmbH: Solid wood slab elements to be used as structural elements in buildings, ETA-06/0138, Gültig bis 09.09.2017
- [71] ETA-09/0036: Mayr-Melnhof Holz Holding AG: Solid wood slab elements to be used as structural elements in buildings, ETA-09/0036, valid until 16.06.2018
- [72] ETA-09/211: Lignotrend AG: Timber units for walls, roofs and ceilings, ETA 09/0211, valid until 27.06.2018
- [73] ETA-11/0189: W. u. J. Derix GmbH & Co. KG: Solid wood slab elements to be used as structural elements in buildings, ETA-11/0189
- [74] ETA-11/0210: Merkle Holz GmbH: Solid wood slab elements to be used as structural elements in buildings, ETA-11/0210
- [75] ETA-12/0327: Eugen Decker Holzindustrie KG: Solid wood slab elements to be used as structural elements in buildings, ETA-12/0327, valid until 05.09.2017
- [76] ETA-14/0349: Stora Enso Wood Products Oy Ltd.: Solid wood slab elements to be used as structural elements in buildings, ETA-14/0349
- [77] ETA-16/0055 “Massive plattenförmige Holzbauelemente für tragende Bauteile in Bauwerken“, Österreichisches Institut für Bautechnik, Wien, 2016.
- [78] Europäisches Bewertungsdokument EAD 13005-000304 – „Massive plattenförmige Holzbauelemente für tragende Bauteile in Bauwerken“, Ausgabe August 2014
- [79] Fitz, M. (2012): *Untersuchung des Schwingungsverhaltens von Deckensystemen aus Brettspertholz (BSP)*, Diplomarbeit an der TU Graz.
- [80] Flaig, M. (2013): *Tragfähigkeit und Steifigkeit von Biegeträgern aus Brettspertholz bei Beanspruchung in Plattenebene*. Dissertation,

Fakultät für Bauingenieur, Geo-und Umweltwissenschaften, Karlsruher Institut für Technologie, Karlsruher Berichte zum Ingenieurholzbau, Bd. 27, KIT Scientific Publishing, Karlsruhe, Germany, 2013.

- [81] Flaig, M. (2015): *Design of CLT beams with large finger joints at different angles*, 2nd INTER Meeting, Sibenik, Croatia, 2015
- [82] Flaig, M.; Blaß, H. (2013): *Shear strength and shear stiffness of CLT-beams loaded in plane*, 46th CIB-W18 Meeting, Vancouver, Canada, 2013
- [83] Flaig, M.; Blaß, H. (2014): *Bending strength of cross laminated timber beams loaded in plane*, In: Proceedings of the World Conference on Timber Engineering 2014, Quebec City, Canada August 10-14 2014.
- [84] Flaig, M.; Blaß, H. (2015): *Keilgezinkte Rahmenecken und Satteldachträger aus Brettsperrholz*, Forschungsbericht KIT, 2015
- [85] Flatscher (2015): *Experimental tests on cross-laminated timber joints and walls*, ICE Journal Structures and Buildings, 2015, 168, 868-877
- [86] Flatscher and Schickhofer (2016): *Displacement-based determination of laterally loaded cross laminated timber (CLT) wall systems*, INTER/49-12-1
- [87] Follesa M., Christovasilis I., Vassallo D., Fragiaco M., Ceccotti A. (2013): *Seismic design of multi-storey cross laminated timber buildings according to Eurocode 8*, Ingegneria Sismica 30(4):27-53, 2013
- [88] Gagnon, S.; Pirvu C. (eds.) (2011): *CLT-Handbook: cross laminated timber*, Canadian edition. ISBN 978-0-86488-553-1, 2011
- [89] Gavric, I., Fragiaco, M., Ceccotti, A. (2015): *Cyclic behavior of CLT wall systems: Experimental tests and analytical prediction models*, In: Journal of Structural Engineering (United States), 141 (11)
- [90] Gereke, T., (2009): *Moisture-Induced Stresses in Cross-Laminated Wood Panels*, Dissertation, ETH Zürich.
- [91] Gereke, T.; Hass, P.; Niemz, P. (2010): *Moisture-induced stresses and distortions in spruce cross-laminates and composite laminates*, In: Holzforschung 64 (1), S. 127-133. DOI: 10.1515/hf.2010.003.
- [92] Görlacher, R. (2002): *Ein Verfahren zur Ermittlung des Rollschubmoduls von Holz*, In: Holz als Roh- und Werkstoff, 60:317-322, 2002

- [93] Guggenberger, W., Moosbrugger T. (2006): *Mechanics of cross-laminated timber plates under uniaxial bending*, WCTE 2006, Portland, USA.
- [94] Halili, Y. (2008): *Versuchstechnische Ermittlung von Querdruckkenngrößen für Brettsperrholz*, Diploma Thesis, Institute of Timber Engineering and Wood Technology, Graz University of Technology, pp179 (in German)
- [95] Hamm, P. (2006): *Warum Decken zu schwingen beginnen*, Bauen mit Holz, 3/2006, S. 24-29.
- [96] Hamm, P. (2008): *Schwingungsverhalten von Decken bei Auflagerung auf Unterzügen*, holzbau, die neue quadriga, 1/2008.
- [97] Hamm, P., Richter, A (2009): *Personeninduzierte Schwingungen bei Holzdecken – Neue Erkenntnisse führen zu neuen Bemessungsregeln*, Ingenieurholzbau – Karlsruher Tage: Forschung für die Praxis, Oktober 2009, Universität Karlsruhe.
- [98] Hamm, P.; Richter, A.; Winter, S. (2010): *Floor vibrations – new results*. In: Proceedings World Conference on Timber Engineering, 2010
- [99] Hasuni, H.K., Al-douri, K., Hamodi, M.H. (2009): *Compression strength perpendicular to grain in cross-laminated timber (CLT)*, Master thesis, School of Technology and Design, Växjö University, Sweden
- [100] Heimeshoff, B. (1997): *Zur Berechnung von Biegeträgern aus nachgiebig miteinander verbundenen Querschnittsteilen im Ingenieurholzbau*, in: Holz als Roh- und Werkstoff45 (1987) 237-241, 1997.
- [101] Horvat, D. (2013): *Stability Behaviour of Cross-laminated Timber (CLT) Columns under Compressive Axial Load*, PhD thesis, University of British Columbia, Vancouver, BC, Canada, 2013.
- [102] Hirschmann, B. (2011): *Ein Beitrag zur Bestimmung der Scheibenschubfestigkeit von Brettsperrholz (in German)*, Master Thesis, Graz University of Technology, Graz (in German).
- [103] Hummel et al. (2013): *CLT wall elements under cyclic loading – details for anchorage and connection*, COST Action FP1004, Focus Solid Timber Solutions – European Conference on Cross Laminated Timber (CLT), The University of Bath, 2013, 152-165

- [104] ISO 2631-2, Evaluation of human exposure to whole-body vibration Part 2: Continuous and shock-induced vibration in buildings (1 to 80 Hz), Genf, Schweiz International Organization for Standardization, 1989.
- [105] Jacobs, A. (2005): *Zur Berechnung von Brettlagenholz mit starrem und nachgiebigem Verbund unter plattenartiger Belastung unter besonderer Berücksichtigung des Rollschubes und der Drillweichheit*, Dissertation, Universität der Bundeswehr, München, 2005
- [106] Jeitler, G. (2004): *Versuchstechnische Ermittlung der Verdrehungskenngrößen von orthogonal verklebten Brettlamellen (in German)*, Diploma Thesis, Graz University of Technology, Graz (in German).
- [107] Jeitler, G., Brandner, R. (2008): *Modellbildung für Duo-, Trio- und Quattro-Querschnitte*, In: Schickhofer, G. and Brandner, R. (eds.) 7. Grazer Holzbau-Fachtagung (7. GraHFT'08): Modellbildung für Produkte und Konstruktionen aus Holz – Bedeutung von Simulation und Experiment. Verlag der Technischen Universität Graz, Graz, 2008
- [108] Jöbstl, R. A.; Schickhofer, G. (2007): *Comparative examination of creep of GLT- and CLT-slabs in bending*, In: Proceedings of CIB W18, Bled, 2007, Paper 40-12-3
- [109] Jöbstl, R.; Bogensperger, T.; Schickhofer, G. (2006): *A contribution to the design band system effect of cross laminated timber (CLT)*, 39th CIB-W18 Meeting, Florence, Italy, 2006
- [110] Jöbstl, R.A., Bogensperger T, Schickhofer G (2008): *In-plane shear strength of cross laminated timber*, CIB-W18/41-12-3, St. Andrews, Canada.
- [111] Jöbstl, R.A., Bogensperger T, Schickhofer G, Jeitler G (2004): *Mechanical Behaviour of Two Orthogonally Glued Boards*, WCTE, Lahti, Finland.
- [112] Karabeyli, E.; Douglas, B. (eds.) (2013): *CLT-Handbook: cross laminated timber*, US edition. ISBN 978-0-86488-547-0, 2013
- [113] Keylwerth, R. (1962): *Untersuchungen über freie und behinderte Quellung – Zweite Mitteilung: Behinderte Quellung*, Holz Roh Werkst. 20: 292-303

- [114] Keylwerth, R. (1968): *Praktische Untersuchungen zum Holzfeuchte-Gleichgewicht*, Holz Roh-Werkstoff 27: 285–290
- [115] Krenn, H. Moosbrugger, T., Bogensperger, T. (2016): *Stability of Cross Laminated Timber (CLT) Beams*, WCTE 2016, Vienna, 2016
- [116] Kreuzinger, H. (1995): *Schwingungen von Fußgängerbrücken – Berechnung und Messung*, In: Informationsdienst Holz, Holzbauwerke STEP 3, Fachverlag Holz, 1995; S. 17/1-17/16
- [117] Kreuzinger, H. (1999): *Flächentragwerke - Platten, Scheiben und Schalen – Berechnungsmethoden und Beispiele*, Fachverlag Holz Düsseldorf, S. 43-60, 1999.
- [118] Kreuzinger, H. (1999): *Platten, Scheiben und Schalen. Bauen mit Holz*, 101. Jahrgang, Heft 1, S. 34-39, 1999.
- [119] Kreuzinger, H. (2000): *Verbundkonstruktionen aus nachgiebig miteinander verbundenen Querschnittsteilen*, In: Ingenieurholzbau Karlsruher Tage. Bruderverlag Karlsruhe, S. 43-55, 2000.
- [120] Kreuzinger, H. (2002): *Verbundkonstruktionen*, In: Holzbaukalender 2002. Bruderverlag Karlsruhe, S.598-621, 2002.
- [121] Kreuzinger, H., (2003): *Schwingungsanalyse*, Holz-Beton-Verbundkonstruktionen, Fachtagung Holz-Beton-Verbundbau, Stuttgart, 13. Oktober 2003.
- [122] Kreuzinger, H., Sieder M (2013): *Einfaches Prüfverfahren zur Bewertung der Schubfestigkeit von Kreuzlagenholz / Brettsper Holz (in German)*, Bautechnik, 90(5):314–316 (in German).
- [123] Kreuzinger, H.; Mohr, B. (1999): *Gebrauchstauglichkeit von Wohnungsdecken aus Holz*, Abschlussbericht Januar 1999, TU München, Fachgebiet Holzbau, Forschungsvorhaben durchgeführt für die EGH in der DGfH.
- [124] Mestek, P. (2011): *Punktgestützte Flächentragwerke aus Brettsper Holz (BSP) – Schubbemessung unter Berücksichtigung von Schubverstärkungen*, Dissertation, Technische Universität München, München, 2011
- [125] Mestek, P. Kreuzinger, H. Winter, S., (2008): *Design of Cross Laminated Timber (CLT)*, In Proceedings of the 10th World Conference on Timber Engineering.

- [126] Mestek, P.; Winter, S. (2011): *Design concept for CLT-reinforced with self-tapping screws*, 44th CIB-W18 meeting, Alghero, Italy, 2011
- [127] Mohr, B. (2001): *Schwingungen von Wohnungsdecken aus Holz, Stahl und Beton – Vorschläge für eine zutreffende Bewertung*, Ingenieurholzbau – Karlsruher Tage, Hrsg.: Universität Karlsruhe (TH), Lehrstuhl für Ingenieurholzbau und Baukonstruktionen und Bruderverlag, Karlsruhe, 2001. S. 81-98.
- [128] Moosbrugger, T., Neumüller, F., Neumüller, A. (2017): *Schwinden und Quellen von orthogonal verklebten Holzprodukten – Teil 1: Globales Schwindverhalten von Blockbohlen und Brettsperrhölzern*, in: holztechnologie 58 (2017) 5, IHD, Dresden, 2017.
- [129] Moosbrugger, T., Guggenberger, T., Neumüller, F., Neumüller, A. (2018): *Schwinden und Quellen von orthogonal verklebten Holzprodukten – Teil 3: Lokales Feuchteverhalten entlang der Plattenränder: Querschnittsverformung*, in: Holztechnologie 59 (2018) 1, IHD, Dresden, 2018.
- [130] Moosbrugger, T.; Bogensperger, T. und Krenn, H. (2015): *Kippen hoher BSP-Träger*, Bauen mit Holz, Heft 12/2015, Bruderverlag Karlsruhe, 2015.
- [131] Moosbrugger, T.; Schickhofer, G., Unterwieser, H., Krenn, H. (2006): 5. Grazer Holzbau-Fachtagung: *Brettsperrholz -- Ein Blick auf Forschung und Entwicklung*, Institut für Holzbau und Holztechnologie der TU Graz – ISBN 3-902020-32-6, 2006
- [132] Murray, T. M., Allen, D. E.; Ungar, E. (2003): *Floor vibrations due to human activity*, Steel design guide series 11, American Institute of Steel Construction, Chicago, Illinois, Oct. 2003.
- [133] Nakajima, S.A., Miyatake, A.b, Shibuwasa, T.b, Araki, Y.c, Yamaguch, N.c, Haramiishi, T.d, Ando, N.e, Yasumura, M. (2014): *Creep and duration of load characteristics of cross laminated timber*" World Conference on Timber Engineering: Renaissance of Timber Construction, WCTE 2014; Quebec City, Canada.
- [134] Niemz, P. (1993): *Physik des Holzes und der Holzwerkstoffe*, DRW-Verlag, ISBN 3-87181-324-9, 1993.

- [135] Niemz, P.; Bärtsch, H.; Howald, M. (2005): *Untersuchungen zur Feuchteverteilung und Spannungsbildung in Holzbauteilen bei Wechselklimalagerung*, In: Schweiz. Z. Forstwes. 156(2005) 3-4: 92-99.
- [136] Niemz, P.; Petzold, H.; Häupl, P. (2003): *Untersuchungen zur Messung und Simulation der Feuchteänderung von dreischichtigen Massiv-Holzplatten bei Klimawechsel*, Holz als Roh- und Werkstoff 61, 1: 8–12.
- [137] OIB-260-001/99-116, *Common Understanding of Assessment Procedure (CUAP): Solid wood slab element to be used as a structural element in buildings*, Version June 2005.
- [138] ÖNORM B 1995-1-1, *Eurocode 5: Bemessung und Konstruktion von Holzbauten, Teil 1-1: Allgemeines – Allgemeine Regeln und Regeln für die den Hochbau*
- [139] ÖNORM B 3012:2003: *Holzarten – Kennwerte zu den Benennungen und Kurzzeichen der ÖNORM EN 13556*, Ausgabe 01.12.2003
- [140] ÖNORM EN 318:2002: *Holzwerkstoffe – Bestimmung von Maßänderungen in Verbindung mit Änderungen der relativen Luftfeuchte*; Ausgabe 01.05.2002
- [141] Park, H.M., Fushitani, M., Sato, K., Kubo, T., Byeon, H.S. (2002): *Bending creep performances of cross-laminated sugi wood" (in Japanese)*, 2002, Mokuzai Gakkaishi 48:166–177.
- [142] Park, H.M., Fushitani, M., Sato, K., Kubo, T., Byeon, H.S. (2006): *Bending creep performances of three-ply cross-laminated woods made with five species*, 2006, J. Wood Sci., 52 (3), pp. 220–229.
- [143] Petersen, C. (1996), *Dynamik der Baukonstruktionen*, Vieweg Verlag, Braunschweig/ Wiesbaden, 1996
- [144] Pirvu, C., Karacabeyli, E. (2014): *Time-dependent behaviour of CLT"*, *World Conference on Timber Engineering*, Renaissance of Timber Construction, WCTE 2014, Quebec City, Canada.
- [145] Pischl, R. (1968): *Ein Beitrag zur Berechnung zusammengesetzter hölzerner Biegeträger*, Der Bauingenieur, 43. Jahrgang, S.448-452, 1968.
- [146] Pischl, R. (1969): *Die praktische Berechnung zusammengesetzter hölzerner Biegeträger mit Hilfstafeln zur Berechnung der Abminderungsfaktoren*, Der Bauingenieur, 44. Jahrgang, S.181-185, 1969.

- [147] Popovski and Karacabeyli (2011): *Seismic Performance of cross-laminated wood panels*. CIB-W18/44-15-7
- [148] Popper, R.; Niemz, P.; Eberle, G. (2004): *Untersuchungen zur Gleichgewichtsfeuchte und Quellung von Massivholzplatten*, In: Holz als Roh- u. Werkstoff 62 (3), S. 209-217. DOI: 10.1007/s00107-003-0461-y.
- [149] R. Brandner, T. Bogensperger, G. Schickhofer, (2013): *In plane Shear Strength of Cross Laminated Timber (CLT): Test Configuration, Quantification and influencing Parameters*“, CIB-W18/46-12-2, Vancouver, Canada, 2013.
- [150] Resch, L., (2010): *DÉVELOPPEMENT D'ÉLÉMENTS DE CONSTRUCTION EN BOIS DE PAYS LAMELLÉS ASSEMBLÉS PAR TOURILLONS THERMO-SOUDES*, (Chapter 1), Phd Thesis, Nancy Universite, France.
- [151] Salzmann C (2010:) *Ermittlung von Querdruckkenngrößen für Brettsperrholz (BSP)*, Master Thesis, Institute of Timber Engineering and Wood Technology, Graz University of Technology, pp198 (in German)
- [152] Schelling, W. (1968): *Die Berechnung nachgiebig verbundener zusammengesetzter Biegeträger im Ingenieurholzbau*, Dissertation TH Karlsruhe, 1968.
- [153] Schelling, W. (1998): *Genauere Berechnung nachgiebig verbundener Holzbiegeträger mit dem γ -Verfahren*, In: Festschrift E. Csiesielski. Werner-Verlag. S 10, April, 1998.
- [154] Schickhofer, G., Bogensperger, T., Moosbrugger, T., Herausgeber (2010): *BSPhandbuch*, Verlag der Technischen Universität Graz, 2. Auflage, ISBN 978-3-85125-109-8, 2010.
- [155] Schickhofer, G.; Bauer, H.; Thiel, A. (2015): *Mit neuen Tragelementen in die Zukunft des Holzbaus*, S-WIN Kurs 2015, S-WIN; c/o Lignum, ZürichBI.
- [156] Scholz, A. (2003): *Ein Beitrag zur Berechnung von Flächentragwerken aus Holz*, Dissertation, TU München, 2003.
- [157] Schwab, E., Steffen, A., Korte, C. (1997): *In-plane swelling and shrinkage of wood-based panels*, Holz als Roh- und Werkstoff, 55:227–233, 1997.

- [158] Serrano, E., Enquist B (2010): *Compression strength perpendicular to grain in cross-laminated timber (CLT)*, World Conference on Timber Engineering (WCTE), Riva del Garda, Italy, pp7.
- [159] SIA 265:2003, *Holzbau*, 2003 by SIA Zürich.
- [160] Silly, G. (2010): *Numerische Studien zur Drill- und Schubsteifigkeit von Brettsperrholz (BSP)*, Diploma-Thesis at Institut für Holzbau und Holztechnologie, Technische Universität Graz, 2010.
- [161] Silly, G. (2014): *Schubfestigkeit der BSP-Scheibe – numerische Untersuchung einer Prüfkfiguration (in German)*, Research Report, holz.bau forschungs gmbh, Graz University of Technology, Graz (in German).
- [162] Silly, G.; Thiel, A. (2013): *Analyse und numerische Simulation zur Entwicklung einer Prüfkfiguration für die Ermittlung der Rollschubkenngrößen von BSP-Elementen*, Präsentation beim COMET area meeting, holz.bau forschungs gmbh Graz, 15. Oktober 2013.
- [163] STSM Bidakov, A., (2017): *Strength properties of CLT in Tension perpendicular to the grain*, 2017, COST Action FP1402, STSM report.
- [164] Susteric, I.; Dujic, B. (2012): *Simplified cross laminated timber wall modelling for linear-elastic seismic analysis*, In: CIB-W18, 45-15-6, Växjö, Sweden, 2012.
- [165] Teknisk handbook (2006): *Bygge med massivtreelementer*, Teknisk handbook, 7 hefter i samleperm, Norsk Treteknisk Institutt, Vol. 1, Oslo, ISBN 82-7120-000-3, 2006
- [166] Thiel, A., Augustin, M., Bogensperger, T., Schickhofer, G. (2014): *Mitwirkende Breite bei Plattenbalken aus BSH und BSP – Kurzfassung und Anwendungsbeispiel*. Forschungsbericht, holz.bau forschungs gmbh, Graz, 2014.
- [167] Thiel, A., Brandner, R., (2016): *ULS Design of CLT Elements – Basics and some Special Topics*, Joint Conference of COST Actions FP1402 and FP1404 Cross Laminated Timber - a competitive wood product for visionary and fire safe buildings, Stockholm, Sweden.
- [168] Thiel, A., Schickhofer, G. (2010): *A software tool for designing cross laminated timber elements: 1D-plate-design*, Proceedings of the World Conference on Timber Engineering, WCTE 2010, Riva del Garda, Italy, 2010.

- [169] Thiel, A.; Schickhofer, G. (2012): *Design methods of Cross Laminated Timber concerning floor vibrations: a comparability study*, holz.bau forschungs gmbh and TU Graz; 2012
- [170] Thiel, A.; Zimmer, S.; Augustin, A. (2013): *CLT and floor vibrations: A comparison of design methods*, In. CIB-Proceedings, 2013
- [171] Tobisch, S. (2006) Methoden zur Beeinflussung ausgewählter Eigenschaften von dreilagigen Massivholzplatten aus Nadelholz. Dissertation, Universität Hamburg
- [172] Tomasi R. (2013): *Seismic behaviour of connections for buildings in CLT*, In: Focus solids timber solutions, European conference on cross-laminated timber (CLT), Graz: University of Bath, UK, 2013, p. 138-151. - ISBN: 1857901819. COST Action FP 1004, Graz, 21-22 may, 2013
- [173] Tredgold, T. (1828): *Elementary Principles of Carpentry*, 2nd Edition, Verlag unbekannt, 1828.
- [174] Unterwieser, H., and Schickhofer, G. (2013a): *Characteristic Values and Test Configurations of CLT with Focus on Selected Properties*, In: R. Harris, A. Ringhofer and G. Schickhofer (eds.) Focus Solid Timber Solutions – European Conference on Cross Laminated Timber (CLT), Proceeding, COST Action FP1004, 2013, ISBN 1857901819, pp. 53-73, Graz, Austria.
- [175] Unterwieser, H.; Schickhofer, G. (2013b): *Characteristic values and test configurations of CLT with focus on selected properties*, In: proceedings of Focus Solid Timber Solutions - European Conference on Cross Laminated Timber (CLT), Editor R. Harris, 21-22. Mai 2013
- [176] van der Put, T.A.C.M. (1991): *Discussion of the failure criterion for combined bending and compression*, CIB-W18/24-6-1, Oxford, United Kingdom.
- [177] van der Put, T.A.C.M. (2008): *Derivation of the bearing strength perpendicular to the grain of locally loaded timber blocks*, Holz als Roh- und Werkstoff, 66:409–417, DOI 10.1007/s00107-008-0258-0
- [178] van der Put, T.A.C.M. (2012): *Restoration of exact design for partial compression perpendicular to the grain*, Wood Material Science and Engineering, DOI 10.1080/17480272.2012.681703

- [179] van der Put, T.A.C.M. (2008): *Derivation of the bearing strength perpendicular to the grain of locally loaded timber blocks*, Holz als Roh- und Werkstoff 66, p. 409-417, Springer-V. 2008.
- [180] Wallner G (2004): *Versuchstechnische Ermittlung der Verschiebungskenngrößen von orthogonal verklebten Brettlamellen*, Diploma Thesis, Graz University of Technology, Graz (in German).
- [181] Wallner-Novak, M., Koppelhuber, J., Pock, K. (2013): *Brettsperrholz Bemessung -- Grundlagen für Statik und Konstruktion nach Eurocode*, Wien: proHolz Austria– ISBN 978-3-902320-96-4, 2013
- [182] Wang, J.; Mohammad, M.; Di Lenardo, B.; Sultan, M. (2016): *CLT panels subjected to combined out-of-plane bending and compressive axial loads*; WCTE 2016
- [183] Watson, C.; van Beerschoten, W.; Smith, T.; Pampanin, S.; Buchanan, Andrew H. (2013): *Shear strength and shear stiffness of CLT-beams loaded in plane*, In: Proceedings of CIB-Meeting, Vancouver, Canada, Paper 46-12-4, 26.–29. August 2013
- [184] Winter, S.; Hamm, P.; Richter, A. (2009): *Zwischenbericht zum Forschungsvorhaben: Schwingungstechnische Optimierung von Holz- und Holz-Beton-Verbunddecken*, DGfH 2009.
- [185] Winter, S.; Kreuzinger, H.; Mestek, P. (2009): *Flächen aus Brettstapeln, Brettsperrholz und Verbundkonstruktionen*, Fraunhofer IRB Verlag, Serie Holzbau der Zukunft, Teilprojekt 19, ISBN 978-3-8167-7875-2, 2009
- [186] Z9.1-482: KLH Massivholz GmbH: *KLH-Kreuzlagenholz*, Allgemeine bauaufsichtliche Zulassung Z-9.1-482, valid until 17.11.2020
- [187] Z9.1-501: Allgemeine bauaufsichtliche Zulassung des Deutschen Instituts für Bautechnik, *Leno Brettsperrholz*, Holder: Merk Timber GmbH, valid until 03.06.2019
- [188] Z9.1-534: Binderholz Bausysteme GmbH: *Binderholz Brettsperrholz BBS*, Allgemeine bauaufsichtliche Zulassung Z-9.1-534, valid until 17.11.2019
- [189] Z9.1-555: Lignotrend GmbH & Co. KG, *Lignotrend Elemente*, Allgemeine bauaufsichtliche Zulassung Z-9.1-555, valid until 26.01.2018

- [190] Z9.1-559: Stora Enso Wood Products Oy Ltd., *CLT-Cross Laminated Timber*, Allgemeine bauaufsichtliche Zulassung Z-9.1-559, 13. valid until 26.01.2017
- [191] Z9.1-576: Woodtec Fankhauser GmbH: „Woodtec“ *Massivholzplatten*, Allgemeine bauaufsichtliche Zulassung Z-9.1-576, valid until 28.04.2020
- [192] Z-9.1-680: Haas Holzprodukte GmbH: *Haas BSP Brettsperrholz*, Haas CLT Cross Laminated Timber HMS-Element. Allgemeine bauaufsichtliche Zulassung, valid until 23.11.2017
- [193] Z9.1-721: Eugen Decker Holz, Industrie KG: *ED-BSP (Brettsperrholz) aus Fichte, Kiefer oder Douglasie*, Zulassung Z-9.1-721, valid until 19.09.2018
- [194] Z9.1-793: Stephan Holzbau GmbH: *Brettsperrholzelemente “Stephan-Flexcross”*, Allgemeine bauaufsichtliche Zulassung Z-9.1-793, valid until 14.06.2016
- [195] Zimmer, Severin; Augustin, A. (2016): *Vibrational behaviour of cross laminated timber floors in residential buildings*, In: Proceedings of the World Conference of Timber Engineering, Vienna, 2016

Literature of PT-background information only

- [Andreolli et al., 2014] Andreolli, M.; Rigamonti, M; Tomasi, R.: *Diagonal compression test on cross laminated timber panels*. 13th World Conference on Timber Engineering (WCTE 2014), Quebec, Canada, 2014
- [Augustin et al., 2009] Augustin, Manfred; Blaß, Hans Joachim; Bogensperger, Thomas; Ebner; Ferk, Heinz J.; Fontana, Mario; Frangi, Andrea; Hamm; Jöbstl, Robert-August; Moosbrugger; Richter, Klaus; Schickhofer, Gerhard; Thiel, Alexandra B.; Traetta, Gianluigi; Uibel, Thomas: *BSPhandbuch. Holz-Massivbauweise in Brettsper Holz*. Editoren Schickhofer, Gerhard; Bogensperger, Thomas; Moosbrugger, Thomas, 2.überarbeitete Auflage, Verlag der Technischen Universität Graz. 2009
- [Augustin, M. et al., 2017] Augustin, M.; Bogensperger, T.; Schickhofer, G. and Thiel, A.: *Lasteinleitung in Wandscheiben aus BSP – Bestimmung der wirksamen Lastverteilung – Kurzfassung und Anwendungsbeispiel*, Report holz.bau forschungsgmbh and TU Graz Graz, 2017.
- [Augustin, M.; Thiel, A., 2017] Augustin, M.; Thiel, A.: *Proposal for the determination of the effective width and the verification of ribbed plates*, Report holz.bau forschungsgmbh and TU Graz Graz, 2017.
- [Augustin et al. 2017] Augustin, M.; Flatscher, G.; Tripolt, M. and Schickhofer, G.: *Messung der Vorkrümmung amplituden von planmäßig mittig gedrückten BSP-Elementen zur Festlegung des Imperfektionsbeiwertes für den Knicknachweis*, holz.bau forschungsgmbh Graz und TU Graz, 2017
- [Bejtka, 2010] Bejtka, Ireneusz: *Cross (CLT) and diagonal (DLT) laminated timber as innovative material for beam elements*. Karlsruher Institut für Technologie (KIT), Lehrstuhl für Ingenieurholzbau und Baukonstruktionen. KIT Scientific Publishing: Karlsruher Berichte zum Ingenieurholzbau 17, ISBN 978-3-86644-604-5, 2010
- [Blaß et al., 2002] Blaß, H.; Görlacher, R.: *Zum Trag- und Verformungsverhalten von Brettsper Holzelementen bei*

Beanspruchung in Plattenebene: Teil 2., Bauen mit Holz, 12: 30-34, Bruderverlag, Karlsruhe, 2002

- [Blaß et al., 2014] Blaß, H., Flaig, M.: *Keilgezinkte Rahmenecken und Satteldachträger aus Brettsper Holz*. Karlsruher Berichte zum Ingenieurholzbau, Bd. 29, KIT Scientific Publishing, Karlsruhe, Germany, 2014.
- [Blaß, 2015] Blaß, H.: *Ermittlung des 5%-Quantils des Produkts aus Elastizitätsmodul und Torsionsschubmodul für Brettschichtholz*. Report Lehrstuhl für Ingenieurholzbau und Baukonstruktionen, KIT, 2015.
- [Bogensperger et al., 2007] Bogensperger, T.; Moosbrugger, T.; Schickhofer, G.: *New test configuration for CLT wall-elements under shear load*. 40th CIB-W18 Meeting, Bled, Slovenia, 2007
- [Bogensperger et al., 2010] Bogensperger, T.; Moosbrugger, T.; Silly, G.: *Verification of CLT-plates under loads in plane*. 11th World Conference on Timber Engineering (WCTE 2010), Riva da Garda, Italy, 2010
- [Bogensperger et al., 2011] Bogensperger, T.; Augustin, M., Schickhofer, G.: *Properties of CLT-panels exposed to compression perpendicular to their plane*: 44th CIB-W18 Meeting, Alghero, Italy, 2011
- [Bogensperger et al., 2012] Bogensperger, T.; Silly, G., Schickhofer, G.: *Comparison of methods of approximative verification procedures for cross laminated timber*, TU Graz, 2012
- [Bogensperger, T., 2014] Bogensperger, T.: *Lasteinleitung in Wandscheiben aus Brettsper Holz*. Forschungsbericht, holz.bau forschungs gmbh, 2014
- [Bogensperger et al., 2015] Bogensperger, T.; Jöbstl, R. (2015), *Concentrated load introductions in CLT*, Proceedings of INTER, Paper 48-12-1 ,INTER, Šibenik, Croatia, 2015.
- [Bosl, 2002] Bosl, R.: *Zum Nachweis des Trag- und Verformungsverhaltens von Wandscheiben aus Brettsper Holz*. Dissertation, Universität der Bundeswehr, München, 2002

- [Brandner et al., 2006] Brandner, R.; Schickhofer, G.: *System effects of structural elements – determined for bending and tension*. 9th World Conference on Timber Engineering (WCTE 2006), Portland, Oregon, United States, 2006
- [Brandner et al., 2008] Brandner, R.; Schickhofer, G.: *Glued laminated timber in bending: new aspects concerning modelling*. Wood science and Technology. 42(5): 401-425, 2008
- [Brandner et al., 2013] Brandner, Bogensperger, T.; Schickhofer, G.: *In plane shear strength of cross laminated timber (CLT): test configuration, quantification and influencing parameters*. 46th CIB-W18 Meeting, Vancouver, Canada, 2013
- [Brandner et al., 2014] Brandner, R.; Schickhofer, G.: *Properties of cross laminated timber (CLT) in compression perpendicular to the grain*. Proceedings of INTER, Paper INTER/47-12-5, Bath / UK, 2014
- [Brandner et al., 2015] Brandner, R.; Dietsch, P.; Dröscher, J.; Schulte-Wrede, M.; Kreuzinger, H.; Sieder, M.; Schickhofer, G.; Winter, S.: *Shear properties of cross laminated timber (CLT) under in-plane load*. Test configuration and experimental study. 2nd INTER Meeting, Sibenik, Croatia, 2015
- [Brandner et al., 2016] Brandner, R., Flatscher, G., Ringhofer, A, Schickhofer, G. and Thiel, A: *Cross laminated timber (CLT) – Overview and development*, In: European Journal of Wood and Wood products, Vol. 74, No. 3, 03.2013
- [Bratulic, 2013] Bratulic, Katarina: *Untersuchung ausgewählter Einflussparameter auf die Querdruckkenngrößen von Brettsperrholz*. Masterarbeit am Institut für Holzbau und Holztechnologie der TU Graz 2013
- [Casagrande et al., 2016] Casagrande D., Rossi S., Sartori T., Tomasi R., *Proposal of an analytical procedure and a simplified numerical model for elastic response of single-storey timber shear-walls*, Construction and Building Materials, ISSN 0950-0618, pp. 1101-1112, 2016
- [Ciampitti, 2013] Ciampitti, A.: *Untersuchung ausgewählter Einflussparameter auf die Querdruckkenngrößen von Brett-*

- sperrholz*, Diploma Thesis, Technische Universität Graz, Graz, 2013
- [CSA 086-14] CSA O86-14, *Engineering design in wood*, Toronto, Canada: CSA, Canadian Standard Association, 2014
- [DIN EN 1995-1-1/NA] DIN EN 1995-1-1/NA, *Nationaler Anhang – National festgelegte Parameter - Eurocode 5: Bemessung und Konstruktion von Holzbauten – Teil 1-1: Allgemeines - Allgemeine Regeln und Regeln für den Hochbau*
- [Dröscher, 2014] Dröscher, Julia: *Prüftechnische Ermittlung der Schubkenngrößen von BSP-Scheibenelementen und Studie ausgewählter Parameter*. Masterarbeit am Institut für Holzbau und Holztechnologie der TU Graz, 17. November 2014
- [Dujic et al., 2008] Dujic B., Klobcar S., Zarnic R., *Shear capacity of cross-laminated wooden walls*, 10th World Conference on Timber Engineering 2008, 3, pp. 1641-1648, 2008
- [EAD 13005-000304] Europäisches Bewertungsdokument EAD 13005-000304 – *Massive plattenförmige Holzbauelemente für tragende Bauteile in Bauwerken*, Ausgabe August 2014
- [Ehrhart et al., 2015b] Ehrhart, T., Brandner, R., Schickhofer, G., Frangi, A.: *Rolling shear properties of some European timber species with focus on cross laminated timber (CLT): test configuration and parameter study*. 2nd Inter-meeting, Sibenik, Croatia, 2015
- [EN 13353] EN 13353, *Solid wood panels (SWP) – Requirements*
- [EN 14080] EN 14080:2013, *Timber structures – Glued laminated timber and glued solid timber – Requirements*
- [EN 14081-1] EN 14081-1, *Timber structures – Strength graded structural timber with rectangular cross section – Part 1: General requirements*
- [EN 16351] EN 16351:2015, *Timber structures – Cross laminated timber – Requirements*

- [EN 408] EN 408, *Timber structures – Structural timber and glued laminated timber – Determination of some physical and mechanical properties*
- [ETA-06/0009] Binderholz Bausysteme GmbH: *Binderholz Brettsperrholz BBS – Multilayered timber elements for walls, ceilings, roofs and special construction purposes*, ETA-06/0009, valid until 20.12.2016
- [ETA-16/0055] Holzbau Unterrainer, *Solid wood slab elements to be used as structural elements in buildings*, ETA-16/0055
- [ETA-06/0138] KLH Massivholz GmbH: *Solid wood slab elements to be used as structural elements in buildings*, ETA-06/0138, valid until 09.09.2017
- [ETA-08/0238] Schilliger Holz-Industrie AG: *Solid wood slab element to be used as a structural element in buildings*, ETA-08/0238, valid until 10.06.2018.
- [ETA-09/0036] Mayr-Melnhof Holz Holding AG: *Solid wood slab elements to be used as structural elements in buildings*, ETA-09/0036, valid until 16.06.2018
- [ETA-11/0189] W. u. J. Derix GmbH & Co. KG: *Solid wood slab elements to be used as structural elements in buildings*, ETA-11/0189
- [ETA-11/0210] Merkle Holz GmbH: *Solid wood slab elements to be used as structural elements in buildings*, ETA-11/0210
- [ETA-11-0464] EGOIN SA: *Solid wood slab element to be used as a structural element in buildings*, ETA-11/0464, issued at 20 April 2017
- [ETA-09/0211] Lignotrend AG: *Timber units for walls, roofs and ceilings*, ETA 09/0211, valid until 27.06.2018
- [ETA-12/0327] Eugen Decker Holzindustrie KG: *Solid wood slab elements to be used as structural elements in buildings*, ETA-12/0327, valid until 05.09.2017
- [ETA-14/0349] Stora Enso Wood Products Oy Ltd.: *Solid wood slab elements to be used as structural elements in buildings*, ETA-14/0349

- [Flaig et al., 2013] Flaig, M.; Blaß, H.: *Shear strength and shear stiffness of CLT-beams loaded in plane*. 46th CIB-W18 Meeting, Vancouver, Canada, 2013
- [Flaig et al., 2014] Flaig, M.; Blaß, H.: *Bending strength of cross laminated timber beams loaded in plane*. In: Proceedings of the World Conference on Timber Engineering 2014, Quebec City, Canada August 10-14 2014.
- [Flaig et al., 2015] Flaig, M.; Blaß, H.: *Keilgezinkte Rahmenecken und Satteldachträger aus Brettsper Holz*, Forschungsbericht KIT, 2015
- [Flaig, 2013] Flaig, M.: *Tragfähigkeit und Steifigkeit von Biegeträgern aus Brettsper Holz bei Beanspruchung in Plattenebene*. Dissertation, Fakultät für Bauingenieur, Geo-und Umweltwissenschaften, Karlsruher Institut für Technologie, Karlsruher Berichte zum Ingenieurholzbau, Bd. 27, KIT Scientific Publishing, Karlsruhe, Germany, 2013.
- [Flaig, 2015] Flaig, M.: *Design of CLT beams with large finger joints at different angles*. 2nd INTER Meeting, Sibenik, Croatia, 2015
- [Flatscher et al., 2016] Flatscher and Schickhofer (2016) *Displacement-based determination of laterally loaded cross laminated timber (CLT) wall systems*. INTER/49-12-1
- [Flatscher, 2015] Flatscher (2015) *Experimental tests on cross-laminated timber joints and walls*. ICE Journal Structures and Buildings, 2015, 168, 868-877
- [Follesa et al., 2013] Follesa M., Christovasilis I., Vassallo D., Fragiaco M., Ceccotti A., *Seismic design of multi-storey cross laminated timber buildings according to Eurocode 8*, Ingegneria Sismica 30(4):27-53, 2013
- [Gagnon et al., 2011] Gagnon, S.; Pirvu C. (eds.): *CLT-Handbook: cross laminated timber*. Canadian edition. ISBN 978-0-86488-553-1, 2011
- [Gavric, 2015] Gavric, I., Fragiaco, M., Ceccotti, A.: *Cyclic behavior of CLT wall systems: Experimental tests and*

- analytical prediction models*, (2015) Journal of Structural Engineering (United States), 141 (11)
- [Görlacher, 2002] Görlacher, R.: *Ein Verfahren zur Ermittlung des Rollschubmoduls von Holz*. In: Holz als Roh- und Werkstoff, 60:317-322, 2002
- [Halili, 2008] Halili, Y.: *Versuchstechnische Ermittlung von Querdruckkenngrößen für Brettsperrholz*. Diploma Thesis, Graz University of Technology, 2008
- [Hamm et al., 2010] Hamm, P.; Richter, A.; Winter, S.: *Floor vibrations – new results*. In: Proceedings World Conference on Timber Engineering, 2010
- [Hasuni et al., 2009] Hasuni, Hesun Kathum; Al-douri, Khamis Adib Sekran; Hamodi, Mohammed Hussein: *Compression strength perpendicular to grain in cross-laminated timber (CLT)*. Växjö Universitet, Thesis no. TD 058/2009, Växjö, Sweden, Mai 2009
- [Hirschmann, 2011] Hirschmann, B.: *Ein Beitrag zur Bestimmung der Scheibenschubfestigkeit von Brettsperrholz*. Diploma Thesis, Technische Universität Graz, Graz, 2011
- [Hummel et al., 2013] Hummel et al. (2013): *CLT wall elements under cyclic loading – details for anchorage and connection*. COST Action FP1004, Focus Solid Timber Solutions – European Conference on Cross Laminated Timber (CLT), The University of Bath, 2013, 152-165
- [Jacobs, 2005] Jacobs, A.: *Zur Berechnung von Brettlagenholz mit starrem und nachgiebigem Verbund unter plattenartiger Belastung unter besonderer Berücksichtigung des Rollschubes und der Drillweichheit*. Dissertation, Universität der Bundeswehr, München, 2005
- [Jeitler et al., 2008] Jeitler, G., Brandner, R.: *Modellbildung für Duo-, Trio- und Quattro-Querschnitte*. In: Schickhofer, G. and Brandner, R. (eds.) 7. Grazer Holzbau-Fachtagung (7. GraHFT'08): Modellbildung für Produkte und Konstruktionen aus Holz – Bedeutung von Simulation und Experiment. Verlag der technischen Universität Graz, Graz, 2008

- [Jeitler, 2004] Jeitler, G.: *Versuchstechnische Ermittlung der Verdrehungskenngrößen von orthogonalverklebten Brettlamellen*. Diploma Thesis. Technische Universität Graz, Graz, 2004
- [Jöbstl et al., 2004] Jöbstl, R.; Bogensperger, T.; Schickhofer, G., Jeitler, G.: *Mechanical behaviour of two orthogonally glued boards*. 8th World Conference on Timber Engineering (WCTE 2004), Lahti, Finland, 2004
- [Jöbstl et al., 2006] Jöbstl, R.; Bogensperger, T.; Schickhofer, G.: *A contribution to the design band system effect of cross laminated timber (CLT)*. 39th CIB-W18 Meeting, Florence, Italy, 2006
- [Jöbstl et al., 2007] Jöbstl, Robert A.; Schickhofer, G.: *Comparative examination of creep of GLT- and CLT-slabs in bending*. In: Proceedings of CIB W18, Bled, 2007, Paper 40-12-3
- [Jöbstl et al., 2008] Jöbstl, R.; Bogensperger, T.; Schickhofer, G.: *In plane shear strength of cross laminated timber*. 41st CIB-W18 Meeting, St. Andrews, Canada, 2008
- [Karabeyli et al., 2013] Karabeyli, E.; Douglas, B. (eds.): *CLT-Handbook: cross laminated timber*. US Edition. ISBN 978-0-86488-547-0, 2013
- [Kreuzinger et al., 2013] Kreuzinger, Heinrich und Sieder, M.: *Einfaches Prüfverfahren zur Bewertung der Schubfestigkeit von Kreuzlagenholz/Brettsperrholz*. In: Bautechnik, 90(5) 314–316, 2013
- [Mestek et al., 2011] Mestek, P.; Winter, S.: *Design concept for CLT-reinforced with self-tapping screws*, 44th CIB-W18 meeting, Alghero, Italy, 2011
- [Mestek, 2011] Mestek, P.: *Punktgestützte Flächentragwerke aus Brettsperrholz (BSP) – Schubmessung unter Berücksichtigung von Schubverstärkungen*, Dissertation, Technische Universität München, München, 2011
- [Moosbrugger et al., 2006] Moosbrugger, Thomas; Schickhofer, Gerhard, Unterwieser, Helene, Krenn, Harald: 5.Grazer Holzbau-Fachtagung: Brettsperrholz – Ein Blick auf Forschung und Entwicklung. Institut für Holzbau und

- [Moosbrugger et al., 2015] Moosbrugger, T.; Bogensperger, T. and Krenn, H.: *Kippen hoher BSP-Träger*. Bauen mit Holz, Heft 12/2015, Bruderverlag Karlsruhe, 2015
- [Moosbrugger e et al., 2017] Moosbrugger, T., Neumüller, F., Neumüller, A. (2017): *Schwinden und Quellen von orthogonal verklebten Holzprodukten – Teil 1: Globales Schwindverhalten von Blockbohlen und Brettsperrhölzern*. In: Holztechnologie, 58 (2017) 5, IHD, Dresden, 2017
- [ÖNORM B 1995-1-1] ÖNORM B 1995-1-1, *Eurocode 5: Bemessung und Konstruktion von Holzbauten, Teil 1-1: Allgemeines – Allgemeine Regeln und Regeln für die den Hochbau*
- [Popovski et al., 2011] Popovski and Karacabeyli (2011) *Seismic Performance of cross-laminated wood panels*. CIB-W18/44-15-7
- [Salzmann, 2010] Salzmann, C.: *Ermittlung von Querdruckkenngrößen für Brettsperrholz (BSP)*, Diploma Thesis, Technische Universität Graz, Graz, 2010
- [Schickhofer et al., 2015] Schickhofer, Gerhard; Bauer, Helene; Thiel, Alexandra: *Mit neuen Tragelementen in die Zukunft des Holzbaus*, S-WIN Kurs 2015, S-WIN; c/o Lignum, Zürich BI.
- [Serrano et al., 2010] Serrano, E.; Enquist, B.: *Compression strength perpendicular to grain in cross-laminated timber (CLT)*, 11th World Conference on Timber Engineering (WCTE 2010), Riva da Garda, Italy, 2010
- [Silly et al., 2013] Silly, G.; Thiel, A.: *Analyse und numerische Simulation zur Entwicklung einer Prüfkonfiguration für die Ermittlung der Rollschubkenngrößen von BSP-Elementen*. Presentation at COMET Area Meeting, holz.bau forschung gmbh Graz, 15. Oktober 2013
- [Silly, 2010] Silly, G.: *Numerische Studien zur Drill- und Schubsteifigkeit von Brettsperrholz (BSP)*. Diploma Thesis at Institut für Holzbau und Holztechnologie, Technische Universität Graz, 2010.

- [Silly, 2014] Silly, G.: *Schubfestigkeit der BSP-Scheibe: Numerische Untersuchung einer Prüfkongfiguration*. Interner Forschungsbericht der holz.bau forschungs gmbh, Graz Jänner 2014
- [Susteric et al., 2012] Susteric, I.; Dujic, B.: *Simplified cross laminated timber wall modelling for linear-elastic seismic analysis*. In: CIB-W18, 45-15-6, Växjö, Sweden
- [Teknisk handbook 2006] *Bygge med massivtreelementer*, Teknisk handbook, 7 hefter i samleperm, Norsk Treteknisk Institutt, Vol. 1, Oslo, ISBN 82-7120-000-3, 2006
- [Thiel, A.; et al., 2012] Thiel, A.; Schickhofer, G.: *Design methods of Cross Laminated Timber concerning floor vibrations: a comparability study*; holz.bau forschungs gmbh and TU Graz; 2012
- [Thiel, A. et al., 2013] Thiel, A.; Zimmer, S.; Augustin, A.: *CLT and floor vibrations: A comparison of design methods*. In. CIB-Proceedings, 2013
- [Thiel, A. et al., 2014] A. Thiel, M. Augustin, T. Bogensperger, G. Schickhofer: *Mitwirkende Breite bei Plattenbalken aus BSH und BSP – Kurzfassung und Anwendungsbeispiel*. Forschungsbericht, holz.bau forschungs gmbh, Graz, 2014.
- [Tomasi, 2013] Tomasi R.: *Seismic behaviour of connections for buildings in CLT*, In: Focus solids timber solutions, European conference on cross-laminated timber (CLT), Graz: University of Bath, UK, 2013, p. 138-151, ISBN: 1857901819. COST Action FP 1004, Graz, 21-22 may, 2013
- [Unterswieser et al., 2013] Unterswieser, H.; Schickhofer, G.: *Characteristic values and test configurations of CLT with focus on selected properties*. In: proceedings of Focus Solid Timber Solutions – European Conference on Cross Laminated Timber (CLT), Editor R. Harris, 21./22. Mai 2013
- [van der Put, 2008] van der Put, T.A.C.M.: *Derivation of the bearing strength perpendicular to the grain of locally loaded*

timber blocks, Holz als Roh- und Werkstoff 66, p. 409-417, Springer-V. 2008.

- [Wallner, 2004] Wallner, G.: *Versuchstechnische Ermittlung der Verschiebungskenngrößen von orthogonal verklebten Brettlamellen*. Master's Thesis, Technische Universität Graz, Graz, 2004
- [Wallner-Novak et al., 2013] Wallner-Novak, M., Koppelhuber, J., Pock, K.: *Brettsperrholz Bemessung – Grundlagen für Statik und Konstruktion nach Eurocode*. Wien: proHolz Austria, ISBN 978-3-902320-96-4, 2013
- [Watson et al., 2013] Watson, C.; van Beerschoten, W.; Smith, T.; Pampanin, S.; Buchanan, Andrew H.: *Shear strength and shear stiffness of CLT-beams loaded in plane*. In: Proceedings of CIB-Meeting, Vancouver, Kanada, Paper 46-12-4, 26.–29. August 2013
- [Winter et al., 2009] Winter, Stefan; Kreuzinger, Heinrich; Mestek, Peter: *Flächen aus Brettstapeln, Brettsperrholz und Verbundkonstruktionen*. Fraunhofer IRB Verlag, Serie Holzbau der Zukunft, Teilprojekt 19, ISBN 978-3-8167-7875-2, 2009
- [Zimmer, S. et al., 2016] Zimmer, Severin; Augustin, A.: *Vibrational behaviour of cross laminated timber floors in residential buildings*. In: Proceedings of the World Conference of Timber Engineering, Vienna, 2016
- [Z 9.1-482] KLH Massivholz GmbH: *KLH-Kreuzlagenholz*. Allgemeine bauaufsichtliche Zulassung Z-9.1-482, valid until 17.11.2020
- [Z 9.1-501] Allgemeine bauaufsichtliche Zulassung des Deutschen Instituts für Bautechnik Z-9.1-501, *Leno Brettsperrholz*, Holder: Merk Timber GmbH, valid until 03.06.2019
- [Z 9.1-534] Binderholz Bausysteme GmbH: *Binderholz Brettsperrholz BBS*. Allgemeine bauaufsichtliche Zulassung Z-9.1-534, valid until 17.11.2019
- [Z 9.1-555] Lignotrend GmbH & Co. KG, *Lignotrend Elemente*, Allgemeine bauaufsichtliche Zulassung Z-9.1-555, valid until 26.01.2018

- [Z 9.1-559] Stora Enso Wood Products Oy Ltd., *CLT-Cross Laminated Timber*, Allgemeine bauaufsichtliche Zulassung Z-9.1-559, 13. valid until 26.01.2017
- [Z 9.1-576] Woodtec Fankhauser GmbH: „Woodtec“ *Massivholzplatten*. Allgemeine bauaufsichtliche Zulassung Z-9.1-576, valid until 28.04.2020
- [Z 9.1-680] Haas Holzprodukte GmbH: *Haas BSP Brettsperrholz, Haas CLT Cross Laminated Timber* HMS-Element. Allgemeine bauaufsichtliche Zulassung Z-9.1-680, valid until 23.11.2017
- [Z 9.1-721] Eugen Decker Holz, Industrie KG: *ED-BSP (Brettsperrholz) aus Fichte, Kiefer oder Douglasie*, Zulassung Z-9.1-721, valid until 19.09.2018
- [Z 9.1-793] Stephan Holzbau GmbH: *Brettsperrholzelemente „Stephan-Flexcross*, Allgemeine bauaufsichtliche Zulassung Z-9.1-793, valid until 14.06.2016

B ***Thematic Contributions***

Fatigue behaviour of CLT under in-plane shear loading

Prof. Dr.-Ing. Mike Sieder
Head of Institute
TU Braunschweig, iBHolz
Braunschweig, Germany

Peter Niebuhr, M. Sc.
Scientific Assistant
TU Braunschweig, iBHolz
Braunschweig, Germany

Summary

The fatigue behaviour of CLT under in-plane shear loading is examined using the test setup according to Kreuzinger and Sieder [1]. The results of four test series with three specimens per series are described with special attention to the observed ultimate number of load cycles. Based on these observations the applicability of current verification concepts (Woehler-curves) for the examined application is discussed. It is shown that the test results indicate a safe applicability of the Woehler-curve according to EN 1995-2 [2] for wooden members under shear. Apart from the results for the fatigue behaviour under shear loading, indications for the fatigue behaviour under tension perpendicular to grain are pointed out.

1. Introduction

Growing demand for sustainable solutions in the construction sector leads to the application of wooden members in cases where traditionally other materials such as steel or reinforced concrete were applied. One of these new or rediscovered application areas is structures that are exposed to frequently recurring loads that are prone to inducing material fatigue. An example for a recent CLT application in a fatigue load situation is wind energy plants with wooden tower structures (see e.g. [3]). These are decisively loaded by in-plane shear and normal loads which occur frequently and demand fatigue verification. Subsequently, tests on the fatigue behaviour of CLT members under in-plane shear loading are described to show an indication of the direction of profound verification equations for CLT members under fatiguing shear loads.

2. Material and methods

2.1 Material – CLT

The examined CLT cross-section consists of 8 layers that are arranged in an L-L-C-L-L-C-L-L pattern, with L and C for longitudinal and cross layer, respectively (see Fig. 1), with respective thicknesses of 40-40-30-40-40-30-40-40 *mm*. This results in a cross-section with an overall thickness of 300 *mm*. With the adjacent

longitudinal layers, the cross-section could be interpreted as a more conventional 5-layer-arrangement with layer-thicknesses of 80-30-80-30-80 mm. All layers are made of lamellas taken from visual grade S10 according to DIN 4074-1 [4] (strength class C24 according to EN 338 [5]) and are manufactured with bonded narrow faces, the board width is 200 mm in all layers. The fabrication of the specimens was part of the regular production process of a commercial CLT manufacturer, representing common fabrication quality, and are taken from one production batch.

2.2 In-plane shear testing method by Kreuzinger and Sieder

Kreuzinger and Sieder [1] described a testing procedure for evaluating the in-plane shear strength of CLT-members where the specimen is cut in a rectangular column-shape oriented under an angle of $\alpha = 45^\circ$ to the main orientation of the CLT-layers (see Fig. 2). The obtained specimen geometry is shown in Fig. 3. A longitudinal compression load F to the specimen results in combined shear and compression stresses (see Fig. 4).

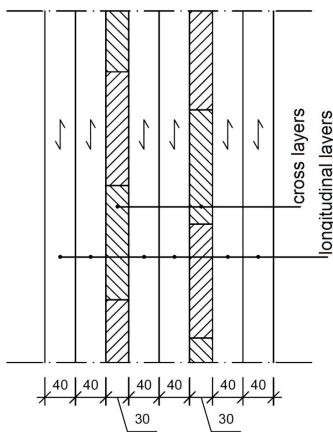


Fig. 1 Examined cross-section

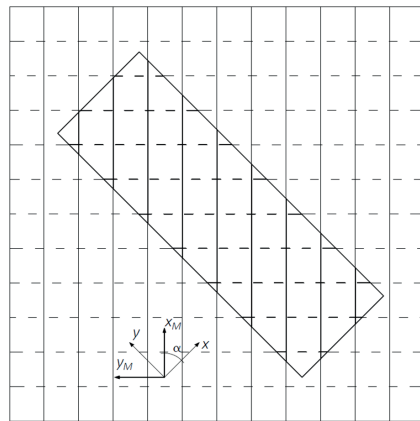


Fig. 2 Specimen orientation in relation to CLT main orientation (adapted from [6])

The shear stress under the load F can be calculated as

$$\tau_{x_M y_M} = \frac{1}{2} \cdot \frac{F}{A_{CLT}} = \frac{1}{2} \cdot \frac{F}{w_{CLT} \cdot t_{CLT}} \quad (1)$$

Since the shear resistance of wood is influenced by stresses perpendicular to grain the shear strength obtained from the Kreuzinger and Sieder setup is not equal to the shear stress given by Eq. (1). Instead, the shear strength can be determined according to Blaß and Krüger [7] (empirically evaluating data from [8]) with Eq. (2) where σ_{90} is negative for compression stresses ([6]).

$$f_{v, gross} = \tau_{xMyM} + 1,15 \cdot \sigma_{90} + 0,13 \cdot \sigma_{90}^2 \quad (2)$$

For the given CLT cross-section (see Section 2.1) this results in Eq. (3). See [6] for a comprehensive description of the calculation of σ_{90} with respect to the anisotropic stiffness properties of the base material. For the determination of Eq. (3) the applied stiffness values were mean values according to EN 338 [5] for strength class C24.

$$f_{v, gross} = 0.832 \cdot \tau_{xMyM} \quad (3)$$

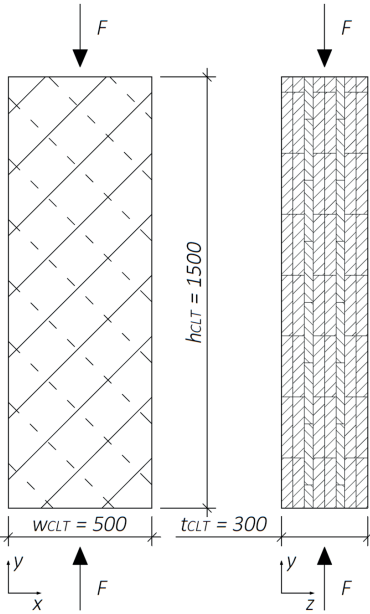


Fig. 3 Specimen geometry

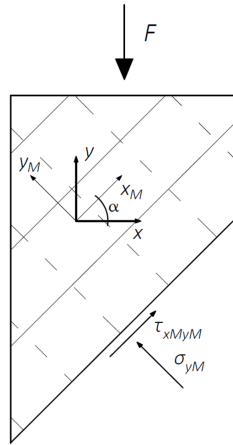


Fig. 4 Internal stresses due to external force F (adapted from [1])

2.3 Test programme

The described specimen geometry was used for four test series, one series (S1) for the determination of the ultimate static load F_{ult} , three series (D1 to D3) for the examination of the fatigue behaviour. In series D1 to D3 the stress level $S = F_{max}/F_{ult}$ was varied between $S = 0.55$ and $S = 0.80$ in order to receive multiple data points on a derived Woehler-curve. Hereby, the ultimate static load was estimated as the mean value of the results of series S1. It would have been beneficial to examine stress levels that are further apart, i.e. investigating configurations with $S < 0.55$. This, however, had to be discarded due to the expected excessive duration of such experiments. In all fatigue tests the stress ratio $R = F_{max}/F_{min}$ was set to $R = 0.1$. Thus, the external load never changes from compression to tension and the internal stresses do not change direction. According

to common assumptions regarding the influence of the stress ratio R this is not the loading that causes the highest damage. Loading situations with $R = -1$, i.e. a complete load reversal during a load cycle, are assumed to be the most damaging ([9]). In the present study, however, a stress ratio of $R = 0.1$ was chosen because of the simplicity of the load application for compression loading only. This setup is close to the most damaging loading of a construction that experiences only loads in one direction or where the dead loads are greater than the variable loads applied in the other direction (*non-reversed loading*: $R = 0$). A good example for this case is bridges which usually do not experience a significant fatigue loading in the vertical upward direction. The loading followed a sinusoidal shape with a frequency in the range of $0.5 \text{ Hz} \leq f \leq 1.1 \text{ Hz}$. The performed test programme is summarised in Table 1.

Table 1 Test programme

Series No.	No. of Specimens	static/dynamic loading	$S = F_{max}/F_{min}$ [-]	R [-]	f [-]
S1	3	static	–	–	–
D1	3	dynamic	0.70	0.1	1.1
D2	3	dynamic	0.80	0.1	0.5
D3	3	dynamic	0.55	0.1	0.8

2.4 Test configuration

All tests were performed on a servo-hydraulic *Schenck* testing machine (type S 56) with a maximum load capacity of 2.5 MN at the *MFPA Leipzig GmbH, Germany*. To allow for free strains perpendicular to the direction of the load a PTFE layer was placed between the specimen and the surface of load application at the top of the specimen and also at the bottom support (see Fig. 5).

To measure the deformations in the $x - y$ -plane, measurement crosses according to EN 408 [10] with a measuring base of $h_0 = 400 \text{ mm}$ were applied on both sides. For series D2 and D3 the deformations in z -direction were measured on both sides at three points equally spaced over the specimen height h_{CLT} . These measurements were taken over the full width of $t_{CLT} = 300 \text{ mm}$. The arrangement of the measuring points is also displayed in Fig. 5, the test configuration is exemplarily shown in Fig. 6.

3. Results

3.1 Observed failure mechanisms

Because of the distinct nature of the loading and consequently the load bearing mechanisms, the observed failure mechanisms will be outlined separately for the static tests (series S1) and the fatigue tests (series D1 to D3).

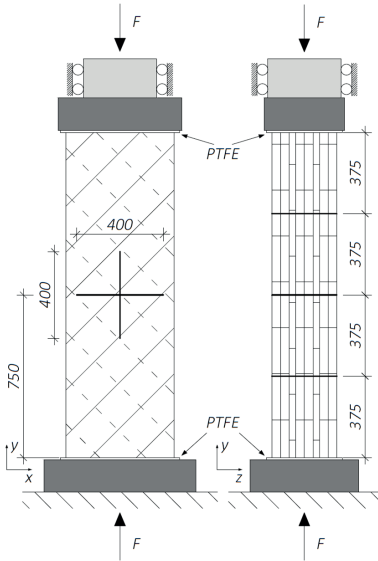


Fig. 5 Test configuration and measurement points (adapted from [6])

Fig. 6 Exemplary display of the test configuration

3.1.1 Static loading (series S1)

All the specimens in series S1 under static loading failed in *gross-shear*. The failure mode is exemplary displayed in Fig. 10. The scatter in the ultimate loads F_{ult} was surprisingly small. The ultimate loads and the resulting observed *gross-shear* strength according to Eq. (3) are given in Table 2. The force-displacement curves of the S1 specimens show a widely linear behaviour with no pronounced loss in stiffness that could be seen as a failure announcement (see Fig. 7).

Table 2 Results of series S1 (static)

Specimen	F_{ult} [kN]	$f_{v,gross}$ [N/mm ²]	$F_{ult,mean}$ [kN]	$f_{v,gross,mean}$ [N/mm ²]	CV [%]
S1-1	1144.7	3.21			
S1-2	1012.9	2.83	1077.2	3.02	6
S1-3	1073.9	3.01			

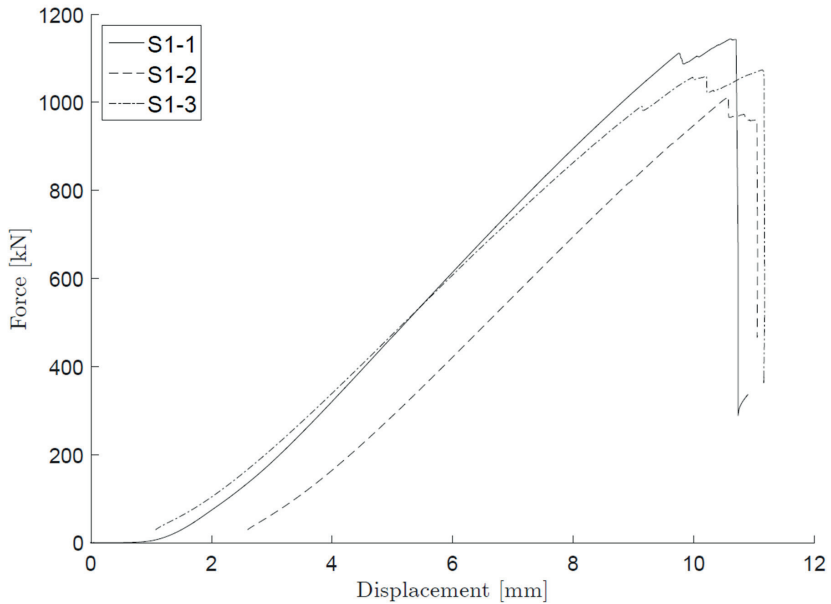


Fig. 7 Force-displacement curves of series S1 (static)

3.1.2 Fatigue loading (series D1 to D3)

Unlike the specimens in static loading, the specimens in fatigue loading (series D1 to D3) showed distinct cracks in the $x - y$ -plane, propagating in the y -direction. These are characteristic for tension stress perpendicular to the grain and occurred mainly in the load application areas, i.e. the top and bottom quarters of the specimen. The cracks appeared to start mainly in the longitudinal-tangential plane ($L - T$ -plane) of the local grain orientation, but propagation and initiation of cracks could also be observed in the longitudinal-radial plane and, especially towards the end of fatigue life, close to the glue surface between layers, indifferent of the grain

orientation. The described cracks are exemplarily displayed in Fig. 8 and Fig. 9. Ultimate failure occurred in *gross-shear*, as in series S1 (see Fig. 11).



Fig. 8 Cracks in x – y-plane in specimen D1-3 (fatigue loading)



Fig. 9 Cracks in x – y-plane in specimen D2-1 (fatigue loading)



Fig. 10 Gross-shear failure in specimen S1-2 (static loading)



Fig. 11 Gross-shear failure in specimen D2-3 (fatigue loading)

3.2 Cycles to failure

The fatigue tests were performed assuming $F_{ult,mean} = 1077 \text{ kN}$ from Table 2 as the maximum bearable static load for all fatigue specimens. The maximum and minimum applied forces were determined with $F_{max} = F_{ult,mean} \cdot S$ and $F_{min} = F_{max} \cdot R = F_{max} \cdot 0.1$. The resultant maximum forces are given in Table 3, which also shows the observed ultimate number of load cycles N of the fatigue tests. Obviously, the scatter in the results of series D2 and D3 is substantial. In series D1, however, the results are surprisingly congruent with a coefficient of variation of only 9 %.

Table 3 Ultimate number of load cycles N of series D1 to D3

Specimen	S [-]	F_{max} [kN]	F_{min} [kN]	N [-]	N_{mean} [-]	CV [%]
D1-1				29150		
D1-2	0.70	750	75	34374	31296	9
D1-3				30365		
D2-1				642		
D2-2	0.80	860	86	11522	5245	107
D2-3				3570		
D3-1				22616		
D3-2	0.55	590	59	41586	21954	91
D3-3				1659		

4. Discussion

4.1 Failure mechanisms under static and cyclic loading

In both, the static and the fatigue tests, the ultimate failure occurred in *gross-shear* which does match the models and findings in [6] and [11]. The additional cracking in the $x - y$ -plane in the fatigue tests, however, did not occur in the static tests. The authors assume that these cracks result from tension stresses perpendicular to grain that are caused by lateral strains in the load application areas where longitudinal compression stresses σ_{yM} and σ_{xM} are assumed to dominate over the (desired) shear stresses τ_{xMyM} (see Fig. 12; [12]).

The influence of lateral strains and resulting tension perpendicular to grain is magnified by the PTFE-layer (see Fig. 5) that minimises the friction between the specimen and the load application surface. Silly's numerical analysis of the Kreuzinger and Sieder test configuration [12] shows that for static loading the friction between the surfaces of load application and the specimen should be reduced to a minimum in order to receive stress distributions that are close to the

theoretical assumption of constant stresses (see Fig. 12). For fatigue testing purposes, however, this practise needs to be rethought. The cracks in the $x - y$ -plane constitute a weakening of the cross-section that supposedly leads to results that are too far on the safe side. Instead of allowing for (quasi) free lateral strains an obstruction of these strains might lead to more realistic results for an assumed shear loading. For static tests the execution of the contact surface between load application and specimen has been found to be without practical relevance ([6]).

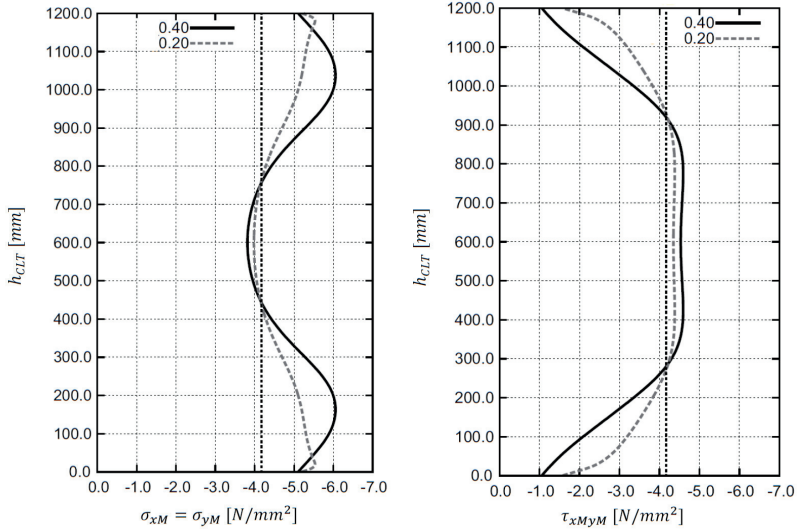


Fig. 12 Results of FE-simulation of longitudinal (left) and shear stresses (right) depending on the coefficient of friction in the load application areas (taken from [12])

The fact that the lateral strains lead to cracks in fatigue testing but are negligible in static loading can give an indication to the relationship between the fatigue behaviour of wood under shear and that under tension perpendicular to grain:

Under the ultimate static load F_{ult} the tension perpendicular to grain $\sigma_{t,90,Fult}$ obviously is smaller than the corresponding strength $f_{t,90}$ because no fracture (i.e. local failure) can be observed:

$$\frac{\sigma_{t,90,Fult}}{f_{t,90}} < 1.0 \quad (4)$$

Since shear failure occurs, the shear stress $\tau_{xMyM,Fult}$ is equal to the shear resistance f'_v (considering the effects of stresses perpendicular to the grain, see Section 2.2), therefore:

$$\frac{\sigma_{t,90,Fult}}{f_{t,90}} < \frac{\tau_{xMyM,Fult}}{f'_v} \quad (5)$$

Under fatigue loading the maximum load is smaller than the ultimate static load ($F_{max} = S \cdot F_{ult}$) and the resulting stresses are smaller by the same amount:

$$\begin{aligned} \sigma_{t,90,max} &= S \cdot \sigma_{t,90,Fult} \\ \tau_{xMyM,max} &= S \cdot \tau_{xMyM,Fult} \end{aligned} \quad (6)$$

Beside the ‘global’ stress level $S = F_{max}/F_{ult}$ a ‘local’ stress level $S_{t,90}$ can be considered. $S_{t,90}$ describes the relation between the maximum tension stress perpendicular to grain and the corresponding strength:

$$S_{t,90} = \frac{\sigma_{t,90,max}}{f_{t,90}} = S \cdot \frac{\sigma_{t,90,Fult}}{f_{t,90}} < \frac{\sigma_{t,90,Fult}}{f_{t,90}} < 1.0 \quad (7)$$

A combination of Eqs. (5), (6) and (7) shows that $S_{t,90}$ is smaller than the global stress level S . In the fatigue tests it was observed that, even though the local stress level $S_{t,90}$ is smaller than S , local failure due to tension perpendicular to grain (i.e. cracks in the $x - y$ -plane) occurred significantly earlier than the global shear failure ($N_{t,90} \ll N$). The described comparison of the fatigue behaviour under shear (global) and tension perpendicular to grain (local) is displayed in Fig. 13. With the known data points at $(x = 1; y = 1)$ (failure under static load) and $(x = N; y = S)$ (global failure of the CLT-specimen) the data point $(x = N_{t,90}; y = S_{t,90})$ can be located qualitatively ($N_{t,90} < N$ and $S_{t,90} < S$). The resulting possible Woehler-curve shows a greater slope than the Woehler-curve for the CLT-specimen under shear loading.

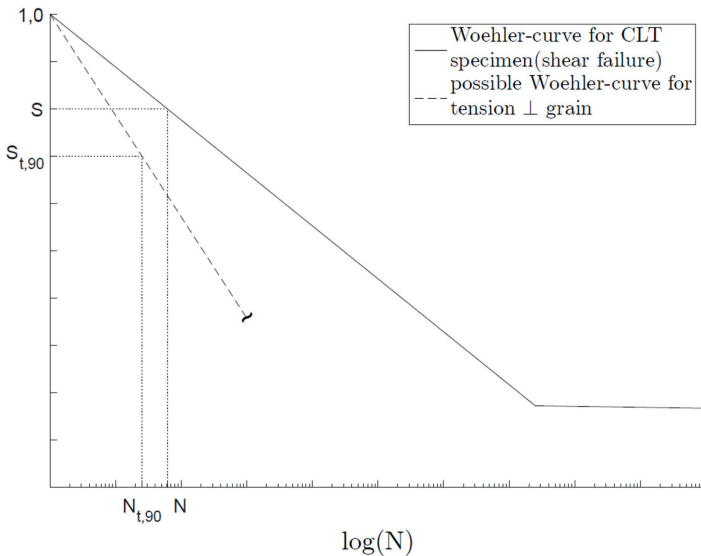


Fig. 13 Comparison of local fatigue due to tension perpendicular to grain and global fatigue of the CLT-specimen under shear loading

The effect of the compression perpendicular to grain in the shear behaviour (see Section 2.2: $f_{v,gross} = 0.832 \cdot \tau_{xMyM}$) is considered to be negligible for this contemplation since both the numerator (F_{max}) and the denominator (F_{ult}) of the ratio S contain the positive effect of the perpendicular compression. An important aspect that was not considered in the previous paragraph, though, is that local shear failure has to be assumed to also occur before the global failure arises. Such local shear damage does not immediately trigger the global failure because of multiple possible load paths (load distribution rearrangement). Hence, the assumption that no shear failure at all has occurred when the cracks in the $x - y$ -plane were detected has to be treated with caution. The declaratives from the previous paragraph and Fig. 13 can, however, be rated as an indication on the fatigue behaviour of wood under tension perpendicular to grain.

4.2 Observed cycles to failure and verification according to EC 5 and Mohr

Fig. 14 shows the observed ultimate number of load cycles N according to Table 3 in relation to the Woehler-curves for wood under shear loading according to EN 1995-2 [2] and Mohr [13]. Additionally, two regression graphs are displayed that represent the mean values of all series (r_2) and of series S1, D1 and D2 (r_1), respectively:

$$r_1: S(N) = 1,0044 - 0,0645 \cdot \log(N) \quad (8)$$

$$r_2: S(N) = 1,0048 - 0,0806 \cdot \log(N) \quad (9)$$

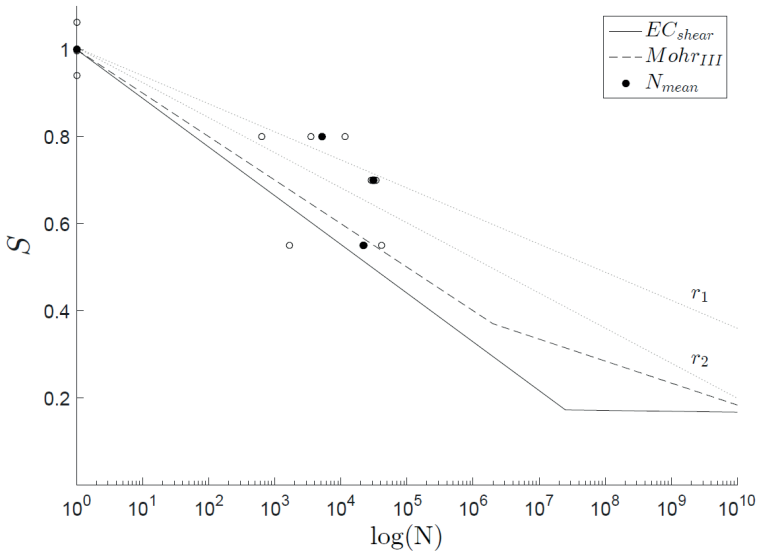


Fig. 14 Woehler-curves according to EN 1995-2 [2] and Mohr [13] for wood under shear loading

It can be seen that the results of series S1, D1 and D2 can be described by a linear function (in the chosen scale) with a high coefficient of determination ($R^2 = 0.987$), whereas the ultimate load cycle numbers of series D3 are unexpectedly small, leading to a coefficient of determination of only $R^2 = 0.765$ for the regression that considers all results.

The reason for the unexpected nature of the results in series D3 could not be found conclusively, although several reasons are conceivable, one of which is natural scatter in the properties of wood. In order for the mean number of load cycles in series D3 to coincide with the regression graph r_1 the stress level had to be at around $S^* = 0.73$. This would be true if the maximum bearable load of the specimens in series D3 had been about 25 % less than the assumed ultimate load of $F_{ult} = 1077 \text{ kN}$, which might be seen as conceivable, especially in the context of F_{ult} being estimated with only three static tests in series S1 and considering the large scatter in the properties of structural lumber as the base material for CLT. Another possible reason for the low load cycle numbers in series D3 is pre-existing damage in the specimens. About seven months passed between the tests in series D2 and D3 during which the D3 specimens were stored under non-standard climatic conditions. Numerous cracks could be observed on the narrow sides of these specimens (i.e. cracks in $x - y$ -plane, showing on the $y - z$ -faces) before any load was applied, which was not apparent on the specimens in series S1, D1 and D2.

In comparison to the displayed Wohler-curves the results from series D1 and D2 are on the safe side. The individual results from series D3, however, are very close to, or even on the unsafe side of the given design curves. The D1 and D2 results suggest that a more favourable Wohler-curve might be applicable, an example being given with r_1 in Eq. (8). It can be seen that the acceptable load cycle numbers according to r_1 are always higher than those according to the compared design suggestions.

When taking the D3 results in full consideration, the EC 5 and Mohr curves for wood under shear loading can still be assumed to be applicable in a safe way according to the results when taking into account that the verification would be performed using the characteristic value of the static strength for the determination of the stress level S . The stress levels of the tests, by contrast, have been determined with the mean value of the static results. This consideration is based on Mohr's evaluation [13] of the cause of scatter in load cycle numbers. It was found that the scatter is mainly based on the scatter in the static strength of the specimens and that a verification with the characteristic values of the static strength and the mean values of the load cycles is sufficiently safe. This, however, was only shown for timber and should be further investigated for engineered wood products.

5. Conclusions

5.1 Test configuration

For the determination of properties under static loads the applicability of the Kreuzinger and Sieder test configuration has been shown in the past ([6, 11, 12]). For the evaluation of fatigue behaviour the configuration could be applied as well, the execution of the load application surfaces, however, does require further refinement to avoid the unwanted local failure due to tension perpendicular to grain. As it stands, the setup is assumed to lead to results on the safe side but more favourable results are believed to be possible with a refined test setup. A restraint of lateral strains in the top and bottom areas of the specimen could bring the desired effect but has not been examined in this study.

5.2 Fatigue verification of CLT under in-plane shear loading

Both, the verification curve from EN 1995-2 [2] and from Mohr [13], seem to be applicable for a safe representation of the observed fatigue behaviour of CLT members under shear loading. The data from series D3 is close to both verification curves but is assumed to allow for an application of the curves considering the safety level that is inherent in a verification based on characteristic values for the static strength. Because of the small number of performed tests and the limited bandwidth in respect to the stress level S , though, the study can only act as an indication to the safe applicability of the mentioned verification curves.

Further studies with a greater number of tests and a greater bandwidth of S should be performed to approve the verification with the Eurocode and Mohr curves. These further investigations could lead to the conclusion that even a more favourable verification curve (similar to r_1 , compare Section 4.2) might be applicable, especially if the additional damage due to lateral strains is suppressed.

6. References

- [1] KREUZINGER, H., SIEDER, M.: *Einfaches Prüfverfahren zur Bewertung der Schubfestigkeit von Kreuzlagenholz/Brettsperrholz*. Bautechnik, Vol. 90 (2013), p. 314–316.
- [2] EN 1995-2:2010: *Eurocode 5: Design of timber structures – Part 2: Bridges*. European Committee for Standardization CEN, 2010.
- [3] SCHRÖDER, C.: *Ermüdungsbeanspruchte Brettsperrholzbauteile am Beispiel eines Turms für Windkraftanlagen*. In: forum-holzbau (ed.): 21. Internationales Holzbau-Forum IHF, 2015.
- [4] DIN 4074-1:2012: *Strength grading of wood – Part 1: Coniferus sawn timber*. DIN Deutsches Institut für Normung e.V., 2012.
- [5] EN 338:2016: *Structural timber – Strength classes*. European Committee for Standardization CEN, 2016.

- [6] BRANDNER, R., DIETSCH, P., DRÖSCHER, J., SCHULTE-WREDE, M., KREUZINGER, H., SIEDER, M.: *Cross laminated timber (CLT) diaphragms under shear. Test configuration, properties and design. Construction and Building Materials, No. 147* (2017), p. 312–327.
- [7] BLAB, H. J., KRÜGER, O.: *Schubverstärkung von Holz mit Holzschrauben und Gewindestangen*. Karlsruhe: KIT Scientific Publishing, 2010.
- [8] SPENGLER, R.: *Festigkeitsverhalten von Brettschichtholz unter zweiachsiger Beanspruchung. Teil 1: Ermittlung des Festigkeitsverhaltens von Brettelementen aus Fichte durch Versuche*. München, 1982.
- [9] KREUZINGER, H., MOHR, B.: *Holz und Holzverbindungen unter nicht vorwiegend ruhenden Einwirkungen*, 1994.
- [10] EN 408:2012+A1:2012: *Timber structures – Structural timber and glued laminate timber – Determination of some physical and mechanical properties*: European Committee for Standardization CEN, 2012.
- [11] BRANDNER, R., DIETSCH, P., DRÖSCHER, J., SCHULTE-WREDE, M., SIEDER, M.: *Scheibenschub von Brettsperrholz. Verifizierung einer Prüfkonfiguration und Parameterstudie. Bautechnik, No. 92* (2015), p. 759–769.
- [12] SILLY, G.: *Schubfestigkeit der BSP-Scheibe – numerische Untersuchung einer Prüfkonfiguration. Forschungsbericht*. Graz, 2014.
- [13] MOHR, B.: *Zur Interaktion der Einflüsse aus Dauerstands- und Ermüdungsbeanspruchung im Ingenieurholzbau*. Dissertation. München, 2001.

COST Action FP1402
Basis of Structural Timber Design:
From Research to Standards

WG 2 – Solid Timber Constructions:
Cross Laminated Timber (CLT)

TG 2 – Testing and Evaluation

A General Motivation, Comments and Overview

Summary

CLT is used in a variety of applications, as floor elements, wall elements and beams and, in addition, both the use of line as well as point supports are common practice. CLT comes in a very large number of lay-ups, depending on the application to which it is optimized, and also *e.g.* depending on prerequisites that the producer might have in terms of available raw materials.

This report relates to testing and verification methods for CLT. Bearing in mind the versatility of the product mentioned above, it is a truly challenging task to summarize in few words how to test and verify the mechanical behavior of CLT. Thus this contribution is by no means complete. But the authors have made an effort to summarize, discuss and evaluate previously proposed test methods from literature and test methods from current standards and European Assessment Document (EAD) 130005-00-0304, the guideline for obtaining a European Technical Assessment for CLT, for those test situations where knowledge is not well established, or where a consensus within the scientific community cannot be said to exist. Thus, this contribution discusses test methods for bending, rolling shear, test methods for in-plane shear and test methods for tension and compression perpendicular to grain.

Apart from discussing and evaluating the test methods, some general knowledge gaps and related needs for additional development and research are highlighted.

1. Introduction¹

1.1 Testing for product properties

TG2 deals with test methods for CLT. The test methods dealt with herein relate primarily to the assessment of essential requirements on *strength and to some extent on elastic properties*, and thus relate indirectly to initial type testing. Test methods specifically designed for factory production control are not dealt with here.

Bearing in mind that the test results are to be compared to the declared properties of the product and these, in turn, are to be used as a basis for the *structural design*, it is of course of utmost importance that the evaluation methods and all relevant testing conditions (specimen geometry and lay-up, time, moisture, load configurations etc.) are consistent and in line with the structural design procedures.

Here, it is of special importance to mention the different mechanical models and the inherent approximations used in structural design, *e.g.* shear-flexible beam- or plate theory or different failure modes for in-plane shear. Due to the use of such approximations, there is in some cases no need for detailed “material” testing. Instead the most important thing is to perform and evaluate the tests under circumstances that are consistent with the structural design requirements and procedures to be used.

1.2 Aims and limitations

A major aim of this work has been to find consensus within the scientific community as regards test methods, identified knowledge gaps and research as well as development needs. An important task has been to find a reasonable level of practical applicability of the outcome. Bearing in mind that the FP1402 title is “From research to standards” focus has been on reviewing test procedures currently in use, or recently proposed, in light of the harmonised standard EN16351:2015, [1]. It has also been necessary to introduce some limitations on the work in terms of type of products being covered. Thus, in addition to the specifications of EN16351:2015, the following limitations have been introduced:

- homogeneous lay-ups (the same strength class in all layers),
- symmetric lay-ups,
- layers of strength graded timber according to EN 14081-1, [2] (EN16351 allows the use of solid wood panel layers).

1.3 Outline

Section 2 presents a general introduction/overview of the topic of defining and testing CLT. The main findings from the work are summarised in Section 3, presenting also recommendations for future work. Details about different loading scenarios and related test methods are presented in detail in the second part of this report as separate contributions from the TG2 members.

¹ Erik Serrano, professor, Structural Mechanics, Lund University, Sweden, erik.serrano@construction.lth.se

2. CLT – considerations regarding denomination and testing²

2.1 Introduction

In timber engineering many novel engineered wood products (EWPs) are used. In the last decades many panel type products have appeared allowing not only to build linear structures in timber but also to think in “solid” wall and floor members spanning in two directions. These products allow to multiply the applications in timber construction. Compared to sawn timber, a higher homogeneity and lower variation of properties between products from different production batches and producers are obtained. Within the last decades, various high-performance load-bearing EWPs entered the market; primary linear members as glued laminated timber (glulam; GLT), solid finger jointed construction timber, duo- and trio-beams composed by two or three boards, but also two-dimensional products as laminated veneer lumber (LVL) and oriented strand boards (OSB). Cross laminated timber (CLT) has been introduced more than two decades ago in central Europe. It is a laminar and large-sized plate-like structural element, which is commonly composed of an uneven number of layers, usually three, five or seven layers. Each layer is made of boards placed side-by-side, which are arranged crosswise to each other, usually at an angle of 90°.

Such elements can be loaded in two ways: as a floor element that is loaded perpendicular to its extension (plate action), or as a wall element that is capable of bearing loads in the plane formed by the panel (panel action). A good definition for the respective loading cases in the engineering sense (panel action / plate action / out-of-plane loading etc.) in-line with other materials like reinforced concrete has still to be found and harmonized to avoid any possible confusion.

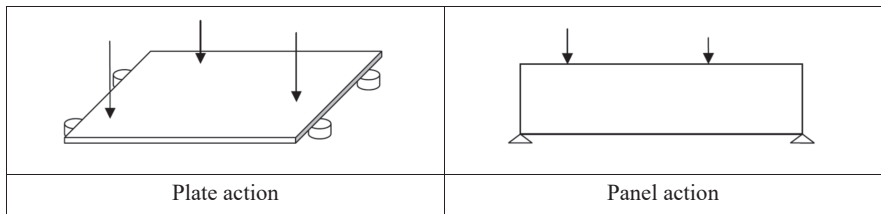


Fig 1 Description and definition of loaded members and corresponding loading, [3]

Thanks to its thickness, CLT can be used as a stand-alone structural element with good strength and stiffness properties. Its large dimensions ease handling and make it versatile in application. CLT opens new markets for timber engineering and allows architecture and engineering to realize (super)structures and monolithic buildings in

² Christophe Sigrist, Dr. PhD., Professor for timber engineering and steel construction, Bern University of Applied Sciences, Architecture, Wood and Civil Engineering, Biel, Switzerland.
christophe.sigrist@bfh.ch, www.ahb.bfh.ch.

timber. The solid structure of CLT also allows using timber species and boards with lower mechanical properties compared to traditional linear structural timber products like glulam. The properties of the final product depend on a multitude of parameters: the strength and stiffness of the input material as well as the number, thickness and arrangement of the layers. The derivation of the parameters for the design is an important issue as well as corresponding test configurations to correctly determine the required properties.

Table 1 CLT strength classes; characteristic values of CLT when loaded perpendicular to its plane [4]

Base material T14; CV $[f_{t,0,t}] =$		25 ± 5 %	35 ± 5 %
Property [-]	Symbol [-]	CL 24h	CL 28h
Bending strength	$f_{m,CLT,k}$ [N/mm ²]	24.0	28.0
Tensile strength perpendicular to grain	$f_{t,90,CLT,k}$ [N/mm ²]	0.5	
Compression strength perpendicular to grain	$f_{c,90,CLT,k}$ [N/mm ²]	3.0	
Shear strength	$f_{v,CLT,k}$ [N/mm ²]	3.5	
Rolling shear strength	$f_{r,CLT,k}$ [N/mm ²]	1.40, for $w_t / t_t \geq 4$	
	$f_{r,lay,k}$ [N/mm ²]	0.80, for $w_t / t_t < 4$	
Modulus of elasticity parallel to grain	$E_{0,CLT,mean}$ [N/mm ²]	11,600	
	$E_{0,lay,mean}$ [N/mm ²]		
Modulus of elasticity perpendicular to grain	$E_{90,CLT,mean}$ [N/mm ²]	300	
	$E_{90,lay,mean}$ [N/mm ²]		
Modulus of elasticity in compression perp. to grain	$E_{c,90,CLT,mean}$ [N/mm ²]	450	
Shear modulus	$G_{0,lay,mean}$ [N/mm ²]	650	
Rolling shear modulus	$G_{r,lay,mean}$ [N/mm ²]	100, for $w_t / t_t \geq 4$	
		65, for $w_t / t_t < 4$	
Elastic & shear properties' 5 %-quantiles	$E_{CLT,05}$ [N/mm ²]	$E_{05} = 5/6 \times E_{mean}$ $G_{05} = 5/6 \times G_{mean}$	
	$E_{lay,05}$ [N/mm ²]		
	$G_{CLT,05}$ [N/mm ²]		
	$G_{lay,05}$ [N/mm ²]		

Table 2 Characteristic strength and stiffness properties in N/mm² and densities in kg/m³ for homogeneous cross laminated timber [5]

Base material		T14	
CV[$f_{t,0,t}$]		25 ± 5 %	35 ± 5 %
		CLT strength class	
Property [-] ^{a)}	Symbol [-]	CL 24h	CL 28h
Bending strength	$f_{m,CLT,k}$ [N/mm ²]	24.0	28.0
Tensile strength	$f_{t,0,CLT,net,k}$ [N/mm ²]	16.0	18.0
	$f_{t,90,CLT,k}$ [N/mm ²]	0.5	
Compression strength	$f_{c,0,CLT,net,k}$ [N/mm ²]	24.0	28.0
	$f_{c,90,CLT,k}$ [N/mm ²]	2.85	
Shear strength (shear and torsion) – in plane	$f_{v,CLT,IP,k}$ [N/mm ²]	5.0	
	$f_{T,node,k}$ [N/mm ²]	2.5	
Shear strength – out of plane	$f_{v,CLT,OP,k}$ [N/mm ²]	3.0	
	$f_{r,CLT,k}$ [N/mm ²]	1.25 ($w_t / t_t \geq 4:1$)	
	$f_{r,CLT,k}$ [N/mm ²]	0.70 ($w_t / t_t < 4:1$)	
Modulus of elasticity	$E_{0,CLT,mean}$ [N/mm ²]	11,000	
	$E_{0,CLT,05}$ [N/mm ²]	9,167	
	$E_{90,CLT,mean}$ [N/mm ²]	300	
	$E_{90,CLT,05}$ [N/mm ²]	250	
	$E_{c,90,CLT,mean}$ [N/mm ²]	450	
	$E_{c,90,CLT,05}$ [N/mm ²]	375	
Shear modulus	$G_{CLT,mean}$ [N/mm ²]	650	
	$G_{CLT,05}$ [N/mm ²]	540	
Rolling shear modulus	$G_{r,CLT,mean}$ [N/mm ²]	65	
	$G_{r,CLT,05}$ [N/mm ²]	54	
Density	$\rho_{CLT,k}$ [kg/m ³]	350	
	$\rho_{CLT,mean}$ [kg/m ³]	385	

^{a)} Properties are calculated on the basis of reference cross sections and definitions given in [5].

The panel properties may be determined by testing a certain number of “basic” properties, some of the remaining properties may be calculated using appropriate mechanical models. Table 1 indicates the large number of strength and stiffness properties required when looking at a CLT plate submitted to bending as an example. It is possible to test CLT and to directly declare the defined characteristic values of strength and stiffness. However, defined and fixed test configurations must be used,

which then allow to compare results from various tests and enables a comparison between products.

The definition of the characteristic material properties of CLT could be presented similarly to the definition of solid timber or glued-laminated timber (GLT). Generally, bearing models based on a limited number of basic material properties can be used. The presentation of characteristic values of strength and stiffness for CLT, as shown in Table 2, shows how CLT can be attributed to strength classes. Table 2 also provides an insight into the characteristic values of strength, stiffness and density considering the example of CLT strength classes CL 24h and CL 28h using the strength class T14 as basic input board material. The situation is rather complex as plate and panel action as well as the load bearing direction – parallel or perpendicular to the arrangement of the boards in the outer layer corresponding to the main load carrying direction – have to be considered and corresponding stress and stiffness values to be indicated.

2.2 Standards and guidelines

Regulations regarding the derivation of performance characteristics, the evaluation of conformity and (CE-) marking of wood-based panels for use in constructions in general are given in EN 13986 “Wood-based panels for use in construction – Characteristics, evaluation of conformity and marking”, [6]. Special conditions may be defined in the specific product standards.

Testing of products and test setups must follow established rules to obtain reliable and repeatable strength or stiffness properties. The testing standard EN 408 “Timber structures – Structural timber and glued laminated timber – Determination of some physical and mechanical properties”, [7] mainly deals with (conventional) linear members. Considering testing of panel material, the testing arrangements in EN 408 may not be adequate. Some panel properties can be obtained applying EN 789 “Timber structures – Test methods – Determination of mechanical properties of wood based panels”, [8]. General rules about what relevant characteristics (essential requirements) to be tested and which ones may be derived by calculation must be established.

Next to mechanical properties, which are the focus of this summary, a big range of physical properties are also needed for design purposes: dimensional stability, reaction and resistance to fire, release of dangerous substances, properties in relation with building physics, surface or durability requirements. Some indications are found in the Common Understanding of Assessment Procedure (CUAP), [3], to address EOTA approval bodies to establish an European Technical Approval (ETA) according to Article 9.2 of the Construction Products Directive. This CUAP has been superseded by a new European Assessment Document EAD that prescribes some test procedures and the test arrangements to be considered in view of deriving mechanical properties of “solid wood slabs elements to be used as a structural element in buildings”, [9], as basis for issuing an European Technical Assessment (ETA).

In EN 16351:2015 a certain number of tests specific to CLT are described specifying test arrangements, as for instance span to thickness requirements, to obtain the desired properties. The size of the test specimen to fully and correctly assess the properties is one of the crucial questions next to the required number of replications to derive characteristic values. The sampling must be carried out in such a way that the production process is correctly represented. As the laminations may comprise grooves to reduce (drying) deformations, or layers which are edge bonded or not, the correct test being on the safe side must be performed.

The tests aiming at providing data regarding the structural design according to EC 5 that intend to give specific design rules are not part of basic test configurations. Specific rules may be needed for diaphragms, plates and beams. Rules for basic applications and correction values for specific applications as for instance the determination of $k_{c,90}$ values to verify stress perpendicular to the panel for various loading situations and geometries, and system factors especially in the case of small elements comprising a limited number of laminations will be needed. Therefore, all testing procedures must be harmonized with design standards specifying the future design approaches. Basic testing configurations as discussed here aim at defining CLT elements with reference dimensions that are tested at reference conditions to determine basic strength and stiffness properties. In the structural design, correction factors for the adjustment of such characteristic product properties are introduced to correctly design CLT elements of other dimensions that are exposed to other conditions. Such factors enable the adjustment of properties in combination with load-bearing models for CLT to respect other sizes, systems (homogenization), stress distribution, moisture content and temperature if required. Predicting the respective behavior of CLT panels requires accurate information about their bending and shear strength as well as their elastic properties.

2.3 Denominations

As structural elements will be used for plate action or panel action new and clear denominations and definitions must be introduced. Fig. 2 shows a floor plate loaded perpendicular to its plane leading to internal forces according to the main axes x and y . Contrary to concrete structures with about isotropic characteristics a clear orthotropic material governs the behavior of CLT plates. A precise denomination is therefore required. Special considerations need to be applied to correctly consider the fiber direction of the layers composing the panel. Finally, a complete setting of product properties by CLT strength class and background information regarding load-bearing models, reference conditions and model assumptions must be provided.

In concrete design the x -direction points in one of the main directions (parallel to one edge) of the plate. Forces act on the section or plane that is situated perpendicular to this axis. The bending moment m_y of the plate creates stresses σ_x that are orientated in the x -direction. These stresses can be combined with the stresses due to normal forces (acting in x -direction, same denomination) also creating stresses σ_x in the x -direction.

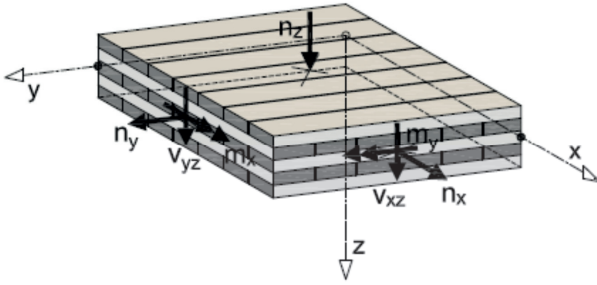


Fig. 2 Definition of axes and denomination of forces [10]

For CLT the main axis x should be defined by the direction of the fibers of the boards in the outer layers of the panel. This is not the case for the panel represented in Fig. 2. The resulting bending stresses $\sigma_{m,x}$ in the main direction “ x ” presented in Fig. 3 are due to a bending moment m_x that rotates around the x -axis which is contrary to the general engineering definition discussed earlier.

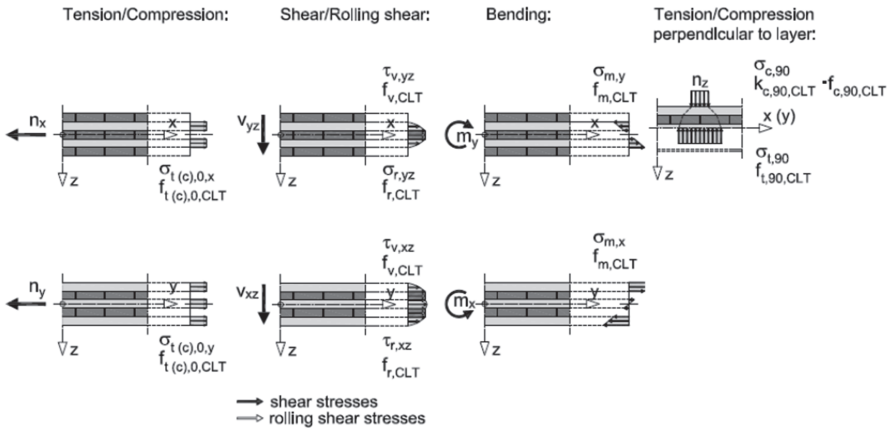


Fig. 3 Definition of axes and denomination of forces [10]

The latest definition of axes and stresses for CLT can be found in the Working Document of prEN 16351, [11]. The x -axis is parallel to the boards composing the outer layers. The first index of the denomination of the stress / force indicates the orientation of the face (perpendicular to the x -axis) considered, the second index relates to the direction of the force. The first index is not necessary to clearly describe the situation; it only leads to complication. For normal forces n_{xx} in particular the double denomination is not really needed. The forces are represented independently for normal forces, shear forces and bending moments. Furthermore, in FEM analysis drilling moments as m_{yy} are usually incorporated into the main bending moment m_{xy} . A simplification in the denomination would be welcome as the source for errors is

quite big: The stress $\sigma_{m,edge,x}$ is due to the in plane bending moment m_{xz} (CLT acting as a panel) and not as indicated due to bending moment m_{zx} . A simplification could be achieved in introducing plate / panel, flat / edge, or other references relating to the loading of the panel that are simple to understand for a designer. Some of this has already been introduced in Fig. 4 and Table 3 as for instance the expression $\sigma_{m,edge,x}$ clearly indicates loading and stress direction.

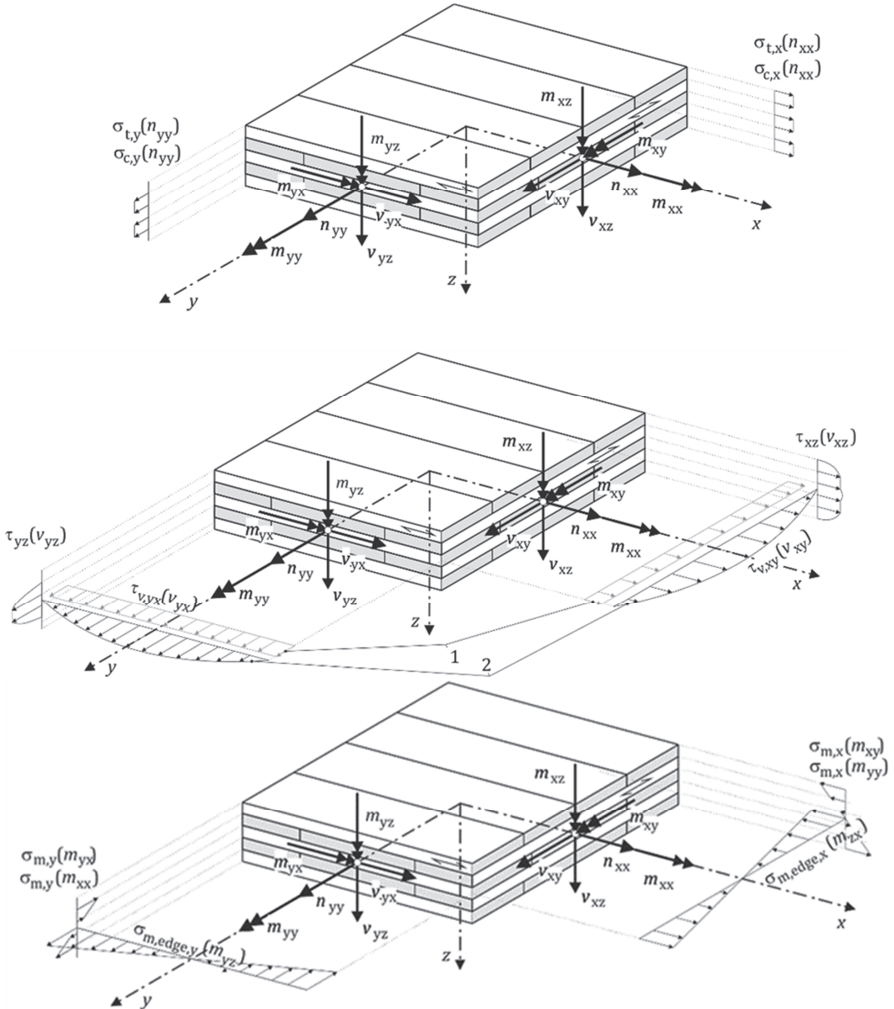


Fig. 4 Definition of axis and denomination of forces [11]

Table 3 Definition of strength and stiffness properties according to Working Document prEN 16351:2018 [11]

Property		Symbol
Bending strength	For bending moments out of plane, see Figure PT.1-8.13, characteristic value	$f_{m,x,k}$ $f_{m,y,k}$
	For bending moments in plane, see Figure PT.1-8.13, characteristic value	$f_{m,edge,x,k}$ $f_{m,edge,y,k}$
Tension strength	In plane, characteristic value	$f_{t,x,k}$ $f_{t,y,k}$
	Perpendicular to the plane, characteristic value	$f_{t,z,k}$
Compression strength	In plane, characteristic value	$f_{c,x,k}$ $f_{c,y,k}$
	Perpendicular to the plane, characteristic plane	$f_{c,z,k}$
Shear strength out of plane	Longitudinal, characteristic value	$f_{v,k}$
	Rolling shear, characteristic value	$f_{r,k}$
Shear and torsional shear strength in plane	Shear strength of the effective cross-section, characteristic value	$f_{v,xy,k}$ $f_{v,yx,k}$
	Torsional shear strength of the glued area of crosswise bonded laminations, characteristic value	$f_{tor,node,k}$
	Rolling shear, characteristic value	$f_{r,k}$
Modulus of elasticity	Loaded in plane, mean value	$E_{x,mean}$ $E_{y,mean}$
	Loaded perpendicular to the plane, mean value	$E_{z,mean}$
Shear modulus	Loaded out of plane, mean value	$G_{xy,mean}$ $G_{yz,mean}$
	Loaded in plane, mean value	$G_{xy,mean}$ $G_{yx,mean}$ $G_{tor,mean}$
	Rolling shear, mean value	$G_{r,mean}$
Density	Characteristic value	ρ_k
	Mean value	ρ_{mean}

2.4 Test configurations

2.4.1 Requirements for bending and shear

EN 789 requires 4-point bending tests on longitudinal specimens presenting a width of 300 mm, generally cut from thin panels. To assure a failure in bending the distance between the supports and the loading points (side span l_2) already equals $16 \times t$, where t is the panel thickness leading to slender specimens with a span to thickness ratio that is well above 32. Comparison of results of bending tests on such specimens with that of full panels shows that neither strength nor stiffness properties derived by specimen with reduced width are appropriate to assess the respective properties of the full panels.

In order to harmonize testing, test setups, specimen type and size as well as number of tests to be performed the following documents and standards have been analyzed:

EN 16351: Timber structures – Cross laminated timber

EN 408: Timber structures – Structural timber and glued laminated timber – Determination of some physical and mechanical properties

EN 789: Timber structures – Test methods – Determination of mechanical properties of wood based panels

CUAP: Common Understanding of Assessment Procedure Solid wood slab element to be used as a structural element in buildings

EAD: Timber structures – Test methods – Determination of mechanical properties of wood based panels

Such comparisons should allow precise recommendations regarding test setups to be given.

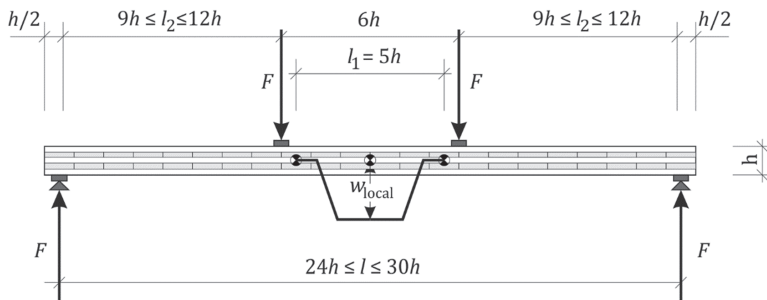


Fig. 5 Bending flat for bending properties (plate action), [11]

Fig. 5 shows the 4-point bending test configuration for cross laminated timber with loads acting perpendicular to the plane (plate action). The longer span compared to the requirements from EN 408 leads to slender panels to ensure that a failure in bending (not rolling shear!) will occur. This configuration can be used to determine both strength and stiffness of the panel.

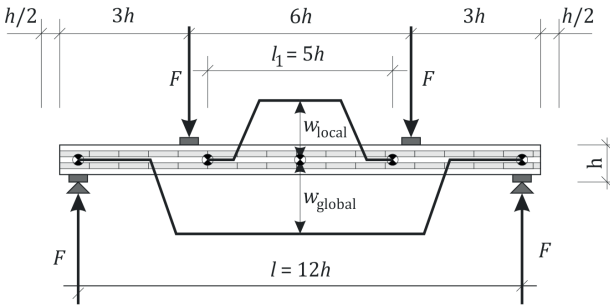


Fig. 6 Bending flat for shear properties (plate action) [11]

Fig. 6 shows the bending test configuration for the determination of rolling shear strength and stiffness (plate action) for cross laminated timber with loads acting perpendicular to the plane. The short span to depth ratio is chosen to ensure that a failure in rolling shear will occur. This configuration can be used to determine both strength and stiffness of the panel.

These two tests are easy to perform and give a clear answer to the problem as long as the above geometrical requirements in combination with basic material properties typical for common European CLT strength profiles are fulfilled.

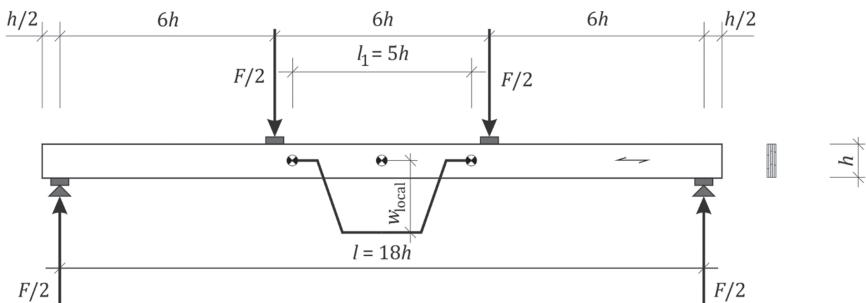


Fig. 7 Bending on edge for bending properties (panel action) [11]

Fig. 7 shows the bending test configuration for the determination of bending strength and stiffness on edge (panel action) for cross laminated timber with loads acting in the plane of the panel. The span corresponds to testing conditions for beams according to EN 408 [7] to achieve a bending failure. This configuration can be used

to determine both strength and stiffness at in-plane bending of the panel. Tests on wider beams presenting $h = 600$ mm that are randomly cut from a panel are currently proposed to be tested.

In EN 16351:2015 a similar test configuration was given, although this had an artificial saw cut to simulate edges without edge gluing. The purpose of that test was to determine in-plane *shear* behavior. For testing direct shear and torsional shear for loading on edge alternative test methods are currently being developed and defined to replace bending tests used earlier.

The outcome of the specification of the test setup and specimen size are twofold: on one side certain characteristics must be physically tested whereas others may be calculated using established models. The “true” behavior of the panels must be evaluated requiring representative and industrially fabricated full-size samples leading to large dimensions and heavy specimens which are awkward to be manipulated and tested. The most important dimension to be defined is the width of specimens to be tested flat and the height of specimens to be tested on edge. In both cases the load sharing effect must be considered in specifying the required width in function of the number of boards / laminations being placed next to each other within one layer. When testing specimens on edge the execution of the lamination edges, i.e. with or without edge gluing, must be considered.

2.4.2 Sample dimensions and testing configurations

To make testing feasible in terms of costs the following strategy is proposed: test as few specimen and types of tests as possible but as many as needed. Furthermore, the test results should be on the safe (conservative) side compared to the real behavior of such large building components. However, this implies defining and fixing test configurations which can be used to compare results from various institutes, producers, etc. and that enable a robust determination of mechanical properties of CLT panels.

The experience has shown that testing CLT panels “flat” for bending considering the geometry proposed by EN 408 would quite often lead to an undesired shear failure. An increase of the span to thickness ratio must therefore be considered. In new standards a ratio of $24 \times h$ to $30 \times h$ will be proposed getting close to panel testing of LVL, plywood or other panel type EWP described by EN 789. The width of the panel to be tested should comprise 3 to 4 adjacent boards / laminations in order to obtain a minimum load shearing effect. This condition already leads to quite wide panels and heavy specimens. Fixed spans and specimen widths of 800 mm to 1500 mm as prescribed by the latest EAD are beyond any reasonable considerations and only lead to very expensive testing campaigns.

Table 4 Comparison of test geometry and sample dimensions

	L_{span} [m]	$B_{specimen}$ [mm]	h [mm]	b_{lam}/t_{lam} [-]	t_{lam} [mm]	n layers [-]
EN 16351 2015	$24 \times h - 30 \times h$	300 or $\geq 2 \times b_{lam}$	≤ 500	≥ 4	6 – 45	representative to production
EN 16351 2018	$24 \times h - 30 \times h$	600 or $\geq 4 \times b_{lam}$	150	≥ 4	30	5
Graz on EN 16351	$21 \times h$	600 or $\geq 4 \times b_{lam}$	150	≥ 4	30	5
EN 408	$15 \times h - 21 \times h$	–	–	–	–	–
EN 789	$32 \times h +$ center span	300	≥ 9 mm	–	–	–
CUAP	$15 \times h - 21 \times h$	–	–	–	–	–
EAD //	fixed 5.5 m	1500	≤ 350	–	–	≥ 3
EAD \perp	fixed 2.3 m	800	≤ 350	–	–	≥ 3

2.4.3 Sampling

The goal is to test industrially produced panels with various layups, layer thicknesses and input board qualities. Layup and target strength class should be representative of the usual production. The geometry of the panels should be such to accommodate all necessary tests required for an eventual accreditation of the product. Matching bending specimens on flat and on edge as well as specimens for delamination and shear tests could be cut from the same panel. Fig. 8 shows the procedure that had been adopted for a specific testing campaign [12] as an example. All specimens had outer boards with the grain direction running longitudinally to the main panel dimension. Specimens with outer layers running across the board length were not tested in this campaign.

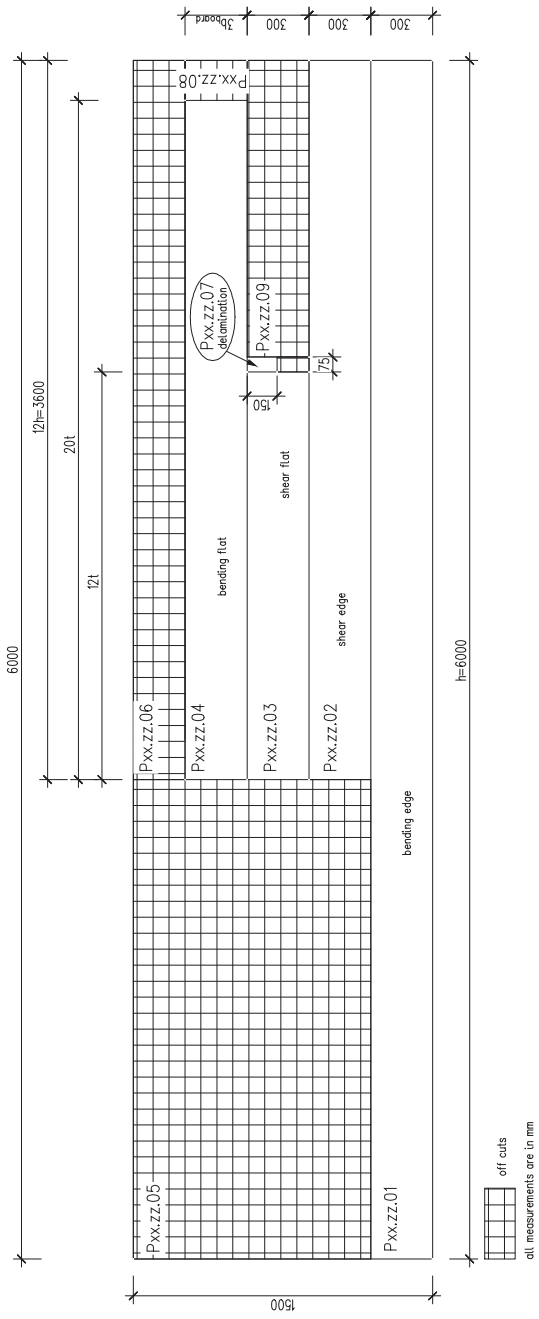


Fig. 8 Organization and cutting scheme of test specimens within one panel and attribution of tests used for developing properties for CLT [12]

Fig. 8 also shows the numbering of the specimen: xx stands for the layup number and zz for the panel number, the last two digits indicate the test procedure (01 bending edge; 02 bending-shear edge; 03 bending-shear flat; 04 bending flat; 07 delamination; 05, 06, 08 and 09 were not subjected to any tests but kept for further investigations). The number was always written on the top left corner of the specimen, therefore the exact position of the specimen in the panels was known. To avoid any influence of the machine operator on the positioning of the specimen the number was always located on the top for the bending tests. All panels were cut according to the same scheme and the specimen after subjected to the same tests. The CLT specimens were at that time tested in four-point bending and shear-bending according to the draft version of prEN 16351:2015 “Timber structures – Cross laminated timber – Requirements”. The local and global bending stiffness, the bending strength and the shear strength were determined. The CLT was tested for plate and panel action as proposed in that draft standard. The specimens for plate action presented a minimum width of 300 mm or three times the board width. The specimens for panel action had a height of 300 mm.

2.5 Conclusion and summary

This section attempts to discuss requirements for the basis of design, the material properties and the characteristic values for strength, stiffness and density of cross laminated timber (CLT) and to link them to testing. The goal for testing is for all properties and configurations to define basic values and to adapt them using modification factors k_{mod} for special design applications. An important point in specifying strength and stiffness properties is to establish reference dimensions for testing (or precise rules if these can't be met) of CLT and to consider the basic characteristics of the boards arranged in the layers, [4], [5]. Based on developments of GLT and from tests, a reference section for boards 150 mm / 30 mm to be used in CLT could be considered, as suggested in [4], [5]. In order to derive panel or plate properties for CLT appropriate models can then be determined that are a function of the base (input) material. Special effects as the variability of the material, size effects and the effect of homogenization may be considered by correction factors. Development of such models would allow certain boundary conditions as lay-up, number of layers, board dimensions, etc. to be defined.

To determine the mechanical properties of CLT, appropriate test configurations are set with corresponding reference dimensions. For the determination of the bending properties the test configuration proposed looks at larger ratios for the free span length than specified in EN 408 to prevent the occurrence of rolling shear failure. Investigations also showed that the local bending modulus of elasticity is much more stable in comparison to the determination of global modulus of elasticity if the span is increased. EN 408 is currently under revision. The above findings will be incorporated and rules / aids developed to simply determine the correct test setup to allow any material to be correctly tested. The test configurations for determination of direct shear and torsional shear strength have still to be defined and are currently being developed.

3. Conclusions and recommendations

3.1 Main findings

This work presents general discussions on test methods and related strategies in light of assuring representative, relevant results using a limited amount of practical methods that will not be too costly. As regards the test methods presented and discussed in the second part the following main findings are highlighted:

Compression perpendicular to grain

Based on test experience, test specimen type and evaluation procedures are recommended, based on a recent research paper by Brandner [13]. The suggested specimen dimensions are: $l_{CLT} \times w_{CLT} \times d_{CLT} = 150 \times 150 \times 150 \text{ mm}^3$ but no greater than $l_{CLT} \times w_{CLT} = 300 \times 300 \text{ mm}^2$.

Rolling shear

The determination of the rolling shear strength and rolling shear modulus by means of the EN 408 alike test setup is seen as an appropriate approach.

In-plane shear

The in-plane shear test method as proposed by Kreuzinger and Sieder [14] and also studied by Brandner et al. [15], is deemed as the most appropriate one. The specimen is a column-like compressive specimen of CLT cut at 45° from the main directions, with proposed dimensions $1500 \times 500 \text{ mm}^2$ (length \times width).

Tension perpendicular to grain

A test configuration and methods similar to those used in tests for solid timber and glued laminated timber are proposed, based on the experimental pilot study presented here.

3.2 Recommendations for future work

Compression perpendicular to grain

The inclusion of CLT in EC5 should involve also compression perpendicular to grain. In [13] it is recommended that a harmonization of the regulations for all timber products and properties as regards the influence of moisture on deformations, and their consequences, at compression perpendicular to grain loading is done.

Rolling shear

Comparative tests for methods for rolling shear as described in EN 16351, with specimens produced from the same raw material, should be performed.

Out-of-plane shear

Adjustment factors to link test results based on different methods for rolling shear, as described in EN 16351, could be developed based on numerical analyses. Further investigations on the size and system effects in serial and parallel acting systems subjected to rolling shear are also needed for a better understanding of the mechanical behaviour of CLT.

In-plane shear

Based on available tests and available basic FE-analyses, additional and more advanced numerical analyses are needed to verify further the in-plane shear test set-up of Kreuzinger and Sieder [14], and Brandner et al. [15]. This approach should also be used to conclude whether torsional tests are at all needed, and if so, suggest a well-defined test method for torsional tests.

Tension perpendicular to grain

Further research efforts as regards CLT strength in tension perpendicular to grain are needed to increase the available amount of data, to include also other lay-ups than the ones the limited pilot study presented herein covered. Of special concern is also the fact that strength properties for tension perpendicular to grain are not yet available in international standards.

4. References

- [1] EN 16351:2015, Timber structures – Cross laminated timber – Requirements.
- [2] EN 14081-1, Timber structures – Strength graded structural timber with rectangular cross section – Part 1: General requirements.
- [3] CUAP:2005, Common Understanding of Assessment Procedure Solid wood slab element to be used as a structural element in buildings.
- [4] Schickhofer, G., Brandner R., Bauer H., “Introduction to CLT: product properties, strength classes”, Conference Paper, Joint Conference of COST Actions FP1402 and FP1404, KTH, Stockholm, Sweden, March 2016.
- [5] Unterwieser, H., Schickhofer, G. “Characteristic Values and Test Configurations of CLT with Focus on Selected Properties”, COST Action FP1004, European Conference on Cross Laminated Timber (CLT), The State-of-the-Art in CLT Research, May 2013.
- [6] EN 13986+A1:2015, “Wood-based panels for use in construction – Characteristics, evaluation of conformity and marking”
- [7] EN 408+A1:2012, Timber structures – Structural timber and glued laminated timber - Determination of some physical and mechanical properties
- [8] EN 789:2004, Timber structures – Test methods – Determination of mechanical properties of wood based panels
- [9] EAD 130005-00-0304:2015, Timber structures – Test methods – Determination of mechanical properties of wood based panels
- [10] Wiegand, T. Current status of European product and design standards for cross laminated timber, Conference Paper, Joint Conference of COST Actions FP1402 and FP1404, KTH, Stockholm, Sweden, March 2016.
- [11] prEN 16351:2018, Timber structures – Cross laminated timber – Requirements, WD 2018-03-26

- [12] Sigrist, C., Lehmann, M., Potential of CLT produced from non-structural grade Australian *pinus radiata*, proceedings WCTE, Quebec City, 2014
- [13] Brandner R., “Cross Laminated Timber (CLT) in Compression Perpendicular to Plane: Testing, Properties, Design and Recommendations for Harmonizing Design Provisions for Structural Timber Products”, *Engineering Structures*, 2018, <https://doi.org/10.1016/j.engstruct.2018.02.076>.
- [14] Kreuzinger, H., Sieder, M. “Einfaches Prüfverfahren zur Bewertung der Schubfestigkeit von Kreuzlagenholz / Brettsper Holz (in German)”. *Bautechnik*, 90(5), pp. 314–316, 2013.
- [15] Brandner, R., Dietsch, P. Dröscher, J., Schulte-Wrede, M., Kreuzinger, H., Sieder, M. Cross laminated timber (CLT) diaphragms under shear: Test configuration, properties and design. *Construction and Building Materials* 147, 312–327, 2017.

B Test Methods – State-of-Art and Future Developments

Some Comments on and Proposals for Determining the Compression Perpendicular to Grain Properties of CLT: Brief Summary of a Recent Publication

Reinhard Brandner
Assistant Professor; Deputy Head of the Institute
Institute of Timber Engineering and Wood Technology
Graz University of Technology
Graz, Austria

1. Proposals for Determining Basic Properties from Testing: Summary of Brandner (2018)

Up to now a standardized definition is missing for reference specimen for determining the basic properties of CLT in compression perpendicular to the plane. The following specifications are proposed: based on own test experience and in respect to the reference CLT cross section, as defined in Unterwieser and Schickhofer [1], Brandner et al. [2] and PT SC5.T1 [3], and by summarizing the findings and proposals recently published in Brandner [4], it is suggested to use prism specimen with dimensions $\ell_{\text{CLT}} \times w_{\text{CLT}} \times d_{\text{CLT}} = 150 \times 150 \times 150 \text{ mm}^3$ but no greater than $\ell_{\text{CLT}} \times w_{\text{CLT}} = 300 \times 300 \text{ mm}^2$. This corresponds to a five-layer CLT element with equally thick layers ($t_\ell = 30 \text{ mm}$) and laminations with a reference width of $w_\ell = 150 \text{ mm}$. To represent the basic properties in a realistic manner also in respect to property variability / uncertainty, it is suggested to cut out specimen arbitrarily from CLT plates so that they feature typical timber growth characteristics (e.g. knots, cracks, etc.) as well as typical CLT product characteristics like gaps and stress reliefs. This is to assure that influences from different laminations within the same layer, featuring e.g. different sawing pattern and annual ring orientation, as also gaps, are represented as its best. For the load application it is advised to use thick, stiff steel plates featuring minimal bending deformations when loaded centrally. Recently, Gasparri and Lam [5] concluded that using steel plates instead of timber elements with grain perpendicular to the loading area reduces the variability in recorded force-displacement curves, i.e. by producing a smoother signal, without impact on the results.

According to EN 408 [6], the modulus of elasticity has to be determined from deformation measurements taken within the central part and over 60 % of member depth. However, there is a certain evidence that the major share of deformations occurs in those zones adjacent to contact areas. Thus, determining the modulus of elasticity from measurements based on deformations measured over the entire member depth is seen to mirror practical design situations more realistically. Föppl [7] already suggested measurements over the entire depth instead of only the central part. Levé et al. [8] and others also have reached the same conclusion.

Following this it is suggested to adapt the regulations in EN 408 [6] accordingly and generally for structural timber and timber products.

With focus on the evaluation procedure, the regulations in EN 408 [6] require to determine $f_{c,90}$ and $E_{c,90}$ iteratively. The reason for this is the definition of $\sigma_{c,90,max}$ by notation as the intersection point between the stress-strain curve and the gradient determined within 0.1 and 0.4 $\sigma_{c,90,max,est}$ with an offset of 1 % of member depth. Brandner [4] reports on the requirement to choose an alternative approach due to frequent occurrence of test data featuring initial successive hardening which exceeded the 10 % limit. The alternative was to determine $E_{c,90}$ within an apparently roughly linear part of the stress-strain curve, based on deformations determined over the whole specimen depth, and by controlling the correlation between stress and strain in that part to be $r \geq 0.999$. The compression perpendicular to grain strength was then determined as stress at the intersection point between the gradient at an offset of 1 % of the total specimen depth and the stress-strain curve. Consequently, an iterative procedure was not required.

Although this alternative approach for evaluating $f_{c,90}$ and $E_{c,90}$ is somehow an improvement compared to the current situation in EN 408 [6] it can still be elaborated further: By accepting the sigmoid, non-linear stress-strain relationship as inherent element of timber tested in compression perpendicular to grain, see Fig. 1 (right), Brandner [4] proposed to evaluate $E_{c,90}$ at the inflexion point of the stress-strain curve, i.e. as $\max[dE_{c,90}]$ within the zone of interest according to Fig. 1 (right). The strength value could then be simply determined at the intersection point between the stress-strain curve and the gradient at this inflexion point shifted by 1 % of overall specimen depth. For analysing the applicability of this approach further investigations are needed, e.g. on filtering of noise in recorded data and on comparative studies between $E_{c,90}$ determined according to EN 408 [6] and the new approach.

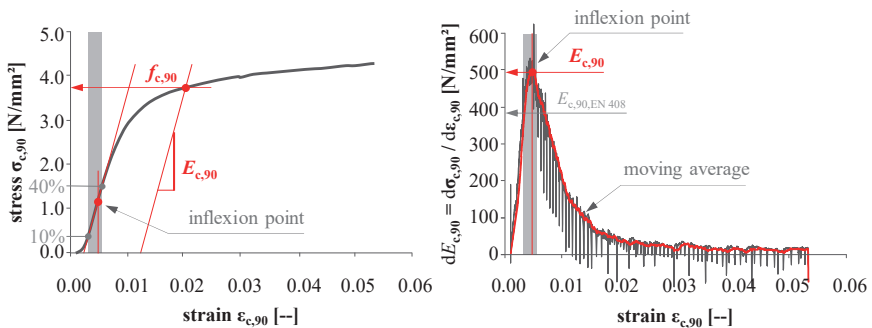


Fig. 1 (left) example of a stress-strain curve of timber loaded in compression perpendicular to grain; (right) change in $E_{c,90}$ per stress / strain-increment vs. strain (from Brandner [4])

In any case, in agreement with EN 408 [6] it is suggested to determine the basic properties at reference conditions, i.e. on specimen which reached their equilibrium

moisture content at 20 °C and 65 % relative humidity, i.e. featuring a reference moisture content of $u_{\text{ref}} = 12$ %. As timber exposed to compression perpendicular to grain is known to be rather sensitive to moisture, based on a literature study and own investigations Brandner [4] suggests to adjust the basic properties determined at moisture contents differing from the reference moisture content by a correction factor of 4 % per percent difference to the reference moisture content.

2. References

- [1] Unterwieser H., and Schickhofer G., “*Characteristic Values and Test Configurations of CLT with Focus on Selected Properties*”, In: R. Harris, A. Ringhofer, and G. Schickhofer (eds.) *Focus Solid Timber Solutions: The State-of-the-Art in CLT Research*. Proceeding of the European Conference on Cross Laminated Timber (CLT), COST Action FP1004, Graz, Austria, 2013.
- [2] Brandner R., Flatscher G., Ringhofer A., Schickhofer G., and Thiel A., “*Cross laminated timber (CLT): overview and development*”, *European Journal of Wood and Wood Products*, Vol. 74, 2016, pp. 331–351.
- [3] PT SC5.T1, “*Working draft of design of cross laminated timber in a revised Eurocode 5-1-1*”, Version: 2017-07-1, 2017.
- [4] Brandner R., “*Cross Laminated Timber (CLT) in Compression Perpendicular to Plane: Testing, Properties, Design and Recommendations for Harmonizing Design Provisions for Structural Timber Products*”, *Engineering Structures*, 2018, <https://doi.org/10.1016/j.engstruct.2018.02.076>.
- [5] Gasparri E., Lam F., and Liu Y., “*Compression perpendicular to grain behaviour for the design of a prefabricated CLT façade horizontal joint*”, Proceeding of the World Conference on Timber Engineering (WCTE), Vienna, Austria, 2016.
- [6] EN 408, “*Timber structures – Structural timber and glued laminated timber – Determination of some physical and mechanical properties*”, European Committee for Standardization (CEN), 2012.
- [7] Föppl A., “*Die Druckfestigkeit des Holzes in der Richtung quer zur Faser*“, Mitt. Mechan.-Techn. Lab. D. K. Techn. Hochsch. München, Vol. 29–32, 1904, pp. 7–25 (in German).
- [8] Levé C. L., Maderebner R., and Flach M., “*Compression strength and stiffness perpendicular to the grain – influences of the material properties, the loading situation and the gauge length*”, Proceeding of International Network on Timber Engineering Research (INTER), 1st Meeting, INTER/47-6-1, Bath, United Kingdom.

Test Configurations for Determining Rolling Shear Properties with Focus on Cross Laminated Timber: A Critical Review

Thomas Ehrhart ^{*)}
PhD Student
ETH Zürich / Empa Dubendorf
Zurich / Dubendorf, Switzerland

Reinhard Brandner ^{*)}
Assistant Professor; Deputy Head of the Institute
Institute of Timber Engineering and Wood Technology
Graz University of Technology
Graz, Austria

^{*)} joint first authorship

Summary

The assessment of mechanical properties requires appropriate, robust, and replicable test methods. International standards, such as EN 408 [1] and EN 789 [2], include test configurations that allow for the determination of most mechanical properties needed for the design of timber structures. Regarding shear stresses in planes perpendicular to the grain, so-called rolling shear stresses, test configurations for the determination of rolling shear strength and modulus of cross laminated timber have been implemented in the recent product-standard EN 16351 [3]. However, several issues of particular relevance are not addressed in the current version of [3]. Furthermore, the occurrence of rolling shear is not only restricted to cross laminated timber. Thus, an appropriate test configuration for the determination of the rolling shear behaviour of further timber products should be also implemented in [1].

A critical review is given on test configurations for the determination of rolling shear properties with focus on cross laminated timber. Configurations proposed in literature are discussed with regard to the resulting stress state, their applicability and versatility, as well as their capability to represent the stress situation in cross laminated timber appropriately.

Finally, (i) concrete steps are suggested for further specification of the regulations given in [3], (ii) a test configuration is suggested to be implemented in [1] for the determination of rolling shear properties of the raw material used for cross laminated timber, glued laminated timber and further timber products, (iii) and research needs are identified.

1. Introduction

The mechanical properties of the cylindrically anisotropic material timber heavily depend on the type and orientation of stresses. Usually, the strength and elastic properties are related to the major axes of timber: longitudinal (L), tangential (T), and radial (R) (Fig. 1, left). With focus on rolling shear, stresses in the TL-plane caused by forces in tangential direction (related shear strength and modulus: $f_{v,TR}$ and G_{TR}), stresses in the RL-plane caused by forces in radial direction ($f_{v,RT}$ and G_{RT}), and all orientations in between induce rolling shear (f_r and G_r as rolling shear strength and modulus, respectively). In the rolling shear failure mode, longitudinally orientated wood fibres typically “roll” off each other along the annual rings or the wood rays without being crushed individually (Fig. 1, middle and right).

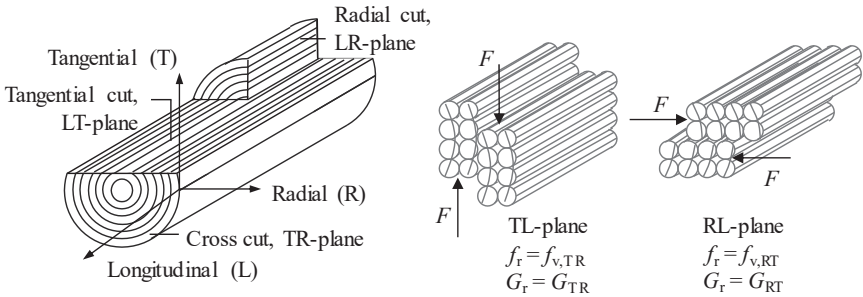


Fig. 1 Principal material axes in a log and fibre bundle (left) and rolling shear planes TL and RL (middle & right).

In the ultimate limit state (ULS) and serviceability limit state (SLS) design of timber structures, there are several cases where rolling shear needs to be taken into consideration. This circumstance has already been recognised, as meanwhile rolling shear properties have been anchored in several product standards, e.g. EN 14080 [4] for glued laminated timber made from softwood and poplar (*Populus spp.*).

Typical design situations where rolling shear might become relevant are e.g. ledgers laterally glued-on main girders and acting as supports for secondary structural elements, and outer glued-on wood-based panels for reinforcing straight girders with notches or holes and of curved, pitched or cambered girders with / without notches and / or holes; see Fig 2.

Rolling shear stresses and strains are inherent to the innovative engineered timber product cross laminated timber (CLT) due to the orthogonal orientation of adjacent layers. The orthogonal structure leads to rolling shear stresses, in particular if CLT elements are loaded out-of-plane (Fig. 3).

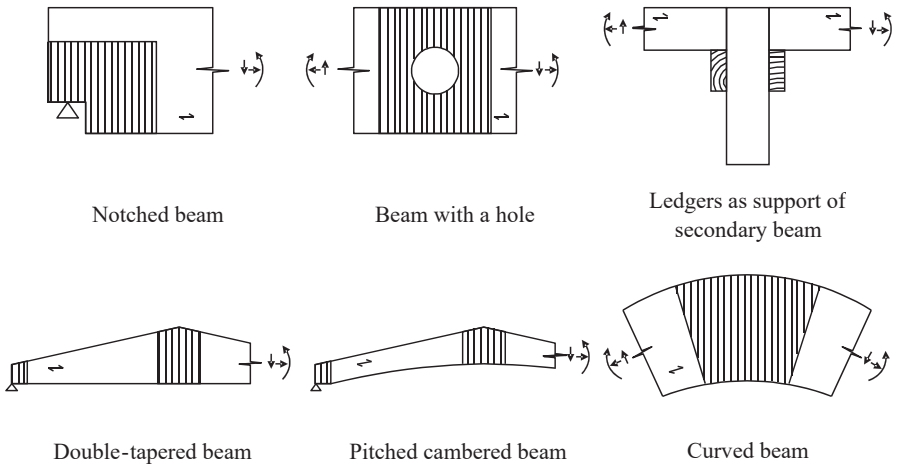


Fig. 2 Some design examples where rolling shear has to be taken into consideration.

Usually, the rolling shear stresses are not a major concern in the design of CLT elements. However, the rolling shear strain contributes a significant amount to the total deflection of CLT elements loaded out-of-plane. It has to be mentioned that the SLS design criteria *deflection* (up to about 4 m span) and *vibration* (spans larger than about 4 m) are of primary concern in the design of CLT floor elements in the majority of cases, not ULS.

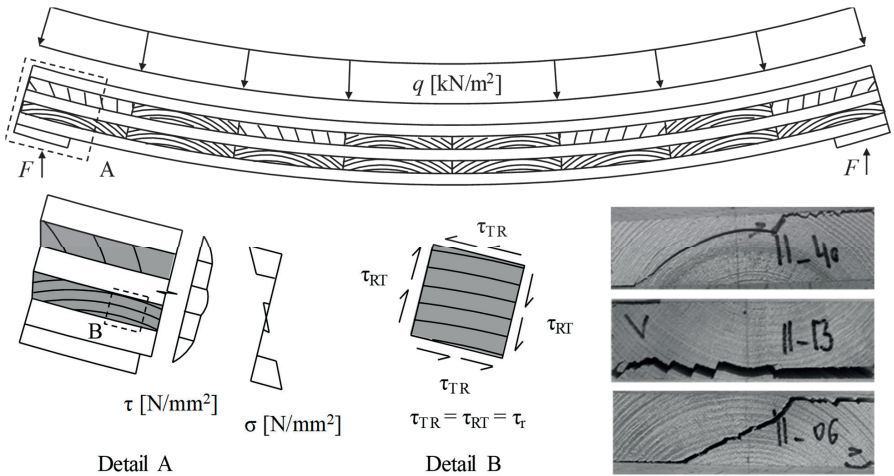


Fig. 3 Out-of-plane loaded five-layer CLT element (top), distribution of bending and shear stresses (bottom, left), dualism of (rolling) shear stresses in a cross layer (bottom, middle), and typical rolling shear failure patterns (bottom, right).

Since some years, another aspect relating to rolling shear strength and modulus has been in focus – optimising the use of timber in CLT-like elements by minimising the amount of laminations in the cross layers, i.e. by creating regularly large spacing between the laminations in the cross layers of CLT-like elements [5]–[7].

Thus, test configurations that allow for the appropriate determination of rolling shear strength and modulus (i.e. mirroring common stress situations and configurations in timber products and constructions in use) together with examination procedures congruent with design approaches are of great importance. As a “pure shear-stress-state” is generally difficult to obtain and, with regard to CLT, the question arises, whether such a stress-state would actually represent the situation within the cross layers and laminations of CLT appropriately, suitable test configurations are not obvious and different approaches imply various disadvantages but also advantages.

In the following, standardised test methods and test setups described in literature are presented and critically discussed regarding their usability for determining the rolling shear properties of CLT with the aim of suggesting one or more configuration(s).

2. Critical View on the State-of-the-Art of Rolling Shear Test Methods

2.1 General Remarks

Initially, test methods for the determination of rolling shear strength and modulus are divided into two different types of approaches: following the *holistic approach*, whole CLT panels are tested using out-of-plane bending tests. This allows for the direct determination of the panel’s strength and stiffness, taking into account all system components like span, height, width, number of laminations, the aspect ratio (width vs. thickness of the laminations), and further parameters. However, although the setup of such tests may be simple, efforts and costs for these tests are rather high, as usually only one product property for strength and stiffness is determined, e.g. rolling shear strength and rolling shear modulus. Furthermore, the results are in principle restricted to exactly the tested product and setup. Hence, variation of any parameter, for example the lamination’s thickness or width, the number of layers or timber strength classes, may lead to a different rolling shear performance of the CLT elements.

Following the *atomistic approach*, single elements of the system CLT (here: single or multiple segments of the cross laminations) are investigated individually. To obtain appropriate values for the rolling shear strength and stiffness of CLT from such tests, the configuration needs to be designed in a way that the resulting stress state is as similar as possible to the actual stress state of the single element within CLT. If all relevant system effects can be described accurately, (atomistic) testing of single elements represents an interesting way to complement or even replace the (holistic) testing of CLT elements.

However, this approach is not completely new and already part of current regulations in standards, i.e. considering the load-bearing model for glulam in bending, which bases on the tensile strength values of the laminations.

In the following, we present and discuss test methods that are related to the base material as well as to the system product CLT separately. The experience gained in applying such test methods are mainly restricted to softwood, in particular Norway spruce (*Picea abies* (L.) KARST.). This circumstance needs to be taken into account when defining the geometry of the specimens in order to prevent other, undesirable failure modes with high probability.

2.2 Test Methods Related to the Base Material – Atomistic Approach

2.2.1 Test Methods for the Determination of Rolling Shear Properties of Clear Wood

For small specimens with straight grain and without any local growth characteristic as present in timber, so called clear wood, and aiming for a pure shear-stress state, several test setups have been presented in literature and discussed in expert's community. The Iosipescu shear test [8]–[11], the Arcan shear test [12], [13], and the single cube apparatus [14] (Fig. 4, left to right) are some of them, partly originally developed for testing other materials than wood, but also shown to be applicable to this material.

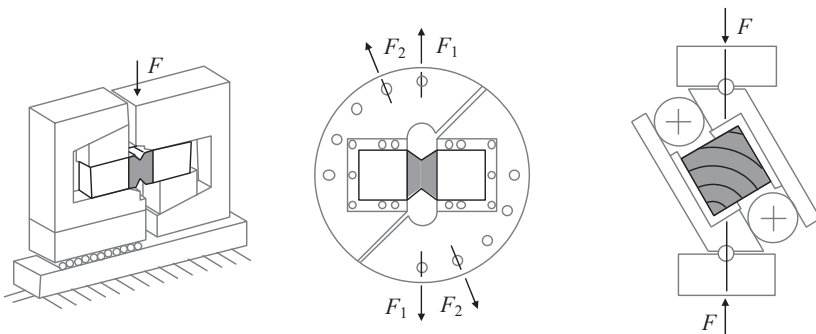


Fig. 4 Test methods for determining rolling shear properties on clear wood according to [8]–[14] (left to right).

Overall, these three test methods are mainly capable of determining the rolling shear modulus rather than rolling shear strength. In comparison to the Arcan shear test and the single cube apparatus, one disadvantage of the Iosipescu shear test method is the eccentric load introduction. This eccentricity induces transverse stresses additionally to the rolling shear stresses. However, due to the heterogeneity of timber, failure does usually not occur exactly at the theoretically foreseen failure plane and, thus, similar problems related to the eccentricity may occur in the Arcan shear tests and when using the single cube apparatus.

The above presented methods are restricted to small-scale tests on clear wood and, in addition, do not allow to appropriately mirror the stress state within cross layers of CLT elements subjected to bending out-of-plane. Thus, these methods cannot be used to investigate several important issues, such as the aspect ratio width vs. thickness of laminations. Furthermore, the potential influences of local growth characteristics and global grain deviations, which are typical for timber, are – by definition – not part of small clear wood specimens.

However, the results obtained from these tests can serve as input parameters for numeric simulations and analytic studies, as stresses and strains in the different material planes can be investigated in detail, i.e. values representing better the cylindrically anisotropic nature of wood and timber. In particular, the rolling shear modulus is known to be remarkably influenced by the annual ring orientation; see e.g. [15]–[18], where for Norway spruce values between 30 and 280 N/mm² for flat grain and annual rings oriented 45° were predicted, respectively.

2.2.2 EN 408 [1] alike Test Setup Used for the Determination of Rolling Shear Properties of Single Lamination Segments

Obviously, rolling shear properties determined on timber are more representative for timber used for structural purposes than properties determined on small clear wood specimens, even if the specimens are short in the longitudinal direction (parallel to the grain). This applies, in particular, if the complete cross section of the sawn timber of interest for later use is tested. Testing the whole timber cross section may also lead to a lower bandwidth in observed rolling shear module than in case of small specimens. This is because the extreme cases of annual ring orientations, i.e. perfect flat or rift grain and 45° orientation [15], are hardly given for the whole cross section.

Additionally, the aspect ratio of the lamination influences the rolling shear modulus due to the changes in the annual ring orientation over the cross section [17], [19]–[21]. Moreover, the *apparent rolling shear strength* decreases significantly for decreasing aspect ratios w_ℓ / t_ℓ , with w_ℓ and t_ℓ as the lamination width and thickness. However, the apparent rolling shear strength seems not to depend on the former position of the lamination segment within the log. The significant decrease in apparent strength for decreasing aspect ratios w_ℓ / t_ℓ is not caused by a decrease in rolling shear strength, the reason why it is called apparent rolling shear strength. Indeed, it may be due to the increasing level of tension perpendicular to grain stresses at the free edges in combination with a larger portion of the cross section needed to build up the shear stresses for smaller aspect ratios w_ℓ / t_ℓ .

The test setup described in EN 408 [1] for the determination of shear properties f_v and G_0 on lamination segments has meanwhile been applied in several studies on the rolling shear behaviour of single lamination segments (e.g. [20]–[23]). From these studies, documented experience with regard to the setup itself and information regarding the following aspects are available:

- Different materials used for the loading plates; apart from steel plates also hardwood species were numerically and experimentally investigated; see e.g. [20]–[23].
- Different angles between force axis and the element; 6°, 10°, 14°; see e.g. [20]–[23].
- Effect of pre-stressing the specimens perpendicular to the grain by loading additionally transversely in tension or compression; see Fig. 6 based on [20].
- Influence of the lamination segment’s width and aspect ratio (width vs. thickness); see e.g. [20]–[23].
- Finite element (FE) analysis on the stress distribution within the specimens regarding the tensile and compression stresses perpendicular to the grain as well as the distribution of rolling shear stresses within the tested element; see [20] and Fig. 5 based on [22].
- Experience with different softwood and hardwood timber species; see e.g. [21]–[24].

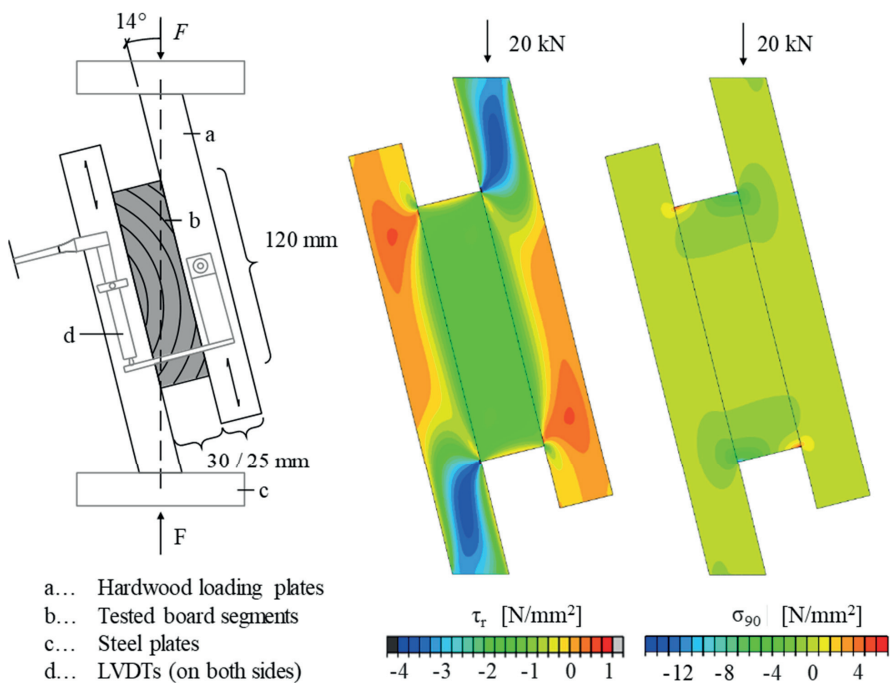


Fig. 5 Test configuration and distribution of shear- and normal stresses (left to right) used in [21], [22].

The main but overall small criticism of the test setups described in EN 408 [1], EN 16351 [3] and EN 789 [2], as well as all configurations based on these three test setups is the presence of stresses perpendicular to the grain, additionally to the rolling shear stress (Fig. 5).

Locally, tensile stresses perpendicular to the grain occur and can lead to initial cracks close to the specimen's edges. However, from the experiences described in [21], the path of ultimate failure was independent from any initial damage due to these stresses. Consequently, influence from transverse stresses on rolling shear properties is only expected in the central part of the specimen, featuring very moderate stresses perpendicular to grain, and not on the edges.

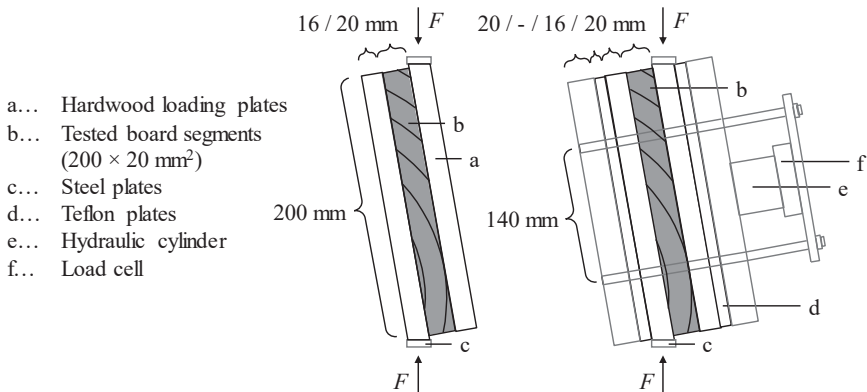


Fig. 6 Test configuration in Mestek [25] used for additional transverse compression or tension loading.

Extensive investigations on the influence of compression stresses perpendicular to the shear plane on the rolling shear strength of lamination segments were carried out in [20]. Fig. 7 shows the results for tests conducted on single lamination segments with and without stress reliefs. In [20], the specimens featured a cross section of $w_\ell \times t_\ell = 200 \times 20 \text{ mm}^2$ and, thus, an aspect ratio of $w_\ell / t_\ell = 10$. An indicative positive effect of increasing compression stresses on the rolling shear resistance was found, but not as significant as found in [26] and [27] for the longitudinal shear resistance.

The EN 408 [1] alike test setup is considered to be a good and reliable candidate for a reference test setup. Its rather simple execution, wide applicability and versatility, and, at least for small inclinations of 10° to 14° (as regulated in EN 408 [1] and applied in [21], [22]), the rather small influence of transverse stresses on the (apparent) rolling shear strength, suggest its use for the determination of rolling shear properties as basis for CLT. Besides CLT, it may be also used for solid timber, glulam and other products based on sawn timber.

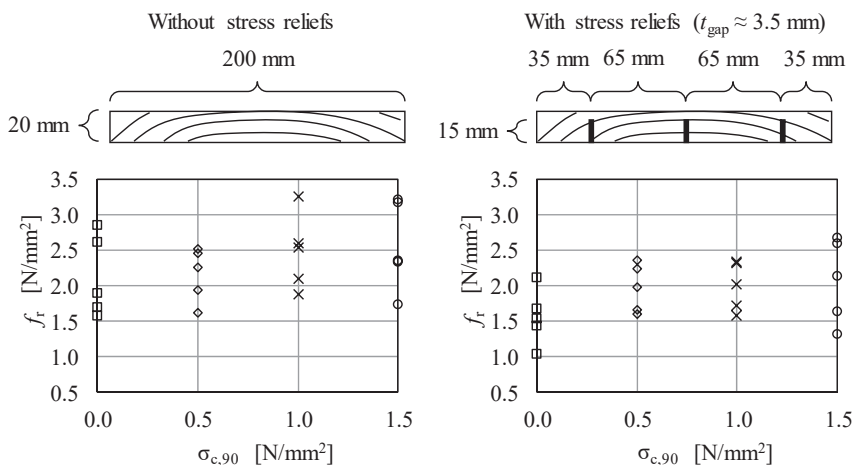


Fig. 7 Rolling shear resistance (apparent rolling shear strength) of single lamination segments without (left) and with stress reliefs (right) depending on the additionally applied transverse stress; based on [20].

Rather small and for timber properties common variability indicates the reliability of this test setup. Regarding the rolling shear modulus, coefficients of variation $CV[G_r]$ from 12 to 27 %, mainly approx. 20 %, and for rolling shear strength $CV[f_r]$ from 8 to 22 %, mainly approx. 10 to 15 %, are found in [21], [22]. For $CV[f_r]$, [20] found in small test series (five specimen each) values between 17 and 28 %.

Compared to tests on CLT elements, as discussed in Chapter 2.3, the specimens are rather small and their preparation is simple and inexpensive. Based on findings in [20] and successful later tests in [21]–[23], instead of steel also hardwood, e.g. lamination segments of beech glued transversely on the specimens, can be used as load introduction plates, which further decreases the effort and costs for the preparation and testing.

2.2.3 Test Methods for the Determination of Rolling Shear Properties of Lamination Segments

The main part of currently available CLT products are without narrow face bonding, i.e. without intended glue-bonding at the edges of adjacent laminations within the same layer. Consequently, test methods considering testing specimens with free edges are principally able to mirror the situation of laminations within CLT elements. In fact, even in CLT with narrow-face bonded laminations, swelling and shrinkage due to unavoidable climatic changes will cause cracks and, thus, again free edges over their lifetime.

Test methods applied and suggested for determining rolling shear properties on short timber specimens are for example described in [28] and [29]; see Fig. 8. However, there are other aspects which provoke some critical view on the test methods applied in [28] and [29]: both test methods comprise already a parallel system of lamination

segments, in [28] two and in [29] four lamination segments. Consequently, the load between the lamination segments is distributed according to their stiffness. Furthermore, potential imperfections in both test configurations regarding load- and support conditions may foster failure of one side of parallel tested elements. As soon as failure of the first segment occurs, moments are induced in the remaining element(s), which, with high probability, provokes a sudden failure. This combined failure mode in the second side influences the maximum estimated rolling shear stress. However, this circumstance could be taken into account in the evaluation procedure as being right-censored at the time the first side fails, e.g. by means of the Maximum-Likelihood method for right-censored data analysis. In this analysis, the parallel action between the lamination segments shall be taken into consideration. Furthermore, in both test configurations the load introduction is in tension. For ease of use, testing in compression would be desirable.

Regarding the setup presented in [28] (Fig. 8, left), the horizontal support by the stiff steel plates, theoretically preventing any lateral deformation of the lamination segments, has to be considered, as this supporting condition is rather different from that of laminations in a CLT plate. Furthermore, the effort and costs of producing and conducting the tests is probably critical as many sets of steel parts are necessary, or only few specimens can be prepared at the same time. A simple improvement could be to use longitudinally loaded lamination segments, i.e. five-layer CLT element, instead of the steel plates for transferring the applied load, as shown in [29].

The test method according to [29] (Fig. 8, right) considers again a system of lamination segments (four) instead of testing a single segment. This might have an influence on the outcomes, at least on the observed variability. In contrast to the test method presented in [28], no lateral support is realised allowing for a stress state that is closer to laminations in CLT plates. The elements required for loading and support can be realised by laminations glued-on orthogonally to the test specimens. In comparison to [28], this simplifies the production and reduces costs in performing the test method.

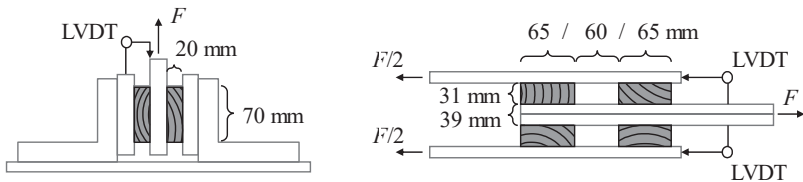


Fig. 8 Test methods for determining rolling shear properties on lamination segments as used in [28] (left) and [29] (right).

- a... Hardwood loading plates
- b... Tested board segments
(120 × 30 mm²)
- c... Steel plates

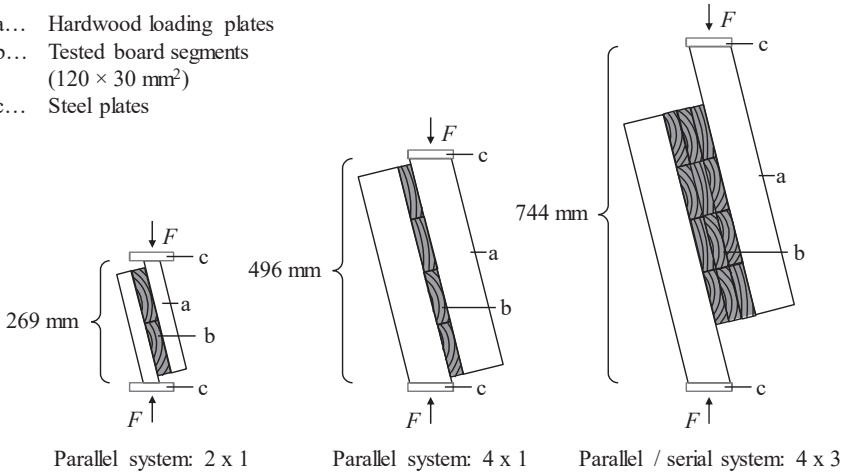


Fig. 9 Rolling shear tests on parallel and serial, sub-parallel acting systems of lamination segments according to [21].

More recently, [21] reported on rolling shear tests using a test configuration based on the shear test configuration implemented in EN 408 [1]. Apart from testing single lamination segments also parallel acting and serial, sub-parallel acting systems of lamination segments were tested; see [21] and Fig. 9. Apart from other aspects, again the necessity to account for the system action between tested lamination segments in the evaluation procedure of the rolling shear test data is required. However, the test configuration based on EN 408 [1] has some advantages when used for testing rolling shear on single lamination segments and CLT elements as well. Therefore, we discuss this EN 408 alike test configuration in more detail in Chapter 2.2.2 and Chapter 2.3.1.

One important aspect of testing systems of lamination segments instead of single lamination segments is the difficulty in investigating single aspects like density, sawing pattern and others as well as their influence on the rolling shear properties.

2.3 Test Methods Related to the Product CLT – Holistic Approach

2.3.1 EN 408 [1] alike Test Setup Used for the Determination of Rolling Shear Properties of CLT Elements

Apart from testing single lamination segments by means of the EN 408 [1] alike test setup, several studies have been conducted for determining the rolling shear behaviour of CLT layers as a system of parallel acting lamination segments; see e.g. [20] and Fig. 10.

As already discussed in Chapter 2.2.2, again some influence from transverse stresses on rolling shear properties occur. In addition to investigations on single lamination segments, extensive investigations on the influence of transverse stresses on the rolling shear properties were carried out in [20].

- a... HEA 100
- b₁... Tested CLT element ($t_{CLT} = 7 \times 17$ mm)
- b₂... Tested CLT element ($t_{CLT} = 7 \times 27$ mm)
- c... Steel plates
- d... Teflon plates
- e... Hydraulic cylinder
- f... Load cell
- g... Critical cross layer

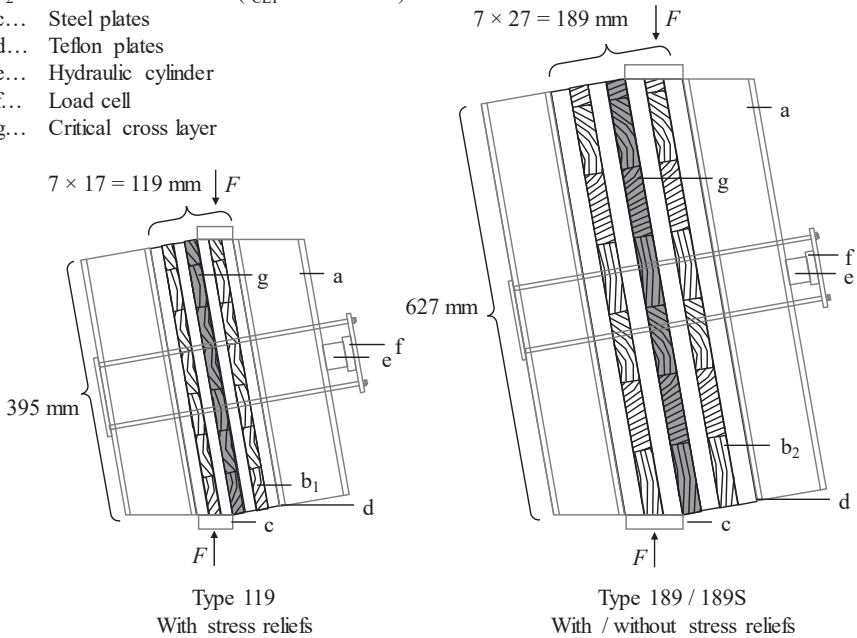


Fig. 10 Shear tests conducted in [20] based on the EN 408 [1] alike setup.

Fig. 11 shows the results for seven layer CLT elements with thicknesses of 119 and 189 mm (constant lamination thickness of 17 and 27 mm, respectively) with and without stress reliefs. Increasing apparent rolling shear strengths (increasing rolling shear resistance) with increasing transverse compression stresses comparable to tests conducted on single lamination segments were found for all sizes and types.

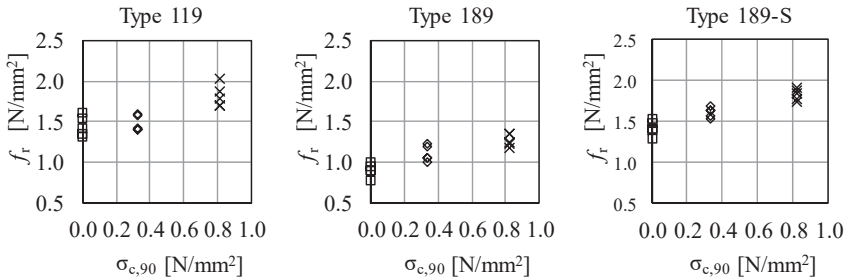


Fig. 11 Apparent rolling shear strength of the middle layer in seven-layer CLT elements depending on the additionally applied transverse stress [20].

The observed variability $CV[f_r]$ in tested series of five specimens each were in the range of 4 to 9 %, thus much smaller than in tested single lamination segments. However, the mean rolling shear strengths agree well with outcomes from testing single lamination segments, as far as approximately equal aspect ratios of laminations are compared, i.e. in case of stress reliefs the ratio between the relief spacing and the lamination thickness; see [1].

2.3.2 Determination of Rolling Shear Properties according to EN 16351 [3] and EN 789 [2]

An alternative test setup for the determination of rolling shear strength and modulus by testing CLT elements or parts of it is described in EN 16351 [3], section F 3.3 (Fig. 12, left). It is very similar to the setup given in EN 789 [2] (Fig. 12, right) and describes a three layer specimen, by using CLT elements directly or parts of CLT elements featuring five or more layers, with a middle layer orientated orthogonal to the force direction. Consequently, this test setup investigates the rolling shear properties of a system of lamination segments representing a CLT cross layer. Due to the parallel shift of the forces' axes, the configuration implies a rotational moment, which is counteracted with horizontally fixed bearings at both ends of the specimen. In this setup, the stresses in the middle layer are very similar to the stress-state in cross layers of a CLT panel subjected to out-of-plane bending. However, the rotational moment and the horizontally fixed bearings imply secondary horizontal forces at both ends of the specimen, which lead to stresses perpendicular to the grain. Although this test setup looks very similar to the test setup alike the shear test configuration according to EN 408 [1], the execution is more difficult requiring higher efforts in preparation of the test setup.

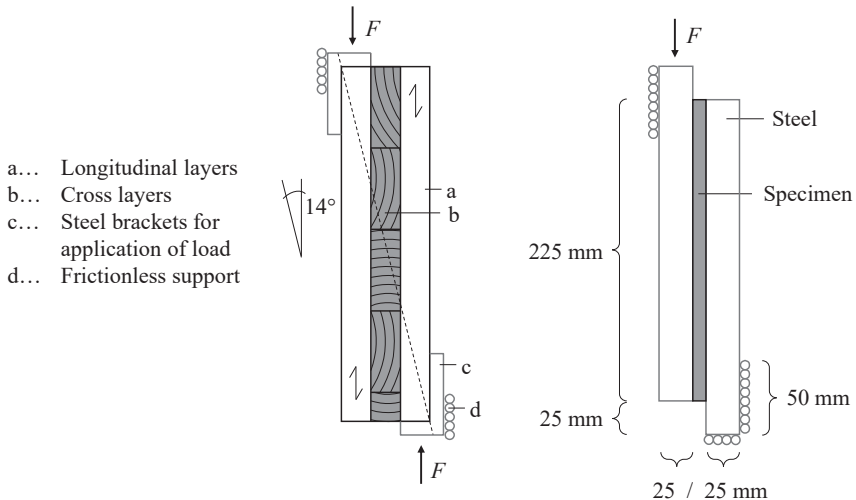


Fig. 12 Shear test setups implemented in the standards EN 16351 [3] and EN 789 [2] (left to right).

Following EN 16351 [3], regarding the geometry of the specimens, only a minimum width of 100 mm (longitudinal dimension of cross layers) is defined. Furthermore, a minimum number of 20 specimens has to be tested for each CLT layout. EN 16351 [3] outlines that results obtained from out-of-plane bending tests, as discussed in Chapter 2.3.3, and the test setup discussed in this chapter can be considered equivalent.

2.3.3 Determination of Rolling Shear Properties by means of Four-Point Bending Test Setups according to EN 16351 [3]

In EN 16351 [3] section F 3.2, the test setups for determining the rolling shear strength and the rolling shear stiffness (Fig. 13, top), and the rolling shear strength only (Fig. 13, bottom) by means of four-point out-of-plane bending tests are described.

The ratio span vs. thickness is reduced to 12 : 1 (9 : 1 for only rolling shear strength determination) compared to bending tests of solid timber and glulam as described in EN 408 [1] ($l = 18 \pm 3 h$) in order to decrease the risk of an undesired premature bending failure in the outermost laminations. For a five-layer CLT panel with a constant lamination thickness of 30 mm ($h = 150$ mm), this means that the following requirement regarding the bending strength $f_{m,CLT}$ and the rolling shear strength $f_{r,CLT}$ of the CLT panel has to be reached to avoid bending failures in most cases: $f_{m,CLT,05} / f_{r,CLT,95} > 18.75$.

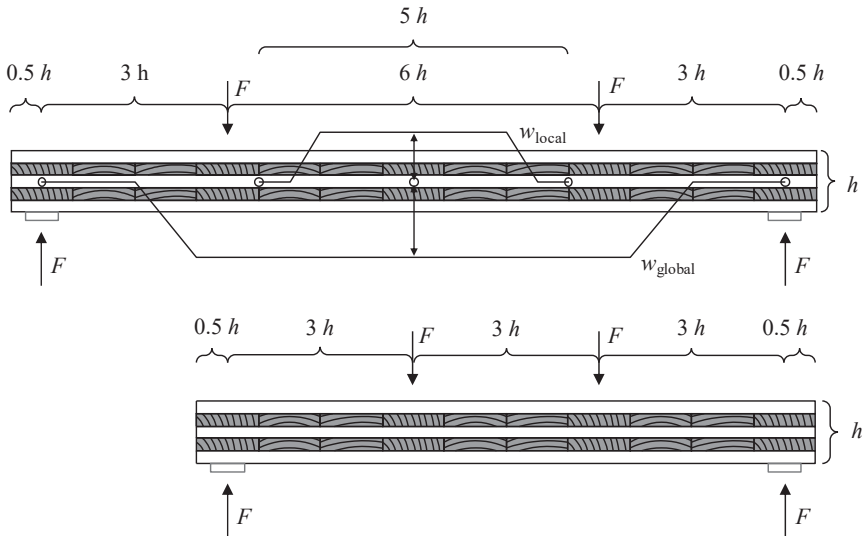


Fig. 13 Bending tests according to EN 16351 [1] for the determination of rolling shear strength and rolling shear modulus (top) and rolling shear strength only (bottom).

The characteristic rolling shear strength given in European technical assessments (e.g. ETA-06/0009 [30], ETA-06/0138 [31], and ETA-10/0241 [32]) lies between

0.85 and 1.5 N/mm². Following this and considering $CV[f_r] = 10\%$, as reasonable assumption following Chapter 2.3.1, and lognormal distribution, the 95 %-quantiles of the rolling shear strength can be estimated with 1.2 to 2.1 N/mm². In fact, outcomes in [20] and [22] indicate higher 95 %-quantile values as these numbers are already reached on average. However, taking these estimates as a starting point, characteristic (5 %-quantile) bending strengths of at least 23 to 39 N/mm² are required to achieve rolling shear failures in most of the cases, i.e. in at least 90 %. Tests at the Lignum Test Center (LTC) of the Institute of Timber Engineering and Wood Technology at Graz University of Technology on several series of CLT elements made of Norway spruce by different CLT producers have shown that applying the test setup dimensions suggested in Fig. 13, premature bending failures occur only rarely. However, when testing CLT made of higher strength class laminations in bending out-of-plane with a span to thickness ratio of 18 to 21, rolling shear failure occurred frequently or even in all specimens of some series before reaching the maximum bending-capacity.

For the determination of the rolling shear strength only, a three-point bending test constitutes an interesting alternative as (i) the section of constant moment (free of shear force) between the loading points, which increases the risk of bending failure, is avoided and (ii) the material use is significantly reduced. However, in order to receive the same level of shear stress as in a four-point bending test, application of a higher force, eventually resulting in problems regarding compression stresses perpendicular to the grain at the loading and support zones, is required.

The test setup in Fig. 13 (top), intended for determining the rolling shear strength and stiffness and according to [3], does not allow for the determination of a reliable rolling shear modulus. Measurement uncertainties of global and local deflections together with influence of the measurement distance, caused by the inhomogeneity in timber, and the necessity for choosing a deterministic value for the longitudinal shear modulus allow only a vague estimation of the rolling shear modulus.

Regarding the width w_{CLT} of the CLT elements, neither a standard dimension nor a reference number of parallel laminations is defined in EN 16351 [3]. However, the required sample size is related to the width: a minimum number of 15 specimens is required for $w_{CLT} < 500$ mm, ten specimens are required for $500 < w_{CLT} < 800$ mm and only seven specimens are required for $w_{CLT} > 800$ mm. As the scatter of the mechanical properties of the system CLT is generally reduced with an increasing number of parallel acting laminations, resulting in a lower CV for strength and stiffness properties, the principle behind this definition of the sample size is reasonable. However, as the width of the single lamination w_l is not defined, an element width w_{CLT} of e.g. 600 mm corresponds to between two and 15 parallel laminations given $40 < w_l < 300$ mm, as currently anchored in EN 16351 [3]. Thus, the sample size should not only be related to w_{CLT} but also to the number of parallel laminations or w_l .

3. Summary and Conclusions

- The determination of the rolling shear strength and rolling shear modulus by means of the EN 408 [1] alike test setup (see Chapter 2.2.2) is seen as an appropriate approach. The preparation of specimens and the test execution are rather simple and can be achieved in an economic way.
- The material to be used for the loading plates in this test configuration has to be defined. Depending on the timber species, different materials appear appropriate according to experiences described in [20] and [21]. For softwood timber species and poplar, loading plates made from hardwoods, e.g. beech (*Fagus sylvatica* L.) or ash (*Fraxinus excelsior* L.), are sufficient and help to reduce the efforts and costs when preparing the specimens. However, when testing hardwoods, it is advisable to use steel loading plates.
- A brief comparison between the rolling shear strength values from testing CLT elements and single lamination segments has shown good comparability. However, the variability in rolling shear properties when testing a layer of several parallel acting lamination segments or CLT elements is significantly lower compared to tests of single lamination segments. This circumstance could be taken into account in a load-bearing model for rolling shear for the adjustment of single lamination segment properties to properties of timber products like CLT by a reduced coefficient of variation.
- Determination of the rolling shear strength of CLT elements by means of four-point bending tests according to EN 16351 [3] (see Chapter 2.3.3) is seen as an appropriate but costly alternative, although, due to the significantly lower variability in rolling shear strength of CLT, the sample size can be significantly smaller in comparison to testing single lamination segments. However, determination of rolling shear modulus based on the suggested four-point bending test setup in EN 16351 [3] is questionable, as unavoidable large epistemic uncertainties are present. Again, the advantages of the EN 408 [1] alike test setup have to be outlined.
- In order to assure comparability between the determined rolling shear properties of different CLT layouts, definition of reference dimensions and a reference cross section are prerequisites. Here, the number of layers, their thickness and the aspect ratio of the laminations are of special importance.
- Overall, in detail regulation of the supporting conditions, the loading protocol and the procedure to measure and calculate the rolling shear strength and modulus have to be defined in order to assure transparency and comparability.

The following research needs have been identified:

- According to EN 16351 [3], the results obtained from out-of-plane bending tests (Chapter 2.3.3) and shear tests (Chapter 2.3.2) can be considered equivalent. Due to the differences between both tests, especially regarding (i) the resulting stress state, (ii) the degree of homogenisation and (iii) the stressed volume (size and system effect), a critical review is necessary to verify or

disprove this assumption. Therefore, single element tests according to EN 16351 [3] F 3.3 and out-of-plane bending tests according to F 3.2 with specimens produced from the same raw material and comparison of the results is suggested.

- Based on (i) a numerical analysis of the stress states in shear tests according to EN 16351 [3] (Chapter 2.3.2) and out-of-plane bending tests (Chapter 2.3.3) and based on (ii) investigations on the interaction between shear and transverse compression or tensile stresses, adjustment factors to directly link the results from both tests, could be developed.
- Further investigations on the size and system effects in serial and parallel acting systems subjected to rolling shear could contribute to a better understanding of the mechanical behaviour of CLT, and would be helpful for the implementation of a load-bearing model.

4. References

- [1] CEN European Committee for Standardization, “EN 408: Timber structures - Structural timber and glued laminated timber - Determination of some physical and mechanical properties“, 2012.
- [2] CEN European Committee for Standardization, “EN 789: Timber structures - Test methods - Determination of mechanical properties of wood based panels,” 2005.
- [3] CEN European Committee for Standardization, “EN 16351: Timber structures - Cross laminated timber - Requirements,” 2016.
- [4] CEN European Committee for Standardization, “EN 14080: Timber structures - Glued laminated timber and glued solid timber - Requirements,” 2013.
- [5] Silly G., Thiel A., and Augustin M., “Options for the Resource Optimised Production of Laminar Load Carrying Members Based on Wood Products“, in *Proceedings of WCTE*, 2016.
- [6] Franzoni L., Lebé A., Lyon F., and Foret G., “Influence of orientation and number of layers on the elastic response and failure modes on CLT floors: modeling and parameter studies“, *Eur. J. Wood Wood Prod.*, Vol. 74, No. 6, 2016, pp. 671–684.
- [7] Franzoni L., Lebé A., Lyon F., and Foret G., “Bending Behavior of Regularly Spaced CLT Panels“, in *Proceedings of WCTE*, 2016.
- [8] Dumail J.-F., Olofsson K., and Salmén L., “An Analysis of Rolling Shear of Spruce Wood by the Iosipescu Method“, *Holzforschung*, Vol. 54, 2000, pp. 420–426.
- [9] Kubojima Y., Yoshihara H., Ohsaki H., and Ohta M., “Accuracy of shear properties of wood obtained by simplified Iosipescu shear test“, *J. Wood Sci.*, Vol. 46, 2000, pp. 279–283.
- [10] Xavier J. C., Garrido N. M., Oliveira M., Morais J. L., Camanho P. P., and

- Pierron F., “A comparison between the Iosipescu and off-axis shear test methods for the characterization of *Pinus Pinaster* Ait,” *Compos. Part A*, Vol. 35, 2004, pp. 827–840.
- [11] Zhang L. and Yang N., “Evaluation of a modified Iosipescu shear test method for determining the shear properties of clear wood“, *Wood Sci. Technol.*, Vol. 51, No. 2, 2017, pp. 323–343.
- [12] Dahl K. B. and Malo K. A., “Linear shear properties of spruce softwood,” *Wood Sci. Technol.*, Vol. 43, No. 5–6, 2009, pp. 499–525.
- [13] Müller U., Ringhofer A., Brandner R., and Schickhofer G., “Homogeneous shear stress field of wood in an Arcan shear test configuration measured by means of electronic speckle pattern interferometry: description of the test setup“, *Wood Sci. Technol.*, Vol. 49, No. 6, 2015, pp. 1123–1136.
- [14] Hassel B. I., Berard P., Modén C. S., and Berglund L. A., “The single cube apparatus for shear testing – Full-field strain data and finite element analysis of wood in transverse shear“, *Compos. Sci. Technol.*, Vol. 69, 2009, pp. 877–882.
- [15] Görlacher R., “Ein Verfahren zur Ermittlung des Rollschubmoduls von Holz“, *Holz als Roh- und Werkst.*, Vol. 60, pp. 317–322, 2002 (in German).
- [16] Aicher S. and Dill-Langer G., “Basic considerations to rolling shear modulus in wooden boards“, *Otto-Graf-Journal*, Vol. 11, 2000, pp. 157–166.
- [17] Jakobs A., “Zur Berechnung von Brettlagenholz mit starrem und nachgiebigem Verbund unter plattenartiger Belastung mit besonderer Berücksichtigung des Rollschubes und der Drillweichheit”, Dissertation, Universität der Bundeswehr München, 2005 (in German).
- [18] Feichter I., “Spannungs- und Traglastberechnungen an ausgewählten Problemen der Holz-Massivbauweise in Brettsperrholz“, Master Thesis, Graz University of Technology, 2013 (in German).
- [19] Scholz A., “Schub beim Brettsperrholz“, *Bauen mit holz*, Vol. 5, 2001, pp. 60–66 (in German).
- [20] Mestek P., “Punktgestützte Flächentragwerke aus Brettsperrholz (BSP) – Schubbemessung unter Berücksichtigung von Schubverstärkungen“, Dissertation, Technical University of Munich, 2011 (in German).
- [21] Ehrhart T., “Materialbezogene Einflussparameter auf die Rollschubeigenschaften in Hinblick auf Brettsperrholz“, Master Thesis, Graz University of Technology, 2014 (in German).
- [22] Ehrhart T., Brandner R., Schickhofer G., and Frangi A., “Rolling Shear Properties of some European Timber Species with Focus on Cross Laminated Timber (CLT): Test Configuration and Parameter Study”, in *Proceedings of INTER - Meeting Forty-Eight*, 2015.

- [23] Aicher S., Christian Z., and Hirsch M., “Rolling shear modulus and strength of beech wood laminations“, *Holzforschung*, Vol. 70, No. 8, 2016, pp. 773–781.
- [24] Bendtsen B. A., “Rolling Shear Characteristics of Nine Structural Softwoods“, *For. Prod. J.*, Vol. 26, No. 11, 1975, pp. 51–56.
- [25] Mestek P. and Winter S., “Cross Laminated Timber (CLT) - Reinforcements with Self-Tapping Screws“, in *Proceedings of WCTE*, 2010.
- [26] Spengler R., “Festigkeitsverhalten von Brettschichtholz unter zweiachsiger Beanspruchung, Teil 1, Ermittlung des Festigkeitsverhaltens von Brett lamellen aus Fichte durch Versuche“, *Berichte zur Zuverlässigkeitstheorie der Bauwerke*, Heft 62, 1982 (in German).
- [27] Hemmer K., “Versagensarten des Holzes der Weißtanne (*Abies Alba*) unter mehrachsiger Beanspruchung“, Dissertation, Karlsruhe, Germany, 1984 (in German).
- [28] Franzoni L., Lebée A., Foret G., and Lyon F., “Advanced modelling for design helping of heterogeneous CLT panels in bending“, in *Proceedings of INTER - Meeting Forty-Eight*, 2015.
- [29] Görlacher R. and Blaß H. J., “Zum Trag- und Verformungsverhalten von LIGNOTREND-Decken- und Wandsystemen aus Nadelschnittholz“, *Bauen mit Holz*, Vol. 104, No. 11, 2002, pp. 30–41 (in German).
- [30] Deutsches Institut für Bautechnik, “European Technical Assessment: ETA-06/0009 Binderholz Brettsperrholz“, Berlin, Germany, 2017.
- [31] Österreichisches Institut für Bautechnik, “European Technical Assessment: ETA-06/0138 K LH-Massivholzplatten“, Vienna, Austria, 2012.
- [32] Deutsches Institut für Bautechnik, “European Technical Assessment: ETA-10/0241 Leno Brettsperrholz“, Berlin, Germany, 2013.

Test Methods for In-plane Shear Tests of Cross Laminated Timber

Erik Serrano

Division of Structural Mechanics, Lund University
Lund, Sweden

Summary

A number of different test methods to characterise the behaviour at in-plane shear loading of cross laminated timber, can be found in literature, including methods already available in standards. This contribution aims at giving a brief overview and discussion about these methods, highlighting their respective benefits and drawbacks. In addition, a more detailed discussion related to test methods to characterise the torsional strength of crossing areas in cross laminated timber is given. Recommendations for which test methods to include in future versions of the harmonised standard for cross laminated timber is given, together with recommendations on further developments necessary and future research topics that should be addressed.

1. Background and introduction

1.1 In-plane shear of cross laminated timber

Due to the structure of cross laminated timber (CLT), the action of CLT elements for in-plane shear loading has traditionally been analysed in relation to three possible failure modes, according to Fig. 1³. Failure mode I, also referred to as gross shear failure, relates to a failure where the laminations of the CLT are in full interaction and thus making possible a pure and equal shear deformation of all layers (*i.e.* edge glued CLT is assumed). Failure mode II, also referred to as net shear failure, relates to the case where the longitudinal (transversal) layers fail in shear along a failure plane coinciding with the gaps (non-edge glued or assumed cracks at the glued edges) between the longitudinal (transversal) layers. Thus, both gross shear and net shear failures involve the shear stress τ_{xy} (τ_{yx}) with directions (x,y) representing the global directions according to Fig. 1. For a single lamination, this shear stress represents longitudinal-transverse shear. Failure mode III involves the torsional shear failure of the glued crossing area between a longitudinal and a transversal layer. The shear stress acting on such a surface can thus be decomposed into components τ_{zx} and τ_{zy} , again making reference to Fig. 1 (z being the direction of the normal of the crossing area). For the glued face of a horizontal lamination, τ_{zx} and τ_{zy} correspond to longitudinal-transverse shear and rolling shear, respectively, while for the glued face of a transversal lamination τ_{zx} and τ_{zy} correspond to rolling shear and longitudinal-transverse shear, respectively.

³ Note that the three failure modes are not consistently numbered throughout literature.

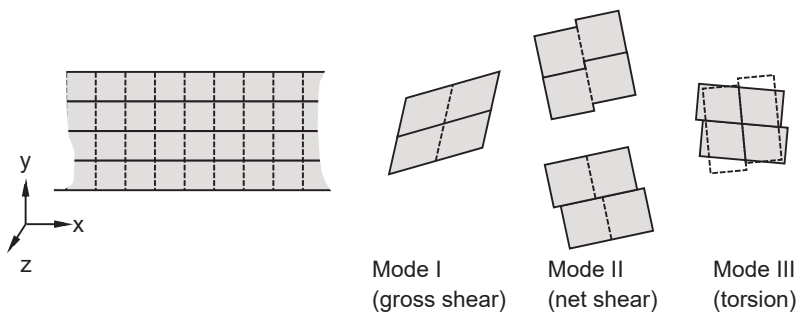


Fig. 1 Definition of three shear failure modes in CLT diaphragms.

It is important to realise that the nomenclature used in describing the behaviour of CLT is intimately connected to the *structural* characteristics of the product, and not to the material characteristics (in a continuum sense). This holds also for the test methods used in characterising CLT and the methods of evaluating the test results. For failure mode III this is elucidated by the fact that the shear capacity of the crossing areas is typically expressed in terms of the sum of the bearing capacity in shear along the lamination directions and the bearing capacity in torsional shear. For these two contributions, different strength values are assumed. In a continuum-based approach, the stress situation would be described in terms of the two perpendicular stress components active in the crossing area, τ_{xz} and τ_{yz} , and of course at a specific material point of interest, without taking into account the loading situation giving rise to these stresses.

1.2 Single node tests vs. “full scale” testing

Several attempts have been made to test CLT at in-plane loading based on larger-scale tests (full-scale CLT-plates involving a large amount of laminations) and introducing shear fields by means of *e.g.* a 3-point bending test [1], by means of (bi-axial) tension or compression tests, [2], [3] and [4], or by tests similar to wall racking tests. Although such test set-ups may seem appropriate they do bring several difficulties related to load introduction, distinction between gross and net shear failure on the one hand and torsional failure on the other hand and, finally, assuring that a state of pure shear is indeed achieved. In addition, such test set-ups are cumbersome to deal with and probably expensive due to cost of labour. A single node test, on the other hand can be designed such that the sought failure mode is achieved, but one issue with these is instead the much higher variability of the test results, as compared to what would be expected for *e.g.* a full size wall element which includes system effects.

2. Current methods

2.1 EN 16351 – Net shear tests and torsional shear

In the standard EN 16351:2015, [5], two methods relating to shear strength at in-plane loading are described in Annex F. The first methods, depicted in Fig. 2, relate

to shear failure of non-edge glued and edge-glued CLT, respectively. The description of the test specimens is limited and nothing is stated in the text regarding expected failure modes or if specific provisions have to be taken to avoid some failure mode.

The testing for the non-edge-glued case is based on a specimen where only one crossing area is tested, and thus, it may result in quite large variability. Taking into account the fact that the test results (most probably) are to be used for determination of product properties and that the product characteristics involves system effects, the in-plane shear strength obtained from this test method would have to be corrected for such system effects. Also, it might be difficult to avoid rolling shear failure at the interface to the glued-on side members. For both set-ups it is unclear from the standard if the intent is to manufacture the specimens by cutting out from CLT plates or if separate specimens are to be manufactured.

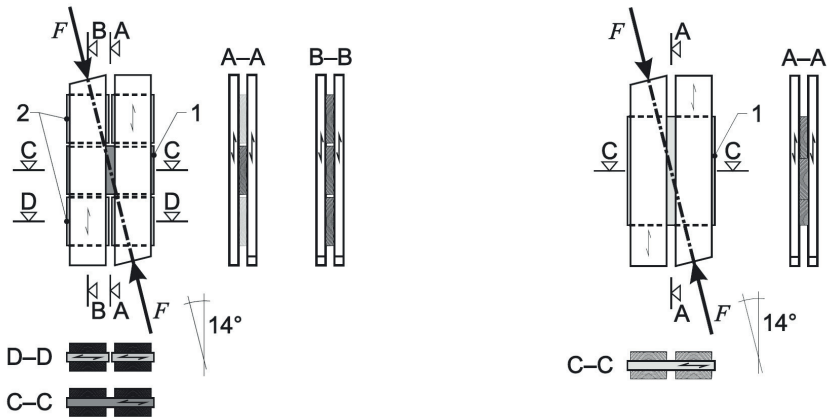


Fig. 2 Shear test according to EN 16351:2015. Left: Non-edge-glued CLT. Right: Edge-glued CLT. From [5].

The second in-plane shear strength method described in EN 16351:2015 is a test method to determine the torsional strength of the crossing areas, see Fig. 3. Here, again the description of the specimen and the test procedure is very rudimentary. The standard says that “The torsional shear strength of cross laminated timber shall be declared by the shear strength $f_{mz,9090}$ in N/mm^2 of the cross laminated timber, calculated by polar moment of inertia of the glued surface and layup”. It is unclear what the reference to “layup” means in this context.

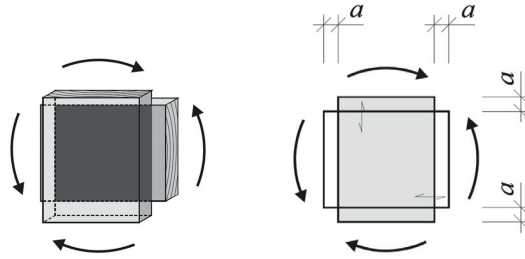


Fig. 3 Test specimen for torsional shear strength of crossing areas as given in EN 16351:2015. The overlap, a , should be 30 mm. From [5].

It is by no means straightforward to arrange this type of test set-up. A torsional testing machine could possibly be used (see below), but it is unclear whether this is what the standard suggests and such a test machine cannot anyhow be regarded as standard test equipment. The conclusion is anyhow that it is cumbersome to arrange the set-up proposed in the standard.

2.2 Other test methods proposed in literature

2.2.1 Single node test methods

Quite a large number of test methods have been proposed by various researchers. As a first example, the test method proposed by Wallner, [6], is shown in Fig. 4. The specimen is a specially manufactured specimen loaded in compression and aimed primarily at testing rolling shear failure of the crossing area although also net shear failures of the horizontally oriented lamination was also observed in some cases.

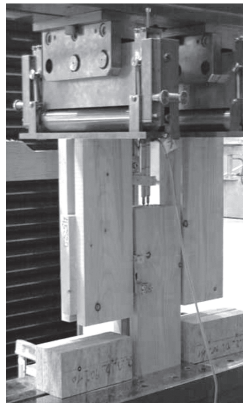


Fig. 4. Test set-up as proposed by Wallner for shear tests of single nodes.

A further developed test specimen was presented by Jöbstl *et al.*, [7], see Fig. 5. This test configuration is capable of producing net shear failures and was successfully used for that purpose as reported in [8].

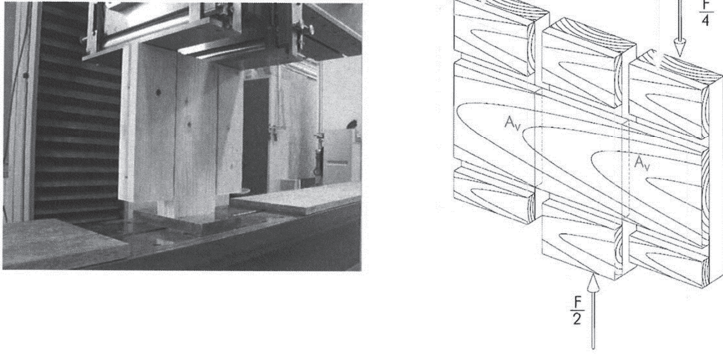


Fig. 5 Test set-up as proposed by Jöbstl et al. for shear tests of single nodes (left). Sketch of the symmetric half of the specimen (right).

Both the above-mentioned test methods/specimens suffer from the same drawback of not being directly cut from a CLT plate. The specimen of Fig. 5 is designed such that it produces right censored results, *i.e.* for each test, only the weakest section of two sections tested (for net shear) will fail. To circumvent this the specimen shown in Fig. 6 was developed, see [9]. This specimen has the advantage of being able to produce by cutting directly from a CLT-plate. Since the state of stress involved is a combination of shear and compression, a slight overestimation of the shear capacity is expected, [10]. The specimen and the set-up was also studied in detail by means of non-linear FE-analyses, which revealed that failure is indeed a combination of failure mode II (net shear) and failure mode III (torsion), see [10].



Fig. 6. Test set-up as proposed by Hirschmann for net shear tests of single nodes
A test method for torsional shear was suggested in the work of Jeitler, [11], [12] see Fig. 7. The method was evaluated in terms of the shape and size of the crossing area

and the orientation of the annual rings in the laminations, by use of elastic stress analyses using finite elements.

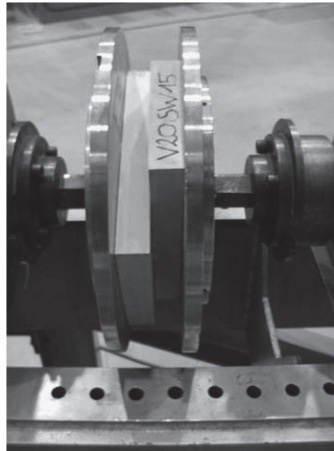


Fig. 7. Test set-up as proposed by Jeitler, for torsional tests of single nodes.

2.2.2 Multiple node test methods

A test set-up in compression with a larger CLT-panel was proposed by Andreolli *et al.*, see [2] and, in a later publication, Nygård *et al.* suggested a similar set-up, see [3]. All three failure modes are reported using this type of specimen, shown in Fig. 8. The method of Nygård *et al.* is also similar to a previous method proposed by Bosl in 2002, [4], who used a tension set-up instead.

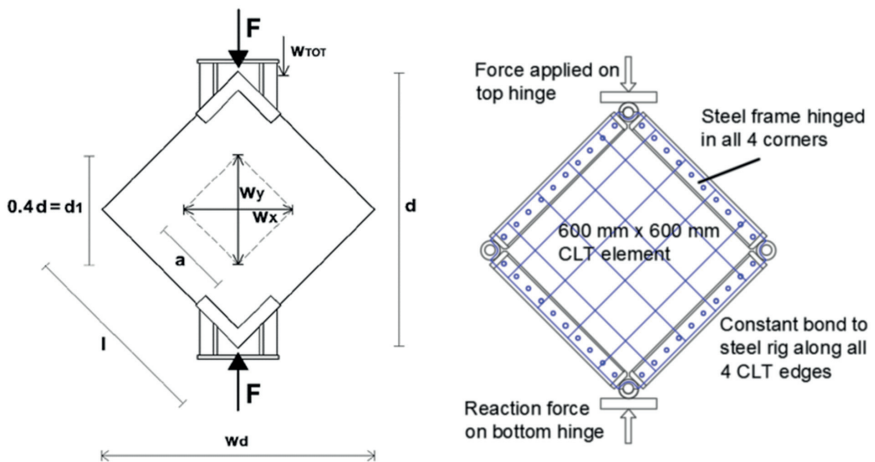


Fig. 8. Test set-ups as proposed by Andreolli *et al.* [2] (left) and Nygård *et al.* [2] (right), for in-plane shear.

A compressive test set-up and test specimen, see Fig. 9, was suggested by Kreuzinger and Sieder [13], and was evaluated by Brandner and Dietsch *et al.* [10], [14]. The rectangular specimen is cut at 45° relative the main board directions of the CLT plates and is loaded in compression. The specimen size must be chosen so as to avoid buckling at testing, and possibly also be chosen in relation to lamination widths. At the supports different conditions have been tested, to investigate potential influence of friction: lubrication, Teflon sheets, roller bearings, and direct steel to timber contact. The test results are evaluated by considering also a small influence of a compressive stress on the shear strength, since the global loads applied represent a combination of bi-axial compression + shear. It is noticeable that the method seems to be capable of distinguishing the failure modes of net shear and gross shear, and also reasonable values for shear modulus can be obtained [10]. Another main advantage is that the test itself is rather easy to perform and that the specimen can be easily cut from standard production. Evaluation of torsional shear strength has not been done with this setup, although nothing contradicts that this should be possible.

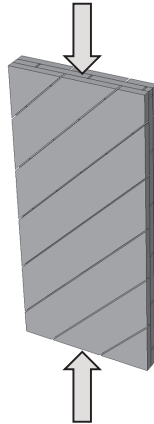


Fig. 9. Test set-up as proposed by Kreuzinger and Sieder for shear tests (net and gross shear capacity).

2.3 Discussion

2.3.1 Test methods for in-plane net shear and gross shear

As regards the currently proposed single node, in-plane shear method of EN 16351 and other single node methods, these are not well-suited to determine gross shear strength and one might anyhow doubt the relevance of those test methods in terms of producing a well-defined stress state which is also relevant for e.g. wall elements.

It is also possible that for some of the single node test methods, torsional shear is introduced, at least after some failure has been initiated.

Single node test specimens can be questioned for net shear, since such test results would have to be corrected for system effects.

As it seems, only the method as proposed by Kreuzinger and Sieder is straightforward to use for the determination of net and gross shear (depending on edge gluing or not) with the same test set-up. This set-up also has the advantage of being based on a specimen that can be cut from a standard CLT-plate. Thus, specimen preparation should be efficient.

2.3.2 A note on shear stress and failure criteria of crossing areas

Especially in applications where CLT is used as a beam, failure mode III has drawn some attention in terms of how to evaluate this failure mode (e.g. finding relevant stress distributions). In the evaluation of the capacity of crossing areas, it has been suggested, see e.g. [15] and [16], that failure criteria according to Eq. 1 should be used

$$\begin{aligned} \frac{\tau_{tor}}{f_{v,tor}} + \frac{\tau_{xz}}{f_R} &= 1 \\ \frac{\tau_{tor}}{f_{v,tor}} + \frac{\tau_{yz}}{f_R} &= 1 \end{aligned} \quad (1)$$

Here, τ_{tor} is the maximum *torsional* shear stress, assumed to be equal to the shear stress along an edge of the crossing area as calculated from linear elastic theory and using the polar moment of inertia of the crossing area. The corresponding strength is denoted $f_{v,tor}$. The shear stresses coming from a relative *translation* between the laminations are denoted τ_{xz} and τ_{yz} and these stress components are evaluated relative the rolling shear strength, $f_{v,R}$. These loading situations are depicted in Fig. 10.

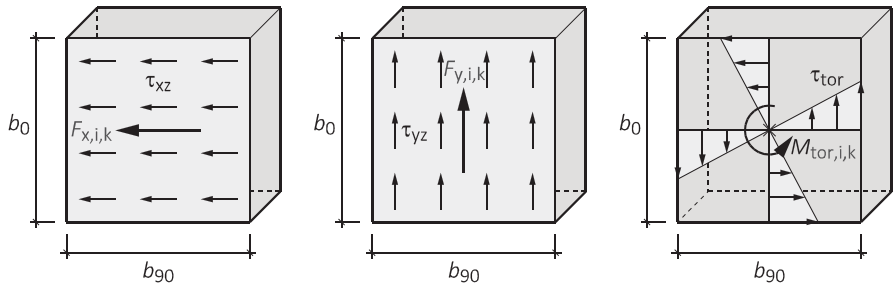


Fig. 10 Shear stress at crossing area of CLT due to shear forces (left and centre) and due to torsion (right).

Obviously, the shear stress acting on a crossing area can be decomposed into two components, the above mentioned τ_{xz} and τ_{yz} . For the one face (e.g. the face of the longitudinal lamination) these stress components correspond to rolling shear and longitudinal shear, respectively. For the other face (the face of the transversal lamination) the stresses τ_{xz} and τ_{yz} correspond instead to longitudinal shear and rolling shear, respectively.

Assuming that the rolling shear strength is less than the longitudinal shear strength, we naturally also assume a rolling shear failure if loading is in the longitudinal or in the transverse direction (*i.e.* corresponding to the situation to the left and in the centre of Fig. 10). The only difference would be at what face the failure is initiated.

For any other type of loading involving stress components τ_{xz} and τ_{yz} , for example a pure torsional loading, the failure could be influenced by interaction with longitudinal shear. This situation is depicted in Fig. 11, where an assumed quadratic interaction between rolling shear and longitudinal shear was assumed. The orange curve represents the failure envelope for the face of a longitudinal lamination and the blue curve represents the failure envelope of a transversal lamination. Furthermore, it is assumed that the rolling shear strength is half the longitudinal shear strength. The grey area would then represent the combined failure envelope. That failure envelope is seen to be quite similar to assuming rolling shear to be the only influencing strength parameter, and assuming no interaction between the two directions of the longitudinal and transversal laminations, respectively, *i.e.* the area bounded by the dashed lines of Fig. 11.

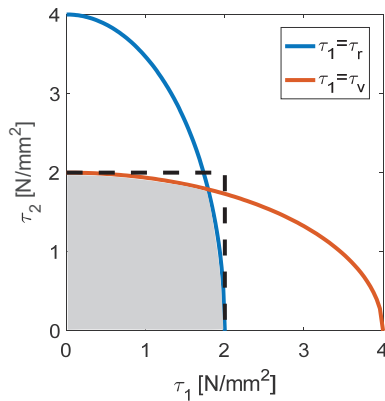


Fig. 11 Failure envelopes for the two faces at a crossing area (orange and blue curves) and the combined failure envelope (grey area).

With the above reasoning in mind, it is obvious that the failure criteria (1) can only be understood in terms of a structural description of the behaviour which, in turn, is a consequence of the test method and evaluation method used in characterisation, a structural description which should also then be adopted to the models used in design. In that sense, the torsional shear strength $f_{v,tor}$ can be seen as a fictitious strength parameter. An interesting question is then if it would be possible to make use of another approach that would use as strength input data *only* rolling shear strength. The rather small influence of longitudinal shear indicated in Fig. 11 indicates that this would be reasonable.

2.3.3 Test methods for torsional shear

As regards tests for torsional shear, the main issue of relevance is the question if there is a need for a separate torsional test at all. Based on the above discussion on strength characterisation of crossing areas, the rolling shear stress as obtained from other test methods, or even the rolling shear strength of the base material should be possible to use directly.

If a torsional test method is to be suggested *e.g.* for inclusion in EN 16351, this must be thoroughly described, as torsional testing machines are not standard equipment in most laboratories.

3. Summary and conclusions/recommendations

- The in-plane shear test method as proposed by Kreuzinger and Sieder, see [10], [13], is believed to be the most appropriate one taking into account its possibilities to distinguish from failure modes I and II, the straightforward specimen preparation and the simplicity of the test set-up.
- If a method for torsional tests is needed, a test method must be described in much more details in coming versions of EN 16351.

The following research and development needs have been identified:

- Based on available tests and available basic FE-analyses, use additional and advanced numerical analyses (and possibly additional tests) to:
 1. verify further the test set-up of Kreuzinger *et al.*
 2. conclude whether torsional tests are at all needed, and if so,
 3. suggest a well-defined test method for torsional tests.

As regards the further numerical work, such analyses should include fracture analyses beyond linear elastic approaches including of course the effects of annual ring orientation and geometry (lay-up) parameters.

4. References

- [1] Bogensperger, T., Moosbrugger, T., Schickhofer, G. “New test configuration for CLT-wall-elements under shear load”. Proceedings of CIBW18. Paper 40-21-2, Bled, Slovenia, 2007.
- [2] Andreolli, M., Rigamonti, M., Tomasi, R. “Diagonal Compression Test on Cross Laminated Timber Panels”. Proceedings, WCTE-2014, Quebec City, Canada.
- [3] Steinsvik Nygård, A., Björnfort, A. Tsalkatidis, T. and Tomasi, R. “Test Method for Determining the In-Plane Shear Strength and Stiffness of Cross Laminated Timber (CLT)”, Proceedings, WCTE-2016, Vienna, Austria, 2016.
- [4] Bosl, R. “Zum Nachweis des Trag- und Verformungsverhaltens von Wandscheiben aus Brettlagenholz.” Dissertation, Universität der Bundeswehr München, Fakultät für Bauingenieur- und Vermessungswesen, 2002 (in German).

- [5] CEN European Committee for Standardization, “EN16351:2015 Timber structures – Cross laminated timber – Requirements,” 2015.
- [6] Wallner, G. “Versuchstechnische Ermittlung der Verschiebungskenngrößen von orthogonal verklebten Brett lamellen (in German).” Master Thesis, Graz University of Technology, Graz, 2004.
- [7] Jöbstl, R. A., Bogensperger, T. and Schickhofer, G. “In-plane shear strength of cross laminated timber. Proceedings of CIB-W18, paper 41-12-3, St. Andrews, Canada, 2008.
- [8] Brandner, R, Bogensperger, T, Schickhofer, G In plane Shear Strength of Cross Laminated Timber (CLT): Test Configuration, Quantification and influencing Parameters. Proceedings of CIB-W18, paper 46-12-2, Vancouver, Canada, 2013.
- [9] Hirschmann, B “Ein Beitrag zur Bestimmung der Scheibenschubfestigkeit von Brettsperrholz (in German)”. Master Thesis, Graz University of Technology, Graz 2011.
- [10] Brandner, R., Dietsch, P., Dröscher, J., Schulte-Wrede, M., Kreuzinger, H, Sieder, M., Schickhofer, G. and Winter, S. “Shear Properties of Cross Laminated Timber (CLT) under in-plane load: Test Configuration and Experimental Study” Proceedings of INTER, paper 48-12-02, Šibenik, Croatia, 2015.
- [11] Jöbstl, R. A., Bogensperger, T., Schickhofer, G. and Jeitler, G. “Mechanical Behaviour of Two Orthogonally Glued Boards.” Proceedings of WCTE-2004, Lahti, Finland, 2004.
- [12] Jeitler, G. “Versuchstechnische Ermittlung der Verdrehungskenngrößen von orthogonal verklebten Brett lamellen (in German). Master Thesis, Graz University of Technology, Graz, 2004.
- [13] Kreuzinger, H., Sieder, M. “Einfaches Prüfverfahren zur Bewertung der Schubfestigkeit von Kreuzlagenholz / Brettsperrholz (in German)”. Bautechnik, 90(5), pp. 314–316, 2013.
- [14] Brandner, R., Dietsch, P. Dröscher, J., Schulte-Wrede, M., Kreuzinger, H., Sieder, M. Cross laminated timber (CLT) diaphragms under shear: Test configuration, properties and design. Construction and Building Materials 147, 312–327, 2017.
- [15] Flaig M (2013): Biegeträger aus Brettsperrholz bei Beanspruchung in Plattenebene. PhD Thesis, KIT, Karlsruhe, Germany.
- [16] Flaig M, Blass HJ (2013): Shear strength and shear stiffness of CLT-beams loaded in plane. In: Proc. CIB-W18, CIB-W18/46-12-3, Vancouver, Canada.

CLT Strength in Tension Perpendicular to Grain

Andrii Bidakov

Dept. of Building Constructions, O.M. Beketov National University of Urban
Economy
Kharkiv, Ukraine

Keywords cross laminated timber (CLT), tension perpendicular to grain strength, test configuration, size of specimens, influencing parameters.

Abstract Cross laminated timber has already been subject of thorough research into different types of stress conditions, such as bending, compression, tension, etc., with only one exception which is tension perpendicular to the grain. The present paper shows the results of experimental investigations of CLT specimens which were carried out for the first time in research practice. It also suggests geometrical parameters of test specimens which are subject to tension perpendicular to the grain. Test arrangements for CLT are based on similar tests for solid timber and glued laminated timber specimens. The paper also contains the analysis of parameters that influence the strength value of solid timber and glued laminated timber in tension perpendicular to the grain. The results of this study provide the characteristic value of CLT panels in tension perpendicular to the grain, which may be used for designing curved CLT panels and connections. Besides, some aspects of CLT structure, such as gaps between boards and stress reliefs are considered in this paper and taken into account in order to evaluate the test results. These details of CLT panel technology expand the area of effective cross section, influence the stress distribution in the volume of test specimens and contribute to the behavior by rupture.

The methods of testing CLT strength in tension perpendicular to the grain and the size of specimens are not described in the European Standard EN 16351:2015, so some points of this paper could be included in the next edition of this normative document.

1. Introduction

Cross laminated timber is a relatively new material in timber design. There is no information on its behavior and strength in tension perpendicular to the grain. The little information available is based only on simple tests for assessing the bearing capacity of some techniques used for installing CLT panels, as it is shown in Fig. 1.

It is well known that tension perpendicular to the grain is the timber strength property with the lowest value. Some national standards for design of timber structures (USA, Russia, Belarus, Ukraine) contain recommendations to avoid situations when timber elements are loaded in tension perpendicular to the grain.

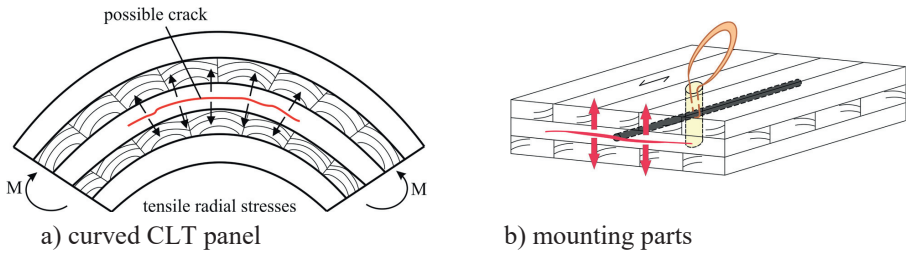


Fig. 1 Examples of tension perpendicular of CLT in practice.

The characteristic value of CLT strength in tension perpendicular is necessary when choosing the appropriate way of reinforcing timber elements which are loaded or stressed that way. Various tests show that brittle failures occur most often in timber in tension perpendicular to the grain, often in interaction with shear. One way to avoid brittle failure mechanisms is achieved by using different types of screws as reinforcement.

The aim of this paper is to show the test results of the strength of CLT plates in tension perpendicular to the grain and to propose a reference specimen and test arrangements which are similar to those for solid timber and glued laminated timber. Moreover, the proposed geometrical parameters of test specimens take into account the specific features of the CLT plate structure including gaps and stress reliefs. The present research also considers the effect of two boards with cross bonding in tests for small specimens in comparison to specimens with two boards with parallel bonding.

1.1 Test configurations for solid timber (ST) and glued laminated timber (GLT)

According to EN 408 [1] GLT strength in tension perpendicular can be tested with two hinged fixing of specimens, as shown in Fig. 2, or with one rigid fixed end to the test machine. Test arrangements for ST and GLT are thoroughly described in a number of publications by Blaß [2], [3], Ranta-Maunus [4], Aicher [5] and others.

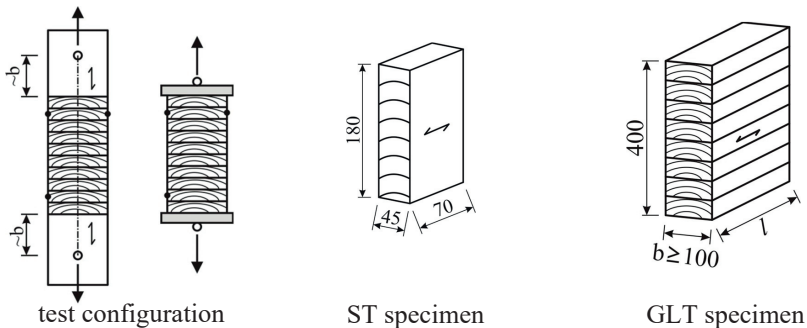


Fig. 2 Test configurations and size of specimens according to EN 408.

The dependence of strength values on the size effect in the cross section parameters of solid timber, glulam and LVL is well known for bending and tension parallel to the grain. Additionally, for GLT exposed to tension perpendicular to the grain a significant volume effect is known [5]. In the revoked standard EN 1193, [6], the test method for determining the tensile strength perpendicular to grain of glulam used the reference volume V_0 where specimen dimensions $90 \text{ mm} \times 275 \text{ mm} \times 400 \text{ mm}$ (Fig. 2) giving a volume of $0.0099 \text{ m}^3 \cong 0.01 \text{ m}^3$.

1.2 Potential parameters influencing tension perpendicular to grain strength

Tension perpendicular to grain strength is dependent on a number of major parameters such as density, volume of tested specimens and annual ring orientation in the cross section of solid timber elements. In today's standards the values of tension perpendicular to grain strength of solid timber and glulam are however no longer considered to be dependent on density.

The characteristic strength value $f_{t,90,g,k}$ is related to the reference volume of $V_0=0.01 \text{ m}^3$. The test method for determining the tensile strength perpendicular to grain of glulam uses this reference volume V_0 and it is taken into account when designing double tapered, pitched cambered and curved beams where tension stresses perpendicular to the grain appear in the apex zone.

According to the former standards EN 338:2003, [7] and EN 1194:1999, [8], strength properties of solid timber and glulam are dependent on timber density. The tensile strength perpendicular to grain for solid timber according to the former versions of standards EN 384:1995 [9] and EN 338:2003, [7] was derived in dependency on the timber density:

$$\text{EN 384:1995} \quad f_{t,90,k} = 0.001 \rho \quad (1)$$

$$\text{EN 338:2003} \quad f_{t,90,k} = \min \begin{cases} 0.6 \\ 0.0015 \rho_k \end{cases} \quad (2)$$

EN 1194:1999 [8] has been revoked and all the data on strength properties of GLT are stipulated in EN 14080:2013 [10], where strength values in tension perpendicular to the grain are changed and considered to be equal for all strength classes. A similar situation occurs in the new version of EN 338:2009, [11] for solid timber, where strength data in tension perpendicular to the grain are also equal. According to EN 338:2009, [11], all strength classes of solid softwood have the value 0.4 N/mm^2 and EN 14080:2013, [10], attributes the value 0.5 N/mm^2 to all strength classes of glued laminated timber.

2. Material and methods

2.1 Material

Small specimens (type A and type B), rather than larger specimens (type C) have been used so far in order to test the tension perpendicular to grain strength of CLT

panels and to consider the system effect on specimens as shown in Fig. 3. The outcomes of cross glued boards were compared with the strength values of longitudinal glued boards, 25 specimens of each type being tested. The results of these tests are summarized in Table 1. Glued boards were 30 mm thick, 150 mm long and 150 mm wide (see Fig. 3). The boards were made of pine wood (*Pinus sylvestris* L.).

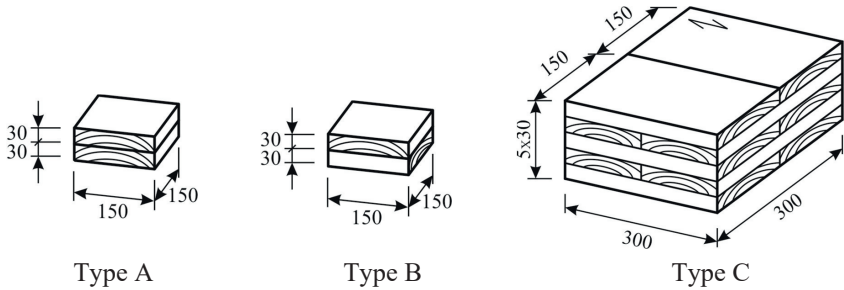
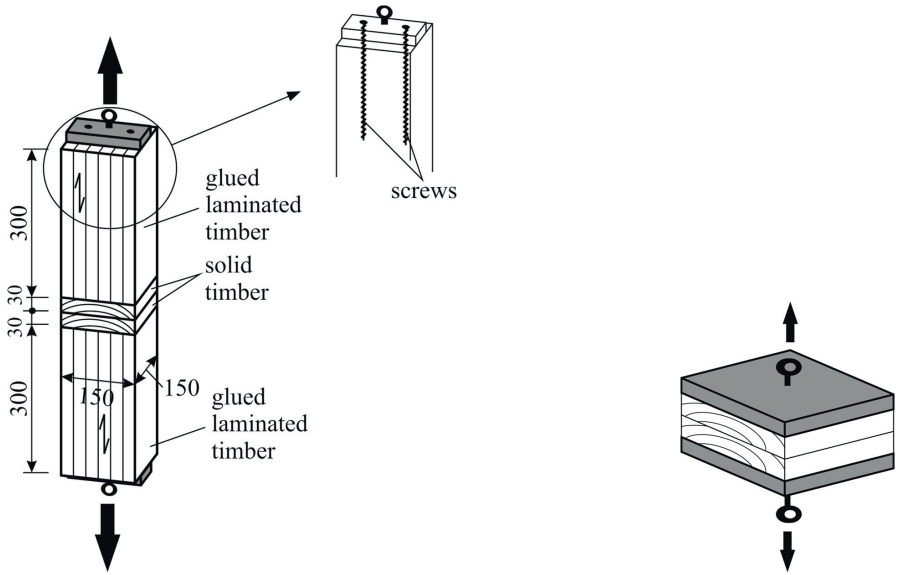


Fig. 3 Test configuration and size of specimens

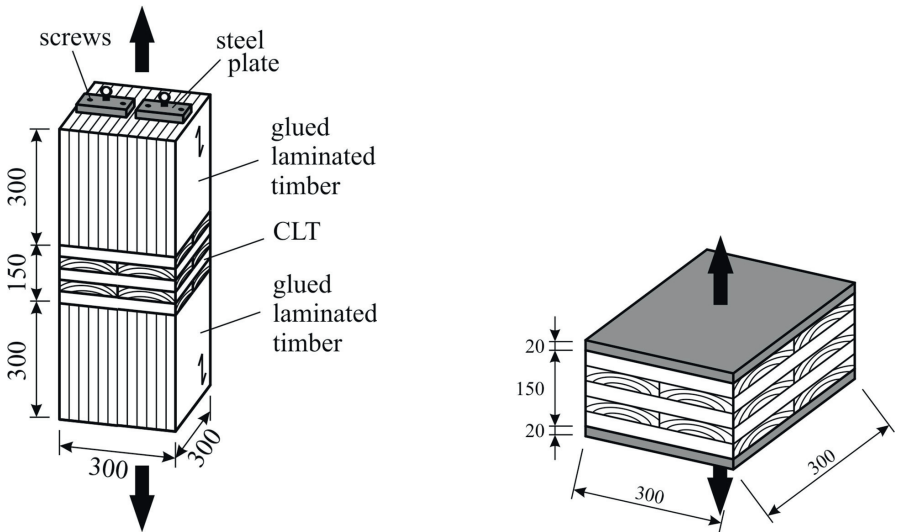
The CLT specimens (type C) had a cross section of 300 mm × 300 mm and were 150 mm thick. CLT specimens were fabricated using 30 × 150 × 300 mm³ boards that were visually graded to avoid cracks, but otherwise were not strength graded. Boards of this kind were only bonded face-to-face during the fabrication process.

2.2 Methods

The tests were carried out in two variants. In the first variant the test specimens were glued to steel plates with two-component epoxy. The steel plates were 30 mm thick. The steel plate in tests for CLT specimens had four steel ribs with holes in them (see Fig. 4). In the second variant the load was transferred to test specimens through bonded intermediate blocks of glulam with grain direction parallel to the load axis as recommended by EN 408 [1]. Intermediate glulam blocks were connected to steel arrangements by means of screws installed parallel to grain of each intermediate block and fixed to the steel plates. The length of the intermediate wooden blocks was 300 mm for both specimens. The glue lines between the test volume and GLT blocks were performed with polyvinyl acetate (PVAc D3/D4) and two-component epoxy. Each intermediate wooden block in small test specimens was cleaned after failure and bonded once again to the next specimen. About 8 % of all specimens failed at the bonded joint between intermediate wooden or steel plates and the test specimen. Failures that occurred in the glued area of the test specimens or in the steel plate interface accounted for less than 20 % of the total area of failure.



a) test configuration for small specimens



b) test configuration for CLT specimens

Fig. 4 Test configuration of small and CLT plate specimens with intermediate wooden blocks and steel plates (left to right)

Tensile strength perpendicular to grain was calculated according to EN 408 [1] using Eq. (3).

$$f_{t,90} = \frac{F_{t,90,max}}{b \cdot l} \quad (3)$$

The load F was applied at a constant rate of cross head movement throughout the test. Using vertical advancing rates of 0.4 up to 0.8 mm/min, F_{max} was reached within 300 ± 120 s. Two measuring devices were attached diagonally, as shown in Fig. 5.

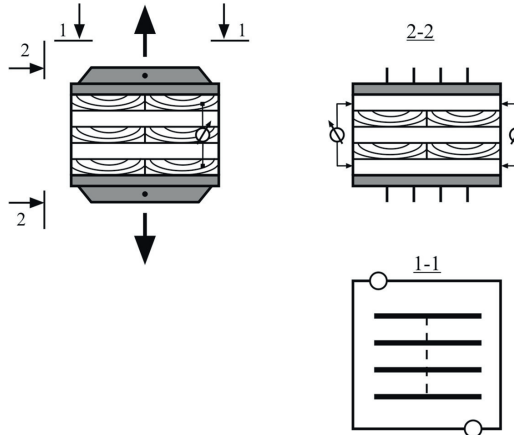


Fig. 5 Placement of measuring devices

3. Results and discussion

3.1 The influence of cross bonded boards in small specimens

The first stage of testing CLT strength properties in tension perpendicular to the grain was carried out using two types of small specimens. The first type contains two parallel bonded solid timber boards and the second type contains cross bonded boards. Fig. 3 shows the geometric parameters of small specimens and the scheme of grain orientation in each type of specimens. The thickness of 30 mm and the width of 150 mm in cross section of these boards comply with the reference parameters of lamellas in CLT elements in accordance with EN 16351, [11]. 25 specimens of each type were used in the tests.



Fig. 6 Test arrangements for small specimens (top) and CLT specimens (bottom)

The major results of the research are summarized in Table 1, which shows different parameters for two groups of tested small specimens. The failure in tension perpendicular to the grain can be characterized as brittle failure, which corresponds to Weibull distribution of test data for solid timber and glued laminated timber specimens [3]. The test results for small and CLT specimens were analyzed in accordance with EN 14358:2016 [13], referring to lognormal distribution of obtained results rather than normal distribution, as was proposed in the former edition of EN 14358, which did not yet differentiate between analyzing test data depending on the type of strength or elastic characteristics. Therefore, EN 14358:2016 does not contain parameters which are necessary for obtaining characteristic values of strength at 2-parameter Weibull distribution.

Table 1 Test results of small specimens

Specimens	Number	Mean [N/mm ²]	Minimum [N/mm ²]	Maximum [N/mm ²]	5%- percentile acc. to EN 14358 [N/mm ²]	Standard deviation [N/mm ²]	COV %
Type A (parallel bonded boards)	25	1,83	1,05	3,02	1,19	0,31	16
Type B (perp. bonded boards)	25	1,78	1,11	3,02	1,15	0,40	23

The analysis of small timber specimens showed a difference of COVs of 7 %. Fig. 7 shows the test results for each small specimen.

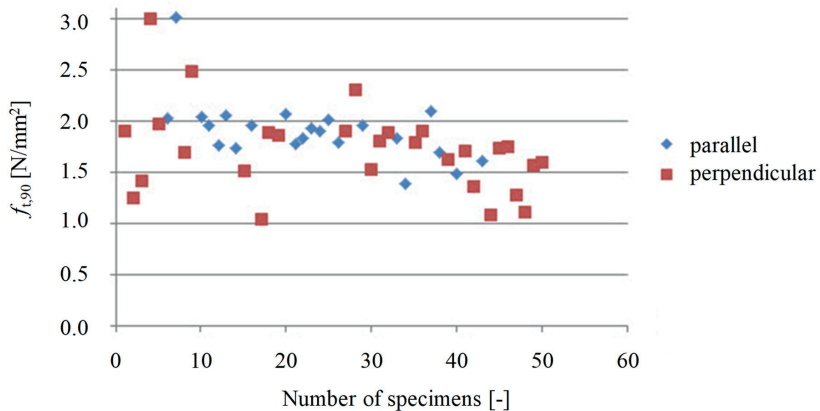


Fig. 7 Strength of small specimens in tension perpendicular

Tension perpendicular failure along one board was observed for most specimens (Fig. 8) regardless of whether those were parallel or perpendicular bonded boards. A possible explanation for this might be found in the different orientation of annual rings which has a certain influence on the tensile strength perpendicular to grain [2].



a) parallel glued boards (type A)



b) perpendicular glued boards (type B)

Fig. 8 Typical failures of small specimens

Specimens with radial annual rings show higher strength in tension perpendicular to the grain than tangentially orientated specimens. It can also be explained by the distance from the pith to the center of the specimen.

3.2 Test results for CLT specimens

Most specimens failed near the bonded joint between the steel plate and the CLT test specimen. The lines of failure of specimens occurred mostly in boards of two adjacent layers and rarely in one layer (see Fig. 9). Different failure behavior is caused by different orientation of annual rings.

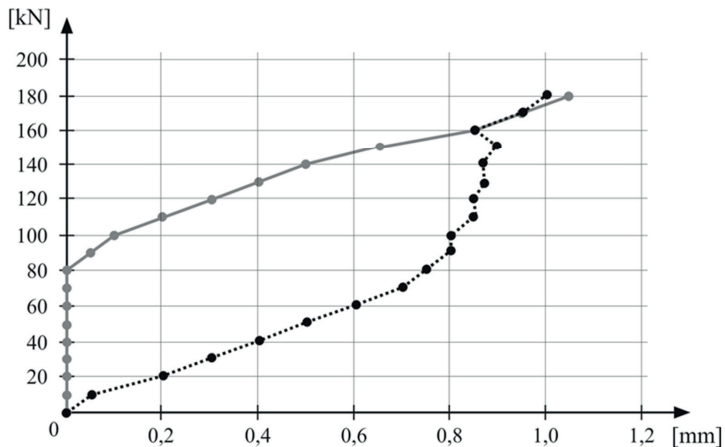
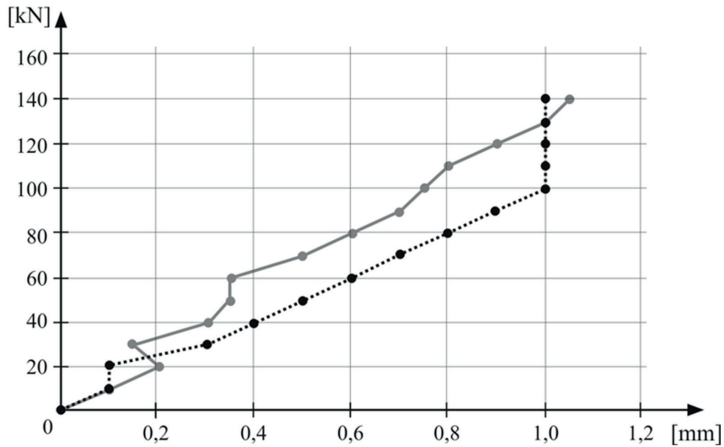


Fig. 9 Typical failures of CLT specimens

The tensile strength perpendicular to the grain of specimens stressed in tangential direction is the greatest. Its value is medium for specimens loaded under the angle of 45° and it is the lowest for specimens stressed in radial direction. The big difference between radial and tangential strength results in anisotropic specimens and causes non-uniform stress distribution in CLT specimens. Table 2 shows the test results for CLT specimens. The tested specimens mostly contained boards with annual ring patterns oriented such that they were stressed in radial direction and under the angle of 45° .

Table 2 Test results for CLT specimens

Number [-]	Mean [N/mm ²]	Minimum [N/mm ²]	Maximum [N/mm ²]	5%- percentile [N/mm ²]	Standard deviation [N/mm ²]	COV [%]
25	1.43	0.56	2.11	0.65	0.46	32



a)

Fig. 10 Load-deformation diagram of CLT specimens. Top: specimen with $F_{max}=150$ kN. Bottom: specimen with $F_{max}=190$ kN

The tested specimens contained boards with knots, and the lines of failure always appeared near the knots. Another imperfection and irregularity of timber structure

lead to non-uniform stress distribution, which eventually makes the failure load F_{max} lower than that in the case of uniform stress distribution.

The difference between two measured displacements was therefore evaluated. Fig. 10 shows the load-deformation diagram of CLT specimens which was obtained from measuring two devices. According to this diagram the cause of this difference lies in the displacement of two sides, which can be explained by the intensive crack propagation on one of the sides.

It is also possible that the crack propagation inside the specimen occurs in the middle. This kind of rupture is caused by the big size of the tested specimen.

4. Conclusions

An important aim of the project was to determine the tensile strength perpendicular to the grain of CLT specimens with geometrical. The test configuration and the methods are similar to those used in tests for solid timber and glued laminated timber. The size of CLT specimens is based on the reference parameters of boards and the number of layers as described in EN 16351 [11] for tests under different stress conditions.

It should be noted that the visually graded wooden specimens used in the tests were without splits or any visible cracks that often occur in structural size timber. Due to cracks, the tensile strength perpendicular to grain in structural timber will be lower than the values given in this publication. Crack formation and delamination should be considered not only during the process of production, but also during the lifetime of the structure. Further research effort could deal with the comparison of CLT strength in tension perpendicular to the grain in case when specimens have boards with stress reliefs and edge gluing.

The information on CLT strength properties in tension perpendicular to the grain is not yet available in international standards. The results of the present research could make a contribution to EN 16351 standards.

5. Acknowledgements

I would like to express my thanks to the National University of Civil Engineering and Architecture (KNUCEA) as well as to the Laboratory of Building Constructions which helped to conduct the tests to explore CLT strength in tension perpendicular to the grain in summer 2017. The publication, as part of the STSM work, was written in the framework of the COST Action FP1402 “Basis of Structural Timber Design – from research to standards”. I would like to thank the representatives of COST office for their Short Term Scientific Mission grant and Karlsruhe Institute of Technology for the warm welcome and positive collaboration during the STSM. The comments and suggestions given by Prof. Blaß during the STSM work in KIT were also highly appreciated.

I wish to acknowledge the research contribution of students Nikita Kuznetsov and Yuriy Kalachev from KNUCEA, as well as the experimental assistance provided by

Bogdan Strashko for the valuable support during all the stages of the project. I am also grateful to Rothoblaas company for providing the screws which were used in this research.

6. References

- [1] EN 408:2010+A1:2012, Timber structures – Structural timber and glued laminated timber – Determination of some physical and mechanical properties, European Committee for Standardization (CEN), 2012.
- [2] Blass, H. J., Schmid, M., «Tensile strength perpendicular to grain according to EN 1193», CIB-W18 / 31-6-2, Proceedings of the international council for research and innovation in building and construction, Working commission W18 – timber structures, Meeting 31, Savonlinna, Finland, 1998.
- [3] Blass, H. J., Schmid, M., «Tensile strength perpendicular to grain of glued laminated timber», CIB-W18 / 32-6-4, Proceedings of the international council for research and innovation in building and construction, Working commission W18 – timber structures, Meeting 32, Meeting 32, Graz, Austria, 1999.
- [4] Ranta-Maunus, A., «Duration of Load Effect in Tension Perpendicular to Grain in Curved Glulam», CIB-W18 / 31-9-1, Proceedings of the international council for research and innovation in building and construction, Working commission W18 – timber structures, Meeting 31, Savonlinna, Finland, 1998.
- [5] Aicher, S. and Dill-Langer, G. «Evaluation of Different Size Effect Models for Tension Perpendicular to Grain Design», CIB-W18 / 35-6-1, Proceedings of the international council for research and innovation in building and construction, Working commission W18 – timber structures, Meeting 35, Kyoto, Japan, 2002.
- [6] EN 1193 Timber structures – Structural timber and glued laminated timber - Determination of shear strength and mechanical properties perpendicular to grain, European Committee for Standardization (CEN), 1998.
- [7] EN 338 Structural Timber – Strength Classes, European Committee for Standardization (CEN), 2003.
- [8] EN 1194 Glued laminated timber – Strength classes and determination of characteristic values
- [9] EN 384, Structural timber – Determination of characteristic values of mechanical properties and density, European Committee for Standardization (CEN), 1995.
- [10] EN 14080, Timber structures – Glued laminated timber and glued solid timber – Requirements, European Committee for Standardization (CEN), 2013.
- [11] EN 338 Structural Timber – Strength Classes, European Committee for Standardization (CEN), 2009.

- [12] EN 16351, Timber structures – Cross laminated timber – Requirements. European Committee for Standardization (CEN), 2015.
- [13] EN 14358: Timber structures - Calculation of characteristic 5-percentile and mean values for the purpose of initial type testing and factory production control; (CEN), 2016.

COST Action FP1402
Basis of Structural Timber Design:
From Research to Standards

WG 2 – Solid Timber Constructions:
Cross Laminated Timber (CLT)

TG 4 – Design of CLT Systems

Foreword

This State-of-the-Art Report (STAR) was written by the core group of Working Group Two, Task Group Four (WG 2 / TG 4) of COST Action FP1402 “Basis of Structural Timber Design – from Research to Standards” and is addressed at all those who are interested in the design of Cross Laminated Timber (CLT) systems.

The following documents contain the state of the art of different aspects of the design, reporting in detail the different approaches, methods and results that can be found in literature (scientific technical papers, MS thesis, PhD thesis, etc.).

The present output is based also on the discussions, presentations and agreements made in past meetings of COST Action FP1402 in Karlsruhe / Germany (03 / 2015), Pamplona / Spain (10 / 2015), Stockholm / Sweden (03 / 2016), Mons / Belgium (09 / 2016), Zagreb / Croatia (03 / 2017) and Graz / Austria (09 / 2017). In addition to these common meetings an intermediate meeting was held in Trento IVALSA (07/2017) for the seismic subgroup of TG4.

All these contributions generated information and knowledge, which also represents essential input of the work of the COST Action FP1402.

Roberto Tomasi, leader of TG 4

A Mechanical Characterization of Floor and Wall Diaphragms

State-of-the-art: Cross Laminated Timber shear wall capacity and stiffness assessment methods

Ildiko Lukacs
PhD Candidate
Faculty of Science and Technology
Norwegian University of Life Sciences (NMBU)
Ås, Norway

Anders Björnfort
Associate Professor
Faculty of Science and Technology
NMBU, Ås, Norway

Roberto Tomasi
Professor
Faculty of Science and Technology
NMBU, Ås, Norway

Summary

Due to its relatively high strength and stiffness, Cross Laminated Timber (CLT) is well suited for multi-story buildings. Being a somewhat new kind of construction material, it is not surprising that CLT buildings are still to some extent being overdesigned. As the absence of an up-to-date code makes it more difficult for engineers to choose the most adequate method in assessing the strength and stiffness of CLT buildings. This paper presents a state-of-the-art of analytical methods to assess the strength and the stiffness of CLT shear walls. For an updated state-of-the art of CLT Shear walls please refer to Lukacs et al. [1].

1. Introduction

Cross Laminated Timber (CLT) is an efficient wood product that is well suited for multi-story timber buildings due to its relative high strength and stiffness. One of the most significant parameters of a building is its horizontal stiffness. In CLT buildings, shear walls form the general stabilizing system that transfer lateral loads to the foundation while stabilizing and reducing the uplift in the building. In the last years, the number of timber buildings are increasing and the absence of a CLT standard makes it more difficult for engineers to use the best suitable method in assessing a CLT shear wall's strength and stiffness. In addition, there is no reference in the Eurocode 5 regarding CLT shear walls, so there is great need to explore different design methods of CLT shear walls.

In general, the design of CLT shear walls is performed by assessing the wall capacity and the wall displacement. However, regarding the CLT shear wall, the behavior of the connections and the loads acting on the wall also have a decisive influence. In the following, different analytical methods are presented that can help to assess the capacity and the displacement of CLT shear walls. The state-of-the-art presents a summary of research regarding analytical methods for strength

and stiffness calculation of CLT shear walls. This report focuses on presenting the methods as thoroughly as possible; the aim at this stage is therefore not to compare the ability of the methods to design CLT shear walls.

2. Capacity of CLT shear wall

The verifications of CLT shear wall strength mainly consists of equilibrium equations primarily based on external loading and wall geometry. To obtain comparable results, the aim is to calculate the peak force that a shear wall can take. In these results, the connections play a decisive role. Figure 1 presents how the single shear wall is composed: a CLT panel (generally from 3 to 5 layers) with connections to the lower floor or foundation. These connections are normally differentiated as hold-down (HD) and shear connections, where the angle bracket (AB) is the most common type of shear connector. Other common connections used are screws and steel plates as well as special connection systems such as the X-RAD connector system by Rothoblaas.

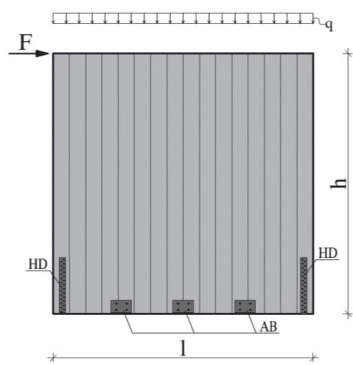


Figure 1. Cross-laminated timber shear wall

First, we need to specify the horizontal and vertical forces acting on the shear wall. When these forces are determined then the internal forces acting on the connections can be determined. In general, two approaches are used (Figure 2). In the first approach (Figure 2a) two different types of connections are used. Hold-downs (HD) are designed to resist the tensile force due to the overturning moment while other connectors, e.g. angle brackets (AB) are used to transfer the horizontal shear force. The angle brackets (AB) thus mainly prevent sliding of the wall, while the hold-downs (HD) mainly prevent rocking of the wall (Figure 2a). In the second approach (Figure 2b) a single connector, e.g. angle brackets (AB) is designed to resist both vertical and horizontal forces. In this case, these connectors resist both sliding and rocking (Figure 2b).

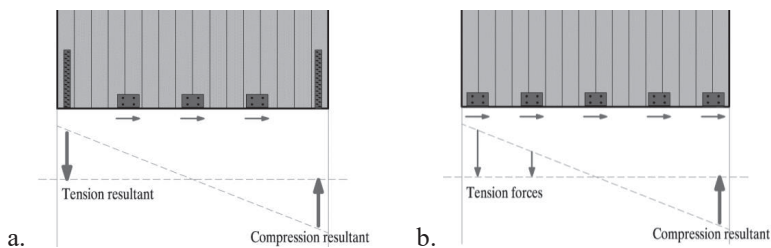


Figure 2. Internal force distribution a. Hold-down for uplift and angle bracket for shear transfer. b. Angle bracket working in both shear and tension

To calculate the lateral resistance of a CLT shear wall, the wall configuration needs to be determined which includes the following data; number of layers of the panel, the geometry of the panel, the type of connectors used, the placement of these connectors and their strength and deformation characteristics. With the capacity evaluation, the main goal is to calculate the maximum lateral resistance of the CLT shear wall. In the literature, four methods, based on static equilibrium equations, are identified for calculating the resistance of a CLT shear wall:

- **Method A** – Casagrande et al. [2]
- **Method B** – Tomasi [3]
- **Method C** – Wallner-Novak et al. [4]
- **Method D** – Pei et.al [5]

Unless specified, this report uses the same notations that are used by the original authors.

2.1. Method A – Casagrande et al. [2]

Casagrande et al. [2] presented an analytical method to evaluate the stiffness of timber shear-walls (Figure 3). In their paper, three main deformation modes are defined as in-plane shear, rigid-body translation and rigid-body rotation. The rigid-body rotation mode has the highest contribution to the deformation of the shear wall. The static equilibrium equation between the internal forces and the overturning moment is illustrated in Figure 3.

To determine the internal forces, an internal lever arm of about 0.9 times the length of the wall was recommended by Casagrande et al. [2]. If a uniformly distributed load, q , is also acting on the top of the wall then the effect of the vertical load on the hold-down can be written as:

$$T = \frac{F \cdot h}{\tau \cdot l} - \frac{q \cdot l}{2} \quad (1)$$

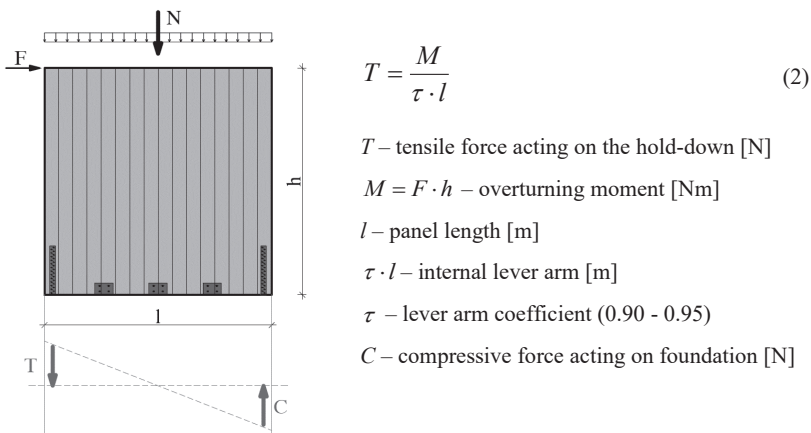


Figure 3. Shear wall layout for method A. Illustration based on [2]

Discussion of Method A

Rigid-body rotation is used as base for method A. By setting the force in the hold-down T equal to the capacity of the hold-down (F_T), the horizontal force F can be determined. Based on the static equilibrium between the hold-down's tensile strength, uniformly distributed vertical load and the resulting overturning moment, the resistance of the shear wall can be calculated as:

$$F = \frac{\left(F_T + \left(\frac{q \cdot l}{2} \right) \right) \cdot 0,9 \cdot l}{h} \quad (3)$$

All the parameters required for the calculation are readily available from the shear wall geometry. In this case $\tau = 0.90$ is used to calculate the lever arm as recommended in [2]. The tensile strength of the hold-downs should be based on test results or taken from the producer.

2.2. Method B – Tomasi [3]

Tomasi [3] proposed a “Stress block” model, where the nonlinear stress distribution for wood in the compression zone is substituted by a rectangular stress block (Figure 4). The unknown terms when using this method are the position of the neutral axis and the tensile force in the hold-down, which are determined by means of translational and rotational equilibrium (Figure 4):

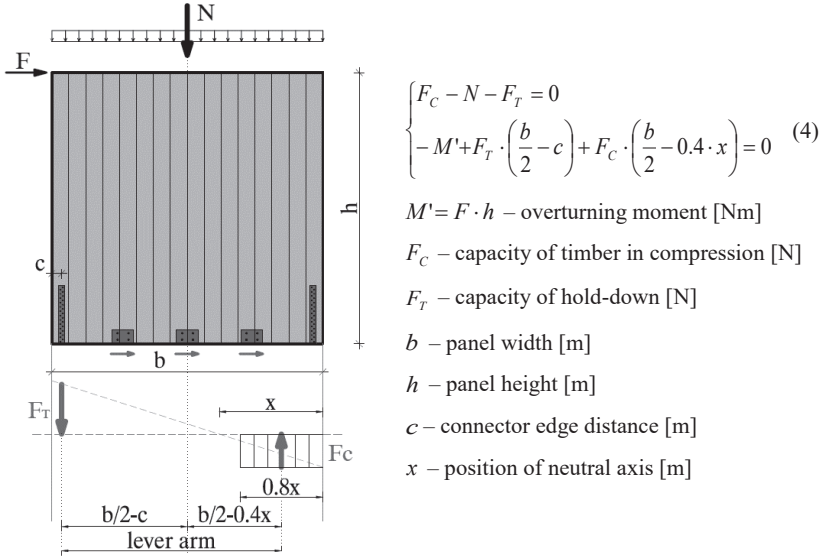


Figure 4. Shear wall layout for method B. Illustration based on [3]

The translational and rotational equilibrium equations are considered in the middle of the wall panel at $b/2$ and the capacity of timber in compression is calculated as:

$$F_C = 0.8 \cdot x \cdot f_{c,d} \cdot s \quad (5)$$

where s [m] is the panel thickness and $f_{c,d}$ [MPa] the timber design strength in compression.

Discussion of Method B

Method B is based on translational and rotational equilibrium with a neutral axis based on the compressive strength of timber. The position of the neutral axis is calculated from translational equilibrium using the hold-down tension force:

$$x = \frac{N + F_T}{0.8 \cdot f_{c,k} \cdot s}, \text{ with } 0 < x \leq \frac{b}{2} \quad (6)$$

If the neutral axis position is higher than $b/2$ then x should be considered equal to $b/2$. The location of the neutral axis is important because the equilibrium equations are considered from this point. In these calculations, the characteristic timber compressive strength is used.

By having the position of the neutral axis (x), hold-down tensile capacity (F_T), compression force (F_C) based on timber strength perpendicular to the grain, wall

geometry (b , h) and the edge distance (c), the horizontal force (F) can be calculated as:

$$F = \frac{F_t \cdot \left(\frac{b}{2} - c\right) + F_c \cdot \left(\frac{b}{2} - 0.4 \cdot x\right)}{h} \quad (7)$$

2.3. Method C – Wallner-Novak et al. [4]

Wallner-Novak et al. [4] presented a method where angle brackets are used to prevent sliding, and hold-downs to prevent rocking of the CLT wall (Figure 5), which is similar to both, Method A and Method B. Although the wall setup, internal force distribution and loading is the same, when it comes to the calculation of tension and shear anchoring of the wall, Wallner-Novak et al. [4] proposed a different length of the compression zone, corresponding to $\frac{1}{4}$ of the wall width and a reduced effect of the vertical load.

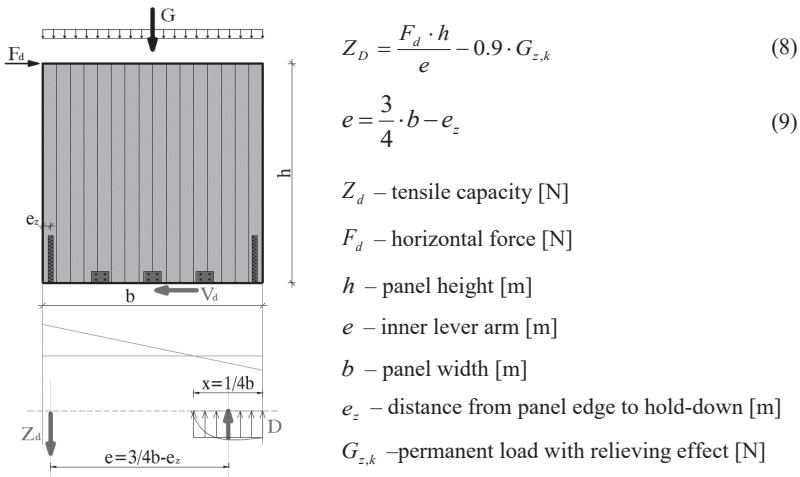


Figure 5. Shear wall layout for method C. Illustration based on [4]

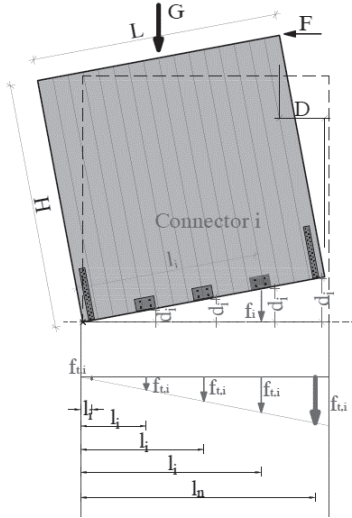
Discussion of Method C

The tensile force is considered as the hold-down tensile strength and a 10 % reduced effect of the vertical load is also taken into account. By setting the compression zone equal to $\frac{1}{4}$ of the wall length, the inner lever arm, will be the remaining $\frac{3}{4}$ length of the wall minus the distance from the wall edge to the position of the hold-down. The horizontal force is calculated as:

$$F = \frac{(F_t + 0.9 \cdot N) \cdot \left(\frac{3}{4} \cdot b - e_z\right)}{h} \quad (10)$$

2.4. Method D – Pei et al. [5]

Pei et al. [5] presented a method that considers the CLT panel rotation as a rigid body rotation, around one of its corners (Figure 6). This simplified kinematic model for the lateral resistance of the CLT shear wall can be used for both connections working in shear and tension, or different connections used to resist sliding and uplift/rocking of the panel.



$$F(D) = \sum_{i=1}^n \frac{l_i}{H} \cdot f_i \left(\frac{l_i}{H} \cdot D \right) + \frac{L}{2 \cdot H} \cdot G \quad (11)$$

$F(D)$ – lateral resistance as function of D [N]

D – lateral displacement at the top of the wall [m]

L – length of the wall panel [m]

H – height of the wall panel [m]

G – gravity load acting in the middle of the panel [N]

n – number of connectors between the wall and floor

$f_{t,i}$ – resistance of the i^{th} connector [N/m]

l_i – distance from the wall corner to the i^{th} connector

l_n – distance from wall corner to the last connector

Figure 6. Shear wall layout for method D. Illustration based on [5]

This method takes into account each connector's resistance in function of its location and the wall panel geometry. Pei et al. [6], Shen et al. [7], and Karakabeyli & Douglas [8] also presented this method with the following general assumptions:

- the wall has in-plane rigid body behavior
- with lateral loading, the wall will rotate around its corner with lateral displacement
- lateral sliding does not occur between wall and floor/foundation
- a vertical force can act at the center of the wall
- the connections are deformed due to the rotation of the panel

Discussion of Method D

To determinate the lateral force, the connector's elongation and stiffness/strength is considered. The tensile strength is proportional with the distance of the connector from the panel edge. A triangular distribution of the connector displacement is considered. It is presumed that the furthest connector (the right

hold-down according to Figure 6) reaches its total elastic tensile strength. The remaining connections will be elongated based on a triangular distribution and thus their tensile capacity ($F_{i,used}$) is proportional with their distance (l_i) from the rotational point. The calculation steps for Method D are as follows:

1. Determine the tensile strength (F_t) of the connector furthest from the point of rotation.
2. Calculate the elongation (d) for F_t .
3. Calculate the elongation (d_i) for each connector based on a triangular distribution.
4. Calculate the tensile strength for each connector based on its stiffness ($F_{i,used} = d_i f_i$).
5. Calculate the total rotational resistance in terms of the total lateral load (F):

$$F = \frac{\sum_{i=1}^n F_{i,used} \cdot l_i}{H} + \frac{G \cdot l_n}{H} \quad (12)$$

2.5. Concluding discussion of approaches presented for calculating shear wall resistance

The first three methods (A, B and C) take into account the effect/strength of the tensile connector (hold-down). Method D considers the tensile strength of all the connectors from the shear wall. Method D seems to more accurately predict the wall capacity as it is able to consider the axial stiffness of all the connectors, which corresponds to the practical behavior of angle brackets that work in two directions.

3. Displacement of CLT shear walls

By knowing the deformation associated to a certain load, the stiffness of the shear wall can be estimated. This chapter presents analytical approaches to assess the displacement of a CLT shear wall. Analytical methods for the displacement of CLT shear wall systems are based on different contributions of deformations. Over the years, researchers have developed different theories and analytical methods regarding how these deformation mechanism influence the shear wall deformation. The next paragraphs present a summary of these approaches.

3.1. Method I – Casagrande et al. [2]

Casagrande et al. [2] developed the UNITN model to calculate the elastic horizontal displacement of a timber shear wall with a simplified equation. In this analytical method, three deformation mechanisms contribute; in-plane shear deformation, rigid-body translation and the rigid-body rotation (Figure 12) as well as the effect of the vertical load is taken into account. Vessby [9] and Reynolds et al. [10] present methods using the same deformation mechanisms.

Regarding the loads acting on the shear wall panel, the influence of the vertical load is used to counteract the rotation of the wall. Together with the uniformly

distributed vertical load, the hold-down stiffness has a major role. For the shear deformation, the considered parameters are the shear area (considering only vertical layers) and the shear modulus. For the translation deformation, the stiffness of the angle bracket gives the highest contribution while for the shear deformation, the CLT properties are decisive. Casagrande et al. [2] concluded that rigid-body rocking has the highest influence on shear wall deformation.

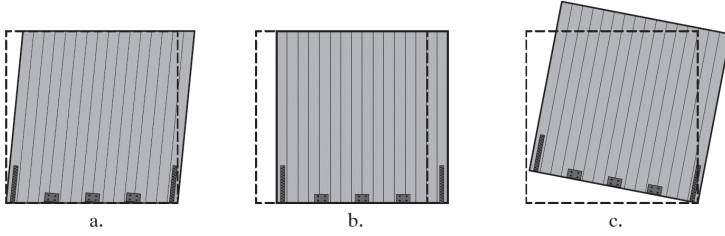


Figure 7. Deformation mechanism for Method I – a) in-plane shear deformation, b) rigid-body translation, and c) rigid-body rotation. Illustrations based on [2]

$$\Delta = \Delta_h + \Delta_a + \Delta_p \quad (13)$$

$$\Delta_h = \gamma \cdot h = \left(\frac{F \cdot h}{\tau \cdot l} - \frac{q \cdot l}{2} \right) \cdot \frac{h}{k_h \cdot \tau \cdot l} \quad (14)$$

$$\Delta_a = \frac{F \cdot i_a}{k_a \cdot l} \quad (15)$$

$$\Delta_p = \zeta \cdot h = \frac{F \cdot h}{G_{CLT} \cdot t_{CLT} \cdot l} \quad (16)$$

Δ – resultant horizontal deformation of a CLT shear-wall

$\Delta_h, \Delta_a, \Delta_p$ – deformation due to rigid-body rotation, translation panel shear respectively

F – applied horizontal force (F)

q – uniformly distributed load (q)

h, l, t_{CLT} – height (h) and length (l) and thickness (t_{CLT}) of the panel

$\tau \cdot l$ – internal lever arm

k_h – stiffness of hold-down (N/m)

i_a – spacing between (i_a) angle-brackets

k_a –stiffness of angle-brackets (k_a)

G_{CLT} – shear modulus of the CLT panel

Discussion of Method I

The UNITN model disregards any bending deformation of the panel as it is argued that the majority of deformations will occur in the mechanical connectors [2]. The lever arm coefficient τ should be taken as 0.9 (based on [2]).

3.2. Method II – Hummel et al. [11]

Method II, based on Hummel et al. [11], has many similarities to method I. Besides shear deformation of the CLT panel, rotation/rocking of the wall panel due to tensile anchoring and contact, and slip of the wall panel caused by the shear anchoring, Method II also considers the bending deformation of the CLT panel (Figure 13). The same contributions of deformations are also presented in Seim et al. [12], Hummel & Seim [13] and in Wallner-Novak et al. [4]. Based on these four deformation mechanisms, the total elastic displacement can be calculated. For the wall rocking, two cases are considered; 1. a rigid foundation (e.g., concrete slab) and 2. an elastic foundation (e.g., timber floor between stories with an elastic intermediate layer).

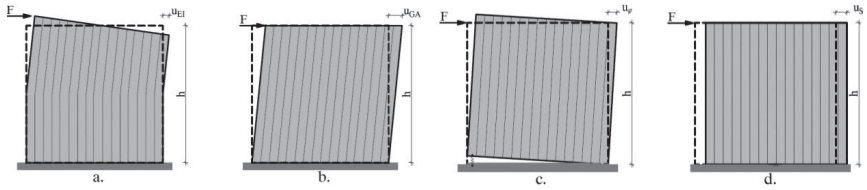


Figure 8. Deformation mechanism for Method II – a) bending, b) shear, c) wall rotation/rocking, and d) slip of wall panel. Illustrations based on [13].

$$u_{tot} = u_{EI} + u_{GA} + u_s + u_\varphi \quad (17)$$

$$u_{EI} = \frac{F \cdot h^3}{3 \cdot EI_{ef}} \quad (18)$$

$$u_{GA} = \frac{F \cdot h}{GA_{ef}} \quad (19)$$

$$u_s = \frac{F}{K_s} \quad (20)$$

$$u_\varphi = \begin{cases} \frac{h}{e} \cdot \frac{Z}{K_z}, Z \approx \max \left\{ F \cdot \frac{h}{e} - \frac{p \cdot l}{2}; 0 \right\} - \text{rigid foundation} \\ \frac{h^2}{l^* - l_c / 3} \cdot \frac{2 \cdot F}{k_D \cdot l_c^2}, k_D = \frac{E_s \cdot b_s}{t_s} - \text{elastic foundation} \end{cases} \quad (21)$$

$$EI_{ef} = E_0 \cdot \left[\sum d_i \cdot l^3 / 12 \right] \quad (22)$$

$$GA_{ef} = G_{eff} \cdot A = \frac{G}{1 + 6 \cdot \left[0,32 \cdot \left(\frac{t}{a} \right)^{-0,77} \right] \cdot \left(\frac{t}{a} \right)^2} \cdot A \quad (23)$$

- $u_{EI}, u_{GA}, u_{\varphi}, u_s$ – deformation caused by bending, shear, rotation and slip respectively
- F, P – applied horizontal force (F) and uniformly distributed load (P)
- h, l, t – height (h) and length (l) and thickness (t) of the panel
- Z – tensile force in the hold-down/tensile anchorage area
- K_z – stiffness of the hold-down connector
- l^* – distance to furthest hold-down (l^*)
- e – inner lever arm (e)
- l_c – length of pressure zone in case of elastic foundation
- t_s, b_s – thickness (t_s) and width (b_s) of the elastic foundation (Figure 9)
- E_s, k_D – modulus of elasticity (E_s) and stiffness (k_D) of the elastic foundation
- a, d_i – average width of the lamellas (a) thickness of the i^{th} vertical lamella (d_i)
- E_0, G – modulus of elasticity parallel to fiber (E_0) and timber shear modulus (G)
- A – gross shear area ($A = t \cdot l$)

In Eq. (19) the shear stiffness is determined based on an effective shear modulus, G_{eff} , and the gross shear area, A . The effective shear modulus is based on Augustin et al. [14] and calculated according to Eq. (23). A typical CLT shear wall with rigid/elastic foundation and the wall rocking deformation is shown in Figure 9. For both foundation types the rocking deformation can be calculated as presented in Eq. (21).

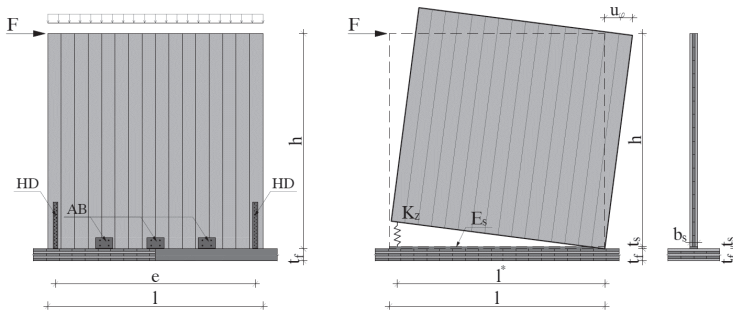


Figure 9. (left) Shear wall with rigid or elastic foundation. (right) Rocking deformation with elastic intermediate layer. Illustrations based on [11]

In the case of the elastic foundation, the width of elastic intermediate layer, b_s , and the E-modulus of the layer, E_s , needs to be known to determine the rocking deformation. Two cases are distinguished for the width, b_s , one for the case of exterior wall and one for interior wall, as summarized in Eq. (24), the E-modulus, E_s , for the elastic material, can be Syldodyn, which is commonly used as a damping material the case of CLT walls. The use of the elastic intermediate layer, leads to

a higher rocking deformation (Eq. 21), due to the reduced stiffness (k_D) of the elastic foundation.

$$b_s = \begin{cases} t + \frac{1}{4}t_f & \text{– for an exterior wall} \\ t + \frac{1}{2}t_f & \text{– for an interior wall} \end{cases} \quad (24)$$

Discussion of Method II

According to Hummel et al. [11], Method II considers the horizontal force acting on the wall (F), wall geometry (l, h, t), CLT characteristics (E, G), stiffness parameters (k_z, k_s), uniformly distributed vertical load (q), and built-up of the CLT panel. For the shear deformation, an effective shear modulus of the CLT wall panel is considered, that is reduced compared to the total shear modulus of the CLT panel. As the only doing so, this approach also considers the increased panel flexibility due to an elastic foundation.

3.3. Method III – Flatscher & Schickhofer [15]

As method III, Flatscher and Schickhofer [15] propose the same deflection mechanisms (Figure 10) as in Method II. This method proved to be difficult to interpret because the input necessary to calculate the displacement is ambiguous. Consequently, this method is not as straight forward to use as the previous methods. No other sources explaining this method have been found in literature. For more information, please refer to Flatscher and Schickhofer [15].

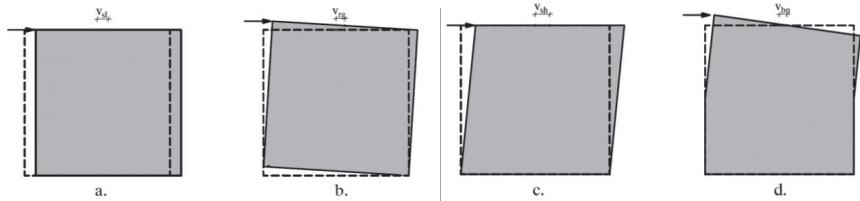


Figure 10. Deformation mechanism for Method II – a) slip, b) rocking, c) shear, and d) bending. Illustrations from [15]

3.4. Concluding discussion of approaches presented for calculating shear wall deformations

Method I does not consider the bending deformation. However, for most practical applications the bending deformation can be even neglected due to the relatively high flexural stiffness of the CLT panel in relation to the mechanical connections. The shear deformation differs only slightly between the two methods. In Method I, the shear deformation is reduced because the full value of the shear modulus is used while method II applied a reduced shear modulus of about half of the total value. The rocking deformation resulting from Method II is slightly lower than

what is obtained from Method I as the lever arm is 10 % larger. Regarding the translation deformation, the values are identical in both methods as both methods use the same principle of translation and the same input parameters.

4. Acknowledgement

The contents presented in this paper is part of the EU-funded COST Action FP1402 working group and part of the Norwegian project “Increased use of wood in urban areas - WOOD/BE/BETTER”, funded by The Norwegian Research Council through the BIONÆR/BIONAER research program. Parts of the contents in this chapter have first been published in the scientific paper submitted to the Special Issue “Basis of Structural Timber Design - from research to standards” of the Engineering Structures journal with title “Strength and Stiffness of Cross-Laminated Timber (CLT) shear walls: State-of-the-art of analytical approaches”.

5. References

- [1] Lukacs, I., Björnfort, A., Tomasi, R., “Strength and Stiffness of Cross-Laminated Timber (CLT) shear walls: State-of-the-art of analytical approaches”, *Engineering Structures*, 2018.
- [2] Casagrande, D., Rossi, S., Sartori, T., and Tomasi, R., “Proposal of an analytical procedure and a simplified numerical model for elastic response of single-storey timber shear-walls”, *Construction and Building Materials*, 102, 2016, pp.1101–1112.
- [3] Tomasi, R. (2013): “Seismic Behavior of Connections for Buildings in CLT. Focus Solid Timber Solutions – Proceedings of the European Conference on Cross-Laminated Timber, TU Graz, 21-22 May 2013. COST Action FP1004, pp. 138-151, 2013.
- [4] Wallner-Novak, M., Koppelhuber, J., Pock, K., “Information Brettsperrholz Bemessung Grundlagen für Statik und Konstruktion nach Eurocode”, *proHolz Austria*, 2013, ISBN 978-3-902926-03-6.
- [5] Pei, S., Lindt, J. V. D., and Popovski, M., “Approximate R-Factor for Cross-Laminated Timber Walls in Multi-Story Buildings”, *Journal of Architectural Engineering*, 19, Issue 4, 2012, pp 245–255.
- [6] Pei, S., Popovski, M., and Van de Lindt, J.W., “Analytical study on seismic force modification factors for cross-laminated timber buildings”, *Canadian Journal of Civil Engineering*, 40(9), 2013, pp. 887–896.
- [7] Shen, Y.-L., Schneider, J., Tesfamariam, S., Stiemer, S. F., and Mu, Z.-G., “Hysteresis behavior of bracket connection in cross-laminated-timber shear walls”, *Construction and Building Materials*, 48, 2013, pp. 980–99.
- [8] Karakabeyli, E. and Douglas, B., “CLT Handbook”. FPInnovations, US edition, 2013.
- [9] Vessby, J., “Analysis of shear walls for multi-storey timber buildings”,

Doctoral Thesis No 45/2011, Linnaeus University, Växjö, Sweden.

- [10] Reynolds, T., Harris, R., Chang, W-S., Bregulla, J., Bawcombe, J., “Ambient vibration test of cross-laminated timber building”, *Proceedings of the Institution of Civil Engineers: Construction Materials*, 168(3), 2014, pp. 121-131.
- [11] Hummel, J., Seim, W., Otto, S., “Steifigkeit und Eigenfrequenzen im mehrgeschossigen Holzbau”, *Bautechnik* 93, 2016, Hef 11 (781-794).
- [12] Seim, W., Hummel, J., Vogt, T., “Earthquake design of timber structures – Remarks on force-based design procedures for different wall systems”, *Eng. Structures*, 76, 2014, pp. 124-137.
- [13] Hummel, J., Seim, W., “Assessment of dynamic characteristics of multi-storey timber buildings”, *Proceedings of the World Conference on Timber Engineering*, 2016, Vienna, Austria.
- [14] Augustin, M., Blass, H.J., Bogensperger, T., Ebner, H., Ferk, H., Fontana, M., Frangi, A., Hamm, P., Jöbstl, R. A., Moosbrugger, T., Richter, A., Schickhofer, G., Thiel, A., Traetta, G., Uibel, T., “BSPhandbuch, Holz-Massivbauweise in Brettsperrholz: Nachweise auf Basis des neuen europäischen Normenkonzepts”, *Verlag der Technischen Universität Graz*, 2. Auflage, 2010.
- [15] Flatscher, G., Schickhofer, G., “Displacement-based determination of laterally loaded cross-laminated timber (CLT) wall systems”, *INTER/49-12-1*, 2016.
- [16] Andreolli, M., Tomasi, R., “Bemessung von Gebäuden in Brettsperrholzbauweise unter Erdbebenbeanspruchung”, *Bautechnik* 93, 2016, Heft 12 (885-898).
- [17] Tomasi, R., “CLT course at “FPS COST Action FP1004 – Enhance mechanical properties of timber, engineered wood products and timber structures”, CLT Training School, University of Trento, 15-17 April 2014.
- [18] Tomasi, R., Smith, I., “Experimental Characterization of Monotonic and Cyclic Loading Response of CLT Panel-to-Foundation Angle Bracket Connections”, *Journal of Materials in Civil Engineering*, ASCE, DOI: 10.1061/(ASCE)MT.1943-5533.0001144, 2014.

State-of-the-art: Timber floor diaphragms

Ildiko Lukacs
PhD Candidate
Faculty of Science and Technology
Norwegian University of Life
Sciences (NMBU)
Ås, Norway

Claudio Pradel
MSc Student
Dpt. of Civil, Environmental and
Mechanical Engineering
University of Trento
Trento, Italy

Anders Björnfot
Associate Professor
Faculty of Science and Technology
NMBU
Ås, Norway

Roberto Tomasi
Professor
Faculty of Science and Technology
NMBU
Ås, Norway

Summary

Building multi-story timber structures is a current trend; many countries are racing to build the highest building. Due to its relatively high strength and stiffness, Cross Laminated Timber (CLT) is well suited for multi-story buildings. The renaissance of timber structures made with CLT and the absence of an up-to-date code in reference to specification of CLT makes it more difficult for engineers to choose the most adequate method in assessing the strength and stiffness of CLT elements. This report presents available methods to calculate the distribution of lateral loads in CLT buildings. The state-of-the-art of floors gives a better understanding how the forces are distributed to the lateral load resisting system, and which modeling technique is most suitable. The emphasis of this state-of-the-art is on presenting the available methods as thoroughly as possible.

1. Introduction

Timber buildings in residential and industrial surroundings are more and more changing city landscapes worldwide. As a building material, glulam post and beams, and Cross Laminated Timber panels (CLT) are generally used. The multipurpose use of CLT panels still raises some questions when it comes to design using a complex material. CLT is an engineered wood product with a quasi-rigid composition making it generally usable in horizontal and vertical diaphragms. CLT has in-plane and out-of-plane load bearing characteristics, which makes it a suitable material for multi-story timber structures.

The increasing number of timber buildings emphasize the lack of timber standards for CLT structures and structural elements. For an engineer to be sure that a CLT structure is properly designed and in accordance with up-to-date standards/codes, it is important to include clear statements regarding CLT wall and CLT floor elements. The Eurocodes currently provide no information on how to design the

lateral load-carrying system of buildings with massive timber elements [1], which means that there is a great need to explore different design methods for CLT shear walls and floor diaphragms, which constitute the main structural elements in tall timber buildings [2, 3].

An issue when designing CLT structures is the estimation of required diaphragm capacity and the determination of the load path in the diaphragms. This report focuses on available analytical and numerical modeling methods to study the behavior of timber floor diaphragms under lateral load. Moreover, attention is given to whether a floor diaphragm should be considered rigid, flexible or semi-rigid. Connections play an important role in determining the diaphragm behavior, in particular panel-to-panel and wall-to-floor connections.

Analytical equations for determining the in-plane deflection under lateral load are contained in standards, taking into account shear and bending deformation of the panel and the deformation of connections. Lateral loads are generally distributed throughout diaphragms and shear walls with the tributary area method or the stiffness method. As part of the research of COST Action FP1402, this paper summarizes available methods to aid in the distribution of lateral loads in buildings composed of CLT elements.

2. Timber floor diaphragms

In the process of designing timber buildings, it is necessary to gain a sufficient understanding of the behavior of the system. The floor diaphragm plays an important role in the load distribution within timber structures. In the following, a brief presentation of floor diaphragms will follow, to give a clear view of how a floor is considered.

2.1. Definition of diaphragms

In accordance with the Advanced Timber Engineering book, by Thelandersson et al. [4], the diaphragms are important in transferring the horizontal forces to shear walls, and then the walls transfer the forces to the floors below and finally to the foundation.

According to Waller-Novak et al. [5], the diaphragms are a requirement when it comes to the stabilization of buildings. In their definition it is also specified that a diaphragm is the result of joining floor panel elements along their side into a plate. This is considered a continuous diaphragm and is needed in the horizontal load distribution to shear walls in the levels below.

Eurocode 5 [6] has a section dedicated to diaphragms built up from wooden plate material connected with fasteners to the vertical resisting elements of the structure.

The CLT Handbook, published by Karakabeyli and Douglas [7], says that the CLT structure's resistance to lateral loads (wind and earthquake) is created through panels as walls and floors that are designed as shear walls and diaphragms

respectively. When CLT panels are assembled together to form the diaphragm, the connections must be able to transfer in-plane diaphragm forces, and maintain the overall safety of the building.

In accordance with the Canadian Standard on CLT [8], a diaphragm is a horizontal system with the main purpose to transfer the lateral loads to the vertical elements.

To conclude, a diaphragm is a horizontal structural element (Figure 1), with the role to transfer the lateral forces to the vertical resisting elements of a structure. The term “diaphragm” is used for both floor and roof elements. The diaphragm contributes to the force transfer, but also in bonding all elements together, structural and non-structural, to form the building. More simply formulated, the diaphragm acts as a horizontal bracing system within the structure.

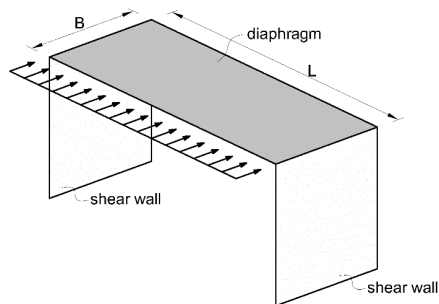


Figure 1. Floor diaphragm

A summary of diaphragm characteristics can be listed as follows:

- transfer horizontal loads;
- provide lateral support;
- embrace out-of-plane forces;
- in-plane stiffness (contributes to the horizontal bracing system).

As Moroder [1] presents, first of all diaphragms (floor and roof) are primarily designed to transmit vertical/gravitational loads for which an out-of-plane behavior is available.

2.2. Types of diaphragms

A typology for timber diaphragms can be differentiated based on material choice and behavior. A general typology of timber floor diaphragms based on material choice can be organized as Light Timber Frame (LTF) diaphragms with (thin) wooden panels, massive timber diaphragms (ex. CLT diaphragm), and hybrid diaphragms made of, for example, Timber-Concrete-Composite (TCC). Much data can be collected regarding timber diaphragms with wooden boards, LTF. However, the use of massive timber elements for diaphragms is not mentioned in any standard, according to Moroder [1].

In the case of massive timber diaphragms, the following definition is generally used: the diaphragm results from the joining of adjacent floor panel elements along their common joints into a plate. In Figure 2, CLT floor diaphragms are presented, such as regular (full) floor, floor as cantilever, floor with opening, etc.

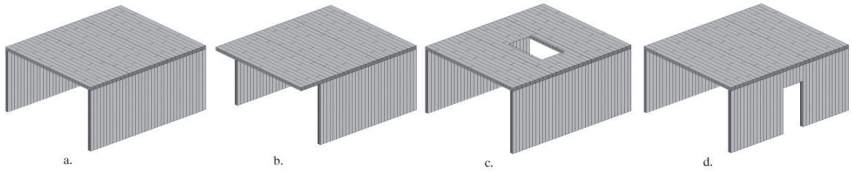


Figure 2. CLT floor diaphragms – a) full floor and shear wall, b) floor as cantilever, c) floor with opening, d) full floor and wall with opening

A general diaphragm typology based on the behavior of the diaphragm is rigid, flexible and semi-rigid diaphragms, which describes the relation between the maximum in-plane deformation of the floor diaphragm ($\Delta_{d,max}$) and the average inter-story drift ($\Delta_{L,ave}$) or shear wall deformation (Figure 3). Countries that have design codes specific for timber design provide definitions of each type of diaphragm (see Table 1).

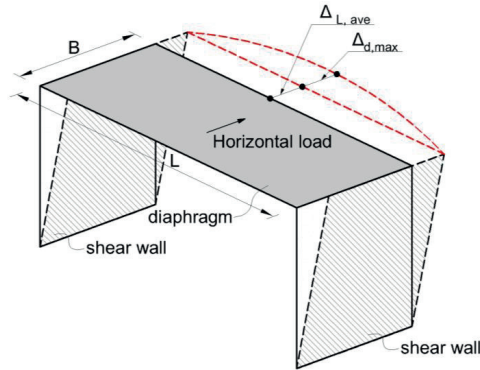


Figure 3. Diaphragm displacement versus inter-story drift

Table 1. Diaphragm definition according to standards

Diaphragm type	EUROPE EN 1998:2010 [9]	USA ASCE 7-10 [10] IBC 2012 [11] SDPWS 2008 [12]
Flexible	$\Delta_{d,max} \geq 1.1\Delta_{L,ave}$	$\Delta_{d,max} \geq 2\Delta_{L,ave}$
Rigid	$\Delta_{d,max} < 1.1\Delta_{L,ave}$	$\Delta_{d,max} \geq 0.5\Delta_{L,ave}$
Semi-rigid	–	$0.5 < \frac{\Delta_{d,max}}{\Delta_{L,ave}} < 2$

2.3. Diaphragm calculation

For the floor diaphragm, the following main parts are enlisted: the plate element, supporting wall/beam, plate-to-plate connection and connections to the lateral load resisting system, i.e., panel-to-panel and panel-to-wall connection. Usually steel connectors are used, the most common is the self-tapping screw.

The total stiffness of the diaphragm (k_{diaph}) is influenced by the effect of a panel stiffness component (k_{panel}) and the connection stiffness component (k_c). The timber panel stiffness can be calculated as follows:

$$k_{panel} = \frac{F}{\Delta_{d,max}} \quad (1)$$

In Eq. (1), F is the horizontal force applied on the diaphragm, and $\Delta_{d,max}$ is the panel deflection at mid-span. The connection stiffness contribution is assessed with Eq. (2):

$$k_c = \frac{V}{\Delta_{con}} = \frac{F}{2 \cdot \Delta_{con}} \quad (2)$$

In this equation, V is the maximum shear force in the diaphragm ($V = F/2$), and the Δ_{con} is the floor-wall connection slip, due to the horizontal force. Based on Eq. (1) and (2), the total stiffness of the diaphragm is evaluated as:

$$k_{diaph} = \left(\frac{1}{k_{panel}} + \frac{1}{k_c} \right)^{-1} \quad (3)$$

2.4. Force distribution methods for diaphragms

Two main methods for the force distribution are used. These are the tributary area method and stiffness method. In the *Tributary area method* panels are considered as simply supported beams and the force in the shear walls is proportional to the tributary area of the corresponding shear wall [13]. According to Chen et al. [13], in the *Stiffness method* the force distribution is dependent on the stiffness of the supporting shear walls. If the force in any wooden shear wall differs by more than 15 % due to the change from flexible to rigid diaphragm assumptions then an envelope force approach should be used, [13], i.e. the shear wall forces based on the highest forces obtained from either the rigid or flexible diaphragm assumption. However, Chen et al. [13] concluded that the design method based on envelope forces might lead to an underestimation of design forces since diaphragms are generally semi-rigid.

2.5. Analysis methods of timber diaphragms

Moroder [1] presents a comparison of methods to analyze the force distribution in concrete respectively timber (see Table 2).

Table 2. Analysis methods for concrete and timber diaphragms, based on [1]

Analysis method	Concrete diaphragm	Timber diaphragm
Deep beam analogy	Used for regular diaphragms	Used for regular diaphragms
Vierendeel truss analogy	Not applicable	Used for unblocked diaphragms and diaphragms with straight boards
Shear field analogy	Used in the form of “stringer-panel method”	Used for regular and to a limited extent to irregular diaphragms
Truss analogy	Applicable, not widely used	Applicable, not widely used
Finite element analysis	Applicable, used for special studies	Applicable, used for special studies

According to Table 2, for timber diaphragms, the following analysis methods are applicable: deep beam analogy, shear field analogy and truss analogy, and finite element analysis. The deep beam (girder) method is commonly used for regular diaphragms; this method is the most widely used, with wide acceptance for timber diaphragms [1], [14]. The shear field method is used for regular and to a limited extent to irregular diaphragms. To provide the methods efficiency, the following features needs to be satisfied: use of metallic fasteners, load applied along the framing element in the load direction. In this shear field analogy, the capacity of the diaphragm is influenced by the failure of the connections.

The truss analogy method is a compromise between a simple approach like the girder analogy and a sophisticated finite element analysis. Even if it is not widely used, this method is applicable to CLT floor analysis, according to Moroder [1]. The FE analysis is the most complex method, and not everyone is comfortable using this. However if a realistic model is considered, this method is the most suitable. For special studies, the most accurate way to analyze diaphragms is the use of FE analysis. According to Follesa et al. [15], diaphragm used in FE analysis are often modelled as rigid.

3. Load distribution in CLT diaphragms

In the literature, two simplified models are available that consider the actual stiffness of floor diaphragms, shear walls and interrelated connections. The purpose of these models is to present how the lateral load acting on the diaphragm can be distributed to the lateral load resisting elements, and how the diaphragm behavior is affecting this. These models can be applied for rigid, flexible and semi-rigid diaphragms. Each should have a different load distribution between the vertical resisting elements of the structure. Both methods have a simplified approach, where diaphragms, walls and connections are modeled as beam and spring element.

Method A – Simplified beam-spring model

The first method is based on Pang and Rosowsky [16]. It was developed for seismic analysis of timber diaphragms. This paper examines the effect of diaphragm flexibility on shear wall deflections by considering the in-plane stiffness of the diaphragm to be semi-rigid. A beam-spring analog model is used to represent the diaphragm-shear wall system where the shear walls are modeled as springs and the diaphragm is modeled as an analog beam that distribute the loads. Here a single-story building with a simple geometry (Figure 4a) is used to explain and to exemplify the use of the model. The simplified beam-spring model of the building is illustrated in Figure 4b.

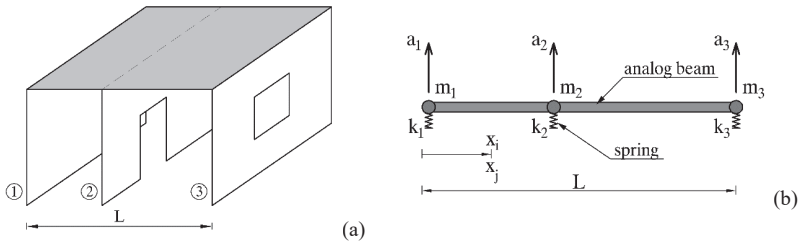


Figure 4. a) Illustration of the simplified single story building (with numbered shear walls). b) Simplified beam-spring model representing the building [16]

The structures setup shows a simple, one story building (Figure 4a) with common geometry, where linear or non-linear spring elements are used for shear wall, and analog beam is used for the diaphragm. The resulting simplified model is presented in Figure 4b. Each spring carries a point load, which is equal to the lumped mass (m) times the spring acceleration (a) which can be approximated by the design spectral acceleration (S_a) specified in building codes. Pang & Rosowsky [16] then proposed a system of equations (Eq. 4) that, when solved, yields the deflections (Δ) of each shear wall, i.e. the inter-story drift necessary for seismic design.

$$\left[\begin{array}{c} \left[\begin{array}{ccccc} 0 & 0 & 0 & 0 & 0 \\ 0 & k_2 & 0 & 0 & 0 \\ \gamma_{i,j} + \lambda_{i,j} & 0 & \ddots & 0 & 0 \\ 0 & 0 & 0 & k_{n-1} & 0 \\ 0 & 0 & 0 & 0 & 0 \end{array} \right] + [I] \end{array} \right] \{\Delta\} = [\gamma_{i,j} + \lambda_{i,j}] \{m_i a_i\} \quad (4)$$

In Equation 4, I is the identity matrix and k is the shear wall (spring) stiffness, which by Pang & Rosowsky [16] was evaluated as the sum of the elastic wall stiffness of walls laying on the same line. Eq. (5) and Eq. (6) represents the stiffness of the fictitious beam elements, given by the $\gamma + \lambda$ matrix, where EI is the in-plane bending stiffness of the diaphragm (beam), x is the shear wall location

measured from the left end of the diaphragm, and L is the length of the diaphragm (see Figure 4b). The notations x_i and x_j represent the x coordinate to the appropriate wall, where i and j are given by the position in the matrix. The application of the simplified beam-spring model is exemplified in Figure 5.

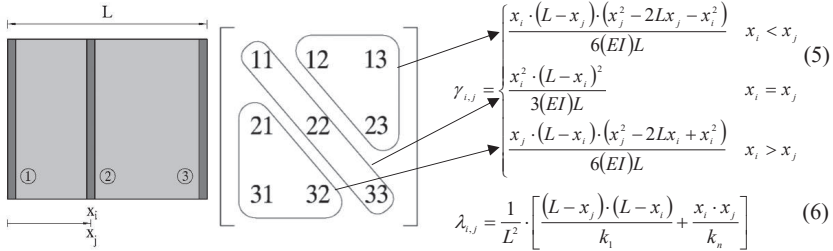


Figure 5. Evaluation of the $[\gamma + \lambda]$ matrix for a one-story building with three shear walls

The in-plane behavior of the floor and roof ceiling was evaluated by a “shear wall” oriented horizontally and its behavior was analyzed by dividing the diaphragm into three segments which are analyzed separately (Figure 5). The diaphragm model employed was a one-way flexible diaphragm model. The relative movement between lines of shear walls was modeled using two-node beam elements (Figure 6) where the axial elongation or compression along the longitudinal direction of the diaphragm was ignored by increasing the beam area.

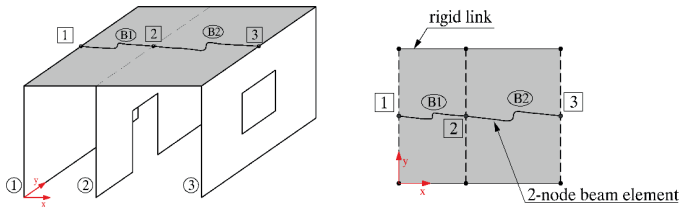


Figure 6. Semi-rigid diaphragm model composed of two-node beam elements with a transversal degree of freedom in each node [16].

Pang & Rosowsy [16] investigated three diaphragm flexibility conditions, i.e. semi-rigid, rigid and completely flexible, by modifying the bending stiffness (EI) of the fictitious beam element from close to zero in the flexible case to an (EI) of 1000 times the semi-rigid stiffness for the case of the rigid diaphragm. It was confirmed that the simplified beam-spring model has the ability to reproduce the deformed shape of actual test data. Thus, it was concluded that the model is suitable for use in a performance-based seismic design framework where accurate prediction of shear wall displacements is needed.

Pang and Rosowsky [16] used this model in a non-linear dynamic time-history analysis, however this can be applied to other types of analysis as well.

3.1. Method B – Multiple spring model

Chen et al. [13, 17] presents a model that is developed to investigate the effect of diaphragm flexibility on the load distribution to lateral load resisting elements (LLREs). According to Chen et al. [13] this model is applicable for all diaphragm flexibility cases: rigid, semi-rigid and flexible. The model is based on the setup of a single-story building, on which a horizontal uniformly distributed load is applied as shown in Figure 7.

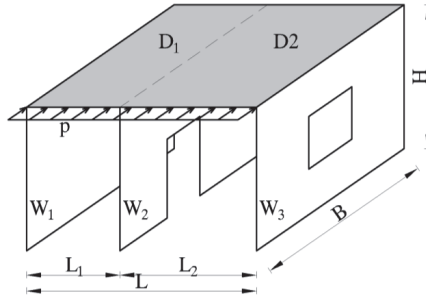


Figure 7. Single story building with diaphragm and shear walls [13, 17]

For simple buildings with only a few lateral load resisting elements, Chen et al. [13] proposed a deep beam-on-spring model where the flexural and shear rigidity of the elastic deep beam represent the diaphragm, whereas shear walls are modeled using a series of linear spring supports. However, as the number of diaphragm elements and shear walls increases, estimation of the load distribution by a mechanical calculating method becomes more tedious. For this purpose, Chen et al. [13] proposed a multiple-spring model.

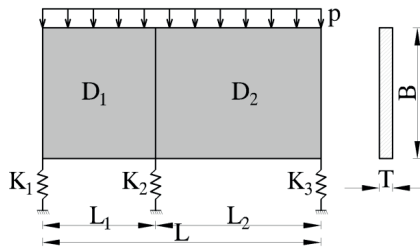


Figure 8. Deep beam-on-spring model setup [13, 17]

The interpretation of Figure 8 is the following: D_i represents the diaphragm, p is the uniformly distributed load, L_i is the distance between the shear walls, L is the total length of the diaphragm and K_i is the stiffness of the shear wall modeled as spring element. However, this model is not applicable when the number of the LLREs increases. For that situation, Chen et al. [13, 17] proposed another model, called multiple-spring model.

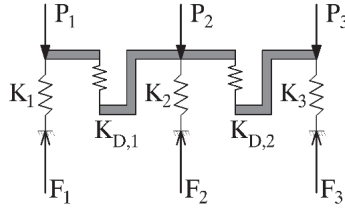


Figure 9. The multiple-spring model with one degree of freedom [13, 17]

In the multiple spring model (Figure 9), the lateral load resisting elements are represented by translational springs with stiffness K_i . The diaphragm between adjacent shear walls is represented by a translational spring with stiffness $K_{D,i}$ connected to the springs of the two adjacent shear walls via a rigid beam with only one degree of freedom in the direction of the applied load. Based on tributary area, the uniform load (p) is converted to a concentrated load P_i acting on each shear wall spring (K_i). In this case, a fully flexible diaphragm implies that $K_{D,i}=0$ resulting in each shear wall carrying a load (F_i) based on tributary area (P_i). Assigning a stiffness for the diaphragms spring ($K_{D,i}$) requires solving a system of equations (Fig. 5). For a rigid diaphragm $K_{D,i}=\infty$, and the force in the LLRE spring, F_i , will be assessed based on the stiffness method. To assess the deformation and reaction of the LLRE spring, in the case of the semi-rigid diaphragm (Figure 9), a system of equations with $2n$ variables has to be solved:

$$\{F\}_{2n} = [D]_{2n \times 2n} \cdot \{U\}_{2n} \quad (7)$$

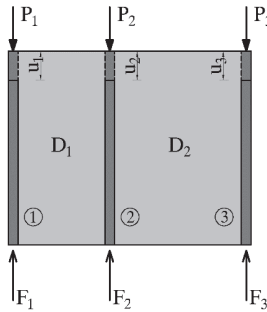


Figure 10. Multiple-spring model setup with one translational DOF for a one story building with three shear walls [13, 17]

Based on Figure 9-10, for the one story building with three shear walls, the Eq. (7) can be calculated with the following equations:

$$\{F\} = \{F_1 \quad -P_1 \quad F_2 \quad -P_2 \quad F_3 \quad -P_3\}^T \quad (8)$$

$$\{U\} = \{0 \quad u_1 \quad 0 \quad u_2 \quad 0 \quad u_3\}^T \quad (9)$$

$$[D] = \begin{bmatrix} K_1 & -K_1 & 0 & 0 & 0 & 0 \\ -K_1 & K_1 + K_{D,1} & 0 & -K_{D,1} & 0 & 0 \\ 0 & 0 & K_2 & -K_2 & 0 & 0 \\ 0 & -K_{D,1} & -K_2 & K_2 + K_{D,1} + K_{D,2} & 0 & -K_{D,2} \\ 0 & 0 & 0 & 0 & K_3 & K_3 \\ 0 & 0 & 0 & -K_{D,2} & -K_3 & K_3 + K_{D,2} + K_{D,3} \end{bmatrix} \quad (10)$$

The stiffness matrix D (Eq. 10) is set up by using the unit deflection method and successively calculating the system response. As the model only makes use of one transitional single degree of freedom, it is generally only suitable for symmetrical buildings with a negligible torsional effect. Therefore, Chen et al. [17] extended the multiple spring model to include a rotational degree of freedom. The torsional effect was modelled by adding a rotational spring ($K_{\theta i}$) to the two ends of the diaphragm segments (Figure 11). The stiffness matrix D is set up in the same manner as previously (see Figure 10). For the one story example building used in Figure 7, the loads acting on the shear walls can be calculated by solving the Eq. (11). Illustration of the multiple spring model with extra rotational DOF is represented in Figure 11.

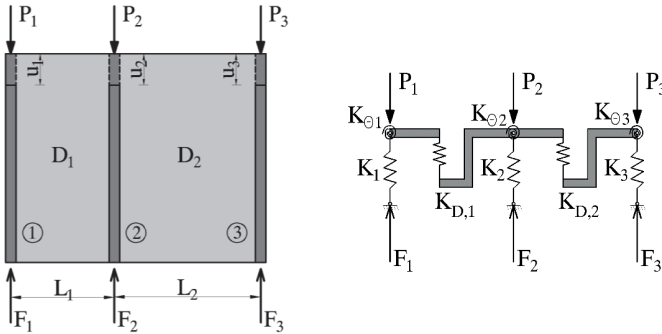


Figure 11. The multiple spring model with a translational (K_i) and rotational ($K_{\theta i}$) degree of freedom for the one-story building with three shear walls [17]

$$\{F\}_{3n} = [D]_{3n \times 3n} \cdot \{U\}_{3n} \quad (11)$$

$$\{F\} = \{F_1 \quad -P_1 \quad 0 \quad F_2 \quad -P_2 \quad 0 \quad F_3 \quad -P_3 \quad 0\}^T \quad (12)$$

$$\{U\} = \{0 \quad u_1 \quad \theta_1 \quad 0 \quad u_2 \quad \theta_2 \quad 0 \quad u_3 \quad \theta_3\}^T \quad (13)$$

$$K_{\theta, i} = (L_i^2 \cdot K_{D, i}) / 3 \quad (14)$$

$$[D] = \begin{bmatrix} K_1 & -K_1 & 0 & 0 & 0 & 0 & 0 & 0 & 0 \\ -K_1 & K_1 + K_{D,1} & (L_1 \cdot K_{D,1})/2 & 0 & -K_{D,1} & (L_1 \cdot K_{D,1})/2 & 0 & 0 & 0 \\ 0 & (L_1 \cdot K_{D,1})/2 & K_{D,1} & 0 & (-L_1 \cdot K_{D,1})/2 & K_{D,1}/2 & 0 & 0 & 0 \\ 0 & 0 & 0 & K_2 & -K_2 & 0 & 0 & 0 & 0 \\ 0 & -K_{D,1} & (-L_1 \cdot K_{D,1})/2 & -K_2 & K_2 + K_{D,1} + K_{D,2} & (-L_1 \cdot K_{D,1} + L_1 \cdot K_{D,2})/2 & 0 & -K_{D,2} & (L_2 \cdot K_{D,2})/2 \\ 0 & (L_1 \cdot K_{D,1})/2 & K_{D,1}/2 & 0 & (-L_1 \cdot K_{D,1} + L_2 \cdot K_{D,2})/2 & K_{D,1} + K_{D,2} & 0 & (-L_2 \cdot K_{D,2})/2 & K_{D,2}/2 \\ 0 & 0 & 0 & 0 & 0 & 0 & K_3 & -K_3 & 0 \\ 0 & 0 & 0 & 0 & -K_{D,2} & (-L_2 \cdot K_{D,2})/2 & -K_3 & K_3 + K_{D,2} + K_{D,3} & (-L_2 \cdot K_{D,2} + L_3 \cdot K_{D,3})/2 \\ 0 & 0 & 0 & 0 & (L_2 \cdot K_{D,2})/2 & K_{D,2}/2 & 0 & (-L_3 \cdot K_{D,2} + L_3 \cdot K_{D,3})/2 & K_{D,2} + K_{D,3} \end{bmatrix}$$

4. Discussion & concluding remarks

For load distribution in CLT diaphragms, the envelope force method is a common approach in calculating the force distribution for CLT diaphragms. With this method, the worst case is usually taken from the two extreme regions, rigid and flexible. However, Chen et al. [13] observed that the forces acting on shear walls in the semi-rigid stiffness range were, in some cases, higher than both the rigid and flexible assumptions, which would indicate that the envelope force method is not always conservative.

This paper presents two models, the simplified beam-spring model by Pang and Rosowsky [16] and the multiple spring model by Chen et al. [13, 17]. Both, are able to consider the actual stiffness of diaphragms in the distribution of forces to shear walls. From the state-of-the-art it can be concluded that:

- The presented models are quite simple mechanical models that mainly work for simple and regular story layouts.
- As the number of shear walls increases and in case of irregular story layouts, the models get increasingly more complex which requires “engineering” simplifications to be made.
- For hand calculations and as a complement to the envelope force method, the semi-rigid models are only appropriate for the simplest story layouts.
- Assignment of stiffness to all included diaphragms and shear walls requires the designer to calculate a stiffness for these elements, a task that can be quite complex by itself.

5. Acknowledgement

The contents presented in this paper is part of the EU-funded COST Action FP1402 working group and part of the Norwegian project “Increased use of wood in urban areas - WOOD/BE/BETTER”, funded by The Norwegian Research Council through the BIONÆR/BIONAER research program.

6. References

- [1] Moroder D., “Floor diaphragms in multi-storey timber buildings”. PhD Thesis, University of Canterbury, Christchurch, New Zealand; 2016.
- [2] Foster RM., Reynolds TP., Ramage MH., “Proposal for defining a tall timber building”, *Journal Structural Engineering*, 2016, DOI 10.1061/(ASCE)ST.1943-541X.0001615
- [3] Lukacs I, Björnfort A., “Structural performance of multi-story cross-laminated timber (CLT) buildings”, In: *Structures and Architecture, Beyond their Limits*, Guimarães, Portugal: Taylor & Francis; 2016, ISBN 978-1-138-02651-3, 2016, pp. 1490-1498.
- [4] Thelandersson, S., Larsen H.J., Ed., “Timber Engineering, Contributions by 18 Scientists from Europe and North America”, *Wiley & Sons*, London, Feb. 2003, ISBN 0-470-84469-8.
- [5] Wallner-Novak M, Koppelhuber J, Pock K., “Information Brettsperrholz Bemessung Grundlagen für Statik und Konstruktion nach Eurocode”, *proHolz Austria*, 2013, ISBN 978-3-902926-03-6.
- [6] European Committee for Standardization, “Eurocode 5: design of timber structures – Part 1-1: General – Common rules and rules for buildings. EN 1995-1-1:2004/A1:2008”, CEN, 2004.
- [7] Karakabeyli E, Douglas B., “CLT Handbook”, FPIInnovations, 2013, US edition, Quebec.
- [8] Canadian CLT Standard, O86-14, “Engineering design in wood”. Published by *Canadian Standards Association*, 2014.
- [9] European Committee for Standardization, “Eurocode 8: design of structures for earthquake resistance – Part 1: General rules, seismic actions and rules for building EN 1998-1:2004/AC:2009”, CEN, 2004.
- [10] ASCE 7-10, “Minimum design loads for buildings and other structures”, American Society of Civil Engineers, 2010; Reston, VA, ISBN 978-0-784-41291-6.
- [11] International Building Code: IBC 2012. International Code Council., USA. ISBN 978-1-60983-040-3, 2012.
- [12] SDPWS-2008 Special Design Provisions for Wind and Seismic standard with Commentary, AF&PA American Wood Council, 2008; Washington, DC, ISBN 0-9786245-9-9.
- [13] Chen ZY, Chui YH, Ni C, Doudak G, Mohammad M., “Load distribution in timber structures consisting of multiple lateral load resisting elements with different stiffnesses”. *Journal Performance of Constructed Facilities*, 2014a; DOI 10.1061/(ASCE)CF.1943-5509.0000587.

- [14] Smith, P.C., Dowrick, D.J. and Dean, J.A., “Horizontal timber diaphragms for wind and earthquake resistance”, *Bulletin of the New Zealand Society for Earthquake Engineering* 19(2), 1986, pp. 135-142.
- [15] Follesa, M., Christovasilis, I. P., Vassallo, D., Fragioacomo, M., Ceccotti, A., “Seismic design of multi-storey cross-laminated timber buildings according to Eurocode 8”, *Ingegneria Sismica*, Special Issue on Timber Structures, Nr. 04 2013, pp. 27-53.
- [16] Pang WC, Rosowsky D., “A beam-spring analog model for seismic analysis of semi-rigid wood diaphragms”, *Proceedings of the World Conference on Timber Engineering*, 2010, Riva del Garda, Italy.
- [17] Chen ZY, Chui YH, Mohammad M, Doudak G, Ni C., “Load distribution in lateral load resisting elements of timber structures”, *Proceedings of the World Conference on Timber Engineering*, 2014b, Quebec, Canada.

Safe design of indeterminate systems in a brittle material

Ishan K. Abeysekera
Structural Engineer
Arup Advanced Technology + Research
London, UK

Andrew J. R. Smith
Structural Engineer
Arup Advanced Technology + Research
London, UK

Andrew C. Lawrence
Associate Director
Arup Advanced Technology + Research
London, UK

Summary

This paper discusses some of the issues engineers may encounter when designing indeterminate systems out of timber, where members and connections often have little or no ductility. The problem is illustrated with a theoretical CLT shear wall building, after which background theory is presented and possible solutions discussed.

1. Introduction

With the increasing popularity of timber in the construction industry there is a growing need for practicing engineers to model ever more complex indeterminate timber structures. Although the structural behaviour of timber elements is well characterised, the stiffness characteristics of timber connections are less well known making it difficult to predict load sharing in an indeterminate (i.e. redundant) structural system. For other common structural materials, such as steel or reinforced concrete, this is generally not an issue because they have significant ductility and can redistribute forces internally. However, timber members and connections often have much less ductility and are frequently characterised by brittle failure, preventing redistribution. Even connections designed following the more ductile Johanssen's modes can often show relatively little ductility in practice [1].

This paper looks at potential challenges faced by engineers when trying to design these indeterminate systems in timber. A building with multiple CLT shear walls is used as an example, but the theory is applicable to any indeterminate timber system such as a grid shell roof.

2. Illustrative Example – Single Storey CLT Shear Wall System

2.1 Behaviour of a single shear wall under in-plane horizontal loads

Before introducing the example it is first important to understand the behaviour of a shear wall consisting of multiple stacked panels with horizontal in-plane forces applied. There are four different mechanisms that contribute to the wall's deflection: bending, shear, sliding and rocking. These are shown in Figure 1.

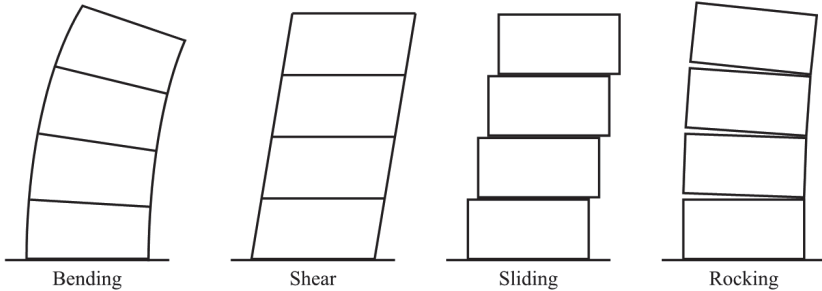


Fig. 1 Mechanisms for deflection for a CLT shear wall.

Although these mechanisms will interact to some degree, this can largely be ignored and the wall can be idealised as a set of four springs in series, one for each mechanism. The total tip deflection, Δ_{Total} can be broken down into a component from each mechanism, as shown in Eq (1).

$$\Delta_{Total} = \Delta_{Bending} + \Delta_{Shear} + \Delta_{Sliding} + \Delta_{Rocking} \quad (1)$$

The total stiffness of the wall, k_{Total} can therefore be calculated from Eq (2).

$$k_{Total} = \frac{1}{\frac{1}{k_{Bending}} + \frac{1}{k_{Shear}} + \frac{1}{k_{Sliding}} + \frac{1}{k_{Rocking}}} \quad (2)$$

In practice, the deflection contributions from sliding and rocking are often ignored as they are governed by connection stiffnesses which are difficult to predict, but these mechanisms can have a significant effect on the overall wall stiffness. As a result, when multiple shear walls are placed in parallel the distribution of forces between them could be significantly different compared to sharing out the loads purely according to shear and bending. This is shown in the following example.

2.2 Example

2.2.1 Building Geometry

Consider a single storey building with a plan as shown in Figure 2. The lateral stability in the N-S direction is provided by three CLT shear walls, two 2 m long and one 4 m long. Diaphragm action is provided by a flat roof which spans in the N-S direction onto the walls oriented E-W, and so the shear walls oriented N-S

take no vertical load from the roof. The 4 m wall has half the thickness of the other two, and therefore all three walls have the same cross-sectional area. All the walls span the full floor to ceiling height of 3 m.

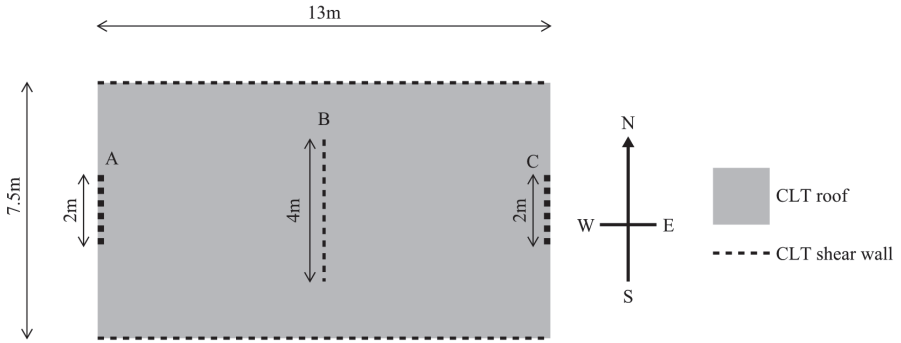


Fig. 2 Plan layout of single storey shear wall system.

2.2.2 Load Distribution Based on Shear Stiffnesses

Since the walls are stocky a practicing engineer is likely to assume that shear deflection governs over bending, and thus would ignore bending, sliding and rocking for simplicity. Therefore, the relative shear stiffness of the walls will govern the lateral load distribution. Assuming a 50 kN design wind load applied at the roof, each wall will resist 16.7 kN because they all have the same effective shear area and therefore the same shear stiffness. Since there is little vertical load on the walls, uplift will occur at the base leading to rocking due flexibility of the tie down connectors. Based on the lateral load of 16.7 kN all three walls would have the same base moment. The walls are restrained from rocking by tie down connectors, each with an assumed lever arm length of $0.7 \times$ the wall length. The tie downs at each end of walls A and C are designed to resist 36 kN in tension (i.e. $[16.7 \text{ kN} \times 3 \text{ m}] / [0.7 \times 2 \text{ m}]$) while the tie downs at the ends of wall B are designed to resist 18 kN of tension at each end.

2.2.3 Load Distribution Based on Rocking Stiffnesses

In reality, testing carried out on connection stiffnesses [2] suggests that the rocking stiffness is an order of magnitude lower than the shear stiffness, and so it is this that mainly governs the lateral load distribution. Assuming the tie down connection stiffness is proportional to the strength, then the tie down connection of wall B will be only half as stiff in tension as those of walls A and C.

From first principles, and the assumption that the tie down lever arm (the distance between the tie down connector and the centroid of the compression zone) is approximately $0.7 \times L$, it can be shown that the rocking stiffness of a particular wall is given by Eq (3), where $k_{Tie-down}$ is the axial stiffness of the wall's tie-down connectors, L is the wall length in plan and h is the wall height.

$$k_{Rocking} = k_{Tie-down} \times \left(\frac{0.7L}{h} \right)^2 \quad (3)$$

Since wall B is twice as long as walls A and C, its rocking stiffness $k_{Rocking,B}$ will therefore be twice that of the other two walls ($k_{Rocking,A} = k_{Rocking,C} = 0.5 k_{Rocking,B}$). If this stiffness distribution governs over shear, bending and sliding stiffnesses then the resulting shear forces in the walls and the axial forces in the tie-downs will be significantly different to the previously calculated values.

2.2.4 Comparison of Results from Different Stiffness Distributions

Table 1 summarises the shear loads in each wall and the resulting axial forces in the tie-downs from the two different stiffness distributions. This shows that if the walls were designed to the initially assumed forces based on relative shear stiffness of the walls then wall B would have been under-designed by 50 %! A more in depth study considering shear, rocking and sliding mechanisms suggests that wall B may actually have only been under-designed by roughly 30 %, depending on various other assumptions, but this is still an unacceptable discrepancy.

Table 1 Wall shear forces and tie-down axial forces for different lateral stiffness distributions.

Wall	Load sharing based on shear stiffness		Load sharing based on rocking stiffness		% Difference
	Wall Shear Force	Tie-Down Axial Force	Wall Shear Force	Tie-Down Axial Force	
A	16.7 kN	36 kN	12.5 kN	27 kN	- 25 %
B	16.7 kN	18 kN	25 kN	27 kN	+ 50 %
C	16.7 kN	36 kN	12.5 kN	27 kN	- 25 %

From the above example it is clear that connection stiffness, which results in rocking and sliding, has a significant effect on the load distribution of indeterminate timber structures.

3. Theory of Indeterminate Structures – Brittle vs Ductile Behaviour

The shear wall system in Figure 2 can be idealised as three springs in parallel in the way it resists a wind force in the N-S direction, as shown in Figure 3. This section compares the load-displacement behaviour of this idealised system for brittle and ductile shear wall failure modes. The total spring stiffness of each wall will be denoted k_A , k_B and k_C . There will be some variation due to construction tolerances, and so all three walls have different stiffnesses and strengths. Any torsional effects are assumed to be resolved by the E-W shear walls and so are neglected.

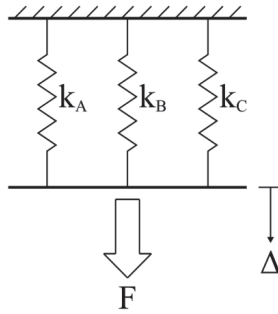


Fig. 3 Idealisation of the shear wall system as 3 springs in parallel.

3.1 Ductile Failure Modes

If each of these springs is characterised as elasto-plastic (linear elastic, then perfectly plastic), with different stiffness and yield strength values, the system of springs would have the load displacement behaviour shown in Figure 4. The springs yield sequentially as load or displacement is applied, and as each spring yields, the residual (tangential) stiffness of the system reduces. This behaviour is the same for both, displacement controlled and force controlled loading.

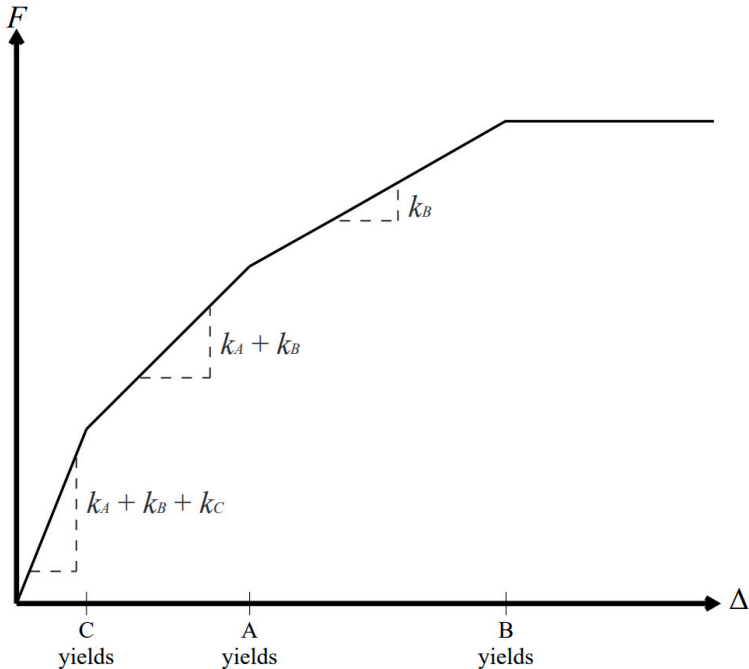


Fig. 4 Load displacement behaviour of a set of elasto-plastic springs.

3.2 Brittle Failure Modes

Now consider the case where the springs are elasto-brittle (linear elastic then perfectly brittle). Such a system is often referred to in reliability analysis as a Daniels system [3], based on original work investigating brittle bundles of threads [4]. Although Daniels' original system assumed equal modulus of elasticity in all springs / fibres, similar principles apply here.

This system will behave differently depending on whether the loading is force controlled or displacement controlled, as shown in Figure 5. If the loading is displacement controlled then failure of one spring will result in the overall force in the system falling to a reduced level; the force in the failed spring is eliminated, but the force in the remaining springs does not change. This is shown by the solid loading line in Figure 5. If the loading is force controlled, as in most real-world scenarios, then the failure of one spring will result in the displacement of the system jumping to a value that puts the total internal force in the remaining springs in equilibrium with the externally applied force. This is shown by the red dashed line in Figure 5.

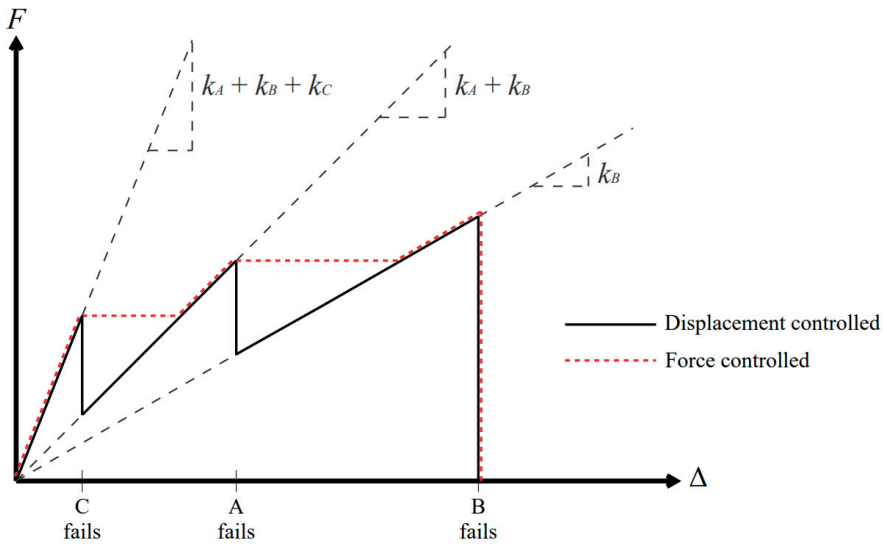


Fig. 5 Load displacement behaviour of a set of brittle springs.

The variation of force in the last spring to fail in the elasto-brittle system is shown in Figure 6. When the other springs fail and the overall displacement jumps, the force and displacement in the last remaining spring (in this case spring B) will jump to a higher value.

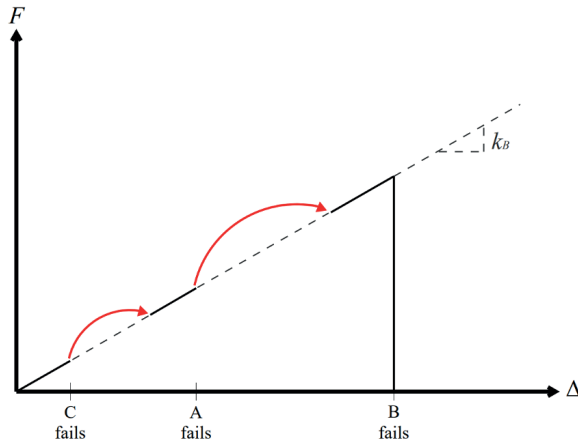


Fig. 6 Load displacement behaviour of the last spring to fail in a force controlled system of brittle springs.

3.3 Premature Full System Failure

In Figure 5, there was sufficient residual strength in the system after the failure of spring C to carry on sustaining the load, albeit at a higher displacement. However, for a different set of spring stiffnesses and strengths it is possible that this would not be the case; in this scenario, once spring C failed the system would not have sufficient residual strength and would suddenly fail under force controlled loading, following the red dashed line in Figure 7.

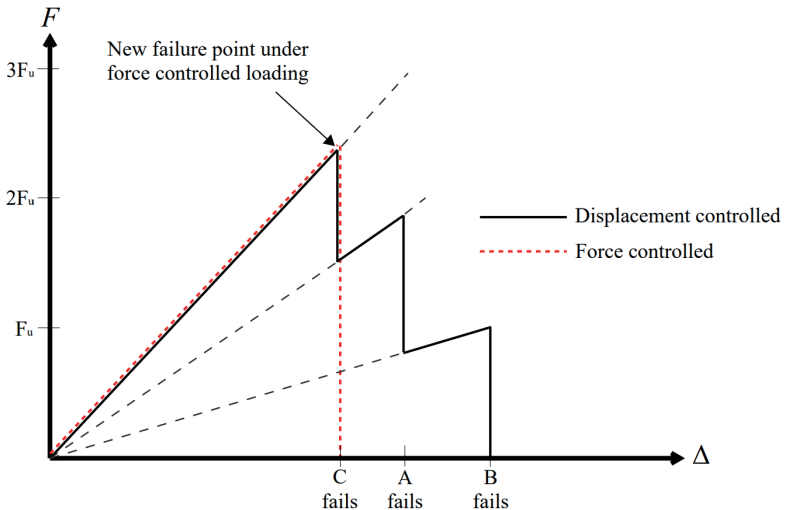


Fig. 7 Load displacement behaviour of a set of three force controlled brittle springs of equal capacity F_u but varying stiffness.

This phenomenon of full system failure upon first elasto-brittle spring failure is particularly likely if all the springs have the same capacity F_u but different stiffnesses. In a real example the spring stiffness variation would be caused by the connection and material stiffness variability in three otherwise identical shear walls. The different stiffnesses will lead to one of the springs attracting more load than the others and failing before the system reaches a force equal to the sum of the capacities of all three springs. Therefore, if mean values of the connection and material stiffnesses are used for the analysis and if only a single elastic analysis of the system is carried out, there is a risk that some of the walls will see more load than predicted by the analysis. If the structure is optimised such that each wall is working close to capacity then there is a high risk of premature failure of the entire wall system if the walls do not have enough ductility to redistribute the applied loads.

4. Design Incorporating Ductility for Redistribution

For redistribution to occur in a structural system, it needs to incorporate sufficient ductility. Plastic design in steel and reinforced concrete is possible because the materials are generally ductile and can be modelled as elasto-plastic. In this case, ductility is commonly defined as the ratio of displacement at first yield to displacement at failure. However, if the construction material has no clear yielding plateau, as with timber elements and some timber connections, then this definition leads to unconservative material idealisations, as shown in Figure 8. In this case, the strength at full ductile displacement is actually weaker than the assumed ultimate strength F_u , resulting in reduced ability to redistribute forces and premature system failure.

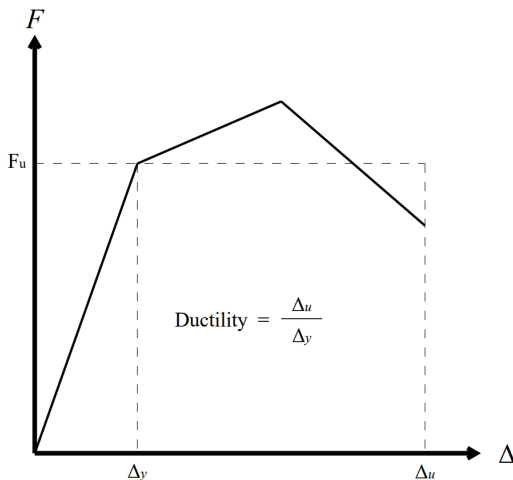


Fig. 8 Unconservative ductility idealisation for a material with no clear yielding plateau.

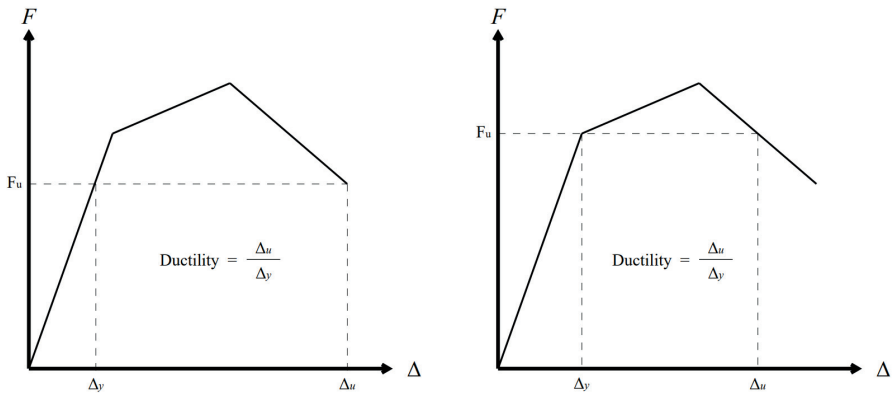


Fig. 9 Two possible conservative definitions of ductility and assumed yield capacity for a brittle material.

In order to ensure that there is sufficient residual strength at the end of the assumed ductile plateau, the definitions of ductility and assumed yield strength (F_u) need to be altered as laid out in Figure 9. This shows that ductility for redistribution of loads needs to be defined as the ratio of displacement at assumed ultimate capacity to the displacement at which the force in the member or connection falls below the assumed yield capacity. This leads to a trade-off between yield strength and degree of ductility – the left-hand side idealised loading curve has a lower yield strength but greater ductility than the right-hand side idealisation. It should be noted that these are two different conservative models of material behaviour; the actual material loading curve does not change. The new idealised behaviour of the material becomes as shown in Figure 10.

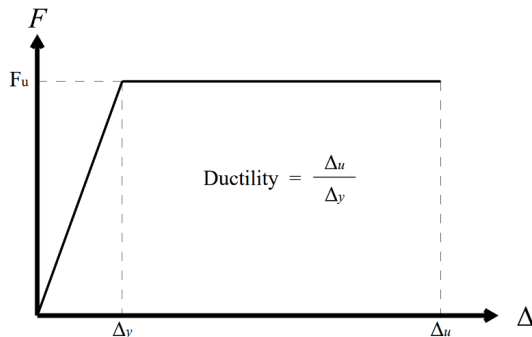


Fig. 10 Conservative ductile idealisation of a material with no clear yielding plateau.

If there is sufficient ductility to redistribute forces internally then the behaviour predicted from the idealised system will be as shown in Figure 11 instead of the brittle failure from Figure 7, ensuring that the system can mobilise the full assumed

capacity of all three springs. The softening behaviour near full capacity is not an issue as long as second-order effects are sufficiently small. For a specific project the engineer will need to decide how much ductility is needed for redistribution.

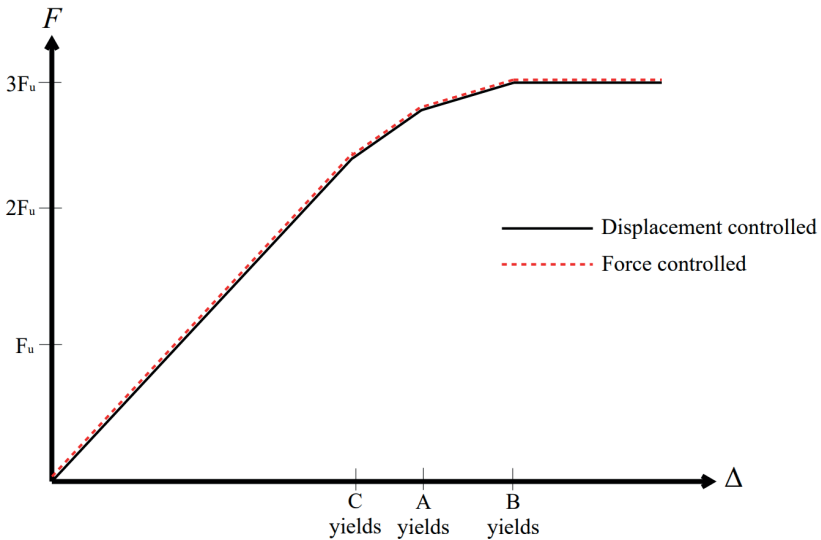


Fig. 11 Load displacement behaviour of a set of three force controlled springs of equal strength F_u but varying stiffness with sufficient ductility to redistribute load.

5. Conclusions

Indeterminate structures are increasingly common in all materials. However, because timber has much less ductility than other materials such as steel, there is a risk that the uncertainties in load distribution highlighted in this paper could lead to sudden failure of a timber structure if it does not have sufficient ductility to enable load redistribution.

Therefore, where a system is indeterminate and where the ultimate strengths of different load paths are governed by a brittle failure mode or have insufficient ductility, the effect of construction sequence, construction tolerances, connection stiffness and element stiffness on load distribution needs to be considered, along with associated uncertainties and variability.

Alternatively, indeterminate structural systems could be designed such that their ultimate strength is governed by ductile failure modes, with sufficient ductility to activate alternative load paths for redistribution. The ductility may be incorporated at the connections (such as through slender dowels in shear) or in ductile non-timber elements. Any brittle failure modes should be designed with a suitable over-strength factor to ensure that these failure modes don't govern. This second option is likely to be far easier in practice.

For engineers to be able to design indeterminate timber systems safely, significant further research is required to either characterise stiffness uncertainties or identify reliable ductile failure mechanisms.

6. Acknowledgements

We would like to thank Arup for supporting this research through the internal Invest in Arup scheme.

7. References

- [1] Brühl F., Kuhlmann U., “Consideration of Connection Ductility within the Design of Timber Structures”, *Proceedings of the Conference of COST Action FP1402*, pp32-45
- [2] Gavric I., Fragiaco M., Ceccotti A., “Cyclic behaviour of typical metal connectors for cross-laminated (CLT) structures”, *Materials and Structures*, Vol. 48, Issue. 6, 2015, pp. 1841-1857.
- [3] Thöns S., Schneider R., “The Influence of Brittle Daniels System Characteristics on the Value of Load Monitoring Information”, *EWSHM 2016, COST Action TU1402 on Quantifying the Value of Structural Health Monitoring*
- [4] Daniels H. E., “The statistical theory of the strength of bundles of threads I”, *Proc. Royal Society Series A*, Vol. 183, Issue. 995, 1945, pp. 405-435

© Arup 2018

B Seismic Design

WG2 “Solid Timber Construction – Cross Laminated Timber” 5th Workshop of “COST Action FP1402”

General rules

Maurizio Follesa
dedaLEGNO
Firenze, Italy

Summary

This paper describes the provisions for the seismic design of CLT buildings included in a recent proposal of revision of Chapter 8 of Eurocode 8. The proposal includes general definitions and design concepts, values of the behavior factors to be used for the seismic design according to the Medium and High Ductility Class, general detailing rules and capacity design rules both at connection and building level, values of the over-strength factors and safety verifications.

1. Introduction

The current provisions for the seismic design of timber buildings are included within Chapter 8 of Eurocode 8 [1] and have been published in 2004. At that time, the development of timber buildings throughout the world was limited only to some countries (mainly USA, Canada, New Zealand, Australia and, even if less widespread, Japan and Central-Northern Europe) and limited only to some structural systems (Light Timber Frame above all) and to a limited number of storeys (maximum 3 or 4). This is one of the reasons why the content of Chapter 8 was limited to only five pages in total, and the few rules included, especially those making reference to the seismic detailing and design of timber buildings, were mostly taken from the research experience and the code provisions of other international Building Codes, mainly those of USA, Canada and New Zealand. The rules were to a great extent the same as included in the first draft of this Chapter, dated 1988 [2].

As for the Cross Laminated Timber (CLT) system, no specific provisions are included, since the technology was not yet widespread at the time these provisions were written, therefore no references to capacity design rules or seismic detailing can be found. However, even if not specifically related to CLT, the system may currently be classified as “Glued wall panels with glued diaphragms, connected with nails and bolts” in Ductility Class Medium and designed with a value of the behavior factor $q=2,0$.

Within the last 13 years the building technology has made great strides in the field of timber structures due several reasons, including: (i) the improvements in the automation process and performance of computer numerical control (CNC) machinery; (ii) the developments reached in the gluing process of wood-based

products; and (iii) the introduction of new types of mechanical fasteners, especially self-tapping screws, which have greatly enhanced the possibility of prefabrication of structural components and made the construction process easier and faster.

At the same time, several important research projects have been conducted (2005-2015) with the aim of investigating above all the seismic performance of medium rise timber buildings built with different structural systems, via both full scale tests on entire multi-storey buildings and numerical investigations.

Noteworthy are: the SOFIE Project (2005-2012) conducted by CNR-IVALSA Italy, NIED, BRI and University of Shizuoka Japan on the seismic performance of multi-storey CLT buildings [3]; the NEESWOOD Project (2004-2010) conducted by Colorado State University, State University of New York at Buffalo, Rensselaer Polytechnic Institute and Texas A&M University, USA on the seismic performance of multi-storey wood-frame buildings [4]; the SERIES Project (2010-2013) conducted by University of Trento, Italy, Graz University of Technology, Austria and University of Minho, Portugal, on the seismic performance of multi-storey CLT, Log House and Light Frame buildings [5], the NEES-Soft project (2011-2014) conducted by Colorado State University, Western Michigan University, Clemson University, Rensselaer Polytechnic Institute and California State Polytechnic University, USA on the seismic retrofit of soft-storey woodframe buildings [6]. Furthermore, two more shaking table tests have been performed in Japan in February 2015 on a 5- and 3-storey full-scale CLT buildings [7]. All these projects have investigated the seismic performance of multi-storey timber building by means of shaking table tests conducted on full-scale buildings with a number of storeys ranging from 2 to 7, built with the most common structural systems currently used in the timber construction practice.

This background led in 2015 to a new proposal of provisions for the seismic design of timber buildings to be included within Chapter 8 of Eurocode 8, which was partly presented in [8] and [9] and is currently under discussion within the CEN/TC250, sub-group WG3 'Timber' of Structural Committee 8 (SC8) 'Design for Earthquake Actions'.

2. A critical review of the current provisions

In the force-based design approach of Eurocode 8 [1], the energy dissipation capacity of the whole structure is implicitly considered by dividing the seismic forces obtained from a linear (static or dynamic) analysis by the behaviour factor q associated to the relevant ductility classification. This approach can be applied only if the following conditions are satisfied:

1. the structural systems are clearly described without any possible misinterpretation.
2. the dissipative zones and the brittle parts to be overdesigned in order to avoid any possible anticipated brittle failure and to achieve the desired energy dissipation capacity are unequivocally identified for each structural system.

3. the over-strength factors to be used for the design of the brittle components are provided.

Conversely, by analysing in detail the content of the current version of Chapter 8 of Eurocode 8, it could be observed that:

- a. the structural systems are not clearly described, the short definition of some of them may be misleading without an explanatory drawing, some systems are repeated twice or refer only to structural components and not to lateral load resisting systems of buildings. Furthermore, as mentioned above, some structural systems such as the CLT system but also the Log House system, which are nowadays widely used in the construction practice are not even mentioned.
- b. the capacity design rules for each structural system are totally missing, only a few prescriptive rules are given regarding joints with dowel type fasteners.
- c. the over-strength factors are not provided. A value of 1.3 is given only regarding the verification of shear stress in carpentry joints.

Therefore, also in order to align the content of the chapter related to timber buildings to the provisions given for the other materials chapters, a fundamental revision is needed, considering that the few rules currently given are left to the interpretation of the structural designer.

3. The new proposal and background research references for the proposed changes

While trying to keep the same order of headings and topics of the former versions also to keep consistency with the other materials chapters within Eurocode 8, the proposed modifications to the current version are substantial. The content of the existing paragraphs was modified and new paragraphs were added, such as the one related to the definitions of the different Structural Types and the one related to the Capacity Design Rules for the different structural systems. Finally, some provisions regarding the non-linear static (pushover) analysis of timber structures, here not reported for the sake of brevity, have been added in a new Annex.

3.1 Definitions and design concepts

Regarding the definition of static ductility, a reference to the definition given in EN 12512 was added, while for carpentry joints a further clarification was given, reporting that “*loads are transferred through special cuttings to the connected elements by means of compression areas*”.

The classification of timber buildings according to the design concept is modified specifying that “*Earthquake-resistant timber buildings shall be designed in accordance with one of the following concepts:*

- a) *High- or Medium-dissipative structural behaviour;*
- b) *Low-dissipative structural behaviour.”*

differently from the current generic distinction between dissipative and low dissipative structural behaviour.

Later it is also specified that “*Other structural types, classified in ductility class M (medium, DCM) or H (high, DCH) may be designed with concept b) provided that the corresponding provisions given in the reference parts of this section for the general rules at building level are satisfied.*”

The possibility of designing every structural type for DCL is given in the relevant chapters of all other materials in Eurocode 8. Regarding the general rules at building level, further specifications are given later within the Capacity Design Rules section.

For the dissipative zones, the current definition specifies that the dissipative zones shall be located in joints and connections, whereas the timber members themselves shall be regarded as behaving elastically. A further clarification is given, more specifically it is stated that “*The energy dissipation is provided by plasticization of metal fasteners combined with embedment of timber at the interface with the fasteners, and for some systems also by friction. Friction can be taken into account only in presence of devices specifically designed for the transmission of horizontal forces through it; in other cases it shall not be considered.*”

A further provision is given later specifying that: “*As an alternative to the design concept provided above, dissipative zones could be located outside of joints and connections in purposely developed energy dissipaters (e.g. lead extruded or hydraulic dampers, dog-bone steel plates, etc.). In this case, both the timber members and the joints and connections shall be regarded as behaving elastically. In order to ensure the correct behaviour of the energy dissipaters, their connections to the timber members should be as stiff as possible. These connections, the other joints and connections between timber members, and all the timber members shall be designed with sufficient over-strength. The appropriate behaviour factor q should not be determined according to Table 8.2 - ‘Structural types and upper limit values of the behaviour factors for buildings regular in elevation’ but will depend on the mechanical properties of the energy dissipaters and the geometrical properties of the structure.*”

3.2 Materials and properties of dissipative and non-dissipative zones

New wood-based materials such as OSB panels, Gypsum Fibre boards and especially CLT panels, which were not included in the current version, have been added, and some existing definitions have been changed. Regarding the structural panels used as structural components or sheathing material for shear walls and diaphragms, the proposal is the following:

- a) particleboard-sheathing (according to EN 312) has a density of at least 650 kg/m³;*
- b) plywood-sheathing (according to EN 636) is at least 9 mm thick and has at least 5 layers;*
- c) particleboard- and fibreboard (according to EN 622)-sheathing are at least 12 mm thick;*

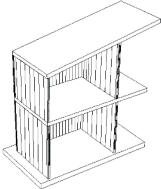
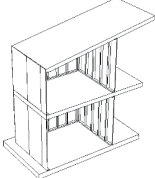
- d) *Oriented Strand Board sheathing (OSB) type 3 or 4 according to EN 300 and has a minimum thickness of 12 mm;*
- e) *Gypsum Fibre boards (GF) sheathing according to EN 15283-2 has a minimum thickness of 12 mm;*
- (5) *CLT panels produced according to EN 16351 have a minimum thickness of 60mm for shear walls and 18 mm for floor and roof diaphragms.*

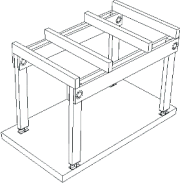
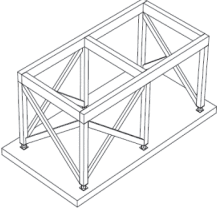
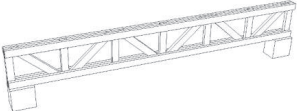
Regarding CLT, the limitation of 18 mm for CLT floor panels is given according to the current specifications included in the European Standard for CLT EN 16351 [11] which states that CLT may be made of timber layers having thicknesses between 6 mm and 60 mm. The limitation to 60 mm of panel thickness for CLT walls is given according to current production of most European producers [12,13].

3.3 Structural types, ductility types and behaviour factors

This part has been completely redrafted with respect to the current version. First of all, a clear definition of the different structural types is given, explained also by means of schematic figures. According to the proposal, nine different structural types are identified and briefly described in Table 1.

Table 1: Structural types for timber buildings and schematic graphical description.

1	Cross laminated timber (CLT) buildings.	
2	Light wood-frame (LF) buildings.	
3	Log House buildings.	

4	Moment resisting frames.	
5	Post and beam timber buildings with vertical bracings made of timber trusses.	
6	Timber framed walls with carpentry connections and masonry infill.	
7	Large span arches with two or three hinged joints.	
8	Large span trussed frames with nailed, screwed, doweled and bolted joints.	
9	Vertical cantilever systems made with structurally continuous Glulam or CLT wall elements.	

The Cross Laminated Timber (CLT) system has been newly introduced together with other “new” structural systems with respect to the current edition, such as the Log House system and the Vertical Cantilever system.

The value of the behaviour factor q given for each structural type and for the corresponding ductility class (Medium or High) are given in Table 2. For structures

designed in accordance with the concept of low-dissipative structural behaviour (DCL), the behaviour factor q should be taken not greater than 1,5.

Table 2: Structural types and upper limit values of the behaviour factors for buildings regular in elevation

Structural type		DCM	DCH
1	CLT buildings	2,0	3,0
2	Light-Frame buildings	2,5	4,0
3	Log House buildings	2,0	-
4	Moment resisting frames	2,5	4,0
5	Post and beam timber buildings	2,0	-
6	Mixed structures made of timber framing and masonry infill resisting to the horizontal forces	2,0	-
7	Large span arches with two or three hinged joints	-	-
8	Large span trusses with nailed, screwed, doveled and bolted joints	-	-
9	Vertical cantilever systems made with glulam or X-Lam wall elements	2,0	-

New values for the behaviour factors have been introduced for the different structural systems, specifying two different values, if applicable, for DCM and DCH ductility classes. The values given for CLT structures are based on research results and numerical investigations conducted within the Sofie Project for buildings designed according to the capacity design rules given in the relevant section (see § 3.4) and referenced in [14], [15] and [16].

3.4 General and Capacity Design Rules

As mentioned above, in order to apply the force-based procedure of Eurocode, (i) a clear description of the structural system is needed, in order to avoid any possible misinterpretation and (ii) capacity design rules are needed for each structural type and material in order to achieve the desired level of ductility and energy dissipation capacity for the whole building and therefore to apply the given values of the behaviour factor q for the different Ductility Classes.

Regarding (i), the provisions included in the new proposal for the Cross Laminated Timber system are the following:

(1) Cross laminated timber buildings are structures in which walls are composed of CLT panels.

(2) The connection of the shear walls to the foundation shall be made by means of mechanical fasteners (e.g. hold-down anchors, steel brackets, anchoring bolts, nails and screws, etc.) and shall adequately restrain the wall against uplift and sliding.

Uplift connections should be placed at wall ends and at opening ends, while shear connections should be distributed uniformly along the shear wall length (Fig. 1).

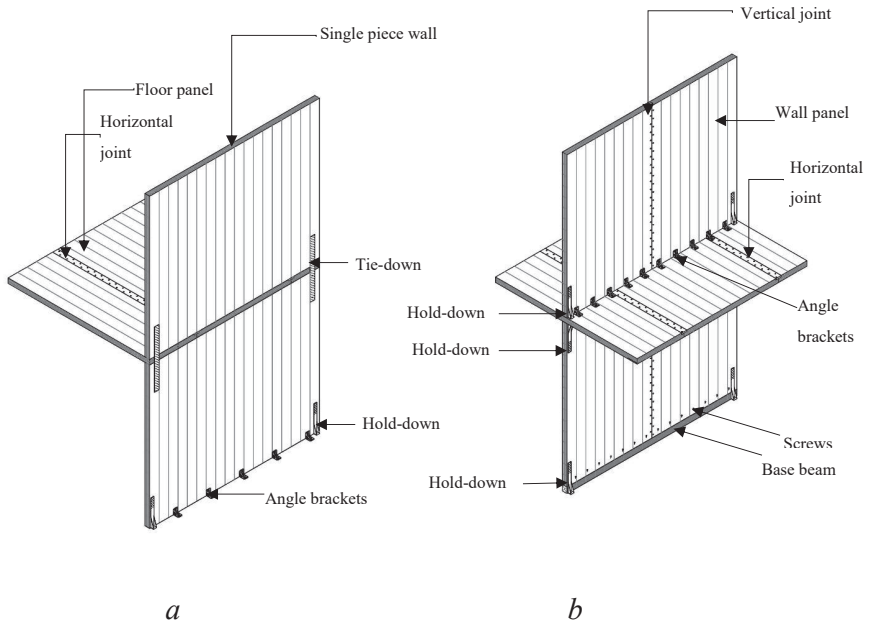


Fig. 1 Walls and floors in monolithic (a) and segmented (b) Cross Laminated Timber buildings.

(3) Walls shall have heights at least equal to the inter-storey height and may be made of a unique element up to the maximum transportable length (Fig. 1 (a)) or may be composed of more than one panel ('segmented wall', Fig. 1 (b)). Each segment shall have width not lower than $0,25h$, h signifying the inter-storey height, and shall be connected to the other segments by means of vertical joints made with mechanical fasteners such as screws or nails. Individual wall-panels with a width of less than $0,25h$ shall not be regarded as a seismic resistant shear wall. Perpendicular walls are connected by means of joints made with mechanical fasteners (usually screws). Horizontal joints between walls should be avoided unless special provisions are taken to ensure adequate out-of-plane restraint (e.g. properly connected to perpendicular stabilizing walls, timber studs, etc.).

(4) Floor and roof diaphragms are made of CLT timber panels connected together by means of horizontal joints made with mechanical fasteners (screws or nails). The floor panels bear on the wall panels and on timber beams if present, to which they are connected with mechanical fasteners (screws or nails).

(5) Other types of floor and roof diaphragms may be used, provided that their in-plane rigidity and resistance is ensured by means of wood-based sheathing panels.

Timber-concrete composite floors may be used provided that they are adequately connected to the lower and upper walls by means of mechanical fasteners. The concrete topping, in particular, shall be connected to the vertical panels to ensure the in-plane shear due to the diaphragm action be transferred to the walls and down to the foundations.

(6) The upper walls bear on the floor panels (platform construction), and are connected to the lower walls using mechanical fasteners similar to those used for the wall-foundation connection. Tie-down connections nailed to the CLT walls may be used for the external walls uplift restraint.

Regarding (ii), as for all other structural types, capacity design rules are provided both at building level and at connection level in order to ensure that the energy dissipation will occur in the ductile components. Regarding the latter, in order to ensure a ductile failure mode characterized by yielding of fasteners in steel-to-timber or timber-to-timber connections, it is specified that any anticipated brittle failure like tensile and pull-through failure of anchor bolts or screws, steel plate tensile and shear failure in the weaker section of hold-down and angle brackets connections or any other brittle failures such as splitting, shear plug, tear-out and tensile fracture of wood in the connection regions should be always avoided.

Table 3 summarizes the Capacity design rules at building level proposed for the CLT system for the two Ductility Classes, while Fig. 2 shows the structural elements and connections to be designed with overstrength criteria.

Table 3: Capacity design rules for DCM and DCH for the different structural types.

Ductility Class Medium (DCM)		Ductility Class High (DCH)	
Components to be oversized	Dissipative components/mechanisms	Elements to be oversized	Dissipative components/mechanisms
<ul style="list-style-type: none"> -all CLT wall and floor panels -connections between adjacent floor panels -connections between floors and underneath walls -connections between perpendicular walls 	<ul style="list-style-type: none"> -Shear-restrain connections at wall base -Uplift-restrain connections at wall ends 	<ul style="list-style-type: none"> -all CLT wall and floor panels -connections between adjacent floor panels -connections between floors and underneath walls -connections between perpendicular walls 	<ul style="list-style-type: none"> -Shear-restrain connections at wall base -Uplift-restrain connections at wall ends -vertical step joints between wall panels in segmented shear walls

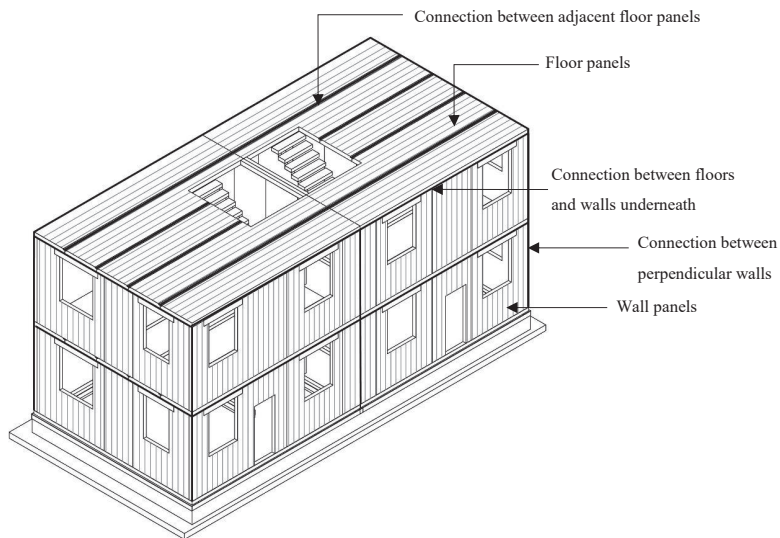


Fig. 2 Structural elements and connections to be designed with overstrength criteria in order to fulfil the capacity design criteria in Cross Laminated Timber buildings in DCM.

The new proposal of capacity design rules defined for each structural type is that *the design strength of the brittle parts $F_{Rd,b}$ should be greater than or equal to the design strength of the ductile parts $F_{Rd,d}$ multiplied by an overstrength factor γ_{Rd} and divided by a reduction factor for strength degradation β_{sd} due to cyclic loading according to the following equation:*

$$\frac{\gamma_{Rd}}{\beta_{sd}} \cdot F_{Rd,d} \leq F_{Rd,b} \quad (1)$$

where the values of γ_{Rd} are provided in Table 4, and the value of β_{sd} is equal to 0,8.

Table 4: Values of the overstrength factors γ_{Rd}

Structural type	Overstrength factor γ_{Rd}
X-Lam buildings, Light-Frame buildings, Log House buildings, High ductility moment resisting frames with expanded tube fasteners, Mixed structures made of timber framing and masonry infill resisting to the horizontal forces	1,3
Moment resisting frames (except for high ductility moment resisting frames with tube fasteners and Densified Veneer Wood), Post and beam timber buildings, Vertical cantilever systems made with glulam or X-Lam wall elements	1,6

The proposed values of over-strength factors are referenced in [17], [18] and [19]. However, the applicability of these values is still under discussion and will be further checked with parametric studies keeping in mind that, especially for taller buildings and considering the characteristic strengths of the connection devices commercially available, such values may lead to unrealistic applications for the lower storeys walls.



Fig. 3 Floor-to-wall connections at the first storey in a 6 storey CLT building, designed for a medium seismicity area.

3.5 Safety verifications

As reported also in [8], the strength values of timber shall be determined considering the k_{mod} -values for instantaneous loading and the partial factors for material properties γ_M for accidental load combinations.

For ultimate limit state verifications of structures designed in accordance with the concept of dissipative structural behaviour (Ductility classes M or H), the strength

degradation of the dissipative zones shall be taken into account by multiplying the characteristic strength in static conditions by the reduction factor β_{sd} . The design strength shall then be calculated as:

$$F_{Rd,d} = k_{mod} \cdot \beta_{sd} \cdot \frac{F_{Rk,d}}{\gamma_M} \quad (2)$$

The strength degradation of the non-dissipative zones may not be taken into account. The design strength should be calculated as:

$$F_{Rd,b} = k_{mod} \cdot \frac{F_{Rk,b}}{\gamma_M} \quad (3)$$

This formulation for the safety verifications is quite different from the one present in the Eurocode 8 version of 2004 version where the partial safety factor γ_M for fundamental load combinations is proposed for ultimate limit state verifications of structures designed in accordance with the concept of low-dissipative structural behaviour and no reduction factor β_{sd} for strength degradation is given.

4. Discussion and conclusions

The provisions for the seismic design of CLT buildings to be included in the future revision of Chapter 8 of Eurocode 8 has been presented. The proposal is markedly different from the previous and current short and outdated version. It is based on the following main modifications: (i) changes in the general definitions and design concepts, (ii) update of the list of wood based and other materials and properties of dissipative and non-dissipative zones, (iii) update of the list of structural types with consideration of new structural widely used types not included in the current version, (iv) modification of the description of the existing structural types with the aid of graphical descriptions, (v) modification of the values of the behaviour factors for the different Ductility Classes, (vi) introduction of capacity design rules for each structural type and of the over-strength factors to be used in the design of the brittle components and (vii) modification of the current equations for the safety verifications.

The revision work is still ongoing within sub-group WG3 'Timber' of CEN/TC250/SC8 'Design for Earthquake Actions'. More research is needed on the applicability of the new provisions on multi-storey buildings also considering other structural systems and especially for medium to high-rise buildings in medium to high seismicity areas, where the common commercially available connection devices seem inapplicable and the seismic design requires a different philosophy or different types of connection devices.

Furthermore, some other paragraphs of the current edition still need improvements, especially those related to the detailing rules and to the control of design and construction.

5. Acknowledgements

The contribution to this work of the other participants, members and observers of CEN TC 250/SC8/WG3 is gratefully acknowledged. Special thanks to Massimo

Fragiacomo, Maurizio Piazza, Daniele Casagrande, Roberto Tomasi, Werner Seim, André Jorissen, Eric Fournely, Thierry Lamadon, Laurent Le Magorou, Eleftheria Tsakanika, Jorge Branco, Wim De Groot, Iztok Sustersic and Andrew Lawrence.

6. References

- [1] Eurocode 8 (2004): Design of structures for earthquake resistance, Part 1: General rules, seismic actions and rules for buildings. CEN. (EN 1998-1-1).
- [2] Commission of the European Communities – Industrial Processes – Building and Civil Engineering [1988] Eurocode 8—Structures in Seismic Regions – Design - Part 1: General and buildings, May 1988 Edition – Report EUR 12266 EN, Directorate-General Telecommunications, Information Industries and Innovation L-2920 Luxembourg.
- [3] Ceccotti A., Sandhaas C., Okabe M., Yasumura M., Minowa C., Kawai N. *SOFIE project – 3D shaking table test on a seven-storey full-scale Cross-Laminated building*. Earthquake Engineering & Structural Dynamics, DOI: 10.1002/eqe.2309, 2013.
- [4] van de Lindt J. W., Pei S., Pryor S. E., Shimizu H., Isoda H. *Experimental Seismic Response of a Full-Scale Six-Story Light-Frame Wood Building*. Journal of Structural Engineering, Vol. 136 No. 10, pp. 1262-1272., 2010.
- [5] Tomasi R., Piazza M. *Investigation of seismic performance of multi-storey timber buildings within the framework of the SERIES Project*. Proc., the International Conference on Structure and Architecture ICESA2013, Guimaraes, Portugal, 2013.
- [6] van de Lindt J. W., Bahmani P., Mochizuki G., Pryor S. E., Gershfeld M., Tian J., Michael D. Symans M. D., Rammer D. *Experimental Seismic Behavior of a Full-Scale Four-Story Soft-Story Wood-Frame Building with Retrofits. II: Shake Table Test Results*. Journal of Structural Engineering, E4014004, doi: 10.1061/(ASCE)ST.1943-541X.0001206, 2014.
- [7] Sato, M.; Kawai, N.; Miyake, T.; Yasumura, M.; Isoda, H.; Koshihara, M.; Nakajima, S.; Araki, Y.; Nakagawa, T.: *Structural design of five-story and three-story specimen of the shaking table test*, CD-ROM Proceedings of the World Conference on Timber Engineering (WCTE 2016), August 22-25, 2016, Vienna, Austria, Eds.: J. Eberhardsteiner, W. Winter, A. Fadai, M. Pöll, Publisher: Vienna University of Technology, Austria, ISBN: 978-3-903039-00-1
- [8] Follesa M., Fragiaco M., Vassallo D., Piazza M., Tomasi R., Casagrande D., Rossi S. *A proposal for a new Background Document of Chapter 8 of Eurocode 8*. Proceedings of the International Network on Timber Engineering Research meeting INTER 2015. Šibenik, Croatia. paper 48-102-1 - ISSN: 2199-9740, 2015.
- [9] Follesa, M.; Fragiaco, M.; Casagrande, D.; Tomasi, R.; Piazza, M.; Vassallo,

- D.; Rossi, S.: *The new version of Chapter 8 of Eurocode 8*, CD-ROM Proceedings of the World Conference on Timber Engineering (WCTE 2016), August 22-25, 2016, Vienna, Austria, Eds.: J. Eberhardsteiner, W. Winter, A. Fadaï, M. Pöll, Publisher: Vienna University of Technology, Austria, ISBN: 978-3-903039-00-1
- [10] EN 12512: *Timber structures – Test methods – Cyclic testing of joints made with mechanical fasteners*. CEN. Brussels, Belgium, 2001.
- [11] EN 16351: *Timber structures – Cross laminated timber – Requirements*. CEN. Brussels, Belgium, 2015.
- [12] Stora Enso CLT Technical brochure. Stora Enso Wood Products GmbH, 2017
- [13] BINDERHOLZ CLT BBS. Binderholz Bausysteme GmbH. 2017
- [14] Ceccotti A., Follesa M. *Seismic Behaviour of Multi-Storey X-Lam Buildings*. Proceedings of 426 COST E29 International Workshop on Earthquake Engineering on Timber Structures, pages 81-95, Coimbra, Portugal, 2006.
- [15] Ceccotti A., Follesa M., Lauriola M.P. *Quale fattore di struttura per gli edifici multipiano a struttura di legno con pannelli a strati incrociati?* XII Convegno ANIDIS L'ingegneria sismica in Italia, Pisa, 2007 (in Italian).
- [16] Follesa M., Christovasilis I., Vassallo D., Fragiaco M., Ceccotti A. *Seismic design of multi-storey CLT buildings according to Eurocode 8*. Ingegneria Sismica, Special Issue on Timber Structures, n. 04/2013, pp. 27-53, 2013.
- [17] Casagrande, D., Sartori, T., Tomasi R. *Capacity design approach for multi-storey timber-frame buildings*. Proc. of the International Network on Timber Engineering Research meeting INTER, Bath, United Kingdom. (paper 47-15-3), 2014.
- [18] Schick, M., Vogt T., Seim W. *Connection and anchoring for wall and slab elements in seismic design*. Proceedings of the 46th CIB-W18-Meeting, Vancouver, Canada. (paper 46-15-4), 2013
- [19] Jorissen, A., Fragiaco, M. *General notes on ductility in timber structures*. Engineering Structures. (Vol. 33, N. 11, pp. 2987-2997), 2011.

The capacity design approach of Cross Laminated Timber structures: a state-of-the-art review

Daniele Casagrande

National Research Council of Italy - Trees and Timber Institute
(CNR IVALSA), Italy

1. Introduction

Seismic design of structures can be performed by adopting a force- or displacement-based design approach. In the first case, the seismic action is represented by external forces, obtained from the product of the inertial masses and the accelerations, at the different levels of the structure. In the second case, the seismic design is carried out by comparing the demand and the capacity in term of absolute and relative displacements.

According to the performance based design (PBD) approach, different limit states of the structures can be considered. Ultimate limit states (ULS) are associated with collapse or with other forms of structural failure, which might endanger the safety of people, whereas Damage limitation states (DLS) are those associated with damage beyond which specified service requirements are no longer met [1]. A reference probability of exceedance of 10% in 50 years, is usually adopted for ordinary buildings at ULS, whereas at DLS the same reference probability is adopted in 10 years.

The resistance and energy-dissipation capacity of structures at ULS is commonly related to their non-linear response. Design seismic forces are obtained by dividing the elastic forces by the values of the *behavior q-factor* (or *reduction R-factor*), depending on the ductility capacity of the structure [2]. The seismic energy dissipation is achieved in specific zones, which are properly designed to ensure a sufficient local ductility. All other structural elements are assumed to behave elastically and, for this reason, are designed with sufficient over-strength, according to the capacity design (CD) approach. A ductile global failure mechanism of the structure is achieved thanks to the hierarchy of resistance between the components, by avoiding local and global brittle failure mechanisms, in accordance with eq. (1):

$$\gamma_{Rd} \cdot F_{Rd,d} \leq F_{Rd,b} \quad (1)$$

where $F_{Rd,d}$ and $F_{Rd,b}$ are the design strength of the ductile and the brittle component respectively, and γ_{Rd} is defined as the over-strength factor.

In timber structures, the seismic energy dissipation is ensured by the yielding of the mechanical connection devices, since timber elements may be characterized by brittle failures. Depending on the structural typology (e.g. Light-timber frame buildings - LTF, Cross Laminated Timber buildings - CLT, Moment Resisting frames, etc.), different energy dissipation capacities are obtained, consistently with the ductility

capacity of the connections, which develop plastic deformations with an adequate low-cycle fatigue strength.

In this document, a general background on the application of the CD approach to CLT structures is presented.

2. Background

Capacity design rules provided for CLT buildings are mainly based on the research experience of the Sofie Project as well as on the experimental and numerical analyses carried out in the last 15 years.

An interesting general overview on the ductility and the over-strength factor of timber structures can be found in [3], where the different contributions for the definition of the hierarchy of resistance are presented.

In [4], the results of a shake table test on a 3-storey CLT building are reported, with specific attention to the assessment of the global energy dissipation and of the q-factor. It was clearly specified that: *“the vertical joints between perpendicular walls and the horizontal joints between floor panels were over-designed and the building was designed in order to reach the energy dissipation first in the vertical joints between wall panels, then in the horizontal connection between walls and floors (steel angles and screws) and last in the hold-down connection”*.

In [5], the importance of using ductile connectors in seismic design is highlighted, by presenting the results obtained from modal response spectrum as well as pushover analyses. With the aim of giving specific provisions for a ductile connection between CLT panels, it is remarked that *“failure of the wall panel due to in-plane loading (shear, bending and axial force) is mostly brittle and should be avoided by designing the panel for the over-strength of the ductile elements (the connectors)”*. On the contrary, it is suggested that *“the connections between adjacent floor panels are considered as non-ductile and designed for the over-strength of the bracket and wall-to-wall connections”*. Moreover, particular attention is given to capacity design at connection level by highlighting that *“the connectors between adjacent panels and between panels and foundation, however, may behave ductile or brittle under shear deformation depending on whether plasticization of the steel fastener (screws and nails) is attained or not”*. Therefore, the paper suggests that all fastener failures with no plastic hinge should be avoided, whereas the failure where two plastic hinges are formed in the fastener should be considered as the most desirable. An over-strength factor of 1.3 is proposed for the design of the brittle mechanism of bracket devices used to bear the wall shear and tensile loads, whereas a value of 1.6 was derived for screws holding together adjacent perpendicular walls.

A list of the connection typologies which should be devoted to the dissipative behavior of CLT buildings is reported in [6], namely: *“step joints between wall panels in case of walls composed of more than one element, connections against sliding between walls and floor below, and between walls and foundation, and anchoring connections against uplift placed at wall ends and at wall openings”*. It was also specified that the CD approach should be applied to timber members and the other connection typologies: connections between adjacent floor, connections between floors and walls

and connections between perpendicular walls. Moreover, in order to ensure a well-distributed energy dissipation along the height of the buildings it is observed that the *seismic resistance of shear walls should be higher at lower storeys and should decrease at higher storeys proportionally to the decrease of the storeys seismic shear, thus leading to the simultaneous plasticization of the ductile connections*". For the applicability of the CD at connection level, it is recommended that failure mechanisms of connections are characterized by the formation of one or two plastic hinges in the mechanical fastener and that "*brittle failures such as splitting, shear plug, tear out and tensile fracture of wood in the connection regions should be always avoided*".

Capacity design rules are presented also in [7], with different levels of applicability, regarding connectors, walls and buildings. It is reported that capacity based design provisions at the connector level in CLT buildings aim to "*ensure ductile failure mechanism of simple fasteners (nails, screws) in hold-downs, angle brackets and vertical screwed joints in coupled walls*". In order to achieve a significant energy dissipation, it is pointed out that the nail plasticization with the formation of at least one plastic hinge should be ensured. As a result, eq. (1) should be applied so that failure modes related only to the embedment strength of timber without the formation of any plastic hinge is considered as brittle failure, whereas the failures with the formation of plastic hinges are assumed as ductile. Moreover, it is specified that all steel parts of mechanical devices (e.g. hold-down, angle brackets, etc.), their anchoring to the foundation as well as CLT wall panels, have to be designed with a sufficient over-strength. Brittle failure modes such as shear plug, splitting of timber, tension of wood, and tear out are assumed to be avoided. At wall level, it is suggested that "*plasticization should preferably occur in the hold-downs and angle brackets loaded in tension, whereas the angle bracket should ideally remain elastic in shear so that there is no residual slip in the wall at the end of the seismic event*". An over-strength factor of 1.3 is proposed in this case.

For multi-panel walls, it is required that the shear capacity of the vertical joints should be lower than the shear capacity related to the panels or other connections (i.e. hold-down, angle brackets). An over-strength factor of 1.6 is suggested in this case. It is also recommended that walls with large openings should be designed "*in such a way that possible brittle failures due to concentration of forces in the corners of the wall openings are avoided*". An over-strength factor of 1.3 is proposed for that. At building level, it is specified that, in order to ensure a box-type behavior, the floor panels should act as non-dissipative rigid diaphragms. Moreover, no energy-dissipation should be achieved in floor panel-to-wall panel connections, floor panel-to-lateral load resisting walls underneath and perpendicular wall-to-wall connections. In all aforementioned cases, an over-strength factor of 1.3 is proposed.

In [8] a conservative proposal of 1.3 and 1.25–1.45 is reported for the over-strength for hold-downs and angle brackets, respectively. In [9], an over-strength factor with an average value of 1.60 is suggested, for panel-to-panel CLT screwed joints.

Important results for the CD applicability to CLT structures are presented in [10], by analyzing the experimental results obtained from full-scale tests on single-panel as well as multi-panel shear walls. It is specifically suggested that at wall level, "*plasticization should preferably occur in the hold-downs and angle brackets loaded in tension,*

whereas the angle brackets should ideally remain elastic in shear so that there is no residual slip in the wall at the end of the seismic event". Three different kinematic behavior types are recognized for two-panel CLT walls with vertical joints depending on the relative weakness of vertical joints in comparison with the anchoring connections: "1- coupled wall behavior, when each wall segment rocks about its lower corner as an independent, individual panel; 2- single-coupled wall behavior, when the wall panels behave as partly fixed panels with semi rigid screwed connection; and 3- single wall behavior, when the wall panels behave as a single wall panel with rigid screwed connection". It is also pointed out that CLT multi-panel walls have a better performance under cyclic lateral loads when they have coupled wall behavior with predominant rocking deformations rather than single-wall behavior.

3. The proposal for the new version of Chapter 8 of Eurocode 8

The current provisions for the seismic design of timber buildings in Europe are reported in the chapter 8 of Eurocode 8 [1]. However, capacity based design rules and detailing provisions for dissipative zones are totally missing for most of the structural types, which, with exception of moment resisting frames, only one ductility class is assigned to. The location of dissipative zones is not clearly defined and the values of over-strength factors are not reported.

For this reason, a draft document for the new version of the chapter 8 of Eurocode 8 is being discussed with the 'Seismic' sub-group WG8 of the committee CEN/TC250/SC5, [11], taking into account most of the research results obtained in the last years in the field of seismic engineering applied to timber structures.

In this draft document, the CLT structural typology is clearly introduced and an upper-limit value of the q-factor, for CLT buildings, equal to 2 and 3 is defined for DCM and DCH ductility classes, respectively. A value of q equal to 1.5 has been maintained for the low ductility class (DCL).

Taking into account the strength degradation due to cyclic loading of dissipative connections, a coefficient β_{sd} , equal to 0.8, was introduced in eq. (1), yielding:

$$\frac{\gamma_{Rd}}{\beta_{sd}} \cdot F_{Rd,d} \leq F_{Rd,b} \quad (2)$$

The design strength of dissipative connections $F_{Rd,d}$ is in fact obtained by considering a reduction of strength equal to 20th of the 5th percentile strength $F_{Rk,d}$ and by assuming a safety factor γ_M equal to 1.0, since seismic load is considered as accidental. For brittle elements, since they behave elastically, the reduction factor related to the strength degradation due to cyclic loading is not taken into account. The design strength of dissipative connections $F_{Rd,b}$ is calculated as the ratio between the 5th percentile strength $F_{Rk,b}$ and the safety factor γ_M , equal to 1.

$$F_{Rd,d} = \beta_{sd} \cdot \frac{F_{Rk,d}}{\gamma_M} \quad (3)$$

$$F_{Rd,b} = \frac{F_{Rk,b}}{\gamma_M} \quad (4)$$

The value of the over-strength γ_{Rd} is assumed equal to 1.3. It is also noted that the design forces in the non-dissipative connections, elements and anchorages to the foundation calculated with eq. (2), need not exceed the design values calculated for q equal to 1.5.

Specific CD rules, based on the research results reported in the previous section, are defined for CLT buildings. Rules at connection level and building level are distinguished.

At building level, it is required that CLT buildings should be regarded as box-type structures and the dissipative connections will use dowel-type fasteners inserted perpendicular to the shear direction. Connections with dowel-type fasteners inclined in the shear direction (e.g. screws inclined in the shear direction) are allowed only in non-dissipative connections. The structural elements which should be designed with sufficient over-strength are:

- *“all CLT wall and floor panels;*
- *connections between adjacent floor panels (or connections of other type of sheathing material like in 8.4.1.1(5)) in order to limit the possible extent of relative slip and to assure a sufficiently rigid in-plane behaviour;*
- *connections between floors and walls underneath thus assuring that at each storey there is a sufficiently rigid floor to which the walls are rigidly connected;*
- *connections between perpendicular walls, particularly at the building corners, so that the stability of the walls themselves and of the structural box is always ensured.”*

The connections designed as dissipative zones for DCM are represented by

- *“shear connections between walls and the floor underneath, and between walls and foundation (usually steel brackets or screwed connections);*
- *anchoring connections against uplift placed at wall ends and at wall openings (usually hold-down anchors).”*

For DCH it is recommended that also *“vertical screwed or nailed step joints between adjacent parallel wall panels within the segmented shear walls”* are designed to dissipate energy. In order to ensure a higher energy dissipation, DCH is admitted only for multi-panel, namely *“segmented”* walls which have to be *“composed by more than one panel, each one of width not lower than 0,25 h, with h signifying the inter-storey height, and not greater than h, connected with joints made with mechanical fasteners (screws or nails) inserted perpendicular to the shear plane”*.

At connection level, in dissipative zones a ductile failure mode characterized by yielding of fasteners (nails or screws) in steel-to-timber or timber-to-timber connections should be achieved and brittle failure mechanisms should be avoided according to eq. (2). It is specifically required that the following failure mechanisms shall be avoided:

- tensile and pull-through failure of anchor bolts or screws;
- steel plate tensile and shear failure in the weaker section of hold-down and angle brackets connections

- other brittle failures such as splitting, shear plug, tear-out and tensile fracture of wood in the connection regions, according to the provisions given in EN 1995-1-1.

4. The Canadian Standard CSA 086 -2014

Specific provisions for seismic design of CLT buildings are included in the Canadian Standard for timber structures [12] in section 11.9.2. A maximum reduction R-factor (the equivalent of the European behavior-factor) of 3 is reported, specifying that “*the energy is dissipated through connections and wall panels which act in rocking or in combination of rocking and sliding*”. For CLT structures with wall panels with aspect ratios (height-to-length) less than 1:1 or acting in sliding only a maximum reduction factor of 1.3 is imposed. If for segmented-walls (multi-panel walls) the same value of the reduction R-factor of the Eurocode 8 is adopted, monolithic CLT walls are not considered as capable to dissipate a significant amount of energy and a low ductility class is imposed.

Energy dissipative connections have to be designed in order that a “*yielding mode governs the resistance, shall have at least moderate ductility in the directions of the assumed rigid body motions of CLT panels and possess sufficient deformation capacity to allow for the CLT panels to develop their assumed deformation behavior, such as rocking, sliding, or combination thereof*”. Non-dissipative connections are required to behave elastically and shall be designed with a sufficient over-strength. As for Eurocode 8, however, their seismic force need not exceed the force obtained using the elastic reduction factor, equal, in this case, to 1.3.

According to capacity design principles at building level, it is required that energy dissipation shall occur in

- *vertical joints between the panels in shear walls;*
- *shear connections between the shear walls and the foundations or floors underneath;*
- *hold-down connections, except for continuous steel rods*

CLT panels that are part of the lateral-force-resisting system shall be designed for seismic forces according to the capacity design rules, but need not exceed the force determined using a reduction factor of 1.3, taking into account the net section effects and openings.

Specific values for over-strength factors of eq. (1) are not reported, requiring that brittle failure modes *shall be designed for seismic forces that are developed when energy dissipative connections in shear walls reach the 95th percentile of their ultimate resistance.*

5. General discussion

Similar outcomes have been obtained in the last years from different researchers, as clearly shown by the fact that similar provisions are included both in Canadian Standard and in the proposal for the new version of the chapter 8 of Eurocode 8.

At building level, it is commonly accepted that the energy dissipation in CLT structures should be achieved in vertical joints between the panels, in shear connections between the shear walls and the foundations or floors underneath, and in the hold-down connections. On the contrary, CLT panels and all other types of connections have to be designed with a sufficient over-strength.

For multi-panel CLT shear walls, a higher behavior factor is adopted than for single-panel CLT walls, due to the energy dissipation achieved in the vertical joints of the panels. [11] considers a medium ductility class for structures with monolithic CLT panel whereas in [12] a low ductility class is provided.

The importance of uniform energy dissipation at different levels, as proposed in [6], is not highlighted by any other authors and is not specifically required in the two discussed Standards. This seems reasonable for a medium ductility class but, on the contrary, for a design based on a high-energy dissipation, specific requirements for a uniform over-strength distribution along the height of the building should be reported, in order to prevent a global failure mechanism associated with a soft-story mechanism. Similar provisions are reported, in fact, for the seismic design of steel braces in European Standard [1] and have been proposed in [13] for light-timber frame buildings when designed according to a high ductility class.

Few analytical rules for the CD approach at building- and at wall- level have been developed. Depending on the structural typologies and the mechanical models of analysis, specific expressions should be provided in order that CD can be applied in the design practice.

At connection level, the scientific community agrees that yielding of fastener shall be achieved with the formation of at least one plastic hinge. Failure mechanisms related to the embedment strength of the wood without the formation of a plastic hinge as well as brittle failures such as splitting, shear plug, tear-out and tensile fracture of wood in the connection regions have to be avoided. All failures related to steel plates and to anchors with the foundation are considered as non-dissipative zones.

The applicability of capacity design rules at connection level is quite simple and eq. (1) can be adopted. Each connection or anchor device can be, in fact, represented by an isostatic mechanical system composed with in-series springs, subjected to the same force. Each component is designed to behave plastically or elastically when assumed as dissipative or non-dissipative, respectively. No other analytical expression than eq. (1) is hence required of the applicability of CD approach. In order that the connection failure mechanism involves the formation of at least one plastic hinge in the fasteners, limits on the maximum fastener diameter are reported in Standards ([1] and [14]).

If a good agreement has been established in the scientific community for the CD at connection level, at building level several aspects should be investigated and discussed. Among these, it seems fundamental to propose simplified analytical expressions capable to relate the ductile design of dissipative zones to the elastic design of brittle components. A list of elements which shall be designed with a sufficient over-strength seems, in fact, not sufficient.

However, since CLT structures are commonly hyper-static systems, and different global failure mechanisms can be achieved, depending on the structural typology of the walls (cantilever wall, wall with openings, etc.) and of mechanical devices, general and rigorous expressions for CD cannot be easily defined by the simple equilibrium on the structural components of the building. Other aspect should, in fact, be taken into account as, for example, the interaction between shear-walls due to continuous lintel elements.

6. References

- [1] EN 1998-1:2013, Eurocode 8 – Design of structures for earthquake resistance part 1: General rules, seismic actions and rules for buildings, 2013. Brussels, Belgium: CEN, European Committee for Standardization.
- [2] Pauley, T., Priestley, M.J.N. – Seismic design of reinforced concrete and masonry buildings. Wiley Ed.; 1992
- [3] Jorissen, A., Fragiaco, M. – General notes on ductility in timber structures, *Engineering Structures*, 33, 2011, pp. 2987-2997
- [4] Ceccotti A., Follesa M. – Seismic Behaviour of Multi-Storey X-Lam Buildings. Proceedings of 426 COST E29 International Workshop on Earthquake Engineering on Timber Structures, 2006, pages 81-95, Coimbra, Portugal
- [5] Fragiaco, M., Dujic, B., and Sustersic, I. – Elastic and ductile design of multi-storey crosslam massive wooden buildings under seismic actions. *Engineering Structures*, Volume 33, Issue 11, 2011, Pages 3043-3053
- [6] Follesa, M., Vassallo, D., Fragiaco, M., Ceccotti, A. – Seismic design of multi-storey clt buildings according to Eurocode, *Ingegneria Sismica* n. 04/2013 “SPECIAL ISSUE -Timber Structures”, 2013
- [7] Gavric, I., Fragiaco, M., and Ceccotti, A. – Cyclic behaviour of typical metal connectors for cross-laminated (CLT) structures, International council for research and innovation in building and construction working commission W18 - timber structures, 2013, Vancouver, Canada
- [8] Gavric, I., Fragiaco, M., and Ceccotti, A. – Capacity seismic design of x-lam wall systems based on connection mechanical properties, *Materials and Structures*, 2015, 48:1841–1857
- [9] Gavric, I., Fragiaco, M., and Ceccotti, A. – *European Journal of Wood and Wood Products*, Volume 73, Issue 2, 2015, Pages 179-191
- [10] Gavric, I., Fragiaco, M., and Ceccotti, A. – Cyclic Behavior of CLT Wall Systems: Experimental Tests and Analytical Prediction Models, *Journal of Structural Engineering*, 2015, 141(11): 04015034

- [11] Follesa, M., Fragiacomò, M., Vassallo, D., Piazza, M., Tomasi, R., Rossi, S., Casagrande, D. – A proposal for a new Background Document of Chapter 8 of Eurocode 8, Proc. of the International Network on Timber Engineering Research meeting INTER / 48- 102- 1, 21015, Sibenik Croatia
- [12] CSA 086-14, Engineering design in wood, Canadian Standards Association, 2014
- [13] Casagrande, D., Sartori, T., Tomasi, R. – Capacity design approach for multi-storey timber-frame buildings. Proc. of the International Network on Timber Engineering Research meeting INTER, 2014, Bath, United Kingdom. (paper 47-15-3).
- [14] Norme tecniche per le costruzioni - D.M. 14 Gennaio 2008, Consiglio Superiore dei lavori Pubblici, Gazzetta Ufficiale, 2008 (*in Italian*)

Assessment of the q-factor for timber buildings with CLT panels: state of the art

Stefano Bezzi
PhD student
Dep. of Civil, Environmental and
Mechanical Engineering
University of Trento
Trento, Italy

Summary

In this paper an overview about the behavior factor to use in CLT buildings is reported. In detail, the methods used to calculate the q-factor, the research carried out on the assessment of the behaviour factor, and a proposal of provisions for the seismic design of timber buildings to be included within Chapter 8 of Eurocode 8 [1] are presented.

1. Introduction

The energy-dissipation capacity of timber constructions under seismic load is adequately known. However, in the current version of Seismic European standard (Eurocode 8 [1]) recommendations and construction details are not yet well defined. In fact, the chapter on timber constructions (Chapter 8) consists of only five pages. The few rules that are reported in this chapter mainly concern some types of timber structural systems (i.e. Light Timber Frame above all), while no recommendations and construction details are reported for the latest typologies of timber construction (i.e. for Cross Laminated Timber buildings).

For this reason, at present, the CLT system is classified as “*glued wall panels with glued diaphragms connected with nails or screws*”. This means that the CLT system falls into the Ductility Class Medium and its design is performed taking as behaviour factor a value equal to 2,0. Therefore, it is clear that the value of the behaviour factor q (or reduction factor R) proposed by the Standard, for the CLT systems, is not well defined and is not correlated to the structural typology, to the material and to the construction details.

In the last years, several research campaigns have focused on the assessment of the behavior factor in CLT structures. Experimental tests and advanced non-linear numerical analyses have been carried out in this sense. Different methodologies were adopted for the definition of the behavior factor, depending on the analysis process used to investigate the non-linear response of the structures.

To choose an appropriate value of the q -factor for CLT buildings, it is necessary to know and compare the work of different researchers. For this reason, in this paper the researches carried out on the assessment of the behaviour factor are presented.

2. Behaviour factor q

The resistance and energy-dissipation capacity of structures at Ultimate Limit States is commonly related to their non-linear response. The seismic energy dissipation is concentrated in specific zones, which are properly designed to ensure a sufficient local ductility. All other structural elements are assumed to behave elastically and, for this reason, are designed with sufficient over-strength, according to the capacity based-design (CD) approach. To avoid an explicit non-linear structural analysis in the design of structures, the capacity of the structure to dissipate energy, through mainly ductile behaviour of its elements and/or other mechanisms, is taken into account by performing an elastic analysis based on a response spectrum reduced with respect to the elastic one, called a "design spectrum". This reduction is accomplished by introducing the behaviour factor q . The values of q -factors are reported in Standards, depending on materials, structural typology and the expected energy dissipation achieved in the structure in a seismic event.

The behavior factor (q -factor for the European Standard [1], also known as seismic reduction factor R) is a reduction factor used to reduce the linear elastic response spectra to the inelastic response spectra. In other words, the behaviour factor is the ratio of the strength required to maintain the structure elastic to the inelastic design strength of the structure. The behaviour factor, therefore accounts for the inherent ductility and the over-strength of the structure and the difference in the level of stresses considered in its design. The value of behaviour q -factor to use in the design of buildings, can be found in the Eurocode 8 [1] for the Europe area. This code refers to the FMD method presented in [2].

For the design of timber buildings, the behavior factor q to be taken to reduce the linear elastic response spectrum is contained in chapter 8 of EC8[1]. The behaviour q -factor is provided for the different categories related to the dissipation capability of the structural system (see *Fig. 1*).

From *Fig. 1*, it is possible to see that the value of the q -factor for the for structures with high capacity to dissipative energy (i.e. light timber frame buildings) is equal to 5. This value is the highest positive value for timber buildings. Many researches have been carried out to get the goodness of this value, one of this is reported in [3]. It was found that the values of the behaviour factor q given by the Standard, are too high compared to the values obtained from the real structures. This is due to material limitations and the absence of appropriate design rules which mean that the structure has a lower ductility, under real conditions.

The author shows that the only method to obtain the maximum ductility of the structure is the application of the capacity design approach and properly design rules.

Analyzing a single wall connected at the ground through hold-downs and angle brackets, the maximum ductility is obtained when the nails or screws used for the sheathing-to-frame connections are over-strength in relation to the other connections (hold-down and angle brackets). Consequently, the failure of the wall due to the failure of the sheathing-to-framing connections is the most ductile. The authors also found that the q-factor is dependent on various parameters such as: the number of storey, the ductility of the nails, the spacing of the nails and the over strength ratio (O.S.R.). In fact, the behaviour factor is not an intrinsic property of the structure, but it is strictly related to the adopted seismic design code and the safety level assumed by designers. They analyzed many cases (3456 different cases), from which they have derived two possible values of the behaviour factor for light timber frame buildings. The first (4.5) for one-storey buildings and the second (3.3) for n-storey buildings.

Table 8.1: Design concept, Structural types and upper limit values of the behaviour factors for the three ductility classes.

Design concept and ductility class	q	Examples of structures
Low capacity to dissipate energy - DCL	1,5	Cantilevers; Beams; Arches with two or three pinned joints; Trusses joined with connectors.
Medium capacity to dissipate energy - DCM	2	Glued wall panels with glued diaphragms, connected with nails and bolts; Trusses with doweled and bolted joints; Mixed structures consisting of timber framing (resisting the horizontal forces) and non-load bearing infill.
	2,5	Hyperstatic portal frames with doweled and bolted joints (see 8.1.3(3)P).
High capacity to dissipate energy - DCH	3	Nailed wall panels with glued diaphragms, connected with nails and bolts; Trusses with nailed joints.
	4	Hyperstatic portal frames with doweled and bolted joints (see 8.1.3(3)P).
	5	Nailed wall panels with nailed diaphragms, connected with nails and bolts.

Fig. 1: Upper limit values of the behaviour factor (table 8.1 of [1])

Therefore, it can be noted that these values are different to upper limit values proposed in Eurocode 8 [1].

According to Fajfar [4], the behaviour factor is the product of q^* and the O.S.R.. The first contribution q^* , takes into account the energy dissipation capacity of the structure, it is defined as the ratio of elastic strength demand to inelastic strength demand, while the second contribution O.S.R. is the overstrength factor, defined as the ratio of the actual strength F_y to the design strength F_{el} .

$$q = q^* \cdot O.S.R. \tag{1}$$

q^* depends on the ductility of the structure. An excellent overview about the ductility factor q^* is reported in Miranda et al. [5].

2.1 Evaluation of q-factor

The methods used to estimate the value of the q-factor can be divided (according to [6]) into two groups: experimental and numerical methods as reported in Fig. 2.

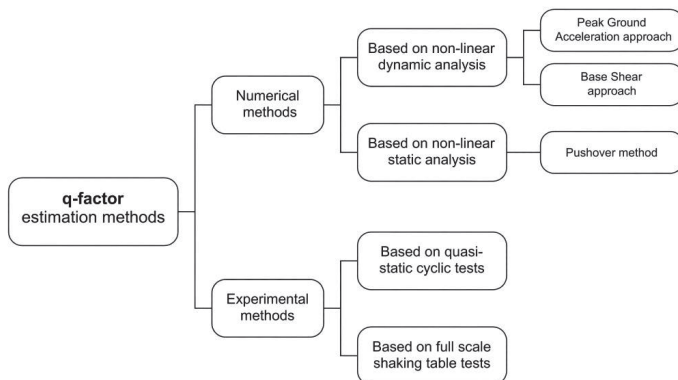


Fig. 2: Flowchart for behaviour factor evaluation [6].

The experimental methods are used to define the dynamic response of an entire timber construction and/or to define the hysteretic behaviour of single walls or single fasteners to use in the numerical analysis. Therefore, these methods can be subdivided into other two subgroups: those based on full-scale shaking tests and those based on quasi-static cyclic tests.

The evaluation of the q-factor by using the method based on full-scale shaking tests is very thorough, because it considers all the parameters that influence the structural system. However, this approach has some disadvantages that limit its use. The q-factor values are dependent on the earthquakes and on the Standards used to design the tested building. Therefore, the established value of behavior factor is only valid for buildings which are in the same conditions of tested structure. Furthermore, these types of test are very costly and time-consuming.

To reduce the test cost, experiments based on the quasi-static cyclic tests can be performed. Through these tests, the behavior factor q can be evaluated by referring to the static ductility concept (i.e. the ratio between the ultimate and the yield displacement). This method is applied on single walls and/or single fasteners in order to characterize the hysteretic behavior of the specimens. It is clear that the established value of q-factor is referred to the single tested element and therefore, to extend the

results to the entire building a numerical method (non-linear static analysis or non-linear dynamic analysis) should be applied.

The evaluation of the q-factor by means of quasi-static tests offers some cost and time benefits, but also some disadvantages. Indeed, a CLT structures does not present a well-defined yield point, and so the behaviour factor is dependent on the methods used to define it. Furthermore, in order to assign a realistic q-factor value extensive tests that take into account different geometry, mechanical properties, different masses and earthquakes should be done.

The methods that allow to perform a considerable number of tests are the numerical one. These tests can be divided in *Non-linear Dynamic Analysis* and *Non-linear Static Analysis*. The evaluation of the q-factor by means of Non-Linear Dynamic Analysis appears to be the most correct numerical method for timber buildings. With this method it is possible to define the global building response and the local response of each fastener and timber element. After the dynamic building response has been derived, two approaches can be used to evaluate the value of q-factor. The first one is based on a Peak Ground Acceleration (PGA) approach while the second one on a Base Shear approach.

The NLDAnalysis is the subtlest, but it is not so easy to apply. Therefore, in order to analyze a large set of cases, the Non-linear Static Analysis (NLSA) can be adopted. This analysis is commonly namely pushover method. This type of analysis allows to define the load-displacement curve of the buildings and so the ductility. In fact, once the curve is obtained it is possible to perform its bi-linearization and evaluate the global ductility of the building.

To evaluate the ductility factor q^* , two methods are used commonly: the first one is known as N2-method, developed by Fajfar [5], while the second one is known as Newmark method.

In the first method the q^* factor depends firstly on the ductility of the structure, but it takes into account the elastic period of the structure and the ground type. Fajfar provides two different equations with respect to the fundamental period of the structure:

$$\begin{cases} q^* = (\mu - 1) \cdot \frac{T}{T_0} + 1 & \text{if } T < T_0 \\ q^* = \mu & \text{if } T \geq T_0 \end{cases} \quad (2)$$

In the previous equations μ is the ductility of the system defined as the ratio between the maximum displacement and the yielding displacement (see Fig. 3), T is the principal elastic period of the structure and T_0 is the transition period which the constant acceleration part of the response spectrum transforms to the constant velocity portion of spectrum. Generally, the transition period T_0 is assumed equal to T_c . To obtain the principal elastic period T of a structure (represented as M-DOF system) the system must be reduced into an idealized S-DOF system and then the period can be written as:

$$T = 2\pi \sqrt{\frac{m \cdot d_y}{F_y}} \quad (3)$$

Where F_y/d_y is the elastic stiffness of the S-DOF and m is the mass of the idealized system.

The second one, known as Newmark method, has the advantage to not correlate the q^* -factor with the dynamic properties of the structure. The q^* value can be evaluated by the following Eq.(4):

$$q^* = \sqrt{(2\mu - 1)} \quad (4)$$

The Newmark method is less accurate than the Fajfar method, because the values provided by it seem to be extremely conservative, therefore it is suggested to evaluate the ductility factor q^* with the N2-method.

The overstrength factor (O.S.R.) may be defined as the ratio of the actual strength F_y to the elastic design strength F_{el} , according to the following Eq.(5)

$$O.S.R. = \frac{F_y}{F_{el}} \quad (5)$$

Fig. 3 shows the parameters for the definition of the behaviour factor.

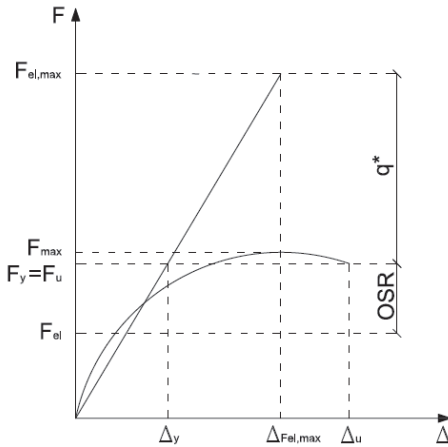


Fig. 3: Parameters for the definition of the behaviour factor.

3. State of the art

In this section, an overview on the researches carried out on the behaviour factor are reported. In addition, a proposal for revision of the current European Standard is presented.

3.1 Research on behaviour factor to use in the design of CLT buildings

Ceccotti & Follesa.[7] presents some results from shaking table tests on full-scale 3 storied XLam building. The test was conducted at the NIED Tsukuba Shaking Table facility in June and July of 2006. The building is square with sides about 7 m and has a height of 10 m (three-storey). The CLT panels used to build the structure were produced in Val di Fiemme, Trentino in North-East of Italy, with spruce wood. The walls present different opening at each floor, at the ground floor the door opening widths varies between 1.2 m to 4.0 m.

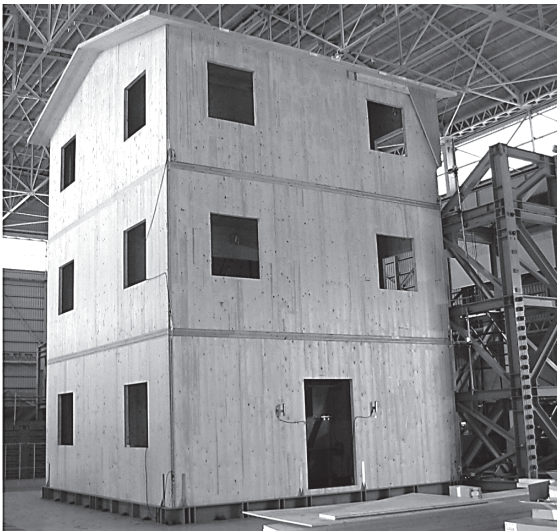


Fig. 4: Three-storey, SOFIE project, taken by [7].

The walls are connected to the steel base using commercial hold-down anchors placed at the end of the wall and in correspondence of the openings and angle brackets placed along the walls. The connections between walls at different level are made by the same systems. The design of the building was made following the rules proposed in the Eurocode 8, in such a way to over-design the horizontal connection (angle brackets) compared to the vertical connection (hold-down). Each building was subjected to three different earthquakes (Kobe, EL Centro and Nocera Umbra) at two growing levels of PGA (0.15g and 0.50g). During the tests the dynamic parameters have been measured to evaluate the behaviour of the structure. The tests results show that the buildings have resisted at the destructive levels of earthquake without undergo several damages. With the measurements performed during the tests subjected to Nocera Umbra earthquake, a value of the behavior factor was estimated.

The value of the behaviour factor in evaluate trough the following equation:

$$q = \frac{PGA_u}{PGA_y} \quad (1)$$

where PGA_u is the peak acceleration that produce the ultimate displacement or rotation and the PGA_y is the acceleration that produce the yielding of the first joint. For this particular case, q is equal to

$$q = 3.4 \quad (2)$$

Furthermore, the authors highlight the importance of using a good mathematical model in order to evaluate the q -factor for different earthquakes and cases.

In Ceccotti et al. [8] the minimum value of the q -factor obtained from the results of the shaking table reported in [7] is estimate. They explain the different methods to determine the q value from the test results and from the mathematical model. In particular, the procedure to estimate the behaviour factor from the test results for a particular building and for a particular ground motion record is:

- Define an appropriate “near collapse” criterion (for example based on a maximum inter-storey drift, or a failure in joints or in timber elements);
- Design the structure using $q=1$ according to the seismic code for a given design PGA (which in this case is both the PGA leading the building to collapse and the PGA which cause the first yielding), and the resistant system according to the relevant codes (seismic and “static” codes) with the design values for seismic actions;
- Analyze the test results and apply the definition of q founding it by the ratio between the PGA value that caused the “real” collapse of the building and the design value of the PGA.

Instead the procedure to estimate the q value from a mathematical calculation (using a non-linear analysis) is:

- Design the structure for a given q value, and the resistant system according to the relevant codes (seismic and “static” codes). At the end of this step the resistant system will be completely anticipated;
- Model the building mechanical behaviour on the base of its mechanical characteristics (obtained by tests, and scaled to 5% percentile based on COV and test mean value, using additional safety coefficients eventually provided by the code for the earthquake load combination);
- Using a suitable non-linear analysis programme capable of following the displacement history of the building under a quake in the time domain (calibrated on the results of shaking table tests), determine the PGA_u that the building will survive without exceeding a given “near collapse” failure limit (for example based on a maximum inter-storey drift, or a rupture in joints or in timber elements);
- Compare this PGA_u against PGA_{code} prescribed by the code.

- Finally, if $PGA_u > PGA_{code}$ the previously chosen design q value is adequate;
- This procedure must be repeated for a series of earthquakes suitable for the design site, in order to have a global picture according to different possible inputs.

Based on the shaking table test results, the authors use the first method, presented above, to determine the minimum value of q for this type of building. They observed that for all tests carried out with a PGA_u equal to $0.50g$, the uplift force in the hold-down was less than the strength design value. Therefore, assuming a PGA_y value equal to $0.35g$ the minimum value of the behaviour factor for this particular building is

$$q = 1.43 \quad (3)$$

Another paper edited by Ceccotti et al., that use test results on a shaking table to evaluate the q factor, is the [9]. This paper provides, in addition of the results of the three-storey building showed in [8] and [9], the results of a seven-storey building tested on the 3D shaking table using all three earthquake components.

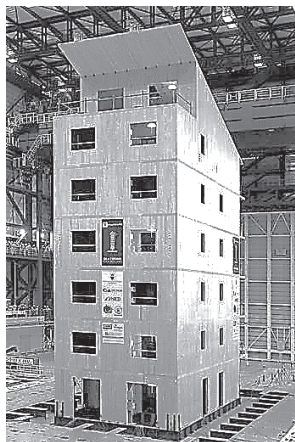


Fig. 5: Seven-storey building, SOFIE project

From analysis of the three-storey building, a behavior factor q equal to 3.4 was determined. Therefore, to design the seven-storey building a behavior factor of $q=3$ was assumed. In addition to this the authors have designed the building with an importance factor $\gamma_I=1.5$ in such a way to consider the building as completely operational even after a destructive quake. The results show that the seven-storey structure has not reached the collapse state and no residual displacement was measured at the final tests. For these reasons, the CLT buildings can be considered as a well performing construction in earthquake zone, while as regards the behaviour factor it was shown that a value of 3 may be considered acceptable for these constructions.

Fragiacomo et al. [10] present a paper in which emphasizes the importance of design parameters. In particular, the importance of the over-strength factor to use in the design phase when the capacity design is adopted. In fact the over-strength factor is another value that is not mentioned in the European code [1]. Some indications can be found in the New Zealand timber standard, where a value of 2 is suggested for the over-strength factor. They carried out linear and non-linear analysis in order to evaluate the overstrength of connections (i.e. hold-down connection, angle brackets connection and panel-to-panel connection). The authors propose a value of 1.3 for shear and uplift based on some preliminary tests. In addition, simple detail rules on the nail length which should not be shorter than 60 mm to avoid brittle failure of connections were provided. An overstrength ratio of 1.6 was derived for self-tapping screws holding together adjacent perpendicular walls.

Popovski et al. [11]–[13], present some results from a series of quasi-static test on CLT wall panels. The number of tests carried out was 32, on 12 configurations of CLT wall. The test results shown the good performance of the CLT walls subjected to horizontal forces. Furthermore, the authors estimated a set of R_d factor and R_0 factor to be used for CLT structures. The values proposed by the authors are more conservative than the value obtained from other ones, in fact they suggest to take a behaviour factor equal to $R_d=2$ and an overstrength factor equal to $R_0=1.5$. If we compare these values with the q-factor, suggested for CLT in Europe, the product between R_d and R_0 must be performed. Thus, we obtain

$$R = R_d \cdot R_0 = 2 \cdot 1.5 = 3 \quad (4)$$

Pei et al. [14] studied the structural behaviour of a ten-storey CLT building with the objective to perform a performance-based seismic design and derive an appropriate strength reduction factor, (R-factor). Focusing on the second part of their work, they used nonlinear analysis to identify a suitable response factor to be used in the equivalent lateral force procedure. The determination of the behaviour factor was performed by means of an incremental analysis, in fact the R-factor was changed manually until the final resistance distribution matched the target resistance. The authors state that, based on the results of analysis, a value of $R=4.3$ can be chosen for the analyzed building and similar CLT building. However, they said that a significantly variation of the R value may exist if different boundary condition change (i.e. different fasteners are used in the brackets and the hold-downs, numbers of storey, ecc.). The R-factor is the product between R_d factor and R_0 factor, therefore this value is a combination of the behaviour factor and the over-strength factor.

Pozza et al. [15], [16] present a series of test on three massive wooden shear-wall system (e.g. Cross Laminated Glued wall, Fig. 6, Cross Laminated Stapled panels, and Layered panels with dovetail inserts, Fig. 7), with the aim to characterize the structures in terms of strength, stiffness, ductility and hysteresis behaviour.

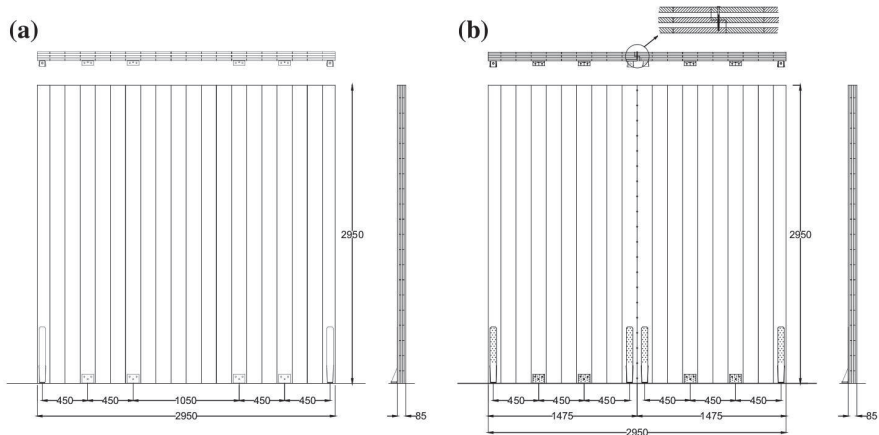


Fig. 6: Glued walls, a) Un-jointed CLT wall, b) Jointed CLT wall, taken from [16].

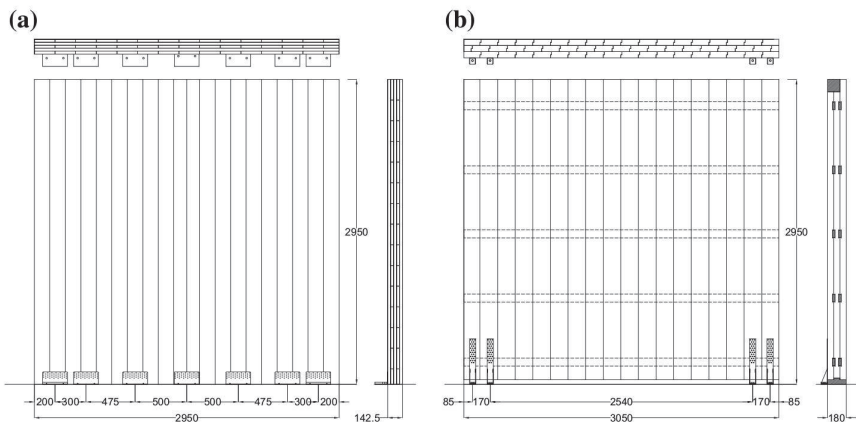


Fig. 7: Non-glued walls, a) Stapled wall, b) Layered wall, taken from [17].

In addition, main steps of numerical modelling are described in order to evaluate the dissipative capacity and to estimate a suitable intrinsic q -factor. The numerical analysis (linear static analysis and non-linear dynamic analysis) was carried out to determine the parameters (PGA_y and PGA_w) to evaluate the q -factor. The value of the behaviour factor was estimated through the equation (1). They have obtained a value equal to $q=2.55$ due to the un-jointed CLT panel, a value of $q=3.16$ for the CLT jointed panels, $q=4.74$ for the Stapled panel and $q=4.64$ for the Layered panel. The high value for Stapled and Layered panels, if compared with CLT walls, is due not only to higher dissipative capacity, but also to the hardening behaviour of those two panels. It must be noted that the values obtained for the Stapled and Layered wall are more widespread than the values obtained for the CLT walls. According to results, the authors propose a q -factor in the range of 2 and 3 for the CLT structures, while a

q-factor value in the range of 3 and 4 for structure that use the Stapled and Layered walls.

Stojmanovska [17] presents a paper in which she summarizes the results of the experimental and analytical research of CLT wall panel systems subjected to seismic excitation. The experimental tests refer to two full-scale CLT systems, see Fig. 8.

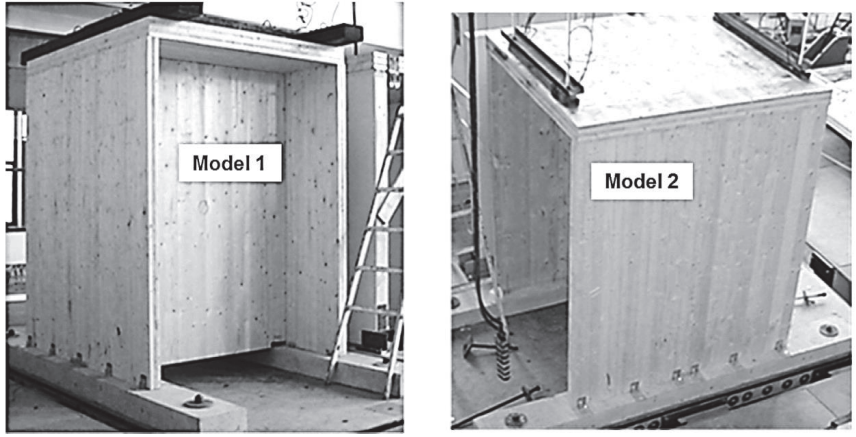


Fig. 8: Test specimens, taken by [17].

The first consisted in two walls jointed by an horizontal CLT panel which simulates the slab floor (model 1 of Fig. 8). The second have the same schema but the vertical wall are composed of two elements jointed together by screws (model 2 of Fig. 8). After the experimental tests an analytical part was carried out. In this part numerical analysis (non-linear static and dynamic analysis) have been performed. The earthquake excitation used in these analyses was the same at the one used in the experimental tests. To evaluate the behaviour factor only the ductility of the system (μ) has been taken into account. Thus, the equation used to estimate the q-factor is:

$$q = \sqrt{2\mu - 1} \quad (5)$$

To determine the failure point and the yielding point from the hysteretic diagrams, in order to obtain the ductility μ of the system, Elastic-Plastic Equivalent Energy model (EPEE) has been applied. The value obtained is in the range between 2.21 and 3.98. The author mentions that if the over-strength is taken into account the above values would be higher than the value of the behaviour factor $q=2$ proposed in the Eurocode 8.

Pozza and Trutalli present a paper [18] in which a parametric study on a several CLT buildings was carried out in order to define the effects of their geometrical and construction features in the seismic response. The results of this study were used to define some proposals correlation between the behavior factor q and the parameters that describe the structure. They studied 24 building configurations with different

geometrical features (i.e. base dimension, number of storey ecc.). The results, obtained from a parametric nonlinear dynamic analysis, were used to propose an analytical formulation to evaluate the behaviour factor based on panel-to-panel joints and walls size. The authors also present a paper [19] in which the in-elevation irregularity in the CLT building is taken into account. The method used to analyze the buildings is the same as that just presented. The results were used to extend the correlation method proposed in [18] to the in-elevation irregular CLT buildings.

3.2 Proposal of revision of Eurocode 8 Part 1

Extensive research on CLT buildings have been carried out at to specify values of behavior factor q for this type of construction system. However, in the current version of Eurocode 8, only a unique value equal to 2 is proposed for regular buildings realized with *glued wall panels with glued diaphragms, connected with nails and bolts*. Therefore, some authors [20], [21], presented a proposal for the revision of Chapter 8 of Eurocode 8. They explained that, based on the capacity design criteria and suitable design rules, the buildings in seismic areas can be subdivided into two class (*Fig. 9*). The first class (DCM) includes the CLT structures that are built with *walls composed of a unique element without joints*, while the second class (DCH) includes the CLT structures that are built with *walls composed of several panels connected with vertical joints made with mechanical fasteners (nails or screws)*.

Table 8.1(New): Design concept, structural types and upper limit values of the behaviour factors for the three ductility classes.

Design concept and ductility class	q	Examples of structures
Low capacity to dissipate energy - DCL	1.5	Vertical cantilever walls. Beams and horizontal cantilevers. Arches with two or three pinned joints. Trusses joined with connectors (e.g. toothed metal plates). Moment resisting frames with glued joints
Medium capacity to dissipate energy - DCM	2.0	Cross laminated buildings with walls composed of a unique element without vertical joints. Log House Buildings. Trusses with screwed, doweled and bolted joints. Mixed structures consisting of timber framing (resisting the horizontal forces) and non-load bearing infill.
	2.5	Moment resisting frames with dowel-type fastener joints
High capacity to dissipate energy - DCH	3.0	Cross laminated buildings with walls composed of several panels connected with vertical joints made with mechanical fasteners (nails or screws) [6]. Trusses with nailed joints.
	4.0	Moment resisting frames with high ductility joints (e.g. densified veneer wood reinforced joints with expanded tube fasteners) [9]
	5.0	Light-frame buildings with nailed walls.

Fig. 9: Proposal of new table 8.1 of EC8, taken from [20], [21].

As can be seen from Fig. 9, CLT buildings shall be included in DCM class (with $q=2$) if the building walls are composed of a unique element without vertical joint, while shall be included in DCH class (with $q=3$) if the building walls are composed of several panels connected with vertical joints made with mechanical fasteners (nails or screws). If the capacity design criteria and the design rules are not respected the upper limits of the behaviour factor are reduced to the values shown in Fig. 10.

Table 8.2 (New): Structural types and reduced upper limits of behaviour factors

Structural types	Behaviour factor q
Cross laminated buildings with walls composed of a unique element without vertical joints.	1.5
Trusses with screwed, doweled and bolted joints.	1.5
Mixed structures consisting of timber framing and non-load bearing infill.	1.5
Cross laminated buildings with walls composed of several panels connected with vertical joints made with mechanical fasteners (nails or screws).	2.0
Moment resisting frames with dowel-type fastener joints	2.0
Trusses with nailed joints.	2.0
Light-frame buildings.	3.0

Fig. 10: Proposal of new table 8.1 of EC8, taken by [20], [21].

4. Conclusion and Outlook

This paper deals with CLT buildings subjected to seismic excitation. In detail, the researches carried out to realize new proposals of the behaviour factor to use in the design of CLT buildings, are presented. From the papers summarized above, it is clear that structures made by CLT panels provide good abilities to withstand earthquakes, without incurring serious damage. This, thanks to high ductility and ability to dissipate seismic energy. However, it must be highlighted that the ductility is not an intrinsic property of the structure, but it is dependent on the design and construction rules.

The following table, Tab 1, summarize the values of the behaviour factor q related to researches presented in Chapter 3.

Reference	q-factor value	Focus of research
Ceccotti et al. [7]	$q=3.4$	The value was obtained from shaking table test of full-scale three-storey CLT building
Caccotti et al. [8]	$q=1.43$	It is the minimum vale of q-factor obtained from shaking table test of full-scale three-storey CLT building
Caccotti et al. [9]	$q=3.0$	The value was obtained from shaking table test of full-scale seven-storey CLT building

Popovski et al. [11]–[13]	R=3.0	The authors suggest to take a ductility factor equal to $R_d=2$ and a overstrength factor equal to $R_0=1.5$. These values are referred to 32 tests, on 12 configurations of CLT walls
Pei et al. [14]	R=4.3	The value was obtained from the numerical analysis of a ten-storey building
Pozza et al. [15], [16]	q=2.0-3.0	For a structure made with glued CLT walls
	q=3.0-4.0	For a structure made with Stapled or Layared walls
Stojmanovska [17]	q=2.2-3.9	These values were obtained from experimental and numerical analysis
Follesa [20], [21]	q=2.0	For a CLT buildings with walls composed of a unique element without joints
	q=3.0	For CLT buildings with walls composed of several panels connected with vertical joints
	q=1.5	For CLT buildings in which the capacity design criteria and the design rules are not respected

Tab 1: Summary of the q-factor values.

The values of the q-factor reported in Tab 1 (referring to [7]–[17]) were derived from specific experimental tests and numerical analysis, therefore the values obtained refer only to a limited number of cases. For this reason, it is essential to continue research in the field of behaviour factor, in order to have a greater number of samples, and then propose a suitable value of the q-factor for CLT buildings.

Another thing to note is that the value of the q-factor (on average, $q=3$) obtained in above researches is generally higher than the value $q=2$ present in the European Standard EC8. It is therefore important that other studies are conducted to identify the parameters that influence the behaviour of the structure, as for example the number of storeys, the overstrength of connections, the number of jointed panels to form a shear wall and the building details, for providing a comprehensive document on CLT buildings.

5. References

- [1] “EN 1998-1:2013, Eurocode 8: Design of structures for earthquake resistance part 1: General rules, seismic actions and rules for buildings, 2013. Brussels, Belgium: CEN, European Committee for Standardization.” 2013.
- [2] A. Chopra, “Dynamics of Structures—Theory and Applications to Earthquake Engineering, Third Edition,” *Earthquake Spectra*, vol. 23, no. 2.

- pp. 491–492, 2007.
- [3] S. Rossi, “Seismic Behaviour and Ductility Evaluation of multi-storey Light timber-frame Buildings by Means of analytical Formulations and numerical Modelling,,” Doctoral dissertation University of Trento, 2015.
 - [4] P. Fajfar, “Design spectra for the new generation of codes,” in *Proceeding 11th World Conference on Earthquake Engineering, Acapulco, Mexico*, 1996.
 - [5] E. Miranda and V. V Bertero, “Evaluation of strength reduction factors for earthquake-resistant design,” *Earthq. spectra*, vol. 10, no. 2, pp. 357–379, 1994.
 - [6] L. Pozza, “Ductility and behaviour factor of wood structural systems,” Doctoral dissertation University of Padova, 2012.
 - [7] A. Ceccotti and M. Follesa, “Seismic Behaviour of Multi-Storey XLam Buildings,” *COST E29 Int. Work. Earthq. Eng. Timber Struct.*, no. January, pp. 81–95, 2006.
 - [8] A. Ceccotti *et al.*, “Which seismic behaviour factor for multi-storey buildings made of cross-laminated wooden panels,” *Proc. 39th CIB W18 Meet. Pap.*, no. 39–15, 2006.
 - [9] A. Ceccotti, C. Sandhaas, and M. Yasumura, “Seismic behaviour of multistory cross-laminated timber buildings,” *Proc. Int. Conv. Soc. Wood Sci. Technol. United Nations Econ. Commission Eur. - Timber Comm.*, no. July, pp. 1–14, 2010.
 - [10] M. Fragiaco, B. Dujic, and I. Sustersic, “Elastic and ductile design of multi-storey crosslam massive wooden buildings under seismic actions,” *Eng. Struct.*, vol. 33, no. 11, pp. 3043–3053, 2011.
 - [11] M. Popovski, S. Pei, J. W. van de Lindt, and E. Karacabeyli, “Force Modification Factors for CLT Structures for NBCC,” in *Materials and Joints in Timber Structures: Recent Developments of Technology*, S. Aicher, H.-W. Reinhardt, and H. Garrecht, Eds. Dordrecht: Springer Netherlands, 2014, pp. 543–553.
 - [12] M. Popovski and E. Karacabeyli, “Seismic Performance of Cross-Laminated Wood Panels,” 44th CIB-W18 Meeting, Alghero, Italy, Paper 44-15-7, August, 2011.
 - [13] M. Popovski and E. Karacabeyli, “Seismic behaviour of cross-laminated timber structures,” *World Conf. Timber Eng. 2012, WCTE 2012*, vol. 2, pp. 335–344, 2012.
 - [14] S. Pei, M. Popovski, and J. W. Van De Lindt, “Seismic design of a multi-story cross laminated timber building based on component level testing,” *World Conf. Timber Eng. 2012, WCTE 2012*, vol. 2, no. April 2016, pp. 244–252, 2012.
 - [15] L. Pozza, R. Scotta, D. Trutalli, M. Pinna, A. Polastri, and P. Bertoni, “Experimental and Numerical Analyses of New Massive Wooden Shear-Wall Systems,” *Buildings*, vol. 4, no. 3, pp. 355–374, 2014.
 - [16] L. Pozza, R. Scotta, D. Trutalli, and A. Polastri, “Behaviour factor for innovative massive timber shear walls,” *Bull. Earthq. Eng.*, vol. 13, no. 11,

- pp. 3449–3469, 2015.
- [17] M. Stojmanovska, “Experimental and analytical research of xlam structural systems,” *COST FP1402 5th Work. Zagreb*, no. March, pp. 1–9, 2017.
 - [18] L. Pozza and D. Trutalli, “An analytical formulation of q-factor for mid-rise CLT buildings based on parametric numerical analyses,” *Bull. Earthq. Eng.*, vol. 15, no. 5, 2017.
 - [19] D. Trutalli and L. Pozza, “Seismic design of floor–wall joints of multi-storey CLT buildings to comply with regularity in elevation,” *Bull. Earthq. Eng.*, pp. 1–19, 2017.
 - [20] M. Follesa, M. Fragiaco, D. Casagrande, M. Piazza, D. Vassallo, and S. Rossi, “The new version of Chapter 8 of Eurocode 8,” World Conference on Timber Engineering, WCTE 2016. Vienna University of Technology, 2016.
 - [21] M: Follesa, M. Fragiaco, D. Vassallo, M. Piazza, R. Tomasi, S. Rossi, and D. Casagrande, "A proposal for a new Background Document of Chapter 8 of Eurocode 8". In INTER 2nd meeting. Karlsruher Institut für Technologie, 2015.

Definition of the most suitable value of the q-factor for XLam structural systems

Marta Stojmanovska,
Assistant Professor
UKIM-IZIIS,
Skopje, Macedonia

Summary

The primary idea of the presented research was to obtain results and findings that will contribute towards improvement of the existing standards for building seismic resistant structures in terms of adding certain information on cross laminated timber structural systems, which are more and more applied in the European construction practice, but for which there are currently no technical regulations for designing and building.

1. Introduction

The main objective of the preformed study is to understand more precisely how XLAM structural systems behave under earthquake events by conducting, first comprehensive experimental testing that includes dynamic tests on full-scale XLAM models, then developing 2D computational models that predict the dynamic response of XLAM structures with relatively good accuracy and finally by evaluation of q value for the investigated systems [1]. Model 1 consisted of one unit wall elements 244/272/9.4cm and Model 2 consisted of two wall elements assembled by screwing together two basic units of 122 cm length (Figure 1).

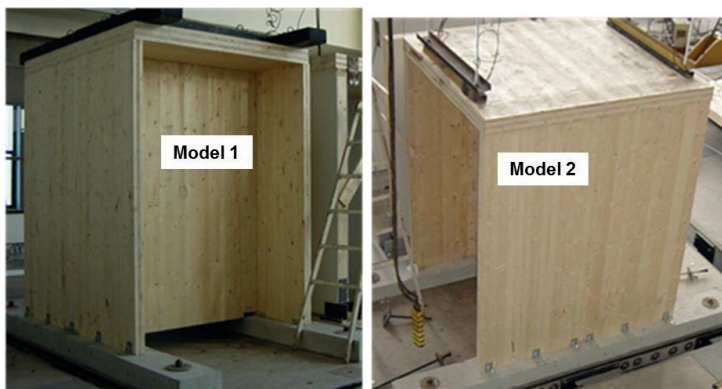


Figure 1. Tested XLam Models

2. Procedure for definition of the most suitable value of q

The final part of the research comes from the fact that although cross-laminated structural systems become very popular on the market, existing standards for designing earthquake resistant timber constructions are very poor and do not provide any recommendations and guidelines, especially with regard to the behaviour factor q . In fact, the technical regulations relating to the design of earthquake-resistant constructions are based on the assumption that a larger number of constructions will withstand plastic deformations under the influence of relatively strong earthquakes, and seismic forces are much smaller than the forces generated in constructions when they preform elastically. In order to avoid nonlinear analysis when designing a structure, undertaking into account their nonlinear response, that is the energy dissipation capacity through the ductile behaviour of their elements, a linear elastic analysis is carried out. This is based on a response spectrum reduced in relation to the elastic response spectrum by introducing the so-called reduction factor or behaviour factor q . Consequently, the behaviour factors q actually expresses the ability of the structure to dissipate energy and withstand large deformations without catastrophic damages.

In this investigation, the developed and experimentally verified numerical models were used to implement dynamic nonlinear analysis. For models' formulation, finite-element approach was followed, treating the system as a continuum (the wooden panels) with discontinuities (anchor links and contact zones). Anchor links and contact zones have been modelled by using the standard link element with zero length, consisting of two points, each having two degrees of freedom-translations in the horizontal and vertical directions (Figure 2).

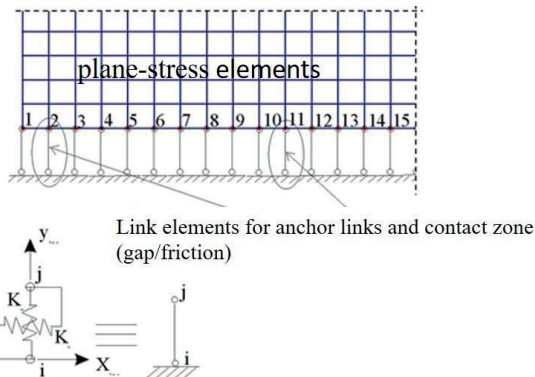


Figure 2. 2D Model with final elements, continuum with discontinuities

Standard boundary conditions have been applied: free translation without rotation was allowed for all nodal points except for the bottom nodal points of the contact

between the panel and the foundations, for which the translations and the rotation have been restrained.

The analyses were carried out with the FELISA / 3M software package, developed in IZIIS, for the same earthquake motions that were applied in performing experimental tests. However, they were scaled to reach the limit state of the system, and as a result, the corresponding hysteresis force-displacement diagrams were obtained. Figure 3 and Figure 4 show the analytically obtained hysteresis force-displacement diagrams for Model 1 and Model 2, corresponding, for selected earthquake motions.

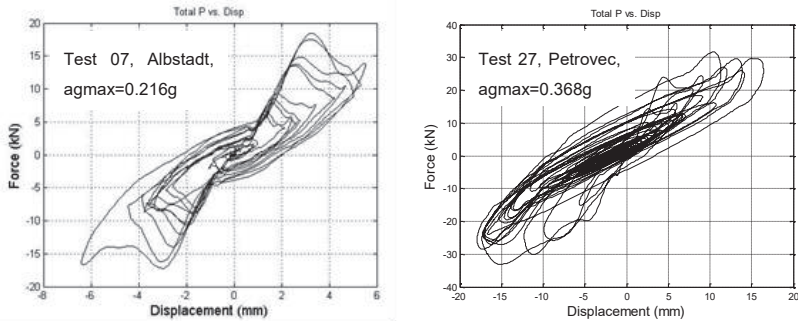


Figure 3. Force – displacement diagrams Model 1

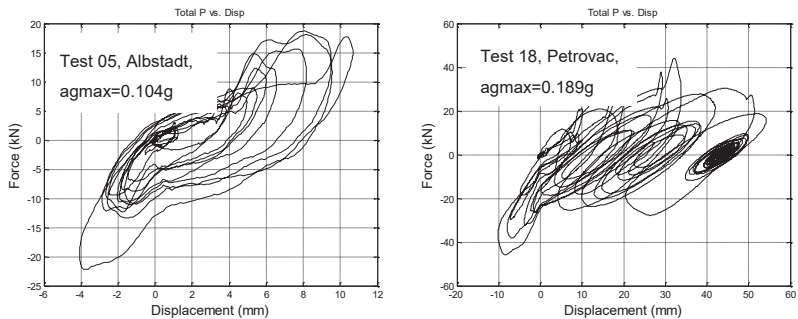


Figure 4. Force – displacement diagrams Model 2

In order to simplify the entire procedure, we determine the behaviour factor only in terms of ductility. Since the natural frequencies of the considered construction systems is less than 0.5s, we apply the following formula

$$R_{\mu} = \sqrt{2\mu - 1} \quad \text{кога} \quad 0.12s < T < 0.5s \quad (1)$$

Ductility μ represents the ratio between the displacement that corresponds to the maximum force that is failure Δ_{\max} , and the displacement that corresponds to the yielding point Δ_y .

For the interpretation of the obtained hysteretic diagrams and determination of the ductility that is the failure point and the yielding point, Δ_{max} and Δ_y , an Elastic-Plastic Equivalent Energy model or EEEP model has been applied (Figure 5).

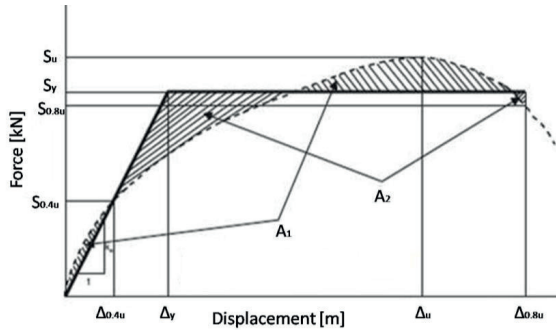


Figure 5. EEEP Model

The EEEP model simplifies the obtained force-displacement curve via a bi-linear model curve that demonstrates linear-elastic behavior of the system up to yielding point and is perfectly plastic up to failure. The obtained values of q for this specific construction system were between 2.21 and 3.98. Taking the overstrength factor into consideration these numbers would be significantly higher than the value of the behavior factor $q=2$ stated as recommendation in the Eurocode 8. This leads to the clear conclusion that constructions made of cross laminated timber, if designed and built properly have high ductility and ability to dissipate seismic energy from earthquakes with high intensities.

3. Discussion

The value of the behavior factor $q = 2$, which is a recommendation in the current version of Eurocode 8, and refers to glued timber elements, does not correspond to the actual capacity for energy dissipation by these systems. The results of the analyzes indicated a value of q greater than 3.

Previous research related to the behavior of structures under earthquake actions has shown that the overstrength factor plays a very important role in the protection of structures against collapse. Therefore taking the overstrength factor into account when defining the behavior factor leads to more realistic and more reliable values.

4. References

- [1] Stojmanovska, M., “Experimental and Numerical Research of Dynamic Response of Wooden Structures Assembled from Cross Laminated Wooden Panels”, Institute of Earthquake Engineering and Engineering Seismology (UKIM-IZIIS), Doctoral Thesis, June, 2015

Assessment of the over-strength factor for CLT structures: a state-of-the-art review

Roberto Tomasi

Professor

NMBU – Norwegian University of Life Science

Ås, Norway

Dag Pasca

PhD student

NMBU – Norwegian University of Life Science

Ås, Norway

Mariano Fiorencis

MsC student

Università degli studi di Trento

Trento, Italy

Summary

The fact that a structure must be able to dissipate energy during a seismic event is a well understood fact today. The adoption of Capacity Design (CD) principles helps engineers to design structures that comply with this requirement. One fundamental aspect of CD principles is that ductile failure mechanisms shall take place before brittle failure mechanisms. This is ensured by designing the elements that are considered non-dissipative with respect not to the external loading, but to the strength capacity of the dissipative elements multiplied with an overstrength factor. Unfortunately, this very important piece of information is missing in the current version of the Section 8 of Eurocode 8.

The goal of this paper is to present a state-of-the-art review on the methods used in the last years to assess this coefficient for timber structures, with particular attention to buildings made of CLT panels. In the first part an introduction on the concept of overstrength is presented, then a brief background on the current regulatory framework adopted in different parts of the world. The third, and main, chapter reports on the review of several relevant scientific articles that treat the assessment of the overstrength factor for timber buildings. Finally, in the last part some suggestions on how to apply Capacity Design principles are given.

1. Introduction

The overstrength is commonly defined as the difference between the design resistance of a material/component/structure, calculated using characteristic values, and the 95th percentile of the strength distribution observed from tests. In the framework of structural engineering this difference has, in most cases, a positive

meaning since it is indicative of a reserve of strength, not taken into account at the stage of design, that further decreases the failure probability. In seismic engineering, or in case of other accidental actions, the overstrength of some element of the structure may lead to negative outcomes. In this context and aiming for an effective and efficient design, a specific hierarchy of resistances of the structural components have to be fulfilled. It is easy to understand that an unexpected overstrength of some parts may undermine this hierarchy.

The behaviour of a building under high intensity accidental loads, such as in the event of an earthquake with high return period, should take place in the post-elastic range in order to assure a cost-effective design. In doing so, a significant energy dissipation is guaranteed due to the cyclic deformations in the plastic range of some components and, at the same time, a decrease of seismic demand is secured because of the reduction of structural stiffness and the consequent increase in its fundamental period of vibration. A necessary condition for this effective post-elastic behaviour is that the structure has sufficient ductility and it is able to withstand the large displacements required.

Consequently, every kind of brittle failure mode that could take place before the complete yielding of the most ductile and dissipative components shall be avoided.

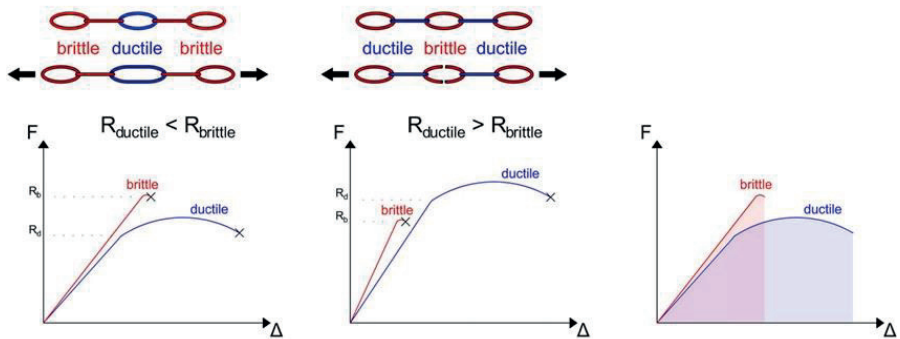


Figure 1: Ductile chain and Capacity Design concept.

Such an approach is called Capacity Design [1] and it aims to ensure the occurrence of the chosen global ductile failure mechanism by avoiding local and global brittle failure mechanisms. The elements susceptible to brittle and non-dissipative failure modes must then show an overstrength with respect to the most ductile elements according to Eq. (1):

$$F_{b,Rd} = \gamma_{Rd} \cdot F_{d,Rd} \tag{1}$$

where $F_{b,Rd}$ and $F_{d,Rd}$ stand for the design resistance of the brittle and the ductile component, respectively, whereas γ_{Rd} is the overstrength factor.

This factor takes into account the variability of the effective resistance of the ductile part with reference to the nominal/design strength. This variability may result in an

unexpected overstrength of the ductile member that could lead to the failure of the brittle components and to a low dissipative behaviour.

The mathematical definition for the factor γ_{Rd} is not univocally established yet and may result from different approaches. If data are available from experimental tests, the overstrength factor is usually calculated as the ratio between the value of the experimental achieved strength (95th percentile) and the design strength.

On the other hand, other methods are based on a probabilistic approach conducted with Monte Carlo simulations. Starting from the statistical distributions of the fundamental properties of the resisting elements, a deterministic analytical model is applied to randomly picked values from these distributions. The procedure is then repeated until a sufficiently regular distribution of results is achieved.

2. Regulatory framework

Eurocode 8 [2] is the reference standard in Europe for the design of seismic resistant structures, and Section 8 deals with the specific rules for timber structures. In the current version this chapter cannot be considered exhaustive due to several reasons. Among them, the code does not treat buildings made of CLT, and this could lead to confusion in the choice of the relevant behaviour factor. Furthermore, despite the standard embracing the capacity design principle and stating (§8.6 (4)P) that non-dissipative zones shall be designed with sufficient over-strength, it fails to provide any values that quantify this over-strength, making de facto the Capacity Design approach not applicable to any kind of timber structure not only the ones made with CLT.

In the context of harmonized European standards, SIA (Swiss Society of Engineers and Architects) has published a new generation of structural standards based on the Eurocodes. The current Swiss code for timber structures [3] deals with the design for seismic loads at §4.6. Although neither the swiss code deals with constructions made of CLT, it gives an indication, for other timber structures, on the overstrength that the non-dissipative zones shall be designed for. Specifically stating at point 4.6.3.1 that the brittle elements shall be oversized by 20 % ($\gamma_{Rd} = 1.2$) with respects to the ductile zones.

If we move outside of Europe, New Zealand has always been a reference point for earthquake engineering, being the place where Capacity Design principles were invented [1]. Although CLT arrived in the region later than in Europe, it is quickly gaining popularity within the engineering community. This delay had though, as consequence that New Zealand too lacks a set of specific rules for the seismic design of CLT structures. With regard to other types of timber constructions the Timber Structures Standard [4] at C4.2.2 states: “The average ultimate strength of nailed connections in single shear is approximately 1.6 times the characteristic strength given in table 4.3. Hence for capacity design, an overstrength factor of $1.6/\phi = 2.0$ should be used”. It should be noted though that resistance values for nailed connections are not derived adopting the European Yield model but given in the standard in the form of tables.

Canada is the only nation so far to have directly implemented criteria for the design of CLT structures in the national timber standard [5]. The code deals with specific verification rules for CLT walls/slabs in Clause 8 and with seismic design consideration for CLT structures in Clause 11.9. With regard to overstrength factor it is stated that non-dissipative connections and CLT panels shall be designed for forces that are induced in them when the energy dissipative connections reach the 95th percentile of their ultimate resistance, with the limitation that the design force need not exceed the force determined using a behaviour factor of 1.3 ($R_d \cdot R_o = 1.3$).

In Europe as a result of the growing interest for engineered wooden products several researches were carried out in the last decade. These confirm the effectiveness of timber as a construction material in seismic prone areas. The draft of the new Section 8 for EC 8 is under development [6]. One of the new features of the draft is the introduction of CLT and an improved description of the different commonly used structural types. With regard to the overstrength factors two values are introduced: 1.3 for CLT buildings, light-frame buildings, and others and 1.6 for moment resisting frames (except for high ductility moment resisting frames with tube fasteners and Densified Veneer Wood), post and beam timber buildings, vertical cantilever systems made with glulam or CLT wall elements.

3. Overstrength factor for timber buildings

In the following, a literature review on the assessment of the overstrength factor for timber structures is presented.

A general overview on ductility and over-strength factors for timber structures can be found in [7]. In this paper the extensive results on the previous work of Jorissen [22] on doweled connections is used in order to evaluate the overstrength factor.

The overstrength ratio is defined by the authors as:

$$\gamma_{Rd} = \frac{R_{d,0.95}}{R_{d,0.05}} \cdot \frac{R_{d,0.05}}{R_{d,k}} \cdot \frac{R_{d,k}}{R_{d,d}} = \gamma_{sc} \cdot \gamma_{an} \cdot \gamma_M \quad (2)$$

where $R_{d,0.95}$ and $R_{d,0.05}$ are, respectively, the 95th and 5th percentile of the ductile component strength distribution; $R_{d,k}$ and $R_{d,d}$ are, respectively, the characteristic and the design values of the analytical prediction of the ductile element strength.

The coefficient $\gamma_{sc} = R_{d,0.95} / R_{d,0.05}$ expresses then the scatter of the experimental connection strength properties and, therefore, gives an indication on the reliability of the connection. The coefficient $\gamma_{an} = R_{d,0.05} / R_{d,k}$ expresses instead the approximation of the analytical formula used to evaluate the strength property. Finally, γ_M is the partial material factor that, for verifications of structures designed in accordance with

the concept of dissipative structural behaviour (DCM, DCH), should be taken from the accidental load combinations (equal to one).

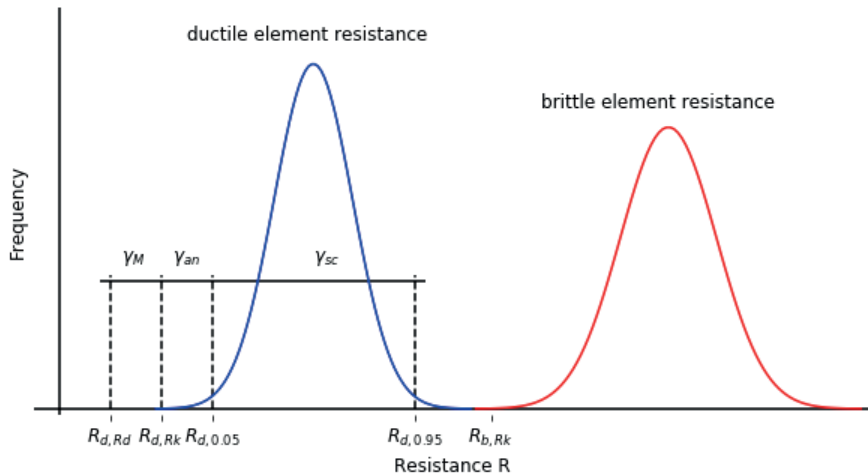


Figure 2: Concept of overstrength according to [7].

The experimental investigation was carried out on doweled timber to timber connections loaded monotonically up to failure in shear parallel to the grain. 14 configurations, varying dowel diameters, number of fasteners, spacing between fasteners and thickness of the wooden elements, were tested. For each configuration 10 to 25 specimens were considered. The average values and standard deviations of the connection strength distribution were calculated according to EN 14358 [8] using a lognormal distribution. From the previously defined formulas the values for γ_{an} , γ_{sc} and γ_{Rd} were calculated, finding that the 5th and 95th percentiles for γ_{Rd} were 1.2 and 1.85 respectively. The authors proposed therefore the use of the mean value 1.6 as overstrength factor for a ductile design.

In [9] a very similar procedure for the evaluation of the overstrength factor is applied on the results of experimental cyclic tests performed by Dujic and Zarnic on timber connections made of angular brackets and screwed connections between perpendicular panels. The difference with [7] is that here the 5th and 95th percentiles were evaluated using a student's t distribution, due to limited amount of experimental data (only 2 to 5 specimens per configuration), and without considering the contribution of γ_{an} . The overstrength factor was, in fact, calculated as $\gamma_{Rd} = R_{c,0.95} / R_{c,0.05}$. The configuration with angle brackets connected to the panels using nails with a diameter of 4 mm and a length of 40 mm, showed a rather brittle behaviour, resulting in an overstrength factor of 2.12 in shear and 1.85 in uplift. Hence the recommendation given to use nails at least 60 mm long so that the brittle failures can be avoided. In fact, the configuration using nails with a diameter of 4 mm and a length of 60 mm, gave instead much lower values for the overstrength factor, namely

1.26 in shear and 1.18 in uplift. In the tests performed on a screwed connection ($\phi 8$, length 160mm) between perpendicular panels, due to a larger scatter of the results, the calculated value for the overstrength factor was 1.63.

In [10] and [11] the results from an experimental programme conducted by CNR IVALSA is presented. The tests were carried out on hold-downs, angle brackets and screwed connections between panels, for a total of 20 different configurations. These different setups were based on the typical connections used within the buildings tested for the SOFIE project [12]. In [10] the results of the tests performed on 12 different configurations of screwed connections between CLT panels is presented. The configurations vary so that the capacity of the screw could be assessed for both a lateral and a withdrawal load. For each of the configurations at least one monotonic and six cyclic tests were performed. Here as well the overstrength factor is defined as the ratio between 95th percentile of the connection strength distribution and the analytical prediction of the design connection strength. However, the final value of the overstrength factor γ_{Rd} was calculated neglecting the contribution of γ_{an} , in fact, as the author state, these results are valid only for experimentally tested connections. The 5th and 95th percentile strength values were calculated assuming two different distribution, namely normal, and log-normal, but using also the procedure from EN14358 for the calculation of characteristic values for the log-normal distribution. A comparison between the three different approaches was then made showing that with the normal and log-normal distribution the factor was ranging from 1.15 to 1.7, with the exception of one configuration that gives a value of 2.3 due to a brittle failure mode (shear plug), so that the high scatter gives a much higher value. The average overstrength value calculated was 1.46. On the other hand, using the approach given in EN 14358 leads to higher values, that range from 1.2 to 1.9, and 3.3 for the configuration that was characterized by a brittle failure mode. The average calculated value was 1.74.

In [11] the results from the tests performed on hold-downs and angle brackets loaded in both tension and shear is presented. The 8 configurations investigated recreates CLT-foundation and CLT-CLT (wall-floor) connection types. Here as well one monotonic and six cyclic tests were performed, while the 5th and 95th percentile values were evaluated according to EN 14358. The overstrength factors, as average values for hold-downs loaded in tension, were found to be 1.3, while when loaded in shear ratios were found between 1.25 and 1.38, depending on the configuration (CLT-CLT and CLT-foundation, respectively). For angle brackets connecting foundation to CLT wall panel, the overstrength factors range from 1.16 to 1.23 depending on the direction of loading (tension and shear, respectively). Angle brackets connecting CLT walls to CLT floors were found to have higher overstrength ratios, namely 1.44 in tension and 1.40 in shear, due to the larger scatter of the experimental results. As noted by the authors, for connections that were not experimentally tested, higher values that take into account the difference between the analytical prediction and the actual experimental values, should be used.

A very similar approach is presented in [13] and [14]. Here the overstrength factor is determined with the following equation:

$$\gamma_{Rd} = \gamma_{mat} \cdot \gamma_{mech} \cdot \gamma_{0.95} = \frac{R_m^*}{R_k} \cdot \frac{R_{exp,m}}{R_m^*} \cdot \frac{R_{exp,0.95}}{R_{exp,m}} \quad (3)$$

where R_k is the design value according to code provisions, R_m^* is the mean value of resistance calculated with the mean values of material properties, $R_{exp,m}$ is the mean value of capacity from testing and $R_{exp,0.95}$ is the 95 % quantile from testing. The partial coefficient γ_{mat} takes then into account the spread between the characteristic resistance calculated according to design provisions and the one calculated using mean values for the material properties. γ_{mech} considers the “hidden reserves” that are present from the difference between calculated and experimental values. Finally, $\gamma_{0.95}$ is defined as the ratio between the 95th percentile and the mean value from testing.

From Eq. (3) it is quite clear that the difference with the definition found in [7] is only in how the various contributions to evaluate γ_{Rd} are defined, but in both the procedures γ_{Rd} depends ultimately only on the ratio $R_{d,0.95}/R_k$.

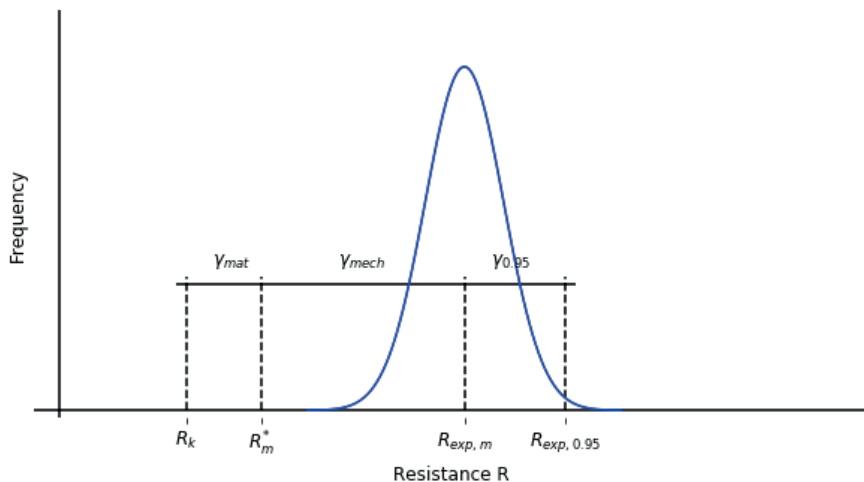


Figure 3: Concept of overstrength according to [13]

Relying on data obtained by experimental investigations on light-frame timber shear walls, the authors calculate the partial factor, as explained above, for every configuration tested, and derived the final overstrength factor as the product of the mean values of the partial factors. The value that was found is: $\gamma_{Rd} = 1.3 \cdot 1.33 \cdot 1.28 \cong 2.2$. Subsequently, they state that γ_{mech} can be decreased to 1.0 if the same mechanical over-strength is expected for the wall element and the connection, decreasing the overstrength factor to: $\gamma_{Rd} = 1.3 \cdot 1.0 \cdot 1.28 \cong 1.65$.

An alternative approach to determine the overstrength factor is presented in [15]. The purely experimental approach is here replaced by a probabilistic analysis conducted

with a Monte Carlo simulation. The authors had previously conducted some investigations on timber beams with joints acting in the middle, the bending moment acting on the connection is split in a compression force transferred via a compressive zone made of steel plates, and a tensile force transferred via doweled joints.

The initial data upon which the simulation is based are the statistical distribution (normal and lognormal) of the basic material properties, taken from the conducted experiments.

A reliability analysis was conducted by defining the limit state function g :

$$g = R - E \quad (4)$$

the terms R and E usually represents the resistance and the effect on the system. In this case, the two terms are respectively set as the resistance of the brittle element (moment resistance of the wooden beam) and the resistance of the ductile one (resistance of the doweled connection) times the OSF. The limit state function becomes then:

$$g = W_{net} \cdot f_m - X_M \cdot \kappa_{cs} \cdot n \cdot F_{v,Rk} = M_{beam} - X_M \cdot \kappa_{cs} \cdot M_{joint} \quad (5)$$

The outcomes of the limit state function g can then be processed by sampling the basic variables (tensile strength of the connector, geometrical data, timber density, bending strength, model uncertainty) at random according to their distribution functions (normal and lognormal). The outcomes might be in the failure domain ($g < 0$) or in the safe domain ($g > 0$). The reliability index ($\beta = \mu_g / \sigma_g$) is determined from the statistical distribution of g obtained from 10^8 calculations, for each input values of κ_{cs} . It should be noted that κ_{cs} is referred to a specific geometrical configuration and therefore it should be normalized with respect to the M_{joint} / M_{beam} ratio.

$$k_{cs} = \kappa_{cs} \cdot \frac{M_{joint,design}}{M_{cs,design}} \quad (6)$$

The authors derive therefore the final relation as:

$$\beta = 7.65 - 7.65 \cdot k_{cs} \quad (7)$$

By imposing the value of β (3.8) that leads to the required failure probability set by regulations, the overstrength factor k_{cs} calculated is equal to 0.5 ($\gamma_{Rd} = 2$).

More recently other articles ([16], [17], [18]) that report the results of experimental investigation programmes have been published. In [16] the mechanical and the hysteretic behaviour of steel-to-timber joints with annular-ringed shank nails was investigated. Average and characteristic values of the experimental strength capacities were evaluated and compared to the analytical predictions determined according to current structural design codes and literature. Furthermore, using the same procedure as presented in [7], the overstrength factor and the strength degradation factor were evaluated. The testing programme consisted of tension and bending tests on nails, monotonic and cyclic shear tests on single fastener joints loaded in parallel and perpendicular direction to the face lamination of the CLT

panels, and withdrawal tests on single nails embedded in the side face of CLT panels. Based on the test results the following values are proposed: $\gamma_{Rd} = 2.0$ and $\gamma_{Rd} = 1.8$ are recommended for nailed joints with annular-ringed shank nails loaded in withdrawal; $\gamma_{Rd} = 1.8$ and $\gamma_{Rd} = 1.3$ are recommended for laterally loaded steel-to-timber joints parallel to the face lamination of the CLT panel, while the values $\gamma_{Rd} = 2.3$ and $\gamma_{Rd} = 1.5$ should be assumed in the perpendicular direction. For each configuration, two overstrength factors are given, this is because one is recommended when the characteristic load-carrying capacity is defined based on general rules, the other is recommended when the design is based on the characteristic strength capacities determined from test results (assuming $\gamma_{an}=1$).

In [17] an evaluation of overstrength based on an experimental study on dowelled connections is presented. In this study a total of 20 connection tests were performed on three different connection layouts. CLT embedment tests and dowel bending tests were also performed to derive embedment strength, the fastener yield moment, as well as component overstrength. Here as well the approach followed to determine overstrength values is the one presented in [7]. Based on the parametric study of component overstrength, the authors calculated an overall theoretical overstrength value of $\gamma_{Rd} = 1.68$. The observed strength in the connection tests did not exceed this value, as the largest observed strength was 1.54 times the predicted characteristic strength.

The fact that the overstrength factor is affected, not only, by the statistical variability of the strength of the ductile element, but also by the analytical method to estimate its characteristic strength, is addressed in [18]. The authors present in this paper an innovative steel bracket developed and tested at the University of Padova. This innovative connector was designed to grant high ductility and energy dissipations capacity. Thanks to a well-defined behaviour of the ductile component and reliable response of the structural steel, not only were the authors able to reduce the scattering of peak force and therefore the γ_{sc} value, but also to improve the accuracy of analytical predictions of the connection strength and therefore to reduce γ_{an} . For their innovative bracket loaded in tension they found: $\gamma_{sc} = 1.04$, $\gamma_{an} = 1.68$, $\gamma_{Rd} = 1.76$. In a shear loading condition, instead they found: $\gamma_{sc} = 1.04$, $\gamma_{an} = 1.11$, $\gamma_{Rd} = 1.15$.

4. Summary of application of overstrength factor for Capacity Design in timber structures

Several suggestions for a correct application of the CD principles are given throughout the previously presented papers and in [19], where the authors take stock of the situation providing a set of indications that will be used as basis for the draft proposal for the new section 8 of EC 8.

A summary of indications and suggestions is also presented in [20]. Here the authors use the results of several previous experimental tests, and critically discuss the typical failure mechanisms of connections and wall systems. Furthermore, they look into the influence of different types of wall behaviour on mechanical properties and

energy dissipation, and provide a guideline on how the CD approach should be used for a proper seismic design.

The importance of the development of a ductile failure mode at connection level is underlined and a guideline on how to achieve such failure mode is presented. First of all, the designer shall ensure that the failure mode of the fastener is ductile, corresponding to either one or two plastic hinge formations. The authors propose to achieve this once again by applying Eq. (1). In this case thus, $R_{d,d}$ is the lowest design shear resistance which presents a ductile failure mode (modes b), d) and e) for steel to timber connections, and modes d), e) and f) for timber to timber connections of Johansen's equations in Eurocode 5 [21]). $R_{b,d}$ is instead the lowest resistance which presents a brittle failure mode (modes a) and c) for steel to timber connections, and modes a), b) and c) for timber to timber connections). In addition, other possible brittle failure modes as shear plug, splitting of timber, tear out, resistance of net section of the metal plate, or withdrawal of the fastener and pull-through resistance of bolts shall be avoided as well.

Once the ductility at the connection level is ensured, it is suggested that, at the wall level, the plasticization should rather occur in the hold-downs and angle brackets loaded in tension, than in angle brackets loaded in shear. This because in this way there will be no residual slip at the end of the seismic event, and the self-weight can act as stabilizing load and re-center the building. This behaviour can be ensured again using Eq. (1), hence ensuring that the total shear resistance of the angle brackets is larger than 1.3 times the design value of the uplift resistance of hold-downs and angle brackets. Nevertheless, still at the wall level, the CLT panel resistance should be larger than 1.3 times the connection resistance.

At the building level some other suggestions are given. In order to ensure a proper uniform distribution of lateral forces from the slabs to the wall panels below, the floor panels should act as non-dissipative rigid diaphragms, and therefore any floor to floor connection should be oversized according to the same principle. Similarly, floor to wall connections should also be oversized to guarantee an efficient transmission of forces. Furthermore, in order to ensure a box-type behaviour perpendicular wall to wall connections should as well be designed in accordance to Eq. (1).

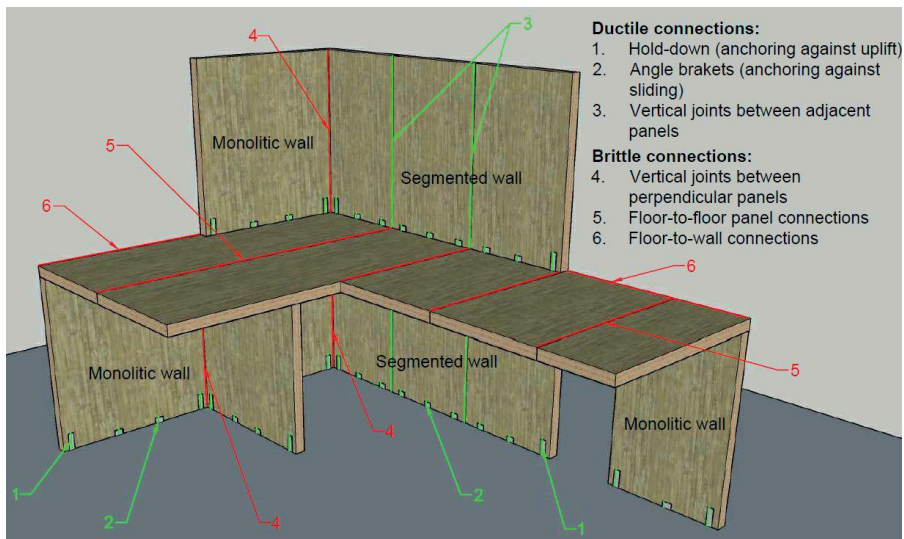


Figure 4: Ductile and brittle connections in a CLT building.

5. Conclusions

Until today most CLT structures have been designed to behave elastically during a seismic event. However, the outcomes of several experimental testing programmes conducted in the last decade shows the good seismic performances of such systems. In order to achieve more cost effective buildings, the non-linear behaviour of these kind of structures should be exploited as it happens for steel and reinforced concrete buildings. The overstrength factor plays a very important role in the framework of a seismic design based on Capacity Design principles. The purpose of this coefficient is in fact, to ensure that the chosen ductile failure mode will activate before any undesired brittle failures, so to achieve the highest possible level of energy dissipation. Since this important piece of information is missing in current regulations, there is an urgent need to further investigate this matter so that this coefficient could be implemented in future version of the structural standards. This paper presents a review of the methods used in the last years to evaluate the overstrength factor for timber structures, and a summary of the reviewed articles is given in Table 1. As it can be noticed in that table, most of the research works are based on experimental testing programmes. Future work could further investigate the approach adopting structural reliability methods. The use of structural reliability analysis with limit state functions through Monte Carlo simulations is in fact widely used for other structural materials, such as steel and concrete.

Table 1: Summary of papers that derive the overstrength factor

Reference	Approach	Connection type	Loading	N° of configurations (n° of specimen per config.)	γ_{Rd}
[7]	$\gamma_{Rd} = \frac{R_{d,0.95}}{R_{d,0.05}} \cdot \frac{R_{d,0.05}}{R_{d,k}} \cdot \frac{R_{d,k}}{R_{d,d}}$ $= \gamma_{sc} \cdot \gamma_{an} \cdot \gamma_M$	Doweled connections timber-to-timber C24	Monotonic shear parallel to the grain	14 (10 ÷ 25)	1.20 ÷ 1.85 Mean 1.60
[13] [14]	$\gamma_{Rd} = \frac{R_m^*}{R_k} \cdot \frac{R_{exp,k}}{R_m} \cdot \frac{R_{exp,0.095}}{R_{exp,m}}$ $= \gamma_{mat} \cdot \gamma_{mech} \cdot \gamma_{0.95}$	Nails and staples in light frame elements (OSB, GFB) - Connection unit - Wall element	Monotonic and cyclic shear	11 (4 ÷ 7) on connections 10 (1 ÷ 4) on wall elements	Mean 2.20 Mean 1.65 (for $\gamma_{mech}=1$)
[9]	$\gamma_{Rd} = \frac{R_{d,0.95}}{R_{d,d}} = \frac{R_{d,0.95}}{R_{d,k}}$ $= \gamma_{sc}$	Nailed connections metal angle brackets on CLT panels Screwed connections perpendicular CLT panels	Cyclic shear Cyclic uplift Cyclic shear	1 (3) 1 (2 ÷ 3) 1 (5)	1.3 1.2 1.6
[10]	$\gamma_{Rd} = \frac{R_{d,0.95}}{R_{d,d}} = \frac{R_{d,0.95}}{R_{d,k}}$ $= \gamma_{sc}$	Screwed connections on CLT panels	Monotonic and cyclic shear and withdrawal	12 (1 M + 6C)	1.2 ÷ 1.9 Mean 1.74
[11]	$\gamma_{Rd} = \frac{R_{d,0.95}}{R_{d,d}} = \frac{R_{d,0.95}}{R_{d,k}}$ $= \gamma_{sc}$	Hold-downs (H-d) steel angle brackets (a-b) nailed on CLT panels	Monotonic and cyclic shear and tension	8 (1M + 6C)	1.3 hold-downs 1.25 ÷ 1.45 angle brackets
[15]	Monte Carlo simulation Reliability analysis	Doweled connections timber-steel-timber GL24h	Bending	3	1.99 for $\beta=3,80$
[16]	$\gamma_{Rd} = \frac{R_{d,0.95}}{R_{d,0.05}} \cdot \frac{R_{d,0.05}}{R_{d,k}} \cdot \frac{R_{d,k}}{R_{d,d}}$ $= \gamma_{sc} \cdot \gamma_{an} \cdot \gamma_M$	Single annular-ringed shank nails on CLT panel	Monotonic and cyclic shear and withdrawal	1 (22) withdrawal 1 (6M + 15C) to grain 1 (5M + 15C) ⊥ to grain	2.0 (1.8 if $\gamma_{an}=1$) 1.8 (1.3 if $\gamma_{an}=1$) 2.3 (1.5 if $\gamma_{an}=1$)
[17]	$\gamma_{Rd} = \frac{R_{d,0.95}}{R_{d,0.05}} \cdot \frac{R_{d,0.05}}{R_{d,k}} \cdot \frac{R_{d,k}}{R_{d,d}}$ $= \gamma_{sc} \cdot \gamma_{an} \cdot \gamma_M$	Doweled connections	Monotonic and cyclic shear	3 (5)	1.68 from parametric study 1.54 from experimental results
[18]	$\gamma_{Rd} = \frac{R_{d,0.95}}{R_{d,0.05}} \cdot \frac{R_{d,0.05}}{R_{d,k}} \cdot \frac{R_{d,k}}{R_{d,d}}$ $= \gamma_{sc} \cdot \gamma_{an} \cdot \gamma_M$	Innovative metal brackets	Cyclic shear and tension	1 (3) tension 1 (3) shear	1.76 (1.04 if $\gamma_{an}=1$) 1.15 (1.04 if $\gamma_{an}=1$)

6. References

1. Paulay, T. and M.J.N. Priestley, *Seismic design of reinforced concrete and masonry buildings*. 1992, New York: Wiley.
2. *EN 1998-1: Eurocode 8: Design of structures for earthquake resistance – Part 1: General rules, seismic actions and rules for buildings*. 2004, CEN.
3. *SIA 265:2012: Holzbau*. 2012, Schweizerischer Ingenieur- und Architektenverein.
4. *NZS 3603:1993.TIMBER STRUCTURES STANDARD*. 1996, Standards New Zealand.
5. *CSA 086-14. Engineering design in wood*. 2016, Canadian Standard Association.
6. *EC8- New Chapter 8 (2017-02-01) - draft proposal*. 2017.
7. Jorissen, A. and M. Fragiaco, *General notes on ductility in timber structures*. *Engineering Structures*, 2011. **33**(11): p. 2987-2997.
8. *EN 14358:2016. Timber structures - Calculation of characteristic 5-percentile values and acceptance criteria for a sample*. 2016, CEN.
9. Fragiaco, M., B. Dujic, and I. Sustersic, *Elastic and ductile design of multi-storey crosslam massive wooden buildings under seismic actions*. *Engineering Structures*, 2011. **33**(11): p. 3043-3053.
10. Gavric, I., M. Fragiaco, and A. Ceccotti, *Strength and deformation characteristics of typical X-lam connections*. *Proceedings of WCTE 2012, Auckland, New Zealand*; 2012.
11. Gavric, I., M. Fragiaco, and A. Ceccotti, *Cyclic behaviour of typical metal connectors for cross-laminated (CLT) structures*. *Materials and Structures*, 2015. **48**(6): p. 1841-1857.
12. Ceccotti, A., et al. *Sofie project–test results on the lateral resistance of cross-laminated wooden panels*. in *Proceedings of the First European Conference on Earthquake Engineering and Seismicity*. 2006.
13. Schick, M., T. Vogt, and W. Seim. *Connections and anchoring for wall and slab elements in seismic design*. In: 46th CIB-W18 meeting, Vancouver, Canada, Paper 46-15-4; 2013.
14. Vogt, T., et al., *Experimentelle Untersuchungen für innovative erdbebensichere Konstruktionen im Holzbau*. *Bautechnik*, 2014. **91**(1): p. 1-14.
15. Brühl, F., J. Schänzlin, and U. Kuhlmann, *Ductility in Timber Structures: Investigations on Over-Strength Factors*, in *Materials and Joints in Timber Structures*. 2014, Springer. p. 181-190.
16. Izzi, M., et al., *Experimental investigations and design provisions of steel-to-timber joints with annular-ringed shank nails for Cross-Laminated Timber structures*. *Construction and Building Materials*, 2016. **122**: p. 446-457.
17. Ottenhaus, L.-M., et al., *Overstrength of dowelled CLT connections under monotonic and cyclic loading*. *Bulletin of Earthquake Engineering*: p. 1-21.

18. Scotta, R., et al. *Capacity Design of CLT Structures with Traditional or Innovative Seismic-Resistant Brackets* in *INTER - International Network on Timber Engineering Research Meeting*. Kyoto, Japan, Paper 50-15-5; 2017
19. Follesa, M., M. Fragiaco, and M.P. Lauriola. *A proposal for revision of the current timber part (Section 8) of Eurocode 8 Part 1*. In *44th CIB-W18 Meeting, Alghero, Italy*. paper 44-15-1; 2011.
20. Gavric, I., M. Fragiaco, and A. Ceccotti. *Capacity seismic design of X-LAM wall systems based on connection mechanical properties*. In: *46th CIB-W18 meeting, Vancouver, Canada, Paper 46-15-2*; 2013.
21. *EN 1995-1-1: Eurocode 5: Design of timber structures - Part 1-1: General - Common rules and rules for buildings*. 2004, CEN.
22. Jorissen, A. J. M. *Double shear timber connections with dowel type fasteners*, Delft University Press Delft, The Netherlands. (1998).

C General Design Issues

An Architectural Perspective on Cross Laminated Timber

Dr. Elizabeth Shotton

Associate Professor

**Architecture, Planning & Environmental Policy, University College Dublin
Dublin, Ireland**

Summary

While there has been considerable research on the mechanical attributes of cross laminated timber (CLT) over the past two decades, research on the environmental profile of the material is less developed. Environmental profiles are critical to architects, as material choices effect the environmental impact of a project as well as its durability and potential for reuse. This paper surveys a selection of recent research in this field, largely sponsored by the adoption of CLT in mid-rise construction.

1. Introduction

The introduction of cross laminated timber products has had a radical impact on architectural design in recent years. Prior to its introduction, timber had long been eclipsed by non-combustible materials such as steel, concrete and masonry for buildings of any significant scale. These material choices were driven, in part, by building regulations and codes that limited the use of timber in public buildings or construction over 4 floors [1] due to its combustibility.

Although various types of load-bearing engineered wood products, such as glued laminated timber, have existed for many decades they were principally used as linear members with limited applications [2]. It is only with the recent development of cross laminated timber (CLT) in the past two decades that a genuine alternative to mineral-based building materials has become available, due to its performance as a stand-alone horizontal or vertical structural element coupled with its fire resistance. A growing concern for the environmental impact of construction has served to accelerate the adoption of CLT in mid- to high-rise construction, as it is generally thought to have a lower embodied energy and carbon footprint than concrete or steel, the leading contenders for construction in this sector, leading to a resurgence in timber building [1].

Research into the structural properties of CLT has been underway for two decades [2] and is in an advanced state, as is the analysis of its performance in fire. Given that significant adoption into the building sector is relatively recent, analysis of this material in terms of its use by architects is less advanced, and less clearly defined due to the breadth and complexity of design decisions made by architects. In 2007 Hegger et al. published a small volume [3] addressing the principles architects use in making material choices, within which they charted the various considerations architects contend with during the design process (Fig. 1).

Material Choice	Perception	Visual
		Tactility
		Thermal
		Acoustic
		Olfactory
	Properties	Thermal
		Mechanical
		Chemical
	Requirements	Suitability for Use
		Ecological Requirements
		Economic Requirements

Figure 1: Principles for the Choice of Materials derived from Hegger et al., 2007 [3]

Engineers contribute research and design across a number of these areas in the design of a building, but with respect to CLT they are principally engaged with the technical properties and, specifically, mechanical properties of the structure. Architects, conversely, must attend to and negotiate between all of these issues, to a greater or lesser extent, on each project. Though superficially independent most categories are inter-related and optimisation of each category is rarely a possibility for an architect coordinating the design and construction of a building, thus trade-offs and compromises are made between all these categories in an attempt to find the optimum solution.

The use of CLT in architecture, being a relatively new phenomenon, carries with it a more than usual amount of uncertainty, as most architects have limited experience with the material or its performative aspects. The publication of various CLT manuals, though helpful in this regard, tend to focus on structural performance attributes, with only 3 of 12 chapters addressing the environmental profile and the indoor environment in the Canadian and US handbooks, symptomatic of the imbalance in research to date.

Although positive commentary regarding the environmental profile of CLT and its impact on tempering of the indoor environment have been made generally in architectural literature, there is a relative absence of research in these fields [4], while the aesthetic qualities of CLT are even less examined [5]. Given the existing comprehensive research on the technical properties of CLT, and for the moment overlooking the economic impact, thermal conditioning and aesthetics as being beyond the scope of this review, this paper will review a selection of current research on two related themes of concern to architectural practitioners: embodied energy and environmental impact; and durability and reuse.

2. The Environmental Profile of CLT

2.1 Embodied Energy & Environmental Impact

As noted by Fernandez et al. (2014) European obligations under the Kyoto Protocol for greenhouse gas emissions have not been entirely met, and a large proportion of these emissions result from the construction industry [6,7]. While energy used in the operation of a building accounts for the bulk of emissions associated with buildings and becomes increasingly dominant as the life span of the building increases [8,9]. As building envelopes have improved and renewable energy generation has increased, the importance of the embodied energy and environmental impacts of building materials has become more significant [10]. Thus, the approach to the selection and deployment of materials within a building becomes an increasing concern for architects.

At the date of publication in 2011, the authors of Chapter 11 of the CLT Handbook published by FPInnovations [4] noted that though the use of CLT is often discussed as being advantageous over comparable concrete systems in terms of environmental impact, there had been very little research to date that offered a credible and quantifiable comparison. Any comparisons which existed at the time tended to refer to light wood-framing rather than mass timber construction, the latter of which they suggested would use at least three times more wood and would include additional processing energy and adhesives [4]. At that date, there had only been two articles published offering a comparative analysis of the environmental profile of CLT from Sweden [9] and New Zealand [11], with a third study underway in Canada [10]. The authors of the Handbook offered a series of approximations using data on glulam as a proxy for CLT, a tactic common among researchers in absence of authoritative data, in an attempt to quantify the environmental footprint without actually doing a full Life Cycle Analysis. They did, however, note that variances in construction methods, design details and transportation between glulam and CLT would influence the reliability of their conclusions [4].

Environmental impact assessments were made based on functionally equivalent units of CLT to reinforced concrete of 1m² of structural floor. In all cases LCA values for glulam were used to represent CLT, as data was not available for CLT. Based on these relatively crude approximations, the authors conclude that CLT would have less impact on the environment than concrete across all measures and have additional benefits as a carbon storage mechanism and biofuel at end of life (Figure 2). Included in the calculations from Mahalle et al. [4], were credits for energy recovery from wood waste generated during CLT manufacturing with subsequent substitution effects for natural gas, and for the stored carbon in the wood, giving CLT a negative cradle-to-gate carbon footprint for global warming. This offsetting of processing energy and the associated carbon emissions by credits given for carbon sequestration and substitution of fossil fuels with biomass is an accepted convention in LCA studies, supported by IPCC guidelines.

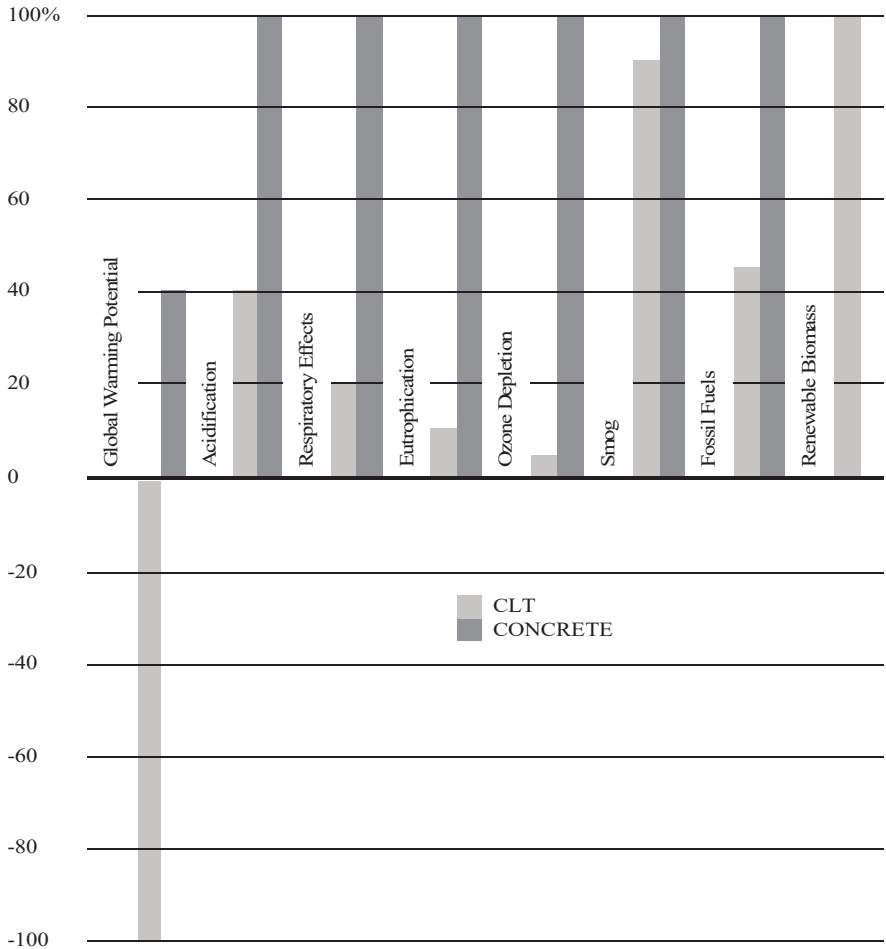


Figure 2: Comparative LCA between 1 square meter of CLT and concrete floor structure, derived from Mahalle et al., 2011 [4]

While the attribution of carbon storage potential to timber is legitimate, including it in the analysis of the direct environmental impacts obscures the clarity of comparative results between CLT and other materials, unless these calculations are offered in a transparent manner. For instance, recent research in concrete [12,13] has indicated that concrete absorbs atmospheric carbon during its life cycle, thus to provide an authoritative comparison would require accounting for the carbon sequestration potential of concrete as well. While this has been acknowledged and accounted for in a number of studies [14,15,16,17,18] it has not been consistent across the entire case study literature. Similarly, the reduction in carbon emissions

(global warming potential) from using waste wood for energy production rather than natural gas, further obscures the comparison, as it is only by virtue of the current IPCC rules that the burning of wood for energy is considered carbon neutral. Increasing opinion among researchers in this field is that since there is still carbon released during this process, biomass for energy use cannot be considered climate neutral [19].

The absolute values associated with the chart (Table 1), adjusted to clarify these assumptions, make apparent that in these approximated calculations the relative impact of CLT and concrete is almost equal in contribution to smog, despite the global warming potential of CLT being negative. This apparent inconsistency is a result of reducing the global warming potential of CLT by attributing carbon sequestration of 248 kg CO₂ and energy substitution of 21.8 kg CO₂, which, if not included (line 4), would result in a positive global warming potential for CLT of 47.25 kg CO₂. Though still lower than that of concrete, it provides a clearer reference figure for comparison.

Table 1: Comparative LCA results for CLT and concrete produced and used in Vancouver adjusted to clarify contribution of carbon sequestration and energy substitution in contribution to global warming, derived from Mahalle et al., 2011 [4]

Impact Category		Unit	CLT 1m ² of floor	Concrete 1m ² of floor
1	Global Warming	Kg CO ₂ eq.	-222.55	90.12
2	Carbon Sequestration	Kg CO ₂ eq.	248.00	No data
3	Energy substitution	Kg CO ₂ eq.	21.80	No data
4	Global Warming (1) adjusted to remove sequestration (2) and substitution (3)	Kg CO ₂ eq.	47.25	90.12
5	Acidification	H+ moles eq.	8.77	23.00
6	Respiratory effects	Kg PM _{2.5} eq.	0.010	0.058
7	Eutrophication	Kg N eq.	0.014	0.115
8	Smog	Kg NO _x eq.	0.21	0.23
9	Non-renewable fossil fuel	MJ eq.	274.3	633.54

A more authoritative comparison between the environmental impact of CLT and reinforced concrete was published in 2012 by Robertson et al. [10], based on a cradle to construction site boundary and using data from a 5 story office building with a reinforced concrete frame structure in comparison to a hypothetical model of a similar size using CLT and glulam. The design values for CLT were derived from a pilot-scale manufacturing facility in Canada, while secondary sources were used for all other materials [10]. In general, the analysis suggested that buildings constructed of CLT had a lower environmental impact in 10 of 11 assessment categories [10], though fossil fuel depletion is higher for the laminated timber option (Figure 3). The authors suggest this last unexpected finding may be a result of using data from a

pilot-scale facility, which could be improved in a full-scale operation. Though the fuel source for the pilot-scale facility is not identified in the paper it would appear that fossil fuels are used as a primary energy source, while waste wood is often used in full-scale engineered timber manufacturing plants. The more generalised LCA study in the CLT Handbook [4] did indicate far less use of non-renewable fuels for CLT, however, when viewed in tandem with the use of renewable fuel use for processing (Figure 2) it would seem both studies suggest that the overall energy use (renewable and non-renewable) for processing is quite high for either construction method.

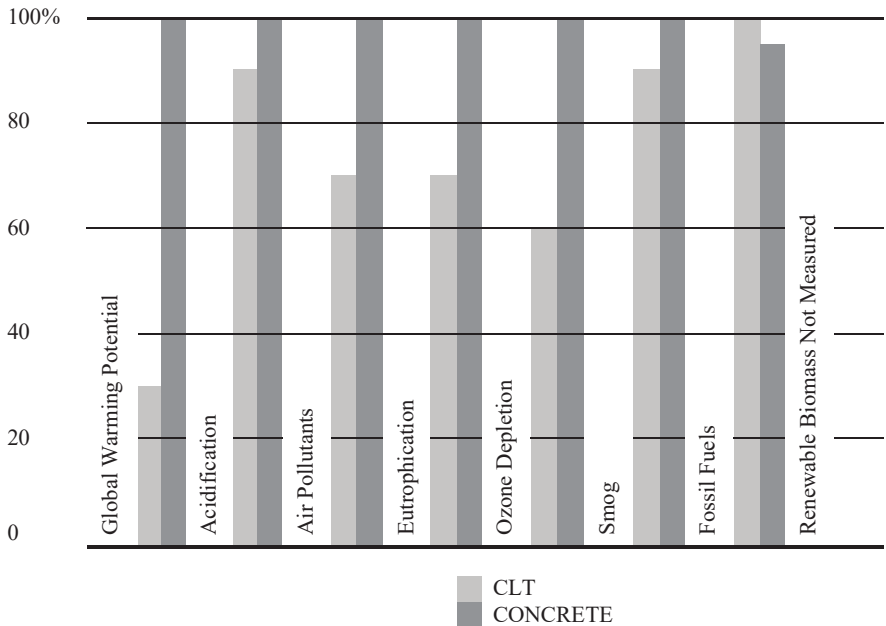


Figure 3: Environmental impact comparison of the concrete and timber design alternatives, derived from Robertson et al., 2012 [10]

As in the earlier study [4] Robertson et al. [10] offset the global warming potential (GWP) for CLT, that is the total amount of CO₂ equivalent associated with the cradle-to-gate emissions, by its capacity to act as a carbon store. Though in this study the GWP for CLT was still positive, unlike the earlier study, it was 70% less than the impact of a comparable reinforced concrete frame building. If the carbon storage property of wood was not included in the GWP calculation this figure drops to 17% [10].

While Robertson et al. estimated that the cumulative embodied energy of the construction materials was 8.2GJ/m² for the CLT and 4.6 GJ/m² for the reinforced concrete frame system (Figure 4), which appears counter-intuitive, the reason for this

is the inclusion of what they describe as ‘feedstock energy’ in the embodied energy figure [10]. Feedstock energy refers to the energy that can be recaptured from the material at end-of-life, by using the timber as biomass for energy production. The summing of feedstock energy, or the energy that could be obtained from the product at the end-of-life, with the processing energy used to manufacture the product into a single figure, as is done in the study by Robertson et al. [10], confuses comparisons between different materials regarding embodied energy and the associated potential climate effects. Though the energy that could be obtained from the product at the end-of-life is critical information that can be used to inform material choices, separating this value from processing energy offers a greater degree of clarity. Nevertheless, what is of interest is that the energy used to process CLT and reinforced concrete is nearly equivalent, an unexpected result. These results are broadly similar to earlier research (Table 2), including the Gustavsson et al. study on the early Limnologen project in Sweden [9]. Although much of this energy may be from renewable sources in the case of CLT, given that the burning of biomass for energy is not climate neutral as it still results in CO₂ emissions to the atmosphere [19], it would appear that developing a more efficient manufacturing process for CLT would be of value and may point to a future area of research.

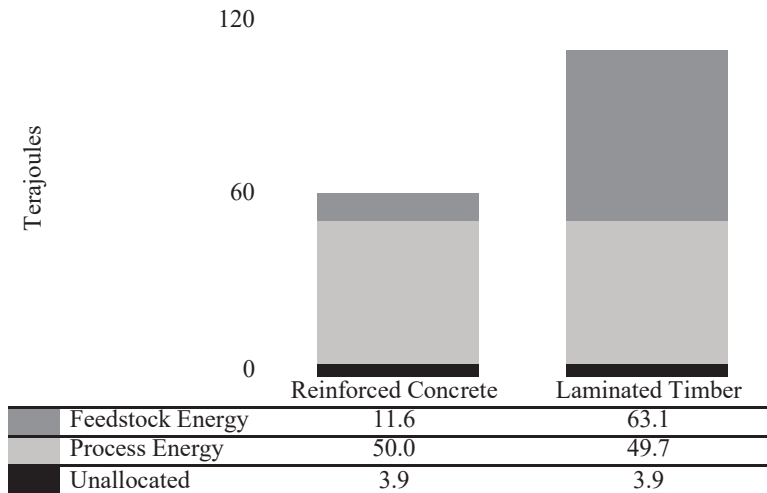


Figure 4: Embodied energy of building materials, derived from Robertson et al. 2012 [10]

More recent comparative studies on the environmental profile of CLT [18,20,21] have extended this research but have employed varying methodologies making comparisons difficult. Santi et al. [20] took as a functional unit a m² unit of wall assembly to compare the Massiv-Holz-Mauer Wall System to a comparable brick wall system and found that the GWP of the CLT wall system was 40% lower than

the brick equivalent at 35.23kg CO₂eq, though it was not explicit as to whether this accounted for carbon sequestration or fossil fuel replacement with biomass. Skullestad et al. [18] recognised the differentials caused by how replacement of fossil fuels with biomass were attributed in the calculations and offered 3 different scenarios that studied the climate change (CC) impact of per m² gross floor area (structure only) of high-rise buildings constructed of CLT and reinforced concrete. With renewable fuel use considered neutral, the reference case GWP varied between 26.3 – 67.3 kg CO₂eq across the case study buildings, which increased to 41.6 – 94.7 kg CO₂eq when carbon emissions from incineration of biomass for energy during manufacturing or at end of life (EOL) was included, and decreased substantially when the use of biomass as replacement for fossil fuel use and its use as fuel at EOL was credited, resulting in negative carbon impact ranging from –140.3 kg CO₂eq to –230.8 kg CO₂eq. The recent study by Passarelli et al. [21] investigated the implications of transport energy on the GWP of CLT. It accounted for GWP for a functional unit of m³ material in the manufacturing stages for the three companies investigated, including credits for carbon sequestration, resulting in a negative GWP. These calculations were to aid in determining the relative impact of transport energy, which in the case of importing European product to Japan was a hefty 60% of the GWP, leading the authors to recommend localised production of the product.

Table 2: Comparison of CLT studies, derived from [4,10,18,20]

Summary of Analyses on Environmental Profile of Cross Laminated Timber					
Study		Impact of Processing		Related Credits	
	Year	Embodied energy	Global Warming Potential	Carbon Sequestration	Renewable Energy used in Processing
		GJ/m ²	kg CO ₂ eqv/m ²	kg CO ₂ eqv/m ²	GJ/m ²
Gustavsson et al.	2010	3.51	89*	N/A	N/A
Lal Mahalle et al.	2011	–	–222.55*	248	21.8
Robertson et al.	2012	3.49	126*	752	N/A
Santi et al.	2016	–	35.23**	N/A	N/A
Skullestad et al.	2016	–	26.3 – 67.3***	N/A	343

* Includes credits for carbon sequestration and use of renewable biomass

** Credits included are unclear

*** Credit for carbon sequestration unclear

To appreciate the complexity of the information offered to designers for decision making, the data drawn from the FPInnovation study [4] in comparison to results from [10,18,20] are tabulated in Table 2. The range of figures for GWP vary

substantially, depending on the functional unit used, the accounting methods for carbon sequestration and renewable biomass use, and the LCA methodologies and databases accessed in the studies, making comparisons difficult.

Architects, as the principal participants in the design and construction of buildings, are responsible for weighing up material choices relative to other design issues and as such need to have a better understanding of the environmental implications of these decisions, if they are to contribute to solutions to global warming [22]. While recent initiatives such as the BREEM and LEED rating systems incentivise architects to examine their designs based on embodied CO₂, clear unambiguous data is not always available due to variations in the methodologies and a lack of transparency among the published data. A recent, comprehensive study of methodologies used to estimate the GWP of buildings and building materials was undertaken by De Wolf et al. [23] that revealed a lack of consistency and comparability among both academic and industry-sponsored studies as a result of: inconsistencies in data; variations between methodologies and underlying assumptions; lack of an agreement on the terminology and which life cycle stages should be included; and a lack of consensus on how to integrate the benefits and loads of reuse, recycling and recovery potentials. Though they argue for the need for embodied CO₂ to be addressed in regulations and labelling, they acknowledge that the variability in the current results, due to a lack of transparency in the methodologies and a paucity of reliable databases, result in the inability to produce useful and reliable benchmarks for the construction industry.

2.2 Durability & Reuse

Though less discussed in both academic and industry literature, architects are also obliged to address issues of durability and reuse within the context of the environmental impact of building. In the often-cited study by Kernan and Cole (1996) on life-cycle energy use in buildings [8], four categories of life-cycle energy use were identified:

- energy to initially produce the building (embodied energy)
- recurring energy to refurbish and maintain the building
- operational energy (lighting, heating, cooling)
- energy associated with demolition and disposal

Noteworthy in the study is that over a typical 50-year building life, the initial embodied energy of the structure, while significant at the time of construction, represents only a relatively small proportion of the total embodied energy over its life-cycle, estimated as 5% or less [8]. This is because the building structure typically lasts the full life of the building with only minor repairs, while services, interior finishes and often the envelope require refurbishment, repair or replacement, leading to recurring embodied energy [8]. The implications are that the more attention must be given to the durability of finishes, envelopes and services.

In this context, the use of CLT could offer some enormous advantages over other frame systems. While an envelope, accounting for up to 28% of the embodied energy, is still required to protect the structure and address the indoor environment requirements, internal finishes could be minimized as the CLT panels used for floors, walls and ceilings could, and have been, left exposed. Though most CLT buildings built to date have covered the floors, walls and ceilings with finishes, one of the earliest CLT projects in Norway took explicit advantage of the singular mass of the CLT and left it exposed. This becomes all the more probable with the recent introduction of CLT with hardwoods applied as the final lamination, or the use of birch for the entire panel, which has a better aesthetic appearance in comparison to the tradition species used such as spruce or pine. Such a substantial reduction in the deployment of finishes in a building has the potential to reduce the initial embodied energy of the project by up to 14% [8], with further reductions in refurbishment and replacement across the lifespan of the building.

Though little research has been identified that clearly quantifies the energy, and implied global warming potential, associated with demolition and disposal of buildings constructed of CLT, Doodoo et al. [16] studied carbon implications over the life cycle of a timber versus concrete frame building, which suggested that the carbon balance for the post use phase was -4.8 tC and -10.7 tC respectively, due to the carbonation of the concrete aggregate post-demolition. CLT has the potential to be disassembled and reprocessed into other products or used for energy at EOL. Given its higher mass than timber frame, the recovery of biomass for energy use would significantly improve its carbon offset at end of life, while reuse or reprocessing would extend the carbon storage potential of the timber, thus improving its environmental profile over the entire life cycle of the building [10].

3. Discussion and Conclusions

Despite the variability in the data reported, there appears to be a clear and growing consensus as to the superior environmental performance of CLT over other structural systems, which increases with the height of construction [18]. The initial embodied carbon, or global warming potential, of the material is consistently lower than concrete alternatives in the reviewed cases and, when coupled with its potential for reuse at EOL, either as a new product or as biomass for energy, makes a very strong case for its use in mid- or high-rise buildings.

However, while the case studies discussed offer invaluable knowledge regarding the differences of environmental impact between construction systems, the variability in methodology and results can serve to confuse rather than enable any decision-making process. Though researchers have identified the need for a clearer decision-making process with regard to the environmental consequences of material choices [24], these still depend on reliable and comparable data from both product manufacturers and life cycle analysis (LCA) studies. As architects are not, in general, masters of

LCA methodologies, a simple approach to identifying key environmental attributes to inform decision making, based on reliable and comparative data, is required.

References

- [1] J. Mayo, *Solid Wood: Case Studies in Mass Timber Architecture, Technology and Design*. Oxon, New York: Routledge, 2015.
- [2] Gerhard Schickhofer, Reinhard Brandner, Helene Bauer, "Introduction to CLT, Product Properties, Strength Classes," in Joint Conference of COST Action FP1402 and FP1404 – Cross Laminated Timber – a competitive wood product for visionary and fire safe buildings, Stockholm, Sweden, 2016.
- [3] Hegger, Manfred, Hans Drexler, Martin Zeumer, *Basics: Materials*. Basel, Boston, Berlin: Birkhauser, 2007.
- [4] Lal Mahalle, Jennifer O’Connell and Alpha Barry, “Chapter 11: Environmental Performance of cross-laminated timber,” in *CLT Handbook*, Ciprian Pirvu, Sylvain Gagnon, Eds., Quebec: FPInnovations, 2011.
- [5] A. K. Bejder, "Aesthetic Qualities of Cross Laminated Timber," PhD, Department of Civil Engineering, The Faculty of Engineering and Science, Aalborg University Aalborg, Denmark, 2012.
- [6] Fernández, M., Martínez, A., Alonso, A., and Lizondo, L.: ‘A mathematical model for the sustainability of the use of cross-laminated timber in the construction industry: the case of Spain,’ *Clean Technologies and Environmental Policy*, 16, (8), 2014, pp. 1625-1636.
- [7] United Nations Environment Programme (UNEP). *Buildings and Climate Change: Summary for Decision-Makers*; UNEP Sustainable Building and Climate Initiative: Paris, France, 2009; pp. 2–11.
- [8] Cole, Raymond and Paul Kernan, "Life-Cycle Energy Use in Office Buildings," *Building and Environment*, vol. 31, 1996, pp. 307-317.
- [9] Gustavsson, L., A. Joelsson, and R. Sathre, "Life cycle primary energy use and carbon emission of an eight-storey wood-framed apartment building," *Energy and Buildings*, vol. 42, 2, 2010, pp. 230-242.
- [10] Adam B. Robertson, Frank Lam, and Raymond J. Cole, "A Comparative Cradle-to-Gate Life Cycle Assessment of Mid-Rise Office Building Construction Alternatives: Laminated Timber or Reinforced Concrete," *Buildings*, vol. 2, 2012, pp. 245-270.
- [11] John, S., B. Nebel, N. Perez, and A. Buchanan. "Environmental impacts of multi-storey buildings using different construction materials." Research Report 2008-02. Christchurch, New Zealand: University of Canterbury, Department of Civil and Natural Resources Engineering, 2009.

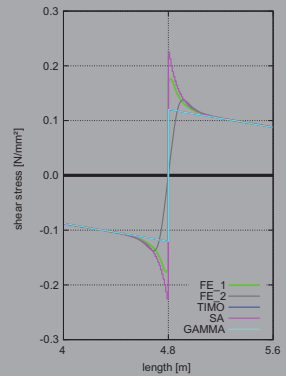
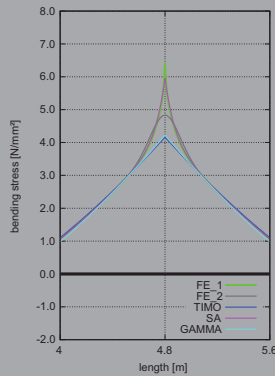
- [12] Lagerblad, B., Carbon dioxide uptake during concrete life cycle – State of the art. Stockholm: Cement och Betong Institutet, 2005.
- [13] Daragh Fitzpatrick, Eanna Nolan, Mark G. Richardson, "Sequestration of carbon dioxide by concrete infrastructure: a preliminary investigation in Ireland," *Journal of Sustainable Architecture and Civil Engineering*, vol. 10, 2015.
- [14] Gustavsson, Leif, and Roger Sathre. "Variability in Energy and Carbon Dioxide Balances of Wood and Concrete Building Materials." *Building and Environment* 41, no. 7, 2006, pp 940-51.
- [15] Gustavsson, Leif, and Roger Sathre. "Energy and Co2 Analysis of Wood Substitution in Construction." *Climatic Change* 105, no. 1, 2011, pp 129-53.
- [16] Dadoo, Ambrose, Leif Gustavsson, and Roger Sathre. "Carbon Implications of End-of-Life Management of Building Materials." *Resources, Conservation and Recycling* 53, no. 5, 2009, pp 276-86.
- [17] Dadoo, Ambrose, Leif Gustavsson, and Roger Sathre. "Lifecycle Carbon Implications of Conventional and Low-Energy Multi-Storey Timber Building Systems." *Energy and Buildings* 82, 2014, pp 194-210.
- [18] Skullestad, Julie Lyslo, Rolf André Bohne, and Jardar Lohne. "High-Rise Timber Buildings as a Climate Change Mitigation Measure - a Comparative LCA of Structural System Alternatives." *Energy Procedia* 96, 2016, pp 112-123.
- [19] Searchinger, T. D., S. P. Hamburg, J. Melillo, W. Chameides, P. Havlik, D. M. Kammen, *et al.*, "Fixing a Critical Climate Accounting Error," *Science*, vol. 326, 2009, pp. 527-528.
- [20] Santi, Silvia, Francesca Pierobon, Giulia Corradini, Raffaele Cavalli, and Michela Zanetti. "Massive Wood Material for Sustainable Building Design: The Massiv-Holz-Mauer Wall System." *Journal of Wood Science* 62, no. 5, 2016, pp 416-28.
- [21] Passarelli, R. N., and M. Koshihara. "CLT Panels in Japan from Cradle to Construction Site Gate: Global Warming Potential and Freight Costs Impact of Three Supply Options." *International Wood Products Journal* 8, no. 2, 2017, pp 127-36.
- [22] Bontinck, Paul-Antoine, Robert H. Crawford, and André Stephan. "Improving the Uptake of Hybrid Life Cycle Assessment in the Construction Industry." *Procedia Engineering* 196, 2017, pp 822-29.
- [23] De Wolf, Catherine, Francesco Pomponi, and Alice Moncaster. "Measuring Embodied Carbon Dioxide Equivalent of Buildings: A Review and Critique of Current Industry Practice." *Energy and Buildings* 140, no. Supplement C, 2017, pp 68-80.

- [24] Crawford, Robert H. and Xavier Cadorel. "A Framework for Assessing the Environmental Benefits of Mass Timber Construction." *Procedia Engineering* 196, 2017, pp 838-46.

Supplemental Material

MMSM 2.2.3 sfem_mat

Comparison of Methods of Approximate Verification
Procedures for Cross Laminated Timber



Research Report

T. Bogensperger
G. Silly
G. Schickhofer

holz.bau forschungs gmbh
Institute for Timber Engineering and Wood Technology
Graz University of Technology



**Competence Center
holz.bau forschungsbau gmbh**

Univ.-Prof. Dipl.-Ing. Dr. techn. Gerhard Schickhofer
Management and Scientific Coordination
Dipl.-Ing. Heinz A. Gach
Management

Mag. Eva Kavelar
Administration & Controlling

Hildegard Weißnar
Administration

Inffeldgasse 24, A-8010 Graz
t: +43 316 873 - 4601
f: +43 316 873 - 4619
e: h.weissnar@tugraz.at
www.holzbauforschung.at

Subarea 2.2_MMSM 2.2.3 sfem_mat

Comparison of Methods of Approximate Verification Procedures for Cross Laminated Timber (Methodenvergleich approximativer Nachweisverfahren für Brettsper Holz)

Project finance / Funding agency

Bundesministerium für Wirtschaft, Familie und Jugend
Bundesministerium für Verkehr, Innovation und Technologie
Land Steiermark, Amt der Steiermärkischen Landesregierung,
Abteilung 14 - Wirtschaft und Innovation
Steirische Wirtschaftsförderungsgesellschaft m.b.H.

Project finance / Industry

Haas Fertigung Holzbauwerk Gesellschaft m.b.H. & Co. KG. / Großwilfersdorf (A)
Holzcluster Steiermark GmbH / Zeltweg (A)
Mayr-Melnhof Kaufmann Holding GmbH / Leoben (A)
Hasslacher Holding GmbH / Sachsenburg (A)

Project partners / Industry

Haas Fertigung Holzbauwerk Gesellschaft m.b.H. & Co. KG.
Dipl.-Ing. Robert A. Jöbstl
Holzcluster Steiermark GmbH
Dipl.-Ing. (FH) Erhard Pretterhofer
Mayr-Melnhof Kaufmann Holding GmbH
Dipl.-Ing. Thomas Lierzer
Hasslacher Holding GmbH
Dipl.-Ing. Georg Jeitler

Project partners / Science

holz.bau forschungs gmbh / Graz
Univ.-Prof. Dipl.-Ing. Dr. techn. Gerhard Schickhofer / Scientific Coordination and Management
Dipl.-Ing. Dr.techn. Thomas Bogensperger / Project processing MMSM 2.2.3
Dipl.-Ing. Gregor Silly / Project processing MMSM 2.2.3

Contents

1	Introduction	1
1.1	General introduction	1
1.1.1	Normative regulations	1
1.1.2	Product approvals given by producers of the cross laminated timber	2
2	Literature Study	3
2.1	Transversal-flexible-in-shear beams	3
2.1.1	Rod theory according to TIMOSHENKO	3
2.1.2	Further research (MOOSBRUGGER)	4
2.2	Flexibly connected beam	4
2.2.1	γ -process according to MÖHLER and SCHELLING	4
2.2.2	Flexibly connected beam according to PISCHL	5
2.3	Approximation method on the basis of coupled rods	6
2.3.1	Shear analogy method according to KREUZINGER	6
2.3.2	Further research (MESTEK)	7
3	Definition of the Verification Method	9
3.1	Transversal-flexible-in shear beams (TIMOSHENKO)	9
3.1.1	General introduction	9
3.1.2	Equations of flexible-in-shear beam theory	9
3.1.3	Bending stiffness of a 1D-slab strip made of CLT – K_{clt}	12
3.1.4	Shear stiffness of a 1D-slab strip made of CLT – S_{clt}	13
3.1.5	Bending- and shear stresses	15
3.1.6	Simplifications using the same material and the same layer thicknesses	16
3.1.7	Advantages and disadvantages of this method, comments	17
3.2	Flexibly connected bending members according to EN 1995-1-1	17
3.2.1	General introduction	17
3.2.2	General formulae according to EN 1995-1-1	19
3.2.3	Special features in the context of determining CLT	20
3.2.4	Advantages and disadvantages of this method, comments	22
3.3	Shear analogy method (SA-method)	23
3.3.1	General introduction	23
3.3.2	Equivalent stiffness	25
3.3.3	Axial stresses	26
3.3.4	Shear stress	26
3.3.5	Advantages and disadvantages of the method, comments	27
3.4	Higher calculation methods	27
3.4.1	General introduction	27
3.4.2	FE-panel (2D)	27
3.4.3	FE-panel (3D)	30
4	Reference Analyses	31
4.1	General introduction	31
4.1.1	Basic system	31
4.1.2	Variation and extension of the basic system	32
4.1.3	Selection of systems	34

4.2	System T1 – single-span girder exposed to uniform load	35
4.2.1	Transversal-flexible-in-shear beam (TIMOSHENKO)	35
4.2.2	Modified γ -process	39
4.2.3	Shear analogy method	42
4.2.4	Summary of results	44
4.3	System T2 – two-span girder exposed to uniform load ($L_1 = L_2$)	47
4.3.1	Dimensions of stiffness.....	47
4.3.2	Summary of the results.....	48
4.3.3	Analyses of the discretisation of the SA-method.....	52
4.3.4	Rounding down of the moment within the supporting area	54
4.4	System T3 – two-span girders exposed to uniform load (L_1, L_2)	58
4.4.1	Dimensions of stiffness.....	58
4.4.2	Summary of results	58
4.5	System T4 – three-span girder exposed to uniform load ($L_1 = L_2 = L_3$)	62
4.5.1	Dimensions of stiffness.....	62
4.5.2	Summary of results	62
4.6	System T5 – three-span girder exposed to uniform load (L_1, L_2, L_3) . .	66
4.6.1	Dimensions of stiffness.....	66
4.6.2	Summary of results	66
4.7	System T6 – three-span girder exposed to uniform load (L_1, L_2, L_3) . .	70
4.7.1	Dimensions of stiffness.....	70
4.7.2	Summary of results	70

5 Further Case Studies 75

5.1	General introduction.	75
5.1.1	5I – variation in the thickness of layers.....	75
5.1.2	7I – application of the γ -process	75
5.1.3	Examined systems and slab structures	76
5.2	System T1 – single-span girder exposed to uniform load ($t_L/t_Q = 2:1$) .	77
5.2.1	Dimensions of stiffness.....	77
5.2.2	Summary of results	77
5.3	System T1 – single-span girder exposed to uniform load ($t_L/t_Q = 1:2$) .	79
5.3.1	Dimensions of stiffness.....	79
5.3.2	Summary of results	79
5.4	System T2 – two-span girder exposed to uniform load ($t_L/t_Q = 2:1$) . .	81
5.4.1	Dimensions of stiffness.....	81
5.4.2	Summary of results	81
5.4.3	Rounding down of moment within the supporting area.....	84
5.5	System T2 – two-span girder exposed to uniform load ($t_L/t_Q = 1:2$) . .	86
5.5.1	Dimensions of stiffness.....	86
5.5.2	Summary of results	86
5.5.3	Rounding down of moment within the supporting area.....	89
5.6	System T1 – single-span girder exposed to uniform load (7I)	91
5.6.1	Determination of the γ -values according to SCHELLING	91
5.6.2	Dimensions of stiffness.....	92
5.6.3	Summary of results	92
5.7	System T2 – two-span girder exposed to uniform load (7I)	94
5.7.1	Determination of the γ -values according to SCHELLING	94

5.7.2	Dimensions of stiffness.....	95
5.7.3	Summary of results	96
6	Summary, Conclusion and Prospect	99
6.1	Summary.....	99
6.1.1	Stress peaks within the supporting area	99
6.1.2	Strength values within the supporting area	100
6.1.3	Bending stresses within abridged L/H-ratios	100
6.1.4	Commentary on the selection of the reference solution	101
6.1.5	Deflections	101
6.2	Conclusion and prospect	102
7	Bibliography	103
A	Appendix A	107
A.1	Solution according to SCHELLING in order to determine the γ -values . . .	107
A.1.1	Determination of stiffness.....	107
A.1.2	Determination of bending stress	108
A.2	2-, 3- and 4-part cross-section according to SCHELLING	109
A.2.1	2-part cross-section	109
A.2.2	3-part cross-section.....	110
A.2.3	4-part cross-section	112
A.3	Examples – flexibly connected bending members	114
A.3.1	2-part cross-section – example 1	114
A.3.2	2-part cross-section – example 2.....	116
A.3.3	2-part cross-section – example 3.....	118
A.3.4	3-part cross-section – example 1.....	120
A.3.5	3-part cross-section – example 2.....	122
A.3.6	3-part cross-section – example 3.....	124
A.3.7	3-part cross-section – example 4.....	126
A.3.8	3-part cross-section – example 5.....	128
B	Appendix B	131
B.1	System T1 „mod“ – single-span girder exposed to uniform load	131
B.1.1	Modified γ -process	131
B.1.2	Determination according to SCHELLING.....	134

1 Introduction

1.1 General introduction

Due to the shear-flexible transversal layers in the context of a one-dimensional design assumption, cross-laminated timber is regarded as beams with flexibly connected layers (cf. EN 1995-1-1, annex B). Generally, this flexibility can be attributed to the prevailing connectors. With regard to CLT the transversal layers show a continuous flexibility and the real connector (= adhesive layer) is seen as almost rigid.

In the context of CLT a manifold variety of design assumptions is used (cf. EN 1995, DIN 1052 and relevant approvals). The most renowned representatives to determine flexibly connected beams are the γ -process and the shear analogy method. This report provides an insight into the results of these design assumptions and analyses their differences as well as their correlations. In this regard it is worth mentioning that the focus of attention is on the stress analysis. Because of its significant importance regarding the deformation analysis, also the deflection is determined in the run-up. However, since there is a strong correlation between the prevailing processes, this issue will not be addressed any further.

The following chapters will provide an insight into the transversal-flexible-in-shear beam according to TIMOSHENKO, the γ -process and the shear analogy method. Added to this, in the context of six practical examples these methods will be compared with the 2D-FE panel solution, which is regarded as reference procedure.

1.1.1 Normative regulations

A verification procedure to determine flexibly connected bending members based on the gamma process (γ -process), which is also used in DIN 1052, chapter 8.6.2 [5], is provided in the annex B of Eurocode EN 1995-1-1 ([6], [21]).

With regard to the national annex of DIN EN 1995-1-1 [7], chapter NCI NA.5.6.3, a design assumption about *areas of flexibly connected layers* is included. Concerning this calculation the shear analogy method according to KREUZINGER, which is extended to laminar members, is used.

1.1.2 Product approvals given by producers of the cross laminated timber

With regard to CLT various verification procedures are described in European Technical Approval (ETA) and „allgemein bauaufsichtlichen“ approvals (Z). Table 1-1 provides an insight into renowned producers of CLT, their product approvals and the suggested design methods.

Tab. 1-1 Details concerning the design methods in the context of the prevailing product approvals

producer	product approvals	EN 1995-1-1	DIN 1052	notes
BINDER	ETA-06/0009 (DIBt)	O	O	
	Z-9.1-534 (DIBt)	O	O	
DECKER	Z-9.1-721 (DIBt)	O	O	
	ETA-11/0189 (DIBt)	O		mod. γ (EN)
FINNFOREST	ETA-10/0241 (DIBt)	O		mod. γ (EN)
	Z-9.1-501 (DIBt)	O	O	
HAAS	Z-9.1-680 (DIBt)	O	O	
HASSLACHER	Z-9.1-576 (DIBt)	O	O	
HMS	ETA-08/0242 (DIBt)	O		mod. γ (EN)
KLH	ETA-06/0138 (OIB)	O		mod. γ (CUAP)
	Z-9.1-482 (DIBt)	O	O	
MERKLE	ETA-11/0210 (DIBt)	O		mod. γ (EN)
MAYR-MELNHOF	ETA-09/0036 (OIB)	O		mod. γ (CUAP)
	Z-9.1-638 (DIBt)	O	O	
STEPHAN	Z-9.1-793 (DIBt)	O	O	
STORA ENSO	ETA-08/0271 (DIBt)	O		mod. γ (EN)
	Z-9.1-559 (DIBt)	O	O	

All product approvals, with the exception of European Technical Approval (ETA), which uses the modified γ -procedure explicitly in formula (cf. tab. 1-1, column notes), refer to EN 1995-1-1 and DIN 1052.

2 Literature Study

In the context of the rapid development of solid timber construction with cross laminated timber the question concerning an adequate verification procedure, especially with regard to the bending of these plates, is raised. In the following chapter, the existent verification procedures, which are relevant to the determination of cross laminated timber, will be presented.

The technical bending theory used in solid cross-section cannot be simply applied to CLT (assembled cross-sections). Based on the assumption that the structural behaviour of assembled beams is set between limiting case A, loosely placed single cross-sections, and limiting case B, rigidly connected single cross-sections, the deflections are determined with reduced second moments of area. Added to this, the edge stresses are calculated with reduced moments of resistance. The used reduction factors result from safety values added up to empirical- and experimental values, which are given by GRAF [12] and later on by GABER [11] (cf. [25]).

2.1 Transversal-flexible-in-shear beams

2.1.1 Rod theory according to TIMOSHENKO

In general, a beam is connected with a rigid-in-shear EULER-BERNOULLI-beam. In this context the following hypotheses are valid: Cross-sections, which are originally orthogonal to the beam axis, remain in this position after any deformation. In the course of a pure bending ($M = \text{constant}$) the cross-sections remain in a position which is perpendicular to the neutral axis since the deflection line corresponds to a circle and the cross-sectional area matches with the radius of the circle. The second hypothesis suggests that with regard to general loads, which are not free from transverse force, the cross-sections are supposed to remain plane. However, if shear stains are taken into consideration, the cross-sectional area is no longer perpendicular to the beam axis. This phenomenon is called the TIMOSHENKO-rod theory. The second hypothesis, which says that cross-sections are supposed to remain plane, is verified applying the previously mentioned TIMOSHENKO-rod theory. Instead of determining the transverse force as moment equilibrium by using the bending moments, as it is done in the context of the classic EULER-BERNOULLI-theory of beams, in the context of the TIMOSHENKO-rod theory, an own constitutive law which determines the transverse force by analysing the shear distortion and the shear stiffness is given careful consideration. As it was mentioned earlier, the TIMOSHENKO-rod theory presupposes plane cross-sections. However, since the cross-sections cannot remain plane because of the shear distortion, the relation between transverse force and rod-shear strain should be regarded as an approximation. In order to analyse the shear stiffness of the TIMOSHENKO-rod theory realistically, the shear correction factor κ is corrected.

Due to the fact that, with regard to cross laminated timber, the shear flexibility of transversal layers is a highly important aspect, it is advisable to take the TIMOSHENKO-rod theory, which includes shear strains, into consideration. Nevertheless, because of the high level of shear flexibility of the transversal layers, the assumption of plane cross-sections is challenged to a greater extent than in the context of a conventional calculation in which the TIMOSHENKO-rod theory is applied.

2.1.2 Further research (MOOSBRUGGER)

MOOSBRUGGER focuses on an elastic theory based determination of the bending stresses of laminated structures (1D) with flexible joints, which corresponds with the one-way 1D slab strip. In this regard, it is worth mentioning that the usual calculation method of rod structures is always based on making assumptions about unknown curvatures (in general curvatures are translational displacements along the longitudinal axis) in cross-sectional plane and on stressing them with certain functions along the rod (e.g. bending-deformation function $w(x)$ and its derivatives). However, in this example, the method is applied in reverse order: The supports are restricted to a simple beam and the loads are separated into Fourier series as function of the x-coordinate, while the curvatures in rod direction are regarded as unknown functions in the context of the cross-sectional coordinate z. Hence, by assuming the non-distortion in cross-sectional plane and these unknown functions of curvatures, the existent problem – the 3D-rod structure, which needs to be solved as a partial differential equation 2nd order coupled with each other in $u(x,y,z)$, $v(x,y,z)$ and $w(x,y,z)$, - is reduced to an ordinary differential equation within one series expansion. This approach, which yields significant results with regard to single-span girders under any loads, shows just a marginal difference compared with the conventional engineering calculation methods also analysed in this report.

2.2 Flexibly connected beam

2.2.1 γ -process according to MÖHLER and SCHELLING

Focussing on a practical calculation method, MÖHLER edits the differential relations of the flexibly connected beam and is able to define a reduction factor of the moment of inertia in the context of a rigid composite (cf. the previously mentioned limiting case B). MÖHLER does not reduce the whole moment of inertia, but only the "Steiner-terms" of the flexibly connected beam, which consists of combined single cross-sections. Nevertheless, his results can be exclusively applied up to three-part cross-sections (cf. [19] and [20]).

SCHELLING ([30], [31], [32]) extends the adaptability of this γ -process to an endless number of single cross-sections. Added to this, by using a Fourier series in the context of the load functions he is able to determine the state of stress and the state of deformation of members when being exposed to load. His results show that the influence of load and of the static system (dependence on length), which MÖHLER regarded as to be ignorable, are definitely relevant (cf. chap. 2.2.2).

In DIN 1052, *Teil 1: Holzbauwerke, Berechnung und Ausführung* of 1969 a design algorithm was developed on the basis of this calculation method in first approximation (only the first part of the Fourier series, which corresponds to a sine-approach to the load, is used). This algorithm can be found in the generally acknowledged rules of technology up to now (cf. e.g. [21], annex B).

Nevertheless, it needs to be mentioned that this approach should be exclusively used in the context of determining single-span girders exposed to sinusoidal load with continuously connected cross-sections in two- or three parts. Regarding actions which are similar to sinusoidal load, such as uniformly distributed loads, this calculation method can be still applied in order to get sufficiently accurate results.

Special form of the γ -process (modified γ -process)

The γ -process is defined in Eurocode *EN 1995-1-1, annex B: Nachgiebig verbundene Biegestäbe* and in *DIN 1052*. Based on this norm, AICHER ET AL use the analogy between the composite of two surface layers, which are connected by shear, and the composite of the in two parts flexibly connected cross-section in order to design a „modified γ -process“ to determine sandwich members (cf. [2], [1] and chap. 3.2.3).

2.2.2 Flexibly connected beam according to PISCHL

R. PISCHL [26] exactly solves the differential equations of continuous, flexibly connected bending members in the context of various load cases (uniform load and one, or rather two, single loads) and is able to define reduction factors of the effective moment of inertia and the effective moment of resistance with regard to the selected load constellations. These factors are based on the whole stiffness and not exclusively on the “Steiner-terms”, as it is the case with MÖHLER and SCHELLING. Regarding a practical calculation, in [27] PISCHL creates tables in order to determine these reduction factors of the effective moment of inertia and the effective moment of resistance exposed to the selected load constellations.

In DIN 1052 [4], the previously mentioned γ -process is defined on the basis of the sine-approach. PISCHL compares a single-span girder with three-part cross-section exposed to uniform load and single load with the results of γ -process ruled by standard and reaches the conclusion:

1. Being exposed to constant uniform load the variation of the maximum bending stress amounts to 1,6 % and the deflection amounts to 0,5 %.
2. Being exposed to a single load in midspan the level of variation is significantly higher. In the context of maximum bending stress the difference amounts to 49,4 % and concerning deflection the variation amounts to 2,4 %.

With regard to the second conclusion it needs to be mentioned that the maximum bending stress is defined at the web and not at the outer flanges. This phenomenon does not occur when being exposed to uniform- or to sinusoidal loads. The reason for this great difference is that in the context of the classic γ -process always just the

first wave $n = 1$ of the sine rule is taken into consideration. With a higher number of waves this error gets more and more insignificant.

In [28] the focus of attention is on the optimal order of connectors. It goes without saying that a reasonable order results in a considerable reduction of connectors, while the level of bending stress is just insignificantly higher.

2.3 Approximation method on the basis of coupled rods

2.3.1 Shear analogy method according to KREUZINGER

At the turn of the last millennium KREUZINGER (cf. [13], [14], [15], [16]) designed another calculation model called „shear analogy model“, which is also highly effective in the context of being implemented in framework programs. The suitability of this process in order to determine laminar flexibly connected structural members, which is also described in the annex of DIN 1052:2008 [5], is verified with regard to constant joint stiffness. This calculation method is also applied by BURGER [3] concerning the roof of the exposition in Hannover (cf. fig. 2-1).

In his dissertation SCHOLZ [33] examines not only the analysis model of the shear analogy in analytically closed form, but especially its applicability regarding stability problems.



Fig. 2-1 Roof of the exposition in Hannover (image left: [34], image right: [35])

As it was mentioned earlier, the shear analogy process is an approximation method. However, due to its widespread applicability in the context of framework programs, a manifold variety of systems with different loads can be determined. Figure. 2-2 shows the basic principle of this process to determine cross laminated timber.

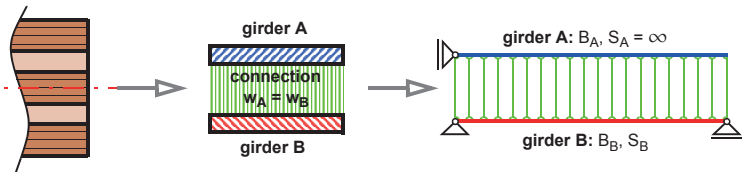


Fig. 2-2 Basic principle of the shear analogy process

2.3.2 Further research (MESTEK)

In chapter 3 of his dissertation [17] MESTEK compares the effective bending stiffness of the shear analogy method with the one of the γ -process. He analyses the single-span girder under sine load and concludes that the stiffness of symmetrical cross laminated timber slabs up to five layers corresponds to those of the exact solution according to the γ -process.

In chapter 4 Mestek determines the longitudinal- and the shear stresses of the systems „single-span girder exposed to axial single load“ (concentrated load introduction, cf. fig. 2-3) and „two-span girder exposed to constant uniform load“. Added to this, he compares them with the stresses of a FE-panel calculation. He concludes that there exist stress peaks at the edge stresses when longitudinal stresses are placed on the direct load application- and supporting areas. However, they subside quickly. The maximum deviation from the results of the panel calculation in the context of single-span girders amounts to below 2 % (cf. fig. 2-4).

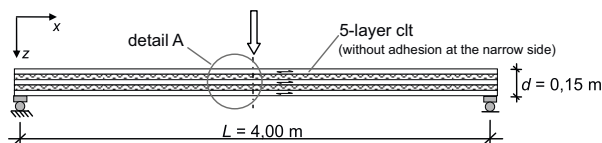


Fig. 2-3 System single-span girder exposed to axial single load (cf. [17], figure 4-1)

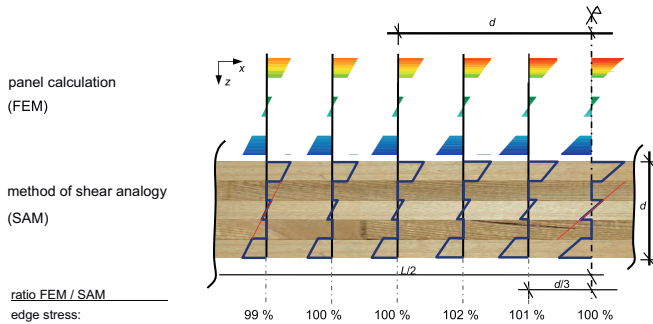


Fig. 2-4 Comparison of longitudinal stress distribution (cf. [17], figure 4-2)

When comparing the shear stresses it becomes evident that, with regard to the shear analogy method, there occur only stresses within the longitude layer of the load introduction (cf. fig. 2-5), which is seen as the result of the assumed shear rigidity of beam A (cf. fig. 2-2). Therefore, it can be said that the shear analogy method produces insufficient results in the context of direct load introduction- and supporting areas. Nevertheless, the deviation of rolling shear stress relevant for design amounts to ca. 3 % in a distance d from the load introduction.

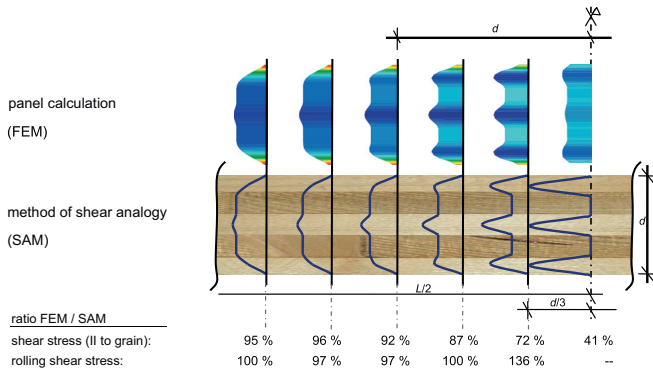


Fig. 2-5 Comparison of the rolling shear stress (cf. [17], figure 4-3)

Note: The approximately constant amount of shear stress in the context of the FE-solution is the result of the continuous load introduction provided within the points of the FE web.

3 Definition of the Verification Method

In this chapter the three mostly used standard methods to determine flexibly connected beams (flexible-in-shear beam theory according to TIMOSHENKO, γ -process, shear analogy method) will be defined in detail. Added to this, a model using the FE-method, which realistically describes the effects of flexibility and load introduction, will be presented. The results of this FE-determination will be used as reference values in comparison with other methods.

3.1 Transversal-flexible-in shear beams (TIMOSHENKO)

3.1.1 General introduction

The TIMOSHENKO-flexible-in-shear beam theory is based on the following assumptions:

1. In contrast to the BERNOULLI-beam, the cross-section is no longer perpendicular to the deformed rod axis.
2. Similar to the BERNOULLI-beam, the cross-section remains plane (NAVIER).
3. When being exposed to transversal force deformation, shear actions and, as a consequence, shear curvatures are produced, which are contrary to assumption 2. Hence, this contradiction leads to discrepancies in determining the shear stress and the shear stiffness.
4. The concept of the shear adjustment factor κ corrects the error in the shear stiffness of elastic behavior.
5. The process of determining the shear stress in cross-section is based on the local longitudinal equilibrium with bending stresses and, consequently, is identical with the one regarding the BERNOULLI-beam. Hence, this phenomenon is also called secondary shear stresses.

In the following section a brief overview of equations which define flexible-in-shear beams will be given.

3.1.2 Equations of flexible-in-shear beam theory

Kinematics of the beam (2D)

The beam of fig. 3-1 is exposed to displacement $w(x)$ in transversal direction (deflection) and to cross-sectional rotation $\beta(x)$, which is independent from the former displacement (cf. fig. 3-1).

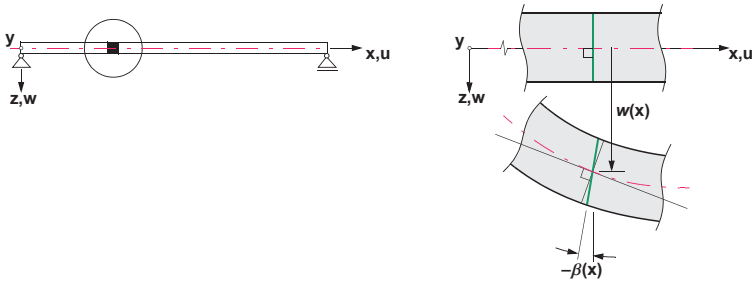


Fig. 3-1 Displaced and rotated beam

The displacements u and w of each rod point are defined by a product ansatz. In this regard, the first factor can be seen as the longitudinal axis x of the rod with the functions $w(x)$ and $\beta(x)$, while the second factor describes the position in cross-section (z -coordinate of the cross-sectional rotation, or rather „1“ of the deflection). Based on the assumed displacements, the deformation of the rod (bending deformation, transverse force deformation) is determined.

$$u(x,z) = z \cdot \beta(x)$$

$$w(x,z) = w(x)$$

$$\varepsilon_x(x,z) = \frac{\partial u}{\partial x} = z \cdot \beta'(x)$$

$$\gamma_{xz}(x,z) = \frac{\partial u}{\partial z} + \frac{\partial w}{\partial x} = \beta(x) + w'(x)$$

Kinetics and constitution

Due to the underlying assumptions concerning the z -direction, the internal forces M_y and Q_z in cross-section can be determined by integrating the stresses σ_x and τ_{xz} .

$$\sigma_x = E(z) \cdot \varepsilon_x(x,z) = E(z) \cdot z \cdot \beta'(x)$$

$$\tau_{xz} = G(x) \cdot \gamma_{xz}(x,z) = G(z) \cdot (\beta(x) + w'(x))$$

$$M_y = \int_A \sigma_x \cdot z \cdot dA = E(z) \cdot \int_A z^2 \cdot dA \cdot \beta'(x) = K_{clt} \cdot \beta'(x)$$

$$Q_z = \int_A \tau_{xz} \cdot dA = G(z) \int_A dA \cdot (\beta(x) + w'(x))$$

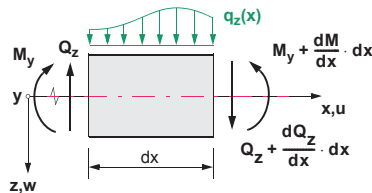
In the context of the equations of the bending moment M_y and the transverse force Q_z the two dimensions of CLT-stiffness, the bending stiffness K_{clt} and the shear stiffness GA , need to be taken under consideration. The longitudinal equilibrium of the shear stresses, which are determined by using the displacement formulation, does not correlate with the one of the bending stresses. As a consequence, this solution for distributing shear stresses needs to be obtained. Hence, the determined shear stiffness GA is inaccurate and needs to be corrected using the shear adjustment factor κ to S_{clt} (cf. chap. 3.1.4). As a result, the equation of transverse force Q_z is modified to:

$$Q_z = \int_A \tau_{xz} \cdot dA \equiv S_{clt} \cdot (\beta(x) + w'(x))$$

$$\text{with } S_{clt} = \frac{GA}{\kappa}$$

Equilibrium

On the basis of the determined internal forces the conditions of equilibrium can be defined.



$$\Sigma V = 0$$

$$q_z(x) \cdot dx + \frac{dQ_z}{dx} \cdot dx = 0 \Rightarrow Q'_z + q_z(x) = 0$$

$$\Sigma M = 0$$

$$M_y \cdot dx - Q_z \cdot dx = 0 \Rightarrow M'_y - Q_z = 0$$

Differential equations of the flexible-in-shear beam

A continuous vertical load $q_z(x)$ forms the load.

Vertical equilibrium

$$Q_z = S_{clt} \cdot (\beta(x) + w'(x)) \Rightarrow$$

$$Q'_z = S_{clt} \cdot (\beta'(x) + w''(x))$$

$$S_{clt} \cdot (\beta'(x) + w''(x)) = -q_z(x)$$

Moment equilibrium

$$M_y = K_{clt} \cdot \beta'(x) \Rightarrow$$

$$M_y' = K_{clt} \cdot \beta''(x)$$

$$K_{clt} \cdot \beta''(x) - S_{clt} \cdot (\beta(x) + w'(x)) = 0$$

As a consequence, they result in a system of two coupled differential equations of 2nd order.

The following sections will describe the determination of the bending stiffness K_{clt} and the shear stiffness S_{clt} of a 1D-slab strip, which are of crucial importance in the context of calculating the stresses and deflections as well as the internal forces of statically undefined systems.

3.1.3 Bending stiffness of a 1D-slab strip made of CLT – K_{clt}

If the assumption of a consistency in layers forms basis of the material parameters, the bending stiffness can be regarded as the sum of the prevailing dimensions of eigen stiffness and the so-called „Steiner-terms“. In tab. 3-1 the decomposition of a 5-layer cross laminated timber-slab is presented.

$$K_{clt} = \sum (E_i \cdot I_i) + \sum (E_i \cdot A_i \cdot e_{s,i}^2)$$

Tab. 3-1 Determination of the bending stiffness of a 5-layer cross laminated timber slab in tabular form

ES	α	E	t	e_s	Component of eigen inertia	Steiner-term
5	0	E_0	$t_5 = t_1$	$e_{s,1}$	$E_0 \cdot b \cdot t_1^3/12$	$E_0 \cdot b \cdot t_1 \cdot e_{s,1}^2$
4	90	E_{90}	$t_4 = t_2$	$e_{s,2}$	$E_{90} \cdot b \cdot t_2^3/12$	$E_{90} \cdot b \cdot t_2 \cdot e_{s,2}^2$
3	0	E_0	t_3	$e_{s,3}$	$E_0 \cdot b \cdot t_3^3/12$	0
2	90	E_{90}	t_2	$e_{s,2}$	$E_{90} \cdot b \cdot t_2^3/12$	$E_{90} \cdot b \cdot t_2 \cdot e_{s,2}^2$
1	0	E_0	t_1	$e_{s,1}$	$E_0 \cdot b \cdot t_1^3/12$	$E_0 \cdot b \cdot t_1 \cdot e_{s,1}^2$
					$K_{clt} = \sum \text{Component of eigen inertia} + \sum \text{Steiner-term}$	

- gravity centre of cross section
- gravity centre of individual layers

with:

$t_1 = t_5$ and $t_2 = t_4$

$e_{s,1} = e_{s,5}$ and $e_{s,2} = e_{s,4}$

$e_{s,3} = 0$

3.1.4 Shear stiffness of a 1D-slab strip made of CLT – S_{clt}

It is absolutely necessary to take the shear deformation into consideration in the context of cross laminated timber, since the dimension of the shear deformation S_{clt} is fairly small due to the shear-flexible transversal layers. In this regard, it is worth mentioning that the shear deformation amounts up to 20 % of the total deformation. Because there exists no exact formulation of shear deformation it needs to be determined directly. In general, the basic shear stiffness S_{clt} is defined as the sum of the products of the dimensions of the individual layers combined with the prevailing shear modulus G . The next step is to divide the basic shear stiffness S_{clt} by the so-called shear adjustment factor κ .

$$S_{clt} = \frac{\sum (G_i \cdot b \cdot t_i)}{\kappa} = \frac{\sum (G_i \cdot A_i)}{\kappa}$$

Shear adjustment factor κ

The shear adjustment factor κ is defined by using the following integral which can be derived from the principle of virtual forces.

$$\frac{\kappa}{\sum_i G_i \cdot t_i} = \frac{1}{K_{clt}^2} \cdot \int_{z = -\frac{t_{clt}}{2}}^{z = \frac{t_{clt}}{2}} \left[\int_{s = -\frac{t_{clt}}{2}}^{s = z} E(s) \cdot s \cdot ds \right]^2 \cdot \frac{dz}{G(z)}$$

The shear adjustment factor κ correlates with the shear stiffness ratio G_{II}/G_R and in the context of the same layer thicknesses can be defined approximately by the following formula and tab. 3-2:

$$\kappa_{(G_{II}/G_R)} \approx \kappa_{10} + \frac{\kappa_{14.4} - \kappa_{10}}{4,4} \cdot \left(\frac{G_{II}}{G_R} - 10 \right)$$

Table 3-2 shows all shear adjustment factors regarding a relation between shear stiffness and rolling shear stiffness of $G_{II}/G_R = 10$ ($= \kappa_{10}$), $G_{II}/G_R = 13,8$ ($= \kappa_{13,8}$) and $G_{II}/G_R = 14,4$ ($= \kappa_{14,4}$).

Tab. 3-2 Shear adjustment factors κ_{10} , $\kappa_{13,8}$ and $\kappa_{14,4}$ of cross laminated timber with the same layer thicknesses of various shear modulus ratios.

number of layers #	main load direction		
	κ_{10}	$\kappa_{13,8}$	$\kappa_{14,4}$
3	4,854	6,468	6,723
5	4,107	5,441	5,652
7	3,873	5,116	5,313

The relation between shear stiffness and rolling shear stiffness of $G_{II}/G_R = 10$ can be found in renowned codes (DIN 1052 [5], EN 338 [22]). In relevant approval documents of CLT, such as ETA 06/0009 [8] or ETA 06/0138 [9], the stiffness $G_{II} = 650 \dots 690 \text{ N/mm}^2$ can be found as direct value. Added to this, it needs to be referred to the features of stiffness of CLT (e.g. Z-9.1-680 [36]). Consequently, the values of DIN 1052 [5], or rather ON EN 1194 [23] with $G_{II} = 720 \text{ N/mm}^2$ (GL 24h) gain importance. With regard to the rolling shear modulus G_R , usually a constant value of 50 N/mm^2 is declared. These values result in the maximum ratio of shear modulus $G_{II}/G_R = 14,4 (= 720/50 \text{ N/mm}^2)$, which is presented in tab. 3-2.

Lay-up parameter

In tab. 3-2 the shear adjustment factor concerning constant ratios of layer thickness is declared. However, this factor depends on the relation between the thicknesses of transversal- and longitudinal layers. This relation is often defined as lay-up parameter t_L/t_Q . With regard to slabs with different layer thickness, this lay-up parameter is determined by taking the mean of the thicknesses of longitudinal- and transversal layers $t_{L,mean}$ and $t_{Q,mean}$ (cf. fig. 3-2).

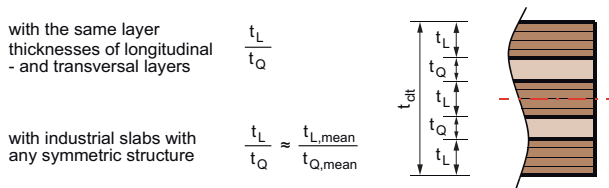


Fig. 3-2 Definition of the lay-up parameter t_L/t_Q

Figure 3-3 shows the shear adjustment factors κ in the context of stresses in main direction of 5 layer CLT panels. The lay-up parameter t_L/t_Q amounts from 0.5 to 2.0.

This image presents all shear adjustment factors κ of CLT panels in demand. Based on the ratios of shear modulus G_{II}/G_R , which are granted in the prevailing approvals, the factors of 64 types of panels (5 layer) are determined.

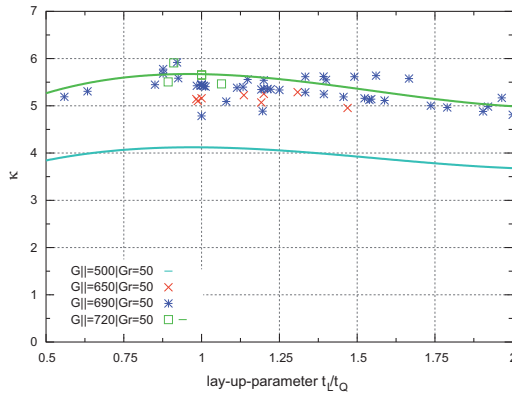


Fig. 3-3 Shear adjustment factors κ of 5 layer CLT panels varying in t_L/t_Q

3.1.5 Bending- and shear stresses

Regarding the determination of stresses of cross laminated timber it is of vital importance to take the laminated structure and the grain orientation rotated by 90° of adjoining layers into consideration. In the context of a 5 layer CLT panel, this results in the bending- shear stresses presented in fig. 3-4. It needs to be mentioned that the high level of orthotropy between the E-modulus (E_0) and the one transverse to grain direction (E_{90}) has already been taken into account. In practical terms, this implies that the bending stress being exposed to the transversal layers is fairly small. Therefore, E_{90} is regarded as approximately 0.

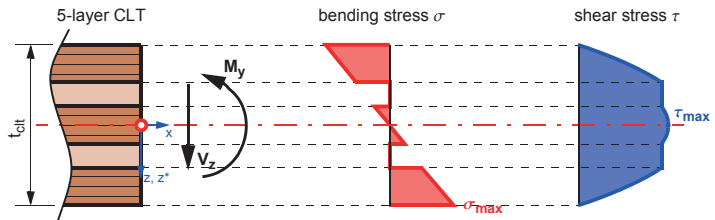


Fig. 3-4 Stresses of CLT exposed to transverse force bending ($E_{90} = 0$)

Bending stress

$$\sigma(x, z) = \frac{M_y(x)}{K_{clt}} \cdot z \cdot E(z) \qquad \sigma_{max} = \frac{M_{max}}{K_{clt}} \cdot \frac{t_{clt}}{2} \cdot E$$

Shear stress

$$\tau(z) = \frac{V_z(x) \cdot \int_{-t_{clt}/2}^z (E(z^*) \cdot z^* \cdot b \cdot dz^*)}{K_{clt} \cdot b}$$

z ... distance between the examined shear stress joint and the gravity centre [mm]

$$\tau_{max} = \frac{V_{max} \cdot \sum (S \cdot E_i)}{K_{clt} \cdot b} = \frac{V_{max} \cdot \sum (E_i \cdot A_i \cdot e_{s,i})}{K_{clt} \cdot b}$$

S ... static moment [mm³]

3.1.6 Simplifications using the same material and the same layer thicknesses

Based on the assumption that $E_{90} = 0$ and $t_i = t$, the dimensions of bending- and shear stiffness can be simplified as follows:

3I

$$K_{clt} = \sum (I_i \cdot E_i) + \sum (A_i \cdot E_i \cdot e_{s,i}^2) = \frac{13}{6} \cdot E_{\parallel} \cdot b \cdot t_i^3$$

$$S_{clt} = \frac{\sum (G_i \cdot b \cdot t_i)}{\kappa_{3s}} = \frac{b \cdot t_i \cdot (2 \cdot G_{\parallel} + G_R)}{\kappa_{3s}}$$

5I

$$K_{clt} = \sum (I_i \cdot E_i) + \sum (A_i \cdot E_i \cdot e_{s,i}^2) = \frac{33}{4} \cdot E_{\parallel} \cdot b \cdot t_i^3$$

$$S_{clt} = \frac{\sum (G_i \cdot b \cdot t_i)}{\kappa_{5s}} = \frac{b \cdot t_i \cdot (3 \cdot G_{\parallel} + 2 \cdot G_R)}{\kappa_{5s}}$$

7I

$$K_{clt} = \sum (I_i \cdot E_i) + \sum (A_i \cdot E_i \cdot e_{s,i}^2) = \frac{61}{3} \cdot E_{\parallel} \cdot b \cdot t_i^3$$

$$S_{clt} = \frac{\sum (G_i \cdot b \cdot t_i)}{\kappa_{7s}} = \frac{b \cdot t_i \cdot (4 \cdot G_{\parallel} + 3 \cdot G_R)}{\kappa_{7s}}$$

3.1.7 Advantages and disadvantages of this method, comments

- [+] It can be extended to slabs (plane plate structures) and to 2D-slab theory (REISSNER-MINDLIN slab theory) without any effort.
- [+] Being aware of K_{clt} and S_{clt} it is perfectly suited to manual calculation using the flexibility method.
- [+] The rod flexible-in-shear is included in most of the software programs of structural analysis. Consequently, it is fairly easy to put this method into practice.
- [+] It can be applied in the context of any systems or loads.
- [+] Regarding the determined deflections it needs to be mentioned that they are approximate values. However, in practical terms it can be said that their accuracy is sufficient when being confronted with usual L/H relations.
- [-] In the context of individual loads and internal supporting points of continuous beams a significant deviation of the determined bending stress within the direct area of load application is identified (cf. chapter 4).

3.2 Flexibly connected bending members according to EN 1995-1-1 (γ -process)

3.2.1 General introduction

The γ -process is used in order to determine continuously connected bending members exposed to any loads. Nevertheless, it is just possible to exactly determine arbitrary loads by applying approaches of Fourier series. In practical terms it can be said that solving the first wave $n = 1$ (sinusoidal load) usually produces sufficient results. In the following section the γ -process corresponds with the norms in Eurocode 5 ([6], [21]) and in SCHELLING [31].

The γ -process is based on the following assumptions (cf. [25]):

1. The bending theory is relevant for all cross-sections. This implies that certain assumptions, such as BERNOULLI beam, HOOK's law and linear stress distribution across the cross-section, need to be made (NAVIER).
2. Deflection as a consequence of shear stress is not taken into consideration.
3. Affine deflection curves of individual beams are presupposed. Hence, the state of deformation can be defined by shifting the gravity centre of the total cross-section.
4. The total cross-section is symmetric concerning this layer, which is exposed to load. This results in the definition of an uniaxial bending.
5. The single cross-sections are connected on the basis of a continuous transmis-

sion of shear with constant shear stiffness. If this is done by using mechanical connectors, such as steel dowel pins and sloped screwed connections, these discrete connectors are regarded as divided up longitudinally between their fixing points.

6. Regarding the structural material of the individual cross-sections and the connectors, a fully elastic structural- and ductile behaviour is supposed.
7. The friction within the connection joints is ignored.

However, it needs to be mentioned that the norms in Eurocode 5 ([6], [21]) slightly differ from SCHELLING [31]. SCHELLING, for example, presents a linear equation system in order to determine the flexibility coefficient (γ -values of each layer). As point of reference he declares the geometric gravity centre, which is based on the total area of the individual cross-sections.

With regard to multipart cross-sections there exists a relatively extensive amount of expressions related to the geometric centre line, which justifies the reference to the effective centre line at least on the subject of manual calculations of types of cross-sections ruled by the standards. This formulation is used in EN 1995-1-1 and in its predecessors, such as in DIN 1052. The effective centre line can also be seen as mechanical centre line since its shear stresses are at the maximum level. Nevertheless, focussing on a completely symmetric cross-section in two parts two solutions of equal importance concerning the position of the mechanical gravity centre are possible. In concrete terms, this means that these positions can be defined above and below this geometric gravity centres (cf. chap. A.3, ex. 1). On the subject of a systematic programming SCHELLING's definition appears to be favourable, whereas in the context of manual calculation the norms of Eurocode 5 are desirable. Added to this, it is of crucial importance to be aware of the sign of the distance a_2 when applying Eurocode 5. Undoubtedly, the signs of the distances a_i ($i = 1, 2, \dots n$) can be determined in a clearer and more systematic way when making use of SCHELLING's approach (cf. appendix A).

The following image provides an insight into both options regarding the determination of the centre line – geometric centre line (SCHELLING) and effective centre line (EC5) – and is taken from [25]:

reference axis	geometric centre line	effective centre line
γ_1	$\frac{I}{I + \frac{\pi^2 \cdot s \cdot EA_1 \cdot a_1}{l^2 \cdot K \cdot a_{1,2}}}$	$\frac{l}{I + \frac{\pi^2 \cdot s \cdot EA_1}{l^2 \cdot K}}$
γ_2	$\frac{l}{I + \frac{\pi^2 \cdot s \cdot EA_2 \cdot -a_2}{l^2 \cdot K \cdot a_{1,2}}}$	1

Fig. 3-5 γ -values of the geometric- and effective centre lines (cf. [25])

For the time being, the focus of interest is on the approach according to annex B of

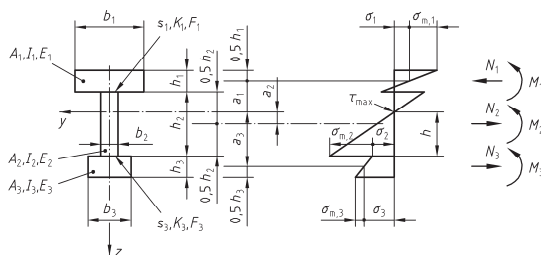
EN 1995-1-1 for flexibly connected bending members. This informative annex describes the renowned γ -process and after a slightly modification can be applied to determine CLT (modified γ -process).

Further information concerning the previously mentioned ambiguous position of the gravity centre within a symmetric cross-section in two parts and the sign of a_2 will be provided in appendix A, in which SCHELLING's approach is described in detail. There examples of rods in two and three parts will be compared in terms of SCHELLING's method and in terms of the norms of Eurocode 5.

Regardless the reference axis it becomes evident that the flexibility factors depend on the span. With a greater system length and consistent conditions an increase of the effective bending stiffness can be identified. After having determined the γ -values of the individual cross-sections, all the other essential values, such as axial-, shear- and connector stresses as well as deflections can be calculated.

3.2.2 General formulae according to EN 1995-1-1

type A



type C

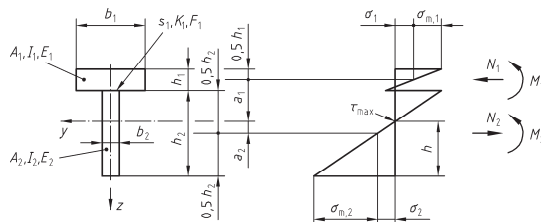


Fig. 3-6 Types of cross-sections according to EN 1995-1-1, annex B

$$(EI)_{ef} = \sum_{i=1}^3 (E_i \cdot I_i + \gamma_i \cdot E_i \cdot A_i \cdot a_i^2)$$

$$A_i = b_i \cdot h_i$$

$$I_i = \frac{b_i \cdot h_i^3}{12}$$

$$\gamma_2 = 1$$

$$\gamma_{i(1,3)} = \frac{1}{1 + \frac{\pi^2 \cdot E_i \cdot A_i \cdot s_i}{K_i \cdot l^2}}$$

$$a_2 = \frac{1}{2} \cdot \frac{\gamma_1 \cdot E_1 \cdot A_1 \cdot (h_1 + h_2) - \gamma_3 \cdot E_3 \cdot A_3 \cdot (h_2 + h_3)}{\sum_{i=1}^3 \gamma_i \cdot E_i \cdot A_i}$$

Note: According to EN 1995-1-1, 4/5 of the span width can be used for the length l with regard to continuous beams.

The distance a_2 is always positive within type C. This implies that the zero point of stress is always situated above the geometric gravity centre of area A_2 . On the subject of type A not only a positive, but also a negative value of a_2 is possible. Concerning the latter option it can be said that a_2 has a negative value, if the determined zero point of stress is situated below the gravity centre of area A_2 .

$$\sigma_i = \frac{N_i}{A_i} = \frac{M}{(EI)_{ef}} \cdot \gamma_i \cdot E_i \cdot a_i$$

$$\sigma_{m,i} = \frac{M_i}{W_i} = \frac{M}{(EI)_{ef}} \cdot \frac{E_i \cdot h_i}{2}$$

$$\tau_{2,max} = \frac{V}{(EI)_{ef}} \cdot \frac{\gamma_3 \cdot E_3 \cdot A_3 \cdot a_3 + 0,5 \cdot E_2 \cdot b_2 \cdot h^2}{b_2}$$

$$\tau_r = \frac{V}{(EI)_{ef}} \cdot \frac{\gamma_3 \cdot E_3 \cdot A_3 \cdot a_3}{b_2}$$

3.2.3 Special features in the context of determining CLT

In order to be able to apply the previously mentioned methods in the context of a verification of cross laminated timber, several adaptations are necessary. Hence, this approach is called „*modified γ -process*“.

Adaptation of cross-sections

3 layer-, or rather 5 layer CLT panels (cf. fig. 3-7) can be deduced from cross-sections in two- or three parts (type C and type A, cf. fig. 3-6). Thus, the flexibility of the connection joints (s_i/K_i) are substituted with shear-flexible transversal layers of cross laminated timber ($h_{s12}/(G_{R,i} \cdot b_i)$). The width of the cross-section b_i of the pre-venailing layers is supposed to be constant within the determination of CLT ($b_i = b$).

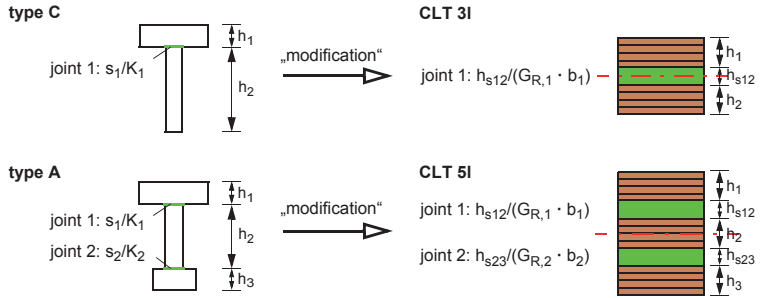


Fig. 3-7 Adaptation of cross-section of 3- and 5-layered CLT.

The formulae according to EN 1995-1-1, annex B can be adapted as follows:

$$\gamma_{i(1,3)} = \frac{1}{1 + \frac{\pi^2 \cdot E_i \cdot A_i \cdot s_i}{K_i \cdot l^2}} = \frac{1}{1 + \frac{\pi^2 \cdot E_i \cdot h_i \cdot b \cdot h_{si}}{G_{90} \cdot b \cdot l^2}}$$

$$\gamma_{i(1,3)} = \frac{1}{1 + \frac{\pi^2 \cdot E_i \cdot h_i \cdot h_{si}}{G_{90} \cdot l^2}}$$

Simplification using the same material and the same layer thickness

$$h_1 = h_2 = h_3 = h \text{ and } h_{s12} = h_{s23} = h$$

3-layered CLT (cf. appendix B)

$$\gamma_1 = \frac{1}{1 + \frac{\pi^2 \cdot E_0 \cdot h^2}{G_{90} \cdot l^2}} \quad \gamma_2 = 1$$

$$a_2 = \frac{\gamma_1 \cdot E_1 \cdot A_1 \cdot \left(\frac{h_1 + h_2}{2} + h_{s12} \right)}{\sum_{i=1}^2 \gamma_i \cdot E_i \cdot A_i} \quad a_1 = \frac{h_1}{2} + h_{s12} + \frac{h_2}{2} - a_2 = 2h - a_2$$

5-layered CLT (cf. chap. 4.2.2)

$$\gamma_1 = \gamma_3 = \frac{1}{1 + \frac{\pi^2 \cdot E_0 \cdot h^2}{G_{90} \cdot l^2}} \quad \gamma_2 = 1$$

$$a_2 = \frac{\gamma_1 \cdot E_1 \cdot A_1 \cdot \left(\frac{h_1 + h_2}{2} + h_{s12} \right) - \gamma_3 \cdot E_3 \cdot A_3 \cdot \left(\frac{h_2 + h_3}{2} + h_{s23} \right)}{\sum_{i=1}^3 \gamma_i \cdot E_i \cdot A_i} = 0$$

$$a_1 = a_3 = \frac{h_1}{2} + h_{s12} + \frac{h_2}{2} - a_2 = 2 \cdot h$$

3.2.4 Advantages and disadvantages of this method, comments

- [+] It is regarded as an established approach, which is applied in Eurocode 5 as well as in almost all product approvals of CLT.
- [-] This method does not only suit to manual calculation on the basis of equations in annex B of EC 5, but also to flexible-in-shear rod theory. However, when being compared, it needs to be mentioned that (a) concerning the former calculation method this approach takes significantly more effort and (b) especially in the context of continuous beams the determination of the γ -value is ambiguous. Added to this, with regard to different span width it might be the case that there occur fields without a moment zero point. Hence, the use of this equivalent length of 4/5 of the span width suggested by the norm is highly dubious (cf. chapter 4.6).
- [-] The standardised approach (effective centre line) can be only applied within 3 layer- or 5 layer CLT. It is highly advisable to make use of the general equations of SCHELLING when being confronted with more layers.
- [-] Although SCHELLING's equations are valid for all systems and loads in general, a single-span girder being exposed to sinusoidal load is needed in practical terms. Needless to say, this has a simplifying effect on the equations, however uniform loads can be just approximately determined. As a consequence, this method shows tremendously high deviations within individual loads and internal supports of continuous beams (cf. [27]).

- [-] Transferring the flexible-in-shear rod theory to a 2D-plate structure causes severe problems.

3.3 Shear analogy method (SA-method)

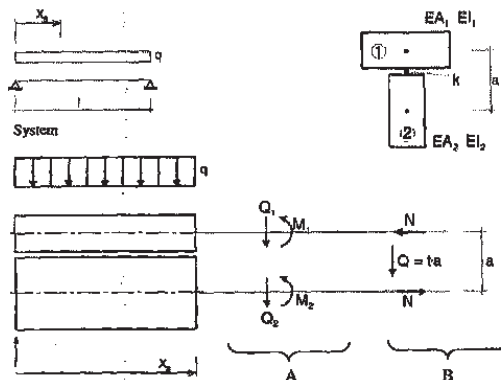
3.3.1 General introduction

The shear analogy method is based on the following assumptions:

1. The structural behaviour is represented by two beams which are coupled by deflection.
2. The bending stiffness of beam A corresponds with the moments of inertia of the prevailing lamellas, whereas the one of beam B corresponds with the “Steiner-terms”. This concept was also applied on the subject of the γ -process.
3. Beam A is supposed to be rigid in shear, while the shear flexibility of beam B results from the flexibility of the transversal layers.

With regard to beams with flexibly connected transversal layers, the most important problems can be seen in connecting the transmission of shear force and in sticking together the individual cross-sections. Generally, it can be said that the shear flexibility is based to a great extent on the shear connection. Concerning the deformation w perpendicular to the rod axis it is the case that all the cross-sectional members are exposed to the same amount of deformation w .

Figure 3-8 shows a beam consisting of two flexibly connected transversal layers (beam A and B) with cross-section, stresses and internal forces.



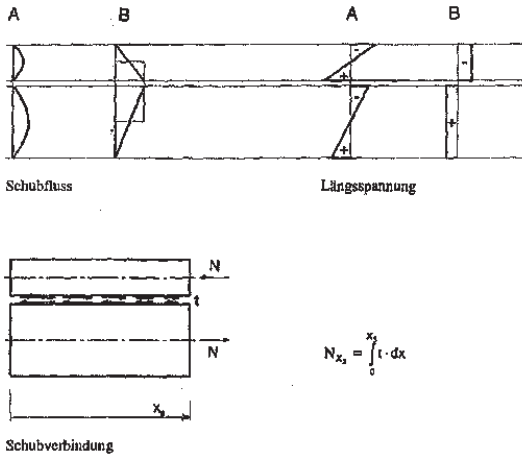


Fig. 3-8 Shear analogy method, taken from [15]

Die Beanspruchung A folgt aus der Eigensteifigkeit der beiden Trägerteile, die Beanspruchung B aus der Schubverbindung. [...] Aus der Überlegung, dass die Nachgiebigkeit der Verbindung durch eine Schubnachgiebigkeit ersetzt wird, könnte der Name "Schubanalogie" entstanden sein. Besteht keine Schubverbindung, muss die Einwirkung über die Beanspruchung A abgetragen werden; ist die Schubverbindung unendlich steif, so erfolgt die Lastabtragung über den Gesamtquerschnitt nach der technischen Biegetheorie. (Zitat aus [15])

[Stress A is based on the eigen stiffness of both elements of the beam, while stress B is based on the shear connection. [...] Based on the assumption that the flexibility of the connection is substituted by shear flexibility, the term „shear analogy“ is coined. However, if there exists no shear connection, the action needs to be transferred to stress A. On the other hand, it can be said that if the shear connection is endlessly stiff, the load transfer takes place via the total cross-section according to the technical bending theory.]

Consequently, in the context of the SA-method the determination of beams based on two flexibly connected cross-sectional members is reduced to a system of two beams (A and B), which are coupled by the common function of deflection $w(x)$. The cross-sectional rotations of the rigid-in-shear beam A are equivalent to the value $-w'(x)$, which again corresponds with the classic BERNOULLI-theory of rod. The cross-sectional rods of the flexible-in-shear beam B form a degree of freedom $\varphi(x)$.

This approach and, consequently, these equations of the shear analogy perfectly correspond with the γ -process in the context of symmetric cross-sections in two- or three parts. Additionally, this can be, at least approximately, assumed for all other cross-sectional members. Hence, the shear analogy method is regarded as an approximate approach, or rather as an approximate solution. Nevertheless, it should be mentioned that loads and arbitrary static systems cannot be defined accurately.

If an analytical solution is sought, a coupled system of differential equations of fourth order with $w(x)$ and of second order with $\varphi(x)$ needs to be solved. In practical terms, however, instead of an analytical solution, KREUZINGER suggests an EDP-assisted calculation of two bending members discretely coupled in deflection. As it was said before, in practical terms the results obtained with this method are sufficient. Regarding the discretisation it can be said that this phenomenon has just an insignificant effect on single-span girders exposed to uniform load. Merely on the subject of individual loads and internal supporting points of continuous beams a finer discretisation is desirable.

The shear analogy method (SA-method) is described in *DIN 1052, annex D.3 – Flächen aus nachgiebig miteinander verbundenen Schichten* in detail.

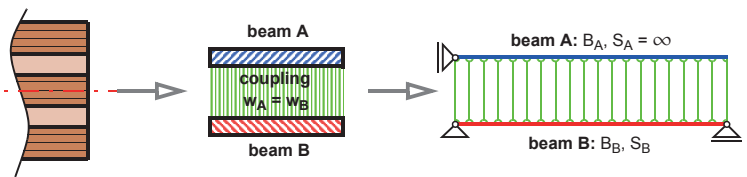


Fig. 3-9 Basic principle of SA-method

3.3.2 Equivalent stiffness

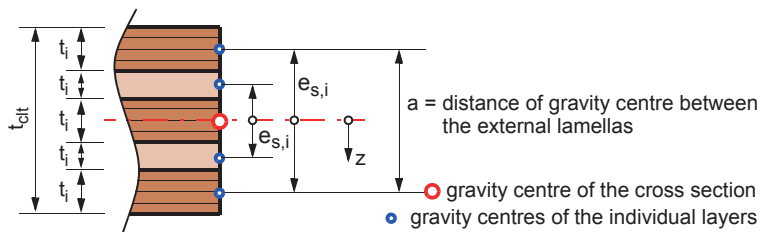


Fig. 3-10 Definition and gravity centres to determine the equivalent stiffness

Beam A: bending stiffness B_A resulting from the inherent shares of inertia

$$B_A = \sum E_i \cdot I_i = \sum E_i \cdot \frac{b \cdot t_i^3}{12} \quad S_A = \infty$$

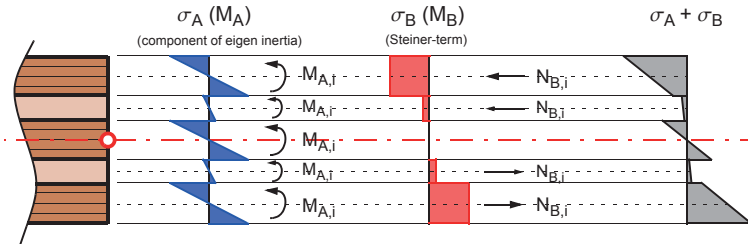
Beam B: bending stiffness B_B resulting from "Steiner-terms" and shear stiffness S_B

$$B_B = \sum E_i \cdot A_i \cdot e_{s,i}^2 = \sum E_i \cdot b \cdot t_i \cdot e_{s,i}^2$$

$$S_B = \frac{a^2}{\frac{1}{b} \cdot \left(2 \cdot G_1 + \sum_{i=2}^{n-1} \frac{t_i}{G_i} + 2 \cdot G_n \right)}$$

3.3.3 Axial stresses

Stresses based on the moments M_A (beam A) and M_B (beam B)



$$M_{A,i} = M_A \cdot \frac{E_i \cdot I_i}{B_A}$$

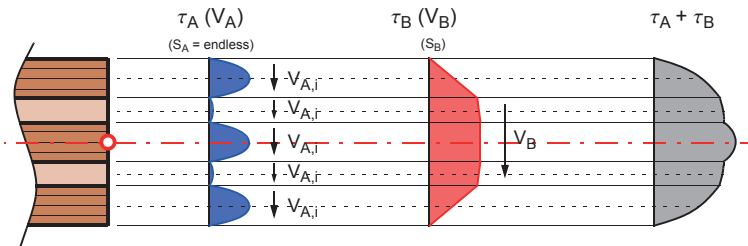
$$\sigma_{A,i} = \pm \frac{M_{A,i}}{I_i} \cdot z_i = \pm \frac{M_A}{B_A} \cdot E_i \cdot z_i$$

$$N_{B,i} = \pm M_B \cdot \frac{E_i \cdot A_i \cdot e_{s,i}}{B_B}$$

$$\sigma_{B,i} = \pm \frac{N_{B,i}}{A_i} = \pm \frac{M_B}{B_B} \cdot E_i \cdot e_{s,i}$$

Note: In the context of the bending stresses, in the illustration above the E-modulus perpendicular to grain (E_{90}) is taken into consideration. However, as it was mentioned in chapter 3.1.5, on the subject of CLT it is highly advisable to approximately pinpoint E_{90} to the value 0.

3.3.4 Shear stress



$$V_{A,i} = V_A \cdot \frac{E_i \cdot I_i}{B_A}$$

$$\tau_{A,i} = -V_A \cdot \frac{E_i}{B_A} \cdot \left(\frac{z_i^2}{2} - \frac{t_i^2}{8} \right)$$

$$\tau_{A,max,i} = \frac{3}{2} \cdot \frac{V_{A,i}}{A_i} = \frac{V_A \cdot E_i \cdot t_i^2}{8 \cdot B_A}$$

$$\tau_{B,i} = \frac{-V_B \cdot E_i \cdot \left(z_i - \frac{t_i}{2} \right) \cdot e_{s,i}}{B_B}$$

$$\tau_{B,max,i} = \frac{V_B \cdot E_i \cdot t_i \cdot e_{s,i}}{B_B}$$

3.3.5 Advantages and disadvantages of the method, comments

- [+] This approach produces exact results compared with the symmetric cross-section in two- or three parts.
- [+] In contrast to the γ -process, it takes arbitrary systems and loads into consideration.
- [+] The determination of influence of the individual loads and internal supporting points of continuous beams is relatively exact. In this context the shear analogy method can be regarded as the exclusive approach which is able to sufficiently determine the existent stress peaks of bending stresses (cf. chapter 4).
- [-] This method is just able to approximately calculate general segmented cross-sections.
- [-] The implementation takes a lot of effort and implies a high amount of discretisation, especially regarding individual loads and internal supporting points of continuous beams.
- [-] The shear stresses within the close-up range of individual loads and internal supporting points of continuous beams cannot be determined exactly. This is seen as the result of the missing shear deformation options of beam A. However, according to MESTEK [17] this error should subside within the space between the thickness of slabs and the individual loads, or rather the internal supporting points.

3.4 Higher calculation methods

3.4.1 General introduction

In the following section design techniques based on the finite element method (FEM) are presented.

3.4.2 FE-panel (2D)

A 2D-FE-calculation with 2D-panel elements can be compared with the results of higher rod theories which are formulated by MOOSBRUGGER [18]. Added to this, supporting situations, such as a wall with contact or specially designed load introductions, can be realistically modelled by using FEM.

Nevertheless, a FE-design on the basis of a 2D-FE calculation with 2D-panel elements cannot be simply compared with the already discussed solutions (rod theory according to TIMOSHENKO, γ -process and shear analogy method), since the results are more precise and, hence, are used as reference values with regard to the pre-

viously mentioned approaches in chap. 4.

In the following sections the designed FE-model is described in detail. The used FE-software program is ABAQUS/standard, version 6.10, or rather 6.11.

Elements

The elements are type CP24 linear panel members with four nodal points used for a plane state of stress. Their dimensions amount to 2/2 mm. Consequently, this FE-web can be seen as extremely fine.

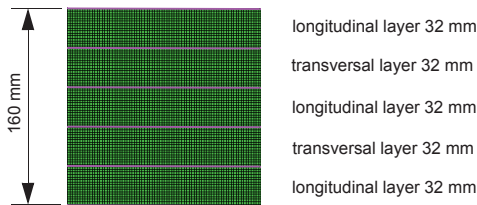


Fig. 3-11 Dimensions of the web of the panel members: 2/2 mm

Material

Wood is an orthotropic material with altogether three E-moduli, three shear moduli and three Poisson's ratios which represent the three anatomical directions (grain direction, radial and tangential). The values of spruce wood correspond with the material parameters of GL 24h (ON EN 1194:1999 [23]). However, on the subject of this 2D panel design a plane, planar 2D state of stress needs to be applied. The used material parameters are presented in tab. 3-3:

Tab. 3-3 Material parameters of board lamellas (GL 24h acc. to ON EN 1194:1999 [23]).

material parameters	abbreviation	value [N/mm ²]
E-modulus in grain direction	E_{II}	11600
E-modulus perpendicular to grain direction	E_{90}	~0
Shear modulus in grain direction	G_{II}	720
Rolling shear modulus	G_R	72

The material parameters of the longitudinal- and transversal layers are defined in the FE software program ABAQUS as follows (attention: units in kN/cm²):

```
*MATERIAL, NAME=WOOD_LR
*ELASTIC, TYPE=LAMINA
1160.0 , 39.0 , 0.0 , 72.0
*MATERIAL, NAME=WOOD_QR
*ELASTIC, TYPE=LAMINA
30.0E-8 , 39.0 , 0.0 , 7.20
```

As it becomes evident in these input lines, the E-modulus perpendicular to grain direction (E_{90}) is numerically set to zero.

Supports

Using the FE-model two different types of supports are created. While the structural support aims at the optimal comparison with the rod designs, the other focuses on the design of a realistic supporting situation. In the course of analysing the latter one, statements concerning the influence of a finite supporting width on the stress distribution within the supporting area can be made. As a consequence, from these statements the condition of the rounding down of the moment can be deduced. Additionally, it needs to be mentioned that the height of the wall has a fundamental influence on the rotation stiffness of the support. Hence, two limiting cases are defined: „real support - free rotatable“ and „real support - fixed“.

structural support (FE_1)

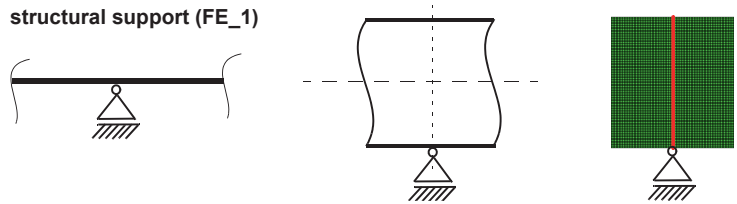


Fig. 3-12 Structural support

„real support“ – free rotatable (FE_2)

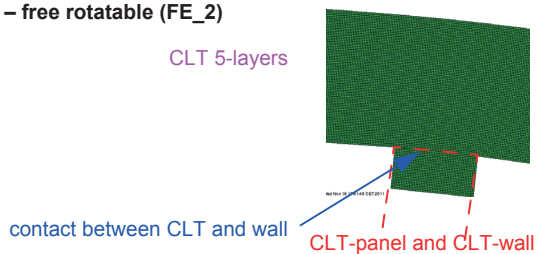


Fig. 3-13 Real support - free rotatable

„real support“ – fixed (fix) (FE_3)

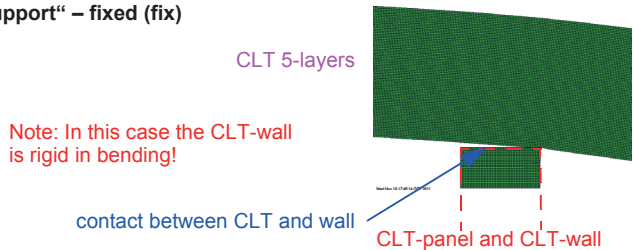


Fig. 3-14 Real support - fixed

Load

The load is regarded as uniform load at the highest load of the CLT panel. Additionally, in this case the dead weight of the CLT panel is defined approximately. To be absolutely correct, the dead weight should be distributed as force per unit volume among the height of the cross-section in all FE-members.

Results

While the results will be presented in chapter 4, this section focuses on a qualitative implication regarding the different longitudinal displacements of the individual layers. These various longitudinal displacements (shear curvatures in structural terms) attract strong criticism against the classic TIMOSHENKO theory). In order to compensate this flaw, other calculation methods have been developed, such as the γ -process and the SA-method.

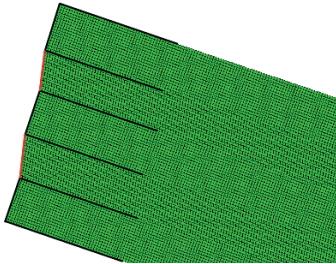


Fig. 3-15 Longitudinal displacement (curvature) within the range of support on the basis of FEM

Note: The curvatures of fig. 3-15 are depicted as extremely superelevated within the longitudinal axis.

3.4.3 FE-panel (3D)

Entire 3D-FE calculations with 3D-volume elements take a lot of effort in the context of designing, calculating and solving the equation system. Nevertheless, the gain is rather modest compared with a 2D-design. Therefore, this report will not go into any further detail concerning this technique.

4 Reference Analyses

4.1 General introduction

In the course of the following calculations the methods to analyse stresses, which were described in chapter 3, are compared with each other by applying them to various static systems. In this regard it is worth mentioning that it is the intention of this report to analyse a representative selection of practical single-, two- and three-span girders. Added to this, special cases, such as balconies (cantilevers), and short span lengths, as it is the case with corridors, will be taken into consideration.

In the context of the check analyses the focus of interest is on the analysis of the maximum bending- and shear stresses. All stresses are determined under full loads on the basis of characteristic loads ($\gamma_f = 1,0$). A field-by-field load position concerning the two- and three- span systems is not investigated.

4.1.1 Basic system

The selected „basic system“ (T1) is a single-span panel with a span length L of 4,80 m. The used 5 layer CLT panel has a constant layer thickness of 32 mm each and, consequently, has a total thickness t_{clt} of 160 mm. These dimensions lead to the in practical terms usual L/H -ratio of 30. The uniform load q_k amounts to 5,0 kN/m² and consists of the dead weight $g_k = 2,0$ kN/m² and the payload $p_k = 3,0$ kN/m².

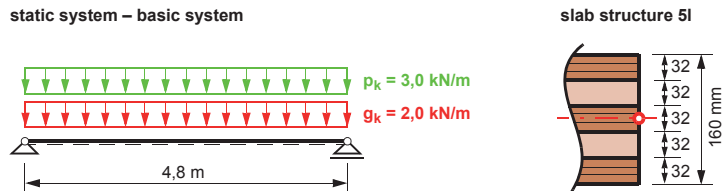


Fig. 4-1 Static system and slab structure of the basic system.

The material data are defined as those of GLT GL 24h, with the exception of E_{90} (= 0). The individual values of stiffness are shown in tab. 4-1.

Tab. 4-1 Material parameters of board lamellas (GL 24h acc. to ON EN 1194:1999 [23])

material parameters	abbreviation	value [N/mm ²]
E-modulus in grain direction	E_{II}	11600
E-modulus perpendicular to grain direction	E_{90}	0
Shear modulus in grain direction	G_{II}	720
Rolling shear modulus	G_R	72

4.1.2 Variation and extension of the basic system

If the available maximum length of slabs of 16 m is taken into account, further static systems (two- and three-span girders) should be designed. It should be mentioned that the slab thickness in comparison to the basic system remains the same and amounts to 160 mm. All in all, 22 different systems are taken into account (cf. fig. 4-2 and fig. 4-3).

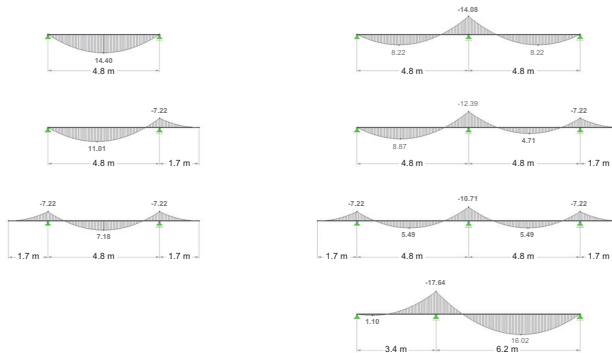


Fig. 4-2 Overview of the systems – analysed single- and two-span girders

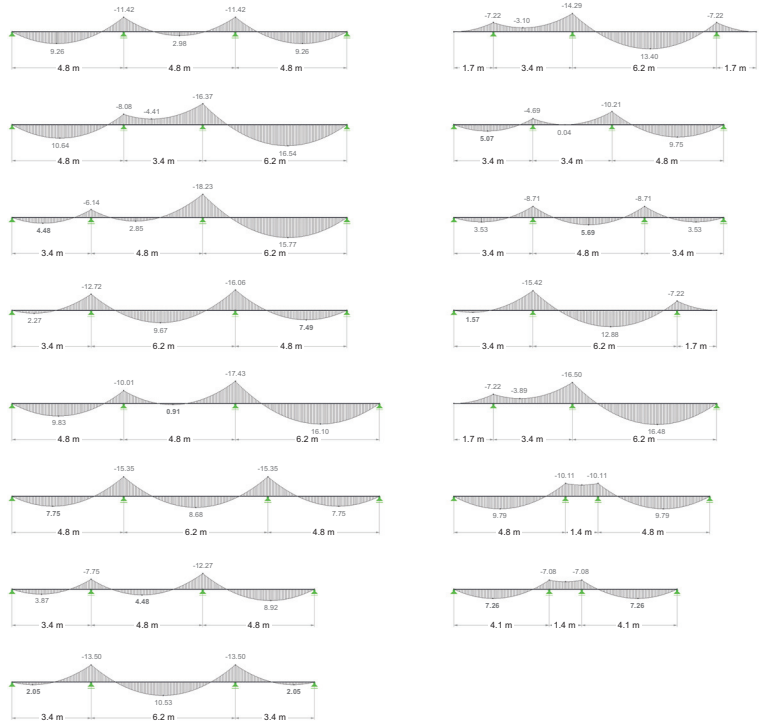
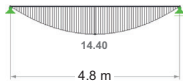


Fig. 4-3 Overview of the systems – analysed three-span girders

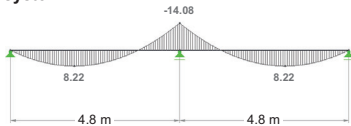
4.1.3 Selection of systems

From the 22 systems presented in fig. 4-2 and fig. 4-3, 6 practical configurations are selected for further analyses on the basis of the maximum span- and support moments.

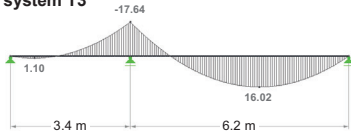
system T1 (basic system)



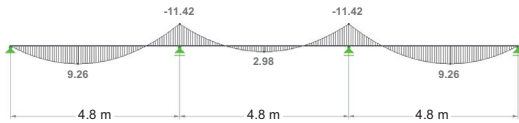
system T2



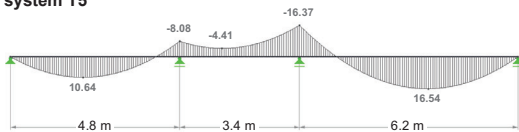
system T3



system T4



system T5



system T6

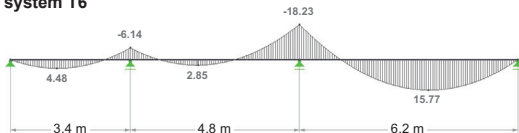


Fig. 4-4 Selection of systems – systems for further analyses

4.2 System T1 – single-span girder exposed to uniform load

The previously mentioned three approximate methods are applied to the „referential configuration“, which defines the single-span girder being exposed to uniform load, in order to illustrate the procedure of the various processes.

4.2.1 Transversal-flexible-in-shear beam (TIMOSHENKO)

Static system | Load

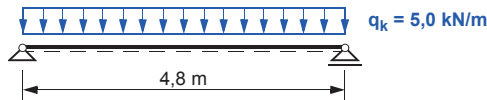


Fig. 4-5 Static system T1 – single-span girder exposed to uniform load

Slab structure | Material data

cf. fig. 4-1 and tab. 4-1

Cross-sectional values

Bending stiffness

Due to the universal layer thickness t_i and the equating to zero of the E-modulus perpendicular to grain direction ($E_{90} = 0$), the bending stiffness of this panel can be determined exactly by making use of the formula defined in chapter 3.1.3:

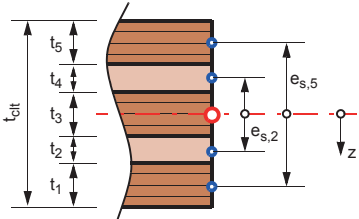
$$K_{\text{clt}} = \sum (E_i \cdot I_i) + \sum (E_i \cdot A_i \cdot e_{s,i}^2) = \frac{33}{4} \cdot E_{\parallel} \cdot b \cdot t_i^3$$

$$K_{\text{clt}} = \frac{33}{4} \cdot 11600 \cdot 1000 \cdot 32^3 = 3,136 \cdot 10^{12} \text{ Nmm}^2$$

As an alternative suggestion the determination of the bending stiffness in tabular form is presented in the following. Thus, the determination of the stiffness with being aware of neither the structure nor the material parameters can be demonstrated.

Tab. 4-2 Determination of the bending stiffness K_{clt} in tabular form

ES	α	E	t	e_s	component of eigen inertia	Steiner-term
[-]	[°]	[N/mm ²]	[mm]	[mm]	[Nmm ²]	[Nmm ²]
5	0	11600	32	64	31675733333	1520435200000
4	90	0	32	32	0	0
3	0	11600	32	0	31675733333	0
2	90	0	32	32	0	0
1	0	11600	32	64	31675733333	1520435200000
Σ					95027199999	3040870400000
$K_{clt} = \Sigma$ component of eigen inertia + Σ Steiner-term					3,136 · 10¹² Nmm²	



○ gravity centre of cross-section
● gravity centres of the individual layers

with:
 $t_1 = t_2 = t_3 = t_4 = t_5$
 $e_{s,1} = e_{s,5}$ and $e_{s,2} = e_{s,4}$
 $e_{s,3} = 0$

Shear stiffness

The shear stiffness S_{clt} is determined by using the formula presented in chap. 3.1.4. On the subject of the existent ratio of shear modulus ($G_{II}/G_R = 10$) the shear adjustment factor κ amounts to 4,107 (cf. tab. 3-2).

$$S_{clt} = \frac{\sum (G_i \cdot b \cdot t_i)}{\kappa}$$

$$S_{clt} = \frac{3 \cdot 720 \cdot 1000 \cdot 32 + 2 \cdot 72 \cdot 1000 \cdot 32}{4,107} = 1,795 \cdot 10^7 \text{ Nmm}^2$$

Internal forces

The next step is to determine the internal forces of the static system (single-span girder) in consideration by analysing the already calculated values of stiffness in an adequate software program for statics. In this regard, it is highly advisable to enter the existent shear deformations into the software program. In the course of conducting this study, the program RSTAB of the firm DLUBAL is used, which offers the following maximum internal forces:

$$M_{max} = 14,4 \text{ kNm} \quad V_{max} = 12,0 \text{ kN} \quad w_{max} = 11,82 \text{ mm}$$

Needless to say, concerning the single-span girder the values of stiffness have no impact on the internal forces, but on the deflection and the eigenfrequencies.

Stresses

The maximum bending- and shear stresses can be determined as follows:

Maximum bending stress

$$\sigma(z) = \frac{M}{K_{clt}} \cdot z \cdot E(z)$$

$$\sigma_{\max} = \frac{M_{\max}}{K_{clt}} \cdot \frac{t_{clt}}{2} \cdot E_0 = \frac{14,4 \cdot 10^6}{3,136 \cdot 10^{12}} \cdot 80 \cdot 11600 = 4,261 \text{ N/mm}^2$$

Maximum shear stress within the centre layer

$$\tau_{\max} = \frac{V_{\max} \cdot \sum(S \cdot E_i)}{K_{clt} \cdot b} = \frac{V_{\max} \cdot \sum(A_i \cdot e_{s,i} \cdot E_i)}{K_{clt} \cdot b}$$

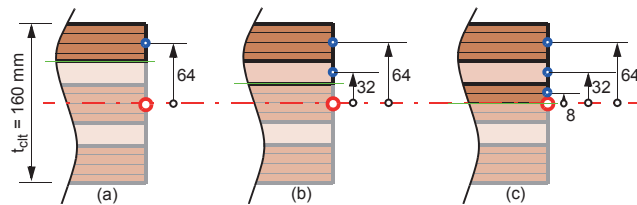


Fig. 4-6 Determination of the static moments

Note: Based on the assumption $E_{90} = 0$, in the context of the static moments (a) and (b) of fig. 4-6 identical values are produced. This phenomenon can be again observed with regard to the constant diagram of shear stiffness in direction of thickness within the transversal layers (cf. fig. 4-7).

$$\tau_{\max} = \frac{12,0 \cdot 10^3}{3,136 \cdot 10^{12} \cdot 1000} \cdot (32 \cdot 1000 \cdot 64 \cdot 11600 + 16 \cdot 1000 \cdot 8 \cdot 11600) =$$

$$= 0,097 \text{ N/mm}^2$$

Maximum rolling shear stress within the transversal layers

$$\tau_r = \frac{V_{\max} \cdot \sum(S \cdot E_i)}{K_{clt} \cdot b} = \frac{V_{\max} \cdot \sum(A_i \cdot e_{s,i} \cdot E_i)}{K_{clt} \cdot b}$$

$$\tau_r = \frac{12,0 \cdot 10^3}{3,136 \cdot 10^{12} \cdot 1000} \cdot (32 \cdot 1000 \cdot 64 \cdot 11600) = 0,0909 \text{ N/mm}^2$$

Stress diagram

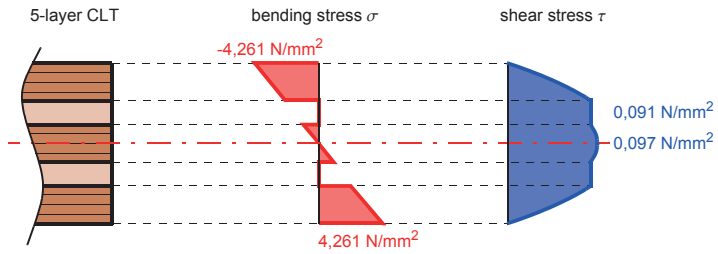


Fig. 4-7 Diagrams of bending- and shear stresses within transversal loads

4.2.2 Modified γ -process

Static system | Load

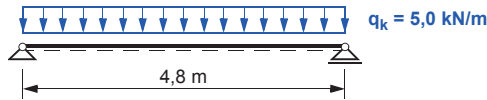


Fig. 4-8 Static system T1 – single-span girder exposed to uniform load

Slab structure | Material data

cf. fig. 4-1 and tab. 4-1

Cross-sectional values

Based on the formulae of chap. 3.2.2 and chap. 3.2.3, the cross-sectional values are determined as follows:

$$A_i = b_i \cdot h_i = 1000 \cdot 32 = 32000 \text{ mm}^2$$

$$I_i = \frac{b_i \cdot h_i^3}{12} = \frac{1000 \cdot 32^3}{12} = 2730667 \text{ mm}^4$$

$$\gamma_2 = 1$$

$$\gamma_{1,3} = \frac{1}{1 + \frac{\pi^2 \cdot E_i \cdot A_i \cdot h_{s,i}}{l^2 \cdot G_{90} \cdot b}} = \frac{1}{1 + \frac{\pi^2 \cdot 11600 \cdot 32000 \cdot 32}{4800^2 \cdot 72 \cdot 1000}} = 0,934$$

$$a_2 = \frac{1}{2} \cdot \frac{\gamma_1 \cdot E_1 \cdot A_1 \cdot (h_1 + h_2) - \gamma_3 \cdot E_3 \cdot A_3 \cdot (h_2 + h_3)}{\sum_{i=1}^3 \gamma_i \cdot E_i \cdot A_i} = 0$$

$$a_{1(3)} = \frac{h_1}{2} + h_{12} + \frac{h_2}{2} - a_2 = \frac{32}{2} + 32 + \frac{32}{2} - 0 = 64 \text{ mm}$$

$$(EI)_{ef} = \sum_{i=1}^3 (E_i \cdot I_i + \gamma_i \cdot E_i \cdot A_i \cdot a_i^2)$$

$$(EI)_{ef} = 3 \cdot 11600 \cdot 2730667 + 2 \cdot 0,934 \cdot 11600 \cdot 32000 \cdot 64^2 = 2,935 \cdot 10^{12} \text{ Nmm}^2$$

Internal forces

The maximum internal forces are again determined by using the software program RSTAB:

$$M_{\max} = 14,4 \text{ kNm} \quad V_{\max} = 12,0 \text{ kN} \quad w_{\max} = 11,77 \text{ mm}$$

Stresses

Maximum bending stress

$$\sigma_1 = \frac{M_{\max}}{(EI)_{ef}} \cdot \gamma_1 \cdot E_1 \cdot a_1 = \frac{14,4 \cdot 10^6}{2,935 \cdot 10^{12}} \cdot 0,934 \cdot 11600 \cdot 64 = 3,402 \text{ N/mm}^2$$

$$\sigma_{m,1} = \frac{M_{\max}}{(EI)_{ef}} \cdot \frac{E_1 \cdot h_1}{2} = \frac{14,4 \cdot 10^6}{2,935 \cdot 10^{12}} \cdot \frac{11600 \cdot 32}{2} = 0,911 \text{ N/mm}^2$$

$$\sigma_{\max} = \sigma_1 + \sigma_{m,1} = 3,402 + 0,911 = 4,313 \text{ N/mm}^2$$

Maximum shear stress within the centre layer

$$\tau_{2,\max} = \frac{V_{\max}}{(EI)_{ef}} \cdot \frac{\gamma_3 \cdot E_3 \cdot A_3 \cdot a_3 + 0,5 \cdot E_2 \cdot b_2 \cdot h^2}{b_2}$$

$$\begin{aligned} \tau_{2,\max} &= \frac{12,0 \cdot 10^3}{2,935 \cdot 10^{12}} \cdot \frac{0,934 \cdot 11600 \cdot 32000 \cdot 64 + 0,5 \cdot 11600 \cdot 1000 \cdot 16^2}{1000} = \\ &= 0,097 \text{ N/mm}^2 \end{aligned}$$

Note: The height h can be defined as $h_2/2 + a_2$. In the context of a 5 layer, symmetric CLT panel, h needs to be substituted by $h_2/2$ (cf. fig. 3-6).

Rolling shear stress

$$\tau_r = \frac{V_{\max}}{(EI)_{ef}} \cdot \frac{\gamma_3 \cdot E_3 \cdot A_3 \cdot a_3}{b_2}$$

$$\tau_r = \frac{12,0 \cdot 10^3}{2,935 \cdot 10^{12}} \cdot \frac{0,934 \cdot 11600 \cdot 32000 \cdot 64}{1000} = 0,0907 \text{ N/mm}^2$$

Stress diagram

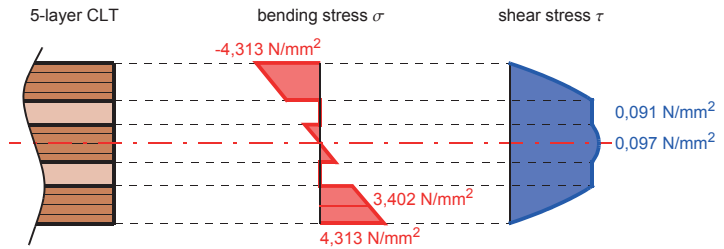


Fig. 4-9 Diagrams of bending- and shear stress within cross-section

4.2.3 Shear analogy method

Static system | Load

As it was mentioned in chapter 3.3, the static system needs to be transferred to two coupled beams.

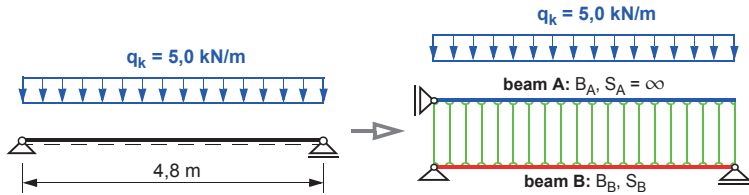


Fig. 4-10 Static system T1 – single-span girder exposed to uniform load and adapted to the SA-method

Cross-sectional values | Dimensions of equivalent stiffness

Beam A

$$B_A = \sum E_i \cdot I_i = \sum E_i \cdot \frac{b \cdot t_i^3}{12} = 3 \cdot 11600 \cdot \frac{1000 \cdot 32^3}{12} = 9,503 \cdot 10^{10} \text{ Nmm}^2$$

$$S_A = \infty$$

Beam B

$$B_B = \sum E_i \cdot b \cdot t_i \cdot e_{s,i}^2 = 2 \cdot 11600 \cdot 1000 \cdot 32 \cdot 64^2 = 3,041 \cdot 10^{12} \text{ Nmm}^2$$

$$S_B = \frac{a^2}{\frac{1}{b} \cdot \left(\frac{t_1}{2 \cdot G_1} + \sum_{i=2}^{n-1} \frac{t_i}{G_i} + \frac{t_n}{2 \cdot G_n} \right)} = \frac{128^2}{\frac{1}{1000} \cdot \left(\frac{32}{2 \cdot 720} + 2 \cdot \frac{32}{72} + \frac{32}{720} + \frac{32}{2 \cdot 720} \right)}$$

$$= 1,676 \cdot 10^7 \text{ Nmm}^2$$

Internal forces

The equivalent system mentioned above together with the already determined dimensions of stiffness is entered into the software program RSTAB. This results in maximum internal forces regarding both beams (A+B). The next step is to determine the maximum stresses. The deflections of both beams w are identical due to the fact that the displacements are rigidly coupled.

$$M_{A,\max} = 0,46 \text{ kNm} \quad V_{A,\max} = 0,72 \text{ kN} \quad w_{\max} = 11,83 \text{ mm}$$

$$M_{B,\max} = 13,94 \text{ kNm} \quad V_{B,\max} = 11,28 \text{ kN}$$

Stresses

Maximum bending stress

$$\sigma_{A,\max,i} = \pm \frac{M_{A,\max}}{B_A} \cdot E_i \cdot z_i = \frac{0,46 \cdot 10^6}{9,503 \cdot 10^{10}} \cdot 11600 \cdot 16 = 0,898 \text{ N/mm}^2$$

$$\sigma_{B,\max,i} = \pm \frac{M_{B,\max}}{B_B} \cdot E_i \cdot e_{s,i} = \frac{13,94 \cdot 10^6}{3,041 \cdot 10^{12}} \cdot 11600 \cdot 64 = 3,403 \text{ N/mm}^2$$

$$\sigma_{\max} = \sigma_{A,\max,i} + \sigma_{B,\max,i} = 0,898 + 3,403 = 4,301 \text{ N/mm}^2$$

Maximum shear stress within centre layer

$$\tau_{A,\max,i} = \frac{V_{A,\max} \cdot E_i \cdot t_i^2}{8 \cdot B_A} = \frac{0,72 \cdot 10^3 \cdot 11600 \cdot 32^2}{8 \cdot 9,503 \cdot 10^{10}} = 0,011 \text{ N/mm}^2$$

$$\tau_{B,\max,i} = \frac{V_{B,\max} \cdot E_i \cdot t_i \cdot e_{s,i}}{B_B} = \frac{11,28 \cdot 10^3 \cdot 11600 \cdot 32 \cdot 64}{3,041 \cdot 10^{12}} = 0,088 \text{ N/mm}^2$$

$$\tau_{\max} = \tau_{A,\max,i} + \tau_{B,\max,i} = 0,011 + 0,088 = 0,099 \text{ N/mm}^2$$

Maximum rolling shear stress within transversal layer

$$\tau_r = \frac{V_{B,\max} \cdot E_i \cdot t_i \cdot e_{s,i}}{B_B} = \frac{11,28 \cdot 10^3 \cdot 11600 \cdot 32 \cdot 64}{3,041 \cdot 10^{12}} = 0,088 \text{ N/mm}^2$$

Stress diagram

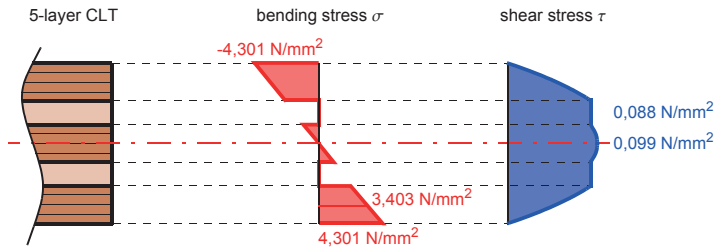


Fig. 4-11 Diagrams of bending- and shear stresses within cross-section

4.2.4 Summary of results

Stiffness

Table 4-3 shows the entire dimensions of bending- and shear stiffness of the prevailing approximate methods. It becomes evident that the level of effective bending stiffness EI_{ef} of the γ -process is lower compared with the one of the TIMOSHENKO-beam. The reason for this can be found in the shear flexibility of the transversal layers, which has already been included in the γ -process. The sum of both dimensions of equivalent stiffness B_A and B_B of the shear analogy method is identical with the K_{clt} of the TIMOSHENKO-beam.

Tab. 4-3 Dimensions of stiffness of the TIMOSHENKO-beam, γ -process and SA-method

	TIMOSHENKO		γ -process		SA-method
	[Nmm ²]		[Nmm ²]		[Nmm ²]
K_{clt}	$3,136 \cdot 10^{12}$	EI_{ef}	$2,935 \cdot 10^{12}$	B_A	$9,503 \cdot 10^{10}$
S_{clt}	$1,795 \cdot 10^7$			S_A	∞
				B_B	$3,041 \cdot 10^{12}$
				S_B	$1,676 \cdot 10^7$

Stress diagrams within the length of beam

Note: The term FE_1  used in the following illustrations and tables corresponds with the structural support, as it was defined in chap. 3.4.2.

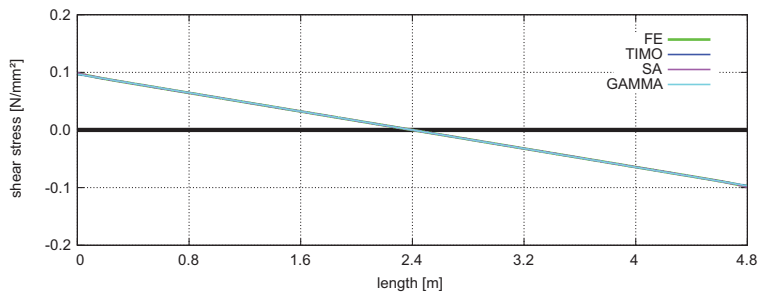
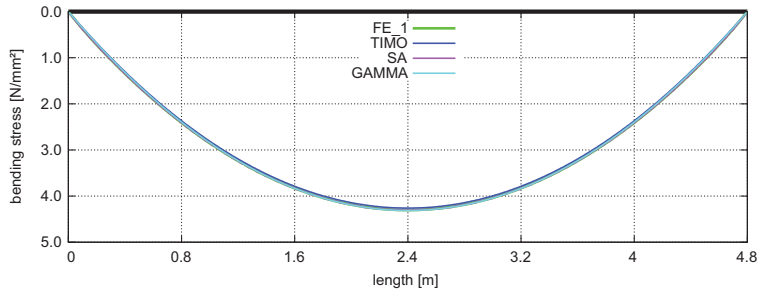


Fig. 4-12 Diagrams of maximum bending- and shear stresses within the length of beam

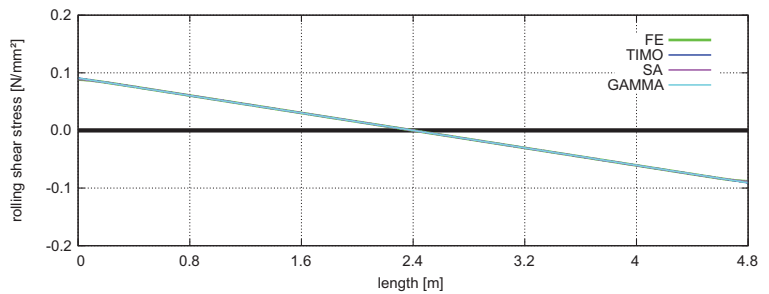


Fig. 4-13 Diagram of maximum rolling shear stress within the length of beam

Table 4-4 shows the maximum bending- and shear stresses and the deflections. Added to this, they are compared with the results of the 2D-FE panel calculation, which are used as reference values.

Tab. 4-4 Comparison and summary of the results

	TIMOSHENKO	mod. γ -process	SA-method	2D-FE_1
	TIMO —	GAMMA —	SA —	FE_1 —
	[N/mm ² , mm]			
σ_{\max}	4,261	4,313	4,301	4,304
τ_{\max}	0,097	0,097	0,099	0,097
$\tau_{r,\max}$	0,091	0,091	0,088	0,088
w_{\max}	11,82	11,77	11,83	11,82
	[%]	[%]	[%]	[%]
σ_{\max}	99,0	100,2	99,9	100
τ_{\max}	100,0	100,0	102,1	100
$\tau_{r,\max}$	103,4	103,4	100,0	100
w_{\max}	100	99,6	100,1	100

Table 4-4, fig. 4-12 and fig. 4-13 show that all approaches produce similar results in the context of exposing the single-span girder to uniform load. In this case a determination with one of the three previously mentioned approximate methods can be regarded as sufficient and convincing.

4.3 System T2 – two-span girder exposed to uniform load ($L_1 = L_2$)

While a statically determined case was analysed with system T1, the focus is now shifted to a statically undetermined two-span girder with the same span lengths ($L_1 = L_2$).

4.3.1 Dimensions of stiffness

For the γ -process the shear flexibility of transversal layers is converted into flexibility between the adjoining rigid layers in grain direction. As a consequence, the effective bending stiffness, which already includes the shear flexibility, is determined approximately. Due to the fact that the γ -process is exclusively valid for analysing single-span girders (to be absolutely correct when being exposed to sinusoidal load), it is suggested that on the subject of multiple-span systems single-span girders with span lengths oriented towards the zero point should be used as an alternative. Within the norms this equivalent length amounts to 80 % of the span length. With regard to this example, the equivalent lengths of the span- and the supporting areas amount to 3,84 m and 1,92 m. On the basis of these equivalent lengths the γ -process results in the following effective distribution of bending stiffness:

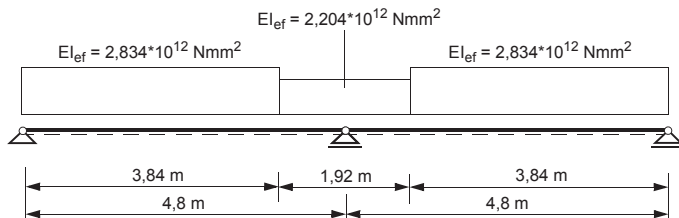


Fig. 4-14 Distribution of bending stiffness applying the γ -process

The dimensions of bending- and shear stiffness of the TIMOSHENKO-beam and the dimensions of the equivalent stiffness of the shear analogy method are independent from the system and, hence identical in all analysed examples (system T1-T6). Table 4-5 summarises all determined dimensions of stiffness of chapter 4.2.

Tab. 4-5 Dimensions of stiffness of the TIMOSHENKO-beam and the shear analogy method

	TIMOSHENKO [Nmm ²]		SA-method [Nmm ²]
K_{cIt}	$3,136 \cdot 10^{12}$	B_A	$9,503 \cdot 10^{10}$
S_{cIt}	$1,795 \cdot 10^7$	S_A	∞
		B_B	$3,041 \cdot 10^{12}$
		S_B	$1,676 \cdot 10^7$

4.3.2 Summary of the results

Stress diagrams within the length of beam

Note: The terms FE_1 — and FE_2 — used in the following images and tables correspond with the structural support and the „real support“ (free rotatable), as it was described in chap. 3.4.2 in detail.

The following illustrations show the diagrams of the bending- and shear stresses of system T2 (two-span girder). Within the field area the individual methods produce – as in system T1 (single-span girder) – sufficient and convincing results, whereas within the supporting area (centre support) they show significant deviations not only in the context of the bending stress, but also regarding the shear stress. Nevertheless, these deviations are limited to a small range.

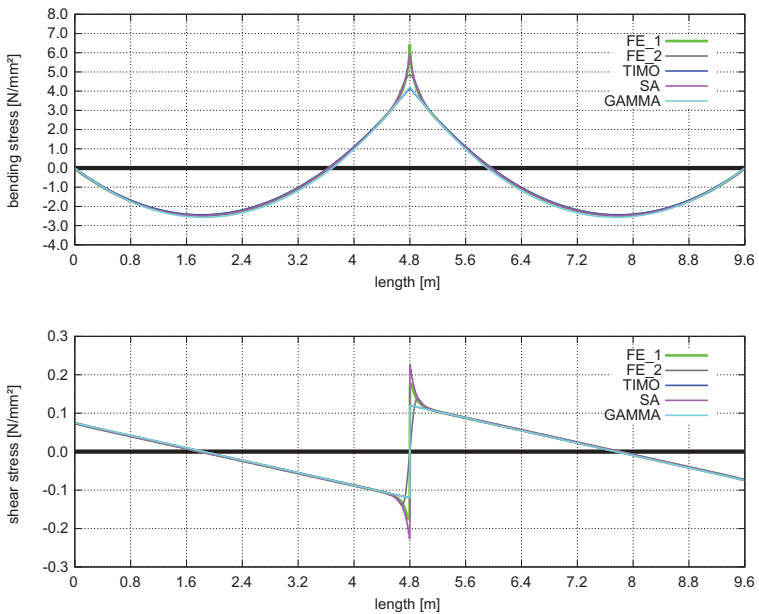


Fig. 4-15 Diagrams of the maximum bending- and shear stresses within the length of beam

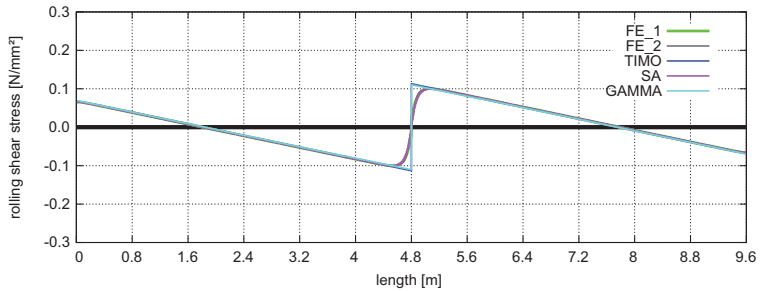


Fig. 4-16 Diagram of the maximum rolling-shear stress within the length of beam

Bending stresses

As it becomes evident in image 4-17, there occur stress peaks at the range of the centre support due to the local load introduction (supporting force). The shear analogy method, as the only one of all the three analysed approaches, is able to produce a good result by showing a deviation of ca. 8 % in comparison with the FE-resolution (FE_1). The differences of the TIMOSHENKO-beam and the modified γ -process amount to 35 % (cf. tab. 4-6). Because of the realistic supporting situation based on the FE-design (free rotatable – chap. 3.4 and FE_2 cf. fig. 4-17) the deviation within the TIMOSHENKO-beam and the γ -process is reduced to ca. 13 %.

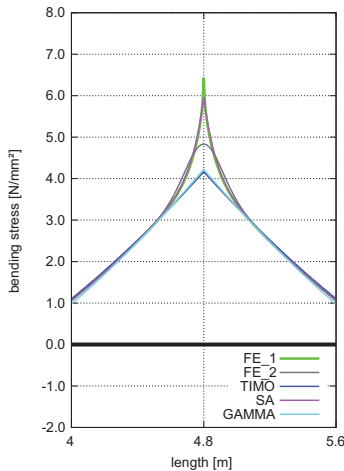


Fig. 4-17 Maximum bending stress within the range of the centre support

Shear stresses

In the context of shear stresses within the range of the centre support the results are similar. The maximum deviations of the TIMOSHENKO-beam and the modified γ -process are equivalent to those of the bending stresses. Interestingly enough, concerning the shear stress the shear analogy method produces „wrong“ results because of the shear rigidity of beam A. However, this error subsides quickly, as it can be seen on the left side of fig. 4-18. Therefore, it seems to be appropriate to determine the shear stress relevant to design within the distance t_{clt} from the edge of the supporting (cf. DIN 1052, 10.2.9 (2) [5]). In this regard, the values highly correlate with those of the FE-solution (cf. tab. 4-6, $\tau_{max(t)}$). Also on the subject of the rolling shear stress of the SA-method, the TIMOSHENKO-beam and the γ -process this procedure obtains convincing results and reduces the deviations to ca. 5 % (cf. tab. 4-6, $\tau_r(t)$).

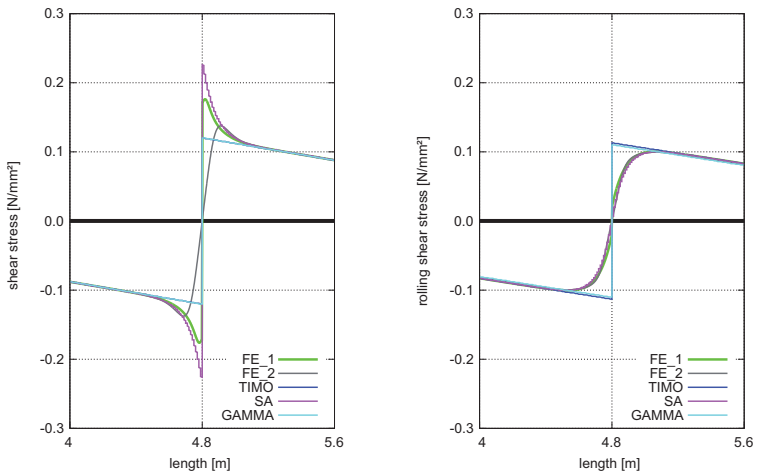


Fig. 4-18 Maximum shear- and rolling shear stresses within the supporting area

Table 4-6 shows the differences of the various calculation methods in detail.

Tab. 4-6 Comparison and summary of the results

	TIMOSHENKO	mod. γ -process	SA-method	2D-FE_1	2D-FE_2
	TIMO —	GAMMA —	SA —	FE_1 —	FE_2 —
	[N/mm ² , mm]				
σ_{\max}	4,167	4,224	5,955	6,432	4,832
τ_{\max}	0,120	0,120	0,226	0,176	0,138
$\tau_{\max(t)}$	0,112	0,112	0,118	0,117	0,120
$\tau_{r(t)}$	0,105	0,103	0,099	0,099	0,099
W_{\max}	5,51	5,50	5,47	5,48	5,48
	[%]	[%]	[%]	[%]	[%]
σ_{\max}	64,8	65,7	92,6	100	75,1
τ_{\max}	68,2	68,2	128,4	100	78,4
$\tau_{\max(t)}$	95,9	95,9	101,0	100	102,4
$\tau_{r(t)}$	106,1	104,0	100,0	100	100,0
W_{\max}	100,5	100,4	99,8	100	100,0

4.3.3 Analyses of the discretisation of the SA-method

In order to identify the influence of the discretisation on the results of the shear analogy method, system T2 is analysed regarding its coupling spaces of 1, 5, 10, 20, 40, 60 and 96 cm.

Stress diagrams within the length of beam

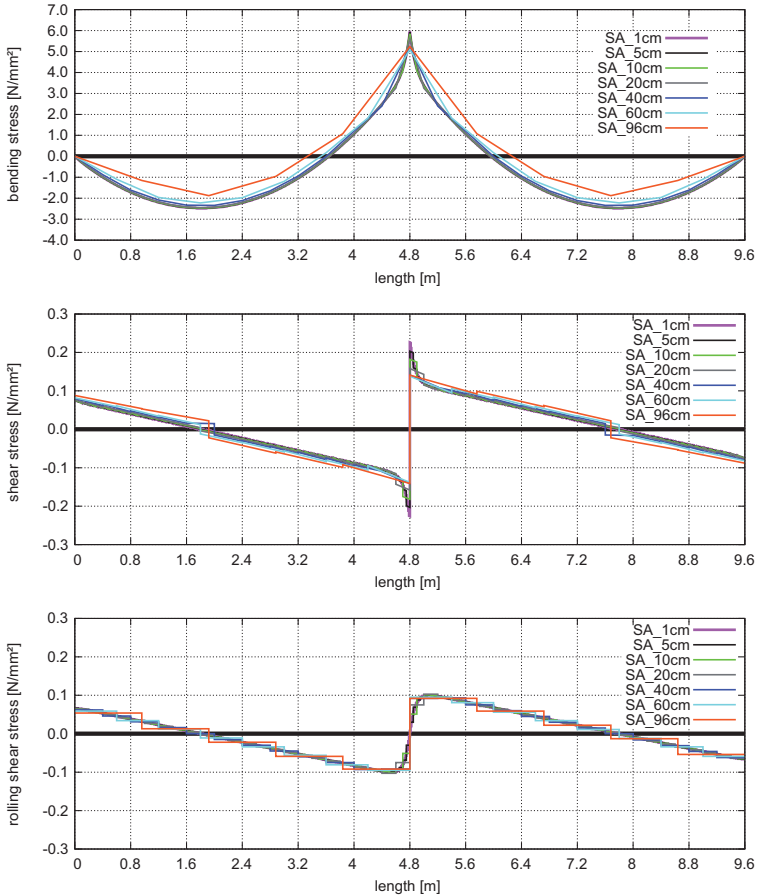


Fig. 4-19 Diagrams of maximum bending-, shear- and rolling shear stresses within the length of beam

Bending stresses

As it becomes evident in fig. 4-20, the selected discretisation plays a significant role in the context of the maximum bending stress within the supporting area. The maximum deviation in comparison with the FE-solution (cf. FE_1, tab. 4-6) amounts to 21 % (cf. tab. 4-7). On the subject of an exact identification of the flexure tension stress within the supporting area using the rounding down of the moment (cf. chap. 4.3.4), the slab thickness t_{clt} as maximum separating distance is highly recommended for the SA-method.

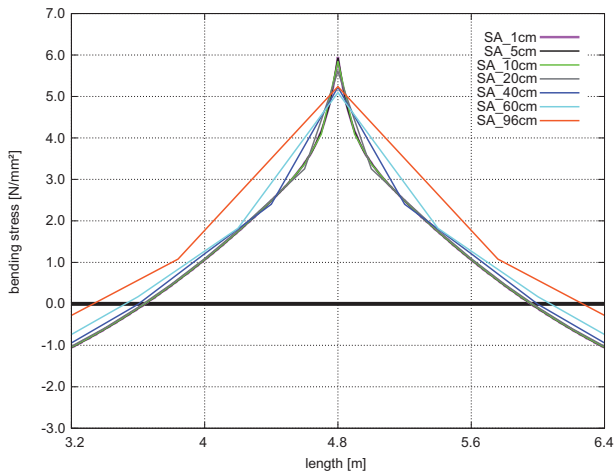


Fig. 4-20 Maximum bending stresses within the centre support

Shear stresses

As it was mentioned in chap. 4.3.2, based on the rigid-in-shear beam A, the shear analogy method shows a higher level of deviation of shear stresses within the centre support. In order to determine the decisive shear stress in distance t_{clt} from the supporting edge, as it is depicted in the previous image, it is highly advisable to again define the thickness of slab t_{clt} as the maximum separating distance.

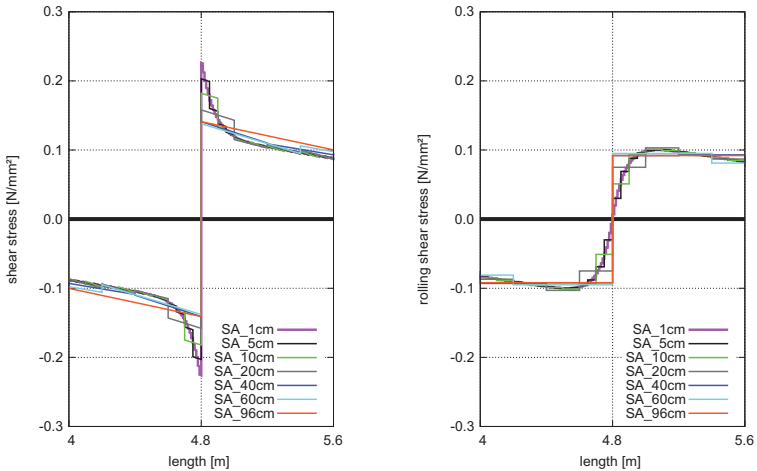


Fig. 4-21 Maximum shear- and rolling shear stresses within the supporting area

Tab. 4-7 Comparison and summary of the results

	SA_1cm	SA_5cm	SA_10cm	SA_20cm	SA_40cm	SA_60cm	SA_96cm	2D-FE_1
								FE_1
	[N/mm ²]							
σ_{max}	5,995	5,931	5,845	5,602	5,227	5,095	5,237	6,432
τ_{max}	0,226	0,203	0,182	0,158	0,141	0,138	0,141	0,176
$\tau_{max(t)}$	0,118	0,118	0,116	0,114	0,125	0,123	0,131	0,117
$\tau_{r(t)}$	0,099	0,099	0,101	0,103	0,092	0,095	0,092	0,099
	[%]	[%]	[%]	[%]	[%]	[%]	[%]	[%]
σ_{max}	92,6	92,2	90,9	87,1	81,3	79,2	81,4	100
τ_{max}	128,4	115,3	103,4	89,8	80,1	78,4	80,1	100
$\tau_{max(t)}$	101,0	101,0	99,3	97,6	107,0	105,3	112,2	100
$\tau_{r(t)}$	100,0	100,0	102,0	104,0	92,9	96,0	92,9	100

4.3.4 Rounding down of the moment within the supporting area

As it becomes evident from the results of chap. 4.3.2 and chap. 4.3.3, the shear analogy method causes bending stresses within the supporting area, which have a high stress gradient among the column. Nevertheless, the results produced in the context of applying this method are remarkably similar to those of the FE-solution with structural supporting (FE_1). The deviation compared with the FE-solution amounts to 7,4 % (cf. fig. 4-22). On the subject of the other two approximate approaches (γ -process and TIMOSHENKO-beam) this increased stress gradient among the supporting area appears to be inexistent. In this regard, the deviation compared with the FE-solution (FE_1) amounts to 35,2 % (cf. fig. 4-22). In the following illus-

trations the bending stresses on the top (flexure tension stress) of the approaches „SA“ and „TIMO“ are depicted in a very small area of the column (± 30 cm) (cf. fig. 4-22).

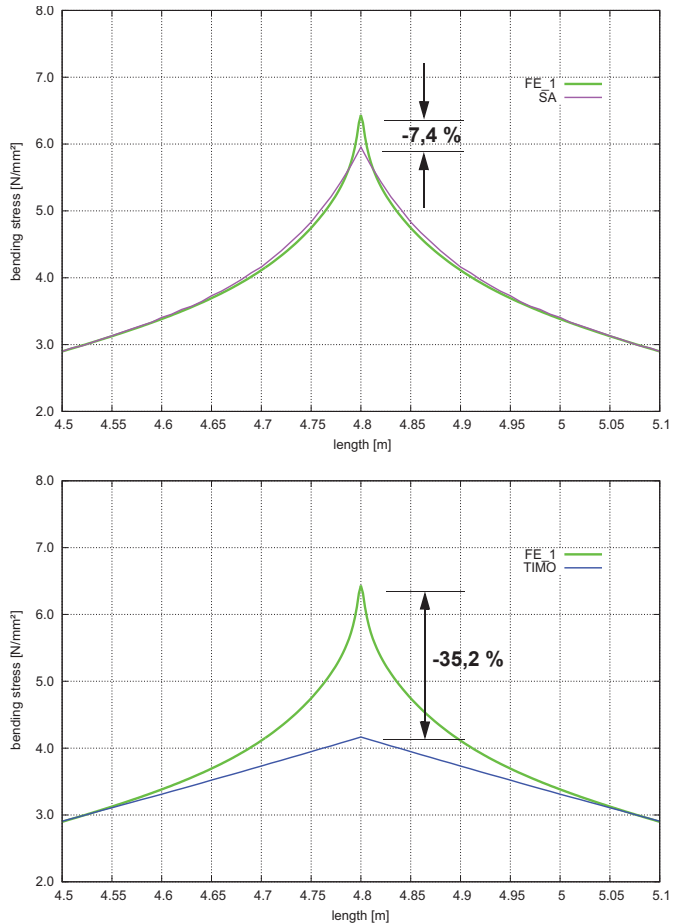


Fig. 4-22 Flexural tension stress within the supporting area, comparing the approaches SA and TIMOSHENKO

The FE-results with „real supporting“ (FE_2) within the supporting area do not share this moment peak depicted in fig. 4-22. However, the rounding down of the moment in wall area and over that item can be detected. In the following illustrations a parabolic rounding down of the moment and, consequently, of the flexural tension stress at the top edge of the slab is analysed within a range of $-(t_{clt}/2 + t_w/$

2 = 130 mm) to $+(t_{clt}/2 + t_w/2 = 130 \text{ mm})$ with t_{clt} (= 160 mm) as thickness of the slab and t_w (= 100 mm) as thickness of the wall. Added to this, the deviation from the „FE-determination“ is defined as „real supporting“ (FE_2).

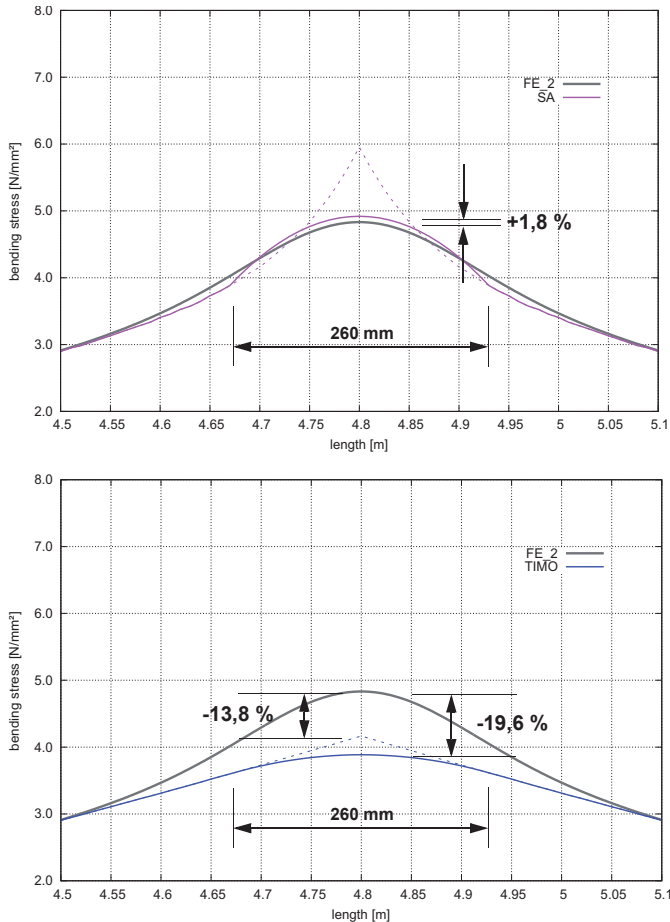


Fig. 4-23 Flexure tension stress within the supporting area, rounded down on the subject of the approaches SA and TIMOSHENKO

The deviation of the rounded down SA-flexure tension stress from the FE-determination with „real supporting“ (FE_2) just amounts to 1,8 % (cf. fig. 4-23), whereas in the context of the TIMOSHENKO-approach the deviation is fairly high and amounts to -19,6 %. If the TIMOSHENKO-results which are not rounded down are taken into consideration, the deviation is reduced to -13,8 % (cf. fig. 4-23). Similar degrees of

deviation can be detected within the γ -process, which is not defined into further detail in this regard. On the basis of these results, the increasing factors of stress ranging from 1,2 for moment diagrams which are rounded down to 1,14 for moment diagrams which are not rounded down could be suggested in order to define two-span girders with the same span width. Using these increased support moments, flexure tension stresses could be determined and cross-sectional verifications could be done.

4.4 System T3 – two-span girders exposed to uniform load (L_1, L_2)

While the same span widths were analysed in the context of system T2, the focus of interest is now shifted to a two-span girder with highly different span widths ($L_1 < L_2$).

4.4.1 Dimensions of stiffness

With regard to the γ -process the effective bending stiffness diagrams need to be determined again. The most effective lengths amount to 2,72 m for the left field, 4,96 m for the right field and 1,92 m for the supporting area. On the basis of these equivalent lengths the distribution of effective bending stiffness within the γ -process amounts to:

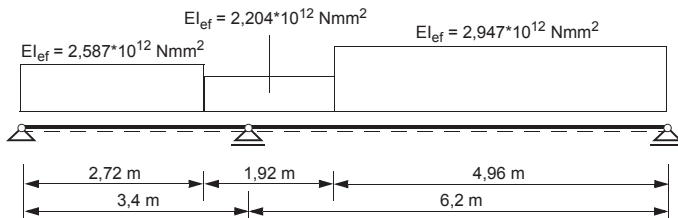


Fig. 4-24 Distribution of bending stiffness when applying the γ -process

The dimensions of stiffness of the other approaches can be found in tab. 4-5.

4.4.2 Summary of results

Stress diagrams within the length of beam

Note: The terms FE_1 —, FE_2 — and FE_3 —, which are used in the following illustrations and tables, correspond with the structural supports of the real supporting (free rotatable) and the real supporting (fixed), as it was mentioned in chap. 3.4.2.

The following illustrations show the diagrams of bending- and shear stresses of system T3. On the subject of the field area, the prevailing methods – similar to system T1 (single-span girder) – produce sufficient results. Nevertheless, within the supporting area (centre support) not only concerning the bending stresses, but also regarding the shear stresses this system shows significant deviations (similar to system T2).

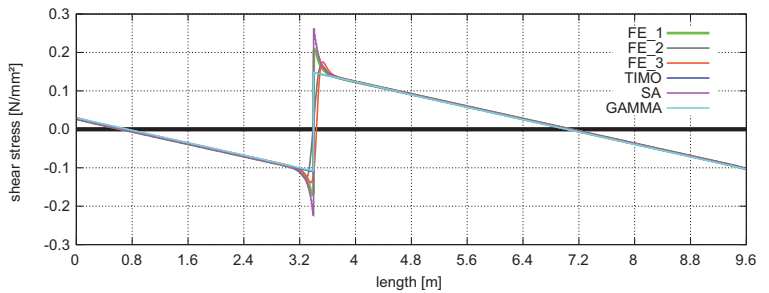
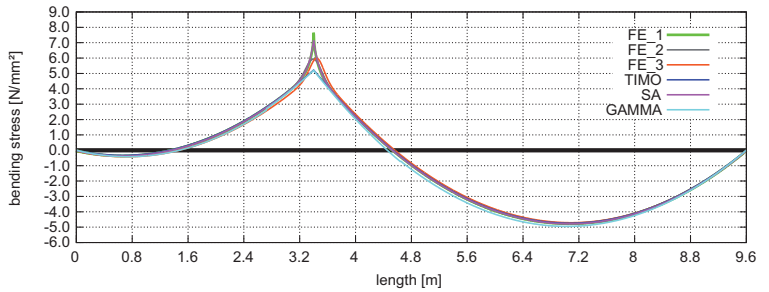


Fig. 4-25 Maximum bending- and shear stress diagrams within the length of beam

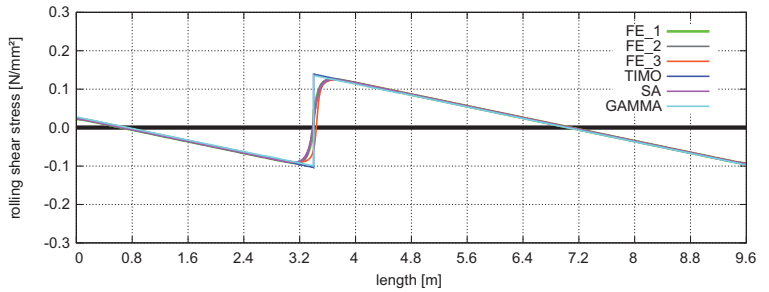


Fig. 4-26 Maximum rolling shear stress diagram within the length of beam

Bending stresses

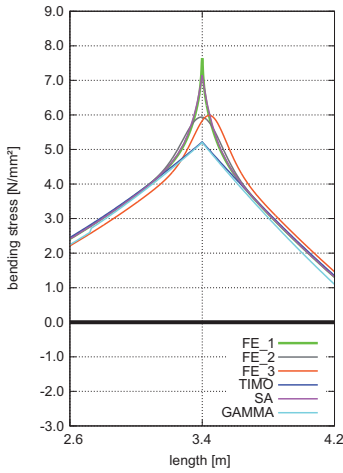


Fig. 4-27 Maximum bending stresses within the centre support

Shear stresses

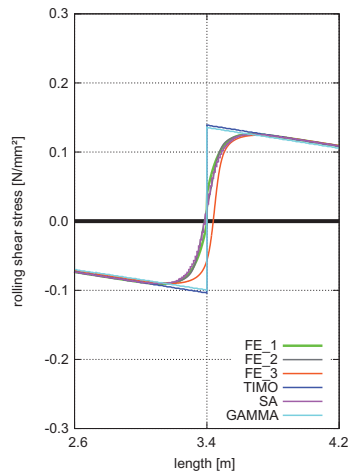
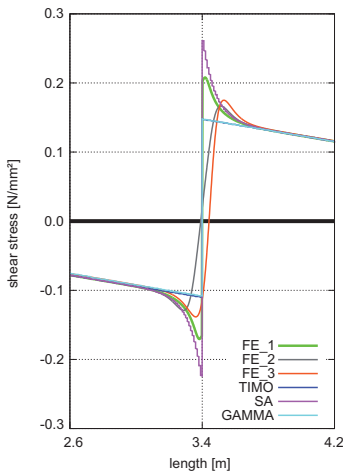


Fig. 4-28 Maximum shear- and rolling shear stresses within the supporting area

Tab. 4-8 Comparison and summary of results

	TIMOSHENKO	mod. γ -process	SA-method	2D-FE_1	2D-FE_2	2D-FE_3
	TIMO —	GAMMA —	SA —	FE_1 —	FE_2 —	FE_3 —
	[N/mm ² , mm]					
σ_{\max}	5,220	5,201	7,148	7,646	5,936	5,986
τ_{\max}	0,148	0,148	0,261	0,208	0,167	0,175
$\tau_{\max(t)}$	0,139	0,139	0,147	0,145	0,148	0,155
$\tau_{r(t)}$	0,131	0,128	0,124	0,125	0,124	0,122
w_{\max}	18,71	19,36	18,67	18,67	18,67	18,19
	[%]	[%]	[%]	[%]	[%]	[%]
σ_{\max}	68,3	68,0	93,5	100	77,6	78,3
τ_{\max}	71,2	71,2	125,5	100	80,3	84,1
$\tau_{\max(t)}$	96,1	96,1	101,7	100	102,1	106,8
$\tau_{r(t)}$	104,8	102,4	99,2	100	99,2	97,6
w_{\max}	100,2	103,7	100,0	100	100,0	97,4

As it becomes evident in tab. 4-8, the deviations of the bending stresses of the TIMOSHENKO-beam and the modified γ -process in comparison with the FE-beam supporting (FE_1) amount to 32 %. In the course of designing a real supporting situation (FE_2 and FE_3) these differences are reduced to ca. 12 %.

4.5 System T4 – three-span girder exposed to uniform load ($L_1 = L_2 = L_3$)

In the following sections there will be conducted a detailed analysis of the three-span girder with same span widths.

4.5.1 Dimensions of stiffness

In the context of the γ -process the effective bending stiffness diagram needs to be again defined. In this regard, the effective lengths amount to 3,84 m for the left and the right fields. Concerning both supporting areas a length of 1,92 m is presupposed due to the zero points of moment. As a consequence, the length of the centre field amounts to 2,88 m (cf. fig. 4-29). On the basis of these equivalent lengths, the following effective distribution of bending stiffness for the γ -process can be defined:

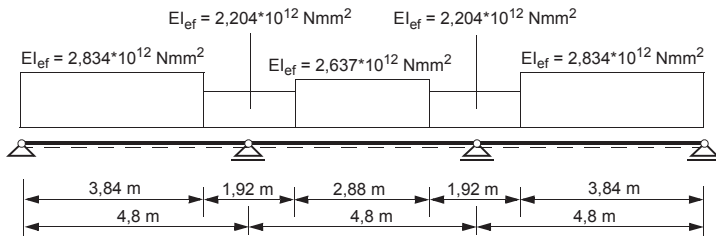


Fig. 4-29 Distribution of the bending stiffness when applying the γ -process

The dimensions of stiffness of the other approaches can be found in tab. 4-5.

4.5.2 Summary of results

Stress diagrams within the length of beam

Note: The terms FE_1 —, FE_2 — and FE_3 —, which are used in the following illustrations and tables, correspond with the structural supports of the real supporting (free rotatable) and the real supporting (fixed), as it was mentioned in chap. 3.4.2.

The following illustrations show the diagrams of bending- and shear stresses of system T4 (three-span girder). On the subject of the field area, the prevailing methods – similar to system T1 (single-span girder) – produce sufficient results. Nevertheless, within the supporting area (centre support) not only concerning the bending stresses, but also regarding the shear stresses also this system shows significant deviations.

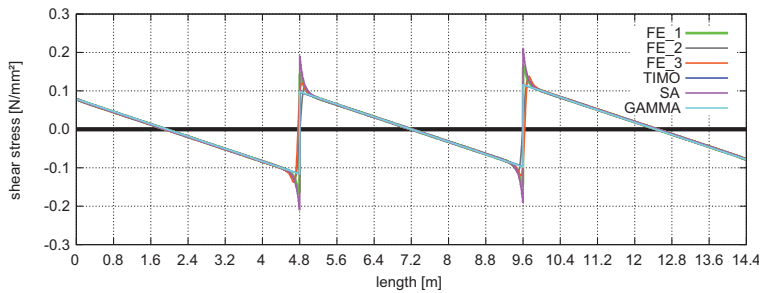
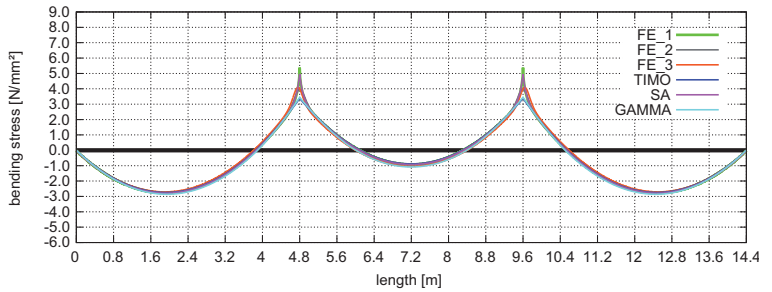


Fig. 4-30 Maximum bending- and shear stress diagrams within the length of beam

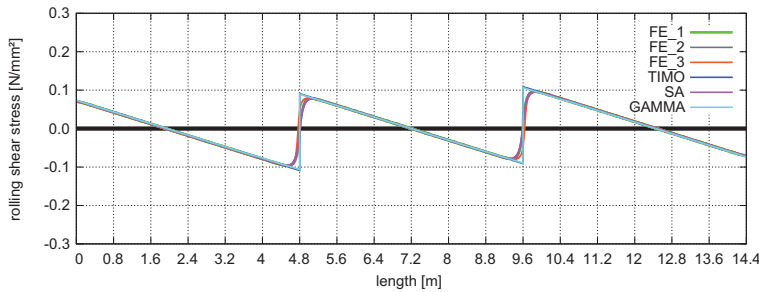


Fig. 4-31 Maximum rolling shear stress diagram within the length of beam

Bending stresses

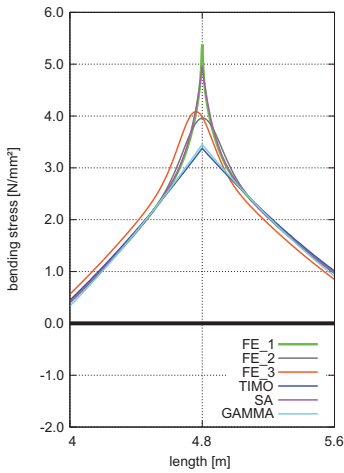


Fig. 4-32 Maximum bending stresses within the centre support

Shear stresses

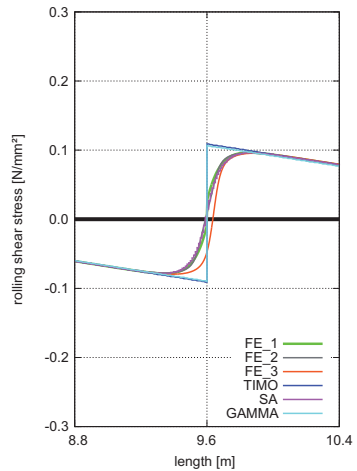
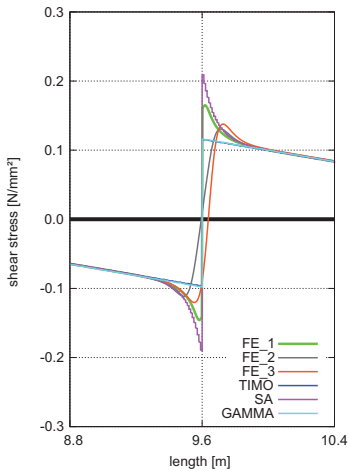


Fig. 4-33 Maximum shear- and rolling shear stresses within the supporting area

Tab. 4-9 Comparison and summary of the results

	TIMOSHENKO	mod. γ -process	SA-method	2D-FE_1	2D-FE_2	2D-FE_3
	TIMO —	GAMMA —	SA —	FE_1 —	FE_2 —	FE_3 —
	[N/mm2, mm]	[N/mm2, mm]	[N/mm2, mm]	[N/mm2, mm]	[N/mm2, mm]	[N/mm2, mm]
σ_{\max}	3,379	3,451	4,961	5,382	3,960	4,083
τ_{\max}	0,116	0,116	0,209	0,146	0,111	0,120
$\tau_{\max(t)}$	0,107	0,108	0,113	0,112	0,114	0,119
$\tau_r(t)$	0,101	0,099	0,095	0,096	0,095	0,094
w_{\max}	6,67	6,71	6,64	6,65	6,65	6,35
	[%]	[%]	[%]	[%]	[%]	[%]
σ_{\max}	62,8	64,1	92,2	100	73,6	75,9
τ_{\max}	79,5	79,5	143,2	100	76,0	82,2
$\tau_{\max(t)}$	95,8	96,7	101,2	100	102,2	106,9
$\tau_r(t)$	105,3	103,2	99,1	100	99,5	98,0
w_{\max}	100,3	100,9	99,8	100	100,0	95,5

As it becomes evident in tab. 4-9, the deviations of bending stresses of the TIMOSHENKO-beam and the modified γ -process in comparison with the FE-beam supporting (FE_1) amount to 36 %. In the course of designing a real supporting situation (FE_2 and FE_3) these differences are reduced to ca. 15 %.

4.6 System T5 – three-span girder exposed to uniform load (L₁, L₂, L₃)

Analogous to the two-span girder the span widths vary within the analysis of the three-span girder. The total length of 14,4 m remains unchanged. In concrete terms this means that the left field has a standard length of 4,8 m, while the length of the centre field is reduced by 30 % and amounts to 3,4 m. The length of the right field, however, is extended by 30 % and amounts to 6,2 m.

4.6.1 Dimensions of stiffness

In the context of the γ -process the effective bending stiffness diagram needs to be again defined. In this regard, the effective lengths amount to 3,84 m for the left field and to 4,96 m for the right field. Concerning the supporting areas and the centre area a length of 5,60 m is presupposed due to the zero points of moment. On the basis of these equivalent lengths, the following effective distribution of bending stiffness for the γ -process can be defined:

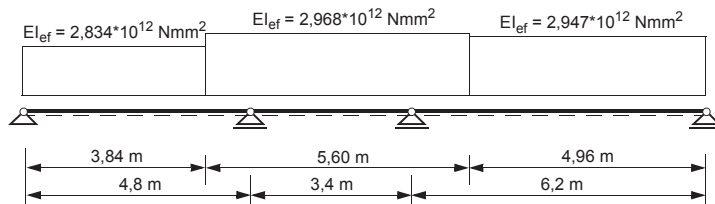


Fig. 4-34 Distribution of bending stiffness when applying the γ -process

The dimensions of stiffness of the other approaches can be found in tab. 4-5.

4.6.2 Summary of results

Stress diagrams within the length of beam

Note: The terms FE_1 —, FE_2 — and FE_3 —, which are used in the following illustrations and tables, correspond with the structural supports of the real supporting (free rotatable) and the real supporting (fixed), as it was mentioned in chap. 3.4.2.

The following illustrations show the diagrams of bending- and shear stresses of system T5 (three-span girder with L₁, L₂ and L₃). On the subject of the field area, the prevailing methods – similar to system T1 (single-span girder) – produce sufficient results. Nevertheless, within the supporting area (centre support) not only concerning the bending stresses, but also regarding the shear stresses also this system shows significant deviations.

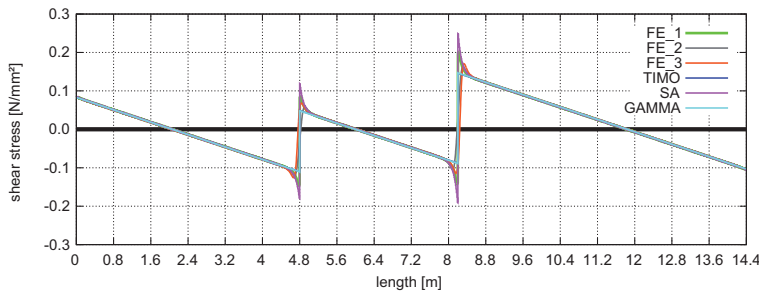
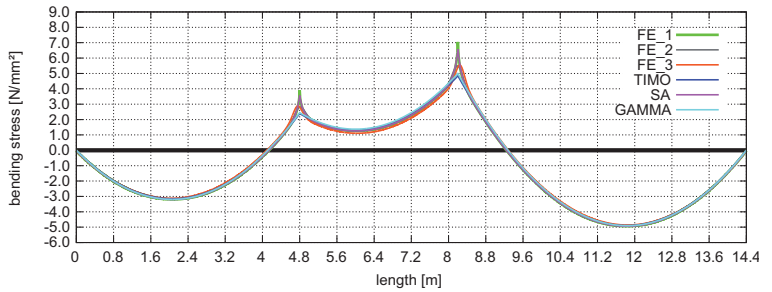


Fig. 4-35 Maximum bending- and shear stress diagrams within the length of beam

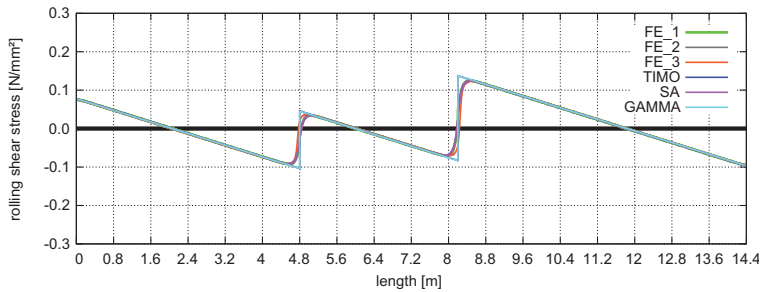


Fig. 4-36 Maximum rolling shear stress diagram within the length of beam

Bending stresses

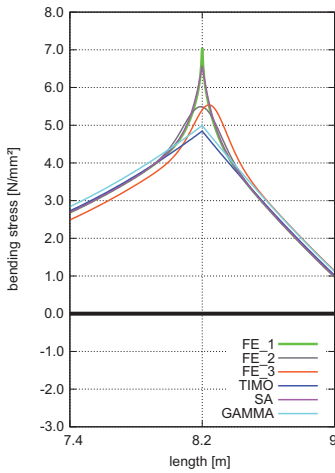


Fig. 4-37 Maximum bending stresses within the right supporting area

Shear stresses

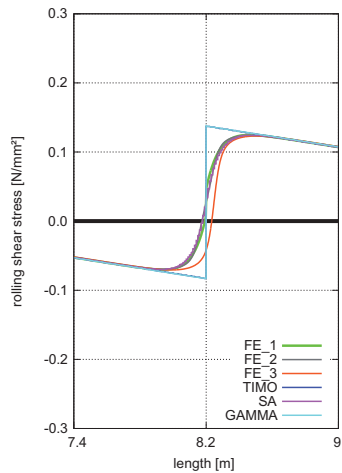
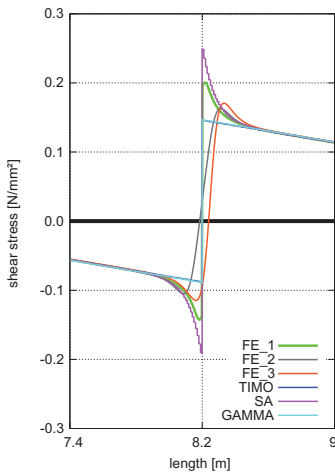


Fig. 4-38 Maximum shear- and rolling shear stresses within the right supporting area

Tab. 4-10 Comparison and summary of results

	TIMOSHENKO	mod. γ -process	SA-method	2D-FE_1	2D-FE_2	2D-FE_3
	TIMO —	GAMMA —	SA —	FE_1 —	FE_2 —	FE_3 —
	[N/mm ² , mm]					
σ_{\max}	4,844	4,991	6,577	7,049	5,491	5,538
τ_{\max}	0,146	0,147	0,249	0,201	0,163	0,171
$\tau_{\max(t)}$	0,138	0,138	0,144	0,143	0,145	0,152
$\tau_{r(t)}$	0,129	0,130	0,123	0,124	0,123	0,121
w_{\max}	19,64	19,22	19,62	19,62	19,62	19,09
	[%]	[%]	[%]	[%]	[%]	[%]
σ_{\max}	68,7	70,8	93,3	100	77,9	78,6
τ_{\max}	72,6	73,1	123,9	100	81,1	85,1
$\tau_{\max(t)}$	96,8	96,8	101,1	100	101,9	106,5
$\tau_{r(t)}$	104,1	104,9	99,3	100	99,5	97,6
w_{\max}	100,1	98,0	100,0	100	100,0	97,3

As it becomes evident in tab. 4-10, the deviations of bending stresses of the TIMOSHENKO-beam and the modified γ -process in comparison with the FE-beam supporting (FE_1) amount to 30 %. In the course of designing a real supporting situation (FE_2 and FE_3) these differences are reduced to ca. 11 %.

4.7 System T6 – three-span girder exposed to uniform load (L₁, L₂, L₃)

With regard to system T6, the arrangement of the span widths varies in comparison to system T5. The total load remains unchanged and amounts to 14,4 m. Added to this, the lengths amount to 3,4 m for the left field, 4,8 m for the centre field and 6,2 m for the right field.

4.7.1 Dimensions of stiffness

In the context of the γ -process the effective bending stiffness diagram needs to be again defined. In this regard, the effective lengths amount to 2,72 m for the left field and to 4,96 m for the right field. The lengths of the supporting areas and the centre area are adjusted to the zero points of moment and can be found in fig. 4-39. On the basis of these equivalent lengths, the following effective distribution of bending stiffness for the γ -process can be defined:

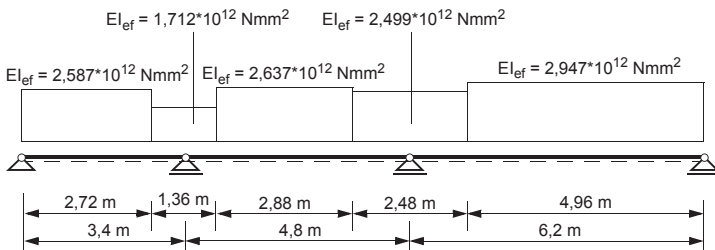


Fig. 4-39 Distribution of bending stiffness when applying the γ -process

The dimensions of stiffness of the other approaches can be found in tab. 4-5.

4.7.2 Summary of results

Stress diagram within the length of beam

Note: The terms FE_1 —, FE_2 — and FE_3 —, which are used in the following illustrations and tables, correspond with the structural supports of the real supporting (free rotatable) and the real supporting (fixed), as it was mentioned in chap. 3.4.2.

The following illustrations show the diagrams of bending- and shear stresses of system T6 (three-span girder with L₁, L₂ and L₃). On the subject of the field area, the prevailing methods – similar to system T1 (single-span girder) – produce sufficient results. Nevertheless, within the supporting area (centre support) not only concerning the bending stresses, but also regarding the shear stresses also this system shows significant deviations.

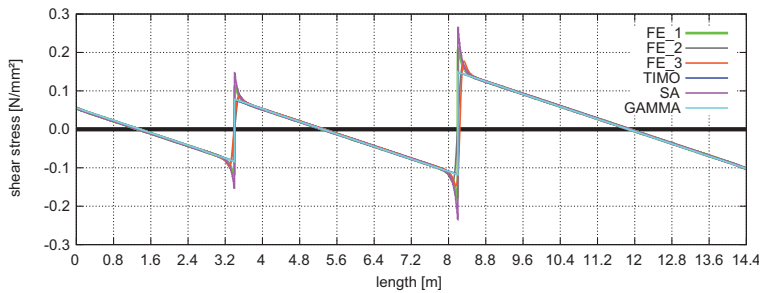
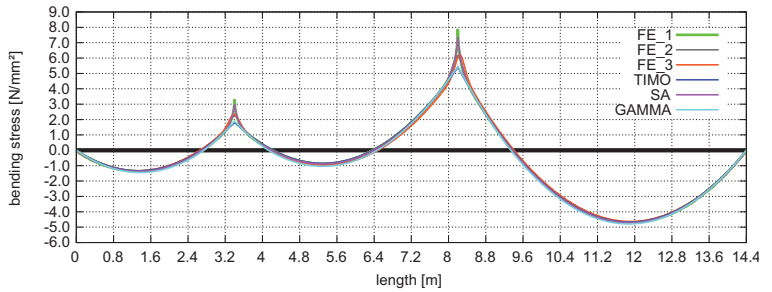


Fig. 4-40 Maximum bending- and shear stress diagrams within the length of beam

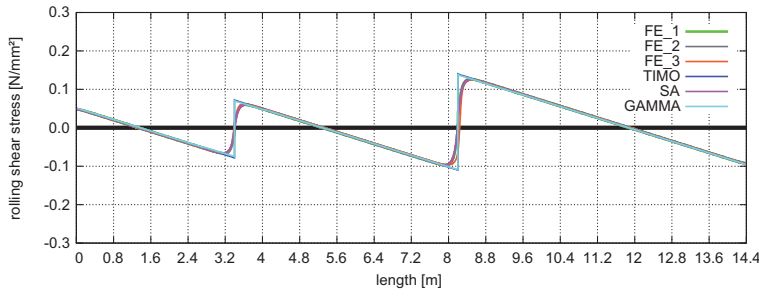


Fig. 4-41 Maximum rolling shear stress diagram within the length of beam

Bending stresses

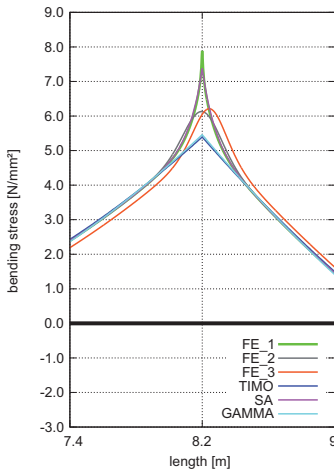


Fig. 4-42 Maximum bending stresses within the right supporting area

Shear stresses

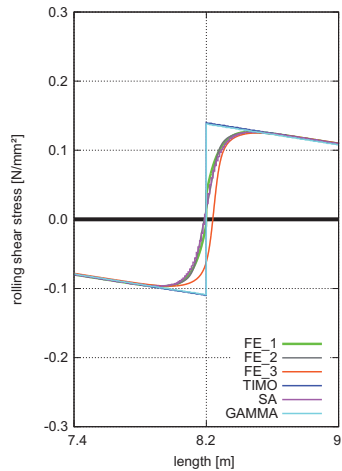
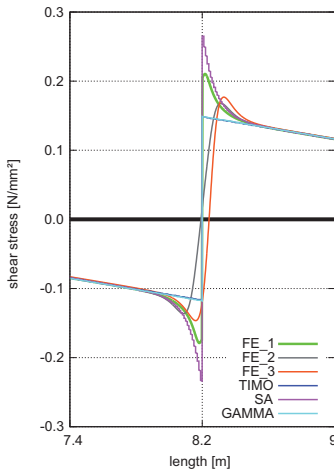


Fig. 4-43 Maximum shear- and rolling shear stresses within the right supporting area

Tab. 4-11 Comparison and summary of results

	TIMOSHENKO	mod. γ -process	SA-method	2D-FE_1	2D-FE_2	2D-FE_3
	TIMO —	GAMMA —	SA —	FE_1 —	FE_2 —	FE_3 —
	[N/mm2, mm]	[N/mm2, mm]	[N/mm2, mm]	[N/mm2, mm]	[N/mm2, mm]	[N/mm2, mm]
σ_{\max}	5,395	5,459	7,375	7,886	6,129	6,211
τ_{\max}	0,148	0,149	0,265	0,210	0,168	0,177
$\tau_{\max(t)}$	0,140	0,140	0,148	0,146	0,149	0,156
$\tau_{r(t)}$	0,132	0,130	0,124	0,125	0,125	0,122
w_{\max}	18,27	18,38	18,24	18,24	18,24	17,71
	[%]	[%]	[%]	[%]	[%]	[%]
σ_{\max}	68,4	69,2	93,5	100	77,7	78,8
τ_{\max}	70,5	71,0	126,2	100	80,0	84,3
$\tau_{\max(t)}$	96,2	96,2	101,7	100	102,2	107,0
$\tau_{r(t)}$	105,3	103,7	98,9	100	99,4	97,4
w_{\max}	100,2	100,8	100,0	100	100,0	97,1

As it becomes evident in tab. 4-11, the deviations of bending stresses of the TIMOSHENKO-beam and the modified γ -process in comparison with the FE-beam supporting (FE_1) amount to 31 %. In the course of designing a real supporting situation (FE_2 and FE_3) these differences are reduced to ca. 12 %.

5 Further Case Studies

5.1 General introduction

In chapter 4 several static systems are determined on the basis of 6 examples (systems T1-T6). In the following sections the influence of various thicknesses of slabs (cf. chap. 5.2 to chap. 5.5) will be analysed. Added to this, the application of the γ -process to a 7-layer CLT panel will be presented (cf. chap. 5.6 and chap. 5.7). However, the focus of interest is shifted to the structure of the slabs. Hence, the variations of system are restricted to the systems T1 and T2. In this context it is also worth mentioning that the material parameters remain unchanged and can be found in tab. 5-1.

Tab. 5-1 Material parameters of board lamellas (GL 24h acc. to ON EN 1194:1999 [23])

material parameter	abbreviation	value [N/mm ²]
E-modulus in grain direction	E_{II}	11600
E-modulus perpendicular to grain direction	E_{90}	0
Shear modulus in grain direction	G_{II}	720
Rolling shear modulus	G_R	72

5.1.1 5I – variation in the thickness of layers

In the course of examining these examples (cf. chap. 5.2 to chap. 5.5) the attempt is made to analyse the results of the prevailing approximate methods on the subject of a cross-sectional design with various layer thicknesses. Thus, the systems T1 (single-span girder) and T2 (two-span girder) are examined concerning both limiting cases using a lay-up parameter t_I/t_Q (cf. chap. 3.1.4) of 2:1, or rather 1:2. The thickness of layer t_{clt} remains unchanged (cf. chapter 4) and still amounts to 160 mm.

Note: Unsymmetrical cross-sectional designs which might occur in special cases, e.g. in the context of a conflagration, are not analysed.

5.1.2 7I – application of the γ -process

Whereas the algorithms on the basis of flexibly-in-shear beams (TIMOSHENKO) and the SA-method cause no changes within the 7 layer cross-sectional design, the solution procedure based on the γ -process significantly modifies the arrangement. Formulae which are defined in relevant norms, such as in EN 1995-1-1, and are applied to 3 layer- and 5 layer CLT panels are inexistent in the context of a 7 layer slab construction. As a consequence, in the following examples (chap. 5.6 and chap. 5.7) the focus of interest is shifted to 7 layer CLT panels. In addition, the general method of analysis according to SCHELLING is applied, which is usually used for segmented flexibly connected bending members.

An accurate presentation and description of the equations according to SCHELLING and a manifold variety of examples regarding 2 layer- and 3 layer flexibly connected bending members are provided in appendix A. Added to this, the significant differences to the existent rules of EC 5 are highlighted and the extension of the fundamental equation system of flexibility coefficients γ_1 for 7 layer CLT panels is explained. It needs to be stressed that on the basis of these extended equations the determination of various segmented slabs, e.g. 9 layer CLT panel, would raise no problems.

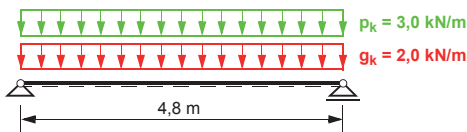
Note: Due to the fact that there is a difference between the γ -process according to EC 5 and the one according to SCHELLING, the latter is defined as γ^* in the following.

5.1.3 Examined systems and slab structures

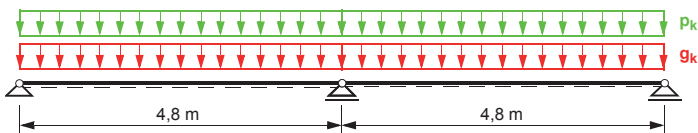
With regard to the following calculations only the systems T1 and T2 (cf. chap. 4.1.3) are taken into consideration. The selected „basic system“ (system T1) is a single-span girder with span width L of 4,80 m. System T2 is a two-span girder with a span width of 4,80 m each. The cross-sectional design of the 5 layer- and 7 layer slabs can be found in fig. 5-1. The lamellas are modified in a way that the L/H-relation still amounts to ca. 30.

On the subject of load, an uniform load $q_k = 5,0 \text{ kN/m}^2$, which consists of the dead weight $g_k = 2,0 \text{ kN/m}^2$ and the payload $p_k = 3,0 \text{ kN/m}^2$, is used again.

system T1

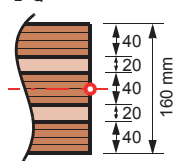


system T2

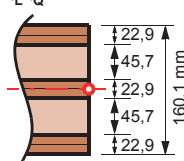


slab design 5l

$t_L/t_Q = 2:1$



$t_L/t_Q = 1:2$



slab design 7l

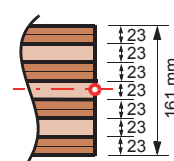


Fig. 5-1 Static systems, load and slab design

5.2 System T1 – single-span girder exposed to uniform load ($t_L/t_Q = 2:1$)

In the following sections the single-span girder exposed to uniform load will be analysed in terms of the ratio 2:1 between the thickness of longitudinal layer t_L and the thickness of transversal layers t_Q . This implies that in this example the thickness of the longitudinal layer is twice the one of the transversal layer (cf. fig. 5-1).

5.2.1 Dimensions of stiffness

Table 5-2 provides an insight into the dimensions of bending- and shear stiffness of the prevailing approximate methods. The calculation is performed according to chapter 4.2.

Tab. 5-2 Dimensions of stiffness of the TIMOSHENKO-beam, the γ -process and the SA-method

	TIMOSHENKO		γ -process		SA-method
	[Nmm ²]		[Nmm ²]		[Nmm ²]
K_{clt}	$3,526 \cdot 10^{12}$	EI_{ef}	$3,352 \cdot 10^{12}$	B_A	$1,856 \cdot 10^{11}$
S_{clt}	$2,427 \cdot 10^7$			S_A	∞
				B_B	$3,341 \cdot 10^{12}$
				S_B	$2,160 \cdot 10^7$

5.2.2 Summary of results

Stress diagrams within the length of beam

The following illustrations show the diagrams of bending- and shear stresses of system T1 (single-span girder) with the ratio of thickness layer t_L/t_Q of 2:1.

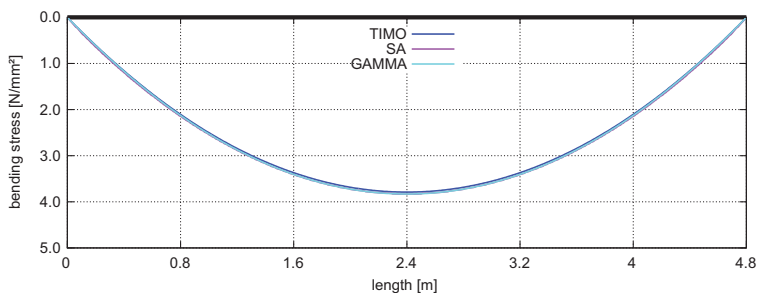


Fig. 5-2 Maximum bending stress diagram within the length of beam

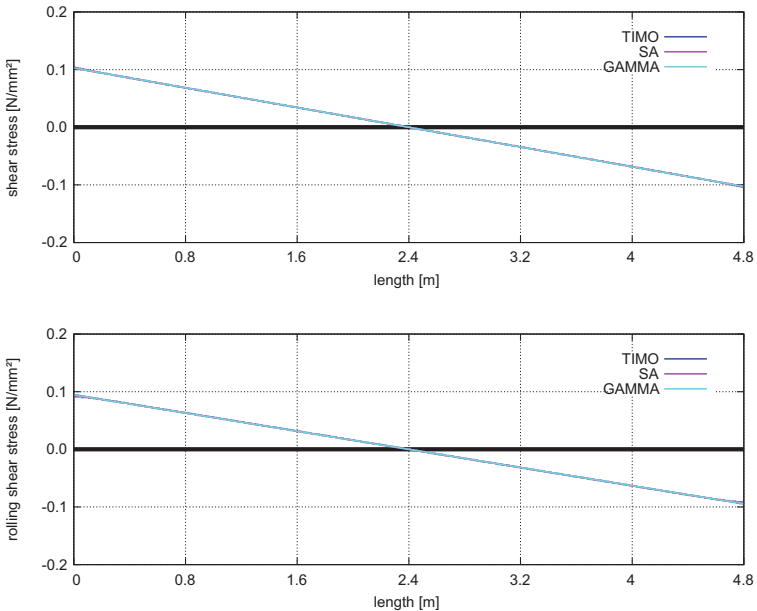


Fig. 5-3 Maximum shear- and rolling shear stresses diagrams within the length of beam

Tab. 5-3 Comparison and summary of results

	TIMOSHENKO	mod. γ -process	SA-method
	TIMO —	GAMMA —	SA —
	[N/mm ² , mm]	[N/mm ² , mm]	[N/mm ² , mm]
σ_{\max}	3,789	3,831	3,833
τ_{\max}	0,103	0,103	0,104
$\tau_{r,\max}$	0,095	0,094	0,091
w_{\max}	10,39	10,31	10,40
	[%]	[%]	[%]
σ_{\max}	100	101,1	101,2
τ_{\max}	100	100,0	101,0
$\tau_{r,\max}$	100	98,9	95,8
w_{\max}	100	99,2	100,1

As it becomes evident in tab. 5-3, fig. 5-2 and fig. 5-3, all methods of calculation produce similar results when analysing single-span girders with different layer thicknesses.

5.3 System T1 – single-span girder exposed to uniform load ($t_L/t_Q = 1:2$)

In the following sections the single-span girder exposed to uniform load will be analysed in terms of the ratio 1:2 between the thickness of longitudinal layer t_L and the thickness of transversal layers t_Q . This implies that in this example the thickness of the longitudinal layer is just half the one of the transversal layer (cf. fig. 5-1).

5.3.1 Dimensions of stiffness

Table 5-4 provides an insight into the dimensions of bending- and shear stiffness of the prevailing approximate methods. The calculation is performed according to chapter 4.2.

Tab. 5-4 Dimensions of stiffness of the TIMOSHENKO-beam, the γ -process and the SA-method

	TIMOSHENKO		γ -process		SA-method
	[Nmm ²]		[Nmm ²]		[Nmm ²]
K_{clt}	$2,535 \cdot 10^{12}$	EI_{ef}	$2,367 \cdot 10^{12}$	B_A	$3,483 \cdot 10^{10}$
S_{clt}	$1,459 \cdot 10^7$			S_A	∞
				B_B	$2,500 \cdot 10^{12}$
				S_B	$1,412 \cdot 10^7$

5.3.2 Summary of results

Stress diagrams within the length of beam

The following illustrations show the diagrams of bending- and shear stresses of system T1 (single-span girder) with the ratio of thickness layer t_L/t_Q of 1:2.

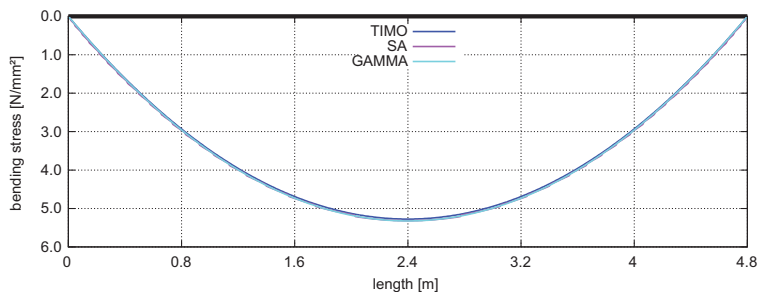


Fig. 5-4 Maximum bending stress diagram within the length of beam

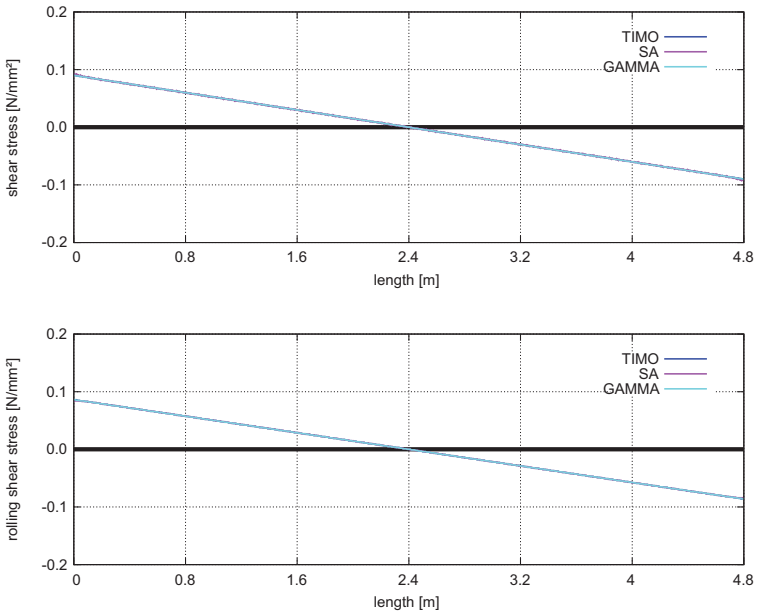


Fig. 5-5 Maximum shear- and rolling shear stresses diagrams within the length of beam

Tab. 5-5 Comparison and summary of results

	TIMOSHENKO	mod. γ -process	SA-method
	TIMO —	GAMMA —	SA —
	[N/mm ² , mm]	[N/mm ² , mm]	[N/mm ² , mm]
σ_{\max}	5,275	5,324	5,317
τ_{\max}	0,090	0,090	0,093
$\tau_{r,\max}$	0,086	0,086	0,084
W_{\max}	14,62	14,60	14,62
	[%]	[%]	[%]
σ_{\max}	100	100,9	100,8
τ_{\max}	100	100,0	103,3
$\tau_{r,\max}$	100	100,0	97,7
W_{\max}	100	99,9	100,0

As it becomes evident in tab. 5-5, fig. 5-4 and fig. 5-5, all methods of calculation produce similar results when analysing single-span girders with different layer thicknesses. To conclude, it can be said that - regardless the cross-sectional design - no significant deviations can be identified within the prevailing approaches concerning the analysis of the single-span girder exposed to uniform load.

5.4 System T2 – two-span girder exposed to uniform load ($t_L/t_Q = 2:1$)

In the following sections the two-span girder exposed to uniform load will be analysed in terms of the ratio 2:1 between the thickness of longitudinal layer t_L and the thickness of transversal layers t_Q . This implies that in this example the thickness of the longitudinal layer is twice the one of the transversal layer (cf. fig. 5-1).

5.4.1 Dimensions of stiffness

For the γ -process the effective diagram of bending stiffness needs to be again determined. The effective lengths amount to 3,84 m for the fields and to 1,92 m for the supporting area. On the basis of these equivalent lengths, the following effective bending stiffness diagram can be deducted with regard to the γ -process:

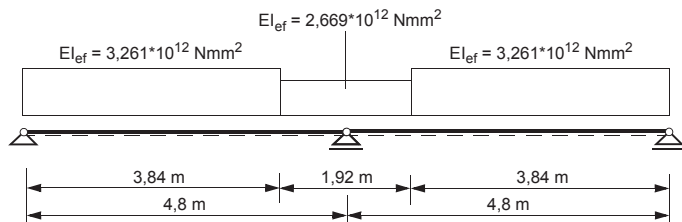


Fig. 5-6 Bending stiffness diagram when applying the γ -process

The dimensions of bending- and shear stiffness of the TIMOSHENKO-beam and the dimensions of equivalent stiffness of the SA-method can be found in tab. 5-2.

5.4.2 Summary of results

Stress diagrams within the length of beam

The following illustrations show the diagrams of bending- and shear stresses of system T2 (two-span girder with the same span widths) with the ratio of thickness layer t_L/t_Q of 2:1.

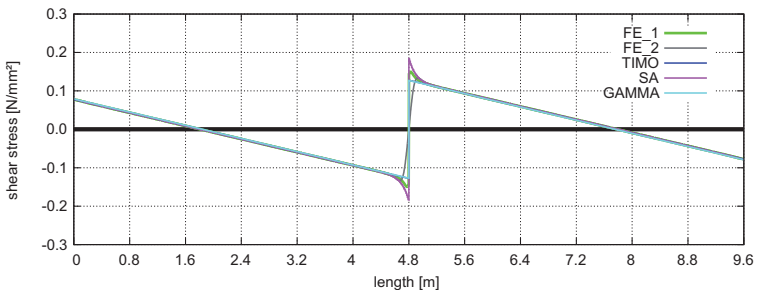
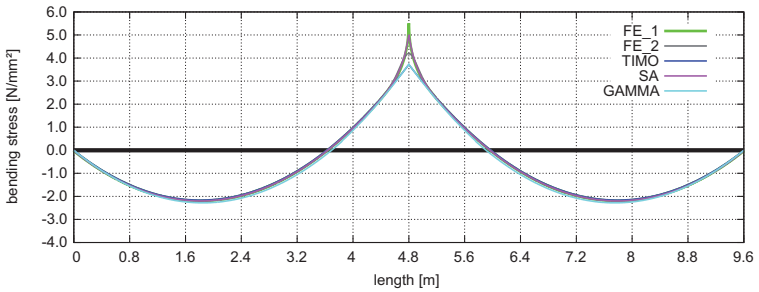


Fig. 5-7 Maximum bending- and shear stresses diagrams within the length of beam

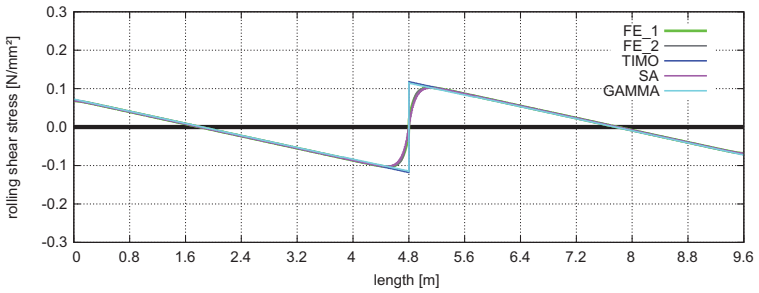


Fig. 5-8 Maximum rolling shear stresses diagram within the length of beam

Bending stresses

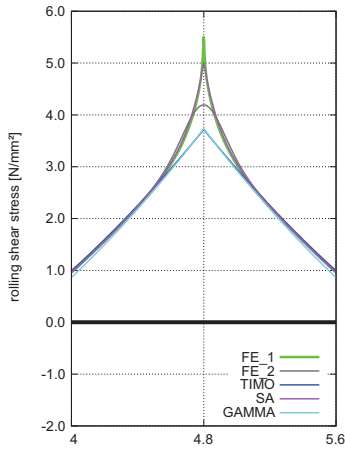


Fig. 5-9 Maximum bending stresses within the centre support

Shear stresses

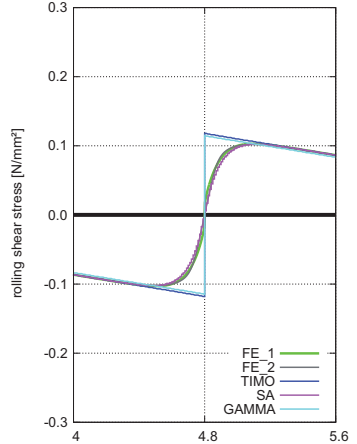
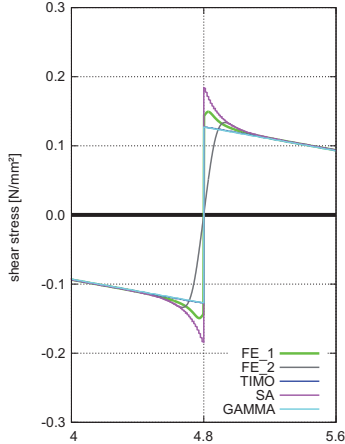


Fig. 5-10 Maximum shear- and rolling shear stresses within the supporting area

Tab. 5-6 Comparison and summary of the results

	TIMOSHENKO	mod. γ -process	SA-method	2D-FE_1	2D-FE_2
	TIMO —	GAMMA —	SA —	FE_1 —	FE_2 —
	[N/mm ² , mm]				
σ_{\max}	3,718	3,732	5,010	5,511	4,192
τ_{\max}	0,128	0,127	0,184	0,149	0,134
$\tau_{\max(t)}$	0,119	0,118	0,124	0,122	0,125
$\tau_r(t)$	0,110	0,106	0,099	0,101	0,100
W_{\max}	4,76	4,70	4,73	4,74	4,74
	[%]	[%]	[%]	[%]	[%]
σ_{\max}	67,5	67,7	90,9	100	76,1
τ_{\max}	85,9	85,2	123,5	100	89,9
$\tau_{\max(t)}$	97,5	96,7	101,6	100	102,5
$\tau_r(t)$	108,9	105,0	98,0	100	99,0
W_{\max}	100,4	99,2	100,2	100	100,0

As it becomes evident in tab. 5-6, regarding the bending stress the deviations amount to ca. 32 % within the FE-supporting (FE_1) and the TIMOSHENKO-beam, or rather the modified γ -process. On the subject of the example „same thickness of layers“ (cf. chap. 4.3) these differences amount to ca. 35 % (cf. tab. 4-6). Hence, it can be said that the modified cross-sectional design has just a marginal impact on the differences in bending stress of the prevailing approaches.

5.4.3 Rounding down of moment within the supporting area

Analogous to chapter 4.3.4 the rounding down of moment within the supporting area is conducted. In the following illustrations the parabolic rounding down of moments and, as a consequence, of the flexure tension stresses on the top of the edge of slab is conducted within the range of $-(t_{clt}/2 + t_w/2 = 130 \text{ mm})$ to $+(t_{clt}/2 + t_w/2 = 130 \text{ mm})$ with t_{clt} (= 160 mm) as thickness of the slab and t_w (= 100 mm) as thickness of the wall. Added to this, the deviation from the FE-determination is defined as „real supporting“ (FE_2).

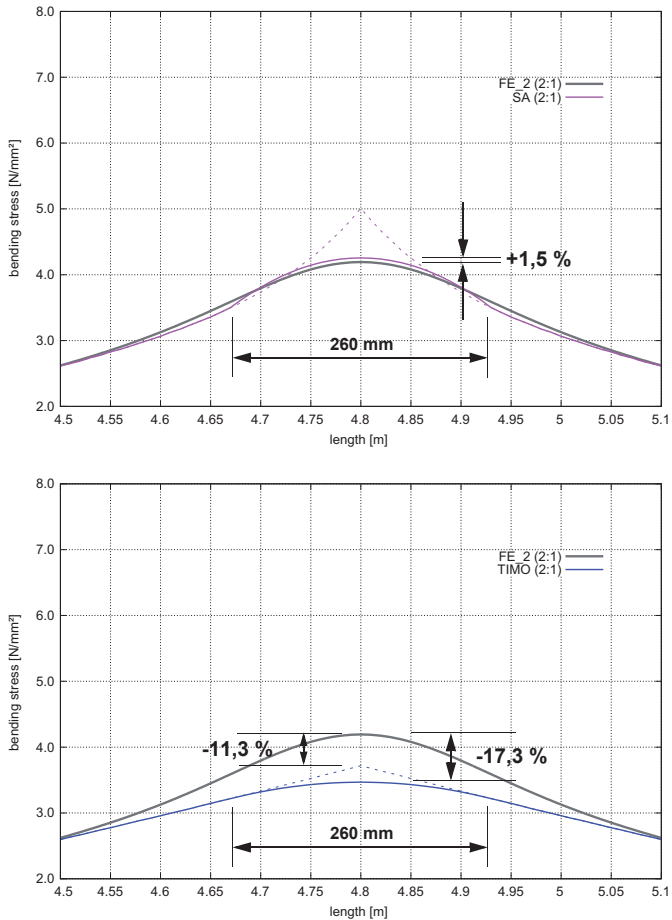


Fig. 5-11 Flexure tension stress within the supporting area, rounded down in the context of the approaches SA and TIMOSHENKO

The deviation of the rounded down SA-flexure tension stress from the FE-determination with „real supporting“ (FE_2) just amounts 1,5 % (cf. fig. 5-11), whereas in the context of the TIMOSHENKO-approach the deviation is fairly high and amounts to -17,3 %. If the TIMOSHENKO-results which are not rounded down are taken into consideration, the deviation is reduced to -11,3 % (cf. fig. 5-11). Similar degrees of deviation can be detected within the γ -process, which is not defined into further detail in this regard. On the basis of these results, increasing factors of stress could be suggested ranging from 1,17 for moment diagrams which are rounded down to 1,11 for moment diagrams which are not rounded down. Using these increased

support moments of the TIMOSHENKO beam, flexure tension stresses could be determined and cross-sectional verifications could be done.

5.5 System T2 – two-span girder exposed to uniform load ($t_L/t_Q = 1:2$)

In the following sections the two-span girder exposed to uniform load is analysed in terms of the ratio 1:2 between the thickness of longitudinal layer t_L and the thickness of transversal layer t_Q . This implies that in this example the thickness of the longitudinal layer is just half the one of the transversal layer (cf. fig. 5-1).

5.5.1 Dimensions of stiffness

For the γ -process the effective diagram of bending stiffness needs to be again determined. The effective lengths amount to 3,84 m for the fields and to 1,92 m for the supporting area. On the basis of these equivalent lengths, the following effective bending stiffness diagram can be deduced with regard to the γ -process:

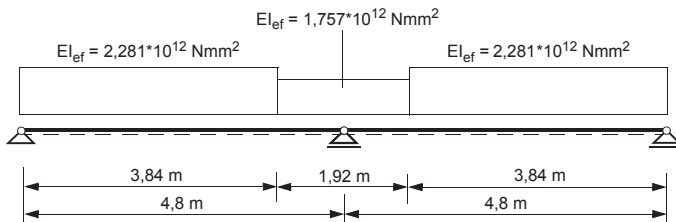


Fig. 5-12 Bending stiffness diagram when applying the γ -process

The dimensions of stiffness of the other approaches can be found in tab. 5-2.

5.5.2 Summary of results

Stress diagrams within the length of beam

The following illustrations show the diagrams of bending- and shear stresses of system T2 (two-span girder with the same span widths) with the ratio of thickness layer t_L/t_Q of 1:2.

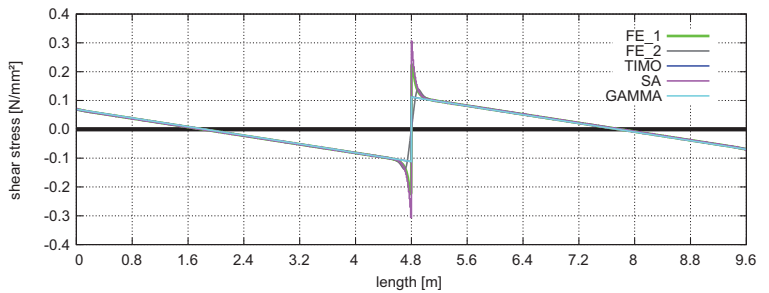
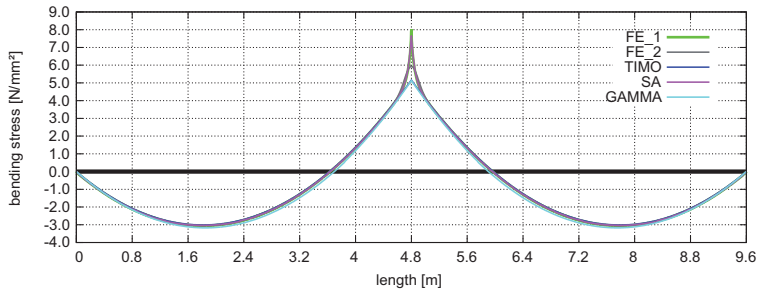


Fig. 5-13 Maximum bending- and shear stresses diagrams within the length of beam

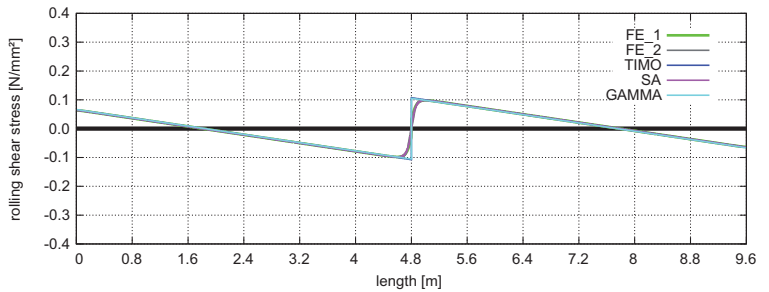


Fig. 5-14 Maximum rolling shear stress diagram within the length of beam

Bending stresses

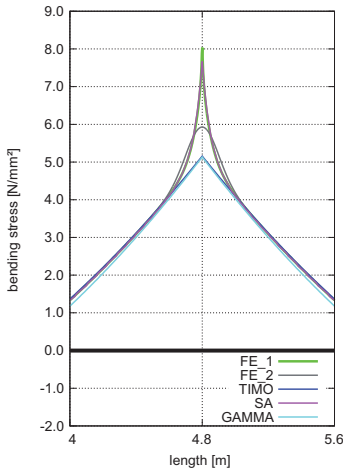


Fig. 5-15 Maximum bending stresses within the centre support

Shear stresses

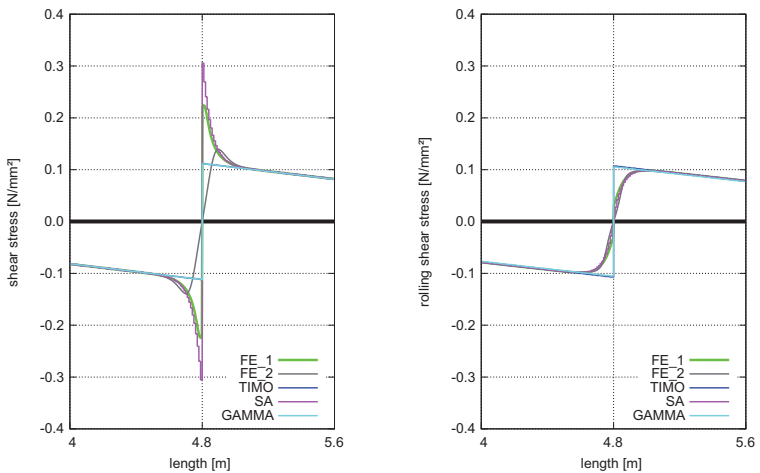


Fig. 5-16 Maximum shear- and rolling shear stresses within the supporting area

Tab. 5-7 Comparison and summary of results

	TIMOSHENKO	mod. γ -process	SA-method	2D-FE_1	2D-FE_2
	TIMO —	GAMMA —	SA —	FE_1 —	FE_2 —
	[N/mm ² , mm]				
σ_{\max}	5,158	5,134	7,669	8,036	5,928
τ_{\max}	0,112	0,112	0,306	0,224	0,139
$\tau_{\max(t)}$	0,104	0,104	0,107	0,107	0,109
$\tau_r(t)$	0,100	0,098	0,098	0,098	0,097
W_{\max}	6,80	6,85	6,78	6,82	6,81
	[%]	[%]	[%]	[%]	[%]
σ_{\max}	64,2	63,9	95,4	100	73,8
τ_{\max}	50,0	50,0	136,6	100	62,1
$\tau_{\max(t)}$	97,2	97,2	100,0	100	101,9
$\tau_r(t)$	102,0	100,0	100,0	100	99,0
W_{\max}	99,7	100,4	99,4	100	99,9

As it becomes evident in tab. 5-7, regarding the bending stress the deviations amount to ca. 36 % within the FE-supporting (FE_1) and the TIMOSHENKO-beam, or rather the modified γ -process. On the subject of the example „same thickness of layers“ (cf. chap. 4.3) these differences amount to ca. 35 % (cf. tab. 4-6). Hence, it can be said that the modified cross-sectional design has just a marginal impact on the differences in bending stress of the prevailing approaches.

5.5.3 Rounding down of moment within the supporting area

Analogous to chapter 4.3.4 a rounding down of moment within the supporting area is conducted. In the following illustrations the parabolic rounding down of moments and, as a consequence, of the flexure tension stresses on the top of the edge of slab is conducted within the range of $-(t_{clt}/2 + t_w/2 = 130 \text{ mm})$ to $+(t_{clt}/2 + t_w/2 = 130 \text{ mm})$ with t_{clt} (= 160 mm) as thickness of slab and t_w (= 100 mm) as thickness of wall. Added to this, the deviation from the FE-determination is defined as „real supporting“ (FE_2).

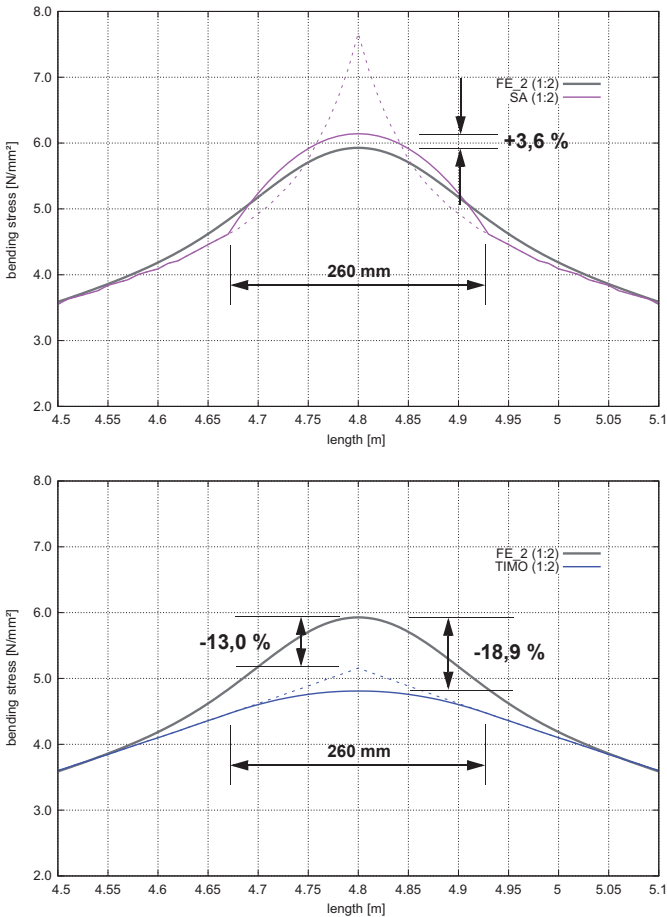


Fig. 5-17 Flexure tension stress within the supporting area, rounded down in the context of SA and TIMOSHENKO

The deviation of the rounded down SA-flexure tension stress from the FE-determination with „real supporting“ (FE_2) just amounts 3,6 % (cf. fig. 5-11), whereas in the context of the TIMOSHENKO-approach the deviation is fairly high and amounts to -18,9 %. If the TIMOSHENKO-results which are not rounded down are taken into consideration, the deviation is reduced to -13,0 % (cf. fig. 5-11). Similar degrees of deviation can be detected within the γ -process, which is not defined into further detail in this regard. On the basis of these results, increasing factors of stress could be suggested ranging from 1,19 for moment diagrams which are rounded down to 1,13 for moment diagrams which are not rounded down. Using these increased

support moments of the TIMOSHENKO beam, flexure tension stresses could be determined and cross-sectional verifications could be done.

5.6 System T1 – single-span girder exposed to uniform load (7I)

5.6.1 Determination of the γ -values according to SCHELLING

The equation system of the single-span girder „system T1“ with 7 layers is defined in appendix A. In this context, the focus of interest is on the numerical values of the equation system used in the course of applying the γ -process. The cross-sectional design consists of 7 layers with the same thickness per layer and a total thickness of 161 mm (cf. fig. 5-1).

E_0	11600	N/mm^2	a_1	69,0	mm
E_{90}	0	N/mm^2	a_2	23,0	mm
G_0	720	N/mm^2	a_3	-23,0	mm
G_{90}	72	N/mm^2	a_4	-69,0	mm
t_1	23	mm			
t_{ges}	161	mm	a_{12}	46	mm
			a_{23}	46	mm
L	4800	mm	a_{34}	46	mm
B	1000	mm			

Values of the individual layers:

$$A_i = B \cdot t_i = 23000 \text{ mm}^2 \qquad I_i = \frac{B \cdot t_i^3}{12} = 1013917 \text{ mm}^4$$

Joint stiffness of the transversal layer:

$$c = 3130,4 \text{ N/mm}^2$$

Solution:

$$\begin{bmatrix} 223885,92 & -72000 & 0 & 0 \\ -216000 & 146628,64 & 72000 & 0 \\ 0 & -72000 & -146628,64 & 216000 \\ 0 & 0 & 72000 & -223885,92 \end{bmatrix} \cdot \begin{bmatrix} \gamma^{*1} \\ \gamma^{*2} \\ \gamma^{*3} \\ \gamma^{*4} \end{bmatrix} = \begin{bmatrix} 144000 \\ 0 \\ 0 \\ -144000 \end{bmatrix}$$

$$\begin{bmatrix} \gamma^{*1} \\ \gamma^{*2} \\ \gamma^{*3} \\ \gamma^{*4} \end{bmatrix} = \begin{bmatrix} 0,942707 \\ 0,931373 \\ 0,931373 \\ 0,942707 \end{bmatrix}$$

As a consequence, the effective bending stiffness EI_{ef} of a slab strip with 1000 mm in width amounts to $2,705 \cdot 10^{12} \text{ Nmm}^2$ (cf. chapter A.1.1).

5.6.2 Dimensions of stiffness

Using the γ -values the effective bending stiffness (cf. chapter A.1.1) is determined. With regard to the single-span girder (system T1), the distribution of the bending stiffness along the rod axis is seen as consistent in the course of determining the internal forces.

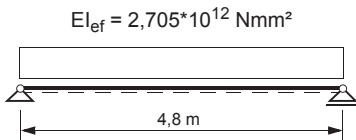


Fig. 5-18 Distribution of bending stiffness when applying the γ -process

5.6.3 Summary of results

Note: The term FE_1 — used in following illustrations and tables corresponds to the structural supporting defined in chap. 3.4.2.

The following illustrations show the diagrams of bending- and shear stresses of the system T1 (single-span girder). Nevertheless, it needs to be mentioned that the focus of attention is on the comparison of results of the stresses based on the γ -process according to SCHELLING (cf. GAMMA —) with the results of the FE-calculation with structural supporting (FE_1).

On the subject of rolling shear stresses, the differentiation between a maximum shear stress distribution and a maximum rolling shear stress distribution is totally unnecessary since in the context of the 7 layer slab the maximum shear stresses within the centre layer are defined as rolling shear stresses.

Tab. 5-8 Comparison and summary of results

	2D-FE_1	mod. γ -process
	FE_1	GAMMA
	[N/mm ²]	[N/mm ²]
σ_{\max}	4,721	4,727
τ_{\max}	0,100	0,106
	[%]	[%]
σ_{\max}	100	100,1
τ_{\max}	100	106,0

As it becomes evident in tab. 5-8, with regard to bending stresses the deviation within the modified γ -process and the FE-calculation with structural supporting is marginal. A slightly higher degree of deviation can be detected in the context of shear stresses.

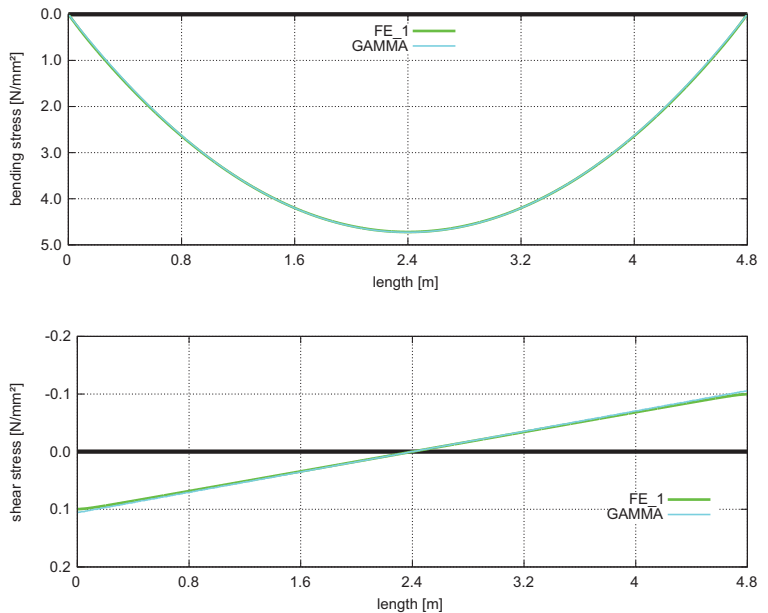


Fig. 5-19 Maximum bending- and rolling shear stresses diagrams within the length of beam

5.7 System T2 – two-span girder exposed to uniform load (7I)

As it becomes evident in example T2, the shear stresses within the supporting areas show different qualities compared with the relevant example of a 5 layer slab. The reason for the fundamental difference in maximum shear stress within the cross-sectional centre between 7 layer- and 5 layer slabs can be detected in the different orientations of their centre layers. In concrete terms this means that the centre layer of the 5 layer slab is turned in the principal direction, whereas the one of the 7 layer slab is perpendicular to this direction. Consequently, the rolling shear stresses can be identified.

5.7.1 Determination of the γ -values according to SCHELLING

On the subject of system T2 with 7 layer design (same layer thickness, 161 mm), two equation systems need to be solved: first within the field area, second within the supporting area; Regarding the field area a relevant length amounting to 80 % of the span width is presupposed. The relevant length of the supporting area consists of the remaining 20 % per internal supporting point - all in all 40 %.

E_0	11600	N/mm^2	a_1	69,0	mm
E_{90}	0	N/mm^2	a_2	23,0	mm
G_0	720	N/mm^2	a_3	-23,0	mm
G_{90}	72	N/mm^2	a_4	-69,0	mm
t_i	23	mm			
t_{ges}	161	mm	a_{12}	46	mm
			a_{23}	46	mm
L_{field}	3840	mm	a_{34}	46	mm
$L_{stütztz}$	1920				
B	1000	mm			

Values of the individual layers:

$$A_i = B \cdot t_i = 23000 \text{ mm}^2$$

$$I_i = \frac{B \cdot t_i^3}{12} = 1013917 \text{ mm}^4$$

Joint stiffness of the transversal layer:

$$c = 3130,4 \text{ N/mm}^2$$

Solution for the field area

$$\begin{bmatrix} 228321,74 & -72000 & 0 & 0 \\ -216000 & 148107,25 & 72000 & 0 \\ 0 & -72000 & -148107,25 & 216000 \\ 0 & 0 & 72000 & -228321,74 \end{bmatrix} \cdot \begin{bmatrix} \gamma_1^* \\ \gamma_2^* \\ \gamma_3^* \\ \gamma_4^* \end{bmatrix} = \begin{bmatrix} 144000 \\ 0 \\ 0 \\ -144000 \end{bmatrix}$$

$$\begin{bmatrix} \gamma_1^* \\ \gamma_2^* \\ \gamma_3^* \\ \gamma_4^* \end{bmatrix} = \begin{bmatrix} 0,913327 \\ 0,896284 \\ 0,896284 \\ 0,913327 \end{bmatrix}$$

Consequently, with regard to the field area the effective bending stiffness EI_{ef} of a slab strip with 1000 mm in width amounts to $2,620 \cdot 10^{12}$ Nmm².

Solution for the internal supporting area

$$\begin{bmatrix} 265286,98 & -72000 & 0 & 0 \\ -216000 & 160428,99 & 72000 & 0 \\ 0 & -72000 & -160428,99 & 216000 \\ 0 & 0 & 72000 & -265286,98 \end{bmatrix} \cdot \begin{bmatrix} \gamma_1^* \\ \gamma_2^* \\ \gamma_3^* \\ \gamma_4^* \end{bmatrix} = \begin{bmatrix} 144000 \\ 0 \\ 0 \\ -144000 \end{bmatrix}$$

$$\begin{bmatrix} \gamma_1^* \\ \gamma_2^* \\ \gamma_3^* \\ \gamma_4^* \end{bmatrix} = \begin{bmatrix} 0,725893 \\ 0,674585 \\ 0,674585 \\ 0,725893 \end{bmatrix}$$

Hence, in the context of the supporting area the effective bending stiffness EI_{ef} of a slab strip with 1000 mm in width amounts to $2,082 \cdot 10^{12}$ Nmm².

5.7.2 Dimensions of stiffness

Using the γ -values the effective bending stiffness (cf. chapter A.1.1) is determined. With regard to the continuous beam (system T2) the distribution of the bending stiffness along the rod axis is regarded as inconsistent. Therefore, there exist a field area and a supporting area (cf. chapter 4.3.1).

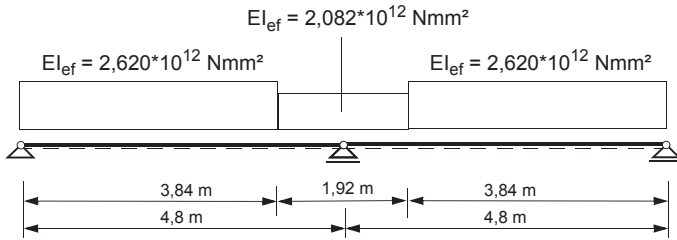


Fig. 5-20 Distribution of bending stiffness when applying the γ -process

5.7.3 Summary of results

Note: The term FE_1 — used in following illustrations and tables corresponds to the structural supporting defined in chap. 3.4.2.

The following illustrations show the diagrams of bending- and shear stresses of the system T2 (continuous beam with the same span widths). Nevertheless, it needs to be mentioned that the focus of attention is on the comparison of results of the stresses based on the γ -process according to SCHELLING (cf. GAMMA —) with the results of the FE-calculation with structural supporting (FE_1).

On the subject of shear stresses, the differentiation between a maximum shear stress distribution and a maximum rolling shear stress distribution is totally unnecessary since in the context of the 7 layer slab the layer within the gravity centre produces rolling shear stresses.

Tab. 5-9 Comparison and summary of the results

	2D-FE_1	mod. γ -Verfahren
	FE_1 —	GAMMA —
	[N/mm ²]	[N/mm ²]
σ_{max}	6,881	4,593
τ_{max}	0,111	0,121
	[%]	[%]
σ_{max}	100	66,7
τ_{max}	100	109,0

As it becomes evident in tab. 5-9, with regard to bending stresses the deviation at the internal support point within the modified γ -process and the FE-calculation with structural supporting is strikingly similar to the one in the comparable example (the deviation from the FE-solution amounts to 35 %, cf. chapter 4.3). The shear stresses resulting from the distance between the slab thickness t_{clt} and the edge of support (in sum 21 cm to the left, or rather to the right, side) are identified as deviations of almost 10 %.

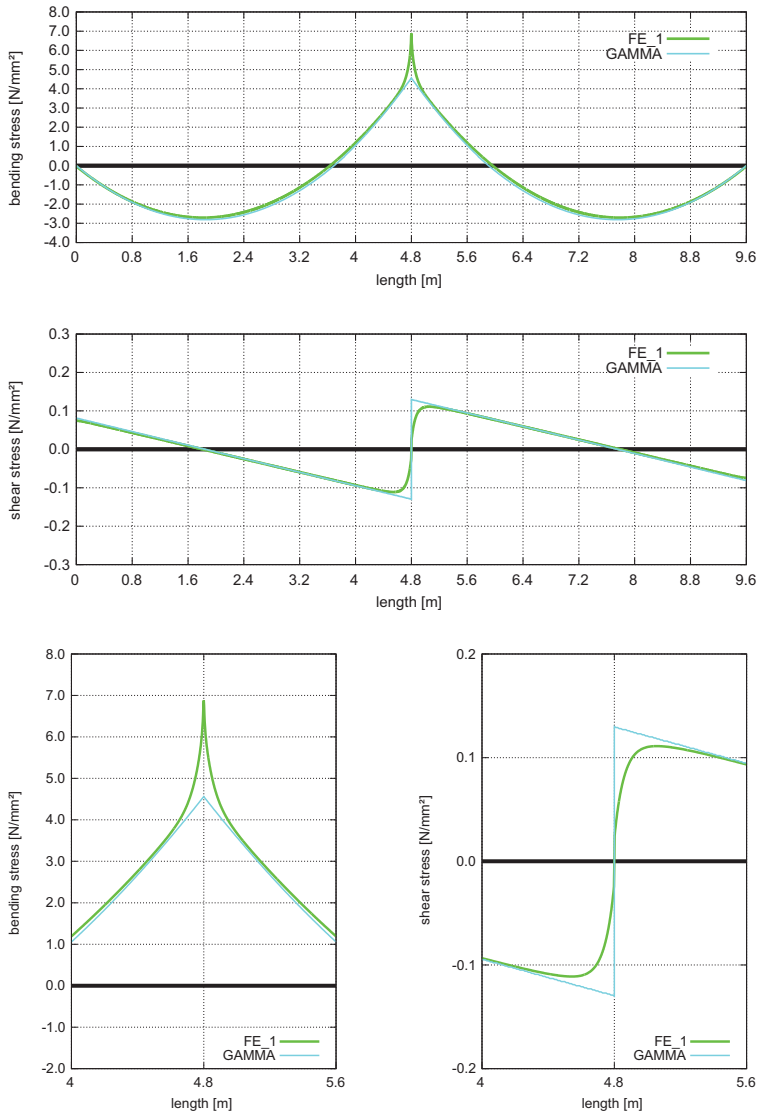


Fig. 5-21 Maximum bending- and shear stresses diagrams within the length of beam

6 Summary, Conclusion and Prospect

6.1 Summary

6.1.1 Stress peaks within the supporting area

By calculating the systems T1-T6 in chapter 4, several static systems are analysed in terms of stress distribution in longitudinal direction. All examples show a strong correlation between the stresses determined by applying the three approximate methods (TIMO, SA, GAMMA) within the field areas of the prevailing system. In the context of the statically defined basic case T1 with the L/H-ratio of 30, the maximum deviation of the bending stresses in comparison with the reference solution (cf. structural supporting, chap. 3.4.2) is regarded as 1 % (cf. tab. 4-4). Concerning all the other cases (T2-T6), which are statically undefined continuous beams, flexure tension stress peaks at the top of the slab are identified within the internal supporting points. In this regard, significant deviations (ca. 35 %) within the FE-solution (FE_1) and the TIMOSHENKO-beam, or rather the modified γ -process, are detected. On the subject of the SA-method, this difference is fairly smaller (ca. 10 %) (cf. tab. 6-1).

Tab. 6-1 Comparison of the maximum bending stresses

	TIMOSHENKO	mod. γ -process	SA-method	2D-FE_1	2D-FE_2	2D-FE_3
	TIMO 	GAMMA 	SA 	FE_1 	FE_2 	FE_3 
	[%]	[%]	[%]	[%]	[%]	[%]
T1	99,0	100,2	99,9	100		
T2	64,8	65,7	92,6	100	75,1	
T3	68,3	68,0	93,5	100	77,6	78,3
T4	62,8	64,1	92,2	100	73,6	75,9
T5	68,7	70,8	93,3	100	77,9	78,6
T6	68,4	69,2	93,5	100	77,7	78,8

Principally, it needs to be mentioned that also the γ -process can be applied in order to determine the stress peaks by solving the differential equation system in an analytical exact way. Due to the formulation of the Fourier series and the coexistent restriction on the first wave (sinusoidal load), other approaches (TIMOSHENKO-beam) are easier in their employment. Regarding the SA-method the differential equation system is solved in terms of a structural analysis and, hence, the previously mentioned weak spots are irrelevant.

In the course of modelling a real supporting situation with the finite element method (FEM) (establishing a contact with a CLT panel with 10 cm in width), it becomes evident that only rounded down stresses occur in the supporting areas (cf. FE-solution FE_2 and FE-solution FE_3). On the basis of this phenomenon, only adjustment factors which cover stress peaks could be defined in the context of the supporting moment. Numerical values of these factors for all three approximate

methods (TIMO/SA/GAMMA) can be found in chap. 4.3.4, chap. 5.4.3 and chap. 5.5.3.

6.1.2 Strength values within the supporting area

However, it is highly questionable whether these stress peaks are relevant to calculation anyway. First, it can be said that with regard to the verification of CLT-panels a global scope needs to be defined in which the results of all three approaches are comparable in practical terms. In addition, there exist local areas near the internal supporting points of continuous beams and single loads which, in a highly limited range, show stress peaks according to the rod theory. In terms of wood technology it might be interesting to analyse whether these stress peaks, which are based on the elasticity theory, can be also verified with locally increased strength values, since just a highly limited volume is concerned in this regard. FRESE reports on these local strength increasing effects in the context of GLT, which would range to 25 % [10]. Nevertheless, it remains unclear whether in the context of CLT a similar increase in strength is expectable. One possible solution is seen in comparing strength values based on the standard 4-point-bending test according to EN 408 with strength values based on the 3-point-bending test with a yet undefined span width. These analyses, however, would go beyond the scope of this report and, hence, are not described in any further detail.

6.1.3 Bending stresses within abridged L/H-ratios

Another aspect, which needs to be clarified, deals with the selection of the static systems. In this project, the focus of attention is on systems which are usually used in the context of the product cross laminated timber (L/H-ratio = 30). Nevertheless, in this regard the verification of the load-bearing capacity is of secondary importance compared with the verification of deflection.

In the course of analysing abridged span widths the disadvantages of the simplified rod theory according to TIMOSHENKO gain the upper hand. Due to the fact that the cross-section remains in plane, the effect of shear flexibility within transversal layers and the causally related impact on the bending stresses are described insufficiently. However, if the span width of example T1 (cf. chap. 4.2) is reduced from 4,8 m (L/H = 30) to 3,2 m (L/H = 20), the error of the maximum bending stress within the midspan is increased from 1,0 % to 2,2 %. In the course of a further reduction of the span width to 1,6 m (L/H = 10) the error increases up to 8,2 %. In the context of system T1 (single-span girder exposed to uniform load) the γ -process should be applied in order to define the position of the bending stresses due to the one-sectional sinusoidal formulation. It needs to be mentioned that this error of almost 10 % occurs among the L/H-ratio of 10, which is very unusual for CLT panels.

Nevertheless, the authors of this report would like to stress the paramount importance of the correct determination of bending stress within the area of internal supporting points of continuous systems, as it is the case with system T2. The stress based on concentrated individual loads perfectly represents the huge demands on CLT panels. As a consequence, in this regard the verification of the load-bearing

capacity is of absolutely essential. As it was described in chapter 4 and chapter 5, there exists a high gradient of longitudinal stress within the internal supporting point. Additionally, abridged span widths intensify this effect of local stress peaks.

On the basis of the FE-method with „real“ supporting (FE-solution FE_2 and FE-solution FE_3), an increase of the maximum flexure tension stress among the internal supporting points can be detected in the context of system T2. In concrete terms this means that the maximum flexure tension stress is increased by 5 %, if the L/H-ratio of 30 is reduced to 20. In contrast to the maximum flexure tension stress of T1, neither the γ -process nor the rod theory according to TIMOSHENKO produces sufficient results. If these local stress peaks are relevant to calculation (cf. chap. 6.1.2) the k-factors need to be defined in the context of the solution for the TIMOSHENKO-theory and the solution for the γ -process. Just the shear analogy method is able to produce relatively sufficient results on the subject of these stress peaks. However, the verifications in which these abridged L/H-ratios are relevant are usually not used within the main field of application of CLT panels. Therefore, the authors strongly suggested that they should be taken into consideration in an additional study.

6.1.4 Commentary on the selection of the reference solution

A point which also needs to be discussed is the selection of the reference solution, which is absolutely necessary for comparing the results. In order to provide an impartial representation of the outcomes, the FE-results with structural supporting (FE_1) are selected as the reference solution. The chosen web of 2/2 mm guarantees the quality of the determined stresses. Just the internal supporting points cause an „obstruction“: In theoretical terms on the subject of the structural supporting there occurs a singularity within the flexure tension stresses, if the vertical displacements of all nodes are blocked at the supporting line (FE_solution, FE_1, cf. chap. 3.4.2). If the dimensions of the web are reduced to 1/1 mm, the flexure tension stresses are increased by 3 %. As a consequence, the unreliability remains with regard to the reference value of the bending stress peaks within the internal supporting points. However in the course of correctly assessing the local stresses within the supporting area, it is highly advisable to prefer a comparison between the stresses using the FE-results of the real supporting design (FE-solution FE_2/3).

6.1.5 Deflections

The determined maximum deflections highly correlate with each other with regard to the three approximate approaches. Concerning the TIMOSHENKO-beam a maximum deviation of 0,5 % (within 6 standard scenarios T1 to T6 according to chap. 4) from the reference solution (FE_1, cf. tab. 6-2) can be detected. The best results are produced by the SA-method, which shows a deviation of just 0,2 % from the FE-solution. In the context of the γ -process the most significant difference can be identified, which amounts to 3,7 %. Nevertheless, it needs to be stated that even the results of the latter method can be regarded as highly accurate, if the distribution of stiffness with the γ -values is perfectly adapted to the moment diagram.

Tab. 6-2 Comparison of the maximum deflections

	TIMOSHENKO	mod. γ -process	SA-method	2D-FE_1	2D-FE_2	2D-FE_3
	TIMO —	GAMMA —	SA —	FE_1 —	FE_2 —	FE_3 —
	[%]	[%]	[%]	[%]	[%]	[%]
T1	100,0	99,6	100,1	100		
T2	100,5	100,4	99,8	100	100,0	
T3	100,2	103,7	100,0	100	100,0	97,4
T4	100,3	100,9	99,8	100	100,0	95,5
T5	100,1	98,0	100,0	100	100,0	97,3
T6	100,2	100,8	100,0	100	100,0	97,1

6.2 Conclusion and prospect

To conclude, it should be again stressed that the TIMOSHENKO-approach can be regarded as sufficient in the context of the calculations of deformation and stresses of the standard scenarios, which are analysed and performed in this report. However, in practical terms special cases, such as high individual load introductions, should be taken into consideration since they are definitely relevant to calculation. In this regard, the authors of this report would like to suggest that these stresses, or rather the stress peaks, are analysed in an additional study. In addition, it is highly advisable to make use of the same quality in the course of examining the stresses as it is applied in this study in order to be able to issue statements on possibly „hidden“ reserves on the subject of defining strength value.

With regard to the modified γ -process it can be said that within the effective lengths of continuous systems it is the attempt to make the best possible adjustment to the norms (0,8·l) and to the prevailing moment diagram. This effort results in a complex distribution of bending stiffness, which, in practical terms, is hardly used. Hence, it is highly possible that there exist errors up to 10 % within the stresses and the deflections. Exact statements on the impact of the effective span width need to be issued in an additional study.

As it was mentioned in the previous section, it is highly advisable to distinguish between global and local load bearing behaviour. In the context of this study it is the attempt to demonstrate that significant stress peaks might occur locally, for example at the internal supports of continuous beams. The question whether, or rather in how far, these stress peaks are relevant to calculation, needs to be answered in an additional study.

7 Bibliography

- [1] AICHER, S.: *Bemessung biegebeanspruchter Sandwichbalken mit dem modifizierten γ -Verfahren* In: Bautechnik; Nr.: 03/1987, S. 79-86.
- [2] AICHER, S.; ROTH, W.: *Ein modifiziertes γ -Verfahren für das mechanische Analogon: dreischichtiger Sandwichverbund-zweiteiliger verschieblicher Verbund* In: Bautechnik; Nr.: 01/1987, S. 21-29.
- [3] BURGER, N.: *Holzschalen in Brettrippenbauweise* In: Ingenieurholzbau Karlsruher Tage. Bruderverlag Karlsruhe, S. 101-119, 2001.
- [4] DIN 1052: *Teil 1: Holzbauwerke; Berechnung und Ausführung*, Oktober 1969.
- [5] DIN 1052: *Entwurf, Berechnung und Bemessung von Holzbauwerken*, Dezember 2008.
- [6] DIN EN 1995-1-1: *Eurocode 5 – Bemessung und Konstruktion von Holzbauten: Teil 1-1: Allgemeines - Allgemeine Regeln und Regeln für den Hochbau*, Dezember 2010.
- [7] DIN EN 1995-1-1/NA: *Nationaler Anhang – National festgelegte Parameter – Eurocode 5: Bemessung und Konstruktion von Holzbauten – Teil 1-1: Allgemeines – Allgemeine Regeln und Regeln für den Hochbau*, Dezember 2010.
- [8] ETA 06/0009: *Binder Brettsperrholz BBS – Mehrschichtige Holzbauelemente für Wand-, Decken-, Dach und Sonderbauteile*, Binder Holzbausysteme GmbH, Deutsches Institut für Bautechnik, Berlin, Oktober 2006.
- [9] ETA 06/0138: *Massive plattenförmige Holzbauelemente für tragende Bauteile in Bauwerken*, KLH Massivholz GmbH, Österreichisches Institut für Bautechnik, Wien, Juli 2011.
- [10] FRESE, M.: *System effects in continuous glulam beams*, Conference Proceedings of the 11th WCTE, Riva del Garda, Italy, 2010.
- [11] GABER, E.: *Sparsame Holzträger: ein Beitrag zum hochwertigen Holzbau*. VDI-Verlag Berlin, 1940.
- [12] GRAF, O.: *Biegeversuche mit verdübelten Holzbalken*. Der Bauingenieur, 11. Jahrgang, S. 157-160, 1930.
- [13] KREUZINGER, H.: *Platten, Scheiben und Schalen*. Bauen mit Holz, 101. Jahrgang, Heft I, S. 34-39, 1999.
- [14] KREUZINGER, H.: *Flächentragwerke - Platten, Scheiben und Schalen – Berechnungsmethoden und Beispiele*. Fachverlag Holz Düsseldorf, S. 43-60, 1999.

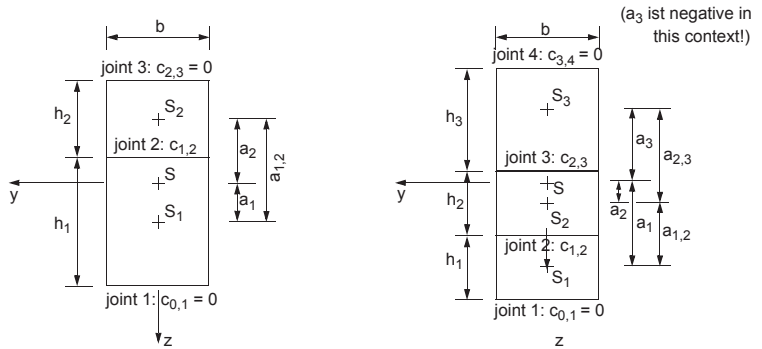
- [15] KREUZINGER, H.: *Verbundkonstruktionen aus nachgiebig miteinander verbundenen Querschnittsteilen* In: Ingenieurholzbau Karlsruher Tage. Bruderverlag Karlsruhe, S. 43-55, 2000.
- [16] KREUZINGER, H.: *Verbundkonstruktionen* In: Holzbaukalender 2002. Bruderverlag Karlsruhe, S.598-621, 2002.
- [17] MESTEK, P.: *Punktgestützte Flächentragwerke aus Brettsperrholz (BSP) – Schubermessung unter Berücksichtigung von Schubverstärkungen*, Dissertation TU München, 2011.
- [18] MOOSBRUGGER, T.: *Elastomechanik von Stäben mit komplexem Querschnittsaufbau und verallgemeinerter Querschnittskinetik (Arbeitstitel)*. Technische Universität Graz, Fakultät für Bauingenieurwissenschaften, Dissertation (geplante Veröffentlichung 2012), Institut für Stahlbau.
- [19] MÖHLER, K.: *Über das Tragverhalten von Biegeträgern und Druckstäben mit zusammengesetzten Querschnitten und nachgiebigen Verbindungsmitteln*. Habilitation TH Karlsruhe, 1962.
- [20] MÖHLER, K.: *Die Bemessung der Verbindungsmittel bei zusammengesetzten Biege- und Druckgliedern im Holzbau*. Bauen mit Holz, 68. Jahrgang, S. 162-164, 1966.
- [21] ÖNORM EN 1995-1-1: *Eurocode 5 – Bemessung und Konstruktion von Holzbauwerken: Teil 1-1: Allgemeines - Allgemeine Regeln und Regeln für den Hochbau*, Juli 2009.
- [22] ÖNORM EN 338: *Bauholz für tragende Zwecke : Festigkeitsklassen*, Juli 2003.
- [23] ÖNORM EN 1194: *Holzbauwerke: Brettschichtholz – Festigkeitsklassen und Bestimmung charakteristischer Werte*, September 1999.
- [24] ÖNORM EN 408: *Holzbauwerke – Bauholz für tragende Zwecke und Brettschichtholz – Bestimmung einiger physikalischer und mechanischer Eigenschaften*, Dezember 2010.
- [25] PETERSON, L. A.: *Zum Tragverhalten nachgiebig verbundener Biegeträger aus Holz*, Berichte des Instituts für Bauphysik der Leibniz Universität Hannover Herausgeber: Univ.-Prof. Dr.-Ing. Nabil A. Fouad; Leibniz Universität Hannover - Institut für Bauphysik Heft 1, April 2008.
- [26] PISCHL, R.: *Ein Beitrag zur Berechnung zusammengesetzter hölzerner Biegeträger*. Der Bauingenieur, 43. Jahrgang, S.448-452, 1968.
- [27] PISCHL, R.: *Die praktische Berechnung zusammengesetzter hölzerner Biegeträger mit Hilfstabeln zur Berechnung der Abminderungsfaktoren*. Der Bauingenieur, 44. Jahrgang, S.181-185, 1969.

- [28] PISCHL, R.: *Die Auslegung der Verbindungsmittel bei zusammengesetzten hölzernen Biegeträgern*. Der Bauingenieur, 44. Jahrgang, S.419-423, 1969.
- [29] PISCHL, R.: *Die direkte Bemessung der Verbindungsmittel bei zusammengesetzten Biegeträgern im Holzbau unter Voraussetzung von DIN 1052, Absatz 5*. Der Bauingenieur, 48. Jahrgang, S.293-296+470, 1973.
- [30] SCHELLING, W.: *Die Berechnung nachgiebig verbundener zusammengesetzter Biegeträger im Ingenieurholzbau*. Dissertation TH Karlsruhe, 1968.
- [31] SCHELLING, W.: *Zur Berechnung nachgiebig zusammengesetzter Biegeträger aus beliebig vielen Einzelquerschnitten* In: EHLBECK, J. (Hrsg.); STECK, G. (Hrsg.): Ingenieurholzbau in Forschung und Praxis. Bruderverlag Karlsruhe 1982.
- [32] SCHELLING, W.: *Genauere Berechnung nachgiebig verbundener Holzbiegeträger mit dem γ -Verfahren* In: Festschrift E. Csiesielski. Werner-Verlag. S 10, April, 1998.
- [33] SCHOLZ, A.: *Ein Beitrag zur Berechnung von Flächentragwerken aus Holz*. Dissertation TU München, 2004.
- [34] www.humbert-online.de/pic/exp004.jpg
- [35] www.heise.de/foto/galerie/Expo-Dach-a70ecedc2d440f8a4043a3b55178534/
- [36] Z-9.1-680: *HMS – Element*, Haas FERTIGBAU GmbH, Deutsches Institut für Bau-technik, Berlin, Januar 2007.

A Appendix A – Examples and comments to the γ -process according to SCHELLING and EN 1995-1-1

A.1 Solution according to SCHELLING in order to determine the γ -values

On the subject of the special case of a rod supported by hinges at both ends exposed to sinusoidal load, an exact solution is obtained by SCHELLING in [30]. The used terms of SCHELLING are provided in the following sketch:



SCHELLING begins with the numbering of the cross-sectional elements within the positive z-range. Added to this, each of the first and the last joints needs to be defined with a joint stiffness of 0. It also needs to be taken into consideration that the spaces a_i are z-coordinates and, consequently, need to be marked with the relevant sign. The $a_{i,i+1}$ values define spaces and, hence, need to be defined as positive numbers.

Note: Due to the fact that the γ -processes differ between EC 5 [21] and SCHELLING [30], [31], [32], the γ -values according to SCHELLING are defined as γ^* .

A.1.1 Determination of stiffness

On the basis of this solution the effective bending stiffness $(EI)_{ef}$ is determined by subdividing it up into dimensions of eigen stiffness and into the so-called „Steiner-terms“:

$$(EI)_{ef} = \sum_i \frac{E \cdot b_i \cdot h_i^3}{12} + \sum_i \gamma_i^* \cdot EA_i \cdot a_i^2$$

The work of SCHELLING forms the basis of the Gamma approach, but the representation within the norm includes another effective gravity centre. Therefore, the γ -values according to the norm differ significantly from the ones according to the original calculation method of SCHELLING, which is presented in the following sections. As a consequence, the γ -values of this equation system are defined as γ^* in this report. The γ^* -values are applied in order to reduce the Steiner-terms, while the dimensions of eigen stiffness contribute significantly to the bending stiffness.

In order to calculate these γ_i -values, SCHELLING provides the following equation system in [31]:

$$\begin{bmatrix} v_{1,1} & v_{1,2} & 0 & 0 & 0 & 0 & 0 \\ v_{2,1} & v_{2,2} & v_{2,3} & 0 & 0 & 0 & 0 \\ 0 & \dots & \dots & \dots & 0 & 0 & 0 \\ 0 & 0 & v_{i,i-1} & v_{i,i} & v_{i,i+1} & 0 & 0 \\ 0 & 0 & 0 & \dots & \dots & \dots & 0 \\ 0 & 0 & 0 & 0 & v_{m-1,m-2} & v_{m-1,m-1} & v_{m-1,m} \\ 0 & 0 & 0 & 0 & 0 & v_{m,m-1} & v_{m,m} \end{bmatrix} \cdot \begin{bmatrix} \gamma^*_1 \\ \gamma^*_2 \\ \dots \\ \gamma^*_i \\ \dots \\ \dots \\ \gamma^*_m \end{bmatrix} = \begin{bmatrix} s_1 \\ s_2 \\ \dots \\ s_i \\ \dots \\ s_{m-1} \\ s_m \end{bmatrix}$$

The number of γ -values corresponds with the number of flexibly connected individual elements of beam of the cross-section (m-cross-sectional elements, (m-1)-cross-sectional joints).

Each line of the matrix consists of 3 values at maximum: the value of the principal diagonal $v_{i,i}$ and both following values $v_{i,i-1}$ and $v_{i,i+1}$. These 3 values, $v_{i,i-1}$, $v_{i,i}$ and $v_{i,i+1}$, and the values of the right side of the equation system s_i can be determined by using the following equations:

$$\begin{aligned} v_{i,i-1} &= -c_{i-1,i} \cdot a_{i-1} \\ v_{i,i} &= \left(c_{i-1,i} + c_{i,i+1} + \frac{\pi^2}{l^2} \cdot E_i \cdot A_i \right) \cdot a_i \\ v_{i,i+1} &= -c_{i,i+1} \cdot a_{i+1} \\ s_i &= c_{i,i+1} \cdot a_{i+1} - c_{i-1,i} \cdot a_{i-1,i} \end{aligned}$$

A.1.2 Determination of bending stress

When being aware of the γ_i -values, the stress of the individual gravity centre of the partial cross-section i and the gradient of the stress put on the layer i with the height h_i can be determined as follows:

$$\begin{aligned} \sigma_{N,i} &= \frac{M}{(EI)_{\text{eff}}} \cdot \gamma^*_i \cdot E_i \cdot a_i \\ \sigma_{M,i} &= \frac{M}{(EI)_{\text{eff}}} \cdot E_i \cdot \frac{h_i}{2} \end{aligned}$$

Edge stresses of the layer i:

$$\sigma_{i, edge} = \frac{M}{(EI)_{ef}} \cdot E_i \cdot \left(\gamma_i^* \cdot a_i \pm \frac{h_i}{2} \right)$$

A.2 2-, 3- and 4-part cross-section according to SCHELLING

A.2.1 2-part cross-section

The individual values of the 2-part cross-section are:

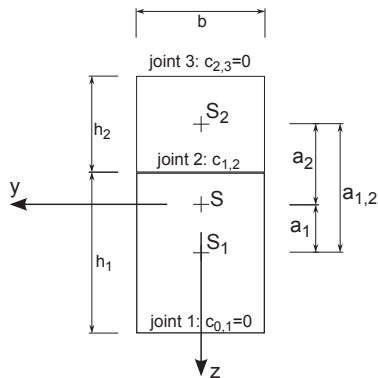


Fig. A-1 2-part cross-section

Tab. A-1 Values of the equation system of the 2-part cross-section

	$v_{i,i-1}$	$v_{i,i}$	$v_{i,i+1}$	s_i
line 1	0	$\left(c_{1,2} + \frac{\pi^2}{l^2} \cdot E_1 \cdot A_1 \right) \cdot a_1$	$-c_{1,2} \cdot a_2$	$c_{1,2} \cdot a_{1,2}$
line 2	$-c_{1,2} \cdot a_1$	$\left(c_{1,2} + \frac{\pi^2}{l^2} \cdot E_2 \cdot A_2 \right) \cdot a_2$	0	$-c_{1,2} \cdot a_{1,2}$

According to SCHELLING the distance $a_{1,2}$ is always positive, the values a_1 and a_2 as coordinates need to be defined with the relevant signs.

Hence, the following equation system of the γ_i^* -values is created:

$$\begin{bmatrix} \left(c_{1,2} + \frac{\pi^2}{l^2} \cdot E_1 \cdot A_1\right) \cdot a_1 & -c_{1,2} \cdot a_2 \\ -c_{1,2} \cdot a_1 & \left(c_{1,2} + \frac{\pi^2}{l^2} \cdot E_2 \cdot A_2\right) \cdot a_2 \end{bmatrix} \cdot \begin{bmatrix} \gamma_{1,2}^* \\ \gamma_{2,3}^* \end{bmatrix} = \begin{bmatrix} c_{1,2} \cdot a_{1,2} \\ -c_{1,2} \cdot a_{1,2} \end{bmatrix}$$

Solution for the $\gamma_{i-1,i}^*$ -values:

$$\gamma_{1,2}^* = \frac{c \cdot L^2 \cdot a_{12} \cdot EA_2}{a_1 \cdot [c \cdot L^2 \cdot (EA_1 + EA_2) + EA_1 \cdot EA_2 \cdot \pi^2]}$$

$$\gamma_{2,3}^* = -\frac{c \cdot L^2 \cdot a_{12} \cdot EA_1}{a_2 \cdot [c \cdot L^2 \cdot (EA_1 + EA_2) + EA_1 \cdot EA_2 \cdot \pi^2]}$$

A.2.2 3-part cross-section

The individual values of the 3-part cross-section are:

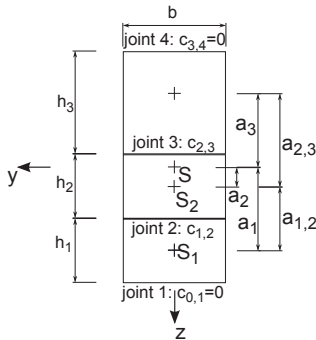


Fig. A-2 3-part cross-section

Tab. A-2 Values of the equation system of the 3-part cross-section

	$v_{i,i-1}$	$v_{i,i}$	$v_{i,i+1}$	s_i
line 1	0	$\left(c_{1,2} + \frac{\pi^2}{l^2} \cdot E_1 \cdot A_1\right) \cdot a_1$	$-c_{1,2} \cdot a_2$	$c_{1,2} \cdot a_{1,2}$
line 2	$-c_{1,2} \cdot a_1$	$\left(c_{1,2} + c_{2,3} + \frac{\pi^2}{l^2} \cdot E_2 \cdot A_2\right) \cdot a_2$	$-c_{2,3} \cdot a_3$	$c_{2,3} \cdot a_{2,3} - c_{1,2} \cdot a_{1,2}$
line 3	$-c_{2,3} \cdot a_2$	$\left(c_{2,3} + \frac{\pi^2}{l^2} \cdot E_3 \cdot A_3\right) \cdot a_3$	0	$-c_{2,3} \cdot a_{2,3}$

According to SCHELLING the distances $a_{1,2}$ and $a_{2,3}$ are always positive, the values a_1 , a_2 and a_3 as coordinates need to be defined with the relevant signs.

Hence, the following equation system of the γ^*_{i-} -values is created:

$$\begin{bmatrix} \left(c_{1,2} + \frac{\pi^2}{l^2} \cdot E_1 \cdot A_1\right) \cdot a_1 & -c_{1,2} \cdot a_2 & 0 \\ -c_{1,2} \cdot a_1 & \left(c_{1,2} + c_{2,3} + \frac{\pi^2}{l^2} \cdot E_2 \cdot A_2\right) \cdot a_2 & -c_{2,3} \cdot a_3 \\ 0 & -c_{2,3} \cdot a_2 & \left(c_{2,3} + \frac{\pi^2}{l^2} \cdot E_3 \cdot A_3\right) \cdot a_3 \end{bmatrix} \cdot \begin{bmatrix} \gamma^*_{1-} \\ \gamma^*_{2-} \\ \gamma^*_{3-} \end{bmatrix} = \begin{bmatrix} c_{1,2} \cdot a_{1,2} \\ c_{2,3} \cdot a_{2,3} - c_{1,2} \cdot a_{1,2} \\ -c_{2,3} \cdot a_{2,3} \end{bmatrix}$$

Solution for the γ^*_{i-} -values in the context of the special case $c = c_{1,2} = c_{2,3}$:

$$\gamma^*_{1-} = \frac{c \cdot L^2 \cdot [a_{12} \cdot (EA_2 + EA_3) + a_{23} \cdot EA_3 + a_{12} \cdot EA_2 \cdot EA_3 \cdot \pi^2]}{a_1 \cdot [c^2 \cdot L^4 \cdot (EA_1 + EA_2 + EA_3) + c \cdot L^2 \cdot \pi^2 \cdot (EA_1 \cdot EA_2 + 2 \cdot EA_1 \cdot EA_3 + EA_2 \cdot EA_3) + \pi^4 \cdot EA_1 \cdot EA_2 \cdot EA_3]}$$

$$\gamma^*_{2-} = \frac{c \cdot L^2 \cdot (-a_{12} \cdot EA_1 + a_{23} \cdot EA_3) + c \cdot L^2 \cdot \pi^2 \cdot (-a_{12} + a_{23}) \cdot EA_1 \cdot EA_3}{a_3 \cdot [c^2 \cdot L^4 \cdot (EA_1 + EA_2 + EA_3) + c \cdot L^2 \cdot \pi^2 \cdot (EA_1 \cdot EA_2 + 2 \cdot EA_1 \cdot EA_3 + EA_2 \cdot EA_3) + \pi^4 \cdot EA_1 \cdot EA_2 \cdot EA_3]}$$

$$\gamma^*_{3-} = \frac{c \cdot L^2 \cdot [a_{23} \cdot (EA_1 + EA_2) + a_{12} \cdot EA_1 + a_{23} \cdot EA_1 \cdot EA_2 \cdot \pi^2]}{a_3 \cdot [c^2 \cdot L^4 \cdot (EA_1 + EA_2 + EA_3) + c \cdot L^2 \cdot \pi^2 \cdot (EA_1 \cdot EA_2 + 2 \cdot EA_1 \cdot EA_3 + EA_2 \cdot EA_3) + \pi^4 \cdot EA_1 \cdot EA_2 \cdot EA_3]}$$

With regard to different joint flexibilities $c_{1,2} \neq c_{2,3}$ the previously presented equation system of the individual γ^*_{i-} -values needs to be solved numerically.

A.2.3 4-part cross-section

The individual values of the 4-part cross-section are:

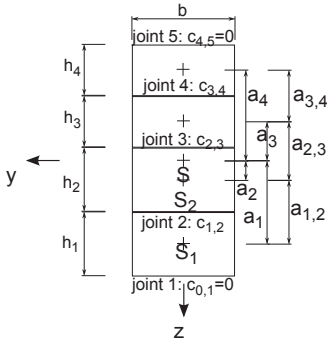


Fig. A-3 4-part cross-section

Tab. A-3 Values of the equation system of the 4-part cross-section

	$v_{i,i-1}$	$v_{i,i}$	$v_{i,i+1}$	s_i
line 1	0	$\left(c_{1,2} + \frac{\pi^2}{l^2} \cdot E_1 \cdot A_1 \right) \cdot a_1$	$-c_{1,2} \cdot a_2$	$c_{1,2} \cdot a_{1,2}$
line 2	$-c_{1,2} \cdot a_1$	$\left(c_{1,2} + c_{2,3} + \frac{\pi^2}{l^2} \cdot E_2 \cdot A_2 \right) \cdot a_2$	$-c_{2,3} \cdot a_3$	$c_{2,3} \cdot a_{2,3} - c_{1,2} \cdot a_{1,2}$
line 3	$-c_{2,3} \cdot a_2$	$\left(c_{2,3} + c_{3,4} + \frac{\pi^2}{l^2} \cdot E_3 \cdot A_3 \right) \cdot a_3$	$-c_{3,4} \cdot a_4$	$c_{3,4} \cdot a_{3,4} - c_{2,3} \cdot a_{2,3}$
line 4	$-c_{3,4} \cdot a_3$	$\left(c_{3,4} + \frac{\pi^2}{l^2} \cdot E_4 \cdot A_4 \right) \cdot a_4$	0	$-c_{3,4} \cdot a_{3,4}$

According to SCHELLING the distances $a_{1,2}, a_{2,3}$ and $a_{3,4}$ are always positive, the values a_1, a_2, a_3 and a_4 as coordinates need to be defined with the relevant signs.

Hence, the following equation system of the γ^* -values is created:

$$V \cdot \begin{bmatrix} \gamma^*_1 \\ \gamma^*_2 \\ \gamma^*_3 \\ \gamma^*_4 \end{bmatrix} = \begin{bmatrix} c_{1,2} \cdot a_{1,2} \\ c_{2,3} \cdot a_{2,3} - c_{1,2} \cdot a_{1,2} \\ c_{3,4} \cdot a_{3,4} - c_{2,3} \cdot a_{2,3} \\ -c_{3,4} \cdot a_{3,4} \end{bmatrix}$$

The left side V is defined as follows:

$$V = \begin{bmatrix} \left(c_{1,2} + \frac{\pi^2}{l^2} \cdot E_1 \cdot A_1\right) \cdot a_1 & -c_{1,2} \cdot a_2 & 0 & 0 \\ -c_{1,2} \cdot a_1 & \left(c_{1,2} + c_{2,3} + \frac{\pi^2}{l^2} \cdot E_2 \cdot A_2\right) \cdot a_2 & -c_{2,3} \cdot a_3 & 0 \\ 0 & -c_{2,3} \cdot a_2 & \left(c_{2,3} + c_{3,4} + \frac{\pi^2}{l^2} \cdot E_3 \cdot A_3\right) \cdot a_3 & -c_{3,4} \cdot a_4 \\ 0 & 0 & -c_{3,4} \cdot a_3 & \left(c_{3,4} + \frac{\pi^2}{l^2} \cdot E_4 \cdot A_4\right) \cdot a_4 \end{bmatrix}$$

A.3 Examples – flexibly connected bending members

In the following sections the approaches according to SCHELLING [31] and the formulations according to EC 5, appendix B [21] are applied to 2- and 3-part cross-sections.

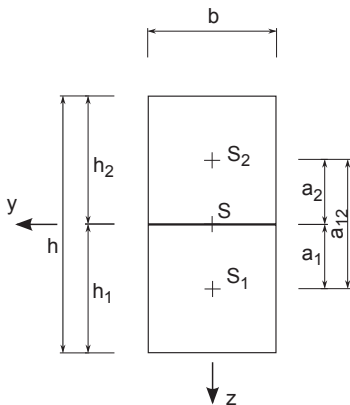
A single-span girder is used as static system. The span width of this girder amounts to 6 m. The dimensions of the 2-part cross-section are defined as $b = 16$ cm and $h = 32$ cm, while those of the 3-part cross-section are regarded as $b = 16$ cm and $h = 36$ cm. The used material is C24 and the E-modulus amounts to 11000 N/mm². Finally, the joint stiffness amounts to 80000 kN/m².

On the left side the notation according to SCHELLING can be found, whereas the one according to EC is placed on the right side.

A.3.1 2-part cross-section – example 1

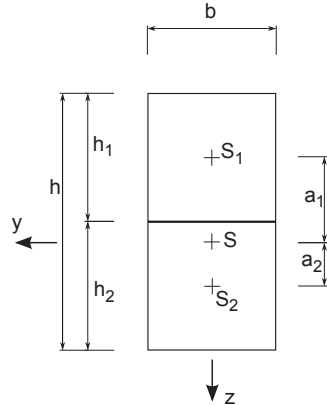
Dimensions of the selected cross-section, position of the gravity centres:

definition according to SCHELLING



$h_1=160$ mm
 $h_2=160$ mm
 $EA_1=281600$ kN
 $EA_2=281600$ kN
 $a_1=80$ mm
 $a_2=-80$ mm
 $a_{12}=160$ mm

definition according to EC 5/appendix B



$h_1=160$ mm
 $h_2=160$ mm
 $EA_1=281600$ kN
 $EA_2=281600$ kN
 a_1
 a_2

$b=160$ mm
 $h=320$ mm
 $L=6$ m
 $E=11000$ N/mm²
 $c=80000$ kN/m²

S ... position of the total gravity centre
 S_1 ... position of the partial cross section 1
 S_2 ... position of the partial cross section 2

Determination of the γ^* -values according to SCHELLING:

$$\gamma^*_{1} = \frac{c \cdot L^2 \cdot a_{12} \cdot EA_2}{a_1 \cdot [c \cdot L^2 \cdot (EA_1 + EA_2) + EA_1 \cdot EA_2 \cdot \pi^2]} = 0,67453$$

$$\gamma^*_{2} = -\frac{c \cdot L^2 \cdot a_{12} \cdot EA_1}{a_2 \cdot [c \cdot L^2 \cdot (EA_1 + EA_2) + EA_1 \cdot EA_2 \cdot \pi^2]} = 0,67453$$

Determination of the effective bending stiffness according to SCHELLING:

$$(EI)_{\text{ef}} = \frac{E \cdot b \cdot h_1^3}{12} + \frac{E \cdot b \cdot h_2^3}{12} + \gamma^*_{1} \cdot EA_1 \cdot a_1^2 + \gamma^*_{2} \cdot EA_2 \cdot a_2^2 = 3632,82 \text{ kNm}^2$$

Despite the symmetry of the cross-section, the determination according to EC 5/appendix B results in a position of gravity centre which cannot be detected in the centre, i.e. within the connection line.

γ -values, a_1 and a_2 , according to EC 5/appendix B:

$$\gamma_1 = \frac{1}{1 + \pi^2 \cdot \frac{EA_1}{c \cdot L^2}} = 0,508899$$

$$\gamma_2 = 1$$

$$a_2 = \frac{\gamma_1 \cdot EA_1 \cdot (h_1 + h_2)}{2 \cdot (\gamma_1 \cdot EA_1 + \gamma_2 \cdot EA_2)} = 0,0539624$$

$$a_1 = \frac{h_1 + h_2}{2} - a_2 = 0,106038$$

Note:
in the context of the 2-part cross-section a_2 is always positive!

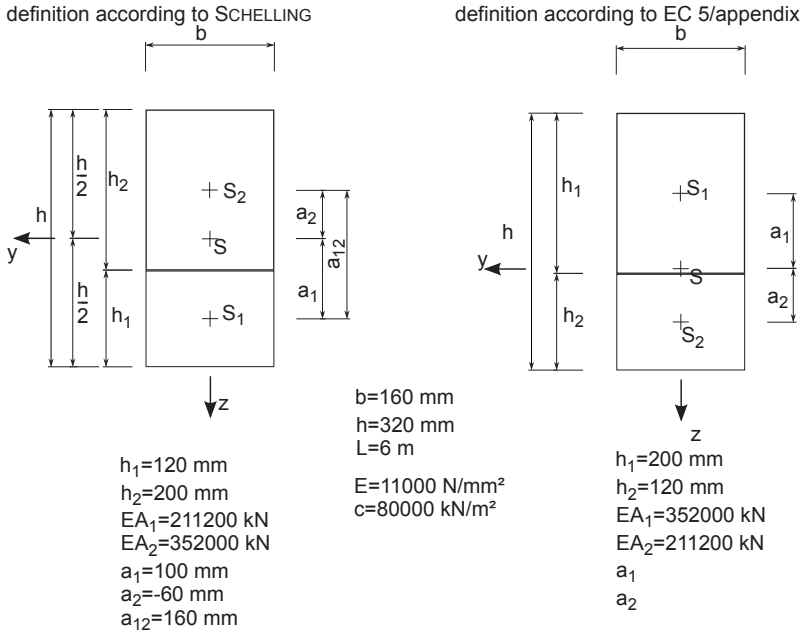
Determination of the effective bending stiffness according to EC 5/appendix B:

$$(EI)_{\text{ef}} = \frac{E \cdot b \cdot h_1^3}{12} + \frac{E \cdot b \cdot h_2^3}{12} + \gamma_1 \cdot EA_1 \cdot a_1^2 + \gamma_2 \cdot EA_2 \cdot a_2^2 = 3632,82 \text{ kNm}^2$$

Although the γ -values and both spaces a_1 and a_2 differ between SCHELLING and EC 5, the determined effective bending stiffness $(EI)_{\text{ef}}$ is identical within both approaches.

A.3.2 2-part cross-section – example 2

Dimensions of the selected cross-section, position of the gravity centres:



S ... position of the total gravity centre
S₁ .. position of the partial cross section 1
S₂ .. position of the partial cross section 2

Determination of the γ^* -values according to SCHELLING:

$$\gamma^*_1 = \frac{c \cdot L^2 \cdot a_{12} \cdot EA_2}{a_1 \cdot [c \cdot L^2 \cdot (EA_1 + EA_2) + EA_1 \cdot EA_2 \cdot \pi^2]} = 0,688536$$

$$\gamma^*_2 = -\frac{c \cdot L^2 \cdot a_{12} \cdot EA_1}{a_2 \cdot [c \cdot L^2 \cdot (EA_1 + EA_2) + EA_1 \cdot EA_2 \cdot \pi^2]} = 0,688536$$

Determination of the effective bending stiffness according to SCHELLING:

$$(ED)_{ef} = \frac{E \cdot b \cdot h_1^3}{12} + \frac{E \cdot b \cdot h_2^3}{12} + \gamma^*_1 \cdot EA_1 \cdot a_1^2 + \gamma^*_2 \cdot EA_2 \cdot a_2^2 = 3753,47\text{ kNm}^2$$

The determination according to EC 5/appendix B results in a position of gravity centre which cannot be detected in the centre of the cross-section.

γ -values, a_1 and a_2 , according to EC 5/appendix B:

$$\gamma_1 = \frac{1}{1 + \pi^2 \cdot \frac{EA_1}{c \cdot L^2}} = 0,453251$$

$$\gamma_2 = 1$$

$$a_2 = \frac{\gamma_1 \cdot EA_1 \cdot (h_1 + h_2)}{2 \cdot (\gamma_1 \cdot EA_1 + \gamma_2 \cdot EA_2)} = 0,0688536$$

$$a_1 = \frac{h_1 + h_2}{2} - a_2 = 0,0911464$$

Note:

in the context of the 2-part cross-section a_2 is always positive!

Determination of the effective bending stiffness according to EC 5/appendix B:

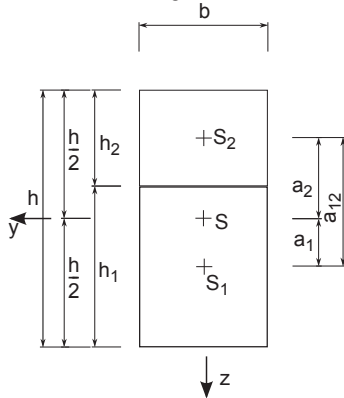
$$(EI)_{ef} = \frac{E \cdot b \cdot h_1^3}{12} + \frac{E \cdot b \cdot h_2^3}{12} + \gamma_1 \cdot EA_1 \cdot a_1^2 + \gamma_2 \cdot EA_2 \cdot a_2^2 = 3753,47 \text{ kNm}^2$$

Although the γ -values and both spaces a_1 and a_2 differ between SCHELLING and EC 5, the determined effective bending stiffness $(EI)_{ef}$ is identical within both approaches.

A.3.3 2-part cross-section – example 3

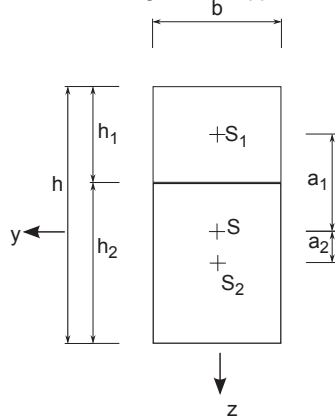
Dimensions of the selected cross-section, position of the gravity centres:

definition according to SCHELLING



$h_1=200 \text{ mm}$
 $h_2=120 \text{ mm}$
 $EA_1=352000 \text{ kN}$
 $EA_2=211200 \text{ kN}$
 $a_1=100 \text{ mm}$
 $a_2=-60 \text{ mm}$
 $a_{12}=160 \text{ mm}$

definition according to EC 5/appendix B



$b=160 \text{ mm}$
 $h=320 \text{ mm}$
 $L=6 \text{ m}$
 $E=11000 \text{ N/mm}^2$
 $c=80000 \text{ kN/m}^2$

$h_1=120 \text{ mm}$
 $h_2=200 \text{ mm}$
 $EA_1=211200 \text{ kN}$
 $EA_2=352000 \text{ kN}$
 a_1
 a_2

S ... position of the total gravity centre
 S_1 .. position of the partial cross section 1
 S_2 .. position of the partial cross section 2

Determination of the γ^* -values according to SCHELLING:

$$\gamma^*_1 = \frac{c \cdot L^2 \cdot a_{12} \cdot EA_2}{a_1 \cdot [c \cdot L^2 \cdot (EA_1 + EA_2) + EA_1 \cdot EA_2 \cdot \pi^2]} = 0,688536$$

$$\gamma^*_2 = -\frac{c \cdot L^2 \cdot a_{12} \cdot EA_1}{a_2 \cdot [c \cdot L^2 \cdot (EA_1 + EA_2) + EA_1 \cdot EA_2 \cdot \pi^2]} = 0,688536$$

Determination of the effective bending stiffness according to SCHELLING:

$$(EI)_{\text{ef}} = \frac{E \cdot b \cdot h_1^3}{12} + \frac{E \cdot b \cdot h_2^3}{12} + \gamma^*_1 \cdot EA_1 \cdot a_1^2 + \gamma^*_2 \cdot EA_2 \cdot a_2^2 = 3753,47 \text{ kNm}^2$$

The determination according to EC 5/appendix B results in a position of gravity centre which cannot be detected in the centre of the cross-section.

γ -values, a_1 and a_2 , according to EC 5/appendix B:

$$\gamma_1 = \frac{1}{1 + \pi^2 \cdot \frac{EA_1}{c \cdot L^2}} = 0,580123$$

$$\gamma_2 = 1$$

$$a_2 = \frac{\gamma_1 \cdot EA_1 \cdot (h_1 + h_2)}{2 \cdot (\gamma_1 \cdot EA_1 + \gamma_2 \cdot EA_2)} = 0,0413122$$

$$a_1 = \frac{h_1 + h_2}{2} - a_2 = 0,118688$$

Note:

in the context of the 2-part cross-section a_2 is always positive!

Determination of the effective bending stiffness according to EC 5/appendix B:

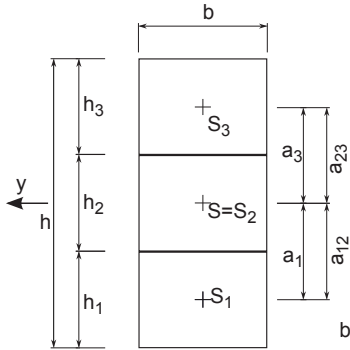
$$(EI)_{\text{ef}} = \frac{E \cdot b \cdot h_1^3}{12} + \frac{E \cdot b \cdot h_2^3}{12} + \gamma_1 \cdot EA_1 \cdot a_1^2 + \gamma_2 \cdot EA_2 \cdot a_2^2 = 3753,47 \text{ kNm}^2$$

This example corresponds to example 2 with one exception: Both partial cross-sections are positioned in a different order. In other words this means that while in example 2 the higher cross-section ($h = 200 \text{ mm}$) is positioned above, in example 3 it is located below. It is expected that this rearrangement has no impact on the bending stiffness, which is also verified by the results. However, it needs to be mentioned that the intermediate results (γ -values, a_1 and a_2) of the method EC 5/appendix B differ between the two examples.

A.3.4 3-part cross-section – example 1

Dimensions of the selected cross-section, position of the gravity centres:

definition according to SCHELLING

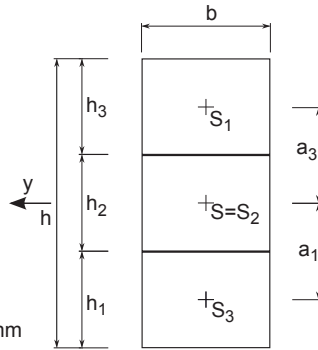


$h_1=120\text{ mm}$
 $h_2=120\text{ mm}$
 $h_3=120\text{ mm}$
 $EA_1=211200\text{ kN}$
 $EA_2=211200\text{ kN}$
 $EA_3=211200\text{ kN}$
 $a_1=120\text{ mm}$
 $a_2=0.00001\text{ h}$ (cf. note)
 $a_3=-120\text{ mm}$ (negative)
 $a_{12}=120\text{ mm}$
 $a_{23}=120\text{ mm}$

$b=160\text{ mm}$
 $h=360\text{ mm}$
 $L=6\text{ m}$

$E=11000\text{ N/mm}^2$
 $c=80000\text{ kN/m}^2$

definition according to EC 5/appendix B



$h_1=120\text{ mm}$
 $h_2=120\text{ mm}$
 $h_3=120\text{ mm}$
 $EA_1=211200\text{ kN}$
 $EA_2=211200\text{ kN}$
 $EA_3=211200\text{ kN}$
 a_2 is 0: consequently, S and S_2 are equal in amount
 a_1, a_3 result from the heights

S ... position of the total gravity centre
 S_1 .. position of the partial cross section 1
 S_2 .. position of the partial cross section 2
 S_3 .. position of the partial cross section 3

Note: SCHELLING states that there exists no regular solution for the equations of the γ^* -values in case of $a_2 = 0$. Therefore, he suggests using a small value for a_2 in this case in order produce a numerically correct solution. Here a_2 is given the value 0.00001 h . Due to the fact that the solution is fairly stable, a_2 could be also given a value which is 10 times higher or lower.

Determination of the γ^* -values according to SCHELLING:

$$\gamma_{1}^{*} = \frac{c \cdot L^2 \cdot [a_{12} \cdot (EA_2 + EA_3) + a_{23} \cdot EA_3 + a_{12} \cdot EA_2 \cdot EA_3 \cdot \pi^2]}{a_1 \cdot [c^2 \cdot L^4 \cdot (EA_1 + EA_2 + EA_3) + c \cdot L^2 \cdot \pi^2 \cdot (EA_1 \cdot EA_2 + 2 \cdot EA_1 \cdot EA_3 + EA_2 \cdot EA_3) + \pi^4 \cdot EA_1 \cdot EA_2 \cdot EA_3]} = 0,580123$$

$$\gamma_{2}^{*} = \frac{c \cdot L^2 \cdot (-a_{12} \cdot EA_1 + a_{23} \cdot EA_3) + c \cdot L^2 \cdot \pi^2 \cdot (-a_{12} + a_{23}) \cdot EA_1 \cdot EA_3}{a_3 \cdot [c^2 \cdot L^4 \cdot (EA_1 + EA_2 + EA_3) + c \cdot L^2 \cdot \pi^2 \cdot (EA_1 \cdot EA_2 + 2 \cdot EA_1 \cdot EA_3 + EA_2 \cdot EA_3) + \pi^4 \cdot EA_1 \cdot EA_2 \cdot EA_3]} = 0,0$$

$$\gamma_{3}^{*} = \frac{c \cdot L^2 \cdot [a_{23} \cdot (EA_1 + EA_2) + a_{12} \cdot EA_1 + a_{23} \cdot EA_1 \cdot EA_2 \cdot \pi^2]}{a_3 \cdot [c^2 \cdot L^4 \cdot (EA_1 + EA_2 + EA_3) + c \cdot L^2 \cdot \pi^2 \cdot (EA_1 \cdot EA_2 + 2 \cdot EA_1 \cdot EA_3 + EA_2 \cdot EA_3) + \pi^4 \cdot EA_1 \cdot EA_2 \cdot EA_3]} = 0,580123$$

Determination of the effective bending stiffness according to SCHELLING:

$$(EI)_{\text{ef}} = \frac{E \cdot b \cdot h_1^3}{12} + \frac{E \cdot b \cdot h_2^3}{12} + \frac{E \cdot b \cdot h_3^3}{12} + \gamma_1 \cdot EA_1 \cdot a_1^2 + \gamma_2 \cdot EA_2 \cdot a_2^2 + \gamma_3 \cdot EA_3 \cdot a_3^2 = 4288,96 \text{ kNm}^2$$

γ -values, a_1 , a_2 and a_3 according to EC 5/appendix B:

$$\gamma_1 = \frac{1}{1 + \pi^2 \cdot \frac{EA_1}{c \cdot L^2}} = 0,580123 \quad \gamma_2 = 1$$

$$\gamma_3 = \frac{1}{1 + \pi^2 \cdot \frac{EA_3}{c \cdot L^2}} = 0,580123$$

$$a_2 = \frac{\gamma_1 \cdot EA_1 \cdot (h_1 + h_2) - \gamma_3 \cdot EA_3 \cdot (h_2 + h_3)}{2 \cdot (\gamma_1 \cdot EA_1 + \gamma_2 \cdot EA_2 + \gamma_3 \cdot EA_3)} = 0$$

$$a_1 = \frac{h_1 + h_2}{2} - a_2 = 0,12$$

$$a_3 = \frac{h_2 + h_3}{2} + a_2 = 0,12$$

Note:

in the context of the 3-part symmetric cross-section a_2 is zero!

Determination of the effective bending stiffness according to EC 5/appendix B:

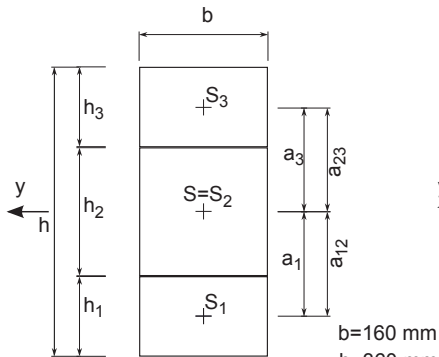
$$(EI)_{\text{ef}} = \frac{E \cdot b \cdot h_1^3}{12} + \frac{E \cdot b \cdot h_2^3}{12} + \frac{E \cdot b \cdot h_3^3}{12} + \gamma_{1}^{*} \cdot EA_1 \cdot a_1^2 + \gamma_{2}^{*} \cdot EA_2 \cdot a_2^2 + \gamma_{3}^{*} \cdot EA_3 \cdot a_3^2 = 4288,96 \text{ kNm}^2$$

In this symmetric example both calculation methods (SCHELLING and EC 5) produce the same results for all γ -values of both external parts 1 and 3. γ_2 is defined as „1“ according to EC 5 appendix B. Based on the equation system of SCHELLING, γ_2 has the value „0“. Both approaches produce the same effective bending stiffness $(EI)_{\text{ef}}$, since the Steiner-term of the intermediate part 2 is zero.

A.3.5 3-part cross-section – example 2

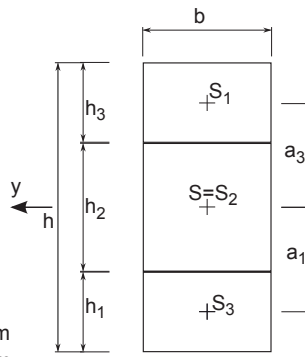
Dimensions of the selected cross-section, position of the gravity centres:

definition according to SCHELLING



$h_1=100\text{ mm}$
 $h_2=160\text{ mm}$
 $h_3=100\text{ mm}$
 $EA_1=176000\text{ kN}$
 $EA_2=281600\text{ kN}$
 $EA_3=176000\text{ kN}$
 $a_1=130\text{ mm}$
 $a_2=0.00001\text{ h}$ (cf. note)
 $a_3=-130\text{ mm}$
 $a_{12}=130\text{ mm}$
 $a_{23}=130\text{ mm}$

definition according to EC 5/appendix B



$b=160\text{ mm}$
 $h=360\text{ mm}$
 $L=6\text{ m}$
 $E=11000\text{ N/mm}^2$
 $c=80000\text{ kN/m}^2$

$h_1=100\text{ mm}$
 $h_2=160\text{ mm}$
 $h_3=100\text{ mm}$
 $EA_1=176000\text{ kN}$
 $EA_2=281600\text{ kN}$
 $EA_3=176000\text{ kN}$
 a_2 is 0: consequently, S and S_2 are equal in amount
 a_1, a_3 result from the heights

S ... position of the total gravity centre
 S_1 .. position of the partial cross section 1
 S_2 .. position of the partial cross section 2
 S_3 .. position of the partial cross section 3

Note: SCHELLING states that there exists no regular solution for the equations of the γ^* -values in case of $a_2 = 0$. Therefore, he suggests using a small value for a_2 in this case in order to produce a numerically correct solution. Here a_2 is given the value 0.00001 h . Due to the fact that the solution is fairly stable, a_2 could be also given a value which is 10 times higher or lower.

Determination of the γ^* -values according to SCHELLING:

$$\gamma^{*1} = \frac{c \cdot L^2 \cdot [a_{12} \cdot (EA_2 + EA_3) + a_{23} \cdot EA_3 + a_{12} \cdot EA_2 \cdot EA_3 \cdot \pi^2]}{a_1 \cdot [c^2 \cdot L^4 \cdot (EA_1 + EA_2 + EA_3) + c \cdot L^2 \cdot \pi^2 \cdot (EA_1 \cdot EA_2 + 2 \cdot EA_1 \cdot EA_3 + EA_2 \cdot EA_3) + \pi^4 \cdot EA_1 \cdot EA_2 \cdot EA_3]} = 0,623775$$

$$\gamma^{*2} = \frac{c \cdot L^2 \cdot (-a_{12} \cdot EA_1 + a_{23} \cdot EA_3) + c \cdot L^2 \cdot \pi^2 \cdot (-a_{12} + a_{23}) \cdot EA_1 \cdot EA_3}{a_3 \cdot [c^2 \cdot L^4 \cdot (EA_1 + EA_2 + EA_3) + c \cdot L^2 \cdot \pi^2 \cdot (EA_1 \cdot EA_2 + 2 \cdot EA_1 \cdot EA_3 + EA_2 \cdot EA_3) + \pi^4 \cdot EA_1 \cdot EA_2 \cdot EA_3]} = 0,0$$

$$\gamma^{*3} = \frac{c \cdot L^2 \cdot [a_{23} \cdot (EA_1 + EA_2) + a_{12} \cdot EA_1 + a_{23} \cdot EA_1 \cdot EA_2 \cdot \pi^2]}{a_3 \cdot [c^2 \cdot L^4 \cdot (EA_1 + EA_2 + EA_3) + c \cdot L^2 \cdot \pi^2 \cdot (EA_1 \cdot EA_2 + 2 \cdot EA_1 \cdot EA_3 + EA_2 \cdot EA_3) + \pi^4 \cdot EA_1 \cdot EA_2 \cdot EA_3]} = 0,623775$$

Determination of the effective bending stiffness according to SCHELLING:

$$(EI)_{\text{ef}} = \frac{E \cdot b \cdot h_1^3}{12} + \frac{E \cdot b \cdot h_2^3}{12} + \frac{E \cdot b \cdot h_3^3}{12} + \gamma^{*1} \cdot EA_1 \cdot a_1^2 + \gamma^{*2} \cdot EA_2 \cdot a_2^2 + \gamma^{*3} \cdot EA_3 \cdot a_3^2 = 4604,79 \text{ kNm}^2$$

γ -values, a_1 , a_2 and a_3 according to EC 5/appendix B:

$$\gamma_1 = \frac{1}{1 + \pi^2 \cdot \frac{EA_1}{c \cdot L^2}} = 0,623775 \quad \gamma_2 = 1$$

$$\gamma_3 = \frac{1}{1 + \pi^2 \cdot \frac{EA_3}{c \cdot L^2}} = 0,623775$$

$$a_2 = \frac{\gamma_1 \cdot EA_1 \cdot (h_1 + h_2) - \gamma_3 \cdot EA_3 \cdot (h_2 + h_3)}{2 \cdot (\gamma_1 \cdot EA_1 + \gamma_2 \cdot EA_2 + \gamma_3 \cdot EA_3)} = 0$$

$$a_1 = \frac{h_1 + h_2}{2} - a_2 = 0,13$$

$$a_3 = \frac{h_2 + h_3}{2} + a_2 = 0,13$$

Note:
in the context of the 3-part symmetric
cross-section a_2 is zero!

Determination of the effective bending stiffness according to EC 5/appendix B:

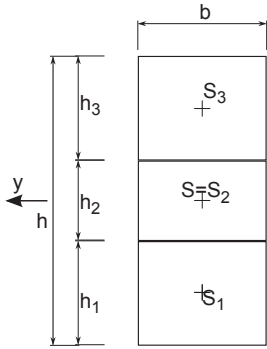
$$(EI)_{\text{ef}} = \frac{E \cdot b \cdot h_1^3}{12} + \frac{E \cdot b \cdot h_2^3}{12} + \frac{E \cdot b \cdot h_3^3}{12} + \gamma_1 \cdot EA_1 \cdot a_1^2 + \gamma_2 \cdot EA_2 \cdot a_2^2 + \gamma_3 \cdot EA_3 \cdot a_3^2 = 4604,79 \text{ kNm}^2$$

In this symmetric example both calculation methods (SCHELLING and EC 5) produce the same results for all γ -values of both external parts 1 and 3. γ_2 is defined as „1“ according to EC 5 appendix B. Based on the equation system of SCHELLING, γ_2 has the value „0“. Both approaches produce the same effective bending stiffness $(EI)_{\text{ef}}$, since the Steiner-term of the intermediate part 2 is zero.

A.3.6 3-part cross-section – example 3

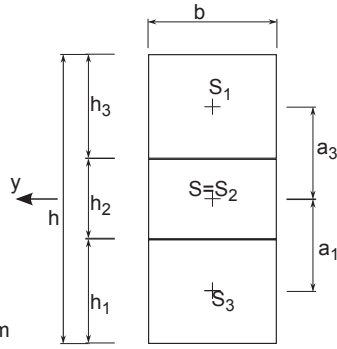
Dimensions of the selected cross-section, position of the gravity centres:

definition according to SCHELLING



$h_1=130\text{ mm}$
 $h_2=100\text{ mm}$
 $h_3=130\text{ mm}$
 $EA_1=228800\text{ kN}$
 $EA_2=176000\text{ kN}$
 $EA_3=228800\text{ kN}$
 $a_1=115\text{ mm}$
 $a_2=0.00001\text{ h (cf. note)}$
 $a_3=-115\text{ mm}$
 $a_{12}=115\text{ mm}$
 $a_{23}=115\text{ mm}$

definition according to EC 5/appendix B



$b=160\text{ mm}$
 $h=360\text{ mm}$
 $L=6\text{ m}$
 $E=11000\text{ N/mm}^2$
 $c=80000\text{ kN/m}^2$

$h_1=130\text{ mm}$
 $h_2=100\text{ mm}$
 $h_3=130\text{ mm}$
 $EA_1=228800\text{ kN}$
 $EA_2=176000\text{ kN}$
 $EA_3=228800\text{ kN}$
 $a_2\text{ is }0\text{: consequently, S and S}_2\text{ are equal in amount}$
 $a_1, a_3\text{ result from the heights}$

S ... position of the total gravity centre
 S_1 .. position of the partial cross section 1
 S_2 .. position of the partial cross section 2
 S_3 .. position of the partial cross section 3

Note: SCHELLING states that there exists no regular solution for the equations of the γ^* -values in case of $a_2 = 0$. Therefore, he suggests using a small value for a_2 in this case in order to produce a numerically correct solution. Here a_2 is given the value 0.00001 h . Due to the fact that the solution is fairly stable, a_2 could be also given a value which is 10 times higher or lower.

Determination of the γ^* -values according to SCHELLING:

$$\gamma^{*1} = \frac{c \cdot L^2 \cdot [a_{12} \cdot (EA_2 + EA_3) + a_{23} \cdot EA_3 + a_{12} \cdot EA_2 \cdot EA_3 \cdot \pi^2]}{a_1 \cdot [c^2 \cdot L^4 \cdot (EA_1 + EA_2 + EA_3) + c \cdot L^2 \cdot \pi^2 \cdot (EA_1 \cdot EA_2 + 2 \cdot EA_1 \cdot EA_3 + EA_2 \cdot EA_3) + \pi^4 \cdot EA_1 \cdot EA_2 \cdot EA_3]} = 0,560511$$

$$\gamma^{*2} = \frac{c \cdot L^2 \cdot (-a_{12} \cdot EA_1 + a_{23} \cdot EA_3) + c \cdot L^2 \cdot \pi^2 \cdot (-a_{12} + a_{23}) \cdot EA_1 \cdot EA_3}{a_3 \cdot [c^2 \cdot L^4 \cdot (EA_1 + EA_2 + EA_3) + c \cdot L^2 \cdot \pi^2 \cdot (EA_1 \cdot EA_2 + 2 \cdot EA_1 \cdot EA_3 + EA_2 \cdot EA_3) + \pi^4 \cdot EA_1 \cdot EA_2 \cdot EA_3]} = 0,0$$

$$\gamma^{*3} = \frac{c \cdot L^2 \cdot [a_{23} \cdot (EA_1 + EA_2) + a_{12} \cdot EA_1 + a_{23} \cdot EA_1 \cdot EA_2 \cdot \pi^2]}{a_3 \cdot [c^2 \cdot L^4 \cdot (EA_1 + EA_2 + EA_3) + c \cdot L^2 \cdot \pi^2 \cdot (EA_1 \cdot EA_2 + 2 \cdot EA_1 \cdot EA_3 + EA_2 \cdot EA_3) + \pi^4 \cdot EA_1 \cdot EA_2 \cdot EA_3]} = 0,560511$$

Determination of the effective bending stiffness according to SCHELLING:

$$(EI)_{\text{ef}} = \frac{E \cdot b \cdot h_1^3}{12} + \frac{E \cdot b \cdot h_2^3}{12} + \frac{E \cdot b \cdot h_3^3}{12} + \gamma^{*1} \cdot EA_1 \cdot a_1^2 + \gamma^{*2} \cdot EA_2 \cdot a_2^2 + \gamma^{*3} \cdot EA_3 \cdot a_3^2 = 4183,2 \text{ kNm}^2$$

γ -values, a_1 , a_2 and a_3 according to EC 5/appendix B:

$$\gamma_1 = \frac{1}{1 + \pi^2 \cdot \frac{EA_1}{c \cdot L^2}} = 0,560511 \quad \gamma_2 = 1$$

$$\gamma_3 = \frac{1}{1 + \pi^2 \cdot \frac{EA_3}{c \cdot L^2}} = 0,560511$$

$$a_2 = \frac{\gamma_1 \cdot EA_1 \cdot (h_1 + h_2) - \gamma_3 \cdot EA_3 \cdot (h_2 + h_3)}{2 \cdot (\gamma_1 \cdot EA_1 + \gamma_2 \cdot EA_2 + \gamma_3 \cdot EA_3)} = 0$$

$$a_1 = \frac{h_1 + h_2}{2} - a_2 = 0,115$$

$$a_3 = \frac{h_2 + h_3}{2} + a_2 = 0,115$$

Anmerkung:
 a_2 ist beim dreiteiligen
symmetrischen Querschnitt null!

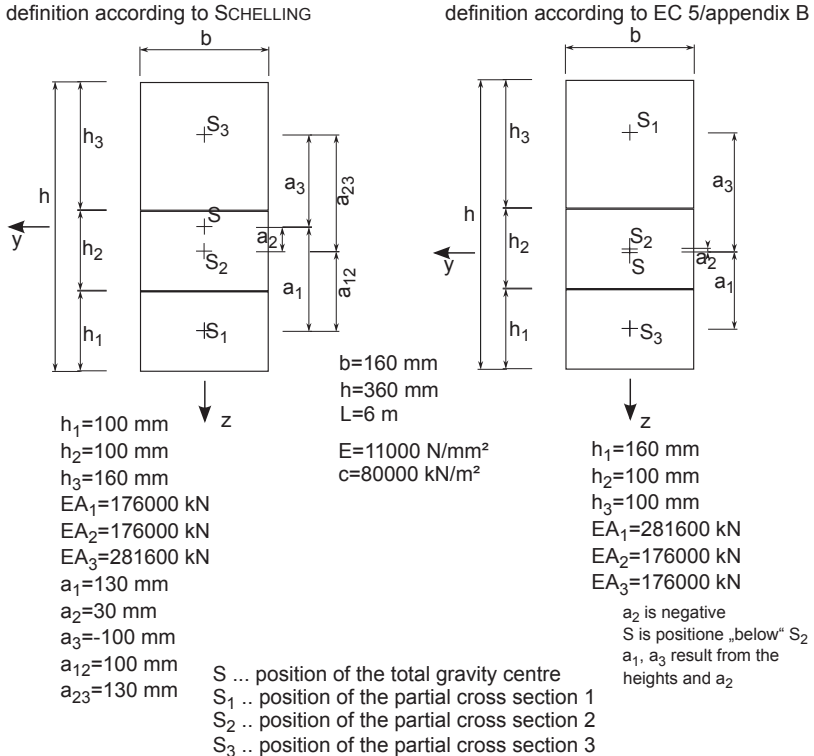
Determination of the effective bending stiffness according to EC 5/appendix B:

$$(EI)_{\text{ef}} = \frac{E \cdot b \cdot h_1^3}{12} + \frac{E \cdot b \cdot h_2^3}{12} + \frac{E \cdot b \cdot h_3^3}{12} + \gamma_1 \cdot EA_1 \cdot a_1^2 + \gamma_2 \cdot EA_2 \cdot a_2^2 + \gamma_3 \cdot EA_3 \cdot a_3^2 = 4183,2 \text{ kNm}^2$$

In this symmetric example both calculation methods (SCHELLING and EC 5) produce the same results for all γ -values of both external parts 1 and 3. γ_2 is defined as „1“ according to EC 5 appendix B. Based on the equation system of SCHELLING, γ_2 has the value „0“. Both approaches produce the same effective bending stiffness $(EI)_{\text{ef}}$, since the Steiner-term of the intermediate part 2 is zero.

A.3.7 3-part cross-section – example 4

Dimensions of the selected cross-section, position of the gravity centres:



In this example a_2 is not zero. This implies that the results directly lead to a regular solution when applying the equations according to SCHELLING.

If the approach EC 5/Annex is used, it is of crucial importance to be aware of the fact that the gravity centre is not placed in the gravity centre of the total area – as it is the case with SCHELLING – but at the position where the highest amount of shear stress is put on.

Determination of the γ^* -values according to SCHELLING:

$$\gamma_1^* = \frac{c \cdot L^2 \cdot [a_{12} \cdot (EA_2 + EA_3) + a_{23} \cdot EA_3 + a_{12} \cdot EA_2 \cdot EA_3 \cdot \pi^2]}{a_1 \cdot [c^2 \cdot L^4 \cdot (EA_1 + EA_2 + EA_3) + c \cdot L^2 \cdot \pi^2 \cdot (EA_1 \cdot EA_2 + 2 \cdot EA_1 \cdot EA_3 + EA_2 \cdot EA_3) + \pi^4 \cdot EA_1 \cdot EA_2 \cdot EA_3]} = 0,565387$$

$$\gamma_2^* = \frac{c \cdot L^2 \cdot (-a_{12} \cdot EA_1 + a_{23} \cdot EA_3) + c \cdot L^2 \cdot \pi^2 \cdot (-a_{12} + a_{23}) \cdot EA_1 \cdot EA_3}{a_3 \cdot [c^2 \cdot L^4 \cdot (EA_1 + EA_2 + EA_3) + c \cdot L^2 \cdot \pi^2 \cdot (EA_1 \cdot EA_2 + 2 \cdot EA_1 \cdot EA_3 + EA_2 \cdot EA_3) + \pi^4 \cdot EA_1 \cdot EA_2 \cdot EA_3]} = 0,594383$$

$$\gamma_3^* = \frac{c \cdot L^2 \cdot [a_{23} \cdot (EA_1 + EA_2) + a_{12} \cdot EA_1 + a_{23} \cdot EA_1 \cdot EA_2 \cdot \pi^2]}{a_3 \cdot [c^2 \cdot L^4 \cdot (EA_1 + EA_2 + EA_3) + c \cdot L^2 \cdot \pi^2 \cdot (EA_1 \cdot EA_2 + 2 \cdot EA_1 \cdot EA_3 + EA_2 \cdot EA_3) + \pi^4 \cdot EA_1 \cdot EA_2 \cdot EA_3]} = 0,570824$$

Determination of the effective bending stiffness according to SCHELLING:

$$(EI)_{\text{ef}} = \frac{E \cdot b \cdot h_1^3}{12} + \frac{E \cdot b \cdot h_2^3}{12} + \frac{E \cdot b \cdot h_3^3}{12} + \gamma_1^* \cdot EA_1 \cdot a_1^2 + \gamma_2^* \cdot EA_2 \cdot a_2^2 + \gamma_3^* \cdot EA_3 \cdot a_3^2 = 4277,36 \text{ kNm}^2$$

γ -values, a_1 , a_2 and a_3 according to EC 5/appendix B:

$$\gamma_1 = \frac{1}{1 + \pi^2 \cdot \frac{EA_1}{c \cdot L^2}} = 0,623775$$

$$\gamma_2 = 1$$

$$\gamma_3 = \frac{1}{1 + \pi^2 \cdot \frac{EA_3}{c \cdot L^2}} = 0,508899(560511)$$

$$a_2 = \frac{\gamma_1 \cdot EA_1 \cdot (h_1 + h_2) - \gamma_3 \cdot EA_3 \cdot (h_2 + h_3)}{2 \cdot (\gamma_1 \cdot EA_1 + \gamma_2 \cdot EA_2 + \gamma_3 \cdot EA_3)} = -0,0178315$$

$$a_1 = \frac{h_1 + h_2}{2} - a_2 = 0,1178315$$

$$a_3 = \frac{h_2 + h_3}{2} + a_2 = 0,1121$$

Note:

in the context of the 3-part symmetric cross-section a_2 is either positive or negative!

Determination of the effective bending stiffness according to EC 5/appendix B:

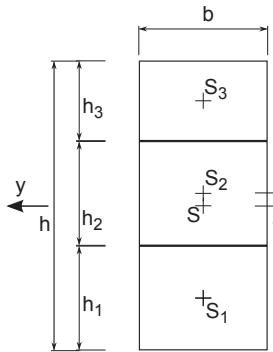
$$(EI)_{\text{ef}} = \frac{E \cdot b \cdot h_1^3}{12} + \frac{E \cdot b \cdot h_2^3}{12} + \frac{E \cdot b \cdot h_3^3}{12} + \gamma_1 \cdot EA_1 \cdot a_1^2 + \gamma_2 \cdot EA_2 \cdot a_2^2 + \gamma_3 \cdot EA_3 \cdot a_3^2 = 4277,36 \text{ kNm}^2$$

Although the γ -values differ significantly, the determined effective bending stiffness $(EI)_{\text{ef}}$ of SCHELLING method is identical with the one of EC 5.

A.3.8 3-part cross-section – example 5

Dimensions of the selected cross-section, position of the gravity centres:

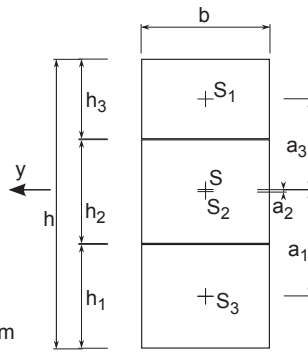
definition according to SCHELLING



$h_1=130\text{ mm}$
 $h_2=130\text{ mm}$
 $h_3=100\text{ mm}$
 $EA_1=228800\text{ kN}$
 $EA_2=228800\text{ kN}$
 $EA_3=176000\text{ kN}$
 $a_1=115\text{ mm}$
 $a_2=-15\text{ mm (negative)}$
 $a_3=-130\text{ mm (negative)}$
 $a_{12}=130\text{ mm}$
 $a_{23}=115\text{ mm}$

$S \dots$ position of the total gravity centre
 $S_1 \dots$ position of the partial cross section 1
 $S_2 \dots$ position of the partial cross section 2
 $S_3 \dots$ position of the partial cross section 3

definition according to EC 5/appendix B



$b=160\text{ mm}$
 $h=360\text{ mm}$
 $L=6\text{ m}$
 $E=11000\text{ N/mm}^2$
 $c=80000\text{ kN/m}^2$

$h_1=160\text{ mm}$
 $h_2=100\text{ mm}$
 $h_3=100\text{ mm}$
 $EA_1=176000\text{ kN}$
 $EA_2=228800\text{ kN}$
 $EA_3=228800\text{ kN}$
 a_2 is positiv
 S is positiond „above“ S_2
 a_1, a_3 result from the heights and a_2

In this example a_2 is not zero. This implies that the results directly lead to a regular solution when applying the equations according to SCHELLING.

If the approach EC 5/Annex is used, it is of crucial importance to be aware of the fact that the gravity centre is not placed in the gravity centre of the total area – as it is the case with SCHELLING – but at the position where the highest amount of shear stress is put on.

Determination of the γ^* -values according to SCHELLING:

$$\gamma^{*1} = \frac{c \cdot L^2 \cdot [a_{12} \cdot (EA_2 + EA_3) + a_{23} \cdot EA_3 + a_{12} \cdot EA_2 \cdot EA_3 \cdot \pi^2]}{a_1 \cdot [c^2 \cdot L^4 \cdot (EA_1 + EA_2 + EA_3) + c \cdot L^2 \cdot \pi^2 \cdot (EA_1 \cdot EA_2 + 2 \cdot EA_1 \cdot EA_3 + EA_2 \cdot EA_3) + \pi^4 \cdot EA_1 \cdot EA_2 \cdot EA_3]} = 0,591372$$

$$\gamma^{*2} = \frac{c \cdot L^2 \cdot (-a_{12} \cdot EA_1 + a_{23} \cdot EA_3) + c \cdot L^2 \cdot \pi^2 \cdot (-a_{12} + a_{23}) \cdot EA_1 \cdot EA_3}{a_3 \cdot [c^2 \cdot L^4 \cdot (EA_1 + EA_2 + EA_3) + c \cdot L^2 \cdot \pi^2 \cdot (EA_1 \cdot EA_2 + 2 \cdot EA_1 \cdot EA_3 + EA_2 \cdot EA_3) + \pi^4 \cdot EA_1 \cdot EA_2 \cdot EA_3]} = 0,577891$$

$$\gamma^{*3} = \frac{c \cdot L^2 \cdot [a_{23} \cdot (EA_1 + EA_2) + a_{12} \cdot EA_1 + a_{23} \cdot EA_1 \cdot EA_2 \cdot \pi^2]}{a_3 \cdot [c^2 \cdot L^4 \cdot (EA_1 + EA_2 + EA_3) + c \cdot L^2 \cdot \pi^2 \cdot (EA_1 \cdot EA_2 + 2 \cdot EA_1 \cdot EA_3 + EA_2 \cdot EA_3) + \pi^4 \cdot EA_1 \cdot EA_2 \cdot EA_3]} = 0,593394$$

Determination of the effective bending stiffness according to SCHELLING:

$$(EI)_{\text{ef}} = \frac{E \cdot b \cdot h_1^3}{12} + \frac{E \cdot b \cdot h_2^3}{12} + \frac{E \cdot b \cdot h_3^3}{12} + \gamma^{*1} \cdot EA_1 \cdot a_1^2 + \gamma^{*2} \cdot EA_2 \cdot a_2^2 + \gamma^{*3} \cdot EA_3 \cdot a_3^2 = 4375,28 \text{ kNm}^2$$

γ -values, a_1 , a_2 and a_3 according to EC 5/appendix B:

$$\gamma_1 = \frac{1}{1 + \pi^2 \cdot \frac{EA_1}{c \cdot L^2}} = 0,560511$$

$$\gamma_2 = 1$$

$$\gamma_3 = \frac{1}{1 + \pi^2 \cdot \frac{EA_3}{c \cdot L^2}} = 0,623775$$

$$a_2 = \frac{\gamma_1 \cdot EA_1 \cdot (h_1 + h_2) - \gamma_3 \cdot EA_3 \cdot (h_2 + h_3)}{2 \cdot (\gamma_1 \cdot EA_1 + \gamma_2 \cdot EA_2 + \gamma_3 \cdot EA_3)} = 0,00866836$$

$$a_1 = \frac{h_1 + h_2}{2} - a_2 = 0,121332$$

$$a_3 = \frac{h_2 + h_3}{2} + a_2 = 0,123668$$

Note:

in the context of the 3-part symmetric cross-section a_2 is either positive or negative!

Determination of the effective bending stiffness according to EC 5/appendix B:

$$(EI)_{\text{ef}} = \frac{E \cdot b \cdot h_1^3}{12} + \frac{E \cdot b \cdot h_2^3}{12} + \frac{E \cdot b \cdot h_3^3}{12} + \gamma_1 \cdot EA_1 \cdot a_1^2 + \gamma_2 \cdot EA_2 \cdot a_2^2 + \gamma_3 \cdot EA_3 \cdot a_3^2 = 4375,28 \text{ kNm}^2$$

Although the γ -values differ significantly between to SCHELLING and EC 5, the determined effective bending stiffness $(EI)_{\text{ef}}$ of the SCHELLING method is identical with the one of EC 5 approach.

B Appendix B – Comparison of the γ -process according to SCHELLING and EN 1995-1-1 on the example of a 3-layered CLT-girder

B.1 System T1 „mod“ – single-span girder exposed to uniform load

B.1.1 Modified γ -process

For the calculation of the 3-layered CLT-plate the span of System T1 was modified so that the L/H-ratio of 30 is still given with a plate thickness t_{clt} of 96 mm.

Static system | Load

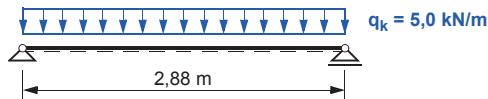


Abb. B-1 Static system T1 „mod“ – single-span girder exposed to uniform load

Slab structure | Material data

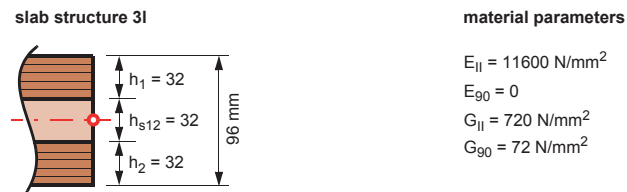


Abb. B-2 Slab structure and material parameters (GL 24h acc. to ON EN 1194:1999 [23])

Cross-sectional values

Based on the formulae of chap. 3.2.2 and chap. 3.2.3, the cross-sectional values are determined as follows:

Values of the single layer

$$A_i = b_i \cdot h_i = 1000 \cdot 32 = 32000 \text{ mm}^2$$

$$I_i = \frac{b_i \cdot h_i^3}{12} = \frac{1000 \cdot 32^3}{12} = 2730667 \text{ mm}^4$$

Determination of the γ -values

$$\gamma_1 = \frac{1}{1 + \frac{\pi^2 \cdot E_i \cdot A_i \cdot h_{si}}{l^2 \cdot G_{90} \cdot b}} = \frac{1}{1 + \frac{\pi^2 \cdot 11600 \cdot 32000 \cdot 32}{2880^2 \cdot 72 \cdot 1000}} = 0,8359$$

$$\gamma_2 = 1$$

Distances from the effective centre line

$$a_2 = \frac{\gamma_1 \cdot E_1 \cdot A_1 \cdot \left(\frac{h_1 + h_2}{2} + h_{s12}\right)}{\sum_{i=1}^2 \gamma_i \cdot E_i \cdot A_i}$$

$$a_2 = \frac{0,8359 \cdot 11600 \cdot 32000 \cdot \left(\frac{32 + 32}{2} + 32\right)}{0,8359 \cdot 11600 \cdot 32000 + 1,0 \cdot 11600 \cdot 32000} = 29,14 \text{ mm}$$

$$a_1 = \frac{h_1}{2} + h_{s12} + \frac{h_2}{2} - a_2 = \frac{32}{2} + 32 + \frac{32}{2} - 29,14 = 34,86 \text{ mm}$$

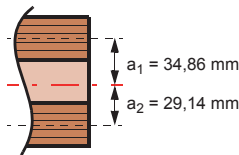


Abb. B-3 Distances from the effective centre line a_1 and a_2

Determination of the effective bending stiffness $(EI)_{ef}$

$$(EI)_{ef} = \sum_{i=1}^2 (E_i \cdot I_i + \gamma_i \cdot E_i \cdot A_i \cdot a_i^2)$$

$$(EI)_{ef} = 2 \cdot 11600 \cdot 2730667 + 0,8359 \cdot 11600 \cdot 32000 \cdot 34,86^2 + 1,0 \cdot 11600 \cdot 32000 \cdot 29,14^2 = 7,556 \cdot 10^{11} \text{ Nmm}^2$$

Internal forces

$$M_{\max} = \frac{q \cdot l^2}{8} = \frac{5,0 \cdot 2,88^2}{8} = 5,184 \text{ kNm}$$

$$V_{\max} = \frac{q \cdot l}{2} = \frac{5,0 \cdot 2,88}{2} = 7,20 \text{ kN}$$

Stresses

Maximum bending stress

$$\sigma_1 = \frac{M_{\max}}{(EI)_{ef}} \cdot \gamma_1 \cdot E_1 \cdot a_1$$

$$\sigma_1 = \frac{5,184 \cdot 10^6}{7,556 \cdot 10^{11}} \cdot 0,8359 \cdot 11600 \cdot 34,86 = 2,319 \text{ N/mm}^2$$

$$\sigma_{m,1} = \frac{M_{\max}}{(EI)_{ef}} \cdot \frac{E_1 \cdot h_1}{2} = \frac{5,184 \cdot 10^6}{7,556 \cdot 10^{11}} \cdot \frac{11600 \cdot 32}{2} = 1,273 \text{ N/mm}^2$$

$$\sigma_{\max} = \sigma_1 + \sigma_{m,1} = 2,319 + 1,273 = 3,592 \text{ N/mm}^2$$

Maximum shear stress

$$\tau_{\max} = \frac{V_{\max}}{(EI)_{ef}} \cdot \frac{\gamma_1 \cdot E_1 \cdot A_1 \cdot a_1}{b}$$

$$\tau_{\max} = \frac{7,20 \cdot 10^3}{7,556 \cdot 10^{11}} \cdot \frac{0,8359 \cdot 11600 \cdot 32000 \cdot 34,86}{1000} = 0,103 \text{ N/mm}^2$$

Stress diagram

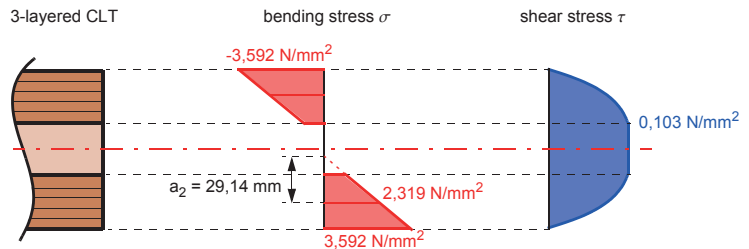


Abb. B-4

Diagrams of bending- and shear stress within cross-section

B.1.2 Determination according to SCHELLING

Static system | Load

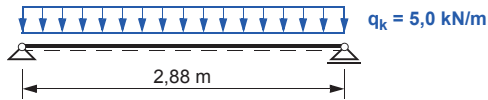
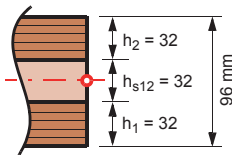


Abb. B-5 Static system T1 „mod“ – single-span girder exposed to uniform load

Slab structure | Material data

slab structure 3I



material parameters

$$E_{II} = 11600 \text{ N/mm}^2$$

$$E_{90} = 0$$

$$G_{II} = 720 \text{ N/mm}^2$$

$$G_{90} = 72 \text{ N/mm}^2$$

Abb. B-6 Slab structure and material parameters (GL 24h acc. to ON EN 1194:1999 [23])

Cross-sectional values

Values of the single layer

$$A_i = b_i \cdot h_i = 1000 \cdot 32 = 32000 \text{ mm}^2$$

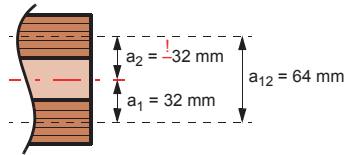
$$EA_i = 11600 \cdot 32000 = 3,712 \cdot 10^8 \text{ mm}$$

$$I_i = \frac{b_i \cdot h_i^3}{12} = \frac{1000 \cdot 32^3}{12} = 2730667 \text{ mm}^4$$

Joint stiffness of the transversal layer

$$c = \frac{G_{90} \cdot b}{h_{s12}} = \frac{72 \cdot 1000}{32} = 2250 \text{ N/mm}^2$$

Distances from the geometric centre line

Abb. B-7 Distances from the geometric centre line a_1 , a_2 and a_{12} Determination of the γ^* -values

$$\gamma^*_1 = \frac{c \cdot L^2 \cdot a_{12} \cdot EA_2}{a_1 \cdot [c \cdot L^2 \cdot (EA_1 + EA_2) + EA_1 \cdot EA_2 \cdot \pi^2]}$$

$$\gamma^*_1 = \frac{2250 \cdot 2880^2 \cdot 64 \cdot 3,712 \cdot 10^8}{32 \cdot [2250 \cdot 2880^2 \cdot (2 \cdot 3,712 \cdot 10^8) + (3,712 \cdot 10^8)^2 \cdot \pi^2]} = 0,9106$$

$$\gamma^*_2 = -\frac{c \cdot L^2 \cdot a_{12} \cdot EA_1}{a_2 \cdot [c \cdot L^2 \cdot (EA_1 + EA_2) + EA_1 \cdot EA_2 \cdot \pi^2]}$$

$$\gamma^*_2 = -\frac{2250 \cdot 2880^2 \cdot 64 \cdot 3,712 \cdot 10^8}{-32 \cdot [2250 \cdot 2880^2 \cdot (2 \cdot 3,712 \cdot 10^8) + (3,712 \cdot 10^8)^2 \cdot \pi^2]} = 0,9106$$

Determination of the effective bending stiffness $(EI)_{ef}$

$$(EI)_{ef} = \frac{E \cdot b \cdot h_1^3}{12} + \frac{E \cdot b \cdot h_2^3}{12} + \gamma^*_1 \cdot EA_1 \cdot a_1^2 + \gamma^*_2 \cdot EA_2 \cdot a_2^2$$

$$\begin{aligned} (EI)_{ef} &= 2 \cdot 11600 \cdot 2730667 + 2 \cdot (0,9106 \cdot 3,712 \cdot 10^8 \cdot 32^2) = \\ &= 7,556 \cdot 10^{11} \text{ Nmm}^2 \end{aligned}$$

Note: Although the g-values and both spaces a_1 and a_2 differ between SCHELLING and EC 5, the determined effective bending stiffness $(EI)_{ef}$ is identical within both approaches.

Internal forces

$$M_{\max} = \frac{q \cdot l^2}{8} = \frac{5,0 \cdot 2,88^2}{8} = 5,184 \text{ kNm}$$

$$V_{\max} = \frac{q \cdot l}{2} = \frac{5,0 \cdot 2,88}{2} = 7,20 \text{ kN}$$

Stresses

Maximum bending stress

$$\sigma_1 = \frac{M_{\max}}{(EI)_{ef}} \cdot \gamma_1 \cdot E_1 \cdot a_1$$

$$\sigma_1 = \frac{5,184 \cdot 10^6}{7,556 \cdot 10^{11}} \cdot 0,9106 \cdot 11600 \cdot 32 = 2,319 \text{ N/mm}^2$$

$$\sigma_{m,1} = \frac{M_{\max}}{(EI)_{ef}} \cdot \frac{E_1 \cdot h_1}{2} = \frac{5,184 \cdot 10^6}{7,556 \cdot 10^{11}} \cdot \frac{11600 \cdot 32}{2} = 1,273 \text{ N/mm}^2$$

$$\sigma_{\max} = \sigma_1 + \sigma_{m,1} = 2,319 + 1,273 = 3,592 \text{ N/mm}^2$$

Maximum shear stress

$$\tau_{\max} = \frac{V_{\max}}{(EI)_{ef}} \cdot \frac{\gamma_1 \cdot E_1 \cdot A_1 \cdot a_1}{b}$$

$$\tau_{\max} = \frac{7,20 \cdot 10^3}{7,556 \cdot 10^{11}} \cdot \frac{0,9106 \cdot 3,712 \cdot 10^8 \cdot 32}{1000} = 0,103 \text{ N/mm}^2$$

Stress diagram

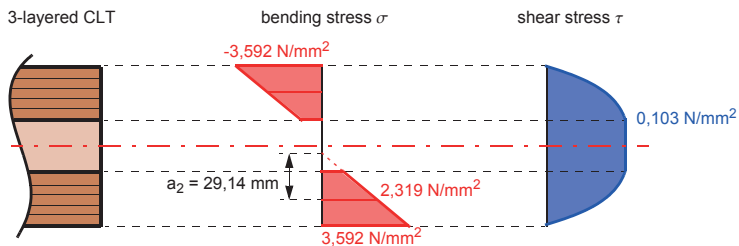


Abb. B-8 Diagrams of bending- and shear stress within cross-section

